Historic Textile and Paper Materials

Published on February 1, 1986 on http://pubs.acs.org | doi: 10.1021/ba-1986-0212.fw001

ADVANCES IN CHEMISTRY SERIES 212

Historic Textile and Paper Materials

Conservation and Characterization

Howard L. Needles, EDITOR
University of California, Davis

S. Haig Zeronian, EDITOR
University of California, Davis

Developed from a symposium sponsored by
the Cellulose, Paper, and Textile Division
at the 188th Meeting
of the American Chemical Society,
Philadelphia, Pennsylvania,
August 27–29, 1984

American Chemical Society, Washington, DC 1986

Library of Congress Cataloging-in-Publication Data

Historic textile and paper materials.
(Advances in chemistry series, ISSN 0065-2393; 212)

"Developed from a symposium sponsored by the Cellulose, Paper, and Textile Chemistry Division at the 188th Meeting of the American Chemical Society, Philadelphia, Pennsylvania, August 27-29, 1984."

Includes bibliographies and indexes.

1. Textile fabrics—Conservation and restoration—Congresses. 2. Paper—Preservation—Congresses.

I. Needles, Howard L. II. Zeronian, S. Haig. III. American Chemical Society. Cellulose, Paper and Textile Division. IV. American Chemical Society. Meeting (188th: 1984: Philadelphia, Pa.) V. Series.

QD1.A355 no. 212 540 s 85-20094
[TS1449] [677'.028]
ISBN 0-8412-0900-6

Advances in Chemistry Series

M. Joan Comstock, *Series Editor*

Advisory Board

FOREWORD

The ADVANCES IN CHEMISTRY SERIES was founded in 1949 by the American Chemical Society as an outlet for symposia and collections of data in special areas of topical interest that could not be accommodated in the Society's journals. It provides a medium for symposia that would otherwise be fragmented because their papers would be distributed among several journals or not published at all. Papers are reviewed critically according to ACS editorial standards and receive the careful attention and processing characteristic of ACS publications. Volumes in the ADVANCES IN CHEMISTRY SERIES maintain the integrity of the symposia on which they are based; however, verbatim reproductions of previously published papers are not accepted. Papers may include reports of research as well as reviews, because symposia may embrace both types of presentation.

ABOUT THE EDITORS

HOWARD L. NEEDLES is professor of textile and materials science and textile chemist in the Experiment Station at the University of California, Davis. He is a graduate of the University of California, Riverside (A.B.), and the University of Missouri, Columbia (Ph.D.). After receiving his degrees, he joined the Wool and Mohair Laboratory of the Western Regional Research Laboratory of the U.S. Department of Agriculture and conducted basic research in the areas of organic, protein, and polymer chemistry. Since becoming a faculty member at the University of California, Davis, in 1969, he has done research on fiber and polymer science, including fiber modification through chemical treatment and polymer grafting, dye-fiber interactions, dye analysis on natural fibers, environmental degradation of undyed and dyed textiles, and fiber-polymer composites. He has published more than eighty papers in these areas. He was visiting professor at North Carolina State University, Raleigh, in 1975–76 and at the University of Leeds, England, in 1982–83. He is currently program chairman for the Cellulose, Paper, and Textile Division of the American Chemical Society.

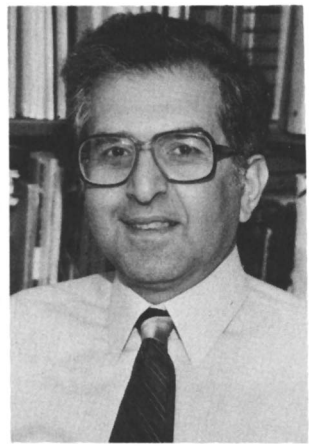

S. HAIG ZERONIAN is professor of textile science and professor of mechanical engineering, as well as textile chemist in the Agricultural Experiment Station and chair of the Division of Textiles and Clothing, all at the University of California, Davis, California. His former posts include research associate in the Research and Development Division of the Columbia Cellulose Company, Canada (1966–68); senior research fellow in nonwoven fabrics at the University of Manchester Institute of Science and Technology, England (1963–66); research fellow in cellulose chemistry at the Institute of Paper Chemistry, Wisconsin; research fellow in fibre bonding at the University of Manchester, England; and research officer at the British Cotton Industry Research Association, Manchester, England. He graduated from Manchester University, England, with a B.Sc. Tech. in textile chemistry (1953), M.Sc. Tech. in textile chemistry (1955), Ph.D. in cellulose chemistry (1962), and D.Sc. in polymer and fibre science (1983).

As well as being a fellow of the Textile Institute since 1979, S. Haig Zeronian was a visiting professor of forest resources at the University of Washington, Seattle, Washington, in 1982, and visiting scientist with the Western Regional Research Laboratory, Berkeley, California, from 1974 to 1975. He has over 70 publications in the scientific literature.

PREFACE

THE CONSERVATION AND CHARACTERIZATION of historic textile and paper materials have been active areas of interest to conservators, chemists, and other physical scientists for several decades. Often studies were conducted with little interaction between conservators and physical scientists because each group tended to present its findings to different societies. In recent years John C. Williams of The Library of Congress organized two symposia for the Cellulose, Paper, and Textile Division of the American Chemical Society dealing with the preservation of paper and textiles of historic and artistic value. These symposia were highly successful in permitting conservators and physical scientists to discuss areas of mutual interest. The ADVANCES IN CHEMISTRY SERIES volumes that resulted from these symposia have been well received by the scientific and conservation community. Because of the success of these efforts, a third symposium concerned with the conservation and characterization of historic textile and paper materials was organized. It differed from the previous two symposia in that papers concerned with the conservation and characterization of textiles were more predominant. This situation reflected a growing interest in this area by textile scientists.

As in the previous symposia, the desired communication between conservators and physical scientists was achieved. We hope that this volume will be received by the conservation and scientific community with the same degree of success as that received by the previous volumes. We thank the researchers who authored the chapters, for without them and their work, this volume would not be possible.

HOWARD L. NEEDLES
S. HAIG ZERONIAN
University of California, Davis
Davis, CA 95616

January 1985

1

Charting the Future: Conservation Principles of Henry Francis du Pont

Margaret A. Fikioris

Conservation Section, Winterthur Museum, Winterthur, DE 19735

Henry Francis du Pont, founder of Winterthur Museum, was a leader in the museum field during his lifetime in acquisitions, display, and care of the collection. He began his American collection in 1923 and was active until 1969. His conservation principles are a synthesis of a late 19th century concern for the care of objects and a 20th century willingness to initiate and encourage modern conservation science and practices. It has now been 16 years since his death, and it seems a fitting time to reflect upon and acknowledge Henry Francis du Pont's contribution to the museum field nationally and to the role of conservation.

THE SEARCH TO UNDERSTAND the conservation principles of Henry Francis du Pont unfolded easily, because he was a great organizer and initiator. Henry Francis du Pont exemplified the well-to-do Victorian household tradition of having a large staff and a formal way of accomplishing routine tasks with instructions given orally. Great loyalty and mutual respect were shared between Mr. du Pont and his staff. Many of the museum employees worked at Winterthur during Mr. du Pont's lifetime, and several of these people generously shared their memories of how things were done in the early transitional years of Winterthur as it changed from a private home and estate to a museum institution and public gardens (Figure 1). Through the letters and instructions of Henry Francis du Pont, one can clearly follow his thought processes and understand his goals of planning the future, maintaining the present, and preserving the past. Many of the principles of how the museum should be cared for were established early in Mr. du Pont's collecting lifetime and served as building blocks for later documents. They were carefully spelled out in the notebook of instructions entitled "Letters and Notes To the Executors and Winterthur Directors [Trustees] Concerning The Winterthur Museum and Winterthur House." This 83-page book was begun before the official opening of the museum in 1951 and was

0065-2393/86/0212-0003 $06.00/0

continually reviewed and reworked; each page has three to five dates in the top margin signifying the many revisions made by Mr. du Pont over the years.

Henry Francis du Pont (Figure 2) worked fervently to get the more than 195 period rooms and display areas completed in his lifetime. Often he would express to his closest staff (*1*), "Do it now because it won't be done after I die." When asked by Harlan B. Phillips in a 1962 oral interview for the Archives of American Art about his feelings on

Figure 1. View of Winterthur House from the east, 1902–28, as it appeared when Henry Francis du Pont inherited it. Courtesy, The Henry Francis du Pont Winterthur Museum.

Figure 2. Patriot's Day ceremonies at Winterthur, April 19, 1955. From left to right: Henry Francis du Pont, Lammot du Pont Copeland, and Delaware Governor J. Caleb Boggs. Courtesy, Harry A. Lemmon.

having to move out of his house to turn it into a public museum, he responded (2):

> *I've always lived in that house, and the more I thought of it as a museum, the more workable I thought it would be. It was just a question of upkeep. It's an enormously big house, and I did want to see it done properly or according to my idea. . . . The best way really was to move out; in fact, I didn't think that many people would come to see it then, that it would evolve by degrees. I['ve] got a big book full of notes for our trustees, executives, and so forth. I kept some of the early pages . . . some of the originals. I thought that they were rather interesting.*

Henry Francis du Pont began his "Letters and Notes To Executors and Winterthur Directors" with the following statement (3): "It is my intention and desire that Winterthur and the surrounding grounds shall be kept in perpetuity as a Museum and arboretum for the education and enjoyment of the public." He continued, "My purpose in leaving Winterthur as a Museum to the public is to afford all those interested an opportunity to view and to study the conditions surrounding the early American home life." Mr. du Pont also wanted the building kept in such a way that it would retain its charm and intimacy. "The reason for this," he stated, "is that the interest of the Museum, quite aside from its furniture, beauty of colors, and upholsteries, lies in the infinite details, . . . and the many, many different ornaments and accessories."

Mr. du Pont did not want the visitors to be hindered in the enjoyment of the room. Thus, he felt that the number of visitors should be restricted. He wrote (3), "There may be two to ten groups seeing the house at the same time, depending on the number of guides available, and each group should be accompanied by a suitable and competent employee guide of the Museum." From his own experience Henry Francis du Pont believed (3) "that three or four people are really all that can go through in one group conveniently and comfortably." Furthermore, limiting the number of groups would help reduce the "wear and tear" on the collection, and this limitation would allow the "furnishings [to] be kept intact for a longer period of years so that those who go through may do so with enjoyment." The guides escorting the visitors through the museum were instructed (3) not to give "a set talk about each room." "Their attitude should be more that of a librarian or well-trained attendant, helpful but not intruding in any way."

Throughout his life Henry Francis du Pont strongly believed that barriers should not be erected in the museum. Visitors were to enjoy an unobstructed view. He explained to Phillips (2), "My idea on what is

wrong with museums in this country is that if you have these things strapped off, you'll lose everything."

Because of the open access to the rooms, guests were instructed at the beginning of each tour not to touch any museum object, especially the historic textiles. Henry Francis du Pont explained to the executors and Winterthur directors (*3*):

> *As I have found that much damage is done by frequent handling of the curtains and upholstery, I have had little cards printed requesting visitors not to lean or put their hands on any upholstered chair or on the curtains. One of these cards is to be shown to each visitor, and should this request be disregarded, the accompanying guide, who should always carry one of these cards with him, should again show it to the visitor. This applies to the Directors and distinguished guests, also.*

Mr. du Pont also forbade sitting on the sofas and chairs in the collections (*3*). "As the years pass by and the old materials begin to wear out, not only from the stretching, but also by use, I realize that the less they are sat upon the better." This rule applied to guests, museum personnel, and even trustees. Certain rooms with more durable pieces were designated sitting rooms for guests. Memorial Library was one such room; however, even here restrictions were found (*3*). "I think it would be wiser for the Directors [Trustees] to use the Memorial Library . . . exclusively for sitting," and Mr. du Pont added, "Please, Directors, sit on the leather pieces and do not lean on the back of the wing chairs." Mr. du Pont also included specific instructions for those staff members who moved upholstered furniture (*3*). They were not to touch the fabric when moving the furniture about the museum and he specified that the wing chairs must [always] be lifted by their legs.

When Winterthur was a private residence prior to 1951, many guests were entertained on weekends at which times special bedspreads, usually of modern fabrics, replaced the historic bedspreads. A delightful story is told by John Sweeney, then Curator, of how Mr. du Pont arranged to have a newly acquired antique bedspread placed on the bed of Miss Mary Allis, a friend and an antiques dealer especially interested in textiles. At dinner, Mr. du Pont asked Miss Mary Allis how she had spent her afternoon. She replied cheerfully that she had had a lovely nap. Henry Francis du Pont paled. Miss Mary Allis then added (*4*), "Oh, don't worry. I didn't sleep on the bed. I took a pillow and slept in the bath tub."

The working operation of the museum was never intended to be seen by the public. On Mondays the museum was closed and major housekeeping tasks were done: floors were vacuumed, waxed, and

polished; new furniture pieces were installed. On the other days of the week half of the museum was opened for tours in the morning and the other half was opened in the afternoon. The furniture in more than 195 rooms was dusted on a daily basis by women who quietly worked through the rooms that were not "on tour". Because each duster worked the same two or three floors everyday, she came to know the locations of important objects, according to Everett Boyce, Museum Buildings Division Supervisor, and was able to spot any moved or missing piece (*5*).

Henry Francis du Pont put a great deal of effort into positioning each object, and in 1964 he wrote (*3*), "I expect the Director and Associate Director and Curator of the Museum, in addition to their conventional duties, to take personal charge of seeing that the furniture and many small objects are kept in their right places and their right angles." When the museum opened in 1951, the task of keeping track of the more than 30,000 museum objects on display was the responsibility of all the offices: curatorial, registrar, housekeeping, and properties. To help them in this task detailed records were made of every room (Figures 3 and 4). About this time Mr. du Pont wrote (*3,6*), "Leslie P. Potts [draftsman and Farm Superintendent] is making a detailed drawing of each room showing the location of each piece of furniture, ornament, etc. . . . I would like him to continue making these drawings until every room has been completed."

In contrast to the fixed placement of furniture and other artifacts, Mr. du Pont wanted the textiles, curtain sets, slipcovers, slip seats, bed dressings, and rugs changed seasonally. He believed that the textile sets needed to "rest" in storage for a period of time and had them stored in

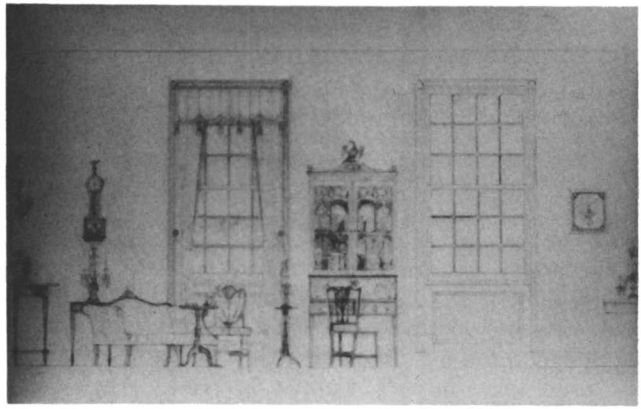

Figure 3. The Baltimore Drawing Room's window wall elevation as executed by Leslie P. Potts, circa 1940. Courtesy, The Henry Francis du Pont Winterthur Museum.

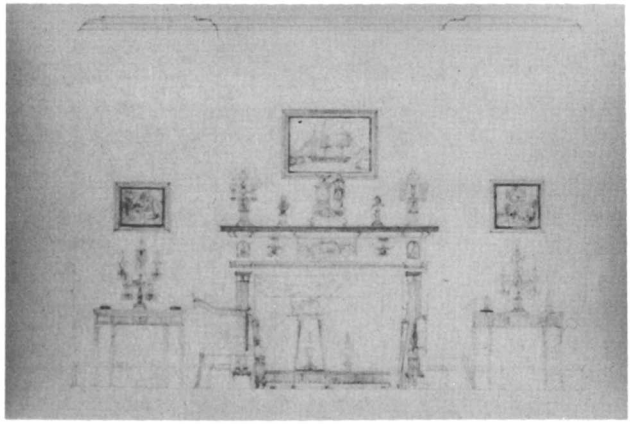

Figure 4. The Baltimore Drawing Room's fireplace wall elevation as executed by Leslie P. Potts, circa 1940. Courtesy, The Henry Francis du Pont Winterthur Museum.

darkness for the 9 months they were not on display (*4*). The rotation of sets also provided an interesting change for visitors returning throughout the year (*5*). Because Mr. du Pont selected the color and texture of the historic fabrics "to coordinate [with] what was seen through the windows," everything had to knit together with the gardens, reflected George Colman who was in charge of the textile changes in the early years of the museum (*1*). Bright, cheerful, colored fabrics were used in spring. In summer the colors were quieter and more subtle. The autumn brought colors to match the brilliant fall foliage. In the winter the colors of the fabrics became deeper and richer to contrast with the outdoors (*1*) (Figures 5–9).

Although Mr. du Pont approached the selection of textiles "visually and intuitively", historical accuracy in curtain design was also very important to him (*4*). Mr. du Pont opined (*3*):

> *The curtains, upholstery, bed hangings and bedspreads at Winterthur are in themselves a textile museum; and the way the materials are draped, upholstered, etc., carries out the best tradition of a museum of decorative arts. Many, many hours have been spent looking at paintings, engravings, and books to find the correct models for the period of each room, and their execution has taken countless hours of hand-sewing. The accurate and minute details of the fringes, tape bindings, tassels, etc., and the ingenuity in making much too short a yardage go in a certain place, the infinite details of the so-called tailoring of curtains and bed valances, have taken endless hours [to execute].*

Figure 5. The Baltimore Drawing Room, which was installed in 1930, circa 1962. Courtesy, The Henry Francis du Pont Winterthur Museum.

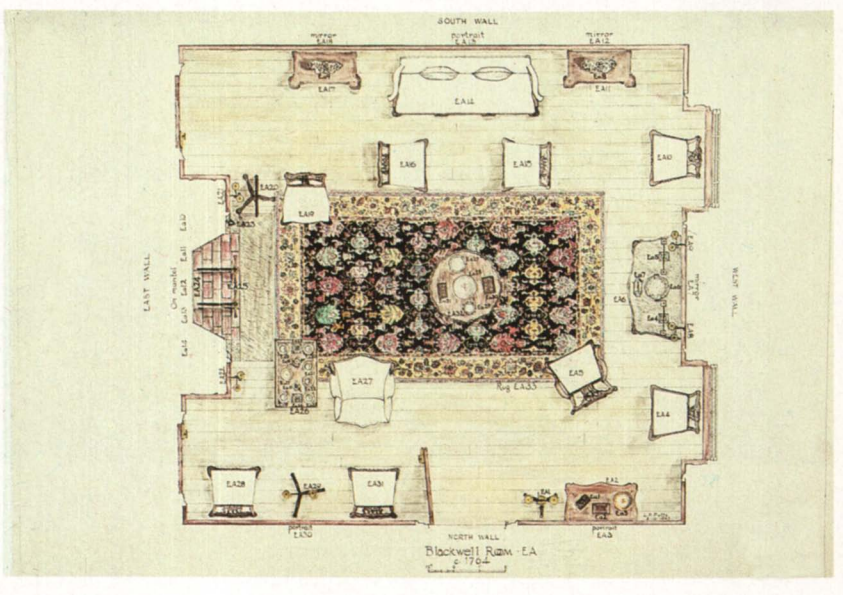

Figure 6. The Blackwell Parlor's furnishing plans as executed by Leslie P. Potts in 1943. Courtesy, The Henry Francis du Pont Winterthur Museum.

Figure 7. The Blackwell Parlor, which was installed in 1940, circa 1955. Courtesy, The Henry Francis du Pont Winterthur Museum.

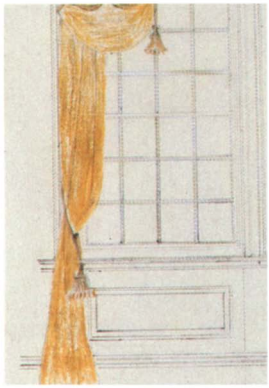

Figure 8. The Port Royal Parlor's textile plan as executed by Leslie P. Potts in the 1940s. Courtesy, The Henry Francis du Pont Winterthur Museum.

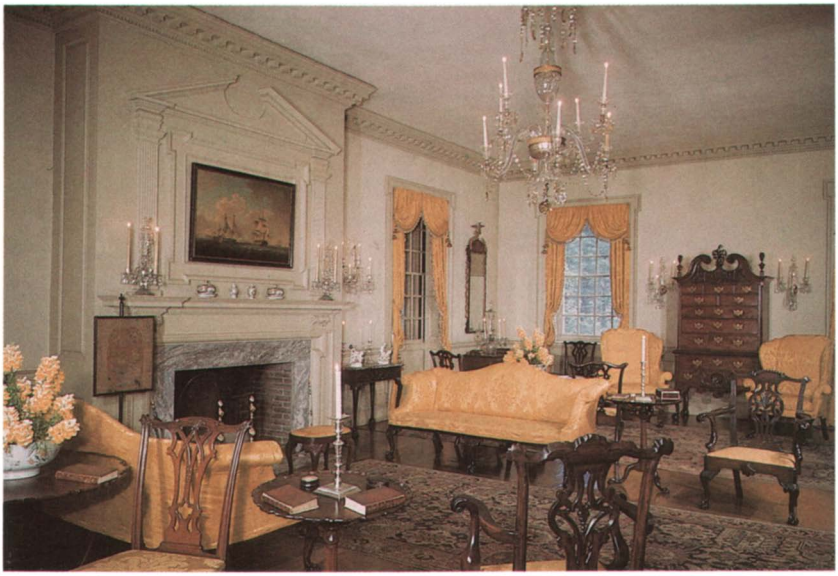

Figure 9. The Port Royal Parlor, which was installed in 1930, showing the winter textile change, circa 1965. Courtesy, The Henry Francis du Pont Winterthur Museum.

Because of the great amount of time and effort that went into assembling the curtain and bed sets and because of the precious nature of the fabrics, Mr. du Pont issued specific instructions on their care and handling (*3*):

> *I want an expert workman to handle the draperies, as they and the bed hangings have to be fastened onto their respective cornices, etc. It is a man's job, and as they are priceless and have cost thousands of dollars to fashion and the materials are unprocurable again, it would be poor economy to have an inexperienced person handle them.*

Careful records were kept concerning the scheduling of seasonal changes. Colman worked with Mr. du Pont and his secretary, Ruth McCollum, on a 223-page loose-leaf book entitled, "Winterthur Fabrics, Bed Hangings, Curtains, Upholstery", first written in 1946 and revised in 1952 (*1*). For each edition, 10 copies were individually typed; these were distributed to the different museum offices (*1*). These change books were organized by category and then by floors. Mr. du Pont explained (*3*):

> *These lists give the correct descriptions of the window curtains, bed hangings, etc., the rooms in which they belong, and the months during which they are to be used in the respective rooms. Each window curtain, bed hanging, bedspread, slipcover, chair seat, and rug has a linen label sewed on it (or tacked on in the case of chair seats) giving the name of the room and the months they are to be used therein.*

The seasonal changes occurred in January, April, July, and October. However, the textiles could not all be moved at once. Mr. du Pont wrote (*3*):

> *I want to make it clear that as the materials are taken down they must be dusted and put away with the greatest care. In other words, I don't want all the curtains, etc., taken down in two or three rooms at the same time and dumped somewhere while the other curtains, etc., in those rooms are being put in place. Each room must be done separately, the curtains, etc., dusted and put away and other curtains hung, etc., before another room is started.*

The storage of the seasonal change sets was an important part of the behind-the-scene activities of Winterthur. Originally the curtains were

stored on the ninth floor, suspended on brass rings from 15-ft wooden poles, and the valances were draped over the rods protected with tissue paper (*1*). The first curtain storage was constructed in 1948. Curtain storage room II was completed in 1957. Bedspread storage and rug storage were constructed in the mid-1960s. In addition, small bins were used to house "every little scrap of material for . . . [each] room" because, as Mr. du Pont explained in 1964 (*3*), "they are most useful for minor repairs." He also set aside "labeled rolls of fabrics and of chintz" and noted (*3*), "these are for replacements in some of the rooms and are so marked and others are [held] for the reupholstering of the furniture."

Mr. du Pont's concerns extended to the care of textiles during storage (*3*): "Every April and October the materials in the room bins in the bedspread room and those in the carpet room are to be dusted and refolded, and all the bins are to be thoroughly cleaned. Also, the carpet room and the curtain and bedspread rooms are to be thoroughly cleaned and should be dusted once a month at least." Moreover, "[t]he rug room, bedspread room, and curtain room . . . are to be kept a uniform moderate temperature both winter and summer, and the air is to be filtered, cooled, etc., and the dirty filter cloth changed every day or so as it is done now. . . . The rug, curtain, and bedspread rooms are not to be shown to the average visitors."

Establishing correct environmental conditions within the museum and in storage became the paramount concern of Mr. du Pont, the trustees, and the staff in the late 1950s and early 1960s. Charles Hummel, now Deputy Director for Collections, recalls that Mr. du Pont became aware of the importance of air conditioning by the mid-1950s (*7*). When burgeoning costs dictated a scaling back of the South Wing addition started in 1956, air conditioning was retained to protect the collection objects (*7*).

The museum's first official director, Charles F. Montgomery, was faced with the construction of the new wing. He also had to stabilize the environment and conditions in the existing nine-story museum building, much of which was built below grade. Years later he recalled the events and the problems of those years of construction (*8*):

> *[I]n 1957 . . . I awakened one night . . . thinking of the responsibility that I as an individual and a director of the museum had for taking care of these things . . . and asked Mr. du Pont if he would be willing to go along with me getting the best person I could get. . . . He said, 'Sure'—he was very good about this kind of thing. . . . So I wrote to [Harold] Plenderleith. . . . Plenderleith . . . came in 1958.*

Harold Plenderleith was director of the British Museum's Research Laboratory and was considered one of the foremost authorities on

conservation in the world. Shortly before Plenderleith's visit, Montgomery outlined what the museum expected him to achieve (*9*):

> *It is my hope that during your visit here you can go over thoroughly our care, handling, and treatment of the objects in our custody with a view to eliminating those practices which are not best for the safest preservation and instituting new ones wherever desirable. I know you will be outspoken and frank in your observations. We feel that we have a great responsibility to care for and preserve these collections. We want to discharge this obligation in light of the best knowledge available.*

After the month-long summertime visit to Winterthur, Plenderleith wrote his comprehensive report concerning the environmental conditions of the museum, fire protection, and treatment recommendations for textiles, leather bindings, Chinese lacquer on wood, painted gesso on furniture, silver, and Sheffield plate (*10*). He had temperature and humidity readings taken in 14 locations in both the museum and the storage areas from July 14th through July 19th and compared them with the daily logs and charts that recorded the high relative humidity in Delaware's summer heat. Plenderleith then made recommendations to stabilize the temperature and humidity within the museum and textile storage. As an outgrowth of Plenderleith's visit, air conditioning of the entire museum, not just the new addition, became a top priority at Winterthur. The Design Division of the Engineering Department of the E. I. du Pont de Nemours and Company produced a feasibility study in 1960, and construction work began the next year (*11*).

Progress was very slow. Mr. du Pont wistfully observed on February 29, 1964 (*3*), "I only hope I may live long enough to see the air cooling in the museum completed." Twenty months later he wrote (*3*):

> *The summer of 1965 will see the beginning of the end, in 1966, of the air cooling for the museum. It has been extremely expensive and very trying and exhausting to move everything out of one room, pack the very "holy" objects, and months later to unpack them and put them where they were. It takes tremendous care and patience, and [George] Colman and now Everett [Boyce] have done a wonderful job, and I shall be always grateful.*

The construction for the air-conditioning project started from the basement of the building and worked up to the ninth floor in vertical sections. Tunnels were dug from a massive air-conditioning unit discreetly positioned on a hillside a hundred or so feet away. Scaffolds were constructed on the outside of the building so workmen and their

equipment would not interfere with the tours. The paneling was removed in each room, and a false wall was installed to hide the work in progress. The construction areas were sealed off to protect the collection objects. Considerable care was taken in positioning the new vents, for once the air conditioning was in operation, Mr. du Pont "did not want to see tassels or curtains moving." Furthermore, he wanted the rooms to look exactly the same as they had before the air-conditioning project began (*1*).

The problem of light damage to collection objects was also a special concern of Mr. du Pont. Even when the du Pont family still lived in the house, the shades were regularly pulled and the shutters were regularly closed to prevent daylight and sun damage. When the museum opened, Mr. du Pont specified that these procedures continue (*3*):

> *There are shades in most of the windows, and I want these kept down both winter and summer when the sun is shining in those particular rooms. When the museum is to be shown, there is to be some [staff member] who is to pull up all these shades before the visitors come. The shades are to be rolled all the way to the top, and on no condition are they to be seen. The rooms and halls that have the early morning sun must have the shades pulled down the night before.*

In addition, Mr. du Pont underwrote installation of the Pittsburgh Plate Glass tinted Pennvernon Graylite storm windows to further protect the rooms from light damage, and this installation became an added bonus of the new air-conditioning system (*4*).

Mr. du Pont, in the early years of the museum's existence, had an aversion to lending any collection objects because he was concerned that they could be lost or damaged. He also believed that loaned objects would leave a visual gap that could not be readily filled. He wrote (*3*):

> *It is my wish that the lending of any portrait, mirror, or piece of furniture, except a sidechair (not the sample chair), for exhibition or other purposes be prohibited. Most museums have articles in reserve to take the place of things temporarily loaned, but this house is furnished as a house and lending of anything will detract from its appearance as a whole, inasmuch as there is nothing in reserve to take the place of such loaned article.*

However, this policy was revised during Mr. du Pont's lifetime at the Board meeting in January 1957 and was recorded as follows (*3*):

> *After discussion, on motion, duly made and seconded, the Board approved the lending to other museums some*

Winterthur Museum objects other than large pieces of furniture, mirrors, and paintings, the Director of the Museum being empowered to make the decision in the case of each request as to what shall or shall not be loaned; requests for large pieces of furniture, mirrors, and paintings shall be referred to the Board in the event that requests are received from some very special exhibition.

In the early years of the collection and museum, Mr. du Pont often sent objects to private firms in New York for repair. A truck was dispatched from Winterthur to deliver the objects and return them. But after one of the trucks carrying a chandelier broke down on the turnpike, Mr. du Pont became increasingly reluctant to risk sending museum objects to New York (*4*, *5*). In fact, he worried about having furniture pieces transported to even another building on the estate for conservation work (*5*). This concern laid the groundwork for incorporating the conservation laboratories into a new facility directly connected to the museum building (*4*). The existing conservation staff had expanded under the first two directors, Charles F. Montgomery (1954–61) and Edgar P. Richardson (1961–66) (*7*). By the mid-1960s the conservation section included two staff members in furniture conservation, two in textile conservation, one in paintings conservation, and one in wood research. During these years, according to Hummel, a growing awareness was seen in the country for the need to establish standards for the conservation of decorative arts (*7*). Responding to this development, the Winterthur staff asked the administration and Mr. du Pont to double the size of the proposed new library building and thereby include two and one-half floors of conservation laboratories to increase the museum's conservation capabilities (*7*). Mr. du Pont agreed. The Louise du Pont Crowninshield Research Building was dedicated on May 12, 1969, just 1 month and 1 day after Mr. du Pont's death (*7*). Plenderleith returned to Winterthur to participate in the dedication and acknowledge Mr. du Pont's contribution to conservation. He began his address (*12*):

Ladies and Gentlemen:

You have honored me by inviting me to join with you today in celebrating a great event in the history of Winterthur. I am delighted to be here again, after an absence of 10 years, and to find myself among so many old friends at the inauguration and the dedication of this fine, new, and important research unit—The Louise du Pont Crowninshield Research Building.

It is no feat of imagination to detect in this memorial and achievement, for such indeed it must be considered, the guiding hand of Mr. du Pont himself, for through the years he

was steadfast in his love for the beauties of nature, the arts, and science—a triumvirate; and this latest building is the consummation of his dream to create a self-contained unit worthy of all three.

The Louise du Pont Crowninshield Research Building was an important indicator of Winterthur's new direction (7). The museum continued to give attention to care of the collection; however, the research facility was also designed to support the establishment of a master's degree training program in art conservation (7). The first class of conservation fellows in the Winterthur-University of Delaware Program in the Conservation of Artistic and Historic Objects was accepted 5 years later in 1974.

Henry Francis du Pont in the last two decades of his life emphasized the expanding role of education at Winterthur Museum. He revealed this evolution of thought in the 1962 interview with Phillips (2):

Our growing days have subsided now. It's never going to be any bigger than this. Some say, "Oh, you'll add on a good many more rooms." I say, "Never" because it's enough now. You can't have everything in the world. Like flowers—you know, there's a limit to the number of flowers that you can have in any one place. People say, "Oh, plant more Azaleas"—well, you can't do it. Probably we'll find some ways, but there's a limit to what you can do. We're going to do a lot in the future about education.

At that time the Winterthur Program in Early American Culture was 12 years old and had already developed an interdisciplinary approach to the study of American civilization. Mr. du Pont continued (3):

I am so impressed by this opportunity for the fellows to receive University and Museum training for an advanced degree, that I really believe this phase of the Museum program is quite as important as the Museum itself. Years after all the books on the Museum have been written, I feel that the training and education of these young people at Winterthur will make the Museum a living force through the age.

During the 1960s only a few rooms were added, but much more was done in the realm of education. Indeed within a dozen years, the museum's conservation facilities and new conservation training program were established at Winterthur. These are the legacy of Mr. du Pont's vision.

Acknowledgments

In gathering material for this article, I would like to express my deepest appreciation to all those individuals who kindly shared their knowledge of Henry Francis du Pont and Winterthur as it developed over the years, especially John Sweeney, George Colman, Everett Boyce, Charles Hummel, Mrs. Edmond du Pont, and Mrs. Leslie Potts. Also I would like to acknowledge the kind assistance of Barbara Hearn, former Museum Archivist; Paul Hensley, current Museum Archivist; Catherine Hutchins, Associate Editor, Publications Office; Ann Clapp, former Paper Conservator; Joyce Hill Stoner, Director, Winterthur–University of Delaware Program in Conservation of Artistic and Historic Objects; and Mrs. Charles Montgomery, former Assistant Curator of Textiles.

Addendum

For a further discussion of textile conservation at Winterthur, see Reference 13.

Notes and References

1. Notes of interview with George Colman by Margaret Fikioris (July 9, 1984) on file in the Textile Conservator's Office. George B. Colman. formerly Supervisor, Mechanical Maintenance and Fire Marshall, worked at Winterthur from 1938 to 1942 and then from 1946 to 1983. He was in charge of the textile changes in the early years of the museum.
2. Transcript of interview with H. F. du Pont by Harlan B. Phillips, April 11, 1962, Winterthur Archives, 74.WC.3/Box 1115, "Phillips, Harlan". Harlan B. Phillips recorded interviews for the Archives of American Art and served as a member of Columbia University Oral History Research Office. He was also associated with the Graduate School of Arts and Science, Brandeis University, and was the author of "Felix Frankfurter Reminisces, recorded in Talk with Dr. Harlan B. Phillips" (Reynal & Company: New York, 1960).
3. Henry Francis du Pont, "Letters and Notes to Executors and Winterthur Directors Concerning The Winterthur Museum and Winterthur House", various revisions 1945 to 1966, Winterthur Archives, Special File.
4. Notes of interview with John Sweeney by Margaret Fikioris (March 2, 1983) on file in the Textile Conservator's Office. John A. H. Sweeney was in the first class of fellows in the Winterthur Program in Early American Culture. He wrote "Winterthur Illustrated" (A Winterthur Book, 1963), the first comprehensive guide to the collection. He was Curator of the museum from 1960 to 1965, Deputy Director from 1966 to 1967, and then Senior Deputy Director for the Collections and Interpretations from 1968 to 1974. He served as Coordinator of Research from 1975 to 1979 and then became Assistant to the Director in 1979 to the present.
5. Notes of interview with Everett Boyce by Margaret Fikioris (February 17, 1983) on file in the Textile Conservator's Office. Everett M. Boyce is currently Supervisor, Museum Services Section. He has worked at Winterthur since 1948. He became Supervisor, Cleaning Maintenance in 1964 and has remained in charge of the cleaning of period rooms since that time.

6. Leslie P. Potts was born at Winterthur in 1905 and lived his entire life there. He received a degree from the University of Delaware in agriculture in 1929 and studied architecture at Temple University in the evenings from 1930 to 1936. He worked as Assistant to the Farm Superintendent and then became Farm Superintendent from 1952 to 1966, the year he died.
7. Notes of discussion with Charles F. Hummel on November 7, 1984. Charles F. Hummel, currently Deputy Director for Collections, was a graduate in the second class of fellows in the Winterthur Program in Early American Culture. He joined the curatorial staff in 1955, becoming Associate Curator in 1961. He served as Associate Curator from 1961 until 1966 and then Curator from 1967 until 1978. He became Deputy Director for Collections in 1979, a position he has held since that time.
8. Foundation of the American Institute for Conservation of Historic and Artistic Works, Oral History File Interview with Charles F. Montgomery, September 27, 1976, by Joyce Hill Stoner on file in the Paintings Conservation Office.

   Joyce Hill Stoner is currently Director, Winterthur-University of Delaware Program in Conservation of Artistic and Historic Objects, a position she has held since 1982. She was Senior Conservator at Winterthur from 1981 to 1982 and Associate Director of the Conservation Program from 1980 to 1982. She has worked with the oral history project of F.A.I.C. from 1974 to the present.
9. Letter dated February 17, 1958, from Charles F. Montgomery to H. J. Plenderleith, Winterthur Archives, Charles Montgomery Papers, Box 563, "Plenderleith".

   Charles F. Montgomery was Director of Winterthur Museum from 1954 to 1961, when he became Senior Research Associate and then Senior Research Fellow, Instructor and Museum Liaison Officer. He was active in teaching and publishing at Winterthur until 1970 when he accepted the position of Curator of the Mabel Brady Garvan and Related Collections of American Art and Professor of Art History at Yale University.

   H. J. Plenderleith was the Keeper of the Research Laboratory in the British Museum and wrote one of the first comprehensive text books on conservation, "The Conservation of Antiquities and Works of Art" (Oxford University Press: London, 1956, reprinted with revisions in 1962; the second edition was published in 1971 and was reprinted in 1974). He became Director of the International Centre for the Study of Conservation and Restoration of Cultural Property, Rome, and was past president of the International Institute for Conservation of Historic and Artistic Works.
10. Report on studies made at Winterthur Museum by H. J. Plenderleith, July 1958, Winterthur Archives, Charles Montgomery Papers, Box 274, "Plenderleith".
11. E. I. du Pont de Nemours and Company, Engineering Department, Design Division, May 9, 1960, "Feasibility of Air Conditioning Winterthur Museum W.R. 425560", prepared by M. G. Kershaw, filed in Winterthur Archives, Charles Montgomery Papers, Box 563, "Air-Conditioning Survey".
12. "The Louise du Pont Crowninshield Research Building at The Henry Francis du Pont Winterthur Museum, Dedicated 12 May 1969", Winterthur, Delaware, 1969.
13. Fikioris, M. In "Preservation of Paper and Textiles of Historic and Artistic Value II"; Williams, J. C., Ed.; ADVANCES IN CHEMISTRY SERIES No. 193; American Chemical Society: Washington, D.C., 1981; pp. 253–74.

RECEIVED for review January 7, 1985. ACCEPTED May 24, 1985.

Age Determination of Textiles from Single-Fiber Creep Measurements

Randall R. Bresee[1], Venkatramana Chandrashekar[1], and Byron W. Jones[2]

[1]Department of Clothing, Textiles, and Interior Design, Kansas State University, Manhattan, KS 66506
[2]Department of Mechanical Engineering, Kansas State University, Manhattan, KS 66506

Physical age characterization using microscopic measurements of tensile creep was investigated as a means of determining the chronological age of short lengths of single textile fibers. An apparatus was constructed to study changes in the creep behavior resulting from physical aging of six cellulosic fiber types. Exponential functions were used to describe relationships between the physical age and changes in creep of each fiber type. These functions may be used to calculate the physical age of a textile from creep measurements of a single fiber. In favorable circumstances, a textile's physical age may be approximately equated to its chronological age, so the technique described may be used to provide an estimate of the chronological age of textiles of unknown origin.

Physical Aging

The chronological age of a material is considered to be the time elapsed since the material originated. On the other hand, the physical age of a material is viewed differently, that is, as the time elapsed (or storage time) since the glass transition temperature, T_g, of the material was last exceeded. The glass transition is considered to be the upper temperature limit, and the next lower thermal transition, T_β, is considered to be the lower temperature limit for rapid physical aging. Thus, physical aging is a general phenomenon that occurs universally in the glassy state, irrespective of the chemical nature of polymers. Struik (*1*) demonstrated that physical aging occurs in similar ways in a large variety of amorphous polymers. He found that aging rates were roughly the same for all samples aged at temperatures between T_g and T_β, aging rates were slow at temperatures below T_β, and aging was "erased" at temperatures above T_g.

0065-2393/86/0212-0019 $06.25/0

Physical aging in glassy polymers has long been a subject of research interest. In thermodynamic terms, physical aging refers to the process occurring when quenched polymeric glasses gradually approach an equilibrium state from a nonequilibrium state with a concurrent loss of volume and enthalpy. The aging process is presumed to occur by an ordering of disordered domains (*2, 3*). Physical aging has been studied in terms of decreases in free volume, heat content, and molecular mobility, and with azochromophoric labels (*1, 4*).

Various views of physical aging on the molecular level have been offered. Struik explained the glassy state as a nonequilibrium state engaged in many dynamic processes (*5*). He used free-volume theory to conclude that, at a constant temperature, physical aging persists for thousands or millions of years at a constant rate, except at temperatures close to T_g. Struik claimed that the thermodynamic and kinetic transformations associated with physical aging occur because overall disorder in the noncrystalline matrix of a polymer is being reduced. Experimental verification that the crystalline matrix of polymer materials remains unchanged during physical aging has been obtained (*6*). However, in a recent study (*7*), the X-ray orientation of cotton fibers aged to about 900 years was found to decrease. Although it was not known whether the cause of this decrease was physical or chemical, the results suggest that crystalline regions of polymer materials may be affected by physical aging.

According to another view, physical aging is related to the fraction of high-mobility polymer segments in regions of large free volume produced by thermal fluctuations (*4*). Fast kinetic processes are thought to decrease with increased aging time in the glassy state at approximately the same time scale as enthalpy relaxation. The aging rate of a material is not expected to be constant as it is in Struik's view because enthalpy relaxation changes exponentially with increasing aging time. Robertson's (*8*) molecular theory of aging based on rotation around short segments of polymer chains also supported a nonconstant aging rate. He suggested that polymers undergo an initial fast volume relaxation, which may be due to molecular rearrangements in regions of particularly high free volume produced by thermal fluctuations. Further evidence of a nonconstant aging rate is that the X-ray orientation angle of cotton fibers aged to about 900 years decreased exponentially rather than linearly (*7*).

Changes in properties of materials during aging form the crux of much research. Changes in thermal and mechanical properties are the most commonly used parameters in studying aging because they are easily detectable. For example, Struik (*1*) studied the effect of physical aging on torsional and tensile creep compliance of about 40 totally amorphous materials, Chapman (*9*) examined the effect of physical

aging on stress relaxation of keratin fibers, and other researchers (*6*, *10*) studied changes in the creep behavior of polypropylene and sulfonated polystyrene samples.

In Struik's extensive study of the physical aging of totally amorphous polymer materials, he clearly demonstrated that thermoreversibility of aging results simply from heating the sample to above T_g where thermal equilibrium is reached (*1*). Upon exceeding T_g, the sample "forgets" its history and any previous aging it may have undergone below its T_g. Thus, the upper temperature limit of aging is realized at the T_g, and erasure of previous aging also occurs at this temperature. When the temperature is again decreased to below the T_g, the clock is "rewound" and aging begins anew.

The general temperature dependence of physical aging of amorphous polymers is illustrated in Figure 1 and may be summarized as follows: At 0 K, aging does not occur because molecular motion does not exist and rearrangement of molecules necessarily is precluded. With increasing temperature, the rate of aging presumably increases very slowly as molecular motions allowing molecular rearrangements to occur are activated. When T_β is reached, molecular motions that are especially effective in reducing free volume are activated, so the rate of aging increases substantially as structural rearrangements occur. Because molecular mobility remains approximately constant from T_β to T_g, the rate of aging also remains approximately constant. Major segmental motions allowing thermodynamic equilibrium to be reached are induced at T_g so the rate of aging quickly decreases to 0 as T_g is attained. Thus,

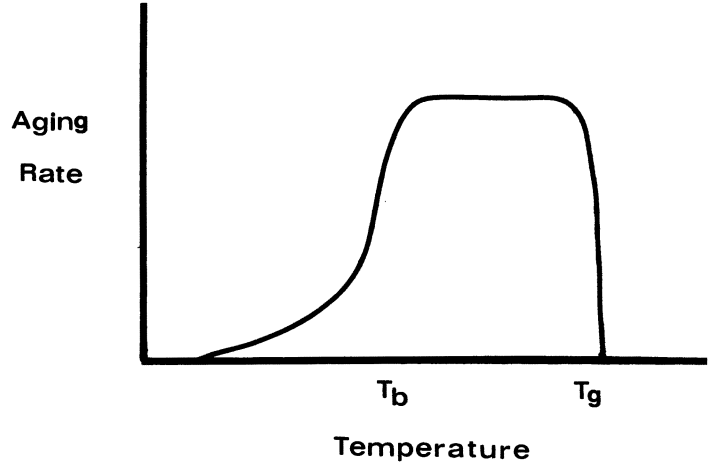

Figure 1. The temperature dependence of physical aging.

physical aging is like most physical phenomena in that it is temperature dependent but the rate of aging remains approximately constant between T_β and T_g.

Effect of Sample Morphology on Physical Aging

Polymeric materials whose physical aging has been studied by tensile creep are mostly unoriented and amorphous. Most textile materials, on the other hand, are oriented and semicrystalline, and the effect of sample morphology on physical aging has not been elucidated. Struik (*1*) hypothesized that the presence of orientation and crystallinity in a sample causes a local decrease in the segmental mobility of the noncrystalline matrix and has the effect of broadening the T_g range within the polymer sample. This hypothesis leads to the conclusion that the presence of orientation and crystallinity will modify the temperature range but not the rate of aging.

Struik performed a limited number of creep measurements on semicrystalline polymers. The physical aging rate observed was the same as that of totally amorphous polymers. This work was viewed as experimental verification of his hypothetical expectation that the presence of orientation or crystallinity would not modify the rate of aging. Consequently, results obtained from studying totally amorphous polymers have been generalized to include all polymer materials, regardless of their morphological structure. However, the influence of sample morphology on physical aging has not been studied enough to adequately test this hypothesis.

Some evidence indicates that the generalization of aging concepts derived for wholly amorphous samples may not be completely valid. For example, other studies found that semicrystalline polymers age at temperatures above their T_g (*11*, *12*). Because totally amorphous materials clearly do not exibit this behavior, it might be concluded that physical aging is affected by sample morphology. In addition, evidence suggests that crystallinity has a long-term effect on the free volume and mobility of amorphous domains. Consequently, the presence of crystallinity might be expected to alter the rate of aging.

Textile Fiber Creep

Creep is a measure of sample length as a function of time when the sample is subjected to a constant load. Normally, creep curves are obtained by plotting data in terms of sample length, strain, or compliance versus log (time), as illustrated in Figure 2. The basic nature of creep curves is explained at the molecular level as a distortion of bond

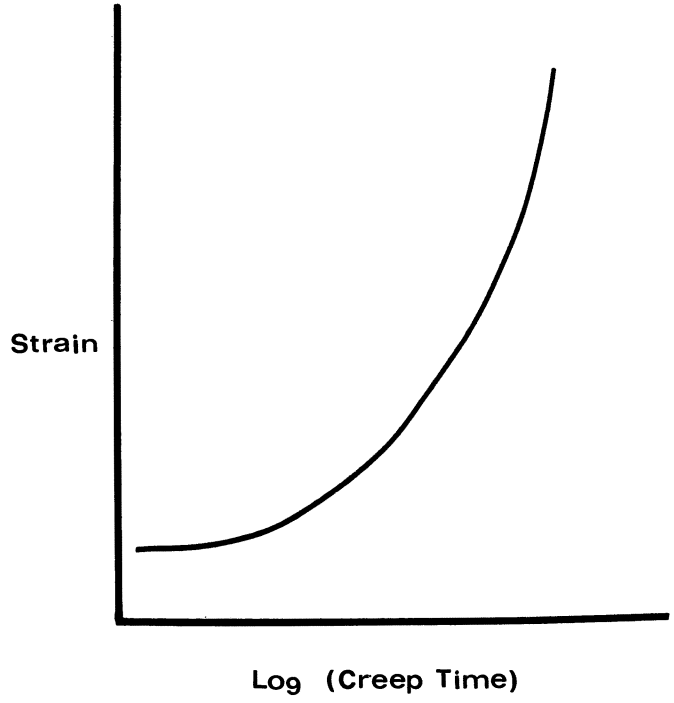

Figure 2. Creep curve.

angles and bond lengths for short creep times and as a reorientation of chain segments at longer times.

Researchers have examined the creep and creep recovery of textile fibers extensively (*13–21*). For example, Hunt and Darlington (*16, 17*) studied the effects of temperature, humidity, and previous thermal history on the creep properties of Nylon 6,6. They were able to explain the shift in creep curves with changes in temperature and humidity. Leaderman (*19*) studied the time dependence of creep at different temperatures and humidities. Shifts in creep curves due to changes in temperature and humidity were explained with simple equations and convenient shift factors. Morton and Hearle (*21*) also examined the dependence of fiber creep on temperature and humidity. Meredith (*20*) studied many mechanical properties, including creep of several generic fiber types. Phenomenological theory of linear viscoelasticity of semicrystalline polymers has been tested with creep measurements performed on textile fibers (*18*). From these works one can readily appreciate that creep behavior is affected by many factors on both practical and theoretical levels.

General Method

A continual change in the structure and properties of materials accompanies increasing aging times at temperatures between T_β and T_g. Consequently, mechanical properties may be used as a gauge for the measurement of physical aging. Although numerous mechanical properties are altered during aging, we chose to employ single-fiber tensile creep as a measure of physical aging in this research. Differences in creep behavior before and after erasure of the physical aging of a sample provided the basis for computing the age of the samples.

The purpose of this study was to develop a microtechnique for measuring creep of short lengths of single fibers and to use this technique to study physical aging of fibers in the cellulosic generic class. The accomplishment of this objective involved constructing a suitable apparatus and measuring the aging rate of six types of cellulosic fibers at three temperatures. In addition, measurements of density and birefringence allowed the effects of crystallinity and orientation on aging to be estimated. Finally, the possibility of using physical aging information to estimate the chronological age of textile fibers from a few days to a few thousand years was evaluated. A single-fiber aging technique would be applicable to most textiles and might offer a practical way to estimate the chronological age of textiles, especially if they have been subjected to relatively constant conditions of temperature and humidity over long periods of time. These conditions may be found in tombs, burials, or sunken ships. Because the T_g of cellulose is estimated to be around 230 °C and the secondary transition is estimated to be near room temperature (*22*), the use of this technique to estimate the chronological age of cellulosic textiles in many applications seemed promising.

The procedure used in this experiment to determine the physical aging rate is empirical and has been defined by Struik (*1*). It requires plotting creep curves consisting of strain versus log(creep time) for different aging times, determining their horizontal shifts from the plots in units of log(creep time) with respect to a reference sample having a small age, plotting values of their shift versus physical age, and calculating their aging rates from the plots of shift values versus physical age in terms of shift per unit of physical age. Figure 3 illustrates creep curves of a sample at three different physical ages in plots of strain versus log(creep time). A specimen having a physical age of 0.5 days is used as the reference for two samples having ages of 10 and 100 days in this figure. The creep curve shifts $\Delta\log(a_1)$ and $\Delta\log(a_2)$ are determined at one particular strain value by finding the differences between values of log(creep time) for the reference specimen and the 10- and 100-day-old samples, respectively. As this figure shows, the increasing physical age of a specimen increases horizontal shifting of its creep curve. Fig-

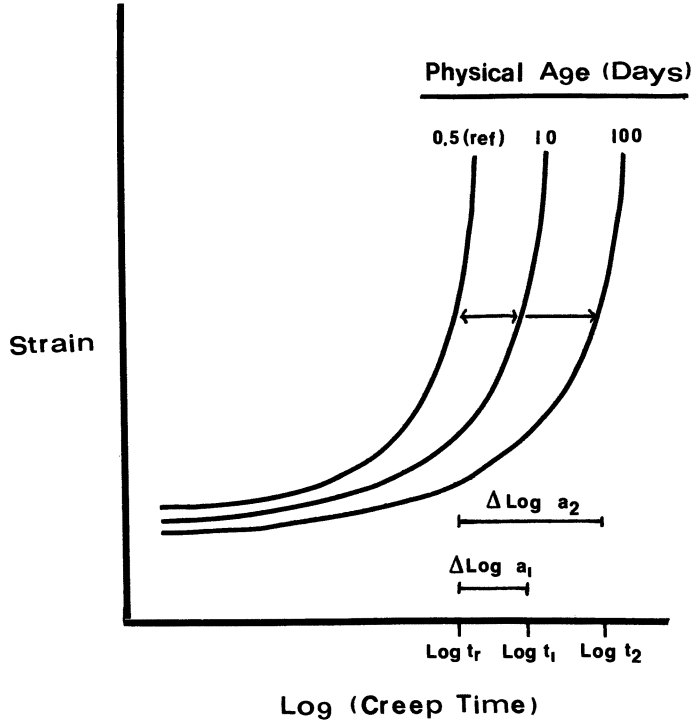

Figure 3. The effect of aging on fiber creep.

ure 4 illustrates a plot of shift versus physical age for which values of shift for different physical age times are obtained from plots such as Figure 3. This figure graphically provides a measure of aging rate over the physical age range plotted. Aging rate is defined mathematically as follows:

$$m = -[d \log(a)]/[d \log(t_e)] \quad (1)$$

where m is the aging rate, $d \log(a)$ is the creep curve shift with respect to the horizontal axis $d \log(a) \cong \Delta\log(a) = \log(\text{creep time})_i - [\log(\text{creep time})_{\text{ref}}]$, and $d \log(t_e)$ is the sample age with respect to a reference age $[d \log(t_e) \cong \Delta\log(t_e) = \log(\text{age time})_i - \log(\text{age time})_{\text{ref}}]$. The direction in which creep properties are affected assumes a negative value for shifts to the right and thereby implies that longer aging times subsequently result in further changes in mechanical properties. Changes in mechanical properties are proportional to aging time. The propor-

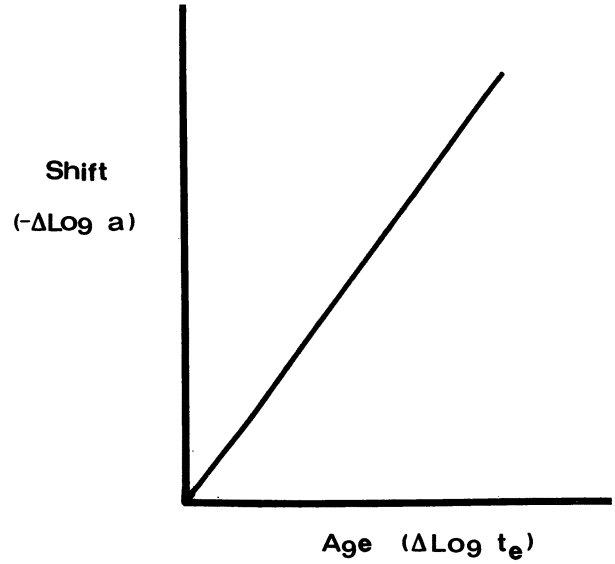

Figure 4. The effect of age on creep shift.

tionality constant is m, which can be calculated if the aging times and creep times are known.

To calculate the physical age of a fiber of unknown age after a plot similar to Figure 4 has been prepared from similar samples of known physical ages, the following steps must be performed: The creep curve of the unknown fiber must be measured and plotted as in Figure 3, the fiber must be subjected to a temperature above its T_g and then conditioned (aged) for a short time at the same temperature used in measuring its previous creep, and then the creep of the fiber must be remeasured and plotted as a reference curve. This plot provides a graph similar to Figure 3 containing one curve of the fiber of unknown age along with a reference curve of the same fiber of known age. From these curves the horizontal shift resulting from the physical age difference of the two states of the sample can be determined. The value of this shift is calculated and then placed on a plot such as Figure 4 to find the physical age.

Limitations of the Method

In considering creep behavior as a measure of physical or chronological age, one finds that the measurement is not simple and is affected by many factors. A rather complex interrelationship exists among the strain

rate, strain temperature along with its relation to T_g, applied stress field with effects of hydrostatic pressure such as that from humidity, changes in chemical constitution such as that accompanying photochemical degradation, thermal history, loading history as described by Boltz mann's superposition principle, and molecular features of the fiber samples. For reasons of simplicity, many of these factors have been assumed to be constant throughout the course of this study.

The presence of thermal transitions occurring above T_g may result in incomplete erasing of former aging when samples are subjected to T_g (*11, 12*). Amorphous polymers are known to exhibit damping transitions that occur at temperatures substantially above their T_g. By subjecting the fiber samples to their T_g to erase previous aging, transitions occurring above the T_g are assumed to not affect physical aging. In reality, the effect of these transitions on aging is not known. If this problem were to be circumvented by selecting a temperature for erasure of aging well above T_g to exceed other possible transitions, melting of small crystals and reformation of new ones might result. These transformations are bound to alter the structure and, consequently, the mechanical properties of the sample, so comparisons of creep before and after erasure of aging would be invalid. A convenient solution to this problem is to temporarily plasticize polymers during aging erasure. Plasticizers have the effect of lowering the T_g without penetrating crystallites, so thermal erasure of aging may be performed at a lower temperature. To illustrate the magnitude of this effect, one only has to consider that the T_g of dry silk is about 197 °C, whereas the T_g of wet silk is depressed by the plasticizer action of water to about 30 °C (*23*). In a study taking advantage of this phenomenon, researchers erased aging of keratin fibers simply by immersing the sample in water at room temperature (*24*). We adopted a similar procedure in this study. However, we used a temperature slightly elevated above room temperature to ensure the erasure of aging. This temperature was determined from calculations of plasticizer-based T_g depression using the theories of Fusek (*23*) and Wortmann et al. (*25*).

Mechanical treatment has been found to accelerate the rate of physical aging (*26*). Researchers have shown that aging is accelerated in both tension and compression, enhanced aging varies with the square of the stress in a creep test and the square of strain in relaxation tests, and enhanced aging persists to zero stress or strain. The effect on aging of stress level during creep measurements has been specifically studied, and a shift in the logarithmic creep times has been shown to result from stress differences (*1*). However, variations due to this change may be reduced to an insignificant level by keeping the stress level low and nearly constant for all fiber samples examined in a study. In addition, creep times usually are small compared to their corresponding aging

times, and the effect of mechanical treatment during creep measurement is negligible.

One might anticipate that, in favorable circumstances, the physical age determined by this procedure would equal the chronological age of the sample, that is, the time elapsed since the textile originated would equal the time elapsed since the T_g of the sample was exceeded. However, in determining the physical age of fibers and claiming their chronological age to be the same, one must assume that the fibers have been subjected to a fairly constant temperature between T_β and T_g and that no other conditions have erased their physical aging.

Several problems might limit this use. For example, small molecules are known to act as plasticizers and change thermal transition temperatures and mechanical properties of the fibers. Consequently, one would expect small molecules to affect physical aging. For example, water in the atmosphere may act as a plasticizer for a hydrophilic polymer, lower the T_g, and thus change its aging rate. These effects may occur in a variety of processes, including laundering, weathering, storage, or use. Because the presence of plasticizers effectively lowers the T_g of polymers, humidity variation during aging of cellulosic materials constitutes a possible source of error in chronological age determinations from physical age data. The effect of this source of error on practical determinations of chronological age has not been determined. However, one would expect that depression of the T_g would not have a major effect on aging rates as long as the ambient temperature was not near T_g or T_β. Meredith (*20*) considered the effects of humidity on the creep of rayon. At relative humidities of less than 40%, the amount of creep was not found to vary considerably for cellulosic fibers. In this study, all tests conducted at the various reference temperatures were subjected to approximately the same humidity level.

Temperature variation during the period of aging occurs in almost all practical circumstances and would be expected to affect the rate of aging. The effect of this source of error on chronological age determinations has not been determined. The rate of aging is assumed to be fairly constant throughout the broad temperature range extending from T_β to T_g, as illustrated in Figure 1. Consequently, temperature variations in this range are not expected to affect the aging rate in a major way. This study included measurements of the temperature dependence of aging to assess this expectation.

Experimental

Large specimens of amorphous polymers that can be subjected to large loads and can produce large displacements in creep generally have been the subject in creep studies of physical aging. Electronic sensing of displacements with sensitive oscillators and amplifiers have been employed in measuring displacements when loads of 1–50 kg were applied.

Small fiber samples with lengths ranging from 2 to 5 cm were tested in this study. All lengths were measured microscopically by using a 7× macroscopic objective on a projecting microscope with no ocular and an eyepiece micrometer. This method of measurement allowed length changes of the order of 10 μm to be detected. Strain was determined by measuring grip displacement. Initial length measurements were determined by extrapolating creep for short times to zero time to circumvent instantaneous creep. A stopwatch with precision to 0.01 s was used to measure creep time. The source and chronological age of fiber specimens tested in this study are listed in Table I.

The apparatus that was constructed and used is illustrated in Figure 5. The dimensions of the box were 18 × 12 × 10 cm. The chamber was built with walls

Table I. Description of Fiber Specimens Tested

Fiber Type	*Source*	*Chronological Age (years)*
Cotton	USDA raw cotton	47
Cotton	Peruvian rug	400
Flax	KSU	68
Flax	KSU	29
Viscose rayon	KSU	29
High-wet-modulus rayon	KSU	24
Cuprammonium rayon	KSU	24
Acetate	KSU	29

NOTE: KSU denotes Kansas State University.

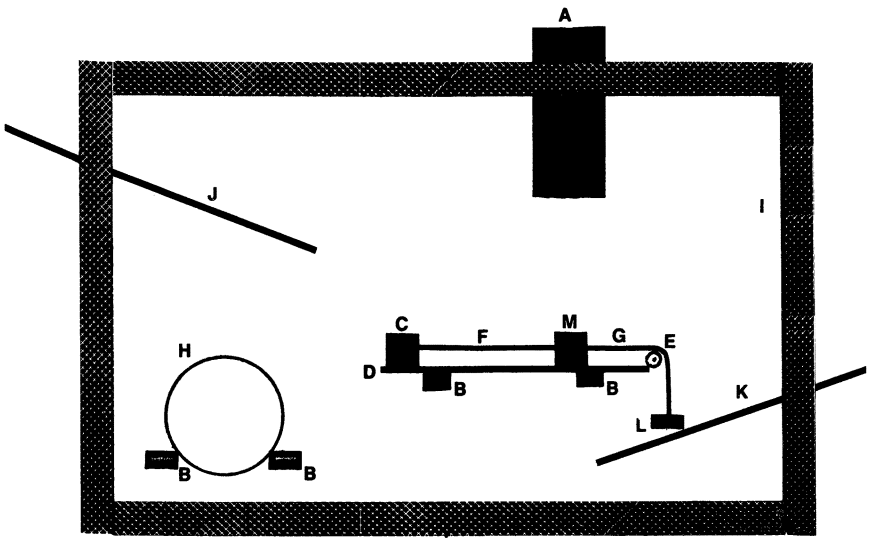

Figure 5. Apparatus elevation: A, microscope objective; B, bar support; C, magnetic clamp; D, platform; E, pulley; F, fiber tested; G, glass fiber; H, heater; I, walls; J, optical fiber; K, lever; L, load; and M, magnetic coupling.

made of 1.6-cm thick foam insulation board and sealed on the edges with aluminum adhesive tape. The chamber contained horizontal aluminum bar supports running across the sides that helped support the fiber mounting platform and a 50-ohm electric heater placed at the bottom of the fiber platform to provide operating temperatures ranging from room temperature to 150 °C. The platform was aluminum, its dimensions were 8 × 2 × 0.5 cm, and it was milled to a smooth and low-friction surface. A thermometer was introduced from the top to monitor temperature. Except for creep measurements at room temperature, the temperature inside the chamber was controlled with a 120-V variable transformer correct to ±2 °C. During testing, one end of a fiber was secured by a pair of hinged magnetic clamps fixed at one end of the sample platform, which was positioned in the focal plane of the microscope objective. Another magnetic piece formed a union between the other fiber end and a glass fiber coupling that passed over a pulley and supported loads of about 0.5 g. A mechanical lever was incorporated so the load could be applied and removed from the fiber without opening the sample chamber. The loads resulted in creep of the cellulosic fiber samples but caused no creep in the other components of the apparatus. The combined frictional drag of the pulley and magnet was 0.110 g. An optical fiber was inserted through the box to illuminate the fiber for length measurements.

The following steps were used in determining the aging rate of each of the six fiber types at three different temperatures: Four specimens of each fiber type were teased from yarns of the textiles of known chronological ages. Three of the specimens were erased of previous aging by immersion in warm water: The temperature of the water was 40 °C for acetate fibers; 50 °C for viscose rayon, high-wet-modulus rayon, and cuprammonium rayon; and 60 °C for cotton and flax. Each of the treated specimens was conditioned (aged) at 25 °C with 65% rh, and 50 and 75 °C with the same absolute rh for an aging period of approximately 48 h. Each of the conditioned specimens was subjected to a creep test at the same temperature at which it was aged. Time intervals for every 0.0014-cm creep were recorded until a maximum creep time of 10^4 s was reached. The specimens were relaxed overnight and again erased of their prior aging by immersion in warm water. Each of the three specimens was subsequently aged and relaxed again for approximately 72 h and then 96 h at the same aging temperatures used for the 48-h aging, and creep data again were collected.

The fourth specimen from each of the fiber types remaining from this procedure was subjected to a creep test at 25 °C without erasure of its age to a strain level identical to that reached by the other specimens. The fiber then was erased of its aging, subsequently aged for 48 h, and then subjected to another creep test.

Birefringence measurements were obtained by the Becke line method, and density measurements were obtained by the sink-float method (*26*).

Results

Increasingly large shifts in creep of samples with increasingly greater physical ages were observed for all samples as expected. An example of this shifting behavior is provided in Figure 6, which shows creep curves for cotton fibers tested at 25 °C and physically aged for short times of approximately 2, 3, and 4 d. All other fiber types exhibited analogous creep shifting. Shifts were determined by measuring the horizontal separation

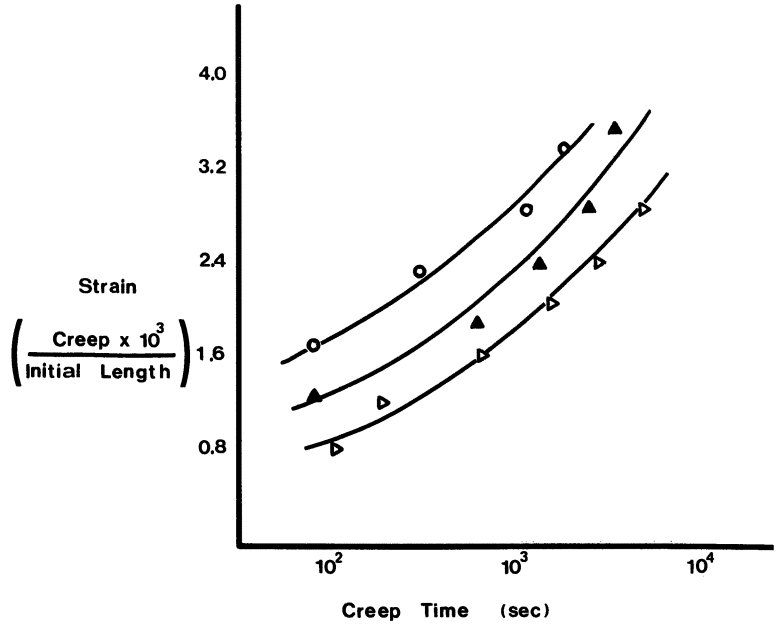

Figure 6. Cotton creep curves, short age times. Age (hours): ○, 28; ▲, 49; and ▷, 105.

of the creep curves in log(creep time) units at five different places and then calculating an average value.

Figure 7 shows the creep curve of a cotton fiber sample having a chronological age of about 400 years. The creep curve of the same fiber after erasure of aging and conditioning for 34 h also is plotted on the graph. As expected, a large shift in the creep curve is observed. However, when these data points are plotted as shift versus age time as in Figure 8, nonlinear behavior becomes apparent at long aging times. Aging rates increase linearly with increasing aging times to several days but then change at an increasingly slower rate. The general form of this behavior is one of an exponentially decaying function.

A function of the following form was fitted to the aging rate data to describe this behavior:

$$y_i = A\,[1 - \exp(-x_i/C)] \tag{2}$$

where y_i is the shift [$y_i = -\Delta\log(a) = \log(\text{creep time})_i - \log(\text{creep time})_{\text{ref}}$], x_i is the age time [$x_i = \Delta\log(t_e) = \log(\text{age time})_t - \log(\text{age time})_{\text{ref}}$], A is a constant corresponding to the asymptotic value of the

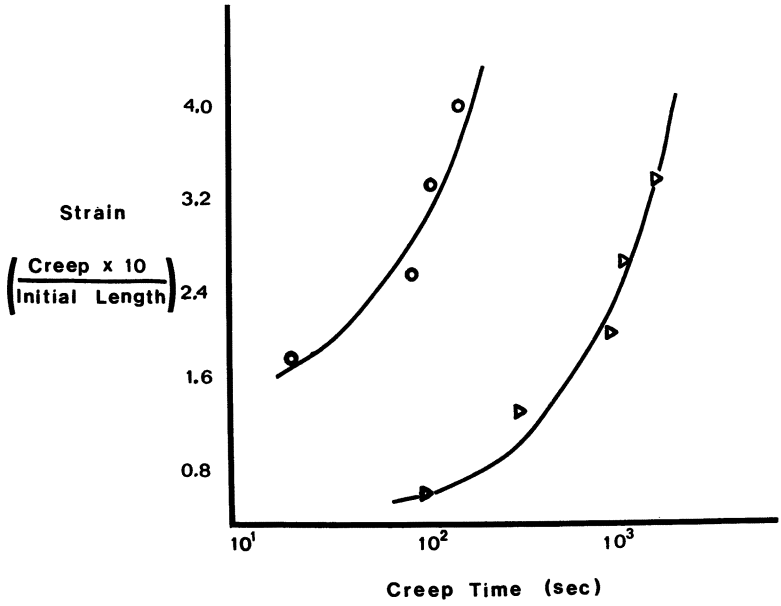

Figure 7. Cotton creep curves, short and long age times. Age (years): ○, 0.004; and ▷, 400.

shift, and C is a constant corresponding to the relative aging rate at short aging times.

The constants A and C were computed for each of the fiber types by using a least squares curve fit. These values are presented in Table II. By substituting values for x_i, y_i, and the constants A and C, plots describing aging rates over a few thousand years can be obtained for each fiber type. Figure 8 is an example of this plot for cotton. Data points actually measured, as well as the fitted function, are included in this figure. Another example of this plot is provided in Figure 9 for flax.

As discussed earlier, previous studies predicted and observed linear behavior in all samples regardless of sample age or morphology (*1*). Nonlinear behavior was not predicted under any circumstances. However, another study indicates that an exponential function such as Equation 2 is applicable to the change in heat content and mobility in polymers with increasing aging time (*4*). Because physical aging occurs with a decrease in heat content and molecular mobility in the polymer, an exponential rather than a linear decay in creep with increasing age might be expected. Apparently, the nonlinear behavior observed here results from the effects of sample morphology. The general effect of orientation and crystallinity is to decrease enthalpy and molecular

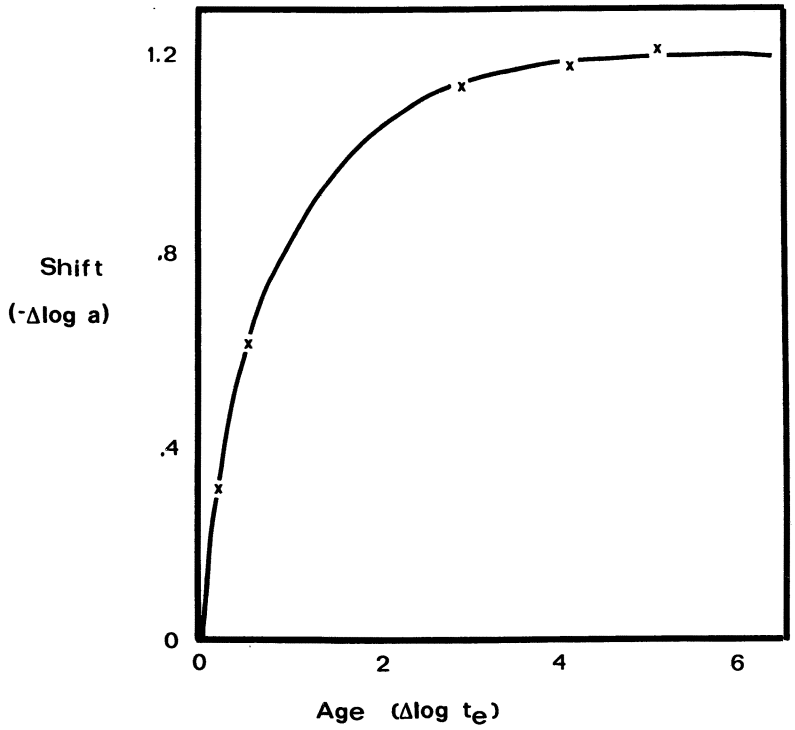

Figure 8. Aging of cotton: —, fitted curve; and ×, data measured.

Table II. Values of Constants *A* and *C*

Fiber Type	A	C
Cotton	1.21	0.82
Flax	1.22	1.66
Viscose rayon	1.14	0.99
High-wet-modulus rayon	1.06	1.05
Cuprammonium rayon	1.10	0.69
Acetate	1.08	0.54

mobility so that the initial linear portion of the exponential curve is shortened and curvature is observed at earlier ages than with totally amorphous samples. These effects have not been thoroughly investigated, however.

Measurements of optical birefringence and density were obtained in an attempt to determine if total polymer orientation and the amount of fiber crystallinity would correlate with aging behavior. These values are presented in Table III. Because the secondary wall of cotton comprises

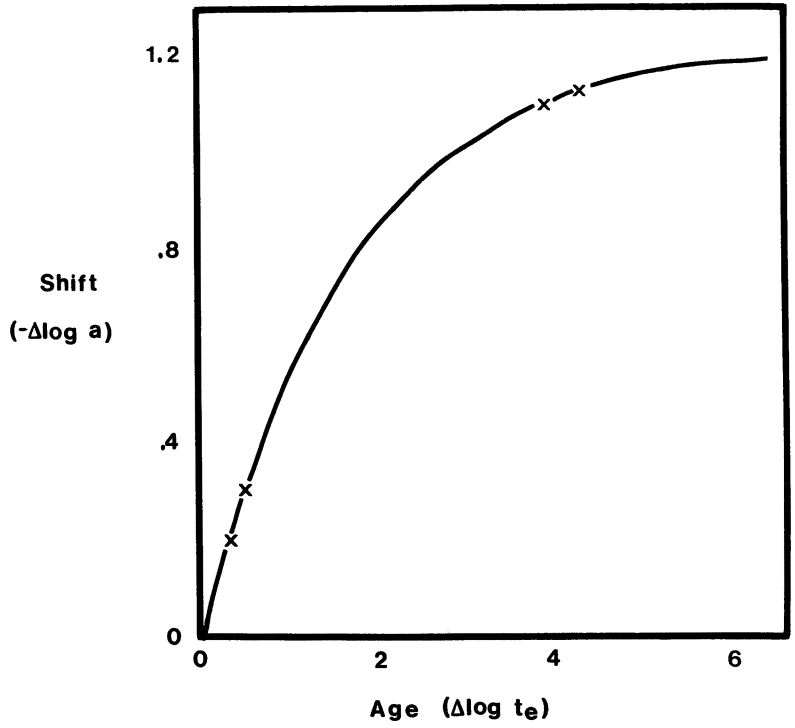

Figure 9. Aging of flax: —, fitted curve; and ×, data measured.

Table III. Birefringence and Density

Fiber Type	*Birefringence*	*Density (g/cm³)*
Cotton	0.028	1.485
Flax	0.060	1.500
Viscose rayon	0.028	1.471
High-wet-modulus rayon	0.030	1.473
Cuprammonium rayon	0.029	1.481
Acetate	0.003	—

the bulk of the fiber and the Becke line method used in this study primarily provides a measure of the fiber cuticle or primary wall, use of a birefringence value of the fiber secondary wall obtained by interference microscopy was more reasonable (27). The linear correlation coefficients for birefringence are 0.03 versus constant A and 0.86 versus constant C, and those for density are 0.64 versus constant A and 0.12 versus constant C. The density of acetate is omitted from this correlation because it would not reflect fiber crystallinity in the same way as it would for other

fiber types. A fairly strong correlation ($r = 0.86$) exists between birefringence and the constant C, although no correlation is found between birefringence and the constant A. This finding suggests that aging is somehow dependent on polymer orientation. A moderate correlation ($r = 0.64$) appears to be present between density and the value of A, although no correlation exists between density and C. This result suggests that aging also is somehow dependent on the amount of crystallinity present in a fiber. However, more data are required to substantiate this hypothesis.

Although some of the experimental results from this study are consistent with the theoretically expected temperature dependence (Figure 1), some disagreement was found. Each of the fiber types exhibited a creep dependence on temperature. The absolute values of creep for each fiber type increased for the same stress at increased temperatures. This result is illustrated for cotton at short aging times in Figure 10. Table IV summarizes aging rates at short aging times for each fiber type at 25, 50, and 75 °C.

Cotton exhibited a consistent aging rate of nearly unity at 25 and 50 °C. At 75 °C, the rate of aging dropped to 0.82. This result indicates that

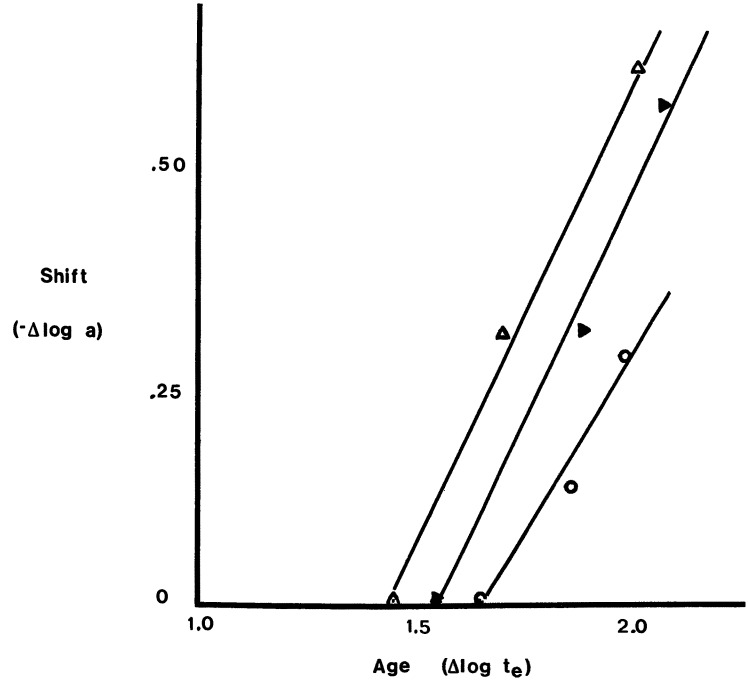

Figure 10. Temperature dependence of cotton aging. Temperature (°C): △, 25; ▶, 50; and ○, 75.

Table IV. Temperature Dependence on Aging Rate

Fiber Type	*Aging Rates*		
	25 °C	*50 °C*	*75 °C*
Cotton	1.04	1.03	0.82
Flax	0.66	0.41	—
Viscose rayon	0.87	0.64	0.58
High-wet-modulus rayon	0.82	0.70	0.68
Cuprammonium rayon	1.11	0.56	—
Acetate	1.06	0.48	0.21

cotton is well between T_β and T_g at 25 and 50 °C but is nearer to T_g at 75 °C.

The aging rate of flax decreased from a value of 0.66 at 25 °C to a value of 0.41 at 50 °C. Flax could not be tested at 75 °C because fiber slippage between the clamps could not be eliminated. However, the nonunity and decreasing aging rate values suggest that T_g is being more closely approached than it is with cotton.

Viscose rayon exhibited an aging rate broadly decreasing from 25 to 75 °C. However, the aging rate is expected to be approximately constant at temperatures between T_β and T_g as illustrated in Figure 1. In addition, aging rates previously measured for a wide variety of amorphous polymers (*1*) indicated that the rate of aging for most materials is expected to be approximately equal to unity. This broad decrease in aging rate is not consistent with the abrupt decrease expected theoretically from Figure 1. One explanation for this behavior might be that the presence of orientation and crystallinity has broadened the T_g range as predicted (*1*) so that fewer amorphous microdomains are below their T_g at progressively higher temperatures. This situation would have the apparent effect of decreasing the aging rate at higher temperatures because fewer microdomains participate in aging. More study of this phenomenon is required, however.

The aging rate of high-wet-modulus rayon was fairly constant at all three testing temperatures. This behavior suggests that the testing temperatures lie in the plateau region of aging illustrated in Figure 1 in which the aging rate is constant and the testing temperatures are not near T_β or T_g.

The aging rate of cuprammonium rayon dropped rapidly from 1.11 at 25 °C to 0.56 at 50 °C. At 75 °C the fiber exhibited irregular changes accompanying shrinkage during creep erasure. Consequently, a proper aging rate value could not be determined because irreversible structural changes accompany shrinkage. The rapid decrease in aging rate indicated

that cuprammonium rayon is approaching its T_g. Because the lower temperature limit of shrinkage is T_g, the presence of shrinkage at 75 °C also supports this conclusion. These data indicate that cuprammonium rayon has the lowest T_g among the fibers examined in this study, lying somewhere between 50 and 75 °C.

Acetate showed a decline in aging rate from a value nearly equal to unity at 25 °C to 0.21 at 75 °C. This finding suggests that acetate has a T_g near but greater than 75 °C. The T_g of acetate has been reported to be 84 °C when conditioned at 65% rh and 70 °F (*23*). However, the broadness of the aging rate decline is inconsistent with expectations associated with Figure 1 as in the case of viscose rayon.

The accuracy and the range of ages obtainable using this method need to be estimated to determine the value of this technique for chronological dating. The lower limit for the age of a sample is set by the requirement that the creep test time be short compared to the sample age. The tests conducted in this study indicate that aging times of 24 h are a practical minimum.

The accuracy of the method depends on the accuracy with which the shift and the slope of the curve can be established. A given uncertainty in the shift will result in a larger error in age as the slope decreases. This relationship can be stated mathematically as follows:

$$\Delta\text{age} = (1/S) \times \Delta\text{shift} \tag{3}$$

where S is the slope of the curve, Δshift is the uncertainty associated with the shift, and Δage is the resulting uncertainty associated with the age. The slope approaches zero as the aging time increases because of the asymptotic nature of the curve. In this case, even a small uncertainty in the shift can cause an error of several orders of magnitude in aging time. The upper limit for sample age then depends upon the slope, the accuracy with which the shift can be determined, and the degree of accuracy required in the dating.

A blind test was conducted with a cotton sample 814 days old. A single creep test was performed and the age was estimated. The result achieved was an estimated age of 214 days. This result seems to indicate a rather large error. However, when the datum is plotted, the point is not very far from the curve. In fact, it is quite consistent with the trend set by the data for 47- and 400-year-old samples and suggests that the curve rather than the 814-day datum is incorrect. In view of the limited number of calibration points used to fit the curves, this explanation seems plausible. Consequently, the curve in Figure 8 represents a curve fitted to all cotton specimens measured, including the 814-day specimen. The fitted equations presented here should be used only to evaluate the

method and not for dating purposes. Considerably more data will be required to accurately define the equations well enough for use in dating textiles.

Conclusive determinations of accuracy and upper age limits cannot be done until more extensive data are available. However, some rough estimates can be made for cotton from the data presented here. The consistency of the trend for the 814-day-old, 47-year-old, and 400-year-old samples indicates that the shifts should be quite consistent from one sample to the next. It is reasonable that these shifts will be repeatable to within ±0.01. The slopes for the aging curve can be estimated from a curve drawn through the data, including the blind test datum. The resulting uncertainty in the age determination can then be estimated. The results are shown in Table V. This table indicates that the method

Table V. Calculated Accuracy Associated with Chronological Age Determinations of Cotton Fibers

Age	$\Delta log(t_e)$[a]	*Slope*	$\Delta log(age)$	*Range in Age Estimate*
100 hours	0.55	1.40	0.007	98–102 hours
100 days	1.93	0.18	0.056	88–114 days
10 years	3.50	0.050	0.20	6.3–15.8 years
100 years	4.50	0.039	0.26	59–181 years
1000 years	5.50	0.028	0.36	430–2280 years

[a] Values are based on a reference age time of 28 h.

should have very good accuracy for fibers having short age times (up to about 1 year) and should provide reasonable discrimination up to several hundred years. For ages greater than this, the method used as described probably will not provide good discrimination, although it still can differentiate between very old and relatively new fibers. However, these conclusions apply only to cotton. Other fibers may have different useful age ranges. For example, the data in Figure 9 indicate that flax would exhibit a much more useful range for age determinations because the asymptotic value is reached considerably more slowly than it is for cotton.

Acknowledgment

The authors thank the Kansas Agricultural Experiment Station and Committee RA75 of the American Association of Textile Chemists and Colorists for support of this work.

Literature Cited

1. Struik, L. C. E. "Physical Aging in Amorphous Polymers and Other Materials"; Elsevier: New York, 1978.
2. Ahmed, A. A.; James, N. H. *Polymer* **1982**, *23*, 1129.
3. Turnbull, D. *J. Chem. Phys.* **1961**, *34*, 120.
4. Sung, C. S. P.; Lamarre, L.; Chung, K. H. *Macromolecules* **1981**, *14*, 1839.
5. Struik, L. C. E. *Rheol. Acta* **1966**, *5*, 303.
6. Weiss, R. A. *J. Polym. Sci. Polym. Phys. Ed.* **1982**, *20*, 73.
7. Kalyanaraman, A. R. *Text. Res. J.* **1984**, *53*, 354.
8. Robertson, R. E. *J. Polym. Sci. Polym. Symp.* **1978**, *63*, 173.
9. Chapman, B. M. *Rheol. Acta* **1975**, *14*, 466.
10. Agarwal, M. K.; Schultz, J. M. *Polym. Eng. Sci.* **1981**, *21*, 776.
11. Cowie, M. G.; McEwen, I. J. *Polymer* **1979**, *20*, 1129.
12. Hedvat, S. *Polymer* **1981**, *22*, 774.
13. Boyd, R. H.; Robertson, M. E.; Johnsson, J. F. *J. Polym. Sci. Polym. Phys. Ed.* **1982**, *20*, 1973.
14. Gupta, V. B.; Satish Kumar. *Text. Res. J.* **1977**, *47*, 647.
15. Ibid. **1979**, *49*, 240.
16. Hunt, D. G.; Darlington, M. W. *Polymer* **1978**, *19*, 971
17. Ibid. **1979**, *20*, 241.
18. Howard, W. H.; Malcolm, L. W. *Text. Res. J.* **1979**, *49*, 647.
19. Leaderman, H. "Elastic and Creep Properties of Filamentous Materials and Other High Polymers"; Textile Foundation: Washington, D.C., 1943.
20. Meredith R. "Mechanical Properties of Textile Fibers"; North Holland: Amsterdam, 1956.
21. Morton, W. E.; Hearle, J. W. S. "Physical Properties of Textile Fibers"; Wiley: New York, 1975.
22. Brandup, J.; Immergent, E. H. "Polymer Handbook", 2nd ed.; Wiley-Interscience: New York, 1975; p. V87.
23. Fuzek, J. K. In "Water in Polymers"; ACS SYMPOSIUM SERIES No. 127; American Chemical Society: Washington, D.C., 1980; p. 515.
24. Robinson, M. S.; Rigby, B. J. *Text. Res. J.* **1981**, *51*, 637.
25. Wortman, F. J.; Rigby, B. J.; Phillips, D. G. *Text. Res. J.* **1984**, *53*, 7.
26. Hall, D. M. "Practical Fiber Identification"; Auburn University: Auburn, Alabama, 1982.
27. Hamza, A. A. *Text. Res. J.* **1980**, *50*, 731.

RECEIVED for review November 26, 1984. ACCEPTED March 25, 1985.

3

Evaluation of Degradation in Museum Textiles Using Property Kinetics

Jeanette M. Cardamone and Peter Brown

Department of Textiles and Clothing, The Ohio State University, Columbus, OH 43210

Methodology was developed to estimate the extent of degradation of historic cotton cloth in terms of "time left" as a viable museum artifact under 50-lux tungsten illumination and 55% rh. A master plot of yarn tensile strength versus half-life was derived from aging contemporary cloth at 190, 160, 130, and 100 °C and by using property kinetics and the Arrhenius equation. The presence of light increased the first-order rate constant by 1.9 and decreased the half-life by 55.5%. The activation energy for the 20 °C degradation rate was 23,486 ± 1312 cal/mol. The half-life plot used comparatively with various historic cotton textiles may provide evaluation of treatments such as consolidation, deacidification, or reduction for effectiveness in conserving the textile and thus in changing time left. Degradation profiles of the yellowness index, oxygen uptake, and weight loss were studied.

MUSEUM TEXTILES PROVIDE PRICELESS DOCUMENTATION of the activities of humans throughout time. They record human interests throughout the ages and serve as invaluable resources for students of many disciplines including anthropology, archaeology, art history, sociology, psychology, architecture, interior design, textile technology, and textile science.

Museum textiles are subject to degradation during storage, on display, or during refurbishing treatments such as cleaning. Textile conservators in the practice of preserving collections may question whether a prescribed treatment slows degradation, stabilizes or alters the condition of the textile, and causes dramatic future changes.

Critical decisions are often made on the basis of subjective observations of each piece coupled with curatorial "experience" with similar pieces. Conservators who embark occasionally on restorative treatments such as fabric consolidation designed to reverse the symptoms of degradation have begun to address the causes and to consider the

0065-2393/86/0212-0041$09.75/0

future fundamental effects of such restoration. Because decisions regarding cleaning and other preservation-restoration procedures often involve a high risk of permanent damage, the need to establish systematic and objective methodology and procedures for the care of textiles is widely recognized.

Research Objectives

The overall objective of this research was to develop a methodology using property kinetics, the Arrhenius rate expression, and half-life to estimate the extent of degradation of contemporary cotton fabric. The ultimate objective was to apply this methodology to historic cotton fabric for the following purposes: (1) to estimate the extent of degradation, (2) to evaluate the time left as a viable museum artifact (the *time left* is the difference between the measured strength of a sample and that of a reference sample whose strength is negligible), (3) to evaluate the appropriateness and effectiveness of a treatment insofar as the time left is altered, and (4) to predict future effects of a treatment designed to slow, stop, or reverse degradation.

Artificial aging experiments on contemporary cotton fabric at 190, 160, 130, and 100 °C when carried out in air under 50-lux tungsten illumination and darkness may lead to the estimation of the extent of degradation and the time left when an end point for degradation is assumed. When half-life values are estimated for 20 °C, they could be used in conjunction with appropriate physical values for a historic fabric to provide an estimate of the useful life of that piece should it be subjected to any predictable regimen. The aim of this research is to provide objective methodology to evaluate the benefit of practices such as enhanced storage or modified display. This methodology is designed to predict the real effect of a given treatment, such as washing, more accurately than subjective evaluation based on the visually apparent effects.

Another objective is to study changes in the degradation effects, the rate constants, and the half-life values of cotton fabric as it ages. Such changes may have a more profound effect on the useful life of the artifact than the more apparent strength losses or gains commonly used to monitor these processes. By developing a methodology, the appropriateness of treatments such as consolidation and deacidification, designed to retard degradation and enhance long-term use, may be evaluated objectively.

Background

Those who document historic artifacts to establish provenance and date or who examine components to assess condition use investigation methods that are as nearly nondestructive as possible. Nondestructive

for the conservator may mean using a scanning mechanism that imparts neither immediate nor latent degradation effects. For the investigator using analytical methods, *nondestructive* means using the smallest sample that fits inside a sample port yet remains unchanged during and after analysis.

Artificial aging has been used to simulate natural aging in various studies including the Shroud of Turin study. In this research we are assuming, as was assumed in the Shroud study, that artificial heat aging can be used to simulate natural aging. For the purposes of preservation, nondestructive scientific investigations were performed on the Shroud in 1969 and in 1973. In 1976, American scientists used surface analysis (*1*), including UV and fluorescent photography (*2*), IR reflectance spectroscopy and thermographic analysis (*3*), and X-ray fluorescence and near UV–vis reflectance (*4*). Pellicori and Chandos, using a portable UV–vis spectrophotometer, simulated the spectral reflectance properties of the yellowed Shroud background on similar contemporary linen cloth by artificially aging it at 150 °C for 4 h. The cause of the more intense body image was proposed to be dehydration due to heat and light, accelerated by foreign substances on those parts of the body in contact with the cloth (*5*). Because surface analysis did not reveal the composition of the blood color, microanalysis was used on fibers withdrawn from the Shroud surface with tape.

In another study to investigate the effects of one preservation treatment, researchers used artificial heat aging of contemporary cloth to simulate the properties of naturally aged cloth (*6*). Although strength levels were matched, not all properties were duplicated, and the overall characteristics of the cloths were not the same (*7*).

Recent approaches directed toward preventing oxidation of cotton cloth included using accelerated aging of alkaline-treated cotton cloth for neutralization of acidic, oxidized, cellulose decomposition components that in cellulosic textiles and in paper are responsible for age tendering and yellowing. Conclusions regarding the relative effectiveness of treatments at room temperature were based on results of treatments at one elevated temperature (*8*). Predictions of long-term effects of these treatments are unknown (*9*).

To cure the effects of degradation, various polymeric consolidation materials were applied to artificially degraded cloth. Because long-term stability and ultimate consequences of treatment were not determined, recommendations for this use were not given (*10*).

By comparison, paper conservators have addressed many of these same issues and may have been somewhat more cause oriented in dealing with specific treatments, such as deacidification, designed to reduce the rate of degradation. Arney and Chapdelaine have widely used the concept of "property kinetics" that is borrowed from chemistry where it was developed (*11*).

Property Kinetics

The degradation reactions involved in the breakdown of cellulose are clearly highly complex, and thus the use of the concept of property kinetics is a bold simplifying analogy. In property kinetics most of the degradation processes are assumed to be temperature dependent. In addition, most or all of these processes are assumed to affect some useful macroscopic property such as tensile strength so that the individual effects of these processes can be subsumed into one unified effect that obeys the Arrhenius equation. Thus property kinetic studies are necessarily empirical and show a much less obvious or demonstrable mechanistic connection than chemical kinetic studies between the presumed cause and the measured effect.

By assuming chemical changes in the aging of cotton become manifest through changes in physical or mechanical properties, a reasonable basis is found for applying the Arrhenius equation to evaluate these changes. A change in property value (p) with time (t) is expressed differentially:

$$dp/dt = k\, f(p) \tag{1}$$

where k is a rate constant and $f(p)$ is some integratable function of the property that is unknown because it has no mechanistic significance. If $f(p)$ is comparable to the chemical kinetic expression

$$A \xrightarrow{k_1} B \tag{2}$$

the rate of A used up is expressed as

$$-dA/dt = k_1(A) \tag{3}$$

This expression is integrated to give

$$A = A_0 e^{-kt} \tag{4}$$

where A is the concentration at time t and A_0 is the concentration at time t_0. By using the property of tensile strength (T.S.), the analogous property kinetic expression is

$$\text{T.S.} = \text{T.S.}_0 e^{-kt} \tag{5}$$

It follows that

$$\ln (\text{T.S.}/\text{T.S.}_0) = -kt \tag{6}$$

then

$$\ln (T.S._0/T.S.) = kt \tag{7}$$

or

$$2.303 \log (T.S._0/T.S.) = kt \tag{8}$$

Plotting 2.303 log ($T.S._0$/T.S.) versus t yields a straight line with a slope equal to the rate constant k_1 typical of first-order kinetics.

Half-life Values

The concept of half-life is well known and can be of use with museum textiles if one assumes that they "decay" steadily if acted upon by their environment. Half-life can be calculated by using Equation 8.

When T.S. = $T.S._0/2$, then

$$\ln[(T.S._0/(T.S._0/2)] = kt_{1/2} \tag{9}$$

Therefore

$$\ln 2 = kt_{1/2} = 0.693 \tag{10}$$

or

$$t_{1/2} = 0.693/k \tag{11}$$

Half-life values, when used with a current value of a property such as tensile strength and with some defined end-point value such as the tensile strength of an extremely weak specimen, may establish the time left in the useful life of a particular historic textile.

Another possible use of this methodology, which is also highly desirable, is the monitoring of ordinary conservation practices, such as cleaning, to determine if the time left is affected by the proposed treatment. Further possible uses include assessing the appropriateness of those treatments such as consolidation and deacidification that have been designed to change the time left to determine if, and to what extent, it has been extended or shortened by the treatment.

The tacit assumption in any consolidation treatment is that by improving the current value of the target property (usually tensile strength) one automatically increases the time left. However, if the half-life were affected negatively by the treatment, the opposite might be

true. For example, one treatment, the use of poly(vinyl alcohol) (PVA) (Rhodoviol BS-125) certainly strengthened the treated fabrics and thus increased the time left with respect to strength. However, PVA attracted dust, became impossible to clean in a very few years, and ruined the artifact as a useful object long before it would have been discarded for weakness (*12*). In that case the degradation process together with the end point simply changed, and appearance, not strength, became the critical factor. The half-life of the new phenomenon, the tendency to attract dust, had it been determined, could have prevented many inappropriate treatments.

In artificial heat aging, property kinetics can be used in conjunction with the Arrhenius rate expression to estimate rate constants at room temperature provided the overall aging behavior, when monitored by a measurable parameter, can be shown to be constant over the temperature range of the study.

Arrhenius expressed the effect of temperature on the rate of a given chemical reaction by

$$d\ln k/dT = E_a/RT^2 \tag{12}$$

where k is the rate constant of the reaction, R is the universal gas constant, T is the absolute temperature, and E_a represents the energy required per mole of reactants for a reaction to occur (E_a is the activation energy). If E_a is assumed to be independent of temperature over the temperature range of study, then the expression can be integrated to

$$\ln k = -E_a/RT + I \tag{13}$$

where I is an integration constant. E_a represents the energy needed to start the reaction. Arrhenius devised and applied his equation to simple chemical reactions for which clear mechanistic reasoning based on the depletion of reactants and thus the decrease in opportunities for reactions to occur could be presented to justify his assertion. Although aging studies are not simple chemical reactions, other researchers have found that certain property values may be used in Arrhenius extrapolations for future predictions of performance.

The Arrhenius treatment has been applied to aging studies on rubber (*13*), to predict the life of a polyester-glass laminate (*14*), to predict product stability of a thermosetting resin alone and in combination with two additives (*15*), in permanence tests on paper (*16*), to multicomponent systems in which the principal component is paper (*17*), and to study the influence of temperature on the relative contributions of the oxygen-independent and oxygen-dependent processes to the total rate of newsprint deterioration (*18–20*).

Experimental

Scope of the Work. Initial stages of the work involved investigations of a nondestructive method, IR photography, for detecting the weakest areas of the cloth so that the weakest yarns could be sampled. To estimate the first-order property kinetics at room temperature, the degradation rates, half-lives, yellowness index, oxygen uptake, percent weight loss, crystallinity index, and tensile strength were examined at 190, 160, 130, and 100 °C under the conditions of light and oxygen (21% air) (LO), darkness and oxygen (21% air) (DO), light and nitrogen (LN), and darkness and nitrogen (DN). Correlations among these parameters were sought to determine which were possible indicators for evaluation of degradation at 20 °C and to understand the aging process so that preventative measures could be determined.

Infrared Photography. The near IR region of the electromagnetic spectrum (0.8–2.5 μm), even though it has limited use, can be important for the study of compounds containing OH, NH, and CH groups. Researchers have reported that the near IR region is useful for the study of hydrogen bonding (*21*). Hydrogen bonding through primary and secondary alcohol groups in cellulose is thought to be the microcellular cement that gives form to the crystalline regions of the molecule. Upon degradation, with bond cleavage, these alcohol groups form carbonyl compounds in oxycellulose formation. In early studies of this research, an attempt was made to record on IR film the selective absorptions of IR radiation by cellulose that was artificially aged. In a series of control experiments, cotton print cloth was artificially aged in the manner of Berry et al. who performed a series of degradation steps on cotton: acid hydrolysis and thermal aging (*22*). Treated and untreated samples from these treatments were photographed sequentially by using high-speed IR black and white film and panchromatic black and white film. Narrow-band IR filters were used to heighten the signal-to-noise ratio, but the method was not sensitive enough to use in locating the weakest areas.

Aging Chambers. To maintain the air and the nitrogen environments during aging, chambers in Figure 1 were devised by using 8-oz clear-glass oval pharmacy bottles with about 30 8-mm diameter solid glass rods inserted into each bottle to reduce the internal volume by 60%. With the reduced ratio of air to mass of the samples, oxygen taken up by the samples attained levels that could be readily measured as oxygen depletion from the enclosed air inside the chambers. To test for leakage the following procedure was carried out: In a glove bag filled with nitrogen and maintained under a positive pressure of nitrogen flow, the custom-made threaded metal caps having a small hole at the top and lined with ⅛-in. silicone discs were screwed firmly in place. The nitrogen filling the bottle chambers had been bubbled through a saturated sodium dichromate salt solution (55% rh). These nitrogen-filled chambers, after 1¾ days at 190 °C, showed an oxygen-free atmosphere. The metal cap of the bottle lined with a fresh silicone disc thus became a reusable chamber.

At each temperature two convection ovens were used and contained 28 aging chambers each; half of these (*14*) contained air and the other half (*14*) contained nitrogen. Half of the air-containing chambers (*7*) and half of the nitrogen-containing chambers (*7*) were placed under 50-lux tungsten light, whereas the others were covered and were in total darkness. Oven temperatures remained uniform throughout all parts of the oven. These temperatures were monitored with calibrated thermistors that remained inside the ovens during the

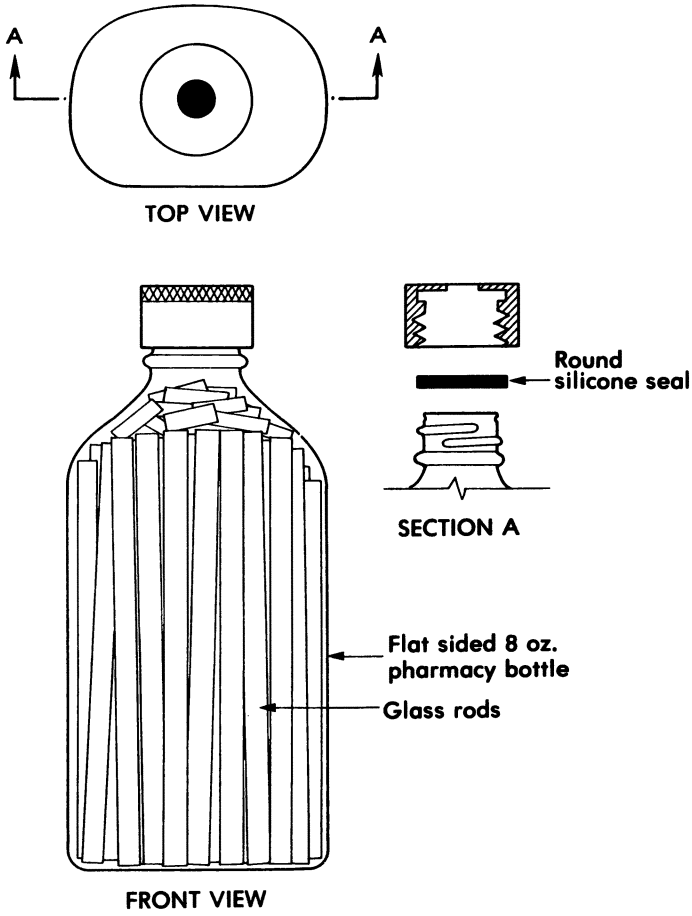

Figure 1. Aging chambers.

aging experiments. Each chamber contained two fabric swatches, approximately 1¾ × 2 in. each. As the experiments proceeded, one chamber from each set was removed at regular intervals throughout the total exposure time to provide a means of monitoring the process of aging for each condition: LO, LN, DO, and DN.

Samples and duplicate samples of unbleached desized cotton print cloth (400 V test fabrics), 80 × 80 count, 3.5 oz/yd^2, and yarn size of 40 singles in warp and weft, were randomly selected after conditioning to 55% rh in a desiccator over potassium dichromate solution. The samples were placed inside the pharmacy bottles along the flat sides so that each bottle contained one sample and one duplicate. When the samples were placed side by side along the flat side of the bottle chambers, they filled the entire flat-sided area. Dark chambers were achieved by wrapping the bottles in aluminum foil to exclude light.

Aging Conditions. To determine the length of exposure times at 190, 160, 130, and 100 °C, the Arrhenius equation was used:

$$\log (k_2/k_1) = (E_a/2.303R)\,[(T_2 - T_1)/T_2T_1] \quad (14)$$

where $k_2/k_1 = (t_{1/2})_1/(t_{1/2})_2$, T_1 and T_2 are in Kelvins, and $R = 1.99$ cal/mol K.

Previous studies of the decomposition of cellulose reported E_a for absorbent cotton as 54.3 kcal/mol at a high-temperature range of 270–310 °C (*23*). For temperatures below pyrolysis, $E_a = 20$ kcal/mol reflects the low-temperature degradation effects of loss of H and OH from adjacent carbon atoms in cellulose (dehydration) and the concomitant creation of C=C bonds (*24*). In another work $E_a = 21$ kcal/mol was estimated from Arrhenius plots of the degree of polymerization versus time for cellulose heated in air at 150–190 °C (*25*).

From Berry's work (*26*) on the strength of cotton print cloths degraded thermally at 168 °C for various aging periods and the plot of strength (percent of original) versus heating time (hours), the estimated half-life for the heat-degradation reaction in air was 24 h. To determine the duration of aging at each temperature (190, 160, 130, and 100 °C) the activation energy for the degradation of cellulose at temperatures below pyrolysis ($E_a = 20$ kcal/mol) was used in the Arrhenius equation (Equation 14) where k_1 and k_2 are rate constants at T_1 and T_2. The value for $(t_{1/2})_2$ is taken from Berry's work as 1 day at T_2(441 °K). The value for $(t_{1/2})_1$ is calculated for the specified temperature (T_1) of the research. By using these values and Equation 14, the calculated aging periods for one half-life are 64 days at 100 °C, 9 days at 130 °C, 2 days at 160 °C, and 8 h at 190 °C (Table I). Six half-life periods of aging were chosen at 190 °C as this period represented an end point for degradation when the fabric became dark brown in color and extremely brittle. The number of half-lives at the other temperatures were determined to allow as much aging as possible so that significant measurable changes were obtained within a reasonable period of time.

The Ovens. Two ovens for the aging experiments were equipped with tungsten bulbs regulated to 50-lux intensity with a dimmer. This light was diffused through sandblasted windowpane glass. Fine-wire mesh screening was used to eliminate any bright spots directly below the light bulbs. The light intensity and spectral distribution were recorded outside the oven by an Instrumentation Specialties Company (ISCO) model SR spectroradiometer that measured μW cm^{-2} nm^{-1} for every 25-nm wavelength from 380 to 1050 nm. For these measurements, the spectroradiometer probe end was adapted to the ends of quartz rods that were at sample levels inside the ovens and that reached through oven vents to the outside. These rods were wrapped in aluminum foil, shiny side in, to increase internal reflectance and thus to deliver sufficient light to the outside of the ovens to the monitoring device.

Table I. Estimated Number of Half-lives Corresponding to Aging Times at Elevated Temperatures (55% rh; LO, DO, LN, and DN)

Temperature (°C)	*Exposure Time (days)*	*Estimated Number of Half-lives*
100	64	1
130	36	4
160	10	5
190	2	6

Properties Monitored

Yellowness Index. The yellowness index provides a measurement related to the yellowing of the cotton cloth that may be due to the isolated or combined effects of heat, light, and/or oxygen. The yellowness index was calculated from the percent reflectance measurements of the aged fabric samples. A Beckman reflectance spectrophotometer with integrating sphere was used to record the percent reflectance of the surface of the fabric samples. Tristimulus values were found from the summation over all wavelengths in the visible range for the energy distribution of the source, reflectance properties of the cloth, and spectral response of the Commission Internationale d'Eclairage (CIE) observer. The yellowness index (Y.I.) is evaluated as (*27*)

$$\text{Y.I.} = (128X - 106Z)/Y$$

where X, Y, and Z are tristimulus values.

Oxygen Uptake. A Carle gas chromatograph model GC 8700 containing an O_2–N_2 detection column was used to measure oxygen uptake. Samples of gas were withdrawn from the test chambers with a 10-μL syringe inserted through the silicone disc. Initial trials indicated that operator error is insignificant and that reliable reproducible results can be obtained so that 0.25% is a more than adequate error allowance.

Percent Weight Loss. Samples were conditioned in a 55% rh environment at 20 °C and weighed until weights were constant. After aging, samples were returned to this atmosphere until the weights were again constant. The percent weight loss was evaluated by using the original weight value.

Crystallinity Index. A Siemens D500 diffractometer was run in the reflectance mode from a Siemens K800 generator. Data on rotating artificially aged cotton cloth samples were collected by using a Siemens LC500 computer interface in the step-scan mode. CuK radiation at 300 mA and 40 kV, 1° divergence slits, a 0.15° receiving slit, and a graphite-reflected beam monochrometer having a 0.15° slit were used in the data collection. Data were obtained at 0.1° intervals from 21° to 25° 2θ from diffractograms in the 18–40° 2θ range by counting 20–30 s/step for most samples.

Tensile Strength. Yarn tensile strength of conditioned samples (20 °C, 65% rh) was measured on an Instron universal testing instrument model 1123 equipped with a 50-g load cell and operating at a 1-in. gauge length and a 2-mm/min crosshead speed. Twenty-five yarns each in

warp and weft directions were required for statistical significance. These yarn samples were arranged in a ladderlike configuration on a special apparatus on the "Jan-Barr" (Figure 2). The purpose of the Jan-Barr was to facilitate the mounting of the 25 yarns accurately in equal lengths of 1 in. and to induce a straight pull on these yarns when they were individually placed between the grips of the Instron and were broken with an applied gram force. Approximately 25 warp yarns and 25 weft yarns from each sample were broken.

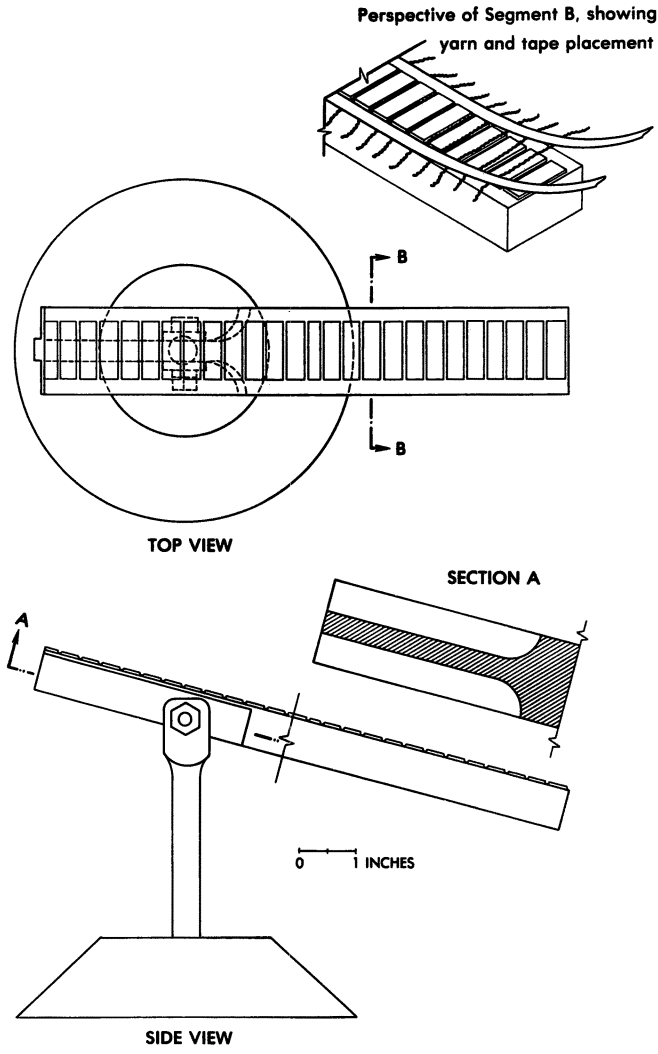

Figure 2. Jan-Barr invention for assembling 1¼-in. yarns for tensile strength.

Results and Discussion

Preliminary Experiments. Pilot studies conducted to test the experimental design at 190 °C showed that yellowness proceeds at a decreasing rate after 15 h of aging. The onset of the decreasing rate coincides in time with the increased uptake of oxygen and increased rate of oxygen uptake of cotton fabric at 190 °C in Figure 3. These results indicate that yellowing may be due appreciably to the loss of water with some oxygen incorporation to form aldehydric cellulose which contributes to yellowing and that this behavior changes when oxygen is taken up at a faster rate.

Studies on the thermal degradation of the cellulose structure have shown that oxidation reactions at 160–180 °C are more important than decarboxylation, but that this state may change at 190 °C (*28*).

Principal Experiments. OXYGEN UPTAKE. Oxygen uptake (millimeters of oxygen per gram of cloth) at 190 °C in Figure 3 appears to proceed at two different rates. At 190 °C, the rate of oxygen uptake up to 14 h of aging (1.7 half-lives) is slower than the rate after this period and up to 24 h of aging (3 half-lives). At 160 °C, in Figure 4, the rate of oxygen uptake up to 2.7 days of aging (1.25 half-lives) is slower than the rate after

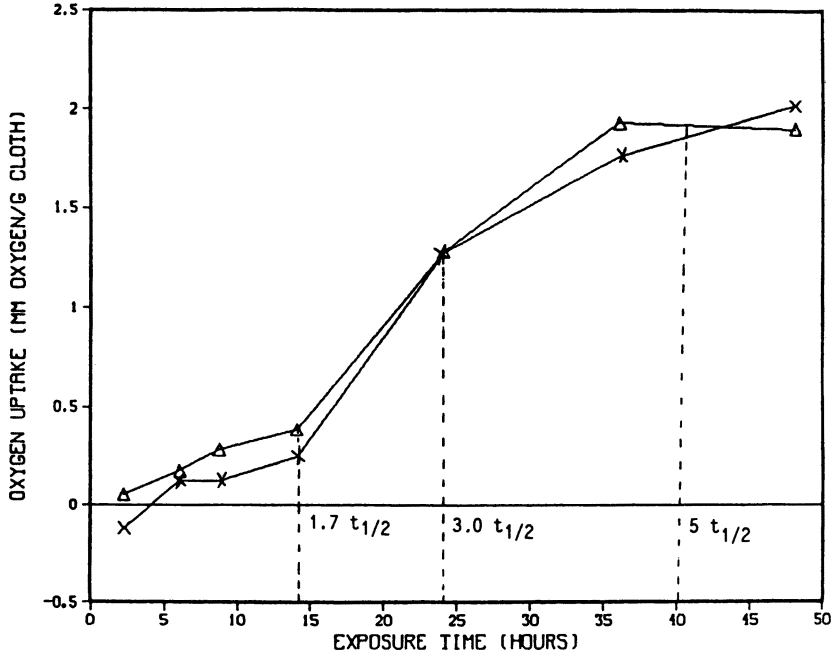

Figure 3. Oxygen uptake vs. exposure time at 190 °C. Key: △, light oxygen; ×, dark oxygen.

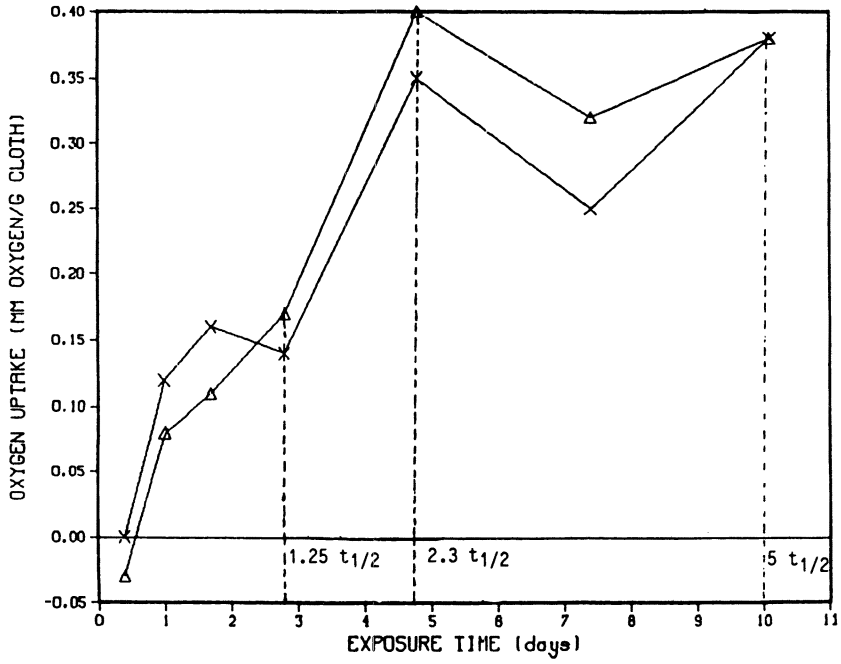

Figure 4. Oxygen uptake vs. exposure time at 160 °C. Key: △, light oxygen; ×, dark oxygen.

this period and up to 4.7 days (2.3 half-lives). The slower rates at 190 and 160 °C may indicate free radical formation and subsequent carbonyl group formation before the onset of autocatalytic behavior when both the amount of oxygen and the rate of oxygen uptake increase sharply with time.

Comparing oxygen uptake at 5 half-lives shows that at 190 °C, 1.8 mm of oxygen/g of cloth is taken up, and at 160 °C, 0.37 mm of oxygen/g of cloth is taken up. Thus, increasing the temperature by 30 °C from 160 to 190 °C causes the oxygen uptake to increase fivefold.

This behavior of cellulose in taking up oxygen at different rates during oxidation degradation reactions is typical of organic materials that oxidize in atmospheric oxygen and have rates of degradation occurring in various stages in which autocatalytic behavior has been described as an inductive stage (29).

PERCENT WEIGHT LOSS. Comparing the percent weight loss of cotton print cloth in Figure 5 at 190 °C to oxygen uptake by cotton print cloth at 190 °C in Figure 3 shows that the reaction rates change at the same periods during aging, that is, at 1.7 and 3 half-lives. When percent weight loss at 160 °C in Figure 6 is compared to oxygen uptake at 160 °C

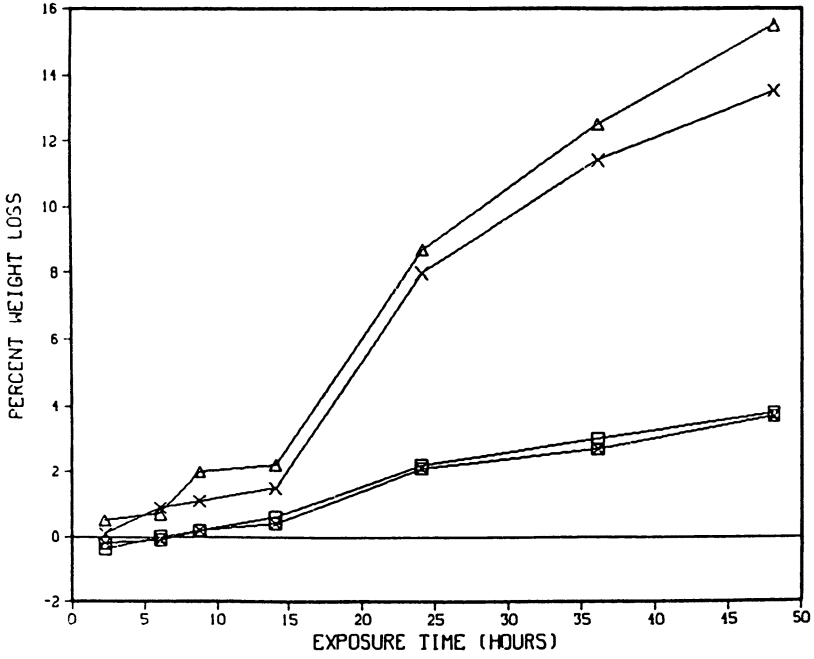

Figure 5. Percent weight loss vs. exposure time at 190 °C. Key: △, light oxygen; ×, dark oxygen; □, light nitrogen; ⊠, dark nitrogen.

in Figure 4, similar rate changes are seen at 1.25 half-lives in air. These results suggest a correlation between oxygen uptake and percent weight loss. In Figure 7, a linear correlation is shown between oxygen uptake and percent weight loss at 190 °C with no difference between aging in light and darkness. These results may indicate that at the faster rate of oxygen incorporation by cellulose, at 190 °C, main-chain scission occurs with resulting weight loss.

In Figures 5 and 6, no appreciable difference in percent weight loss is seen between light and darkness in air or in nitrogen. The nitrogen environment represents the isolated heat effect or the contribution that heat makes to the property change. At 190 °C, heat causes a percent weight loss of 3.8%. At 160 °C, heat causes a percent weight loss of 2.7%. By subtracting the heat effect, when percent weight loss in air at 160 °C is compared to percent weight loss in air at 190 °C, the 30 °C temperature increase from 160 to 190 °C is seen to cause a fivefold increase in the percent weight loss due to oxidation by air.

Because of the long aging periods at 130 and 100 °C, a nitrogen environment could not be maintained inside the enclosed chambers. As a result, LN and DN effects at 130 and 100 °C could not be measured.

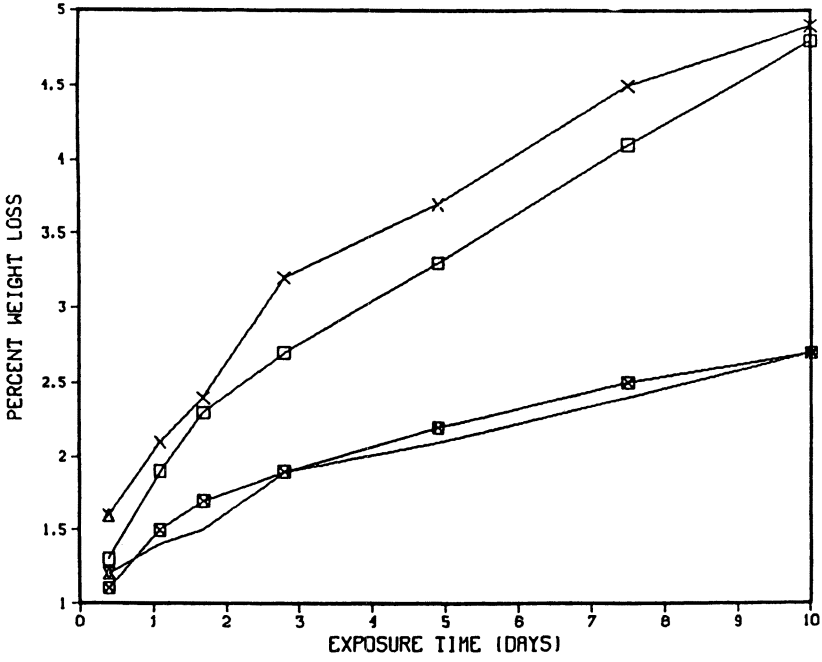

Figure 6. Percent weight loss vs. exposure time at 160 °C. Key: X, light oxygen; □, dark oxygen; ⊠, light nitrogen; XX, dark nitrogen.

Other studies have shown that in the thermal treatment of cellulose at temperatures below 300 °C, the rate of weight loss can be accelerated by oxidation reactions such as the degradation of cellulose by atmospheric oxygen. When cotton cellulose was heated at 190 °C for 50 h, carboxyl and carbonyl groups formed at a linear rate. When rates of glycosidic bond scission at 170 °C in nitrogen and in air were compared, the rate in nitrogen was close to one-half of the rate in air (*30*).

CRYSTALLINITY INDEX. The crystallinity indexes for specimens heated under each set of conditions (LO, DO, LN, and DN) at each temperature from the first exposure time (t_1) to the last or seventh exposure time (t_7) in hours at 190 °C and in days at 160, 130, 100 °C were not significantly different. The crystalline reference was untreated cloth, and the amorphous or least crystalline reference was a sample heated at 200 °C for 14 days. The 112 samples representing seven exposure times at each temperature for the four conditions were of intermediate crystallinity. By using this system, measurement of the crystallinity index did not reveal differences among samples that could be used to show changes in structural order with aging.

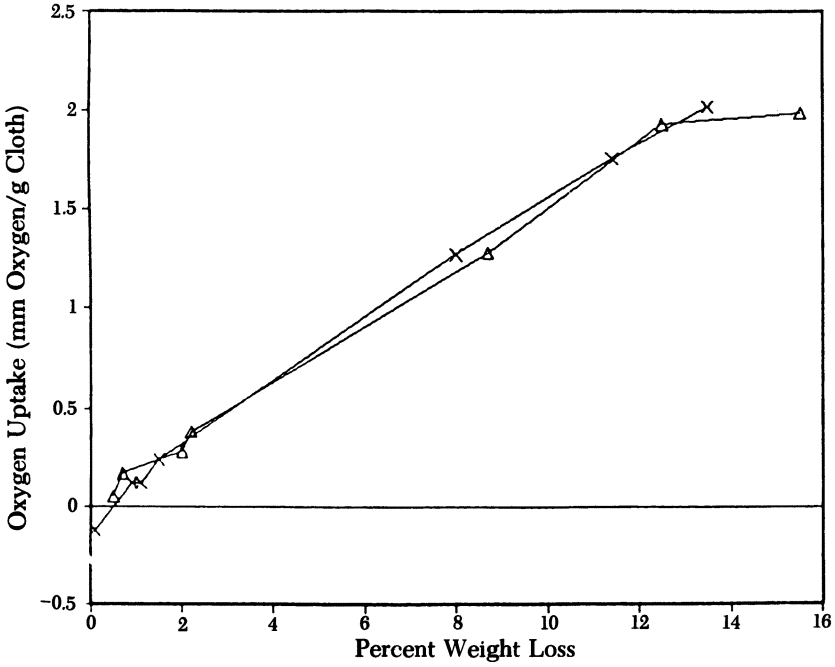

Figure 7. Oxygen uptake vs. percent weight loss at 190 °C. Key: △, light oxygen; X, dark oxygen.

Other researchers have evaluated the crystallinity index by using IR spectrophotometry. This method requires the KBr pellet technique of sampling. The X-ray diffraction method was investigated for its potential as a nondestructive technique for recording changes in cellulose as it ages.

TENSILE STRENGTH. Figures 8–11 show the decay of yarn tensile strength as exposure time increases at each aging temperature (190, 160, 130, and 100 °C) for warp yarns under light and dark conditions. No apparent difference was found in specimens heated in light or dark air at 190 and 160 °C or in light or darkness in nitrogen at 190 and 160 °C. The half-life at 190 °C in air is 2 h compared to about 8 h in nitrogen in Figure 8. The half-life at 160 °C in air is 14 h compared to 43 h in nitrogen in Figure 9.

At 130 °C in Figure 10, LO and DO lines diverge and converge within error limits and show no real difference in strength under light and dark conditions. At 100 °C, in Figure 11, even though LO and DO lines diverge, a light effect cannot be assumed because the extent of divergence of these lines is small. These slightly divergent lines may converge and even cross at exposure times beyond the 70 days monitored. Consequently, a light effect at 100 °C cannot be determined unequivocally, but neither can such an effect be discounted.

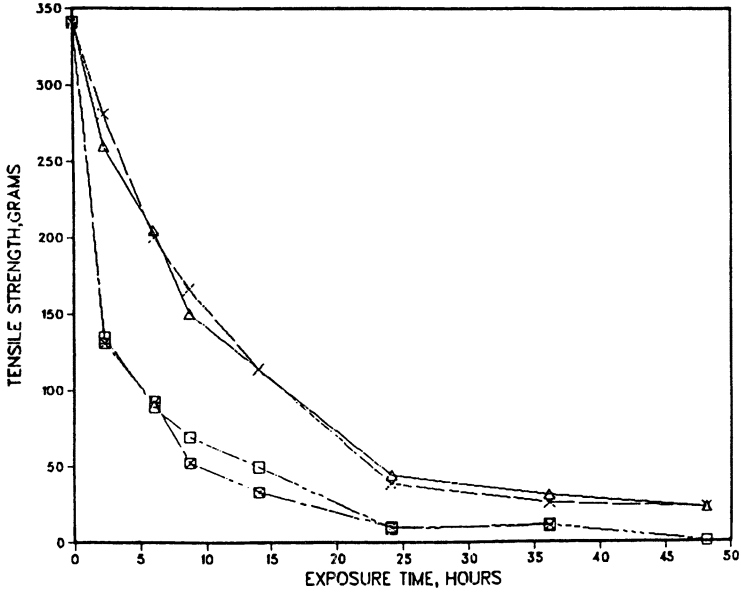

Figure 8. Tensile strength vs. exposure time at 190 °C for warp yarn. Key: △, dark nitrogen; ×, light nitrogen; □, dark oxygen; ⊠, light oxygen.

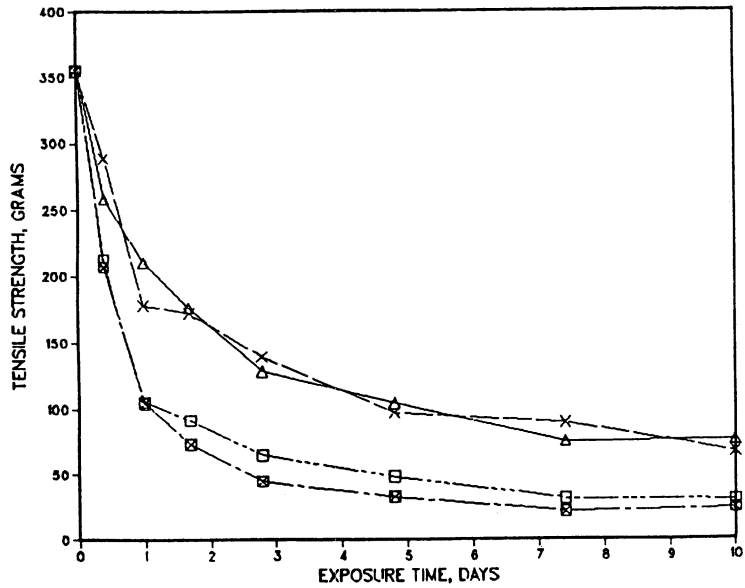

Figure 9. Tensile strength vs. exposure time at 160 °C for warp yarn. Key: △, dark nitrogen; ×, light nitrogen; □, dark oxygen; ⊠, light oxygen.

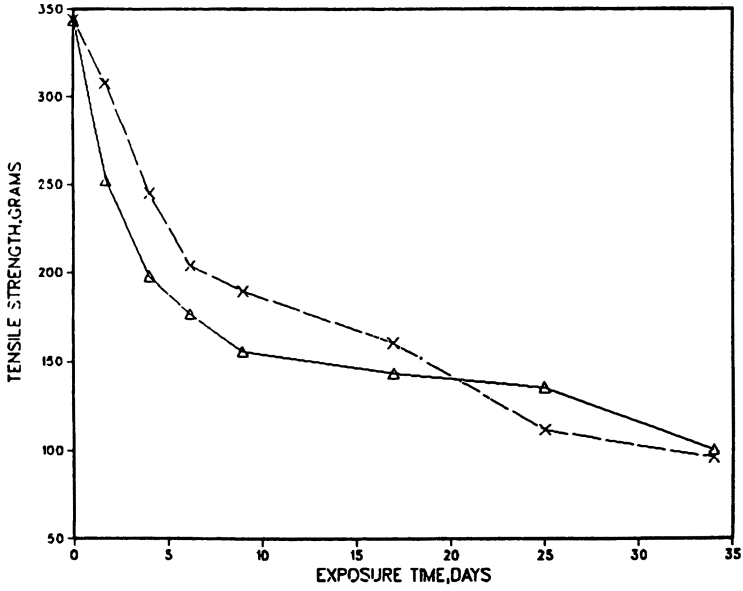

Figure 10. Tensile strength vs. exposure time at 130 °C for warp yarn. Key: △, dark oxygen; ×, light oxygen.

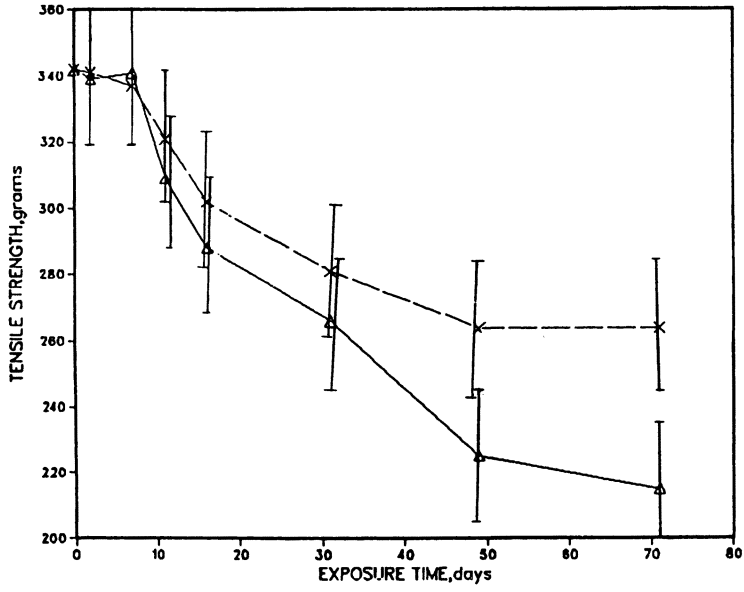

Figure 11. Tensile strength vs. exposure time at 100 °C for warp yarn. Key: △, light oxygen; ×, dark oxygen.

To compare the loss of tensile strength at each temperature, graphs of the percent tensile strength loss versus the number of half-lives were constructed from the LO and LN data in Table II. This treatment was used to normalize tensile strength differences resulting from aging. Coordinating the percent loss of tensile strength with the number of half-lives allowed comparisons of results at different temperatures and showed similar behavior among all temperatures within each half-life period.

PROPERTY KINETICS. To estimate the first-order rate constants for the exponential decay curves, the log plot of the original tensile strength divided by the tensile strength after treatment versus the exposure time was taken so the slope of the best straight line portion could be used in Figures 12–15. These log plots of tensile strength versus time show more than one linear portion from which rate constants can be obtained. Table III provides a summary of rate and half-life values for rates of degradation at 190, 160, 130, and 100 °C. Several considerations led to the choice of the rate portions from exposure times of 1 to 4 or 5 h or d at each temperature. These considerations are as follows: In Grassie's illustration, "Possible Stages of Oxidative History" in the oxygen update versus time plot for oxidative organic depolymerization reactions (*31*), kinetic data are evaluated from the maximum or steady state. At the maximum or steady state, the rate of reaction is slow enough to permit the measurement of the rate constant. A linear portion was taken from the experimental data of the log plots of tensile strength versus time and was used in comparison to this steady state stage of the overall reaction of degradation. From a consideration of the shape of the log forms of the decay curves, a rate degradation rate between time 1 (t_1) and time 4 (t_4) to time 5 (t_5) of aging was determined to be most representative of the particular steady state in the aging process. Correlation coefficients among these data points (t_1 to t_4 or t_5) from the plot of 2.303log (TS_0/TS) versus time were > 0.999. Time t_0 was not included in the estimation of the first-order rate constant. When it was included, LO and DO warp lines converged on the Arrhenius plot, whereas they did not converge when t_0 was excluded in Figure 16. Time t_0 may have been part of the inception stage of the reaction and as such would not be included in the steady state analysis.

Rate constants at 190, 160, 130, and 100 °C for the LO and DO degradation reactions were used to estimate the rate constants at 20 °C. The Arrhenius rate expression was applied with the plot of ln$k$ versus $1000/T(K^{-1})$. A linear relationship was obtained with a correlation coefficient > 0.999 in Figure 17 in which LO and DO are represented.

After obtaining rate constants at 20 °C for the degradation in light and darkness in the presence of oxygen, half-life determinations were made:

$$t_{1/2} = 0.693/k_1$$

Published on February 1, 1986 on http://pubs.acs.org | doi: 10.1021/ba-1986-0212.ch003

Table II. Warp Yarn Tensile Strength Loss During Artificial Aging

Sample	*Aging Time (days)*	*Half-life Period (days)*	*Aging Temp. (°C)*	*Aging Condition*	*Tensile Strength Loss (% of original)*
1	0.10	0.012	190	LO	61.0
				LN	20.7
	0.40	0.20	160	LO	41.0
				LN	22.8
	1.7	0.19	130	LO	18.6
	2.0	0.030	100	LO	0.58
2	0.25	0.032	190	LO	73.3
				LN	40.6
	1.0	0.50	160	LO	70.6
				LN	45.4
	4.0	0.44	130	LO	35.5
	7.0	0.11	100	LO	0.88
3	0.37	0.046	190	LO	82.0
				LN	53.7
	1.7	0.85	160	LO	76.8
				LN	51.0
	6.2	0.69	130	LO	44.5
	11.0	0.17	100	LO	7.9
4	0.59	0.075	190	LO	87.9
				LN	66.6

Published on February 1, 1986 on http://pubs.acs.org | doi: 10.1021/ba-1986-0212.ch003

	2.8	1.4	160	LO	84.6
				LN	62.3
	9.0	1.0	130	LO	49.7
	16.0	0.25	100	LO	13.7
5	1.0	0.13	190	LO	97.1
				LN	87.7
	4.8	2.4	160	LO	88.6
				LN	71.7
	17.0	1.9	130	LO	55.5
	31.0	0.48	100	LO	19.9
6	1.5	0.19	190	LO	96.8
				LN	91.6
	7.4	3.7	160	LO	92.6
				LN	76.8
	25.0	2.8	130	LO	64.0
	49.0	0.77	100	LO	28.4
7	2.0	0.25	190	LO	96.7
				LN	93.2
	10.0	5.1	160	LO	92.3
				LN	80.2
	34.0	3.8	130	LO	71.2
	71.0	1.1	100	LO	29.8

NOTE: The half-life periods were calculated from determinations of aging times in Table I. Tensile strength loss was not calculated under LN conditions at 130 and 100 °C because of the inability to contain a nitrogen environment over long exposure times.

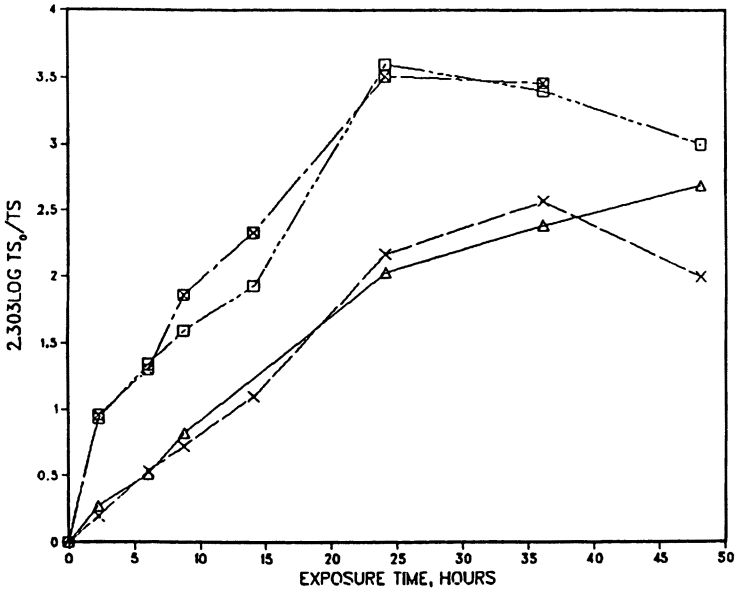

Figure 12. 2.303 log (TS_0/TS) vs. exposure time at 190 °C for warp yarn. Key: △, dark nitrogen; ×, light nitrogen; □ dark oxygen; ⊠ light oxygen.

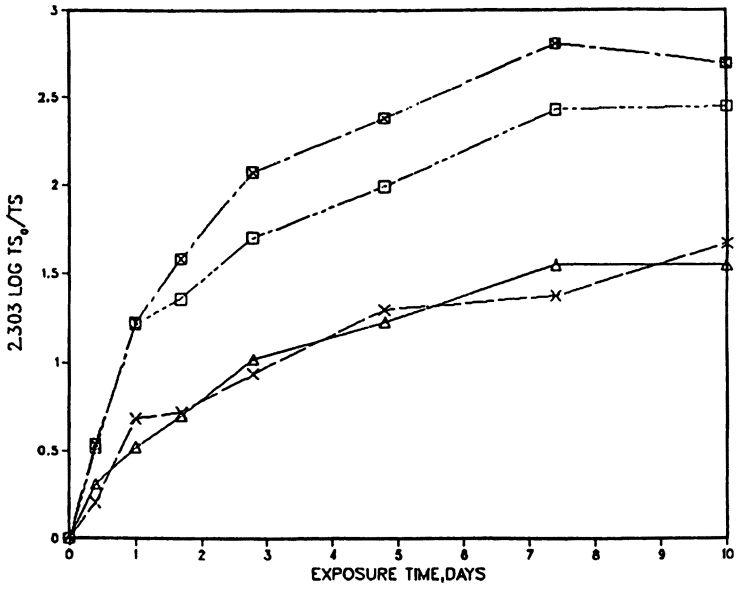

Figure 13. 2.303 log (TS_0/TS) vs. exposure time at 160 °C for warp yarn. Key: △, dark nitrogen; ×, light nitrogen; □ dark oxygen; ⊠ light oxygen.

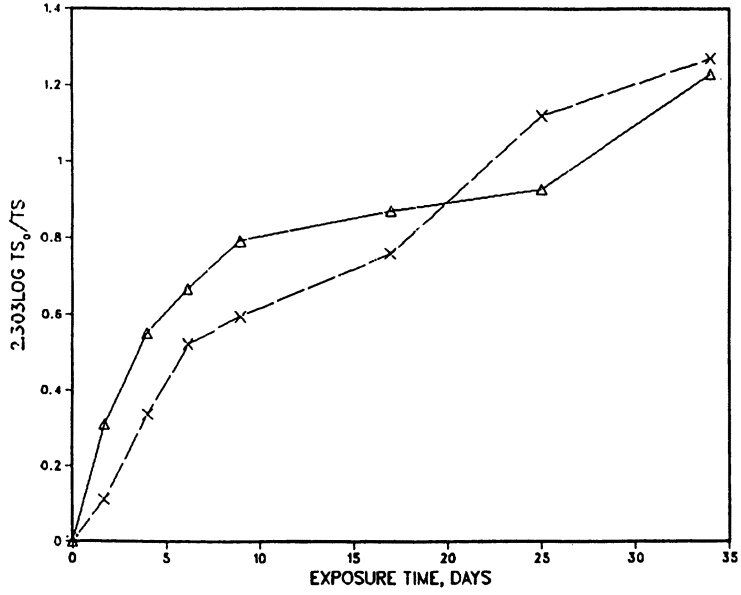

Figure 14. 2.303 log (TS_0/TS) vs. exposure time at 130 °C for warp yarn. Key: △, dark oxygen; ×, light oxygen.

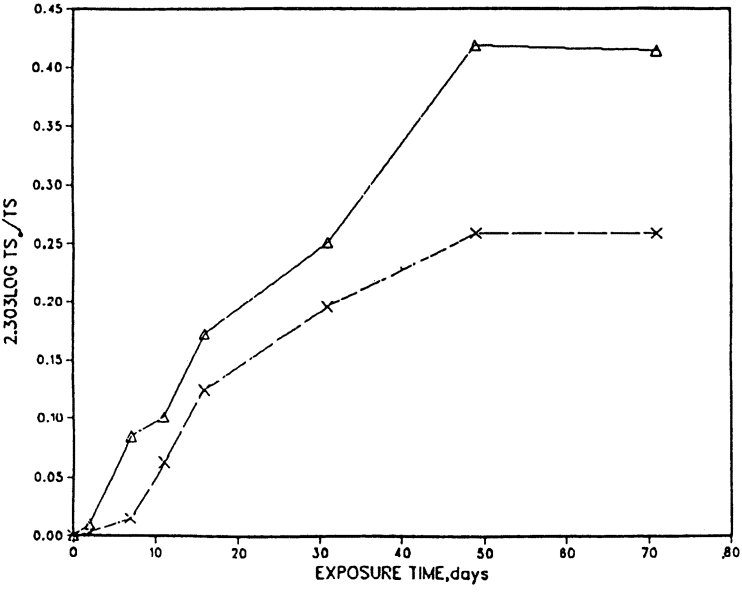

Figure 15. 2.303 log (TS_0/TS) vs. exposure time at 100 °C for warp yarn. Key: △, light oxygen; ×, dark oxygen.

Table III. Rate Constants (k_1) and Half-life Values ($t_{1/2}$) Calculated from Tensil Strength of Yarns Aged at 55% rh

Aging Temperature (°C)	*Aging Condition*	*Correlation Coefficient* (r)	k_1 *(days*$^{-1}$*)*	$t_{1/2}$ *(days)*
Warp				
190	DN	0.985	1.99	0.348
	LN	0.998	1.82	0.380
	DO	0.990	2.02	0.343
	LO	0.996	2.83	0.244
160	DN	0.999	0.289	2.40
	LN	0.897	0.269	2.58
	DO	0.926	0.447	1.55
	LO	0.972	0.607	1.14
130	DO	0.976	0.064	10.83
	LO	0.999	0.092	7.53
100	DO	0.975	0.0040	173
	LO	0.992	0.0061	114
Weft				
190	DN	0.999	2.64	0.26
	LN	0.987	2.62	0.27
	DO	0.994	2.66	0.26
	LO	0.979	2.38	0.29
160	DN	0.974	0.339	2.04
	LN	0.963	0.314	2.21
	DO	0.997	0.740	0.936
	LO	0.946	0.743	0.933
130	DO	0.975	0.093	10.75
	LO	0.948	0.073	9.49
100	DO	0.975	0.0052	133
	LO	0.998	0.0076	91

Arrhenius kinetic data at 20 °C (E_a, k_1, and $t_{1/2}$) are summarized in Table IV.

The half-life plot of tensile strength versus time used to evaluate degradation in museum textiles is found in Figure 18. The value of t_y is taken from Table V.

SCANNING ELECTRON PHOTOMICROSCOPY. At 190 and 160 °C, samples aged in nitrogen were significantly less yellowed and stronger than those aged in air. The distinctively different modes of fractures in fibers tested in the different environments are visually apparent in Figures 19-21 (*40*).

Comparison of photomicrographs of fibers aged at 190 °C and LO (Figure 20), 190 °C and LN (Figure 21), and unaged (Figure 19) shows definite and discrete differences in fine structure. In Figure 19, the cotton control is an open structure with a well-defined central canal and loosely fibrillated internal planes. In Figure 20, in the cotton fiber aged

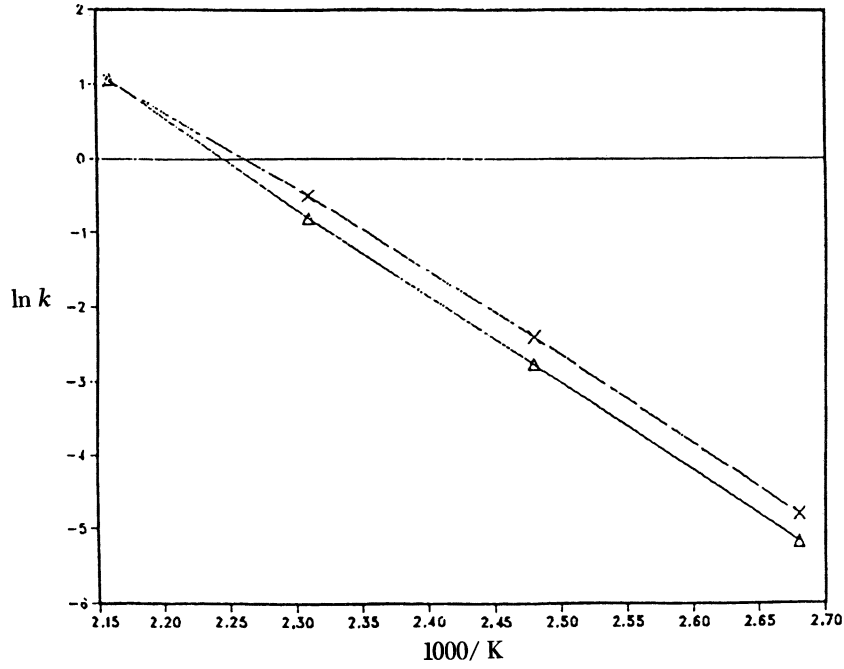

Figure 16. Arrhenius plot of ln k *vs. 1000/*T *(K) for warp yarn under conditions of DO and LO. Key:* △*, dark oxygen;* ×*, light oxygen.*

in air at 190 °C with light, a delamination of fibrillar planes and yet a foliatelike internal structure is apparent. In Figure 21, aging at 190 °C in nitrogen with light, internal planes appear to have fused to a more compact and closed structure. At 160 °C under light and nitrogen, fibers were partially fused but less compact and had a granular appearance at the fiber end. This observation suggests thermal cross-linking possibly through the OH and O groups in different cellulosic planes.

Conclusions

Yarn tensile strength is a macroscopic property that can be used to monitor degradation in cotton cloth. Although the results of degradation also include changes in other properties such as yellowness, oxygen uptake, and percent weight loss, these properties are not as good as yarn tensile strength at indicating degradation. The drawback, of course, to using yarn tensile strength is that a sample of 25 yarns taken from the weakest areas is then destroyed by the tensile test. This destruction may be a discouraging obstacle when applied to museum textiles.

Even though IR photography proved too insensitive for recording molecular components that form during the degradation process, the

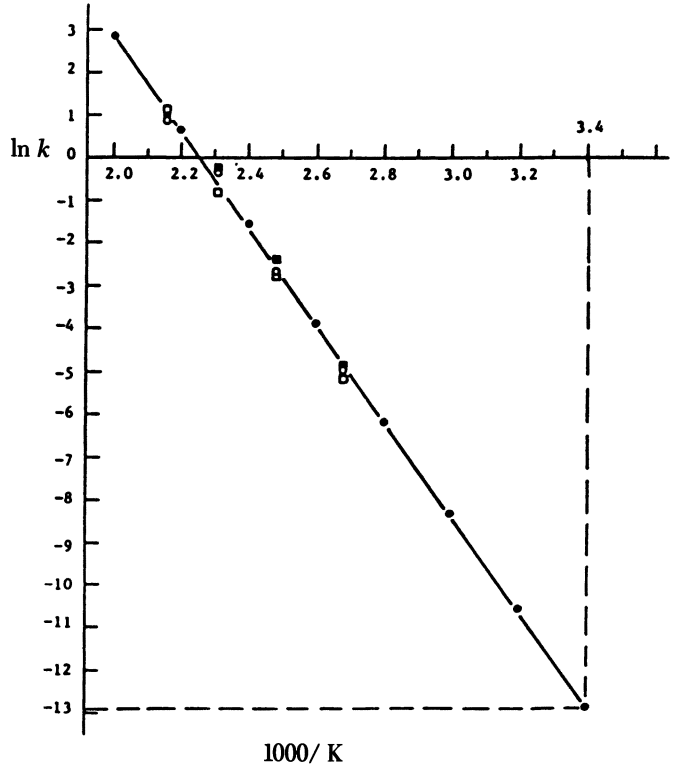

Figure 17. Arrhenius extrapolation of ln k *vs. 1000/*T *(K). Key:* ●, *light oxygen, warp;* ○, *light oxygen, weft;* ■, *dark oxygen, warp;* □, *dark oxygen, weft.*

theoretical validity for this use indicates the future possibility that with advances in modern technology, more sophisticated image enhancement in the near IR region under investigation may provide the method for quantifying the extent of degradation. Baer and Low reported that new analytical instrumental techniques based on computer-assisted image enhancement may hold wide acceptance for conservators (*32*). In the advent of these developments it may be possible to find the "magic ray" to monitor the surface to find the weakest areas upon which to prescribe care. If a method were found to quantify weakness while making correlation with tensile strength, the methodology developed here could be used nondestructively.

Although the yellowness index, oxygen uptake, and percent weight loss were not valid indicators for evaluating the extent of degradation at

Table IV. Linear Regressions: Extrapolations to 20 °C

T (°C)	$1/T(K^{-1})$	$k_{obs}(days^{-1})$	*ln* k	k^a_{calc} $(days^{-1})$	*Half-life*
		Warp Yarn, LO[b]			
190	0.00216	2.83	1.04	3.27	0.245 days
160	0.00231	0.607	−0.499	0.560	1.14 days
130	0.00248	0.092	−2.39	0.074	7.53 days
100	0.00268	0.0061	−5.10	0.007	114 days
20	0.00340	0.0000015	−13.44	0.0000013	1266 years
		Weft Yarn, LO[c]			
190	0.00216	2.38	0.867	2.94	0.291 days
160	0.00231	0.743	−0.297	0.539	0.933 days
130	0.00248	0.073	−2.62	0.077	9.49 days
100	0.00268	0.0076	−4.88	0.0080	91.1 days
20	0.00340	0.0000022	−13.00	0.0000020	863 years
		Warp Yarn, DO[d]			
190	0.00216	2.02	0.703	2.4	0.343 days
160	0.00231	0.447	−0.805	0.399	1.55 days
130	0.00248	0.064	−2.75	0.051	10.8 days
100	0.00268	0.0040	−5.52	0.0047	173 days
20	0.00340	0.0000009	−13.98	0.0000007	2110 years
		Weft Yarn, DO[e]			
190	0.00216	2.66	0.978	3.50	0.261 days
160	0.00231	0.740	−0.301	0.572	0.936 days
130	0.00248	0.093	−2.38	0.071	7.45 days
100	0.00268	0.0052	−5.26	0.0064	133 days
20	0.00340	0.0000011	−13.75	0.0000009	1726 years

NOTE: Extrapolations were done by using plots of ln k vs. $1/T$ in accordance with the Arrhenius equation, $\ln k = -E_a RT + I$.

[a] k_{calc} values were obtained by substituting E_a values calculated from the slopes of plots into the Arrhenius equation.

[b] $I = 26.65$, $-E_a/R = -11{,}790$, $r = 0.998$, and $E_a \pm$ t SE = 23,463 ± 2845 cal/mol (95% confidence).

[c] $I = 25.59$, $-E_a/R = -11{,}348$, $r = 0.996$, and $E_a \pm$ t SE = 22,583 ± 3764 cal/mol (95% confidence).

[d] $I = 26.73$, $-E_a/R = -11{,}972$, $r = 0.997$, and $E_a \pm$ t SE = 23,824 ± 3186 cal/mol (95% confidence).

[e] $I = 27.39$, $-E_a/R = -12{,}101$, $r = 0.994$, and $E_a \pm$ t SE = 24,083 ± 4713 cal/mol (95% confidence).

20 °C, correlations among these parameters helped elucidate the mechanisms of aging. After approximately 15 h of aging at 190 °C, these parameters show this distinctive kinetic behavior: The oxygen uptake and percent weight loss are autocatalytic when the oxygen uptake and rate are linear with time, and the yellowness index is autoretardant when the yellowing of the cotton fabric proceeds at a decreasing rate with aging. At 190 °C up to about 15 h, the contribution of oxygen to yellowing is apparently small. When enough oxygen is taken up by the cloth to catalyze further oxygen uptake, the rate of yellowing decreases. This

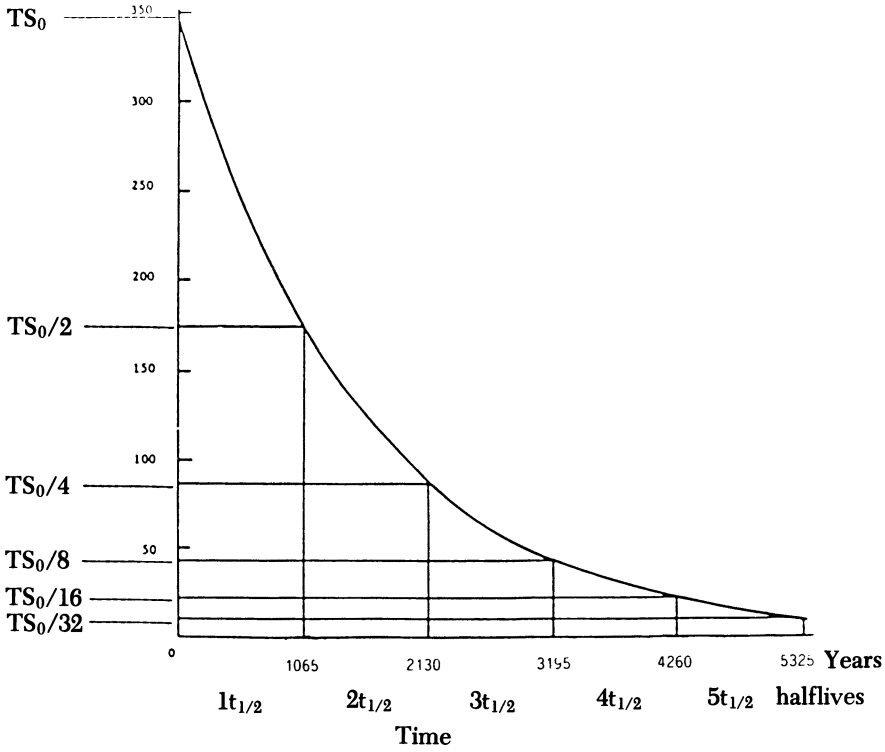

Figure 18. Half-life plot of tensile strength vs. time.

Table V. Summary of Activation Energies, Rate Constants (20 °C), and Half-lives (20 °C)

Yarn Type, Condition	$E_a \pm t$ *SE (cal/mol)*[a]	K *(day*$^{-1}$*)*	$t_{½}$ *(years)*
Warp, LO	22,463 ± 2845	1.5×10^{-6}	1266
Weft, LO	22,583 ± 3764	2.2×10^{-6}	863
Mean		1.9×10^{-6}	1065 ± 201
Warp, DO	23,824 ± 3186	0.9×10^{-6}	2110
Weft, DO	24,083 ± 4713	1.1×10^{-6}	1726
Mean		1.0×10^{-6}	1918 ± 192

[a] The average of the E_a values of all four samples is 23,486 ± 1312 cal/mol.

autocatalytic cellulose oxidation profile is typical of hydrocarbon oxidation behavior for which, at the induction stage, property values change slowly yet are detected before the maximum or steady state at which kinetics are applied at the onset of the faster autocatalysis rate. During the induction stage of deterioration, preservation treatment can be ap-

Figure 19. Scanning electron micrograph of an unheated cotton fiber (control) (8,320×).

plied to extend the time left. Beyond this point, a historic textile may not be viable as a museum artifact, that is, its condition may be so weakened that preservation treatment cannot be performed. Herandi found evidence of the inductive stage in studies of oxygen uptake by paper; the induction periods grew larger with lower aging temperatures: 190 °C, 1½ h; 160 °C, 2 h; and 130 °C, 9 h (*33*).

When cellulose is exposed to the unlimited supply of oxygen present as 21% of the air, unstable peroxide radicals form. In the autocatalytic reaction of cellulose oxidation, decomposition of peroxide forms cellulose radicals that react with oxygen to form $RO_2\cdot$ radicals. These radicals attack other cellulose molecules to form oxycelluloses (carbonyl, aldehyde, and carboxyl acid groups) along with more cellulose free radicals (*34*).

Heat catalyzes free radical formation in cellulose. Aldehydes form from C_2 and C_3 hydroxyls. Aldehydes oxidize to carboxyls, and with dehydration, carbon monoxide (CO) and carbon dioxide (CO_2) form as well as conjugated carbonyl-ethylenic chromophoric groups that selectively absorb blue light and impart yellowness (*35*). During the induction stage of cellulose oxidation, yellowness may increase steadily with selective carbonyl and ethylene group formation. By artificially aging

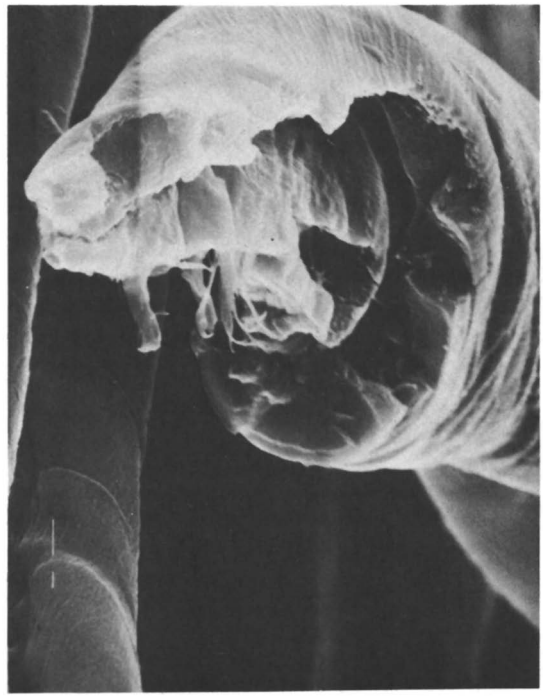

Figure 20. Scanning electron micrograph of a cotton fiber aged at 190 °C under conditions of LO (8,640×).

cotton cloth at 100 °C in air up to 20 days, appreciable carbonyl content has been found, but appreciably fewer carbonyl groups formed during heating in nitrogen (*36*). Twenty days of heat aging at 100 °C may fall within the inception stage for oxygen uptake for which the rate proceeds at a slow rate. In the present study 20 days of aging would represent only approximately a 1/3 half-life period. During the inception stage, enough oxygen must be taken up for carbonyl formation to contribute to yellowness, but as the reaction proceeds with carboxyl group formation and glucosidic scission with concomitant weight loss, the amount of yellowing and the rate of yellowing decline.

Although studies performed at an elevated temperature hold little validity for 20 °C predictions, this previous work may indicate a long induction time for the reaction of oxygen uptake at 100 °C. The findings of the present work showing percent weight loss at 190 and 160 °C, although autocatalytic and having a linear correlation and dependence upon oxygen uptake, hold little validity for 20 °C predictions. The longer inductive stages at the lowest temperatures may represent time periods when cotton cloth is stronger than at a later stage of degrada-

Figure 21. Scanning electron micrograph of a cotton fiber aged at 190 °C under conditions of LN (8,480×).

tion, even though it may be yellowing. To stop yellowness, treatment may involve preventing ketone and aldehyde groups from oxidizing to carboxyl groups. To cure yellowness, treatment may involve the use of reducing agents to convert these functional groups back to hydroxyl groups. The findings of this research suggest that after oxidation autocatalysis when carboxyl groups predominate, treatment may be at a high risk because of an appreciable loss of soluble monomeric residues. Currently, treatments are being prescribed for arresting, retarding, or reversing degradation. These prescriptions have been based on the results of aging studies under one isolated condition (*37*, *38*). Use of results of studies at one elevated temperature to make predictions at room temperature may lead to false predictions because the differences in the E_a values for the treatments that are being compared have to be considered. Even though aging experiments at 100 °C on alkaline buffered cotton cloth show decreases in carbonyl and carboxyl groups, this treatment may not be effective at 20 °C, and the long-term effects remain unknown (*39*).

A better way to make predictions for treatment at 20 °C than single-temperature aging studies is to study certain behavior over a temperature range of aging. In this study, the overall effects of aging as

monitored by the yarn tensile strength loss over time seem not to have changed from 190 to 100 °C as indicated by the linear relationship between ln k (ln of the rate constant at each temperature) versus $1/T$ (reciprocal of the absolute temperature for each rate constant). By linear regression of the straight line of ln k versus $1/T$ and the application of the Arrhenius rate expression, the contribution of ambient oxygen in light and darkness was found as well as E_a, the temperature sensitivity of the rate constant. At 20 °C no apparent difference in rate was seen between warp and weft for either LO or DO. However, the average rate constants of warp and weft may be significantly different for LO and DO; the average value for LO = 1.9×10^{-6}/day and that for DO = 1.0×10^{-6}/day. A light effect on the rate of degradation at room temperature may occur. The presence of light, regardless of intensity, imparts energy that may exceed the energy requirements for bond formation. The difference in half-lives, LO $t_{1/2}$ = 55.5% DO $t_{1/2}$, taken from the average values reported supports current awareness of benefits in exhibiting and storing textiles in the dark.

No apparent difference was found between warp and weft in E_a values for LO and DO. This finding indicated that the temperature sensitivities for these reactions may not be affected by the presence of light. Because E_a values (LO, DO) lie within percent error, 12.20% ($E_a \pm$ t SE) (t SE = standard error of the estimate) at the 95% confidence level, they were considered as one. E_a = 23,486 ± 1312 cal/mol.

The determination of E_a based strictly on the degradation of cellulose in textile form has practical significance. For E_a = 23,486 ± 1312 cal/mol, a 5 °C rise (20 to 25 °C) causes the new rate, k_2, to increase to 1.3 k_1. A 10 °C rise (20 to 30 °C) results in $k_2 = 1.8\ k_1$, and for a 20 °C rise, $k_2 = 3.1\ k_1$. For a 50 °C rise (20 to 70 °C) which may arise in photographing, $k_2 = 16.8\ k_1$.

The practical use of the proposed methodology to determine the extent of degradation is for comparative measurement of a historic cotton fabric's specific yarn tensile strength with that of a similar contemporary aged fabric used to formulate the half-life plot in Figure 17. This figure shows the exponential decay of strength with time and assigns real values for the condition age for cloth of a known tensile strength. The condition age of a historic cotton fabric indicates the difference between the measured value in years on the x-axis as determined from yarn tensile strength measurements positioned on the half-life decay curve and the end point in years on the x-axis of the half-life plot. This difference is the time left or the extent of degradation. An end point for degradation of 5325 years or 5 half-lives was assigned which, as seen in Figure 18, represents negligible strength. Textiles of this age, although viable in the sense that they may be exhibited in the nearly pulverized state, would not be subjected to any prescribed conservation regimen. This methodology has been designed

not only as a means of monitoring the effects of current conservation practice on the strength of a historic textile, but also as a system for establishing the effectiveness of a specific treatment for a specific condition age. These uses support the recognition among conservators that each historic textile receiving treatment must be considered individually.

When a historic textile is accepted for treatment, yarn tensile strength could be evaluated by cutting away samples from the weakest areas. Presumably this procedure would leave small open areas that then must be consolidated with support fabric. The weakest areas may be identified visually by using aids such as transmitted light, perhaps, or by some nondestructive method of detection. By positioning the yarn tensile strength value on the curve in Figure 18, the value for the half-life can be estimated. The difference between this value and the end point represents time the time left, a real value that may be influenced positively or negatively by treatment. After treatment, tensile strength measurements may position the textile at a new place on the half-life axis if the time left has been extended or shortened by treatment.

Many aspects of this research will be pursued in future work. Half-life boundaries will be well defined so that "risk ratings" may be given to historic cloth before specific conservation treatment is performed. Through the use of this methodology, prediction of the effects of the most commonly accepted treatments for specific textile degradation states may be possible so that only initial tensile strength testing may be necessary.

As an extension of this research, the appropriateness and effectiveness of those treatments designed to actually change half-life (deacidification, consolidation, and selective functional group reduction) will be evaluated.

Acknowledgments

R.D. Weizel, Principal Scientific Research Lab Machinist, University of Minnesota, is responsible for the aging chambers and invented the Jan-Barr. We are grateful for his work in designing new chambers that hold a nitrogen environment over the prolonged aging times at the lower temperatures.

This research was supported by a University of Minnesota Foundation Doctoral Dissertation Grant and by Sigma Xi, The Scientific Research Society.

Literature Cited

1. Pellicori, S.; Evans, M. S. *Archaeology* 1981. *34*, 34–43.
2. Gilbert, R. Jr; Gilbert, M. M. *Appl. Opt.* 1980, *19* (*12*), 1930.
3. Accetta, J. S.; Baumgart, J. S. *Appl. Opt.* 1980, *19* (*12*), 1921.

4. Pellicori, S. F.; *Appl. Opt.* **1980**, *19* (*12*), 1913.
5. Pellicori, S. F.; Chandos, R. A. *Ind. Res. Dev.* **1981**, 186-9.
6. Berry, G. M.; Hersh, S. P.; Tucker, P. A.; Kerr, N.; McElwain, D. M. "Properties of Some Archaelogical Textiles"; presented at the 5th Triennial Meet. Proc. ICOM Comm. Conserv., Zagreb, 1978.
7. Berry, G. M.; Hersh, S. P.; Tucker, P. A., Walsh, W. K. In "Preservation of Paper and Textiles of Historic and Artistic Value"; Williams, J. C., Ed.; ADVANCES IN CHEMISTRY SERIES No. 164; American Chemical Society: Washington, D.C., 1977; p. 228.
8. Kerr, N.; Hersh, S. P.; Tucker, P. A.; Berry, G. M. In "Durability of Macromolecular Materials"; Eby, R. K., Ed; ACS SYMPOSIUM SERIES No. 95; American Chemical Society: Washington, D.C., 1979; p. 357.
9. Kerr, N.; Hersh, S. P.; Tucker, P. A. *Proc. Sci. Technol. Serv. Conserv.* **1982**, 100.
10. Berry, G. M.; Hersh, S. P.; Tucker, P. A.; Walsh, W. K. In "Preservation of Paper and Textiles of Historic and Artistic Value"; Williams, J. C., Ed.; ADVANCES IN CHEMISTRY SERIES No. 164, American Chemical Society: Washington, D.C., 1977; p. 249.
11. Arney, J. S.; Chapdelaine, A. H. In "Preservation of Paper and Textiles of Historic and Artistic Value II; Williams, J. C., Ed.; ADVANCES IN CHEMISTRY SERIES No. 193, American Chemical Society: Washington, D.C., 1981; p. 189.
12. Finch, K. *Proc. Conserv. Restoration Text.* **1980**, 82.
13. Juve, A. E.; Schock, M. G., Jr. *ASTM Bull. No. 195.* **1954**, *54.*
14. Doyle, C. P. *Mod. Plast.* **1956**, *33*, 143.
15. Steiger, J. H. *Am. Dyest. Rep.* **1958**, *47*, (*9*), 287.
16. Gray, G. G. In "Preservation of Paper and Textiles of Historic and Artistic Value"; Williams, J. C., Ed.; ADVANCES IN CHEMISTRY SERIES No. 164; American Chemical Society: Washington, D.C., 1977; p. 286.
17. Baer, N. S.; Indictor, N. In "Preservation of Paper and Textiles of Historic and Artistic Value"; Williams, J. C., Ed.; ADVANCES IN CHEMISTRY SERIES No. 164; American Chemical Society: Washington, D.C., 1977; p. 336.
18. Arney, J. S.; Jacobs, A. J.; Newman, R. *J. Am. Inst. Conserv.* **1980**, *18*, 34.
19. Arney, J. S.; Jacobs, A. J. *Tappi* **1980**, 63, 71.
20. Arney, J. S.; Jacobs, A. J., *Tappi* **1980**, 62, 89.
21. Lambert, J. B.; Shurveil, H. F.; Verbit, L.; Cooks, R. G.; Stout, G. H. In "Organic Structural Analysis"; MacMillan Publishing Co: New York, 1976, p. 156.
22. Berry, G. M.; Hersh, S. P.; Tucker, P. A.; Walsh, W. K. In "Preservation of Paper and Textiles of Historic and Artistic Value"; Williams, J. C., Ed.; ADVANCES IN CHEMISTRY SERIES No. 164; American Chemical Society: Washington, D.C., 1977; 234.
23. Chatterjee, P. K; Conrad, Carl M. *Text. Res. J.* **1966**, 36, 487.
24. Bahn, G. S. *1969 WSS/CI* 69-28, *Chem. Abstr.* 1967-1970, 72, 102023.
25. Shafrizadeh, F.; Bradbury, A. G. W. *J. Appl. Polym. Sci.* **1979**, *23*, 1436.
26. Berry, G. M.; Hersh, S. P.; Tucker, P. H.; Walsh, W. K. In "Preservation of Paper and Textiles of Historic and Artistic Value"; Williams, J. C., Ed.; ADVANCES IN CHEMISTRY SERIES No. 164; American Chemical Society: Washington, D.C., 1977; p. 235.
27. Billmeyer, F. W.; Saltzman, M. "Principles of Color Technology"; Wiley: New York, 1966; p. 51.
28. Hebeish, A.; El-Aref, A. T.; El-Alfli, A.; El-Rafie, M. H. *J. Appl. Polym. Sci.* **1979**, *23*, 453.

29. Feller, R. J. In "Preservation of Paper and Textiles of Historic Value"; Williams, J. C., Ed.; ADVANCES IN CHEMISTRY SERIES No. 164; American Chemical Society: Washington, D.C., 1977; p. 314.
30. Shafrizadeh, F.; Bradbury, A. G. W. *J. Appl. Polym. Sci.* **1979**, *23*, 1436.
31. Grassie, N. "Chemistry of High Polymer Degradation Processes"; Interscience: New York, 1956; p. 201.
32. Baer, N. S.; Low, M. J. D. *Proc. Sci. Technol. Serv. Conserv.* **1982**; 4.
33. Hernadi, S. *Sven. Papperstidn.* **1976**, *79*, 418–423.
34. Shafizadeh, F.; Bradbury, A. G. W. *J. Appl. Polym. Sci.* **1979** 23, 1441.
35. Bikales, N. M.; Segal, L., Eds.; "Cellulose and Cellulose Derivatives." Interscience: New York, 1971; Vol. 5, p. 1037.
36. Kerr, N.; Hersh, S. P.; Tucker P. A. *Proc. Sci. Technol. Serv. Conserv.* **1982**, 102.
37. Hackney, S. J.; Hedley, C. A. *Proc. Sci. Technol. Serv. Conserv.* **1982**, 151.
38. Block, I. *J. Am. Inst. Conserv.* **1982**, *22*, 25.
39. Kerr, N.; Hersh, S. P.; Tucker, P. A. *Proc. Sci. Technol. Serv. Conserv.* **1982**, 100.
40. Cardamone, J. M. and Whitmoyer, R. E. *Ohio Rep.* **1984**, *69*, 45–47.

RECEIVED for review November 26, 1984. ACCEPTED March 15, 1985.

4

Studying the Cause and Type of Fiber Damage in Textile Materials by Scanning Electron Microscopy

S. H. Zeronian, K. W. Alger, M. S. Ellison[1], and S. M. Al-Khayatt[2]
Division of Textiles and Clothing, University of California, Davis, CA 95616

Scanning electron microscope use to assist in diagnosing the cause of fabric wear or failure by mechanical means is considered. The types of fiber failure discussed are those induced by tensile, twist, and flex stresses and by wear during use. Cotton, wool, and polyester fibers are used to illustrate the discussion.

SCANNING ELECTRON MICROSCOPES (SEM) became available commercially in the 1960s. Since then, several studies on fiber fractography have provided a much better understanding of the type of fiber damage caused either by different forms of mechanical stress (for example, tensile, fatigue, and abrasion) or by degradation due to such factors as light exposure, insects, heat, and chemical reagents.

Only small amounts of sample are required for examination by SEM. Thus, this technique can be used to obtain valuable information that can be of use when characterizing fabrics to determine how they should be conserved or when attempting to elucidate the cause of the damage for historical purposes. The purpose of this chapter then is to describe the potential use of the SEM in such activities. Discussion will be limited to mechanical stress damage. Comparisons are made when possible between fibers damaged in actual use and those fractured under controlled laboratory conditions. Examples are selected from work we have done in our laboratories on some commonly used fibers namely cotton, polyester, and wool. Reports on light (*1*) and insect (*2*) damage can be found elsewhere.

[1]Current address: School of Textiles, Clemson University, Clemson, SC 29631.
[2]Current address: Department of Mechanical Engineering, University of Baghdad, Baghdad, Iraq.

0065-2393/86/0212-0077 $06.00/0

Experimental

For microscopy, fabric samples (0.5 × 0.5 cm) were mounted on standard specimen stubs with silver paint (T. Pella Co.). The stubs were then placed on a rotating, tilting platform in a sputter coater and coated with gold. Observations were made with an International Scientific Instruments model DS130 microscope operating in the secondary mode at an accelerating voltage of 10 kV. The fractured surfaces of fibers were prepared for examination in the following manner: A metal wire, approximately 2 mm in diameter, was fixed to the specimen stub with silver paint. Fibers were mounted on the stub with their fractured ends projecting 2–3 mm beyond the wire. They were secured to the wire by silver paint before coating.

Results and Discussion

In laboratory studies, fibers are fractured under controlled conditions. Thus, such studies are useful when attempting to diagnose the cause of damage present in used textiles. Hearle et al. have done extensive studies on fiber fracture. They have presented a classification consisting of six types of fiber failure that occur in laboratory tensile tests (*3*). With respect to this discussion, Types 2, 3, 5, and 6 are relevant.

Type 2 is ductile crack propagation with the crack opening to form a V-notch. Finally, the crack becomes catastrophic. It is found in nylon and other melt-spun synthetics. Classical illustrations of this type are readily available (*3*, *4*). However, variations can occur. Figures 1a and 1b show a polyester fiber subjected to tensile stress in which, after the V-notch formed, failure continued along a plane parallel to the fiber axis before eventually crossing the fiber. Thus, a split-level transverse break had occurred.

Type 3 occurs at high rates of testing when the fracture surface of fibers such as nylon changes to a mushroom shape (*3*).

Type 5 takes place when transverse discontinuities are present between structural units of the fiber and are sufficient to stop direct crack propagation. Breaks then occur with a granular surface roughly perpendicular to the fiber axis, as shown in our example of wool-fiber tensile failure (Figure 2). Once again, split-level transverse breaks are possible (*5*).

Type 6 happens in wet cotton fibers. In air-dried cotton fibers, tensile failure starts when fibrils split apart. The break generally occurs adjacent to a reversal, and the splitting is caused by untwisting effects. Finally, a tear develops along the fiber and joins up the split which follows the helical path of the fibrils around the fiber (Figures 3a and 3b). In wet cotton, a weaker attraction exists between fibrils, and the break appears as a gradually thinning out due to separate breaks. In completely dry or cross-linked cottons, the fracture runs across the fiber

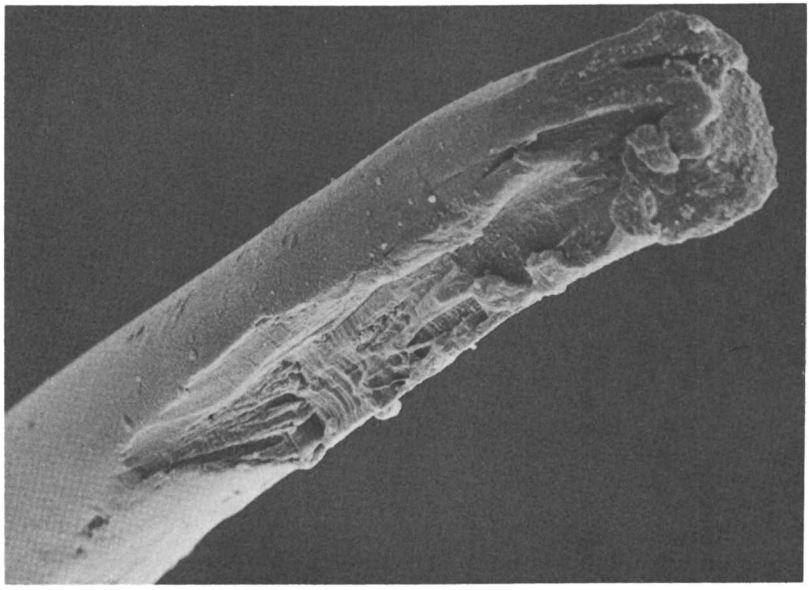

Figure 1a. Tensile fracture of a polyester type 54 fiber taken from a heat-set polyester fabric. Sample was fractured at 65% rh and 21 °C (2,665×).

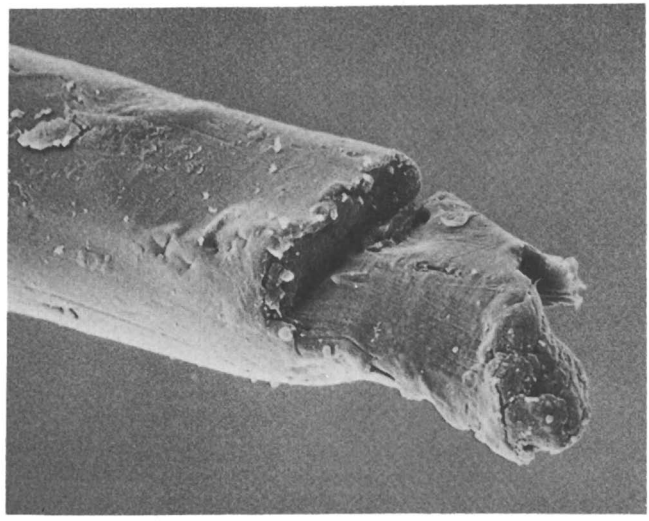

Figure 1b. Counterpart fracture of fiber shown in Figure 1a (2,600×).

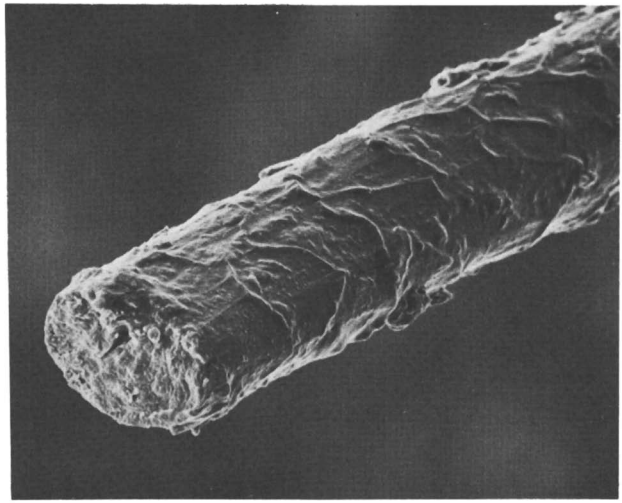

Figure 2. Tensile fracture of a wool fiber taken from a scoured worsted yarn. Sample was fractured at 65% rh and 21 °C (565×).

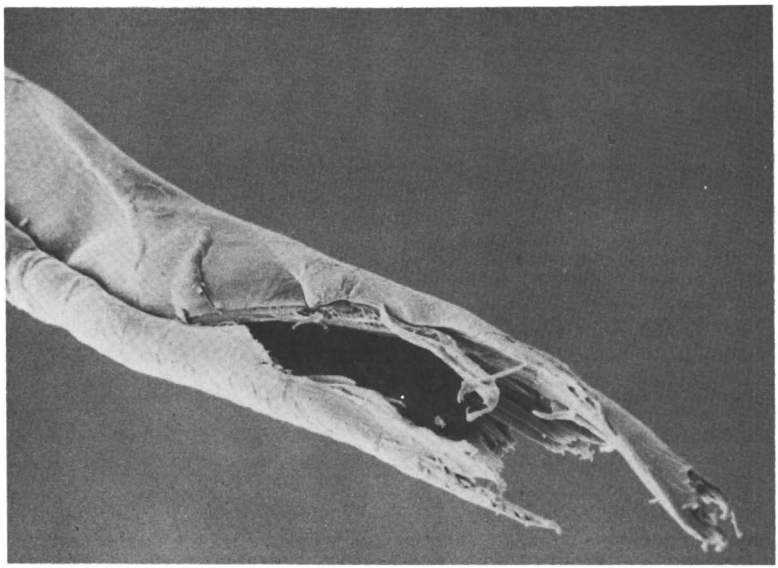

Figure 3a. Tensile fracture of a scoured Deltapine-Smoothleaf cotton fiber. Sample was fractured at 65% rh and 21 °C (1365×).

Figure 3b. Counterpart fracture of fiber shown in Figure 3a (1300×).

and little splitting occurs (*6*, *7*), that is, it is a Type 5 fracture. The studies of Hearle et al. (*6*, *7*) have demonstrated the effect of test conditions and the presence of finishes on fiber fracture. Again, even if all the test conditions are the same, and ostensibly the same fibers are being tested, identical breaks will not be obtained each time. This result is especially true for natural fibers such as cotton which are nonuniform.

Types 1 and 4 tensile failures, which are of less interest to conservationists at this time, are caused by brittle crack propagation and by long axial splits, respectively. Such fractures can occur in ceramic and elastomeric fibers (both Type 1) and highly oriented aramids (Type 4).

Many times under normal end-use conditions, tensile stress will not be the cause of fiber failure. Thus, the effect of stresses other than tensile stress are studied in laboratories. One form of single-fiber testing consists of subjecting the fibers to twisting and measuring the twist at rupture. From the number of turns to rupture, the breaking twist angle (BTA) can be calculated. The BTA gives an indication of the shear behavior of fibers. The fracture morphology of fibers subjected to this test generally appears to have some similarities to that of the same fibers ruptured by tensile tests. However, the presence of a skin-core structure shows up more clearly on the BTA-tested fibers. Thus, the cuticle of the BTA-tested wool fiber is torn off in parts (cf. Figures 2 and 4), and the presence of a skin is seen more clearly on the BTA-tested polyester than

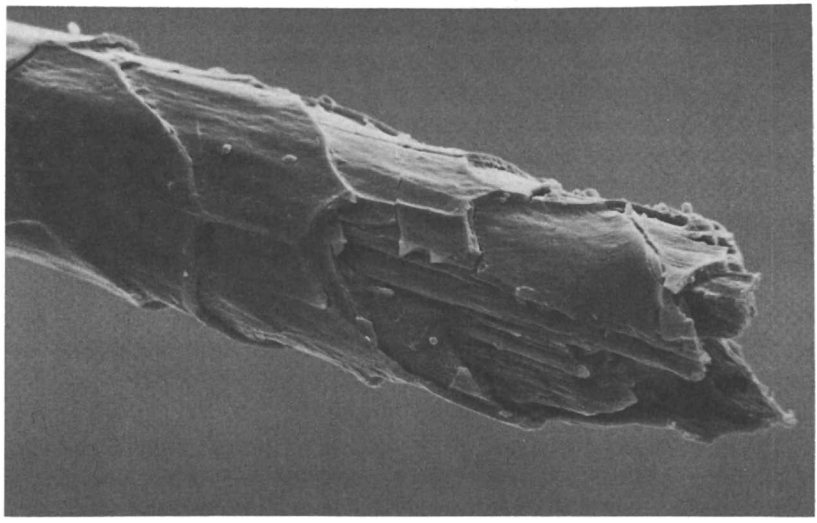

Figure 4. Breaking twist angle fracture of a wool fiber of similar type to that of Figure 2. Sample was fractured at 65% rh and 21 °C (1235×).

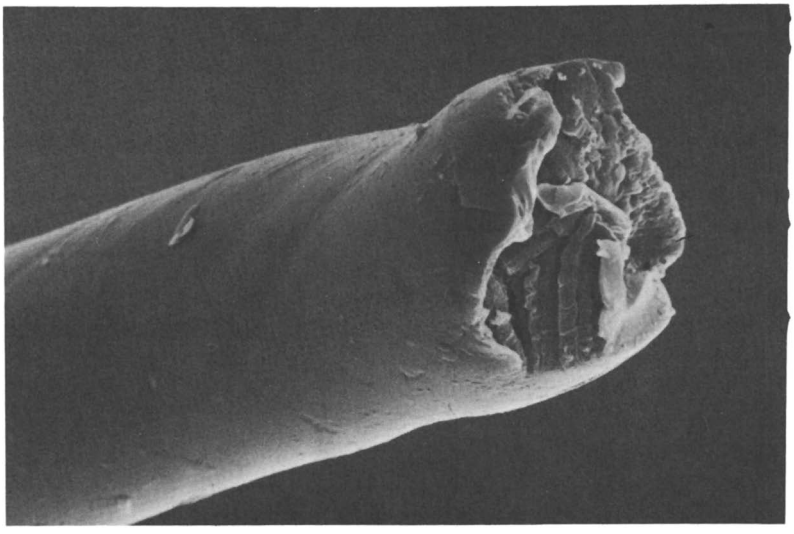

Figure 5. Breaking twist angle fracture of a polyester fiber of similar type to that of Figure 1. Sample was fractured at 65% rh and 21 °C (2275×).

on the tensile-tested counterpart (cf. Figures 1 and 5). A skin is not observed on the cotton fiber. Tearing apart of the fibrils appears to have occurred more often during the stressing of BTA-tested cotton fibers than during the stressing of tensile-tested fibers (cf. Figures 3 and 6).

Single-fiber flex fatiguing is studied also. Researchers have sug-

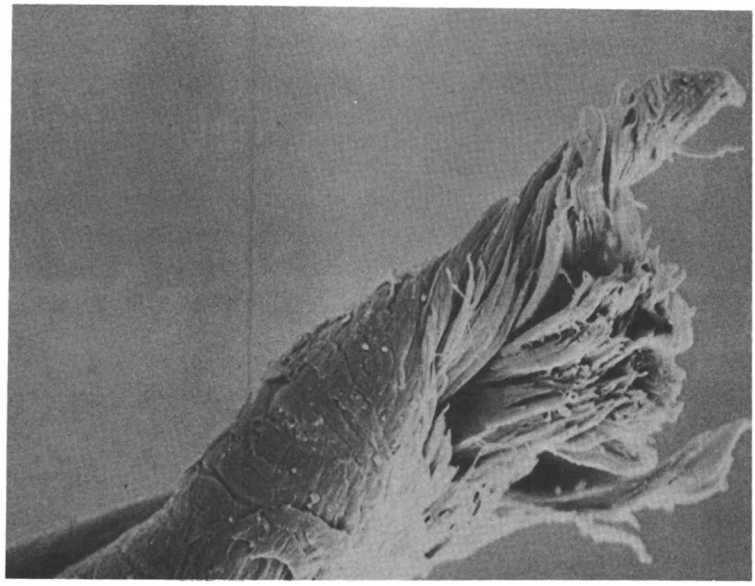

Figure 6. Breaking twist angle fracture of a cotton fiber of similar type to that of Figure 3. Sample was fractured at 65% rh and 21 °C (2665×).

gested that cyclic-bending fatigue is important in the context of abraded fabric failure (*8*). Different types of laboratory single-fiber flex testers appear to fracture fibers differently (*8, 9*). Hearle et al. (*3, 9*) claim that biaxial-rotation tests simulate the forms of fiber fracture that are found in used shirts, trousers, and socks. With our instrument the resistance of fibers to cyclic 180° bending is measured. The fiber is wrapped around a fine wire as mandrel. On its inner radius, the fiber is alternatively compressed and relaxed, while on its outer radius, it is alternatively extended and relaxed. In cotton, failure appears to occur with the fracture running roughly perpendicular to the fiber axis on one side; on the other side failure results in an extended tongue (Figure 7a and 7b). For wool, failure takes place after multiple axial splitting has occurred (Figure 8). In polyester, the fiber splits into larger units (Figure 9). Abrasion damage can be observed on the inner radius of all the fibers where they were in contact with the mandrel (Figures 7a, 8, and 9).

In addition to resins, a number of factors such as aging and exposure to high-energy radiation and sunlight may increase the brittleness of a fiber. If the brittleness increases before the fiber is subjected to physical testing, its fracture morphology may be affected. We have discussed the effect of high-energy radiation and sunlight on nylon 6 elsewhere (*4, 10*). Treatments such as mercerization can affect fracture morphology also (*6–9*).

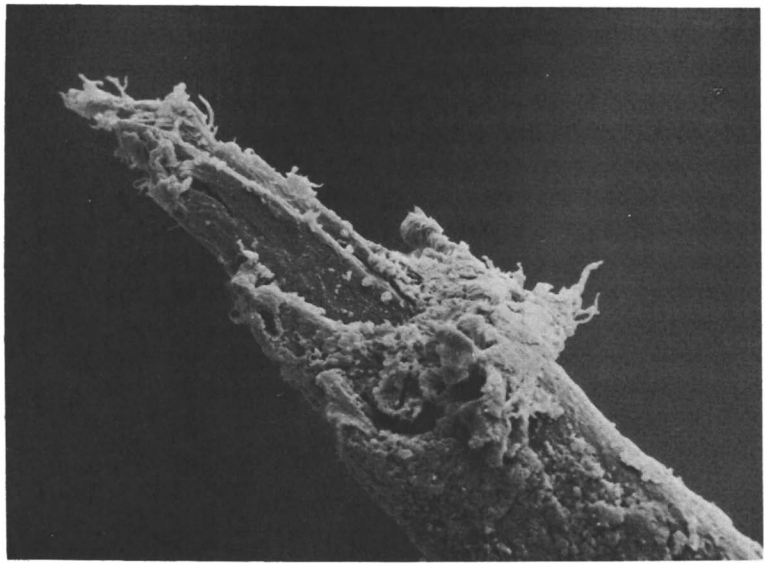

Figure 7a. Fracture by flex fatigue of a cotton fiber of similar type to that of Figure 3. Sample was fractured at 65% rh and 21 °C (1365×).

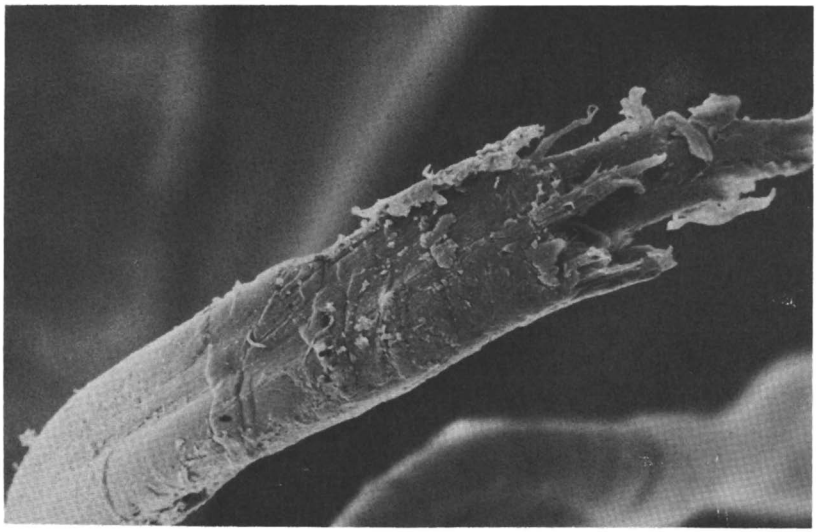

Figure 7b. Another example of a flexural fatigue fracture of cotton (1105×).

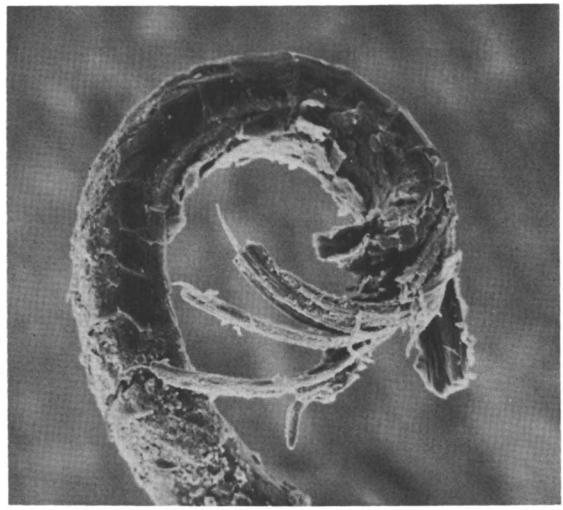

Figure 8. Fracture by flex fatigue of a wool fiber of similar type to that of Figure 2. Sample was fractured at 65% rh and 21 °C (442×).

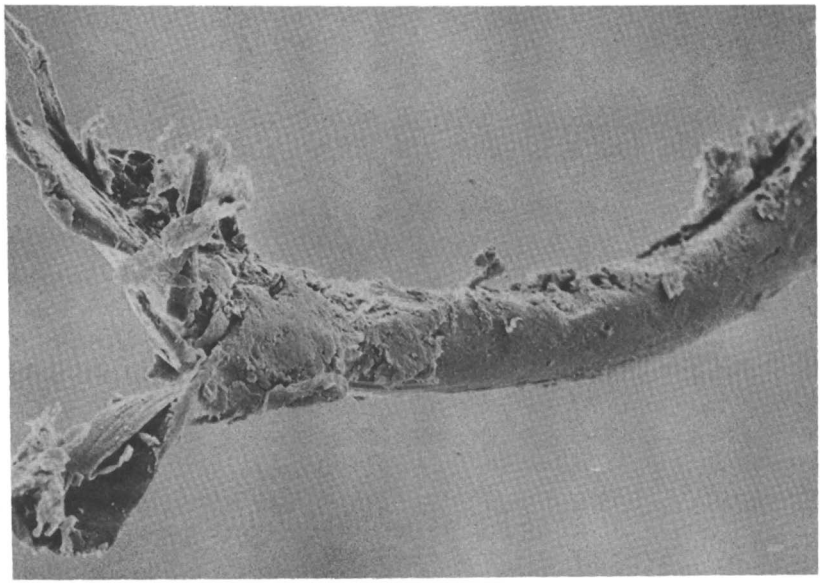

Figure 9. Fracture by flex fatigue of a polyester fiber of similar type to that of Figure 1. Sample was fractured at 65% rh and 21 °C (845×).

Apparel is susceptible to damage during cleaning as well as when in actual use. Goynes and Rollins (*11*) studied untreated and chemically modified cotton fabrics that had been laboratory abraded by machine washing (wet abrasion) and tumble drying (dry abrasion). They reported that generally abrasion patterns were not different from those normally associated with any wet or dry abrasion. Wet fibers, gray or cross-linked, were found to splinter or fibrillate on abrasion, but the fibrillation of cross-linked fibers occurred more in sheets of fibrils than in small bundles characteristic of gray fibers. Gray or cross-linked dry fibers cracked or broke on abrasion. A slight amount of peeling of fibrillar sheets occurred in dry gray fibers, also. The effect of prolonged drying on untreated cotton fibers was to convert their interfibrillar bonding character to one similar to that of cross-linked fibers.

With relatively minor variations, many types of fiber including cotton, wool, polyester, nylon, and acrylic break down in a similar manner when subjected to wear (*9*). Characteristic features for changes in wool fibers during fabric wear consist of cuticular damage (Figure 10a), fibrillated fibers (Figure 10b), fibrillated fiber ends (Figure 10c), and rounded fiber ends (Figure 10d) (*12*). Transversely fractured fiber ends are also observed (Figure 10e). They may have been ruptured by tensile stress (cf. Figures 4 and 10e). The effect of chemical treatments

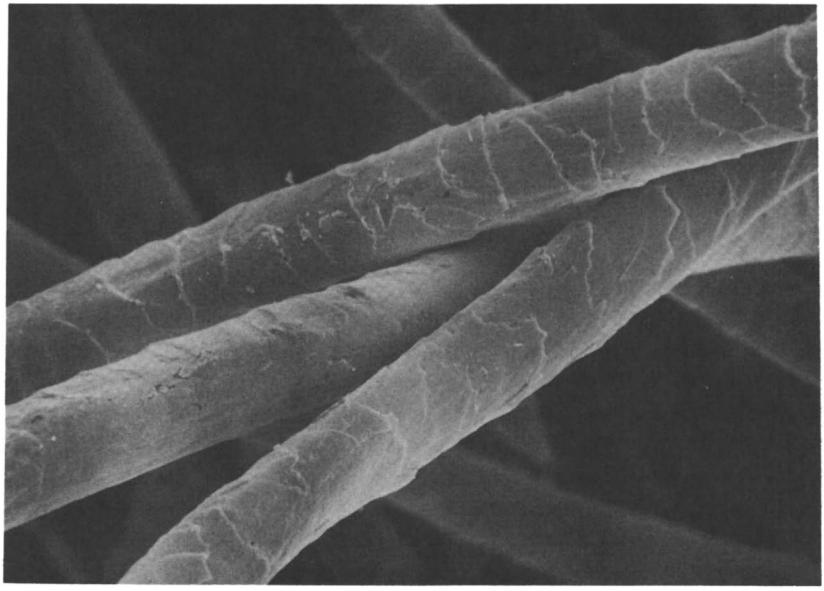

Figure 10a. Fibers present in a worn portion of a wool sock (650×).

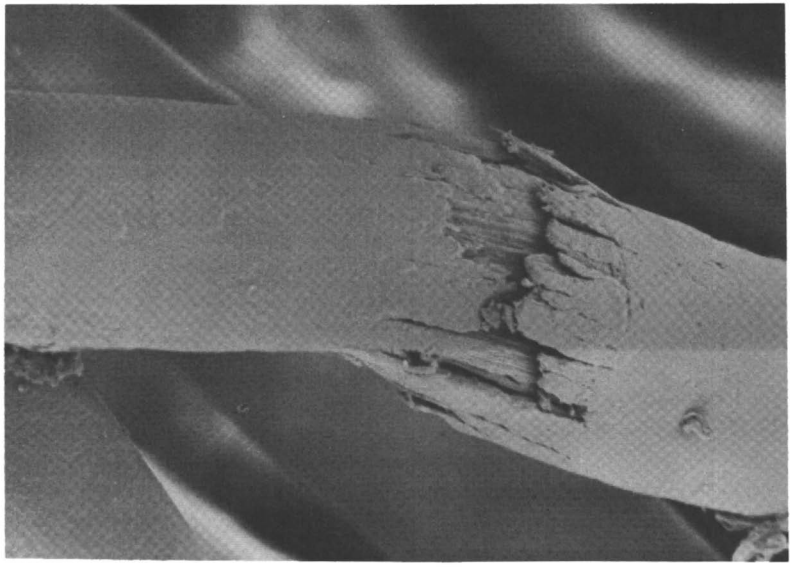

Figure 10b. Fibers present in a worn portion of a wool sock (1300×).

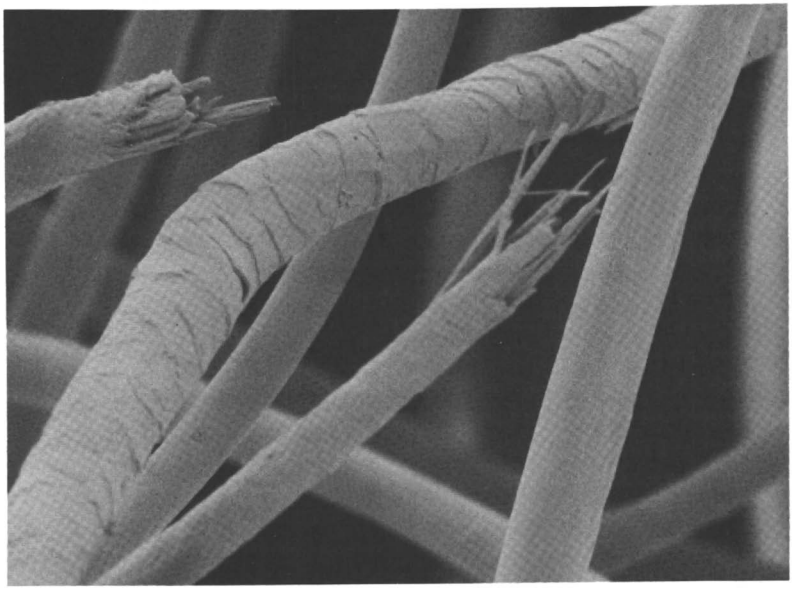

Figure 10c. Fibers present in a worn portion of a wool sock (520×).

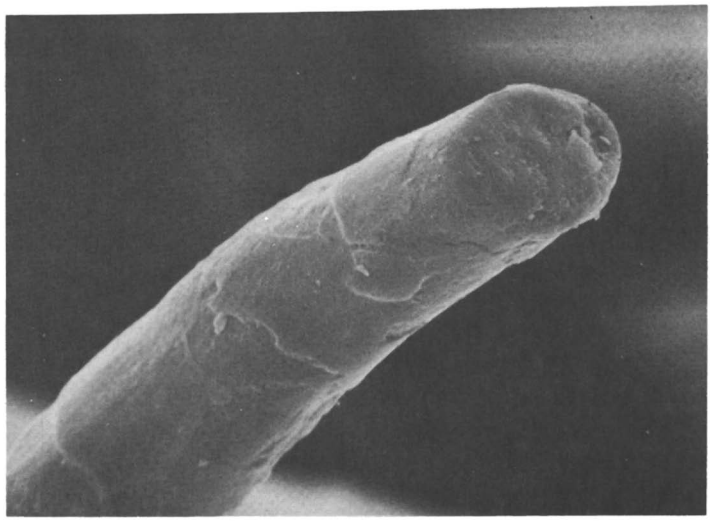

Figure 10d. Fibers present in a worn portion of a wool sock (2015×).

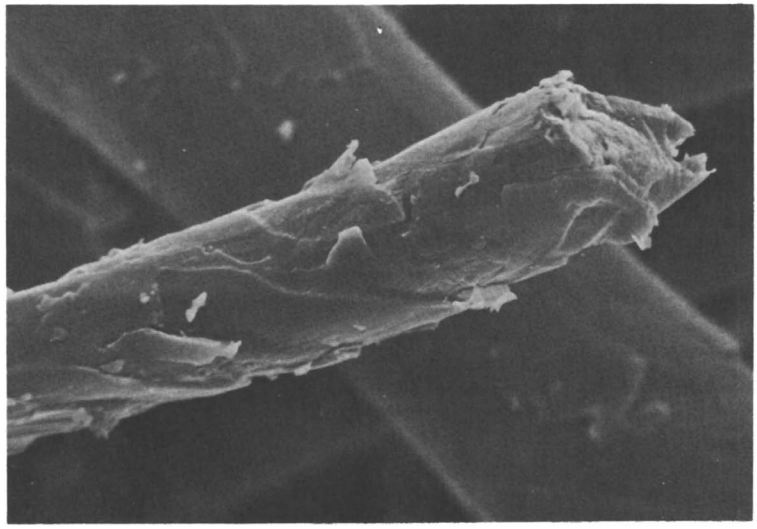

Figure 10e. Fibers present in a worn portion of a wool sock (1365×).

on morphological changes caused during wool abrasion has been discussed by Anderson et al. (*13*).

For polyester, the fiber balloons (Figure 11a) before multiple splits are observed (Figure 11b). Ballooning and splitting are followed by brushlike formations (Figure 11c) as the fiber breaks. Fibers with rounded tips can be observed (Figure 11d). The rounded tips are

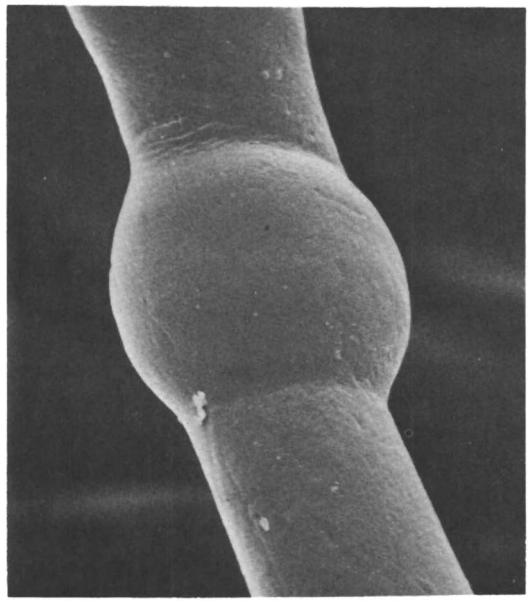

Figure 11a. Fibers present in a worn portion of a polyester fabric taken from a child's sleepwear (2210×).

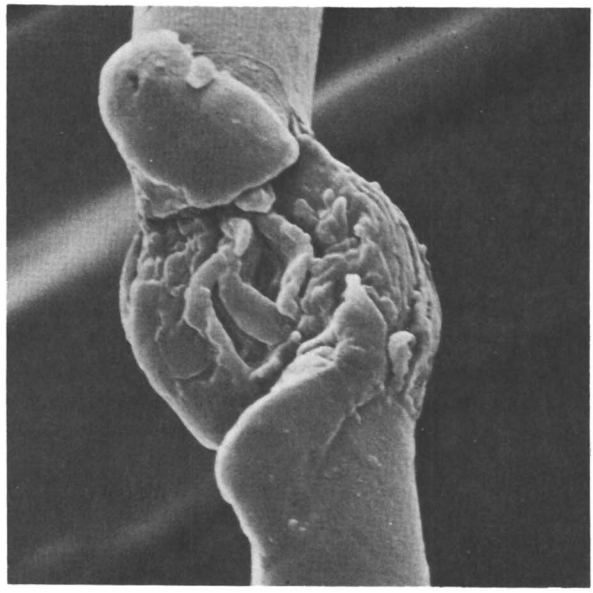

Figure 11b. Fibers present in a worn portion of a polyester fabric taken from a child's sleepwear (2210×).

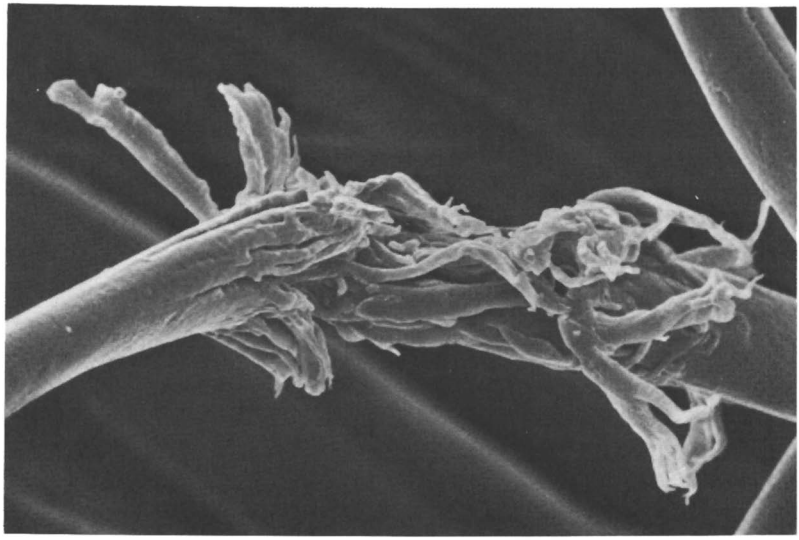

Figure 11c. Fibers present in a worn portion of a polyester fabric taken from a child's sleepwear (1105×).

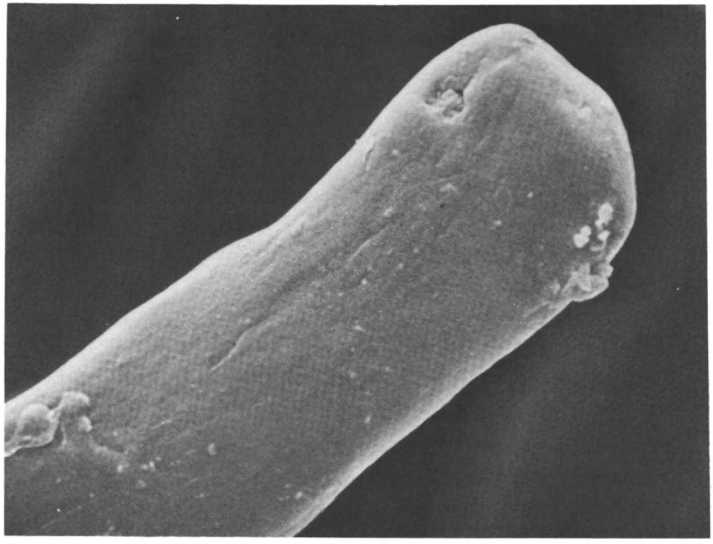

Figure 11d. Fibers present in a worn portion of a polyester fabric taken from a child's sleepwear (2145×).

probably due to a wearing away of the fibrillated ends. Presumably ballooning takes place in regions of high stress as the fibers are flexed during use. Cohesion between fibrillarlike units of the fiber appears to have decreased in these regions and thus resulted in a disordered structure of higher volume.

Multiple splitting, rupture of individual fibrils to yield brushlike fiber ends, and possibly a subsequent wearing of the fiber ends to round them off have been reported for cotton (9). In recent days much apparel containing cotton has been chemically modified by the application of resins to make it either wrinkle resistant or fire resistant. These treatments might affect the fracture morphology. However, multiple splits and frayed, as well as rounded, ends can still be observed (Figures 12a and 12b and Figures 13a and 13b). The fracture surface that can be observed in Figure 13a is similar to that of a cotton fiber taken from a fabric found in the Gramalote site in north Peru and dated about 1000 B.C. (Figure 14 in Reference 14). This similarity indicates that the Gramalote fabric had been subject to wear. In each of the cases of wear just presented, the fibrillation or splitting that happened to the fibers was reminiscent of the damage that occurred to their flex-ruptured counterparts.

Conclusions

The SEM can be a valuable tool to assist in the diagnosis of the cause of fabric wear or fiber failure by mechanical means. Because a variety of factors such as chemical treatments and conditions of use can affect

Figure 12a. Cotton fibers present in a worn portion of a used cotton–polyester sock (617×).

Figure 12b. Cotton fibers present in a worn portion of a used cotton-polyester sock (572×).

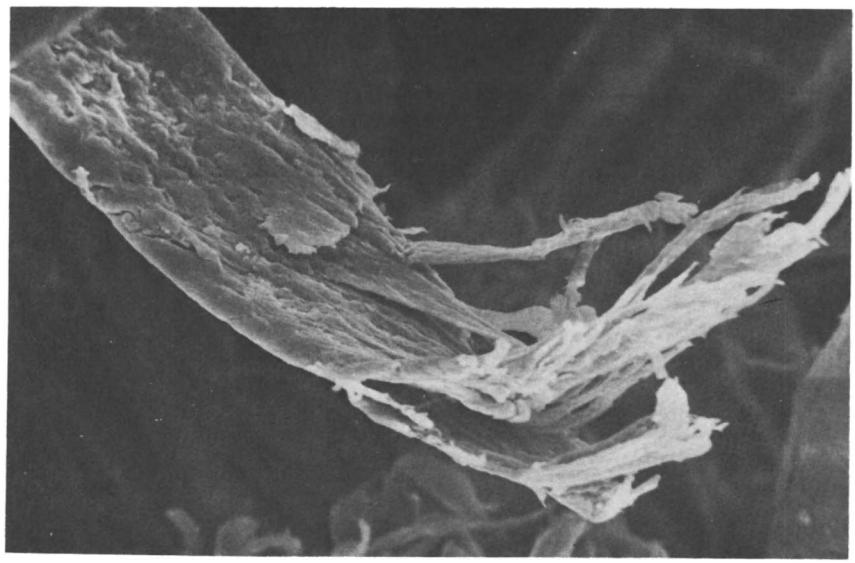

Figure 13a. Cotton fibers present in a worn portion of a used cotton-polyester denim fabric taken from a child's jeans (1300×).

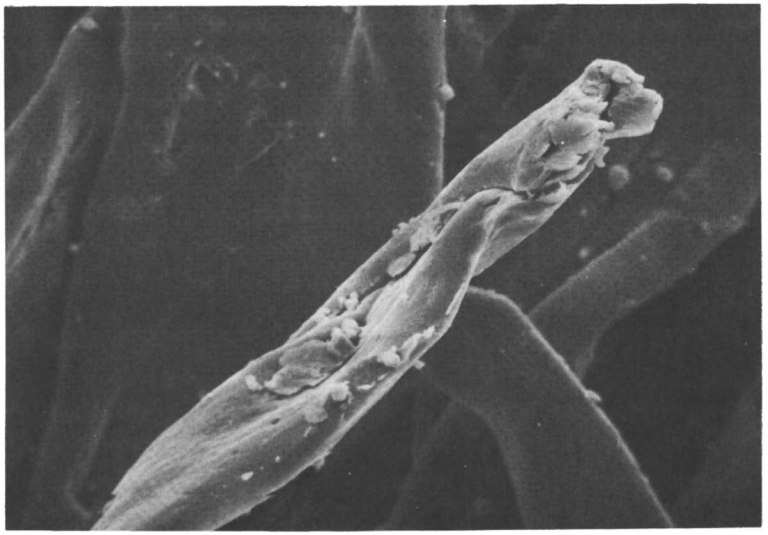

Figure 13b. Cotton fibers present in a worn portion of a used cotton-polyester denim fabric taken from a child's jeans (1300×).

fracture morphology, knowledge of available information on the fiber and fabric is important. Also, a set of micrographs consisting of fibers that have been fractured under known conditions is necessary. This chapter together with the articles we have cited will assist in preparing such a set.

Literature Cited

1. Zeronian, S. H. In "Surface Characteristics of Fibers and Textiles"; Schick, M. J., Ed., Dekker: New York, 1975; Part I, pp. 365–86.
2. Anderson, C. A.; Hoskinson, R. M. *J. Text. Inst.* **1970**, *61*, 355.
3. Hearle, J. W. S.; Buckley, C. P.; Lomas, B. "Fracture, fatigue and wear of man-made fibers." Presented at the Int. Man-made Fibre Conf., Dornbirn, Austria, June 1979.
4. Ellison, M. S.; Zeronian, S. H.; Fujiwara, Y. *J. Mater. Sci.* **1984**, *19*, 82.
5. Hearle, J. W. S.; Jariwala, B. C.; Konopasek, L.; Lomas, B. *Proc. Int. Wool Text. Res.Conf. 5th* **1975**, *2*, 370–80.
6. Hearle, J. W. S.; Sparrow, J. T. *Text. Res. J.* **1971**, *41*, 736.
7. Hearle, J. W. S.; Sparrow, J. T. *Text. Res. J.* **1979**, *49*, 268.
8. Chauhan, R. S.; Shah, N. M.; Dweltz, N. E. *Text. Res. J.* **1979**, *49*, 61.
9. Hearle, J. W. S.; Hasnain, N. *Cotton in a Competitive World. Annu. Conf. Text. Inst. 63rd,* **1979**, 163–83.
10. Ellison, M. S.; Fujiwara, Y.; Zeronian, S. H. In "Physicochemical Aspects of Polymer Surfaces." Vol 2; Mittal, K. L., Ed.; Plenum Press: New York, 1983; pp. 843–60.
11. Goynes, W. R.; Rollins, M. L. *Text. Res. J.* **1971**, *41*, 226.
12. Anderson, C. A.; Robinson, V. N. *J. Text. Inst.* **1971**, *62*, 281.
13. Anderson, C. A.; Leeder, J. D.; Robinson, V. N. *J. Text. Inst.* **1971**, *62*, 450.

14. Berry, G. M.; Hersh, S. P.; Tucker, P. A.; Walsh, W. K. In "Preservation of Paper and Textiles of Historic and Artistic Value"; Williams, J. C., Ed.; ADVANCES IN CHEMISTRY SERIES No. 164; American Chemical Society: Washington, D.C., 1977; pp. 228–48.

RECEIVED for review November 26, 1984. ACCEPTED March 14, 1985.

Fractography of Historic Silk Fibers

Randall R. Bresee[1] and Gail Elizabeth Goodyear[2]

[1]Department of Clothing, Textiles, and Interior Design, Kansas State University, Manhattan, KS 66506
[2]Department of Home Economics, California State University, Chico, CA 95929

Twenty-eight historic silk fabrics dating from 1880 to 1980 were fractured by tensile stress, and scanning electron microscopy was used to examine the morphology of fractured fiber ends. Fractures were interpreted in terms of interfibrillar cohesion, fiber surface flaws, and fiber ductility-brittleness. This interpretation led to the conclusions that accelerated laboratory heat stress results in embrittlement and a marked loss of interfibrillar cohesion, whereas accelerated laboratory light stress results in an increase of fiber surface flaws. The fracture of naturally aged fibers suggests that natural aging occurs by a more complex mechanism than simple laboratory heat or light exposure of newer samples. Fragility of naturally aged historic samples is more accurately described as resulting from a decrease in interfibrillar cohesion rather than from excessive embrittlement.

HISTORIC COSTUME AND TEXTILE COLLECTIONS frequently contain items made from silk. The myriad of uses for silk include garments and accessories, vestments, tapestries, painting canvases, and interior-furnishing fabrics. Regardless of the end use, silks or any other fabric is subject to deterioration. The care and preservation of historic silk textiles are concerns of most museum curators-conservators because silks housed in museums generally are valuable and irreplaceable. Museums seek to preserve objects in a usable state, but control of the museum environment to eliminate deterioration of silk textiles is not possible. These items become more fragile every day and eventually become unusable. The longer the deterioration proceeds unchecked, the greater the loss. Little headway has been made in understanding silk-fiber deterioration. Although a substantial amount of research involving the structure and properties of new silk fibers has been conducted for commercial application, little understanding of the structure and properties of aged silk fibers has been attained.

0065-2393/86/0212-0095 $06.00/0

Work is needed to help understand silk-fiber aging and enable the development of improved methods for the conservation and restoration of historic silk textiles.

The Structure of Modern Silk

Silk fibers are continuous filaments composed of a proteinaceous fibrous biopolymer called fibroin and another proteinaceous nonfibrous biopolymer called sericin (*1*). Fibroin constitutes the fibrous core of silk fibers, whereas sericin acts as a gummy coating that encapsulates two fibroin filaments. Many animals in the phylum *Arthropoda,* classes *Insecta* and *Arachnida,* extrude these complex filaments. However, most commercial silk fibers are produced by one animal—the *Bombyx mori* caterpillar (*2*). The fibroin polymer is composed of 17 different amino acids and has a molecular weight somewhere between 50,000 and 150,000 (*3*). Although researchers disagree somewhat on the exact amino acid composition of silk proteins, they generally agree that more than 80% of the amino acids found in *Bombyx mori* fibroin are the following three small, compact peptides: glycine, alanine, and serine (*4*). However, a few large amino acids also are found in appreciable amounts. To accommodate both compact and bulky amino acids, scientists believe that *Bombyx mori* filament fibroin exists as a block copolymer. Wide-angle X-ray diffraction measurements of fibroin fibers indicate a moderate 40–60% axial orientation of amino acids forming crystalline blocks in the bipolymer (*3*). The shear forces produced by the stretch-spinning motion of the silkworm's head are believed to introduce this orientation and form the fibroin biopolymers into fibrils in the fiber. Each fibroin fiber is believed to consist of 20–30 bundles of highly oriented fibrils (*3*). Fibrils measure 100 Å in diameter and 3500 Å long and are grouped into concentric rings (*3*). The fibrils presumably are held together through interfibrillar tie molecules such as those present in the fringed micelle theory of fiber structure. On the other hand, some evidence indicates that fibrils in fibroin are held together with an adhering, less organized material called "cuticolina" (*3*). Interfibrillar cohesion is an important contributor to the mechanical properties of silk fibers.

Polymer Aging

Changes in the physical and chemical composition of historic textiles usually are attributed to the treatment and care they receive after fiber formation. The most commonly reported effects of silk-fiber aging are those involving changes in mechanical properties, such as strength, elongation, and elasticity (*5*). Overall, these effects generally are said to result in a fabric that is fragile and characterized by increased stiffness and brittleness.

Polymer aging, which may be either physical or chemical, is a complex process that results from the interplay of a large number of different events. *Physical aging* results from the gradual continuation of glass formation and occurs at temperatures below the glass transition temperature of all polymer materials (*6*). Physical aging occurs because amorphous regions of the polymer are not in thermodynamic equilibrium at temperatures below the glass transition temperature. No additional thermal or chemical energy needs to be supplied for aging to occur as long as a polymer material is at a temperature below its glass transition temperature. Because physical aging is strictly a function of temperature, it may occur in the most gentle of chemical environments. Physical aging increases fiber stiffness and brittleness. Fortunately, however, this process may be reversed by exceeding the glass transition temperature of the fiber.

The principal component of degummed silk is fibroin. The glass transition temperature of dry fibroin is 175 °C as measured by differential scanning calorimetry (*7*). Consequently, storage under nonwet conditions and ambient temperatures of 20–25 °C places the fiber well below its glass transition temperature, and physical aging would be expected to occur. Silk fibers are commonly claimed to become brittle during storage; at least some of the stiffness found in historic silk textiles certainly results from physical aging. However, because physical aging is a reversible process, this stiffness may be eliminated by exceeding the glass transition temperature. If desired, plasticizers such as water may be used to depress the glass transition temperature of silk to a lower temperature for more gentle erasure of physical aging.

Chemical aging, on the other hand, involves the making and breaking of covalent bonds and is largely irreversible. Energy must be supplied to make or break bonds during chemical aging. The most common energy sources are heat, light, and nonfibrous chemical substances. Most textiles are repeatedly subjected to these energy sources during their lifetime. Silk, like most proteinaceous substances, suffers degradation when exposed to heat or light. The most important general chemical-aging reactions that occur are polymeric chain scission and cross-linking. Chain scission occurs when polymeric skeletal bonds are broken and thus results in a lower polymeric molecular weight and a broadened molecular weight distribution. Losses in tensile strength, elongation, and elasticity are associated with chain scission. Cross-linking, on the other hand, involves the formation of covalent-bond linkages between polymeric chains. At low reaction levels, cross-linking results in increased fiber strength and toughness, whereas substantially decreased elongation and increased brittleness result from higher cross-linking levels.

The chemical reactivity of silk has been investigated predominantly from an industrial standpoint. Some of the knowledge gained from this

research may be related to the natural chemical aging of historic silk textiles, although differences in chemical and physical conditions to which historic textiles normally are subjected during their lifetimes make direct application of this research sometimes difficult. That is, information resulting from relatively simple laboratory studies employing a small number of short-term stresses of large magnitude must be applied to natural aging during which a great number of milder stresses act on textiles over a very long period of time in a complex manner. Nevertheless, two useful reactions that have been studied are hydrolytic chain scission and oxidative cross-linking (2). Hydrolysis of the amino acid linkages in fibroin may occur in boiling water and in steam containing either alkalies or acids. These conditions may resemble commercial dyeing and finishing as well as some care treatments. Consequently, the amount of hydrolysis found in a collection of historic silk textiles would be expected to be widely variable and may be substantial in some cases. A wide variety of oxidizing agents also may induce cross-linking of silk fibroin (2). Because a large number of common substances such as air contain oxidizing agents, the amount of oxidative cross-linking found in a collection of historic textiles also would be expected to vary over a large range and may be substantial in some cases. The net result of these considerations is that a random sample of historic silk textiles would be expected to exhibit chemical aging that is quite variable and considerably more diverse than that exhibited by laboratory-aged samples.

Fiber Fracture

Studies using scanning electron microscopy (SEM) have been used effectively to examine the morphological details of fiber fracture. Hearle et al. (8) have used this analytical technique to classify fiber fracture into 10 types, as illustrated in Figure 1. Type 1 results from brittle crack propagation and appears as a smooth break perpendicular to the fiber axis. Type 2 is a cracked opening that forms a V-notch and results from controlled ductile crack propagation or tearing. Type 3 is described as a mushroom shape and is caused by large amounts of plastic deformation. Enough heat is generated to soften the material, which is then flattened into a mushroom shape by snapback after rupture (9). This type of fracture results from very high straining rates. Type 4 occurs from long axial splits that eventually cross the fiber. This pattern is more likely to occur if externally induced mechanical stresses are present across the axial plane. Type 4 fractures can occur with highly oriented fibers, which resist stresses parallel to the fiber axis but are susceptible to stress in any nonaxial direction. Type 5 is typified by a moderate loss of cohesion between fibrils or other supermolecular structural units and is characterized by a rough surface appearance defined by groups of the morphological units. Type 6 fractures are typified by a major loss of

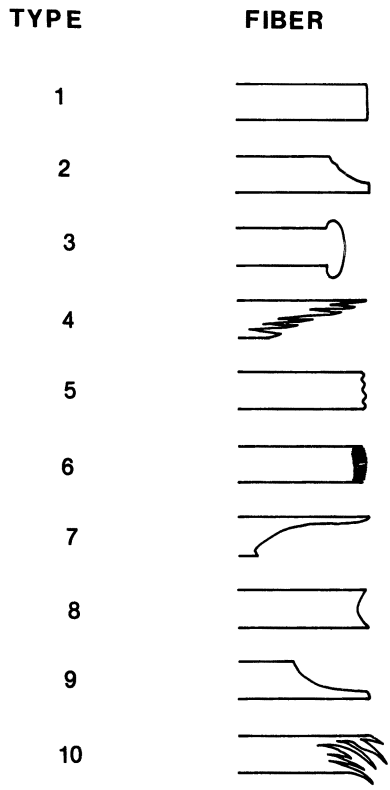

Figure 1. Schematic drawings of Hearle's classification of fiber fracture types. (Reproduced with permission from Ref. 8.)

cohesion between morphological units and occur when these units are so weakly linked that they break independently. The fracture surface consists of independent morphological units. Type 7 is a long axial split that develops from a surface flaw and leaves a tail on one fractured end that is stripped from the other end. Type 8 results from kink bands that eventually split open so the final failure is angular shaped. This failure may occur from fiber flexing. Type 9 is due to abrasion wearing away the fiber surface until it can no longer support stress. Type 10 is initiated by multiple splits along the fiber. This failure results in a frayed appearance of the fracture and occurs in some fibers that have been subjected to biaxial rotation. As can be seen from these descriptions, a wide variety of fiber structural information may be obtained from studies of fiber fracture.

Experimental

Fabrics. Twenty-four fabric samples dating from 1880 to 1973 were obtained from textile collections at Kansas State University, California State University (Chico), and the Fort Riley Kansas Military Museum. Curators from participating museums were requested to submit 5- × 5-cm samples of plain-

weave, silk-lining fabrics for the study. Sample selection was based on age, fabric-construction characteristics, size, and fiber content. A sample of modern degummed silk crepe (*10*) dated 1980 also was included.

To remove surface dirt and oils, each silk sample was agitated gently in tetrachloroethylene for 2 min at 25 °C, conditioned at 21 ± 1 °C and 65 ± 2% rh for 24 h, agitated in a 0.05% aqueous solution of the nonionic surfactant Merpol LF-H at 25 °C, dried, and then reconditioned for 3 days prior to tensile fracture. This treatment was expected to erase the effects of physical aging because fibroin is plasticized by water and its glass transition temperature is depressed to room temperature when completely wet (*11*). Consequently, the effects of aging on fractures observed in this study resulted only from chemical aging and not from physical aging.

Samples of the modern silk fabric measuring 30.5 × 30.5 cm also were heated for 6 h at 60 ± 2 °C in a laboratory convection oven. Specimens of comparable size were cut from the center of the silk fabrics after heating and conditioning.

Other samples of the modern silk fabric measuring 26.5 × 18 cm were exposed to carbon arc radiation for 320 AATCC* fading units following procedures specified in AATCC Test Method 111C-1975, "Weather Resistance: Carbon Arc Lamp Exposure Without Wetting" (*12*). Specimens were mounted in open-back metal frames positioned with the warp in the vertical direction and exposed to continuous light in an Atlas carbon arc weather-ometer. The black panel temperature and relative humidity during exposure were 37.8 ± 6 °C and 80 ± 5% rh. AATCC blue wool lightfastness standards were used to determine the number of AATCC fading units to which the silk specimens were exposed, following the procedures specified in AATCC Test Method 16-1978, "Colorfastness to Light: General Method" (*12*).

Tensile Fracture. Specimens measuring 1 × 5 cm and having the long dimension parallel to the warp were prepared from each of the silk fabrics. Adhesive tape was applied to the ends of the specimens to facilitate placing them between the clamps of a Scott tensile-testing machine having a constant rate of extension. Because of the limited specimen size, the distance between the clamps was 1 cm at the start of the test. The general procedures in American National Standards Institute-American Society for Testing and Materials (ANSI-ASTM) D1682-64, constant traverse speed of 30.5 ± 1 cm/min was used.

Scanning Electron Microscopy. Unbroken ends of short lengths of approximately 25 fractured fibers from each broken fabric were embedded vertically in carbon paste on scanning electron microscope (SEM) specimen holders by using an optical stereo microscope and tweezers. The specimens were evaporatively coated first with carbon and then with a 60-40 gold-palladium alloy. Three fractured fiber ends morphologically representative of the 20 mounted fibers from each historic fabric were photographed in the SEM. Thus, a total of 72 fractured fibers were photographed from the 24 historic fabrics. In addition, 10 representative fibers were photographed from the modern fabric, heat-exposed modern fabric, and light-exposed modern fabric specimens for a total of 30 more fibers. Consequently, more than 100 fractured fiber ends were examined in this study.

Results

The fractured surfaces of the broken silk fibers were classified according to Hearle's system of fiber fracture morphology (*8*). Most fractured

*American Association of Textile Chemists and Colorists

ends observed in our study fit this system. However, some of the fractured surfaces could not be classified as any of the 10 types used by Hearle. An 11th type of fracture that resulted from the presence of a large internal void was added. In addition, some fibers were classified as "combination" because the fracture event appeared to be governed by a combination of more than one fracture type rather than dominated by one particular type. A summary of the fracture types assigned to each of the groups of silk specimens evaluated in this study, as well as their percent frequency, is presented in Table I. Examples of each of the fracture types observed are provided in Figures 2–8.

Fracture Types 3, 4, 6, 9, and 10 were not found in any of the specimens examined. The absence of Type 3 fractures was expected because they are characterized by a large amount of plastic deformation and have been observed only in nylon fibers fractured at very high strain rates for which heat buildup is sufficient to cause melting of polymeric material. The tensile loading rate used in this study was very low, and little heat buildup occurred. Type 4 fractures are observed when discontinuities along planes perpendicular to the fiber axis are present in fibers that are very highly oriented axially and exhibit little interpolymeric attraction perpendicular to the fiber axis. Because fibrillar orientation in silk fibroin is moderate but not great, and fibroin polymers form extensive intermolecular hydrogen bonds, the absence of Type 4 is not surprising. Type 6 is observed when fibrillar units are united so weakly that they break independently. We had anticipated observing some of these fractures because some of the historic fabrics examined in this study were extremely fragile. However, this type of fracture has only been observed in wet cotton fibers in which hydrogen bonds responsible for interfibrillar attraction were broken by wetting. The absence of Type 6 fractures in our study suggests that interfibrillar cohesion of historic silk fibers is greater than that of wet cotton. Silk fibers fractured after wetting might have exhibited this type of fracture morphology. Type 9 fractures are characterized by a wearing away of the sides of the fiber by surface abrasion until fracture occurs. Because we examined fiber failure under tensile stress and not surface abrasion, Type 9 fractures were not present. We did not observe Type 10 fractures, which result from biaxial rotation, because this study involved fracture by tensile deformation.

The modern silk sample not subjected to heat or light stress displayed fracture Types 2, 5, 7, and 11. The dominant fracture type exhibited by these fibers was Type 7; 50% of the modern silk fractures were of this type. This finding indicates that surface flaws largely govern the fracture mechanism of modern silk. A smaller number of fracture Types 2, 5, and 11 were observed. This observation indicates that at least some of these fibers also exhibit ductility, a moderate loss of interfibrillar cohesion, and large internal voids, although their influence in fiber fracture is considerably less than that of surface flaws.

Published on February 1, 1986 on http://pubs.acs.org | doi: 10.1021/ba-1986-0212.ch005

Table I. Fracture Types of Silk Fibers

	Frequency of Fractures (%)						
Fiber	*Type 1 Brittle*	*Type 2 Ductile*	*Type 5 Cohesion*	*Type 7 Surface*	*Type 8 Flex*	*Type 11 Void*	*Combination*
Modern (1980)	—	20	20	50	—	10	—
Modern (1980), accelerated heat stress	10	10	50	10	10	10	—
Modern (1980), accelerated light stress	—	10	—	70	10	10	—
Historic (1880–1973) naturally aged	—	14	42	21	11	3	10

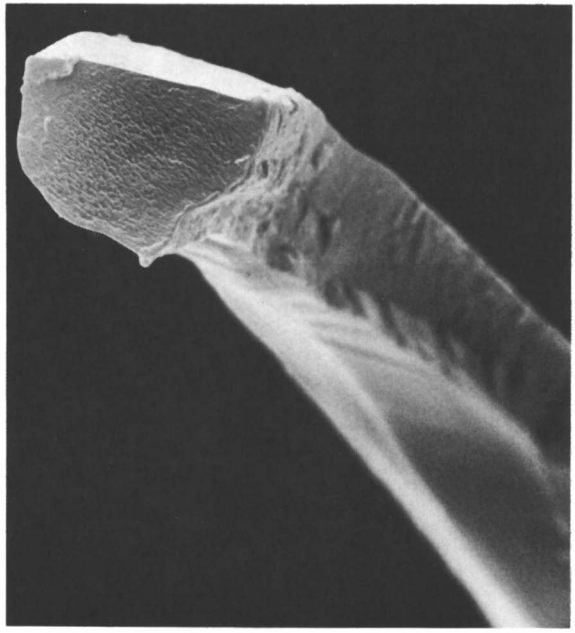

Figure 2. SEM photomicrograph of a Type 1 (brittle) fracture (2600×).

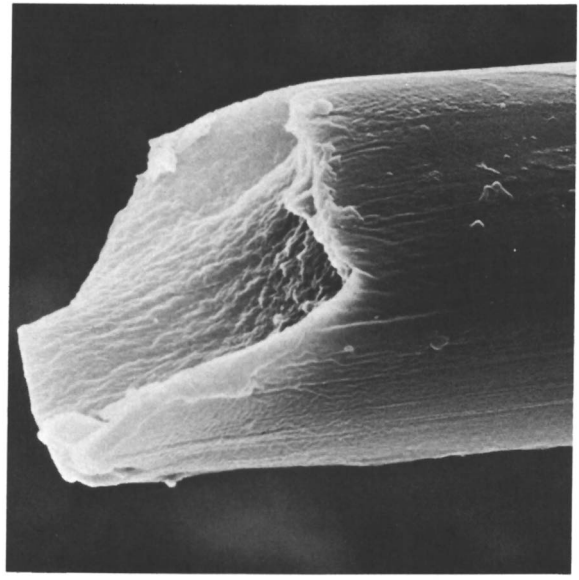

Figure 3. SEM photomicrograph of a Type 2 (ductile) fracture (2600×).

Figure 4. SEM photomicrograph of a Type 5 (loss of interfibrillar cohesion) fracture (2600×).

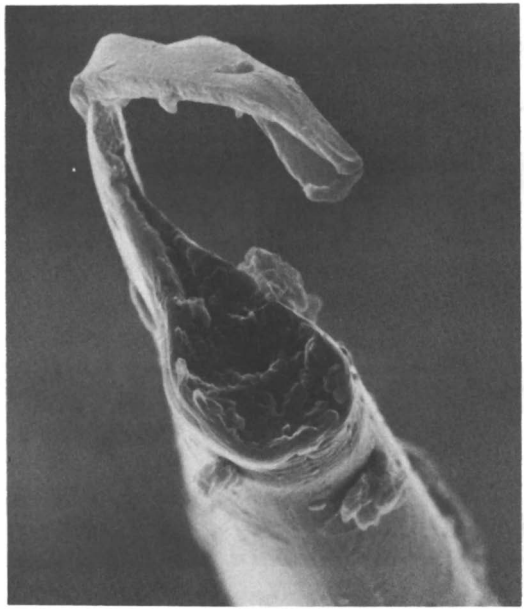

Figure 5. SEM photomicrograph of a Type 7 (surface-flaw-influenced) fracture (2600×).

Figure 6. SEM photomicrograph of a Type 8 (shear) fracture (2600×).

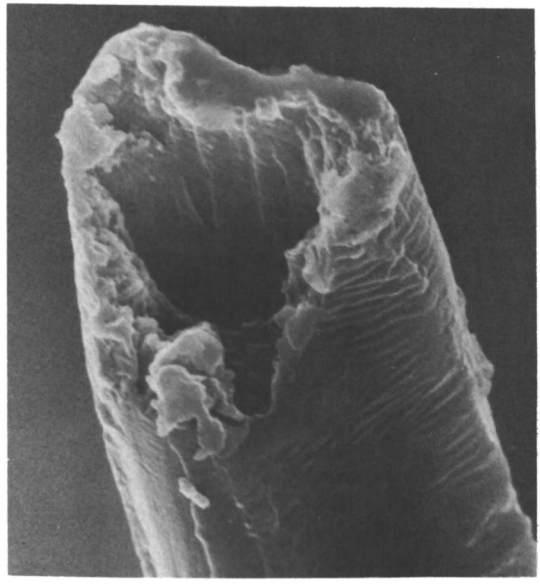

Figure 7. SEM photomicrograph of a Type 11 (void) fracture (2600×).

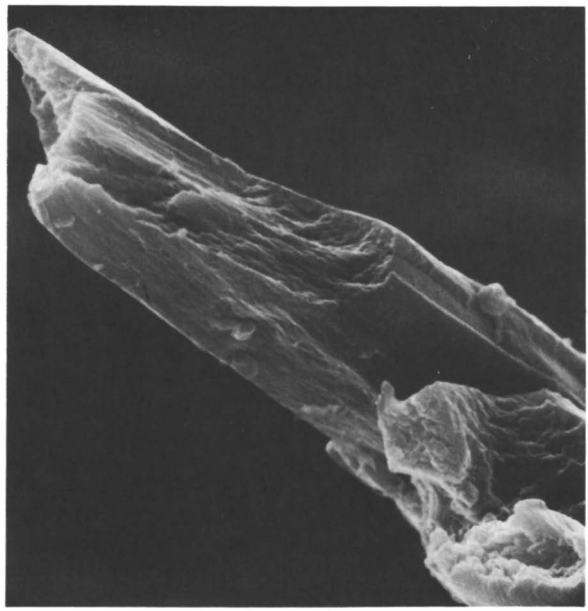

Figure 8. SEM photomicrograph of a combination-type fracture (2600×).

The modern silk fabric stressed by heat displayed a marked shift from a predominance of Type 7 fractures to a predominance of Type 5 fractures. Because Type 5 fractures indicate reduced interfibrillar cohesion, heat stress apparently results in decreased interfibrillar cohesion in silk. This decreased cohesion could be due to degradation (such as chain scission) of interfibrillar tie linkages, fibrillar surfaces, or cuticolina. In addition, the heat-stressed sample displayed a decrease in the number of Type 2 ductile fractures and an increase in the number of Type 1 brittle fractures. Changes in the frequencies of Types 1 and 2 were not large, and a greater number of textiles must be examined to interpret these differences with confidence. Nevertheless, an attempt to interpret changes in the data available is appropriate. Type 1 fractures result from brittle crack propagation along a single fracture plane perpendicular to the fiber axis when a fiber acts as a single homogeneous unit. Silk fibroin possesses a fibrillar morphology and thus is structurally heterogeneous in the supramolecular size range. Consequently, transverse fracture planes of silk fibers would be expected to follow lines of fibrillar structure rather than a single fault line. However, severe degradation could result in a decrease in the physical integrity of the morphological structure that is sufficient to homogenize fiber structure so that Type 1 brittle fractures occur. These observations

suggest that damage sustained by samples during heating for 6 h at 60 °C is severe enough for degradation to occur and for brittleness to increase. The presence of large voids in silk is indicated by Type 11 fractures. Type 8 fractures also were observed in the heat-stressed samples. This fracture type probably was observed because fabrics rather than single fibers were broken in our study, and the interlacing of yarns causes fibers to be bent over yarns to produce a shear stress instead of a true tensile stress.

The modern, light-stressed samples displayed an increase in the proportion of Type 7 surface-flaw-dominated fractures in comparison to the modern sample not stressed by light or heat. Seventy percent of the light-stressed fibers broke with Type 7 fractures. Silk is known to absorb light and suffer chemical degradation as a consequence. One naturally would expect the most absorption to occur at the fiber surface. The fracture behavior observed in this study suggests that degradation resulting from light absorption produces numerous new surface flaws or enhances flaws already present on silk fibers so that these flaws play a more dominant role in the mechanism of fiber breakage. The presence of Type 2 fractures indicates that the light-stressed silks still exhibit ductility. In addition, the presence of large internal voids is indicated by Type 11 fractures. All three samples of modern silk (unstressed, heat stressed, and light stressed) exhibited the same frequency of fractures dominated by large internal voids (10%). This result indicates that a reasonably random sampling of fibers was achieved because the same fabric was the source of all three samples. Type 8 fractures also were observed as in the heat-stressed samples.

The naturally aged historic silk samples displayed a greater diversity of fracture types than the modern samples. This result could be attributable to the better control in modern production facilities of numerous factors such as diet and weather that affect silk structure. Alternatively, the greater diversity of the historic silk samples could result from the greater complexity and variation of natural aging schemes in comparison to the simple laboratory heat or light stressing of modern silk textiles. Because many reactions, such as those resulting in hydrolytic chain scission and oxidative cross-linking, are expected to occur quite variably in historic textiles, this conclusion is not unexpected. Structural diversity of the historic samples is evident from the fact that 10% of the historic samples were classified as a combination fracture, that is, they were governed by a combination of more than one fracture type. None of the modern samples, on the other hand, exhibited this behavior.

The most common fracture event observed among the historic samples was Type 5; this observation indicated a greater loss of interfibrillar cohesion than that found in the modern silk samples. Because the modern samples stressed by heat at 60 °C also showed

decreased interfibrillar cohesion, thermal energy may be a principal component of stress resulting in deterioration of interfibrillar structure during natural aging. The decrease in interfibrillar cohesion exhibited by the historic samples appears to be less severe than that experienced by the laboratory-treated modern samples in which more Type 1 brittle fractures and fewer Type 2 ductile fractures were observed. This situation may result from a lower temperature applied over a longer time during natural aging than during the conditions used for laboratory aging. Observation of similar numbers of Type 1 and 2 fractures for the historic samples and the modern samples was surprising. This result suggests that silk textiles are not excessively embrittled during natural aging and actually are approximately as ductile as modern silk textiles. This observation is consistent with a fracture study involving another polyamide fiber for which both severely light-degraded and nondegraded nylon fibers exhibited ductile tearing during fracture (*13*). Therefore, rather than embrittlement, a more accurate description of deterioration in naturally aged silk fibers is a loss of interfibrillar cohesion. This statement implies that conservation and restoration treatments of historic silk textiles should not emphasize reducing fiber brittleness but instead should concentrate on increasing interfibrillar cohesiveness. Recall that all samples fractured in this study were washed to erase the effects of physical aging. Because physical aging is known to cause embrittlement, the lack of excessive brittleness observed for the samples is likely due partly to the erasure of physical aging prior to fracture. It still may be concluded, however, that chemical aging does not cause excessive brittle fracture because embrittlement resulting from chemical aging still would be observable in the samples fractured. Fracture Types 7, 8, and 11 also were observed for the historic samples.

Among the historic samples, the fracture behavior observed for each different textile was compared to the chronological age of the textile. No correlation between fracture behavior and chronological age was found. If a larger number of samples were analyzed, they might show a correlation. However, a lack of correlation suggests that the most important factor affecting historic silk fiber breakage is fabric treatment and care rather than chronological age.

Acknowledgments

The authors gratefully acknowledge the Kansas Agricultural Experiment Station for support of this work. In addition, curators of collections at the Fort Riley Military Museum, Kansas State University, and California State University (Chico) who graciously donated historic fabrics for use in this study are gratefully acknowledged.

Literature Cited

1. Truter, E. V. "Natural Protein Fibers"; Harper and Row: New York, 1973.
2. Asquith, R. S. "Chemistry of Natural Protein Fibers"; Plenum: New York, 1977.
3. Lucas, F.; Shaw, J. T. B.; Smith, S. G. In "Advances in Protein Chemistry"; Anfinsen, C. B.; Anson, M. L.; Bailey, K.; Edsall, J. T., Eds., Academic: New York, 1958; Vol. 13, p. 107.
4. Peters, R. H. "Textile Chemistry"; Elsevier: Amsterdam, 1963; Vol. I.
5. Scott, W. M. *Am. Dyest. Rep.* **1931**, *20*, 517.
6. Struik, L. C. E. "Physical Aging in Amorphous Polymers and Other Materials"; Elsevier Scientific: Amsterdam, 1978.
7. Magoshi, J.; Nakamura, S. *J. Appl. Polym. Sci.* **1975**, *19*, 1013.
8. Hearle, J. W. S.; Lomas, B.; Clarke, I. E. "Fracture, Fatigue, and Wear of Fibers", presented at the Conference of Helenic Cotton Board, Athens, Greece, September 1979.
9. Hearle, J. W. S. *Text. Manuf.* **1972**, *99*, 26.
10. Style #601, Testfabrics, Inc., 200 Blackford Ave., Middlesex, New Jersey 08846.
11. Fuzek, J. F. In "Water in Polymers"; ACS SYMPOSIUM SERIES No. 127; American Chemical Society: Washington, D.C., 1980; p. 515.
12. "AATCC Technical Manual" Am. Assoc. Text. Chem. Color.: Research Triangle Park, North Carolina, 1978.
13. Hearle, J. W. S.; Cross, P. M. *J. Mater. Sci.* **1970**, *5*, 507.

RECEIVED for review November 26, 1984. ACCEPTED March 25, 1985.

6

Degradation of Silk by Heat and Light

R. V. Kuruppillai, S. P. Hersh, and P. A. Tucker
School of Textiles, North Carolina State University, Raleigh, NC 27695-8301

The degradation of silk produced by dry heat and radiation from a xenon arc lamp is explored. Degradation was assessed by measuring the breaking strength and the concentration of amino groups in the silk. Conditions for exposing to light and heat were established to produce measurable changes in these parameters over reasonable exposure times. Three additives were examined to determine whether they would retard thermal degradation: a deacidifying agent and two antioxidants. The relationship between strength decrease and amino group increase is similar for both light and heat degradation. On the basis of the changes in breaking strength, the degradation by heat and light is of the first order. None of the three additives retarded the heat degradation as measured by breaking strength. In contrast, the two antioxidants did seem to retard the formation of amino groups. At this stage, general conclusions cannot be drawn regarding the effect of these agents on silk degradation.

THE SCIENTIFIC BASE NEEDED TO SUPPORT APPLIED RESEARCH on the conservation and preservation of irreplaceable textiles is inadequate. In recent years, growing awareness and concern have developed about this problem. For textiles, major routes of natural deterioration involve oxidation, hydrolysis, and chain cleavage resulting from exposure to heat, moisture, radiation, mechanical stress, enzymes, and microbiological agents. The effects of such deterioration are strength loss, decreased molecular weight, increased solubility, oxidation, crystallinity changes, and alterations in appearance and hand. After textiles have suffered severe natural deterioration, they are weak and brittle and will often turn to powder at the slightest movement.

To contribute to the fundamental knowledge that must underlie the development of better and more acceptable conservation methods, several studies focusing on the conservation and restoration of cotton have been carried out in our laboratories (*1–8*). The most fragile textile, however, is generally agreed to be silk. (*See* References 9 and 10 for recent reviews.) Its great sensitivity to light has long been recognized

0065-2393/86/0212-0111 $06.00/0

(*11*). A major factor that has added significantly to the fragility of silk is the practice of "weighting" that has been conducted for at least 300 years (*12*, *13*). Weighting is the application of 30–300% of inorganic salts of aluminum, iron, lead, tin, or zinc to silk fabrics to increase the body, drape, weight per unit area, etc. The practice originated primarily, it is believed, as a fraudulent means of increasing the value of the product that is sold by weight. By the late 1800s, weighting had become an accepted method of preparing silk before its final use.

Textile technologists and conservators express a general understanding that unlike cellulosic fibers, which are more easily damaged by acids than by alkalies, proteinaceous fibers such as silk are more easily damaged by strong alkalies than by strong acids (*14*). The damage caused by strong acids, however, is quite severe. Under milder conditions, the light stability of unweighted silk is greatest at about pH 10 but decreases rapidly as the fabric pH becomes greater than 11 or less than 3 (*15*). Because most weighting compounds are highly acidic, one might expect that weighted silks would be even less stable than unweighted silks. This sensitizing effect of weighting has indeed been shown to occur and is far more detrimental to silks exposed to light than to fabrics stored in the dark (*16*, *17*). However, damage even during dark storage is severe.

Silk deterioration takes place via two main mechanisms: oxidation and hydrolysis. Harris (*15*) has shown that degradation by exposure to light results largely from oxidation and is accompanied by the formation of "ammonia" nitrogen. Degradation by hydrolysis, on the other hand, is accompanied by the formation of "amino" nitrogen. In this way, Harris has been able to separate the portions of fiber deterioration that can be attributed to oxidation and hydrolysis.

The ultimate objective of this study is to develop a technique for preventing, or at least retarding, the degradation of silk by applying additives to the silk and to seek consolidants for silk. Before progress can be made in achieving this goal, however, a system for artificially degrading silk and reproducibly measuring the extent and nature of the degradation must be developed. The primary purpose of this chapter, thus, is to examine the nature of the degradation of silk produced by exposure to dry heat and to light from a xenon arc lamp. Because silk degradation can occur as a result of both oxidation and hydrolysis, some preliminary experiments are described in which an antioxidant or alkaline buffering agent is applied to silk to determine the effect of these compounds on the degradation induced by heating. The three stabilizers selected for this initial screening were chosen because of their extensive commercial use. Additional studies of this type and of the influence of these additives and UV light absorbers on the degradation caused by light are currently under way.

Experimental

Selection of Silk for Use as Test Material. In preliminary experiments, contemporary yarn and fabrics were shown to have reasonably uniform tensile properties; hence, either material is suitable as base material for this study. Measuring the tensile properties of yarns, however, is faster and easier than measuring those of fabrics because the preparation of fabric specimens requires cutting the fabrics and then raveling them to the proper dimensions. Artificial aging of yarns by heating in an oven, however, proved to be impractical because the air currents in the forced convection oven blew the yarn around to form a tangled mass. Winding the yarns on a variety of holders also proved impractical, not only because of the extra effort, but also because of resulting nonuniform heating. To take advantage of the ease of handling fabrics combined with the ease of testing yarns, the evaluation method chosen was to treat and age fabrics and then to measure the tensile properties of yarns extracted from the fabrics.

The silk fabric selected for this work was an unweighted plain woven Chinese silk habutae (Testfabrics, style 605) having 126 ends/in. (37.6 denier) and 117 picks/in. (32.1 denier) and weighing 1.11 oz/yd^2. The fabric as received had been degummed, as was confirmed by extraction with a soap solution. Fabric samples were obtained at two different times and are identified as Lots 1 and 2 to distinguish between them.

Artificial Aging. THERMAL. Conditions were selected to degrade the test fabric to levels having a wide range of strengths after reasonable exposure times. The procedure developed was to place 15- × 15-cm pieces of fabric in a forced convection laboratory oven preheated to 150 °C on racks covered with a Fiberglas screen (7- × 3-cm mesh). The screen was used to prevent direct contact of the silk with the metal rack which might lead to enhanced degradation at the points of contact. After heating for the desired times (up to 6 days), the fabric specimens were immediately placed in a desiccator containing silica gel to keep them dry while cooling.

LIGHT. For exposure to light, 15- × 7-cm pieces of fabric were mounted in standard specimen holders as specified in AATCC* test method 16E-1982, "Colorfastness to Light: Water-Cooled Xenon Arc Lamp, Continuous Light" (*18*). These were then placed in a water-cooled xenon arc fading apparatus, model 25FT, (Atlas Electric Devices) and exposed to light for up to 8 days. The apparatus was operated at 53 °C, 75% rh, and an arc power of 2100 W. The light intensity reaching the samples was not measured in these exploratory experiments.

Parameters to Measure Degradation. BREAKING STRENGTH. Warp and weft yarns were extracted from fabrics, and their breaking loads were determined at a gauge length of 2.0 cm and a rate of extension of 5.1 cm/min on a tensile-testing machine (Instron, model 1123) as specified by ASTM† Test Method D2256-80, "Breaking Load (Strength) and Elongation of Yarn by the Single-Strand Method" (*19*). Normally 21 breaks were made on each yarn type.

AMINO GROUP CONTENT. The relative concentration of ($\alpha + \varepsilon$)-amino groups was determined colorimetrically by reaction with ninhydrin (*20*). In this method, the ninhydrin reacts with the α- and ε-amino groups in silk to form a blue-colored compound having a maximum absorption at 570 nm.

*American Association of Textile Chemists and Colorists
†American Society for Testing and Materials

For analysis, a stock solution of ninhydrin was prepared by combining 20.18 g of sodium propionate, 9.3 mL of propionic acid, 50 mL of 2-methoxyethanol (Methyl Cellosolve), and 2 g of ninhydrin. The solution was brought to a volume of 100 mL with deionized water. The fabric specimens to be analyzed were first ground in a Wiley mill fitted with a Number 40 mesh screen. Four samples of the ground specimen each weighing 20 mg were introduced into individual 20-cm long Diels-Alder pressure test tubes to which 2 mL of 2-propanol-water (10-90, v-v), 2 mL of pyridine-water (10-90, v-v), and 4 mL of ninhydrin solution were added. The tubes were capped tightly with bottle caps and placed in an oil bath at 100 °C. After heating for 60 min, the tubes were removed from the bath and uncapped, and immediately 20 mL of deionized water was introduced. After cooling for 15 min, the contents of the tubes were transferred to a 100-mL volumetric flask and diluted to 100 mL with deionized water. A small portion of this solution was collected in a test tube after passing through filter paper to remove the undissolved silk.

The transmittance of the solution was then measured at 570 nm on a Spectronic 20 spectrophotometer (Bausch and Lomb); a solution submitted to the treatment just described but to which no silk was added was used as a blank. Two samples of each filtered solution were measured, and the averages of two readings were reported.

To evaluate the linearity of the analysis with the amount of silk contained in the reaction tubes, several fabric solutions were prepared by adding 10 and 30 mg of the ground specimen, as well as the standard 20 mg, to the reaction tubes.

Application of Additives to Silk. DEACIDIFYING AGENT. This material is ethoxymagnesium ethyl carbonate dissolved in trichlorotrifluoroethane (Wei To Associates). It has been extensively used as an alkaline buffering agent to protect paper and cellulosic textiles from aging (*7,8,21*). Samples were dipped one at a time in the solution for 30 s and then dried flat on a sheet of poly(methyl methacrylate). The treated samples had an add-on of approximately 3% and were relatively stiff.

COMPOUND I. This compound is a trifunctional hindered phenol (Goodrite 3125, BF Goodrich). Compound I is insoluble in water but soluble in aromatic

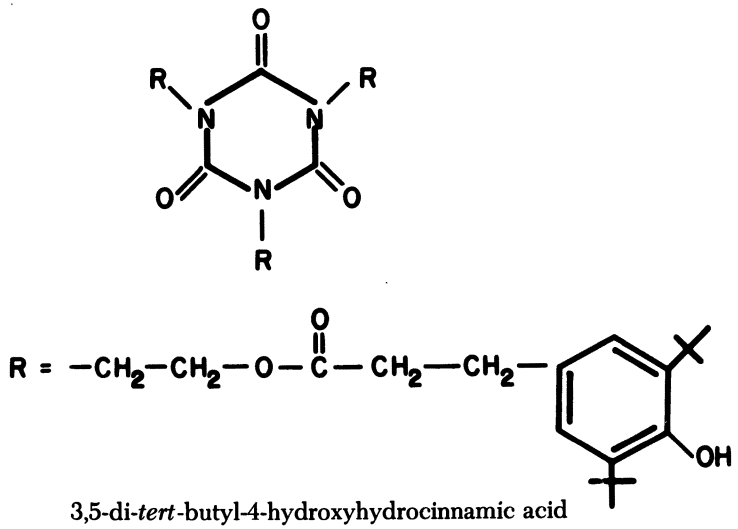

3,5-di-*tert*-butyl-4-hydroxyhydrocinnamic acid triester with 1,3,5-tris(2-hydroxyethyl)-*s*-triazine-2,4,6(1*H*, 3*H*, 5*H*)-trione

solvents such as benzene and toluene. Preliminary experiments showed that of the possible solvents, benzene had the greatest swelling effect on silk; hence, it should be a suitable solvent for transporting the compound into the fiber. The fabrics to be treated were immersed for 30 min in a solution containing 18.71 g of Compound I per 100 mL of benzene (one-third of the concentration of a saturated solution) and then were dried. The average add-on was 33%.

COMPOUND II. This compound is also a hindered phenol antioxidant (Cyanox 1790, American Cyanamid). Compound II is insoluble in water but has a solubility of 4.6 g/100 mL of ethanol. A saturated solution of this compound in ethanol was prepared, and the fabric pieces were immersed in this solution for 30 min. The samples were then dried in the same manner described in the preceding section. The average add-on was 9%.

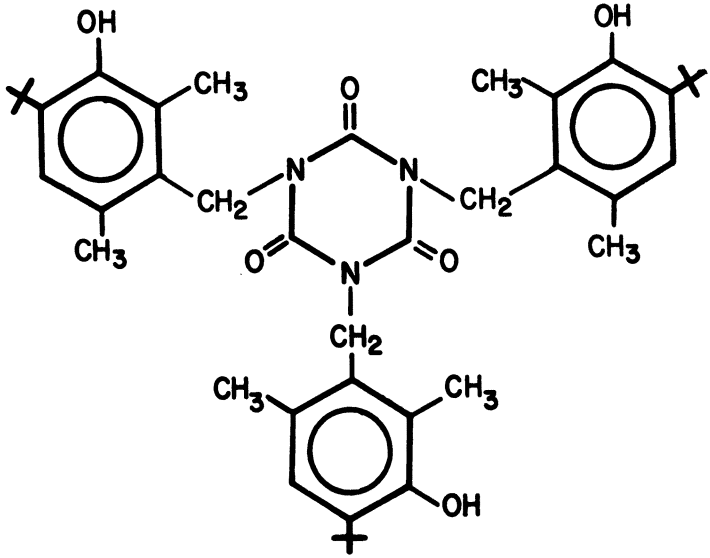

1,3,5-tris(4-*tert*-butyl-3-hydroxy-2,6-dimethylbenzyl)-1,3,5-triazine-2,4,6-(1*H*,3*H*,5*H*)-trione

Results and Discussion

Heat Degradation. STRENGTH. The breaking strengths retained of yarns extracted from the fabric (Lot 1) after heating at 150 °C are shown in Figure 1. The strength retained is based on the breaking load of the unheated, untreated fabric. The curves for both the warp and weft yarns show a rapid initial loss in strength followed by a reduced rate of degradation. Such a curve is typical of first-order reactions in which the rate of decomposition (or degradation) of a material is directly proportional to the amount of material present at any given time, that is,

$$ds/dt = -ks \quad (1)$$

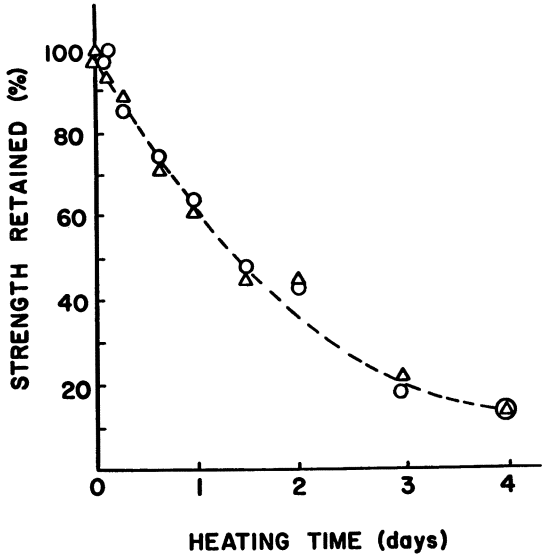

Figure 1. Strength retained of warp and weft yarns from fabric 605 (Lot 1) as a function of heating time at 150 °C. Key: ○, warp; △, weft.

where s is the strength retained, t is the time, and k is the first-order rate constant.

A plot of the logarithm of the degradation as a function of time for a first-order reaction produces a straight line. Such plots for the warp and weft yarns are shown in Figure 2. The plots are nearly linear and suggest that the degradation is indeed first order. As is well known in kinetics, the rate constant can be estimated from the slope of the line whose equation is given by

$$\ln s = -kt + a \tag{2}$$

where k is the slope of the line and a is the intercept on the s-axis.

That the slope k in Equation 2 is the same as the rate constant k in Equation 1 can be shown by differentiating Equation 2 with respect to t:

$$(1/s)\ (ds/dt) = -k \tag{3a}$$

and

$$ds/dt = -ks \tag{3b}$$

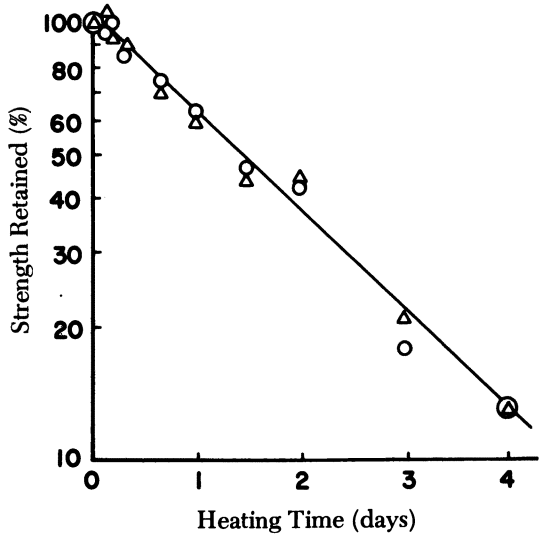

Figure 2. Logarithm of strength retained of warp and weft yarns from fabric 605 (Lot 1) as a function of heating time at 150 °C. Key: ○, warp; △, weft.

Hence, the rate of change of strength for a first-order reaction is given by the slope of the plot in Figure 2. A least-squares regression analysis of the data in Figure 2 gives $k_{warp} = -0.0221$/h and $k_{weft} = -0.0219$/h, both with intercepts of $a = 4.65$ [$s = \exp(4.65) = 104.7\%$]. Thus, the silk fabric degrades at a rate of about 2%/h when heated at 150 °C.

Heating silk at 150 °C therefore seems to be reasonable for thermally aging silk. The strength is reduced to about one-tenth of its original value after 4 days of heating. Furthermore, the rate of degradation appears to be first order, a relationship that will permit the extent of degradation to be calculated for any heating time on the basis of measurements made after only a few different heating times as shown in Table I and Figure 3. These data were obtained on Lot 2 of the test fabric at heating times of 1, 2, 3, and 6 days. The degradation rates were found to be $k_{warp} = -0.0194$/h and $k_{weft} = -0.0224$/h, only 12% and 2% different from the values found for the more extensive study carried out on Lot 1 of the test fabric reported in Figures 1 and 2.

AMINO GROUP CONTENT. The relative amino group concentrations measured on fabric Lots 1 and 2 are listed in Table II and are shown in Figure 4. These data include measurements made on ninhydrin solutions containing 10, 20, and 30 mg of ground fiber.

Published on February 1, 1986 on http://pubs.acs.org | doi: 10.1021/ba-1986-0212.ch006

Table I. Breaking Load of Warp and Weft Yarns Extracted from Treated and Untreated Silk Fabric Lot 2 After Heating at 150 °C

		Warp Breaking Load					*Weft Breaking Load*				
Treatment	*Heating Time (days)*	*Mean (gf)*	*S.D. (gf)*	*C.V. (%)*	*Strength Retained (%)*	*Deg. Rate (%/h)*	*Mean (gf)*	*S.D. (gf)*	*C.V. (%)*	*Strength Retained (%)*	*Deg. Rate (%/h)*
None	0	127.9	9.48	7.41	100.0	−1.94	121.8	7.54	6.18	100.0	−2.24
	1	86.9	5.50	6.38	67.9		86.5	9.72	11.23	71.0	
	2	49.8	8.49	17.05	38.9		53.0	7.67	14.46	43.5	
	3	20.6	3.11	15.09	16.1		21.4	1.88	8.78	17.6	
	6	8.6	1.54	17.85	6.8		5.5	1.18	21.58	4.5	
Deacidifying agent	0	128.1	14.94	11.66	100.1	−2.74	118.8	7.82	6.58	97.5	−2.29
	1	77.9	10.40	13.36	60.8		74.2	8.42	11.35	60.9	
	2	34.3	4.69	13.66	26.8		39.6	5.75	14.54	32.5	
Compound I	0	146.6	12.38	8.50	114.6	−2.93	137.0	10.05	7.33	112.4	−2.33
	1	83.5	10.33	12.38	65.2		79.5	5.74	7.21	65.3	
	2	36.0	5.73	15.93	28.1		44.8	6.69	14.9	36.8	
	3	14.5	2.88	19.84	11.3		17.1	2.68	15.7	14.0	
Compound II	0	128.5	8.52	6.63	100.4	−2.59	129.2	12.84	9.94	106.0	−2.73
	1	87.6	11.18	12.76	68.5		81.8	5.99	7.32	67.1	
	2	37.0	4.76	12.87	28.9		34.8	2.84	8.15	28.6	
Pooled S.D.			8.48					7.19			

NOTE: The breaking load is the mean of 21 breaks. S.D., C.V., and gf denote standard deviation, coefficient of variation, and gram-force, respectively. Deg. is degradation.

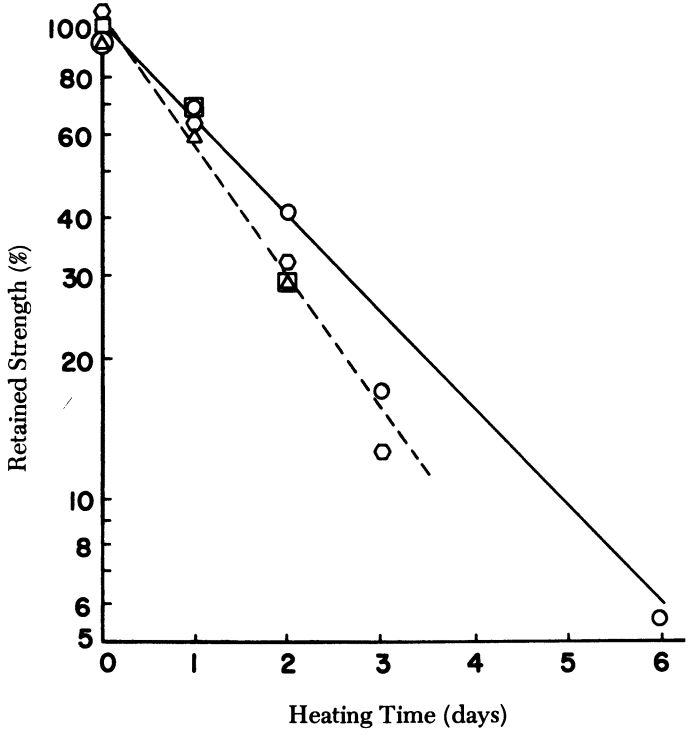

Figure 3. Logarithm of strength retained of yarns from untreated fabric and fabrics treated with the deacidifying agent and the two antioxidants as a function of heating time at 150 °C (Lot 2, average of warp and weft). Key: ○, untreated; △, deacidifying agent; ⬡, Compound I; □, Compound II.

As is known from the Beer-Lambert law, the absorbance A of a solution is the product of the absorption coefficient ϵ, the optical path length of the solution l, and the concentration of the colored species c, that is,

$$A = \epsilon lc \tag{4}$$

Because the path length and absorption coefficient are constant in the amino group analysis, a plot of A versus the amount of fiber added to the solution should be a straight line passing through the origin. Except for two outliers, these plots are linear with zero intercepts. This result suggests that the test procedure is a reasonable one. Also, within experimental error, fabric Lots 1 and 2 are equivalent in amino group content. The amino group content as a function of heating time is shown in Figure 5 (together with some additional data to be referred to later). The absorbance of the fabric from Lot 1 (filled circles) is nearly linear up to

Table II. Absorbance of Ninhydrin Solution Obtained from Silk Fabrics After Heating at 150 °C

Heating Time (days)	Fiber Conc. (mg/100 mL)	Absorbance					
		Fabric Lot 1			Fabric Lot 2		
		Mean	S.D.	C.V. (%)	Mean	S.D.	C.V. (%)
0	10	0.105	0.0185	17.5	0.090	0.0037	3.7
	20	0.210	0.0119	5.6	0.216[a]	0.0155	7.2
	30	0.221	0.0084	3.8	0.323	0.0041	1.4
1	10	0.140	0.0046	3.3	—	—	—
	20	0.298	0.0141	4.7	0.300	0.0062	2.1
	30	0.433	0.0551	12.7	—	—	—
2	10	0.157	0.0041	2.6	—	—	—
	20	0.354[b]	0.0113	3.2	0.378	0.0099	2.6
	30	0.544	0.0184	3.4	—	—	—
3	10	0.203	0.0093	4.6	—	—	—
	20	0.449	0.0044	9.9	0.388	0.0386	9.9
	30	0.607	0.0562	9.3	—	—	—
4	10	0.203	0.0097	4.8	0.241[c]	0.0162	6.7
	20	0.457	0.0117	2.6	0.498[c]	0.0038	7.6
	30	0.669	0.0378	5.7	0.594[c]	0.0702	11.8
Pooled S.D.			0.0240			0.0258	

NOTE: The absorbance is the mean of four observations except where indicated otherwise. S.D. and C.V. denote standard deviation and coefficient of variation, respectively.
[a]Mean of 8 observations.
[b]Mean of 12 observations.
[c]6-day heating time.

3 days of heating time and that from Lot 2 is nearly linear for up to 2 days of heating time. Even though results are not linear for the entire heating range, in both cases the absorbance increases monotonically with heating time. This increase indicates that the concentration of amino groups is increasing.

Because (1) the amino groups present in silk occur only at the ends of the molecular chains and on the lysine and arginine side chains, and (2) the number of side chains can be assumed to remain constant, the increase in amino groups indicates that the chain length of the silk molecules decreases with heating time. Such a result would of course also reduce the breaking strength of the fiber as was indeed observed. Until the absolute number of amino groups of each type originally present in the silk can be determined or estimated, calculation of the change in length of the silk molecules with heating will not be possible. Adequate approximations, however, might be made on the basis of calibration curves of reference amino acids and published lists of the amino acid composition of silk.

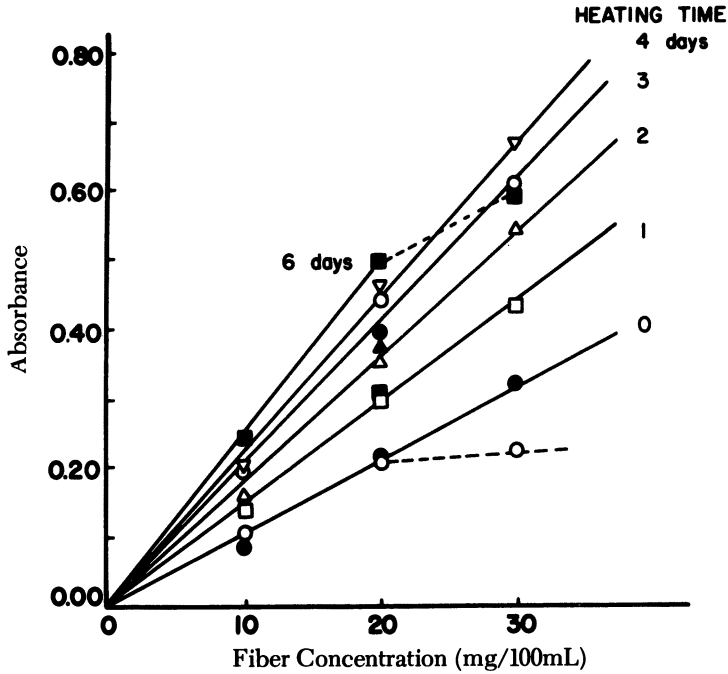

Figure 4. Absorbance of ninhydrin solution obtained from fabric 605 (Lots 1 and 2) after heating at 150 °C as a function of fiber concentration. Key: open symbols, Lot 1; filled symbols, Lot 2.

Light Degradation. STRENGTH. The breaking strengths of yarns extracted from the silk fabric after irradiation with the xenon arc lamp are shown in Table III and Figure 6. The strength retained is based on the breaking load of the fabric that was not irradiated.

On the basis of the arguments presented earlier concerning heat aging, the rate of decrease in strength of silk yarn exposed to light is a first-order reaction. A regression analysis of the data in Figure 6 gives $k_{warp} = -0.130$/day and $k_{weft} = -0.143$/day with intercepts of 108.9% and 113.3%, respectively. Thus, the rate of degradation is about 13%/day or about 0.5%/h, which is only about one-fourth of that (2.2%/h) produced by heating at 150 °C.

AMINO GROUP CONTENT. The amino group concentrations measured on the silk fabric exposed to light are shown in Table III and Figure 7. A regression analysis of these data indicates that the absorbance increases linearly with exposure time at the rate of 0.0179 absorbance units/day, which is about 22% of that (0.081 units/day, Table IV) produced by heating at 150 °C. Thus, exposure to heat at 150 °C degrades the strength and increases the amino group content of silk about five

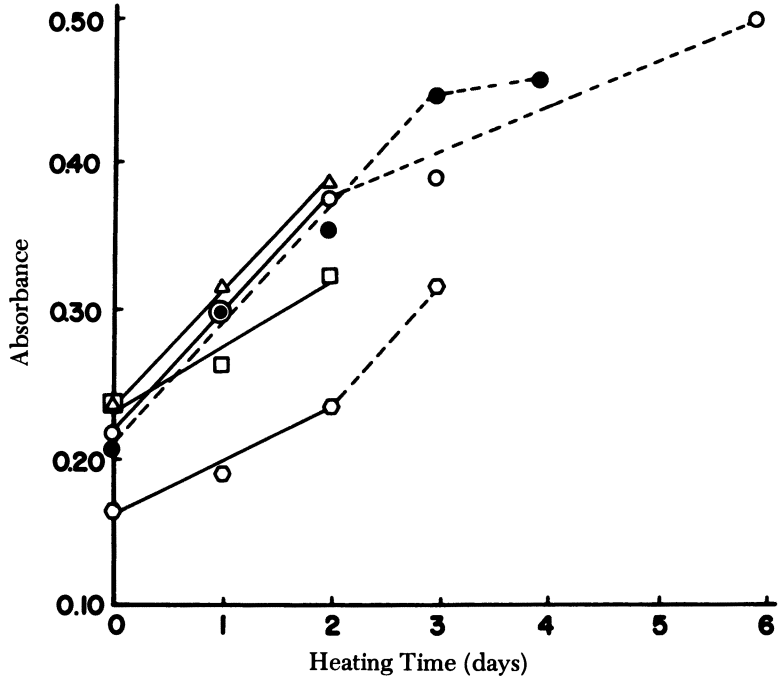

Figure 5. Absorbance of ninhydrin solution obtained from untreated fabric and fabric treated with the deacidifying agent and the two antioxidants as a function of heating time at 150 °C (Lots 1 and 2). Key: ●, untreated Lot 1; ○, untreated Lot 2; △, deacidifying agent; ⬡, Compound I; □, Compound II.

times as fast as does exposure to the xenon arc lamp under the conditions employed here. The relationship between strength decrease and amino group increase is therefore similar for both light and heat exposure.

Effect of Additives on Heat Degradation. The effects of applying the additives to silk on the breaking strength and absorbance are shown in Tables I and IV and in Figures 3 and 5. From these data, particularly from the values of rate constants for strength loss given in Table I, it is evident that none of these additives retard the degradation as measured by breaking strength. However, the silk fabrics were greatly stiffened by the application of the additives, which might have affected the breaking strength. In contrast, the two hindered phenol antioxidants do seem to retard the formation of amino groups. Caution is needed in interpreting the effect of Compound I, however, because some evidence suggests that this compound has interfered with the ninhydrin reaction (by the consistent drop of 0.05 in absorbance, Figure 5). This observation may not be entirely unexpected because the add-on of Compound I was unrea-

Published on February 1, 1986 on http://pubs.acs.org | doi: 10.1021/ba-1986-0212.ch006

Table III. Breaking Load of Warp and Weft Yarns and Absorbance of Ninhydrin Solution Obtained from Silk Fabric Lot 2 After Exposure to Xenon Arc Lamp

Exposure Time (days)	*Breaking Load Warp*[a]				*Breaking Load Weft*[b]				*Absorbance*[c]		
	Mean (gf)	*S.D. (gf)*	*C.V. (%)*	*S.R.*[d] *(%)*	*Mean (gf)*	*S.D. (gf)*	*C.V. (%)*	*S.R.*[d] *(%)*	*Mean*	*S.D.*	*C.V. (%)*
0	127.9	9.48	7.41	100.0	121.9	7.54	6.18	100.0	0.216	0.0155	7.2
2	113.8	8.19	7.19	88.9	115.6	12.00	10.38	94.9	0.245	0.0061	2.5
5	84.3	7.28	8.63	65.9	73.2	9.50	12.98	60.1	0.283	0.0032	1.1
6	62.6	6.60	10.55	48.9	59.7	7.20	12.05	49.0	0.308	0.0031	0.9
7	60.3	6.74	11.17	47.1	53.5	4.01	7.51	43.9	0.346	0.0073	2.4
8	43.5	5.42	12.47	34.0	38.1	5.04	13.21	31.3	0.359	0.0073	2.0
Pooled S.D.		7.40				8.00				0.0082	

NOTE: The breaking load is the mean of 21 breaks, and the absorbance is the mean of four observations. S.D., C.V., and gf denote standard deviation, coefficient of variation, and gram-force, respectively.
[a]The degradation rate was −13.0%/day.
[b]The degradation rate was −14.3%/day.
[c]The rate of increase was 0.0179 A/day.
[d]S.R. is strength retained.

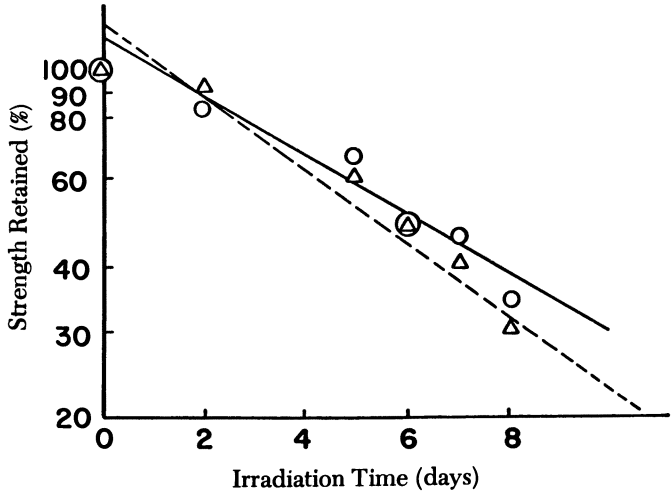

Figure 6. Logarithm of strength retained of warp and weft yarns from fabric 605 (Lot 2) as a function of irradiation time.
Key: —○, warp; ---△, weft.

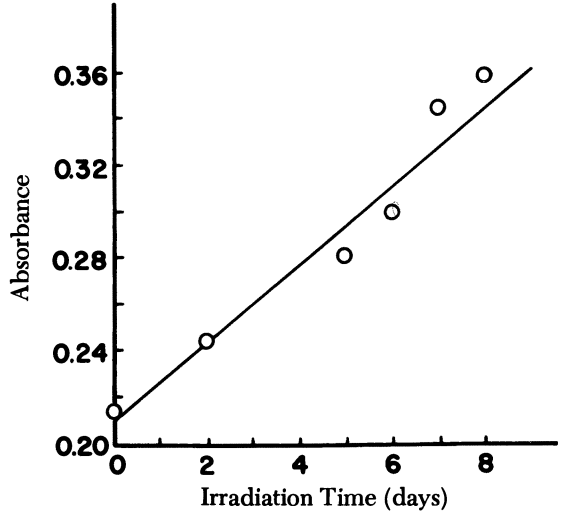

Figure 7. Absorbance of ninhydrin solution obtained from fabric 605 (Lot 2) as a function of irradiation time.

Table IV. Absorbance of the Ninhydrin Solution Obtained from Treated and Untreated Silk Fabric Lot 2 After Heating

Treatment	*Heating Time (days)*	*Absorbance*			*Rate of Increase* $m = (A_2 - A_0)/2$ *(day^{-1})*
		Mean	*S.D.*	*C.V. (%)*	
None	0	0.216	0.0155	7.2	0.0810
	1	0.300	0.0062	2.1	
	2	0.378	0.0099	2.6	
	3	0.388	0.0386	9.9	
	6	0.498	0.0038	0.8	
Deacidifying agent	0	0.236	0.0084	3.6	0.0750
	1	0.316	0.0014	0.4	
	2	0.386	0.0015	0.4	
Compound I	0	0.164	0.0047	2.9	0.0355
	1	0.190	0.0024	1.2	
	2	0.235	0.0108	4.6	
	3	0.314	0.0227	7.2	
Compound II	0	0.233	0.0093	4.0	0.0445
	1	0.261	0.0061	2.4	
	2	0.322	0.0042	1.3	
Pooled S.D.			0.0136		

NOTE: The absorbance is the mean of four observations. S.D. and C.V. denote standard deviation and coefficient of variation, respectively. A_0 and A_2 are the absorbance before heating and after heating 2 days, respectively.

sonably high (33%). In contrast, the deacidifying agent has little effect on the absorbance.

Thus, none of these additives show any great promise at this stage of the study. Investigations of other compounds, application procedures and concentrations, and evaluation procedures, however, could lead to useful stabilizers.

Conclusions

The rate of degradation of silk as measured by strength loss produced by heating dry at 150 °C and exposing to light appears to be first order, a relationship that will permit the extent of degradation to be calculated for any heating or exposure time on the basis of measurements made after only a few different heating times. This result was confirmed by measurements made on two different lots of silk. The rate of degradation as measured by the formation of (α + ϵ)-amino groups increased linearly with heating time. However, amino group formation did not proceed far enough to establish the degradation kinetics.

The three additives as applied are not effective in retarding degradation as measured by breaking strength; however, the two hindered

phenol antioxidants did seem to retard formation of amino groups. This inconsistency in behavior might be attributed to the fact that the fabrics were greatly stiffened by the additives, a change that could lower the breaking strength. Further, the effectiveness of the additives might have been increased if the fabrics were heated in the presence of moisture as was seen in an earlier study made on cotton (*4*). In cotton a deacidifying agent did not protect the fabric against strength loss under dry aging conditions, but it did in the presence of moisture. A similar effect might be occurring with the materials examined in this study.

Studies are continuing to further elucidate the degradation mechanisms and to evaluate additional compounds as possible stabilizers. The effect of additive type, concentration, and application procedures will be determined as well as that of other aging conditions and evaluation methods.

Acknowledgments

This investigation was supported in part by the National Museum Act, which is administered by the Smithsonian Institution. We are grateful for this assistance. We also wish to express our gratitude to Kathryn Dowling who carried out many of the reported experiments.

Literature Cited

1. Berry, G. M.; Hersh, S. P.; Tucker, P. A.; Walsh, W. K. In "Preservation of Paper and Textiles of Historic and Artistic Value"; Williams, J. C., Ed.; ADVANCES IN CHEMISTRY SERIES No. 164; American Chemical Society: Washington, D.C., 1977; pp. 228–48.
2. Berry, G. M.; Hersh, S. P.; Tucker, P. A.; Walsh, W. K. In "Preservation of Paper and Textiles of Historic and Artistic Value"; Williams, J. C., Ed.; ADVANCES IN CHEMISTRY SERIES No. 164; American Chemical Society: Washington, D.C., 1977, pp. 249–60.
3. Tucker, P. A.; Hersh, S. P.; Berry, G. M.; Kerr, N.; McElwain, D. M. In "Electron Microscopy 1978, Vol 1, Physics"; Sturgess, J. M., Ed.; Microscopical Society of Canada: Toronto, 1978; pp. 494–95.
4. Kerr, N.; Hersh, S. P.; Tucker, P. A.; Berry, G. M. "In Durability of Macromolecular Materials"; Eby, R. K., Ed.; ACS SYMPOSIUM SERIES No. 95; American Chemical Society: Washington, D.C., 1979, 357–69.
5. Hutchins, J. K.; Hersh, S. P.; Tucker, P. A.; McElwain, D. M.; Kerr, N. In "Preservation of Paper and Textiles of Historic and Artistic Value II"; Williams, J. C., Ed.; ADVANCES IN CHEMISTRY SERIES No. 193; American Chemical Society: Washington, D.C., 1981; pp. 315–32.
6. Hersh, S. P.; Hutchins, J. K.; Tucker, P. A.; Kerr, N. *Proc. Int. Conf. Conserv. Restoration Text., Como, Italy, 1980,* C.I.S.S.T., Lombardy Section, Milan, 1982., 87–95.
7. Kerr, N.; Hersh, S. P.; Tucker, P. A. *Prepr. Wash. Congr. Sci. Technol. Serv. Conserv.* 1982; Brommelle, N. S. and Thomson, G., Eds.; The International Institute for Conservation of Historic and Artistic Works: London, 100–3.

8. Kerr, N.; Hersh, S. P.; Tucker, P. A. *Prepr. ICOM Comm. Conserv. 7th Triennial Meet.* **1984**, Copenhagen, Denmark, 84.9.25-84.9.29.
9. Tucker, P.; Kerr, N.; Hersh, S. P. "Photochemical Damage of Textiles"; presented at the 1980 Textile Preservation Symposium: Textiles and Museum Lighting, Harpers Ferry Regional Textile Group, Washington, D.C., December 1980.
10. Vigo, T. L. In "Preservation of Paper and Textiles of Historic and Artistic Value"; Williams, J. C., Ed.; ADVANCES IN CHEMISTRY SERIES No. 164; American Chemical Society: Washington, D.C., 1977; pp. 189-207.
11. Rutherford, H. A.; and Harris, M. *Am. Dyest. Rep.* **1941**, *30*, 345-46, 363-64.
12. Tyler, A. G. *Text. J. Aust.* **1949**, *24*, 404-7, 464.
13. Bogle, M. M. "The Deterioration of Silks Through Artificial Weighting," Textile Conservation Center Notes, No. 11; Merrimack Valley Textile Museum: North Andover, Mass., 1979.
14. Ross, J. E.; Johnson, R. L.; Edgar, R. *Text. Res.* **1936**, *6*, 207-16.
15. Harris, M. *Am. Dyest. Rep.* **1934**, 23, 403-404.
16. Roberts, N. M.; Mack, P. B. *Rayon Melliand Text. Mon.* **1956**, *17*, 49-53.
17. D'Olier, A. A.; Mack, P. B. *Rayon Melliand Text. Mon.* **1956**, *17*, 102.
18. "AATCC Technical Manual"; American Association of Textile Chemists and Colorists: Research Triangle Park, North Carolina, 1982, Vol. 57, pp. 160-62.
19. *Annu. Book ASTM Stand.* **1983**, *07-01*, 401-10.
20. Knott, J.; Grandmaire, M.; and Thelen, J. *J. Text. Inst.* **1981**, *72*, 19-25.
21. Kelly, G. B.; Tang, L. C.; Krasnow, M. K. In "Preservation of Paper and Textiles of Historic and Artistic Value"; Williams, J. C., Ed.; ADVANCES IN CHEMISTRY SERIES No. 164; American Chemical Society: Washington, D.C., 1977; pp. 62-71.

RECEIVED for review November 26, 1984. ACCEPTED March 15, 1985.

7

A Systematic Method for Differentiating Between 18th Century Painted-Printed Chinese and Western Silks

Maruta Skelton[1] and Leanna Lee-Whitman[2]

[1]The Henry Francis du Pont Winterthur Museum and Gardens, Winterthur, DE 19735
[2]CIGNA Museum and Art Collection, Philadelphia, PA 19103

Problems of classification of 18th century painted-printed Chinese and Western silk textiles are discussed with emphasis on how nondestructive X-ray fluorescent (XRF) analyses of pigment-dye pastes and paints can be combined with visually observable physical characteristics, painterly techniques, and art historical research to separate Chinese silks from Western ones. This unique documentation process is the result of our joint, 2-year study and shows how textile connoisseurship can be reinforced with scientific data. Thirty painted-printed 18th century silks from the textile and costume collections of the Cooper-Hewitt Museum; The Metropolitan Museum of Art in New York; Musée Historique des Tissus in Lyon, France; National Museum of American History; Philadelphia Museum of Art; Rhode Island Historical Society; and The Henry Francis du Pont Winterthur Museum were examined and analyzed by XRF for this study.

ART HISTORICAL RESEARCH on 18th century plain and patterned silks (*1*) combined with scientific data from the X-ray fluorescent (XRF) analyses of coloring matter on 18th century painted and printed silks is presented in this chapter. This study produced a systematic method for differentiating between Chinese and Western silks of the 18th century (*2*).

Historic Reasons for Existing Separation Problem

To see how the existing Chinese or Western silk separation problem developed, a brief look at the 18th century Chinese export silk trade is necessary.

0065-2393/86/0212-0131$06.25/0

In England, the British East India Company had a monopoly on trade with the East. An established sailing pattern for the British East India Company ships was to leave, in midwinter, from London for Canton, China, and return 13–14 months later. Meticulous records of this company's trade, as a result of silk being an important commodity imported directly from China, are housed at the India Office Library and Records in London. These records provide valuable information and documentation for several of the Chinese silk characteristics.

The influx of silks from the East produced several reactions in Europe. France and England, to protect internal silk and wool industries, issued prohibition acts forbidding the importation of Eastern silks and cottons for home use. To comply with these laws, English merchants bought the fabrics at British East India Company sales in London and then promptly reexported them in accordance with both the law and specific orders to merchants in the British North American colonial ports and elsewhere. Another European reaction to Eastern imports was that the popular taste for exotic Oriental patterns prompted European adaptations of Chinese styles, and elements such as pagodas, priests, and parasol canopies set the pattern and tone for these so-called "chinoiserie" decorations (Figure 1). In France, Holland, and Flanders special factories were set up for the painting and printing of chinoiserie textiles (3). Also prevalent were the practice of sending back to China

Figure 1. Western chinoiserie design on an 18th century French painted-printed silk moire. (Acc. No. 57.1277, courtesy of The Henry Francis du Pont Winterthur Museum.)

samples of the Western chinoiserie designs for Chinese artisans to copy and the smuggling of painted and printed Chinese silks back into England and France.

It is no surprise then that American and European collections now house large numbers of 18th century silks that, on the basis of their appearances, could be of either Chinese or Western origin. The results of this study are addressed to the question of the provenance, that is, the documented origin, of these silks.

Physical Characteristics of Chinese Silks

The four physical characteristics of silks of Chinese origin (Table I) are the result of Lee-Whitman's research on plain and patterned silks (*1*) and our observations of the Chinese silks available to us for study.

The critical selvedge-to-selvedge measurements for Chinese silks are given in British East India Company records as 2–2.2 covids (a covid is equivalent to approximately 14.1 in.). Extant 18th century Chinese silks measure consistently between 28 and 31 in. Western silks are characteristically narrower; their selvedge-to-selvedge widths range from 19½ to 23 in.

In Chinese silks of both plain weave and satin weave, the selvedges were observed to contrast in color, and at times in weave, from the ground color of the fabric. (White Chinese silks often had yellow or green selvedges.) Such a contrast was not regularly found on Western silks.

Table I. Summary of Physical Characteristics of Chinese and Western Silks

Characteristic	*Chinese Silks*	*Western Silks*
Selvedge-to-selvedge width	28–31 in.	19½–23 in.
Contrasting selvedge	always contrasting in color and sometimes in weave from ground	contrasting colors and weaves sometimes present
Temple holes	2–5 sequential holes ($^1/_{32}$–$^3/_{32}$ in. in diameter) in the selvedges	randomly placed holes, pressure marks, or sequentially distributed pin-sized holes in the selvedges
Fabric finish	soft sheen and feel	sometimes soft sheen and feel, but not to the same extent as Chinese silks

SOURCE: Reproduced with permission from Ref. 2. Copyright 1984 The Textile Museum.

Temples are weaving tools consisting of two crossed rods having pin points protruding at each end. Chinese weavers placed the temple rods on an already woven portion of fabric while it was still on the loom so that the end pins pierced the material's selvedges and kept the fabric evenly stretched. This procedure produced permanent, evenly spaced, temple holes in the selvedges of Chinese silks (Figure 2). None of the Western pieces that we examined had such repeating, sequential temple holes in the selvedges.

The fourth physical characteristic of Chinese silks, a soft "hand", we feel is the result of calendering, which is a characteristic mechanical method for finishing silks in China (Figure 3). This process involves a stone base plate, a wooden roller, and a heavy rocking stone. The silk fabric is placed on a roller and subjected to intense pressure as a workman rocks back and forth on a rocking stone. This process leaves an unmistakable sheen and soft clinging hand that can distinguish Chinese silks from Western ones.

Figure 2. Temple holes in the selvedge of an 18th century Chinese painted silk gauze. (Acc. No. 68.48, courtesy of The Henry Francis du Pont Winterthur Museum.)

Figure 3. Chinese workman standing on a calendering stone. (Reproduced from Ref. 13.)

Painterly and Coloration Characteristics of Chinese and Western Silks

The seven painterly and coloration characteristics of Chinese and Western silks (Table II) are the result of research into Chinese painting methods and XRF analyses of the pigment and dye pastes and paints on the 30 painted and printed silks included in this study.

Painting-Printing Techniques. The calligraphic brush stroke is a painting characteristic unique to Chinese hand-painted silks.

Table II. Summary of Painterly and Coloration Characteristics of Chinese and Western Silks

Characteristic	*Chinese Silks*	*Western Silks*
Calligraphic brush stroke	present	none
Printed outline	overpainted, seeps through to reverse	clearly evident as part of design
Consistency of coloring matter	very thick paint and pigment-dye pastes	less viscous pigment-dye pastes
Use of white paint and/or ground	lead white and chalk or oyster shell white pigments	no use of white paint or ground
Copper green pigment	probably malachite	probably verdigris
Brown pigment	iron oxide pigments	organic pigments
Silver	outlines and accents	none

SOURCE: Reproduced with permission from Ref. 2. Copyright 1984 The Textile Museum.

Chinese brush strokes have precisely formed beginnings, and if a tailing off occurs, it must be controlled equally well, as illustrated in Figure 4. Western brush strokes are quite different and leave lines that vary in sharpness and distinctiveness.

A difference is also apparent in how designs were laid out and then painted or printed on the Chinese and Western silks.

Figure 4. Some Chinese brush strokes. Note in particular the nail-headed rat tails (E). (Reproduced with permission from Ref. 14. Copyright 1962 Charles E. Tuttle.)

The Chinese first printed an outline for use as a spacing guide. The ink they used for this outline must have been quite watery because it had seeped through to the back of all the Chinese silks we examined (Figure 5). This black-ink outline provided a large design area having open regions to be filled in with smaller design elements. Colors and calligraphic lines were then painted-printed over this printed outline covering it entirely.

Western silks tend to have very obvious printed outlines that are replicated exactly in the repeat motifs. No attempt is made to cover the outlines because they are an integral part of the design (Figure 6). Western printed black outlines do not seep through to the back of the silk (2) like the Chinese outlines do.

XRF Pigment Analyses. The last five painterly and coloration characteristics listed in Table II are the result of XRF pigment analyses and show how these data can be used to extend and reenforce the visually observable physical characteristics and painting techniques.

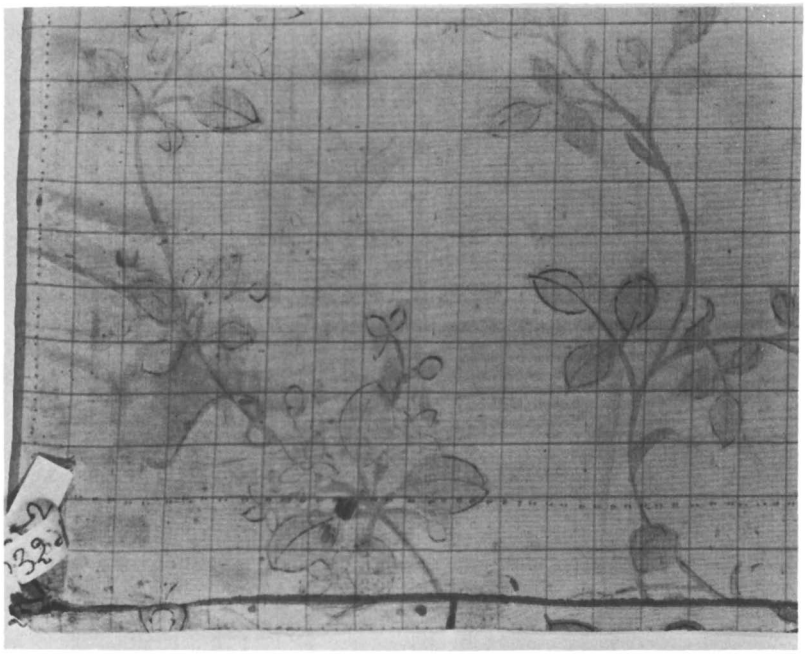

Figure 5. Seepage of the black-ink outline to the back of an 18th century Chinese silk. (Acc. No. 18032, courtesy of the Musée Historique des Tissus, Lyon.)

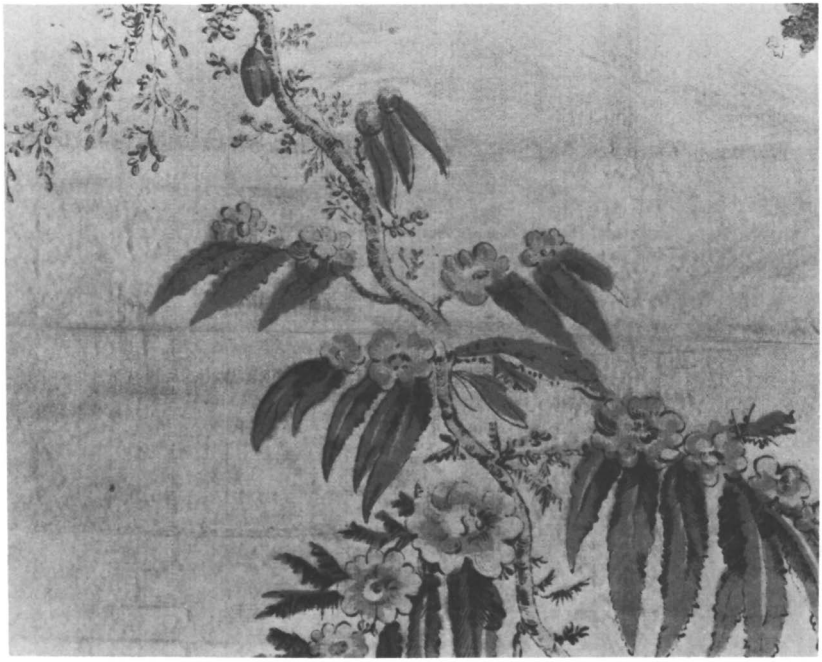

Figure 6. Western printed black outline as part of the design on an 18th century French painted-printed silk. (Acc. No. 1640/1, courtesy of the Musée Historique des Tissus.)

Experimental

XRF is a physical process involving the emission of characteristic radiation from the atoms of a material that has been stimulated by incident radiation (Figure 7). By analyzing this response, the inorganic constituents of any object may be identified (*4*).

The nondestructive nature, speed, and high sensitivity of this technique, particularly useful in worn and fragile paint areas, makes it ideal for the study of pigment characteristics of old silks.

The analyses were performed at The Henry Francis du Pont Winterthur Museum on a Kevex 4525P energy dispersive XRF spectrometer; low-level radioactive isotopes were used for the incident radiation (*4*). The pigment area analyzed was successively irradiated by an iron-55 source, an americium-241 source, and a cadmium-109 source. A qualitative pigment analysis takes only 6 min. Neither the coloring matter nor the silk fabric is altered in any way by the measurement. Figure 8 shows our XRF system setup for the analysis of pigments on painted and printed silks.

Special precautions had to be taken in handling the fragile, 200-year-old silks so that we could obtain the necessary scientific data without further damaging the fabrics in any way.

The analysis area must be as level as possible so as to properly support the textile. All areas of contact between equipment and fabric were lined with

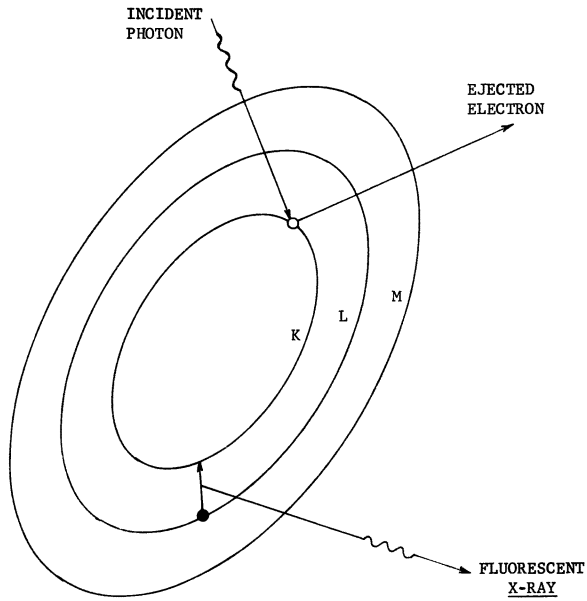

Figure 7. Mechanism for the generation of fluorescent X-rays.

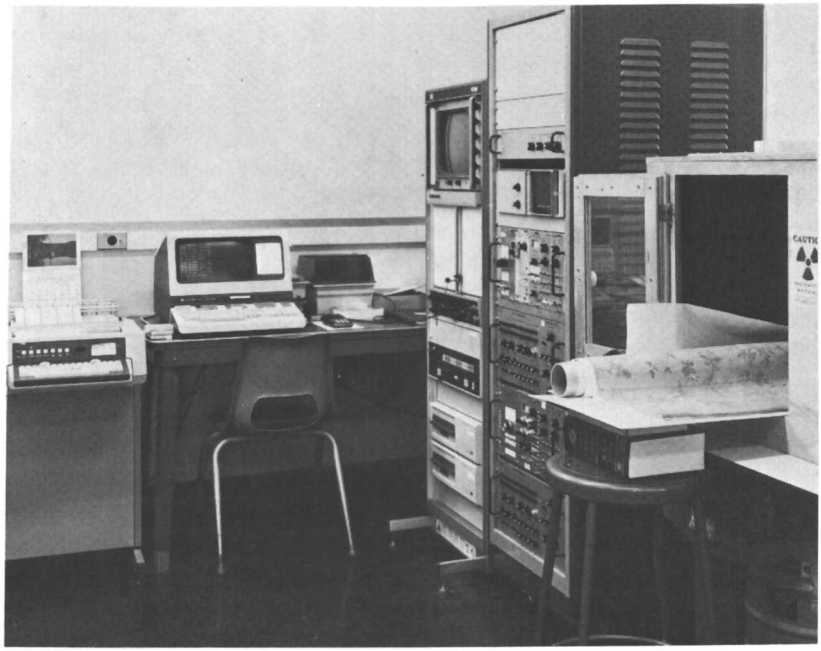

Figure 8. The Henry Francis du Pont Winterthur Museum's analytical laboratory setup for the analysis of pigments on painted silk. (Courtesy of The Henry Francis du Pont Winterthur Museum.)

white, acid-free paper. The painted silk pieces, which had been carefully stored on acid-free rolls, were unrolled only to the areas containing the pigments to be analyzed, and only that pigment area was carefully placed over the radioactive source for irradiation. In the case of the painted silk gown in Figure 9, only the pigments in the hemline area were analyzed.

XRF analyses were performed on the pigments of 22 Chinese and 8 Western painted and printed silks from the silk and costume collections of the Cooper-Hewitt Museum; The Metropolitan Museum of Art in New York; Musée Historique des Tissus in Lyon, France; National Museum of American History; Philadelphia Museum of Art; Rhode Island Historical Society; and The Henry Francis du Pont Winterthur Museum.

Paint and Pigment-Dye Paste Considerations

Even though we found that similar, visual colors were used on both the Chinese and Western silks, detectable differences in pigment-dye application and composition do exist and can be used for characterization.

Consistency of Coloring Matter. With the exception of the underlying ink outline, all surface coloration on Chinese silks appears to be due to the use of thick and opaque paints or pigment and dye pastes.

Figure 9. The Henry Francis du Pont Winterthur Museum's analytical laboratory and conservation staff preparing an 18th century painted silk gown for pigment analysis. (Acc. No. 42-33-2, Philadelphia Museum of Art; courtesy of The Henry Francis du Pont Winterthur Museum.)

The coloration remains on the surface of the fabric. The pigment and dye pastes used to print Western silks were much less viscous than the paints and pastes used on Chinese silks.

Visual Colors and Pigment Formulas. Organic blues, reds, pinks, purples, yellows, and greens are common to both Chinese and Western coloration, as are also the inorganic copper blues and greens, vermilion, and Prussian blue. Even though the minerals azurite, malachite, and cinnabar have been traditional Chinese pigments for centuries, all the pigments listed in Table III were in use in both China and Europe in the 18th century (*5*).

Pigment Composition. XRF pigment analysis picks up only the inorganic elements in the pigment formulas. This type of analysis was sufficient to establish the following four typically Chinese pigment characteristics (characteristics 4–7 in Table II): (1) the use of white lead pigment as a white paint or ground layer, (2) the use of a "jade green" copper pigment, (3) the use of iron oxide brown pigments, and (4) the use of silver paint for outlines and accents on flower petals and leaves.

Table III. Known 18th Century Pigments Used in China and Europe

Pigment	*Color*	*Chemical Formula or Source*
Inorganic		
White lead	white	$2PbCO_3 \cdot Pb(OH)_2$
Chalk	white	$CaCO_3$
Azurite and blue verditer	blue	$2CuCO_3 \cdot Cu(OH)_2$
Prussian blue	blue	$Fe_4(Fe(CN)_6)_3$
Vermilion (cinnabar)	red	HgS
Red lead	red	Pb_3O_4
Realgar	orange-red	As_2S_2
Orpiment	yellow	As_2S_3
Malachite	green	$CuCO_3 \cdot Cu(OH)_2$
Verdigris	green	$Cu(C_2H_3O_2)_2 \cdot 2Cu(OH)_2$
Iron oxides (sienna and ochre)	brown	$Fe_2O_3 \cdot H_2O$, clay, etc.
Bone black	black	$C + Ca_3(PO_4)_2$
Silver	silver	Ag
Organic		
Indigo	blue	*Indigofera tinctoria*
Madder	red	*Rubia tinctoria*
Gamboge and rattan yellow	yellow	*Garcinia*
Plant green or herb green	green	indigo + gamboge or rattan yellow
Lampblack or carbon black	black	soot (C)
Asphaltum	brown	natural oil deposits
Sepia	brown	*Sepia officinalis*

SOURCE: Reproduced with permission from Ref. 2. Copyright 1984 The Textile Museum.

THE CHINESE WHITE TECHNIQUE. The most apparent pigment characteristic found on 18th century Chinese painted and printed silks is the use of a ground layer of white paint beneath most of the colors. XRF analyses showed that the Chinese white-painted ground layer, in most cases, contains white lead pigment. Table IV summarizes the elements detected by XRF for the pigments that were present on the painted silk illustrated in Figure 10 and gives a possible pigment identification based on these data. Note the use of a white lead ground layer under almost all the colors.

This painting technique is related to a centuries-old Chinese tradition for naturalistic flower painting in which white paint is used to form a base to give greater depth to the paint laid over it. Also, details can be painted onto the white paint without a loss of clarity, and it can be mixed with other colors to alter the strength of the tones (*6*). All 22 Chinese silks available for study showed this particular characteristic.

WESTERN WHITE TECHNIQUE. When the Chinese use of white color on 18th century silks is compared to the use of white color on 18th

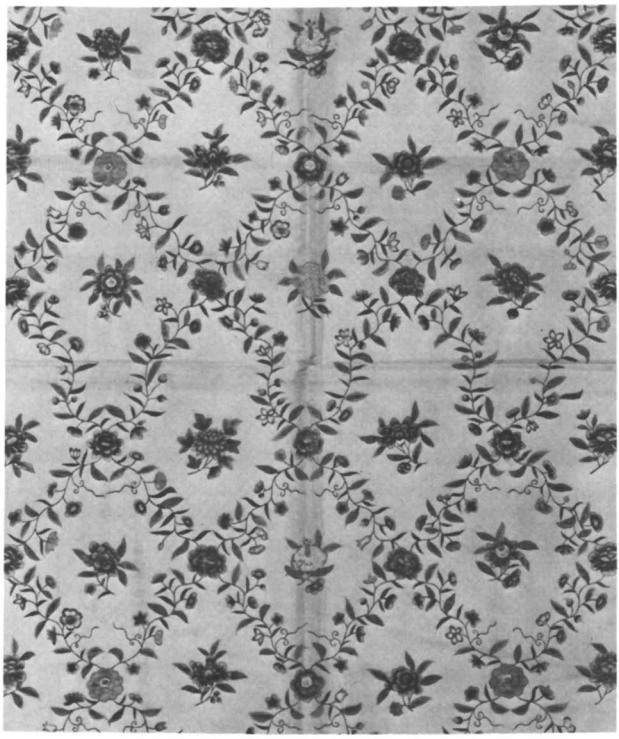

Figure 10. An 18th century painted Chinese silk showing heavy use of white lead ground layer and copper green pigment. (Acc. No. 32554, courtesy of the Musée Historique des Tissus, Lyon.)

Published on February 1, 1986 on http://pubs.acs.org | doi: 10.1021/ba-1986-0212.ch007

Table IV. Pigment Analysis Data for Figure 10

Color	*Elements Detected*[a]	*Possible Pigment*
Blue	***Pb, Cu,*** Ag, ***Fe,*** Sn, Ba, Sb	azurite + Prussian blue and lead white
Red	***Pb,*** Ag, Sn, ***Hg,*** K, Cu, Ba, Sb	vermilion and lead white
Purple	***Pb,*** Ag, K, Sn, Ba	organic compound and lead white
Orange	***Pb,*** Ag, ***Hg,*** K, Sn, Ba, Cu	vermilion and lead white
Yellow	***Pb,*** Ag, K, Ba, Sn	gamboge and lead white
Dark green	Ca, Ag	plant green
Jade green	***Pb, Cu,*** Ca, Ag, Fe, Sn	malachite and lead white
White	***Pb,*** Ag, Ba, Sn, Sb	lead white

[a]Detected elements are listed in order of decreasing concentration, and major pigment elements are italicized. Silver outlines or highlights are present on every color.

century Western silks, the major difference found is that the Western technique uses the white fabric itself for white coloration rather than white pigment (Figure 14 and Table VIII).

COPPER GREEN PIGMENTS. The next Chinese pigment characteristic involves a type of mineral green pigment used by the Chinese. Chinese and Western artisans used organic and inorganic green pigments on silks. Even though XRF analyses showed that the pigment element of both the Chinese and Western inorganic greens was copper, it appears that a visual distinction can be made between the two pigment possibilities of malachite, a copper carbonate; and verdigris, a copper acetate (*see* Table IV and Figure 10 for XRF analysis data for Chinese greens and Table V and Figure 11 for XRF analysis data for Western greens). Because copper acetate is susceptible to hydrolysis, a dark brown product, probably CuO, is formed upon its subsequent oxidation. We found that the copper greens of the Western pieces seemed to have such

Table V. Pigment Analysis Data for Figure 11

Color	*Elements Detected*[a]	*Possible Pigment*
Red	—	organic red (madder)
Purple	Ca, Sn	organic compound or pigment
Yellow	—	organic yellow (gamboge)
Dark brown	K	organic brown pigment
Brown-pink	K	organic compound
Green	*Cu*, K	verdigris

[a]Detected elements are listed in order of decreasing concentration, and major pigment elements are italicized.
SOURCE: Reproduced with permission from Ref. 2. Copyright 1984 The Textile Museum.

Figure 11. An 18th century painted Western silk showing the presence of discolored copper green pigment and the use of an organic brown pigment-dye paste or paint. (Acc. No. 26592, courtesy of the Musée Historique des Tissus, Lyon.)

a brown discoloration, but the copper greens on the 22 Chinese pieces were not discolored in this manner.

Positive wet microchemical and microscopic identifications were permitted for the copper greens on only two of the Chinese silks. In both cases the result was the copper carbonate pigment malachite, which confirmed that Chinese copper greens were malachite and the Western ones were verdigris. A positive identification should be performed whenever conservation conditions permit it and trained personnel are available (7).

BROWN PIGMENTS. A distinction is also apparent between the brown pigments used on the Chinese and Western painted and printed silks that were available to us for study. XRF analyses revealed that the various shades of brown present on the Chinese silks were iron oxide pigments, whereas the brown colors present on the Western silks were organic pigments (*see* Table V and Figure 11 for Western browns and Table VI and Figure 12 for Chinese browns).

SILVER OUTLINES ON CHINESE FLORAL MOTIFS. Perhaps the most fascinating Chinese pigment characteristic is the use of silver outlines and accents on floral motifs.

The detection of silver by XRF on some 18th century Chinese painted silk fragments is what began our full-scale inquiry into the possible separation of Chinese and Western painted silks. The difficulty that delayed the explanation of this finding was that the silver paint used to outline flower petals and leaves had either worn off or had tarnished to such a degree that what remained looked like just an underlying black-ink outline. Only the high sensitivity of the XRF technique to silver revealed its presence on the silk fragments.

Table VI. Pigment Analysis Data for Figure 12

Color	*Elements Detected*[a]	*Possible Pigment*
Blue	*Pb*, Ag	indigo and white lead ground
Red	*Pb*, *Hg*, Ag	vermilion and white lead ground
Purple	*Pb*, Ag	organic compound or pigment and white lead ground
Brown	*Pb*, *Fe*, Ag	iron oxide pigment and white lead ground
White	*Pb*, Ag	white lead
Light green	*Cu*, Ba, Ag	malachite
Medium green	*Cu*, Ba, Ag	malachite
Dark green	*Ca*, Ag	plant green with chalk as ground or opacifier
Gray	*Pb*, *Ag*	silver and white lead ground

[a]Detected elements are listed in order of decreasing concentration, and major pigment elements are italicized. Silver highlights are present on every color.
SOURCE: Reproduced with permission from Ref. 2. Copyright 1984 The Textile Museum.

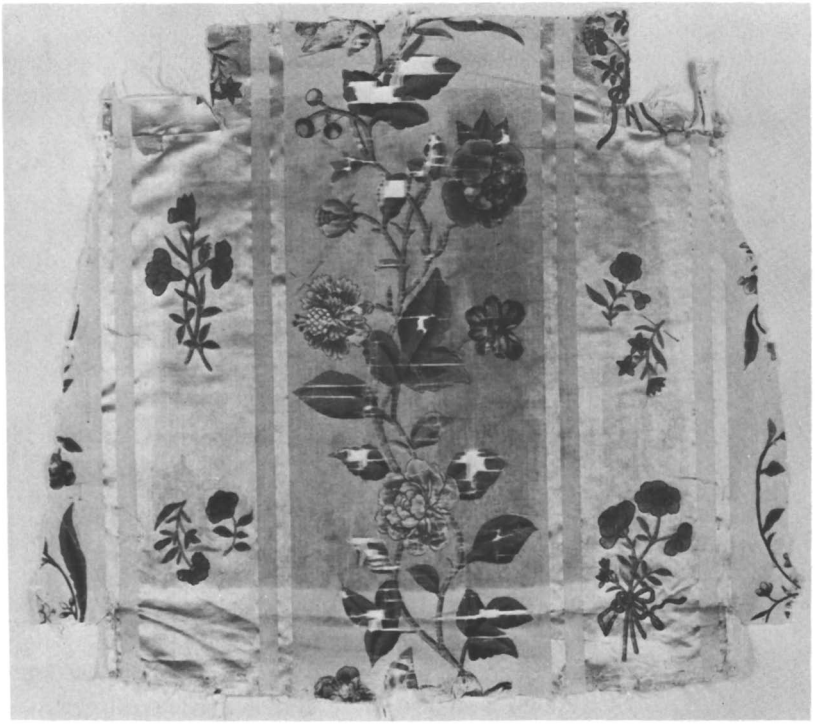

Figure 12. An 18th century painted Chinese silk on which an iron oxide brown pigment was used. (Acc. No. 1981.0008, courtesy of the Smithsonian Institution.)

The addition of painted silver outlines and accents to floral motifs was observed to be a pervasive practice unique to Chinese 18th century painted silks. Flower petals, veins of leaves, wandering tendrils, and even stems have overpainted silver outlines; yet, because silver tarnishes so readily upon exposure to air, most remaining silver pigmentation is barely visible. Only on the rare unused silk length can the full glittering effect of the silver embellishment be seen, and not until we had actually seen the silver on the piece in Figure 13 was the mystery solved. In Table VII, note the detection of silver on every color of this beautifully preserved 18th century Chinese painted silk.

None of the Western silks in this study were found to have silver used for either outlining or accents. Only localized outlining in gold was found on a few painted and printed Western silks (Table VIII and Figure 14).

PRECEDENT FOR SILVER OUTLINE TECHNIQUE. After many interesting but false leads into Indian textiles (*8*) and Chinese (*9, 10*) and

Table VII. Pigment Analysis Data for Figure 13

Color	*Elements Detected*[a]	*Possible Pigment*
Blue	*Pb*, Ag, *Cu*, K, *Fe*	azurite + Prussian blue and white lead ground
Red	*Pb*, Ag	organic red and/or red lead and white lead ground
Purple	*Pb*, Ag	organic compound or pigment and white lead ground
Dark green	*Pb*, *Cu*, Ca, Ag	malachite and white lead ground
Medium green	*Cu*, Ag, Pb	malachite
Olive green	*Pb*, Ag, *Cu*	malachite and white lead ground
White	*Pb*, Ag	white lead

[a]Detected elements are listed in order of decreasing concentration, and major pigment elements are italicized. Silver highlights are present on every color.
SOURCE: Reproduced with permission from Ref. 2. Copyright 1984 The Textile Museum.

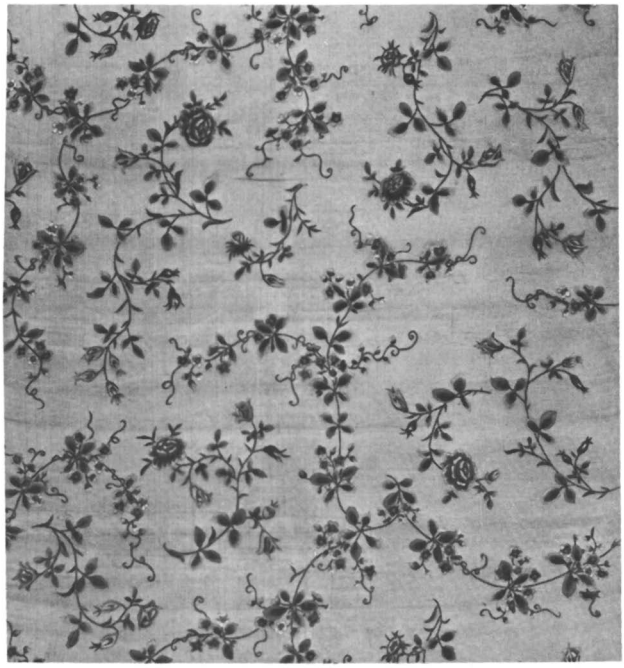

Figure 13. An 18th century painted Chinese silk gauze with visible silver outlines. (Acc. No. 68.48, courtesy of The Henry Francis du Pont Winterthur Museum.)

Table VIII. Pigment Analysis Data for Figure 14

Color	*Elements Detected*[a]	*Possible Pigment*
Blue	*Fe*, Ca, Au	Prussian blue
Red	Ca, *Hg*, Au	vermilion
Light brown (flowers)	Sn, Ca, Au	organic brown (ashphaltum)
Dark brown (stem)	Ca	organic brown
Green	*Fe*, Ca, K, Au	green earth

[a]Detected elements are listed in order of decreasing concentration, and major pigment elements are italicized. Gold highlights are present on every color except dark brown for the areas analyzed.
SOURCE: Reproduced with permission from Ref. 2. Copyright 1984 The Textile Museum.

Figure 14. An 18th century painted-printed Western silk with gold accents. (Acc. No. 29015, courtesy of the Musée Historique des Tissus, Lyon.)

Indian (*11*) painting techniques, we now believe that the precedent for the use of silver in this manner on Chinese textiles is of considerable antiquity.

In the 1920s, numerous painted and embroidered silk icons and banners made for Buddhist patrons during the T'ang Dynasty (9th–10th centuries A.D.) were discovered in the central Asian rock temple caves of Dun'huang by Sir Aurel Stein, the English explorer. On some of the Dun'Huang fabrics, silver paint was used over the entirety of the outlines of the composition to create an overall glittering image (*12*).

Examples of silver used for outlines and accents are also found in woven and brocaded Chinese textiles. The Metropolitan Museum of Art Study Collection has an early 17th century Chinese sutra cover that has

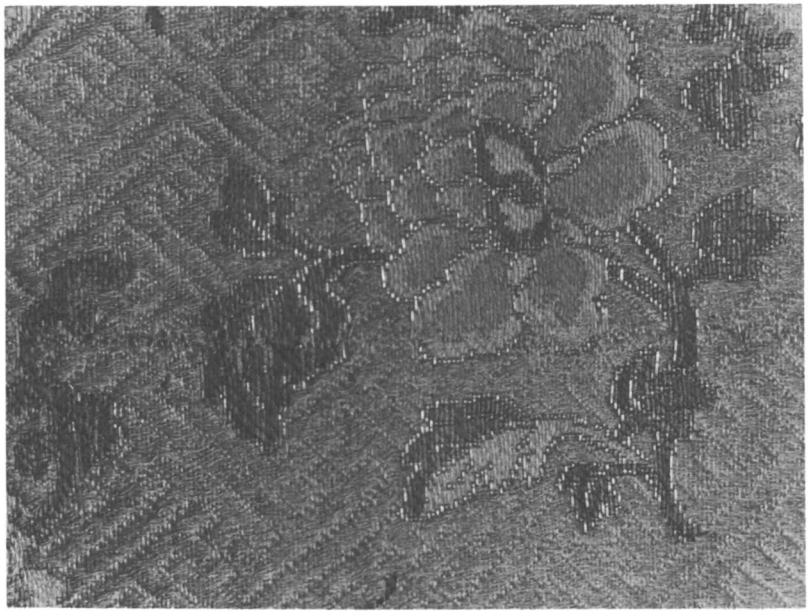

Figure 15. Woven silver outline visible in flower petals and leaves on an 18th century Chinese silk fragment. (Acc. No. 42.115.29, courtesy of The Metropolitan Museum of Art. Gift of Nellie B. Hussey, 1942.)

woven silver outlining in its stylized floral motif; the 18th century Chinese export silk fragment in Figure 15, also from The Metropolitan Museum of Art Study Collection, even has brocaded floral sprays for which silver was used on flowers and leaves in exactly the same places it was used on the Chinese 18th century painted and printed silks (Figure 16).

Conclusion

Our study of the physical and coloration characteristics of 18th century silks has to be classified as an ideal study. We were able to closely examine a wide cross-section of textiles for all the clues that they contain. This type of cooperation involving the question of provenance, which is so difficult to determine for textiles because design migration and readaptation are so prevalent, has produced a systematic method for an approach to the documentation of 18th century Chinese and Western painted and printed silks (Tables I and II).

Figure 16. Overpainted silver outline on flower petals on an 18th century Chinese silk. (Acc. No. 18037, courtesy of the Musée Historique des Tissus, Lyon.)

Literature Cited

1. Lee-Whitman, L. *Winterthur Portfolio* **1982**, *17*, 21–41.
2. Lee-Whitman, L.; Skelton, M. *Text. Mus. J.* **1984**, *22*, 33–52.
3. Reichwein, A. "China and Europe, Intellectual and Artistic Contacts in the Eighteenth Century"; Knopf: New York, 1925; p. 39.
4. Hanson, V. F. *Appl. Spectrosc.* **1973**, *27*, 309–334.
5. Gettens, R. J.; Stout, G. L. "Painting Materials A Short Encyclopaedia"; Dover Publications: New York, 1966; pp. 147–148c.
6. Hulton, P.; Smith, L. "Flowers in Art from East and West"; British Museum Publications: London, 1979; p. 50.
7. Butler, M. H. *Microscope* **1973**, *21*, 101–5.
8. Irwin, J.; Hall, M. "Indian Painted and Printed Fabrics"; S. R. Bastikar: Ahmedabad, 1971; Vol. I, p. 146.
9. Cahill, J. "Parting at the Shore, Chinese Painting of the Early and Middle Ming Dynasty, 1369–1580"; John Weatherhill: New York, Tokyo, 1978; p. 77.

10. Sze, M-m. "The Mustard Seed Garden Manual of Painting"; Princeton University; Princeton, 1963; p. 40.
11. Beach, M. C. "The Imperial Image Paintings for the Mughal Court"; Freer Gallery of Art: Washington, D.C., 1981; p. 93, 174.
12. Whitfield, R. "The Art of Central Asia, The Stein Collection in the British Museum"; Kodansha International: Japan, 1983; Vol. II, pl. 322, Stein painting 127.
13. Hsiung, C. D., et al. *J. Soc. Dyers Colour.* 1939, *55*, (8), 418.
14. van Briessen, Fritz "The Way of the Brush"; Charles E. Tuttle: Tokyo, 1962; p. 66.

RECEIVED for review November 26, 1984. ACCEPTED March 18, 1985.

8

Identification of Dyes in Historic Textile Materials

Helmut Schweppe

BASF Aktiengesellschaft, D-6700 Ludwigshafen, Federal Republic of Germany

Some of the natural dyes that are suitable for dyeing textile materials can be identified very easily with chromatographic or spectroscopic methods even when the object to be investigated is very old. Such identification applies to the two natural vat dyes indigo and purple, and also to mordant dyes belonging to the class of the hydroxyanthraquinones, for example, madder, cochineal, kermes, and lac dyes. If, however, the dyeings were produced with natural dyes that have relatively poor lightfastness, for example, yellow dyeings with hydroxyflavones or red dyeings with orchil or brazilwood, specific color reactions to identify the small proportion of undestroyed dye are usually the more rapid and more reliable method. It is advisable to begin the investigation with these color reactions, and then to attempt to confirm the results thus obtained by the use of chromatographic or spectroscopic methods.

MICROMETHODS ARE EMINENTLY SUITABLE for the identification of dyes in historic textile materials because in most cases only very small samples are available for an analysis.

Chromatographic methods (*1–25*), in particular thin-layer chromatography (TLC) (*5–17, 20–25*) and more recently high-performance liquid chromatography (HPLC) (*21, 22, 25*), preferably are used. If dye mixtures are present, as is the case with madder dyeings, chromatographic comparisons are the best method of distinguishing the individual components.

Spectroscopic methods in the visual (*1, 7, 22, 24, 26–28*) and in the IR region (*7–9, 11, 12, 28*) have also been used for investigating dyeings with outstanding success. In plotting the spectra in the visual range, colorless impurities do not have an interference effect. With this method, however, it is only possible to distinguish a part of the organic dyes, but it is a very simple method for identifying the principal natural dyes, for example, indigo, purple, madder, cochineal, and brazilwood.

0065-2393/86/0212-0153 $06.25/0

With the aid of IR spectroscopy, organic dyes can be clearly identified, provided that they have been precleansed adequately. Before plotting an IR spectrum, it is necessary to separate as far as possible not only the colored, but also colorless secondary components. However, as all accumulation methods involve some loss of substance, the amount of material available for testing historic textile materials is often too small for plotting the IR spectrum.

On pre-Columbian textiles found in the Andes, natural dyes have been identified with the aid of mass spectrometry (*29*).

In mordant dyes, inorganic mordants can be detected to a high degree of sensitivity by flameless atomic absorption spectrometry (*20, 22*).

In addition to the chromatographic and spectroscopic methods, sensitive color reactions are in many cases very useful for the specific identification of various natural dyes (*30–33*) or for recognizing individual dye classes (*34, 35*). In testing very old dyes, these reactions are sometimes able to yield results when most of the dye has already been destroyed by the action of light and all other identification methods fail.

For all identification methods, for comparison purposes, the following are required: a collection of known natural dyes in the purest form possible, dyer's plants or extracts of these plants, and dyeings produced with these substances by the recipes commonly used in the past. The question remains, however, whether an old dyeing that has faded under the influence of light can in all cases be compared in its analytical behavior with a new dyeing. It is always useful, therefore, to have textile material at our disposal that is still dyed and is no longer required for restoration work because of irreparable damage that it has undergone. Such dyeings, however, must first undergo a dye identification test before they can be used for comparison purposes. Generally speaking, however, the amount of material available for testing is sufficient to permit identification of the dyes without difficulty. Reference material from restoration work can be replaced, with certain restrictions, by natural dyeings that have been prepared and subjected to the customary (fade-ometer) exposure test.

Analytical Scheme

To obtain results as rapidly as possible and with minimum labor and costs in investigating old textile dyeings, the individual tests must be carried out in the correct order. Further tests are unnecessary when a specific test has clearly shown the identity of a dye. However, identification beyond any doubt of the exact dyer's plant that was used to produce the dyeing under investigation is not always possible.

Textile materials dating from the second half of the 19th century that were dyed with synthetic as well as natural dyes also can be

regarded as historic objects. For this reason, I have included the early synthetic dyes in my analytical scheme.

In investigating an old dyeing, the first step is to carry out a few simple preliminary trials to determine the chemical and dyeing class of the natural or synthetic dyes contained in the dyed material. The next analytical step includes determination of the shade of the dyeing to be investigated in the analytical scheme. In testing a red dyeing, for instance, I use a different procedure than that used for a blue dyeing. The analytical process can be accelerated drastically by basing the procedure on the shade of the dyeing to eliminate reactions that are not typical for the identification of dyes with other shades. Whenever possible and necessary, the results of these preliminary color reactions are confirmed by TLC comparisons on polyamide layer material.

Preliminary Tests

Solvent Stripping Tests. The first preliminary test is to investigate the bleeding of a dyeing by boiling a small sample in a test tube in water, ethanol, glacial acetic acid, and ammonia, one after the other. The degree of staining of the individual decoctions gives some indication of the presence of certain classes of dyes. Of the synthetic dyes, the acid and direct dyes bleed to a certain extent in water and more heavily in ammonia. The basic dyes, in contrast, stain the ethanol and glacial acetic acid extracts heavily. Synthetic metal complex dyes, including the chrome-developing and mordant dyes, stain only the ammonia extract lightly. In dyeings of this type, chromium and/or cobalt is found in the residue on ignition (*36*, *37*).

Most of the natural dyes treated in this manner bleed only lightly or not at all because they belong to the class of mordant dyes and are present in the dyeings as sparingly soluble color lakes of aluminum, iron, or chromium and, in a few cases, as copper or tin lakes.

Exceptions are dyeings with safflower (C.I.[1] Natural Red 26) (*38*) made from the leaves of the dyer's thistle (*Carthamus tinctorius* L.). The red dye carthamin (C.I. 75140) (*38*) goes into solution when it is boiled in water. When this solution is poured through a paper filter after it has cooled, the paper is stained red, whereas the filtrate is colorless or is stained light yellow by safflower yellow (C.I. Natural Yellow 5), a second dye of the safflower. When the red stained filter is boiled in 1% ammonia, it becomes irreversibly colorless.

Dyeings with indigo sulfonic acid (C.I. Natural Blue 2), which were produced from indigo and sulfuric acid since 1740, also bleed

[1]In the "Colour Index" (C.I.), a multiple-volume, English reference work (*38*), the names, commercial denominations, constitutions, and dyeing properties of synthetic and natural dyes are listed. Each dye has a generic name, and, if the constitution is known, a constitution number.

heavily when treated with ammonia. Dyeings with Berlin blue (C.I. Pigment Blue 27) (an iron lake of ferrocyanic acid) become colorless.

The glacial acetic acid extract can be stained by indigo (C.I. Natural Blue 1) in a blue shade, by berberine (C.I. Natural Yellow 18), the only basic natural dye, and sometimes by madder (C.I. Natural Red 8) in a yellow shade.

Dyeing Tests. These tests are carried out to determine the class of the dye according to its dyeing behavior. When the dyeing to be investigated is boiled in water, ethanol, glacial acetic acid, and ammonia, and heavy bleeding gives reason to assume that the dyeing was produced with synthetic dyes, I can determine whether this dye is an acid or a basic dye by dyeing from acetic acid solution on wool and on cotton mordanted with tannic acid and potassium antimonyl tartrate. Acid dyes dye the wool in a deeper shade, whereas basic dyes stain the mordanted cotton more heavily. Direct dyes can be identified in a separate dyeing test; when they are applied from a neutral solution containing sodium sulfate, they stain unmordanted cotton in relatively deep shades (*15, 36, 37*).

Tests for Identification of Some Synthetic Dyes. Two very simple reactions can confirm the presence of synthetic dyes. In the solvent stripping test, if the ammonia solution is heavily stained and it becomes irreversibly colorless upon the addition of zinc dust even at room temperature, the presence of an azo dye with sulfo group or groups is indicated (an acid or direct dye) (*36, 37*). The color of the solution in concentrated sulfuric acid can also be an important indication for identifying synthetic dyes. In this test, a few drops of concentrated sulfuric acid are dripped on a small sample of the dyeing, and the color of the sulfuric acid is observed after a few minutes. Intensive magenta red, red-violet, violet, blue, and green solutions indicate the presence of synthetic dyes (*36, 37*).

Group Reactions for Natural Dyes with 10% Sulfuric Acid. Another method of determining if certain types of natural dyes are present is to boil a sample of the dyeing for a short time in 10% sulfuric acid. This test is only carried out for dyeings that have shown little bleeding in the boiling tests in water, ethanol, glacial acetic acid, and ammonia. In this test, the following reactions are typical:

1. Natural dyes belonging to the class of the hydroxyflavones (C.I. Natural Yellow 1, 2, 4, 10, 11, 12, and 13) become almost colorless. Upon addition of ammonia to the previously washed dyeing, the original yellow shade returns. Upon subsequent boiling, after addition of a small amount of sodium dithionite, the yel-

low color remains (clear identification of hydroxyflavones and hydroxyisoflavones).
2. Iron tannate dyeings become almost colorless. Iron can be detected in the sulfuric acid solution.
3. Brazilwood and logwood dyeings bleed an intensive red shade.
4. Red and violet madder dyeings on alum or iron sulfate mordant turn orange; the dye bleeds a yellow shade, and after it has been shaken with ethyl acetate, it can be used for TLC comparisons.
5. Dyeings with the red insect dyes cochineal (C.I. Natural Red 4), kermes (C.I. Natural Red 3), and lac dye (C.I. Natural Red 25) bleed an orange shade. After shaking with ethyl acetate and pentanol (1:1), the dye solutions can be used for TLC comparisons.

Vatting with Sodium Dithionite. An indication of the presence of natural vat dyes is obtained by treating a sample of the dyeing with sodium dithionite and ammonia at the boiling temperature. Vat dyes are insoluble in water, ammonia, and dilute mineral acids. Upon reduction at alkaline pH, they go into solution, and this change usually is accompanied by a change in shade. Upon reoxidation in the air, the original shade returns. The natural vat dyes indigo (C.I. Natural Blue 1) and purple [natural (vat) dye] have a yellow vat, and Chinese green (C.I. Natural Green 1) has a magenta red vat. Natural dyes from the class of hydroxynaphthoquinones, for example, walnut shells (C.I. Natural Brown 7), henna (C.I. Natural Orange 6), and alkanna (C.I. Natural Red 20), also can be reduced, and the color of the vat is yellow.

Dyeings with orchil (C.I. Natural Red 28), the natural dye obtained from lichens, become colorless when they are treated with sodium dithionite; the original magenta red shade returns when they are aired.

When very old and yellowed dyeings produced with natural yellow dyes belonging to the class of the hydroxyflavones are treated with sodium dithionite and ammonia, their shade becomes more brilliant. It may be assumed that the yellowing products of dyeings with moderate lightfastness are removed reductively by this treatment.

Identification of Natural Mordant Dyes

In dyeing with natural mordant dyes, widely varying shades are usually obtained, depending on the mordant that was used to pretreat the textile material to be dyed. Madder dyeings on an alum mordant are red, whereas those on an iron sulfate mordant are brown-violet to violet.

Old dyeing recipes sometimes recommend that a dyeing be obtained in a different shade by aftertreating a mordant dyeing with a different mordant. This possibility of conversion also can be used for identifying natural mordant dyes. This identification is done by boiling small

samples of the unknown dyeing in dilute solutions of tin(II) chloride, aluminum sulfate, iron(II) sulfate, copper sulfate, and uranyl acetate and letting the solutions stand for a few minutes (*15*). During the process, the corresponding color lakes form on the fiber, and the shades of these color lakes depend not only on the salt used for the aftertreatment, but also on the mordant dye present. Provided that a corresponding assortment of comparative dyeings on the five different mordants just named is available, an identification is possible even in the case of very faded yellow dyeings with natural dyes of the hydroxyflavone class and in cases where other methods of identification have failed completely.

Figure 1 shows the shades of these color lakes obtained from dyeings produced with the principal yellow natural dyes: dyer's rocket (C.I. Natural Yellow 2), quercitron (C.I. Natural Yellow 10), unripe buckthorn berries (C.I. Natural Yellow 13), fustic (C.I. Natural Yellow 11), curcuma (C.I. Natural Yellow 3), and kamala (C.I. Natural Yellow 25). These lakes, which differ markedly in their shades from the others, are marked with a cross. They are the tin lakes of quercitron and curcuma, the curcuma iron lake, and the copper lakes of dyer's rocket, unripe buckthorn berries, and fustic. A report on these methods has been published (*15*). The natural yellow dyes are shown in Figure 1 as examples of the lakes produced.

Identification of Natural Dyes by TLC

Hydroxyanthraquinones from Madder Dyer's Plants. Often, distinguishing among very similar natural dyes is possible by TLC on polyamide layer material. When the dyes consist of several different components, in many cases identification of a definite dyer's plant that was used to produce the dyeing is even possible. Figure 2 shows how madder can be distinguished by this method from other similar dyer's plants. Madder root (*Rubia tinctorum* L.), hedge bedstraw (*Galium mollugo* L.), South American madder or relbun root (*Relbunium ciliatum* L.), root bark of the Indian "mang-kouda" (*Morinda umbellata* L.), the dye "karamu" of the Maoris in New Zealand, the coprosma root (*Coprosma lucida* L.), and the Indian dye "pitti" (*Ventilago madraspatana* L.) can be clearly distinguished from one another in this manner.

The separation is carried out on Mikropolyamid F 1700 (Schleicher & Schüll) with the solvent mixture toluene–glacial acetic acid (9:1). The uranyl lakes of the individual hydroxyanthraquinone dyes, which vary widely in their shades, are obtained on the chromatogram under standard conditions (chamber saturation) by subsequent dipping in a dilute solution of uranyl acetate (*15*). Table I shows the hR_f values of the principal hydroxyanthraquinones contained in the various madder types.

Hydroxyanthraquinone from Red Insect Dyes Figure 3 shows how to distinguish among the three red insect dyes cochineal (C.I. Natural

Table I. hR_f Values of Hydroxyanthraquinones from Madder Dyer's Plants

Hydroxyanthraquinone	hR_f *Value*	*Color of Stain*
Alizarin (1,2-dihydroxyanthraquinone)	42	violet-blue
Purpurine (1,2,4-trihydroxyanthraquinone)	33	gray
Pseudopurpurine (1,2,4-trihydroxyanthraquinone-3-carboxylic acid)	6	gray
Xanthopurpurine (1,3-dihydroxyanthraquinone)	14	orange-red
Rubiadine (1,3-dihydroxy-2-methylanthraquinone)	22	red
Munjistin (1,3-dihydroxyanthraquinone-2-carboxylic acid)	2	red
Morindone (1,5,6-trihydroxy-2-methylanthraquinone)	45	green-blue
Emodin (1,6,8-trihydroxy-3-methylanthraquinone)	16	magenta

Red 4), lac dye (C.I. Natural Red 25), and kermes (C.I. Natural Red 3) on Mikropolyamid F 1700 with the solvent butanone–formic acid (7:3), followed by identification with uranyl acetate.

In the case of lac dye, clearly the separation of the laccaic acids A, B, C, D, and E (*39–42*) can be seen, and in the case of kermes, the separation into kermesic acid (green spot) and flavokermesic acid (red spot) can be seen. References 39–42 describe the determination of the constitutions of the laccaic acids A–E and indicate their constitutions.

Before the discovery of America by Columbus and long before the cochineal (*Dactylopius coccus*) from Central and South America was known in Europe, kermes was an important red insect dye in the whole Mediterranean region. In the literature, it is pointed out almost exclusively that the two kermes species "*Kermes vermilio* (PLANCH.) TARG." and "*Kermes ilicis* L." are suitable for dyeing purposes. Only Pfister (*43*) cites M. Balachowski (Directeur de la Station Centrale d'Entomologie agricole de Versailles), who states that only *Kermes vermilio* is suitable for dyeing purposes and must, therefore, be regarded as the kermes dye known from classical antiquity. Born (*44*) considers that *Kermes vermilio* was the most important species of kermes for dyeing in former times. As Figure 4 shows, TLC comparison proves that only *Kermes vermilio* contains the dyes kermesic acid and flavokermesic acid, which are essential for dyeing; *Kermes ilicis* L. does not contain these acids.

Table II lists the hR_f values of the hydroxyanthraquinone com-

Table II. hR_f Values of Hydroxyanthraquinones from Red Insect Dyes

Hydroxyanthraquinone	hR_f *Value*	*Color of Stains*
Karminic acid (1,3,4,6-tetrahydroxy-2-D-gluco-3-pyranosyl-8-methylanthraquinone-7-carboxylic acid)	45	green
Kermesic acid (1,3,4,6-tetrahydroxy-8-methylanthraquinone-7-carboxylic acid)	33	green
Flavokermesic acid (constitution unknown)	37	red
Laccaic acids A, B, C, D, and E (Because samples of the pure laccaic acids A–E are not available, a classification of the individual compounds by hR_f value is not possible.)	27	gray-green
	34	gray-green
	45	gray-green
	51	gray-green
	60	gray-green

pounds contained in the red insect dyes. These data were obtained by TLC on Mikropolyamid F 1700 with the solvent butanone–formic acid (7:3). Chromatography was performed under standard conditions (chamber saturation), and the color reaction was obtained with uranyl acetate.

Natural Dyes Belonging to the Class of Hydroxyflavones. Figure 5 shows that the principal yellow natural dyes belonging to the class of the hydroxyflavones can be distinguished by TLC on Mikropolyamid F 1700 with the solvent chloroform–methanol–butanone–formic acid (6:2:1:1). Chromatography was performed under standard conditions (chamber saturation) and the color reaction was obtained with uranyl acetate.

In this example, no data regarding the hR_f values are provided. Reference is made to a previous publication (*11*).

Table III lists some solvent mixtures that are particularly suitable for separating natural dyes of various classes on Mikropolyamid F 1700 as the layer material.

Testing of Natural Dyeings

Testing of Yellow Natural Dyeings. When a yellow dyeing is boiled in glacial acetic acid (cf. solvent stripping tests), berberine (C.I. Natural Yellow 18), the only natural basic yellow, is dissolved. This dye can be identified by TLC comparison on silica gel with the solvent butanol–glacial acetic acid–water (5:1:2).

The most important natural dyes used for dyeing textile materials belong to the class of the hydroxyflavones. Dyeings of this type become

Table III. Suitable Solvents for Separating Various Natural Dyes on Mikropolyamid F 1700 as the Layer Material

Class of Natural Dye	*Suitable Solvents*[a]
Madder dyes	1, 2, and 4
Red insect dyes	3 and 6
Hydroxyflavone dyes	5
Vegetable tannins	3 and 6
Santalin A, B, and C from sandalwood	2 and 4
Curcuma dyes	4[b]

[a]The solvents corresponding to the numbers in the table are the following: 1, toluene–acetic acid (9:1); 2, butanone–formic acid (95:5); 3, butanone-formic acid (7:3); 4, chloroform-methanol (95:5); 5, chloroform–methanol–butanone–formic acid (6:2:1:1); and 6, butanone–methanol–formic acid (65:30:5).
[b]The layer material is silica gel.

almost colorless when boiled in 10% sulfuric acid. If, after the sulfuric acid has been washed out with water, ammonia is added to the dyeing, the original yellow returns and it remains unchanged upon subsequent addition of sodium dithionite and boiling.

When the dyeing treated in this manner is heated with tin, aluminum, iron, copper, and uranyl salts after it has been washed out with water, flavone dyes that contain luteolin as the main component can be identified fairly easily from the color of the lakes. In such cases, one can assume that dyer's plants such as dyer's rocket and dyer's greenwood (both C.I. Natural Yellow 2) were mainly used.

Very brilliant orange-colored tin lakes indicate the presence of quercetin and its glycosides, hydroxyflavones that often occur in the vegetable kingdom. The leading natural dyes quercitron (C.I. Natural Yellow 10), Chinese yellow berries (*Sophora japonica* L., C.I. Natural Yellow 6), and unripe buckthorn berries (C.I. Natural Yellow 13) yield orange-colored tin lakes. More precise information regarding the natural dye that was used is obtained by TLC comparison when other hydroxyflavones as well as quercetin are present, for example, in dyeings made with unripe buckthorn berries.

Testing of Red Natural Dyeings. Of the red dyeings made with natural dyes, those produced with safflower (C.I. Natural Red 26) can be identified in the extraction tests with water and with ammonia (colorless), as indicated earlier. Dyeings with sandalwood (C.I. Natural Red 22) can also be identified at this early stage because they turn dark violet when they are boiled in ammonia. When they are washed with water, the original red shade returns.

Upon boiling in 10% sulfuric acid, the solution obtained from madder dyeings turns yellow (fibers are orange), whereas solutions from dyeings with cochineal, lac dye, and kermes turn orange (fibers are orange-red to red) and solutions from brazilwood dyeings (C.I. Natural Red 24) turn red (fibers are yellow-orange).

Upon reduction with sodium dithionite and ammonia, dyeings made with orchil (C.I. Natural Red 28) become colorless, and they turn magenta red when they are reoxidized in the air; early synthetic dyes belonging to the azo series become irreversibly colorless when they are vatted. Purple dyeings turn yellow when they are vatted, but the original shade returns upon reoxidation in the dark; upon reoxidation under the UV lamp, the two bromine atoms split off from the 6,6′-dibromoindigo, and the blue indigo is obtained (*14, 30*).

Testing of Blue Natural Dyeings. Of the blue dyes, Berlin blue (C.I. Pigment Blue 27) and indigosulfonic acid (C.I. Natural Blue 2) were produced as early as the 18th century. They are often found on old dyeings. Both of them change in the boiling test with ammonia.

Berlin blue, which was used mainly for dyeing silk and for printing on cotton, turns light brown-yellow to colorless in the boiling test. A few drops of 4% caustic soda solution are then added, and the solution is poured through a paper filter. After filtration, iron can be identified on the filter, and ferrocyanide can be identified in the filtrate.

Indigosulfonic acid goes mostly into solution during the extraction test with ammonia, and then it can be identified by TLC comparison on silica gel with the solvent butyl acetate-pyridine-water (4:4:2).

Indigo turns yellow when it is vatted with sodium dithionite and ammonia. When the vat is shaken with ethyl acetate, the supernatant ethyl acetate layer turns blue (*33*).

Testing of Black Natural Dyeings. Black dyeings are first boiled in tin(II) chloride solution (*15*). During this treatment, dyeings with iron tannate (C.I. Natural Brown 6) become almost colorless, whereas dyeings with tanner's sumach (*Rhus coriaria* L., *Herba*, C.I. Natural Brown 6) turn yellow-orange because of their quercetin content.

If the dyeing was produced with logwood black (C.I. Natural Black 1), the solution turns magenta red and the dyeing becomes violet.

If the dyeing remains unchanged when it is treated with tin(II) chloride solution, it is washed out with water and then boiled in *N,N*-dimethylformamide. During this treatment, indigo forms a blue solution. This decoction is repeated until the *N,N*-dimethylformamide remains colorless. If the remaining fibers are then brown, they are boiled in sodium dithionite and ammonia. If the fibers remain brown, this result proves that the material is wool with a inherent brown color.

Testing of Violet Natural Dyeings. Violet dyeings are first boiled in 10% sulfuric acid. If the dye dissolves with a yellow color, a madder dyeing on iron mordant is indicated. If the sulfuric acid turns orange and a blue remains on the fiber, the dyeing is a mixture of cochineal and indigo, which can be identified separately by the methods described earlier.

If the violet dyeing becomes only somewhat paler when treated with 10% sulfuric acid, the specimen is washed out with water and vatted with sodium dithionite and ammonia. If the dyeing then turns yellow and is reoxidized in the air to a blue, this dyeing is one with alkanna (C.I. Natural Red 20) on alum mordant.

A sample of the dyeing is tested separately for the presence of logwood with which violet shades can be dyed on alum and tin mordants. The dyeing is boiled in a solution of tin(II) chloride. If the solution turns magenta red and the dyeing remains violet, this dyeing is one with logwood.

Testing of Green Natural Dyeings. Green shades dyed with natural dyes, in most cases, were produced with mixtures of indigo and dyer's rocket or unripe buckthorn berries. After identification of the indigo by vatting and shaking with ethyl acetate, the indigo proportion is removed by repeated boiling in *N*,*N*-dimethylformamide (as described earlier), and the yellow remaining on the fiber is identified as a dye belonging to the hydroxyflavone class by its behavior towards 10% sulfuric acid, ammonia, and sodium dithionite (as described earlier). Dyer's rocket and unripe buckthorn berries can be distinguished by the formation of the various lakes on the fiber (as described earlier).

Testing of Orange Natural Dyeings. Orange shades, in most cases, were dyed with madder and yellow hydroxyflavone dyes. When these dyeings are boiled in 10% sulfuric acid, the madder goes into solution with a yellow color, and after shaking with ethyl acetate, it can be identified by TLC comparison. The yellow hydroxyflavones, most of which have remained on the fiber, are then dissolved in concentrated sulfuric acid at room temperature, and after dilution with water and shaking with ethyl acetate, this solution can be used for a TLC comparison.

Testing of Brown Natural Dyeings. When brown dyeings produced with natural dyes become much lighter in shade upon boiling in 10% sulfuric acid, usually the presence of iron tannate is indicated. In such cases, iron can be identified in the sulfuric acid. If an excess of ammonia is added to the sulfuric acid decoction, the fiber regains its original brown shade.

When a separate sample is boiled in tin(II) chloride solution, if the dyeing was produced with a dyer's plant that contained tannin and at the same time hydroxyflavones, the shade turns yellow to orange. Many dyer's plants of this kind are found in nature.

When a brown natural dyeing turns yellow upon vatting with sodium dithionite and ammonia and the original shade returns upon reoxidation, the dyeing probably was produced with walnut shells (C.I. Natural Brown 7) or some other hydroxynaphthoquinone.

If the dyeing remains unchanged upon vatting, this result indicates that the material is wool or some other animal fiber having a brown inherent color.

Testing of Historic Objects

The usefulness of the analytical method for the identification of dyes in old textile materials is demonstrated in the following. Figure 6 illustrates a fragment of a woven fabric from the south coast of Peru, probably from the valley of the Rio Nazca. This object is dated A.D. 100–200. We have investigated this sample for the Museum für Völkerkunde in Hamburg, West Germany.

The red threads of the Peruvian fabric fragment were tested in the following manner: upon boiling in 10% sulfuric acid, a large part of the dye dissolved and produced a yellow color, and it was shaken out quantitatively with ethyl acetate. TLC comparison on Mikropolyamid F 1700 with the solvent toluene–acetic acid (9:1) showed the presence of purpurine and pseudopurpurine, but no trace of alizarin. The South American relbun roots, for example, *Relbunium ciliatum* L., which was available as a reference material, have a composition of this kind.

In the dark blue threads, indigo readily was identified by vatting. In addition, a large proportion of indirubine (C.I. 75790), an isomer of indigo, was present. The indirubine was dissolved by acetic ester extraction and was identified by TLC comparison on silica gel with the solvent toluene–acetic acid (9:1).

Indirubine is formed from the primary indigo of the indigo plants to an increased degree when fermented indigo plants are applied in a relatively weak alkaline vat for dyeing. This situation seems to have been the case with the dark blue threads of the Peruvian sample.

For the yellow threads of the Peruvian cloth, all that could be determined was that they were dyed with a natural dye belonging to the class of the hydroxyflavones.

Figure 7 shows a piece of 16th century Mameluke carpet from Cairo. The red threads in this carpet were dyed with the insect dye lac dye (C.I. Natural Red 25). The mordant was identified as aluminum and a small amount of iron and copper compounds. However, as copper also was

identified in the other dyed shades of the sample, it can be assumed that the copper came from a dyeing vessel that was made of this metal.

Lac dye is obtained in the production of shellac from "stick-lac" in India, and it was used in the past on a large scale for dyeing purposes. In Mameluke carpets of the 16th century, this dye often is found. I have been able to identify it on four different objects.

The lac dye was identified by TLC comparison on Mikropolyamid F 1700 with the solvent butanone–formic acid (7:3) and was confirmed with uranyl acetate. The dye was removed from the fiber with 10% sulfuric acid. After shaking with ethyl acetate–pentanol (1:1), the extract was used for TLC.

The blue in the Mameluke carpet easily was identified as indigo by the vatting test. In the yellow and the green threads (after removing the indigo by extraction with *N,N*-dimethylformamide), I identified a hydroxyflavone dye containing luteolin as the main component, in all probability dyer's rocket, by comparison with the tin, aluminum, iron, copper, and uranyl lakes.

Figure 8 shows an Italian 17th century velvet fabric from a liturgical vestment of natural silk.

The preliminary tests indicated that the yellow threads were dyed with a hydroxyflavone dye containing luteolin as the main component, probably dyer's rocket. This finding was confirmed by TLC comparison. The salmon-colored silk threads were dyed with safflower (C.I. Natural Red 26). When the water extract of these threads is filtered, the filter paper is stained red, and the filtrate is light orange. When the red filter is treated with dilute ammonia, it becomes colorless. The red threads were dyed with cochineal (C.I. Natural Red 4). The results of the preliminary tests indicated that one of the three red insect dyes was present. TLC comparison confirmed that no lac dye or kermes was present, but cochineal was identified. On the green threads, indigo was identified by vatting and then stripped from the fiber with *N,N*-dimethylformamide. The yellow remaining on the fiber was identified by the preliminary tests and by TLC comparison as hydroxyflavone containing luteolin as the main component. Also in this case, dyer's rocket probably was used for dyeing.

The left half of Figure 9 shows the face of the tapestry on which the red has faded almost completely. On the right side of Figure 9 is a piece of the back on which the original red shade is still fairly visible.

The threads on the face of the carpet that have faded (because of their moderate lightfastness) become colorless when they are vatted with sodium dithionite and ammonia, and they turn magenta upon subsequent reoxidation in the air. This dyeing is, therefore, one made with orchil (C.I. Natural Red 28). This dye was known as "French purple", and very often it was used in tapestries in the 16th–19th centuries despite its poor lightfastness.

On the yellow threads, hydroxyflavones containing luteolin as the main component, probably dyer's rocket, were identified. The same yellow is present on the green threads alongside indigo.

Figure 10 shows printed cloth from the early 19th century from Mulhouse (mélüz) in Alsace (France). The blue print was produced with Berlin blue (C.I. Pigment Blue 27). This pigment was found in 1704 by Diesbach, who kept it secret until 1724. Chemically, it is ferric ferrocyanide. Berlin blue often was used in the 18th and 19th centuries for silk dyeings and for cotton prints.

To identify the blue shades on the printed cloth, a small sample of the blue print is boiled in a test tube in 4% caustic soda solution. The print turns brown, and the solution is yellow. After the solution is filtered, iron is identified on the filter with a sulfuric acid solution of potassium ferrocyanide. Ferrocyanide in the filtrate is identified with a sulfuric acid solution of iron(III) chloride.

Figure 11 shows the Sicilian coronation robe of the Hohenstauffen emperors. This coronation robe of the Roman-German emperors was made in 1133–34 for King Roger II of Sicily, as indicated by the Kufic (ancient Arabic) letters decorating the edge of the robe. Saracen artists created this representation of royal power on red silk material. The design on the two sides of the fabric is a mirror image of a lion killing a camel.

In the past, it was assumed that Tyrian purple was used for dyeing this coronation robe. However, Max Saltzman (University of California, Los Angeles) doubted that it was a purple dyeing. He obtained a small piece of a thread from the coronation robe in the Weltliche Schatzkammer of the Vienna Hofburg. In my laboratory and in that of Max Saltzman, by means of several color reactions, we were able to prove that this dyeing was produced with a red insect-derived dyestuff.

Figure 12 shows, for shade comparison, a purple dyeing on cotton that was produced from the secretion of the hypobronchial gland of the purple snail "*Purpura patula pansa Gould*" in 1971 by Indians in the area of Oaxaca, Mexico. The shades of purple dyeings may vary from violet-red to red-violet, but they cannot match the shade of the coronation robe.

Acknowledgments

Thanks to the undaunted efforts of Max Saltzman, I was able to obtain a few specimens of the almost extinct kermes species from the cochineal insect researcher Imre Foldi of Paris. I also would like to thank Rotraud Bauer of the Kunsthistorisches Museum in Vienna for providing Max Saltzman and me with a sample of the Sicilian coronation robe of the Hohenstauffen emperors.

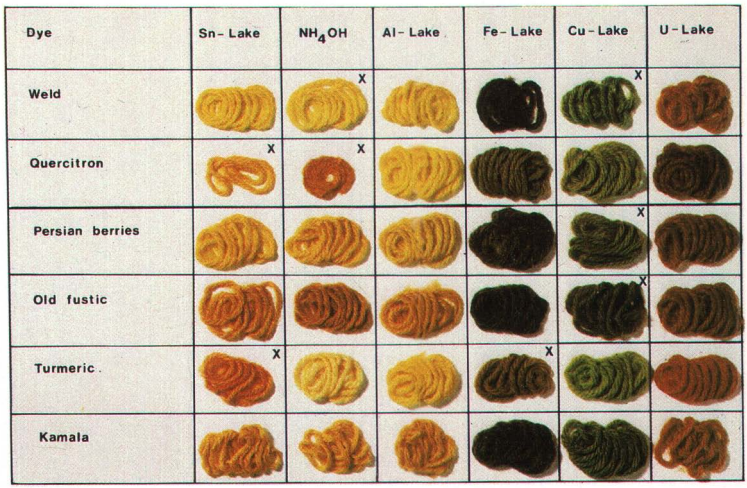

Figure 1. Lakes of yellow natural dyes. (Reproduced with permission from Ref. 15. Copyright 1980.)

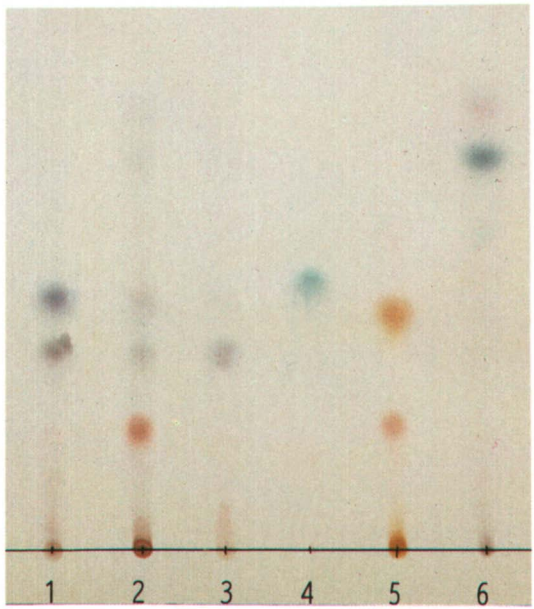

Figure 2. TLC of hydroxyanthraquinones from dyer's plants of the madder type. 1, madder (Rubia tinctorum *L.); 2, hedge bedstraw* (Galium mollugo *L.); 3, relbun root* (Relbunium ciliatum)*; 4, mang-kouda* (Morinda umbellata *L.); 5, karamu or coprosma root* (Coprosma lucida *L.); and 6, pitti* (Ventilago madraspatana *GAERTN.).*

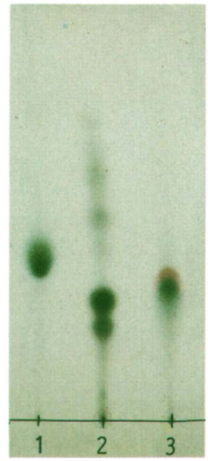

Figure 3. TLC of hydroxyanthraquinones from red insect dyes. 1, cochineal; 2, lac dye; and 3, Kermes vermilio.

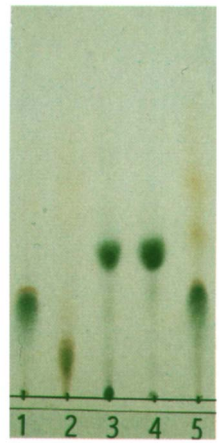

Figure 4. Distinction of hydroxyanthraquinones from kermes types by TLC. Layer material: Mikropolyamid F 1700; solvent: butanone-formic acid (7:3); and color reaction: uranyl acetate. 1, Kermes vermilio; 2, Kermes ilicis; 3, *"kermes" (Iran 1979); 4, cochineal; and 5,* Kermes vermilio.

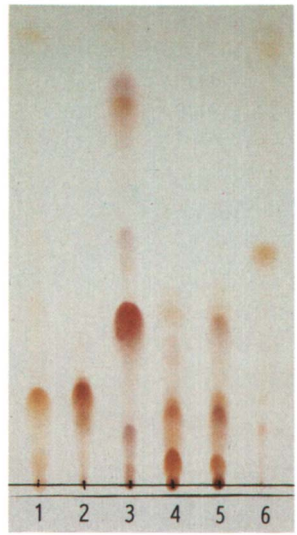

*Figure 5. TLC of hydroxyflavone dyes. 1, dyer's rocket (*Reseda luteola *L., C.I. Natural Yellow 2); 2, young fustic (*Cotinus coggygria *SCOP., C.I. Natural Brown 1); 3, buckthorn berries (*Rhamnus cathartica *L., fructi immaturi, C.I. Natural Yellow 13); 4, old fustic (*Chlorophora tinctoria *GAUD., C.I. Natural Yellow 1; 5, osage orange wood (*Maclura pomifera, *C.I. Natural Yellow 8); and 6, bastard hemp (*Datisca cannabina *L., C.I. Natural Yellow 12).*

Figure 6. Fabric fragment from Peru, A.D. *100–200.*

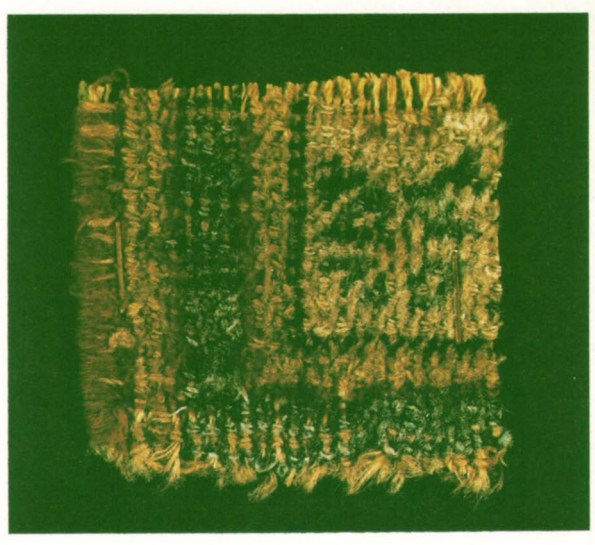

Figure 7. A 16th century Mameluke carpet from Cairo.

Figure 8. A 17th century Italian velvet fabric from a liturgical vestment of natural silk (private property of D. Lehmann, PR 402/57).

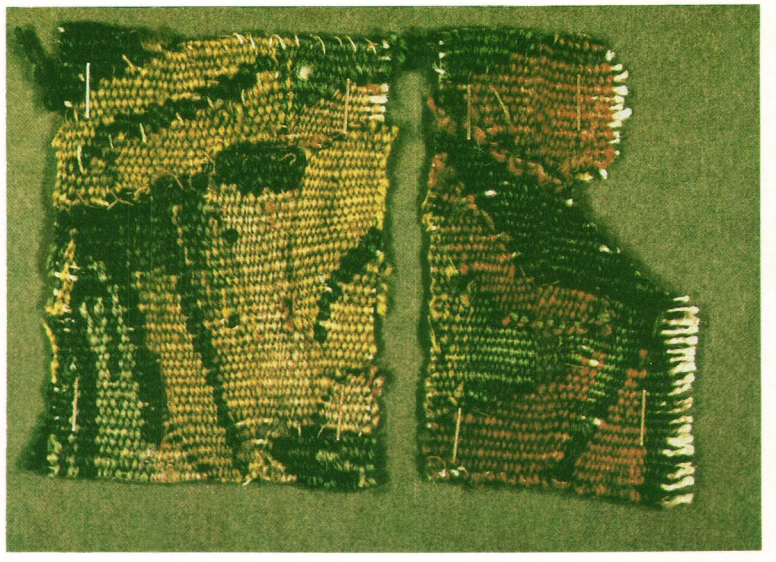

Figure 9. Tierverdüre tapestry produced at the end of the 16th century (private property of D. Lehmann, PR 336/38).

Figure 10. Early 19th century printed cloth from Mulhouse in the Alsace (France).

Figure 11. Sicilian coronation robe of the Hohenstauffen emperors.

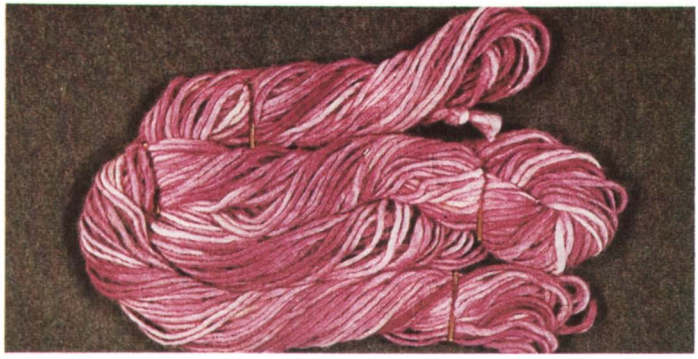

Figure 12. Tyrian purple dyed on cotton by Indians near Oaxaca, Mexico.

Literature Cited

1. Kashiwagi, K.M. *Bull. Chem. Soc. Jpn.* **1976**, *49(5)*, 1236-9.
2. Paris R.; Rousselet, R. *Ann. Pharm. Fr.* **1958**, *16*, 747-56.
3. Shibata, S.; Takito, M.; Tanaka, O. *J. Am. Chem. Soc.* **1950**, *72*, 2789.
4. Boutrop, J. Ingenieurarbeit, Textilingenieurschule, Krefeld, Federal Republic of Germany, 1970.
5. Hofenk-De Graaf, J.H.; Roelofs, W.G.H. "On the occurrence of red dyestuffs in textile materials from the period 1450-1600"; ICOM Plenary Meeting; Madrid. Oct. 1972.
6. Masschelein-Kleiner, L. *Microchim. Acta* **1967**, *6*, 1080-5.
7. Masschelein-Kleiner, L.; Heylen, J.B. *Stud. Conserv.* **1968**, *13*, 87-97.
8. Masschelein-Kleiner, L.; Maes, L. *Bull Inst. R Patrimoine Art.* **1970**, *t.XII*, 34-41.
9. Masschelein-Kleiner, L.; Znamensky-Festraets, N.; Maes, L. *Bull. Inst. R Patrimoine art.* **1969**, *t.XI*, 269-72.
10. Roelofs, W.G.Th. "Thin-layer chromatography, an aid for the analysis of binding materials and natural dyestuffs from the works of art"; ICOM Plenary Meeting: Madrid, Oct. 1972.
11. Schweppe, H. *Z.anal. Chem.* **1975**, *276*, 291-6.
12. Schweppe, H. *Die BASF (Aus der Arbeit der BASF Aktiengesellschaft)* **1976**, *26*, 29-36.
13. Schweppe, H. *Mikrochim. Acta* **1977** *II*, 583-96.
14. Schweppe, H. *HALI (Int. J. Orient. Carpets Text.)* **1979**, *Vol. II, No. 1*, 24-7.
15. Schweppe, H. *J. Am. Inst. Conserv. Hist. Art. Works* **1980**, *19*, 14-23.
16. Böhmer, H. *HALI (Int. J. Orient. Carpets Text.)* **1979**, *Vol. II, No. 1*, 30-33.
17. Brüggemann, W.; Böhmer, H. "Teppiche der Bauern und Nomaden in Anatolien", Verlag Kunst und Antiquitäten GmbH: Hannover, 1980; pp. 88-118.
18. Furuya, T. *J. Chromatogr.* **1965**, *19*, 607-10.
19. Furuya, T.; Shibata, S.; Iizuka, H. *J. Chromatogr.* **1966**, *21*, 116-8.
20. Mushak, P. *Orient. Rug Rev.* **1983**, *Vol. III, No. 4*, 3-5.
21. Mushak, P.; O'Bannon, G.W. *Orient. Rug Rev.* **1982**,*Vol. II, No. 10*, 6-8.
22. Ibid **1983** *Vol. III, No. 2*, 16-9.
23. Whiting, M.C. *HALI (Int. J. Orient. Carpets Text.)* **1978**, *Vol. I, No. 1*, 39-43.
24. Whiting, M.C. *HALI (Int. J. Orient. Carpets Text.)* **1979**, *Vol. II, No. 2*, 28-9.
25. Whiting, M.C. *Chemie in unserer Zeit* **1981**, *15*, 179-89.
26. Saltzman, M.; Keay, A.M.; Christensen, J. *Dyestuffs* **1963**, *44*, 241-51.
27. Saltzman, M. In "Archaeological Chemistry—II"; Carter, G.F., Ed.; ADVANCES IN CHEMISTRY SERIES No. 171; American Chemical Society: Washington, D.C., 1978, pp. 173-85.
28. Abrahams, D.H.; Edelstein, S.M. *Am. Dyest. Rep.* **1964**, *53*, 19-25.
29. de Wong, O.A.: "The identification of natural dyes in pre-Columbian Andean textiles by mass spectroscopy." Submitted in partial fulfillment of the requirement for the Degree of Master of Science at the Massachusetts Institute of Technology, 1977.
30. Driessen-Hengelo, L.A. *Melliand Text.* **1944**, *25*, 66.
31. Stein, W. *Dinglers polytech. J. (Berlin)* **1870**, *196*, 70-1.
32. Ibid **1871**, *200*, 51-72.
33. Hofenk-De Graaf, J.H. *Stud. Conserv.* **1974**, *19*, 54-5.
34. Fol, F. *Dinglers polytech. J. (Berlin)* **1874**, 212, 520-4.

35. Wagner, J. *Dinglers polytech. J. (Berlin)* **1876**, *220*, 444-5.
36. Schweppe, H. In "Ullmanns Encyklopädie der technischen Chemie, 4th Ed."; Verlag Chemie: Weinheim, West Germany, 1976, Vol. 11, pp. 146-72.
37. Schweppe, H. In "The Analytical Chemistry of Synthetic Dyes"; Venkataraman, K. Ed.; Wiley: New York, 1977, pp. 389-430.
38. "Colour Index 3rd Ed."; The Society of Dyers & Colourists: Bradford, United Kingdom, 1971.
39. Pandhare, E.D.; Rama Rao, A.V.; Shaikh, I.N. *Indian J. Chem.* **1969**, *7*, 977-86.
40. Bhide, N.S.; Pandhare, E.D.; Rama Rao, A.V.; Shaikh, I.N.; Srinavasan, R. *Indian J. Chem.* **1969**, *7*, 987-95.
41. Rama Rao, A.V.; Shaikh, I.N.; Venkataraman, K.; *Indian J. Chem.* **1969**, *7*, 188-9.
42. Mehandale, A.R.; Rama Rao, A.V.; Shaikh, I.N.; Venkataraman, K. *Tetrahedron Lett.* **1968**, 2231-4.
43. Pfister, R. "Teinture et alchemie dans l'orient Hellénistique", Seminarium Kondakovianum VII; Institut Kondakov: Prag, 1935, pp. 1-50.
44. Born, W. *Ciba-Rundsch.* **1936**, *7*, 218-28.

RECEIVED for review November 26, 1984. ACCEPTED March 13, 1985.

Analysis of Natural Dyes on Wool Substrates Using Reverse-Phase High-Performance Liquid Chromatography

Cynthia Walker and Howard L. Needles

Division of Textiles and Clothing, University of California, Davis, CA 95616

The separation and identification of natural dyes from wool fibers using reverse-phase high-performance liquid chromotography (HPLC) were performed on a C-18 column. Two isocratic four-solvent systems were developed on the basis of the Snyder solvent-selectivity triangle concept: (1) 10% acetonitrile, 4% alcohol, and 2% tetrahydrofuran in 0.01 M acetic acid and (2) 7% acetonitrile, 8% alcohol, and 5% tetrahydrofuran in 0.01 M acetic acid. Samples were also eluted in 30% acetonitrile. Spot tests and thin-layer chromatography were performed on all samples to confirm HPLC results. The systems also were found to be potentially useful in the identification of early synthetic dyes. A system of sample preparation that minimizes the reaction of samples was discussed. The application of this HPLC separation technique to samples from 20th century Caucasian rugs and American samples unearthed from the foundation of Mission San Jose was examined.

MUCH WORK HAS BEEN DONE in the past few decades on thin-layer chromatography (TLC) and wet chemical analysis of naturally dyed textile samples (*1–3*). Many good analytical schemes have been developed by using these techniques, particularly for red and blue dyes. Yet, reverse-phase high-performance liquid chromatography (HPLC) is now generally regarded as the most effective means of separation of polyphenolic compounds, and natural dyes almost exclusively are polyphenolic compounds (*4–5*). We have developed two four-solvent systems and one two-solvent system that can be used to obtain "fingerprint" chromatograms of dyes, isomers, and minor products present in sample extracts. Samples were also eluted in the two TLC systems outlined in the experimental section, and appropriate spot tests were performed when R_f values from the two systems compared well

0065-2393/86/0212-0175$06.00/0

with a previously tabulated value from TLC runs of standard samples. In conjunction with TLC and spot-test results, the data from the three HPLC system trials led to identification of dyes from ancient textile samples. In this chapter we discuss the development of the solvent systems used, the results of the technique when it was applied to two sets of ancient textile samples, and the possibilities and limitations of reverse-phase HPLC in natural dye analysis.

Experimental

Samples first were washed in water with manual agitation in a Buchner funnel and then were successively rinsed with methanol, chloroform, methanol, and water. During this process, particulate debris separated from the fibers, and it was assumed that loosely attached water-, methanol-, and chloroform-soluble impurities largely washed out with the filtrate. Preliminary extraction tests for the presence of synthetic dyes were conducted as follows: Samples were first boiled in water. If the solution colored, the water extract was analyzed with HPLC, and the sample was then boiled in dilute ammonia. If the ammonia extracts were strongly colored (natural dyes with the exception of very few do not extract into water or dilute ammonia), they were shaken with zinc dust, and if the ammonia extract reduced to a completely colorless solution, it was concluded that the sample was an azo dye (*1*). Early synthetic dyes often bleed into boiling water, and azo groups will reduce in the presence of zinc dust.

An acid extraction was prepared on all samples and was carried out in the manner described later. After extraction, all samples were filtered with 0.45-μm fluorocarbon filters. Twenty microliters of solution was used for each analysis on a Perkin-Elmer series 10 HPLC. Each sample was allowed to run 20 min, and the results were printed by computer. The column used was a 10-cm C-18 reverse-phase 10-μm Perkin-Elmer column with an Alltech precolumn attached. The detector used was a Perkin-Elmer model LC-15 UV detector set at 254 nm.

Three solvent systems were used: System 1, 10% acetonitrile (Baker UV spec grade), 4% alcohol (Baker HPLC grade alcohol, 95% ethanol, 5% methanol), and 2% tetrahydrofuran (Aldrich gold label) in 0.01 M aqueous acetic acid; System 2, 7% acetonitrile, 8% alcohol, and 5% tetrahydrofuran in 0.01 M aqueous acetic acid; and System 3, 30% aqueous acetonitrile. The water used was distilled double-deionized water (Millipore MilliQ system, type 1 water, Bedford, Mass.) degassed by boiling. Once prepared, the solvent system was filtered through a Millipore Durapore membrane 0.45-μm filter.

To test for indigo, a sample was warmed in a standard reducing solution (1 g of NaOH, 1 g of sodium dithionite, and 100 mL of water) until fibers and solution were yellow. A few drops of ethyl acetate was then added, and the tube was shaken gently. If indigo was present, the ethyl acetate layer became blue as any indigo present was reoxidized. Comprehensive outlines of spot tests for other natural dyes can be found in References 1 and 2.

TLC systems that were found to separate natural dyes well were (1) 30% acetonitrile and (2) 5% tetrahydrofuran and 10% alcohol. Both solvent mixtures were used with Baker 10% acetylated cellulosic plates.

Dye samples were pressed into KBr pellets and scanned on a Perkin-Elmer 281 IR spectrophotometer.

Solvent System Development

The technique used to develop the four-solvent systems was based on procedures elucidated by Lehrer (*6*), Rohrschneider (*7*), and Glajch (*8*). After trials with individual solvents chosen from the corners of the Snyder solvent-selectivity triangle—a system of classification of solvents by the degree to which they function as proton donors, proton acceptors, or dipole interactors—an ideal solvent system was calculated. Ethanol, acetonitrile, and tetrahydrofuran were the reverse-phase solvents used, and water was the carrier solvent. Once the ideal solvent strength of one solvent-water combination was empirically determined, that of the other combinations could be estimated by use of the following equation (*9*):

$$S_T = s_i \psi_i \tag{1}$$

where S_T is the total solvent strength, s_i is the strength weighting factor, and ψ_i is the volume fraction of the solvent. After determining with one solvent-water combination the solvent strength that resulted in the elution of the most strongly retained sample at a predetermined capacity factor (k') (10 was chosen for this study), S_T was calculated. The k' value represents the ratio of the retention of the solute to the amount of time an unretained substance takes to elute. From S_T, ψ_i of the other two solvents was determined by substituting their s_i values into Equation 1 (*10*). The s_i values for ethanol, acetonitrile, tetrahydrofuran, and water are 2.6, 3.2, 4.5, and 0, respectively.[1]

As an initial approximation of the ideal solvent strength for HPLC, the results of TLC studies on acetylated cellulosic plates with various methanol-water mixtures and natural dye extractions were graphed (R_f vs. methanol concentration). An acetylated cellulosic TLC system is not directly comparable to a C-18 HPLC system, but TLC results were nonetheless useful as a rough estimate of solvent strength. In practice, approximately two-thirds of the solvent strength required to elute natural dyes with TLC was necessary to achieve a similar separation of major sample components with HPLC. After individual solvent concentrations were determined, samples of known dyes extracted from wool were eluted in each of the three pairs of solvents (the concentration used for each individual solvent-water system was reduced by one-half) and adjustments were made until each sample eluted with a k' value no larger than 10. Retention times and k' values are equivalent expressions of relative retention of a sample on the column if the flow rate is the same for all trials. With a flow rate of 1.4 mL/min, the maximum time

[1] The s_i value for methanol was used here for ethanol because these values are only rough approximations.

that was still within the k'-value limit was approximately 20 min which was the length of time all samples were allowed to run. The data from these trials were then averaged to arrive empirically at an optimum isocratic four-solvent system, System 1.

Natural dyes are almost entirely napthoquinoid, anthraquinoid, or flavonoid compounds having one or more hydroxyls as the primary functional group. Considerable variation in structure occurs among natural dyes, and a single HPLC system that could separate all natural dye samples was not found. Nevertheless, several workable systems were found in which all dye components eluted except for indigo-carmine, which eluted with the solvent, and indigo and turmeric, which remained on the column. For an isocratic system, we consider this situation to be very satisfactory.

Because most natural dyes are phenolic, they are somewhat acidic. Tailing can occur with such compounds in neutral solvents (*4*). To minimize tailing, the solvent can be acidified to keep the sample in the un-ionized state in which it will tail less. The four-solvent systems were brought to the limit of pH tolerance of the column with acetic acid (0.01 M = pH of approximately 3.4). The four-solvent system arrived at empirically was System 1. Both 20% and 30% acetonitrile were also found to be useful solvent systems. By using the strength of 20% acetonitrile, as determined with Equation 1, another four-solvent system was calculated to arrive at a system having the same overall strength of 20% acetonitrile, but showing better selectivity. The components of this calculated system, System 2, have approximately equal solvent strength. System 2 and System 3 (30% acetonitrile) were used to supplement the original, empirically derived four-solvent system, System 1. All samples were analyzed in all three systems. The fingerprint chromatograms obtained from the HPLC analysis of each historic sample extract in the two four-solvent systems as well as in 30% acetonitrile were compared to those of dye standards extracted from wool to establish the identity of the unknown samples. Sixteen wool samples dyed with known natural dyes were available as standards. Pure samples, not extracted from wool fibers, of the major coloring matter of each of the wool-extracted standard samples (reagent grade chemicals) were also chromatographed in each of the systems. After HPLC analysis, TLC and spot tests were performed as confirmatory analytical techniques.

Results and Discussion

Sixteen textile samples from Caucasian rugs were analyzed with the systems just discussed, as were thirteen American samples of textile fragments found buried in the foundation of Mission San Jose. Results are summarized in Tables I and II. Five of the Caucasian rug samples

Table I. Caucasian Sample Results

Color of Wool	*Identity*
Brown	—
Dark green	not an acid dye
Red	acid azo dye
Orange	orange II
Red	madder
Red	acid azo dye
Green-gold	weld
Orange	—
Gold-orange	same as orange wool above, but not identified
Brown	madder
Red	acid azo dye
Orange	madder
Green with purple tips	—
Orange	acid azo dye
Orange-brown	—
Purple	acid azo dye

were found to be synthetic through preliminary extraction tests and through identification of an azo group by reduction with zinc dust. (Extraction tests and azo group tests are described in the experimental section.) One of these was found to be Orange II (acid orange 7) on the basis of TLC, IR, and spot-test results. Of the remaining samples, one was identified as weld, and three were identified as madder. The rest, many of which are suspected to be synthetic, have not yet been

Table II. Mission San Jose Sample Results

Description	*Identity*
Brown wool	cutch
Red wool	brazilwood
Green wool	—
Bright-green wool	—[a]
Black-brown silk	cutch
Brown cotton velvet	cutch
Red cotton	madder
Blue cotton	—
Brown wool	—
Green wool	—
Tan wool	—
Purple wool	—
Brown wool	—

[a]This sample responded exactly like an acid azo dye to extraction tests, although all samples were alleged to be definitely of presynthetic dye vintage.

identified. Of the Mission San Jose samples, one was identified as madder, one was identified as brazilwood, and three were identified as cutch. The other sample chromatograms did not match well with any of the standard chromatograms. Almost all of the unknown samples, even though they were not identified, produced good chromatograms. Those samples found to be of synthetic origin resulted in particularly well-defined peaks.

The Caucasian samples were from 20th century rugs, and it is quite likely that those samples that were not identified were synthetic. Two known early synthetic dyes which were available for analysis, Ponceau R and Amaranth, responded well in the HPLC systems used. Because the Caucasian sample extracts identified as synthetic and the two synthetic dye standards all eluted quite well, the solvent systems developed here fortuitously may be useful for the analysis of early synthetic dyes as well as natural dyes. Once the appropriate synthetic dye standards are found, identification of the samples that did not correspond with known standards will most likely follow.

Two of the Mission San Jose samples were blue and several were green or purple, although spot tests and chromatographic evidence showed that none were logwood, indigocarmine, or, surprisingly, indigo. The presence of indigo was determined by the method developed by Hofenk de Graaf (*11*) (*see* experimental section). TLC studies confirmed the absence of indigo in all samples.

Natural dyes possessing several component substances as colorants, such as fustic, St. John's wort, or madder were the easiest samples to identify because they produced more distinctive patterns of peaks on HPLC analysis rather than a single peak. Significant dye peaks can often be small which, like the HPLC analysis of all natural product samples, can be a source of confusion because impurities and minor sample components can elute in the same k'-value range as the dye sample. Transparent overlays of dye standard chromatograms were superimposed over those of unknown samples to assess not only the actual retention times of the coloring components but also their relative proportions. Comparison by this technique allowed one to determine by visual inspection whether the relative peak heights and spacing of peaks in a sample chromatogram were consistent with those of a known sample, although actual retention times varied slightly because of small changes in solvent composition if the two were not run in the same batch of solvent. Particular care must be taken in solvent preparation to minimize this effect. After each batch of solvent was prepared, the pH of the resulting solution was measured and was found to consistently be between 3.2 and 3.4 (calculated pH = 3.4). As an additional test of consistency between solvent mixtures, brazilin dissolved in ethanol was chromatographed as the first and again as the final sample of each batch

of solvent prepared. The retention time of brazilin was found to vary between batches of solvent by not more than 40 s and to vary by approximately 10 s between the chromatogram of a fresh mixture (500 mL) of solvent and the last chromatogram from the same mixture.

A disadvantage to analysis with HPLC that was not found to as great an extent in TLC is the elution of water- and alcohol-soluble fatty acids, which are easily extracted from wool fibers along with the coloring compounds. In addition to this disadvantage, many natural dye samples were found to be quite sensitive to acid extraction. The majority of yellow, green, and brown dyes are flavonoids, which are well known to convert into one of several compounds in the presence of either heat and water or dilute acids (*12*). One probable reaction is the polymerization of the flavonoid by the reaction shown in Scheme I (*13*). This product can, in turn, further polymerize to form a complex tannin. When a few milligrams of catechin was dissolved in 0.5 mL of alcohol and was warmed for approximately 5 min after the addition of a few drops of 10% HCl, the most obvious change noticed between the IR spectrum of the reaction product and that of the starting material was the dramatic reduction in the size of the ether linkage C–O stretching vibration peak at 1050 cm^{-1}, which is in agreement with the proposed reaction product (Figure 1). The spectra of the acid-hydrolyzed and untreated samples match those published by Samejima and Yoshimoto (*14*) of polymerized and unpolymerized catechin, respectively. Non-flavanoid dyes often also undergo reactions that are not reversible by neutralization alone when heated even briefly in dilute HCl (Figure 2). In the case of walnut (juglone) the conversion product elutes well, but more typical is the formation of a large initial peak similar to that which occurs when catechin, the coloring matter of cutch, is heated even briefly in acid (Figure 3). Extracts must be analyzed when they are fresh because, even after neutralization, the samples can undergo conversion reactions if they are allowed to stand longer than a day or two and will then no longer exhibit the same chromatographic behavior. In addition to reactions of the coloring matter itself, compounds extracted from the wool fiber can also cause a large tailing initial peak which can obscure small early-eluting compounds.

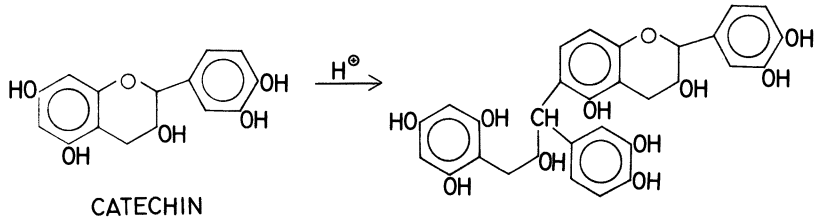

CATECHIN

Scheme I

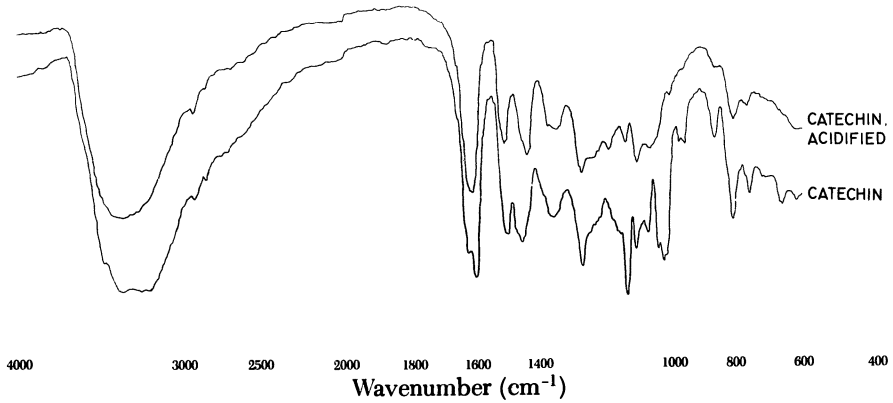

Figure 1. IR spectra of untreated and acid-hydrolyzed catechin.

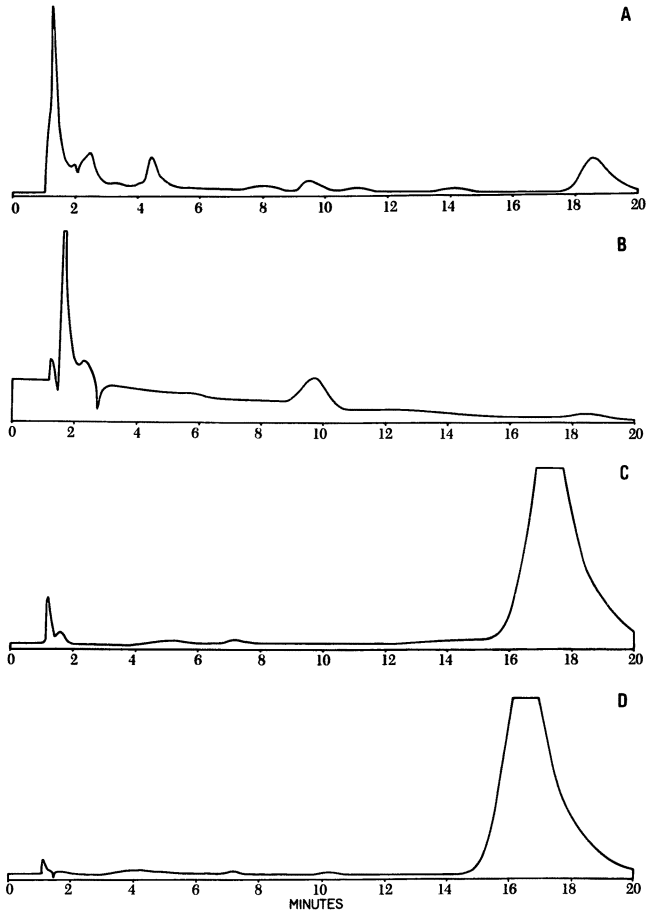

Figure 2. Chromatograms: A, walnut extracted from the fiber; B, juglone untreated; C, juglone after acidification; and D, C after neutralization. All samples were eluted in System 1.

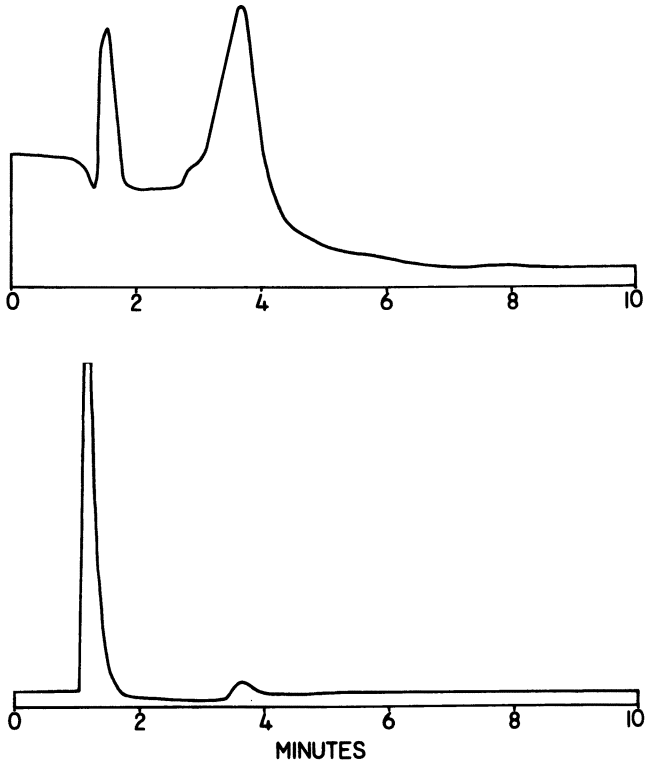

Figure 3. Chromatograms: top, catechin untreated; bottom, catechin after acidification. Both samples were eluted in System 1.

To counter the situations just mentioned, dyes were extracted from samples as follows: Fibers were allowed to soak in a minimum of cold 1 M HCl for approximately 5 min, after which methanol was added (about three or four times the volume of the fibers), and the samples were carefully neutralized with 1 M NaOH until litmus paper did not change color with time after being spotted with the extraction solution. The sample was then placed in a water bath that was just below the boiling point of the solution and was allowed to stand for 5–10 min. This procedure was used on standards as well as unknown samples. The technique was found to extract all samples well and to result in clean chromatograms with smaller initial peaks than those obtained with other sample preparation methods attempted. A variety of nonacidic and aprotic solvents were explored as possible substitutes for acid extraction, but none were found to be effective.

When baseline separation of peaks in a chromatogram is achieved, the individual compounds can be collected as they elute from the

column in essentially pure form. However, with an analytical scale column, the quantity retrieved even from large peaks is well below the detection limit of most other analytical techniques and can be collected only as an extremely dilute solution.

Purified samples, dissolved in alcohol, of the major coloring compounds of each of the natural dyes studied were also chromatographed in the same manner as the extracted known samples whenever they were available. These chromatograms were used to establish which of the several peaks that often eluted from the dye sample was the principal dye component. Peaks corresponding to the primary colorants of samples extracted from wool fibers were often quite small and often not the major peak (Figure 2). Small peaks must not be neglected when interpreting sample chromatograms. The mildest successful extraction technique was employed, yet even this technique has resulted in the partial conversion of components of dye samples into other products.

Conclusions

The isocratic systems used in this study do succeed in characterizing the components of most natural dye samples. Even a sample that elutes with the solvent or remains on the column provides a clue to its identity and an indication of its relative polarity. Yet, when gradient elution is available, even better separations can be achieved.

Sample preparation presented the most likely source of potentially misleading chromatographic results. We are continuing to work on improved extraction techniques and are also continuing to explore the applicability of the systems studied for early synthetic dye analysis.

Acknowledgments

We wish to acknowledge Cathryn Cootner of the DeYoung Museum in San Francisco and Stephen Dietz of Archeological Consulting and Research Services for the generous donation of samples. Thanks also to K. Alger and R. Okamoto for many helpful discussions. We also wish to thank B. Anderton and G. Sensabaugh for providing one of us (C. W.) with the inspiration and means to begin natural dye research.

Literature Cited

1. Schweppe, H. *J. Am. Inst. Conserv.* **1980**, *19*(1), 14.
2. Hofenk de Graaf, J. *ICOM News* **1967**, Brussels.
3. Whiting, M. *Hali* **1979**, *2*(1).
4. Tittel, G.; Wagner, H. *Proc. Int. Bioflavanoid Symp.* **1981**, 299.
5. Wilson, E. *J. Sci. Food Agric.* **1981**, *32*, 257-264.
6. Lehrer, R. *Am. Lab.* **1981**, *13*(10), 113ff.
7. Rohrschneider, L. *Anal. Chem.* **1973**, *45*, 1241.

8. Glajch, J.; Kirkland, J.; Squire, K.; Minor J. *J. Chromatogr.* **1980**, *199*, 57ff.
9. Goldberg, A.; Lehrer, R. *Techscan* **1981**, *1*(4), 2.
10. *Ibid*, p. 6.
11. Hofenk de Graaf, J. *Stud. Conserv.* **1974**, *19*, 54.
12. Freudenberg, K.; Weinges, K. In "The Chemistry of Flavonoid Compounds"; Geissman, T., Ed.; New York, 1962; p. 209.
13. Ref. 8, p. 208.
14. Samejima, M.; Yoshimoto, T. *J. Jpn Wood Res. Soc.* **1979**, *25*, 671.

RECEIVED for review November 26, 1984. ACCEPTED March 18, 1985.

10

3600 Years of Purple-Shell Dyeing: Characterization of Hyacinthine Purple *(Tekhelet)*

I. Irving Ziderman

Israel Fiber Institute, P. O. Box 8001, 91080 Jerusalem, Israel

Purple wools, dyed using hypobranchial mucus from muricacean shellfish, were widely known in many ancient civilizations among their most precious treasures, particularly the bluish hyacinthine purple (biblical Hebrew, tekhelet*). Unknown since the seventh century,* tekhelet *has been an enigma to modern scholars, who have been uncertain as to how it is to be distinguished from the redder Tyrian purple* (argaman) *that is identified as 6,6′-dibromoindigotin. Evidence from chemical, biological, archaeological and talmudic studies indicates that* tekhelet *was prepared from banded dye-murex,* Trunculariopsis trunculus. *As prepared with this species, the dye is a mixture of approximately equal amounts of 6,6′-dibromoindigotin and indigotin; indigotin is a blue dyestuff that is fortuitously chemically identical to vegetable indigo. Authentic* tekhelet *accordingly has been characterized in a textile remnant from Palmyra that is some 1700 years old.*

RANKING WITH GOLD AND SILVER among the more precious treasures of antiquity were three colored woolen fabrics, each dyed with a colorant of animal origin. Two of these were purple materials prepared from shellfish: one was a blue-tinted shade called hyacinthine purple and the other, of reddish hue, was called Tyrian purple (*1*). The third material, a scarlet or crimson, was dyed with kermes, which is extracted from scale insects living on certain oak trees (*2*). The importance of these textiles in international trade and tribute and as adornment of sovereigns and sanctuaries is well documented in Mesopotamian texts from some 3½ millenia ago and in Near Eastern records (*3*) until the end of the classical period. The first archaelogical record of purple dyeing is from 1600 B.C. (Crete).

In the Bible, too, these three colored threads are mentioned scores of times, particularly in connection with the priestly apparel and the

0065-2393/86/0212-0187$06.00/0

tabernacle's awnings in Chapters 25–40 of Exodus and for use in the transportation of the sacred vessels in Chapter 4 of Numbers.

Because the use of kermes for crimson dyeing has continued through modern times, the nature of the raw material and how it is used is well known. In contrast, however, the purple industry largely collapsed by the seventh century, and since then its most important features have been forgotten, namely the identities of the snail species used and the actual colors of the authentic dyes.

Intensive modern studies have successfully identified Tyrian purple (*1*, *4*). Two related species of marine snails that inhabit the Mediterranean littoral were used by the Phoenicians in Tyrian purple manufacture, namely spiny dye-murex (***Bolinus brandaris***) and the rock shell ***Thais haemastoma*** that are shown in Figure 1 in the center and to the right, respectively. The chemical structure of the major colorant in the dye is that of 6,6′-dibromoindigotin (Structure **I** in Scheme I). The pigment is not found in the living murex, but it is actually an artifact formed by the action of air and sunlight on a colorless extract of the hypobranchial gland of the snail. Ancient textiles dyed with Tyrian purple have been uncovered by archaeologists in particular abundance at Palmyra (*5*), and potsherds colored with the dye have been uncovered at Tell Shikmona (*6*).

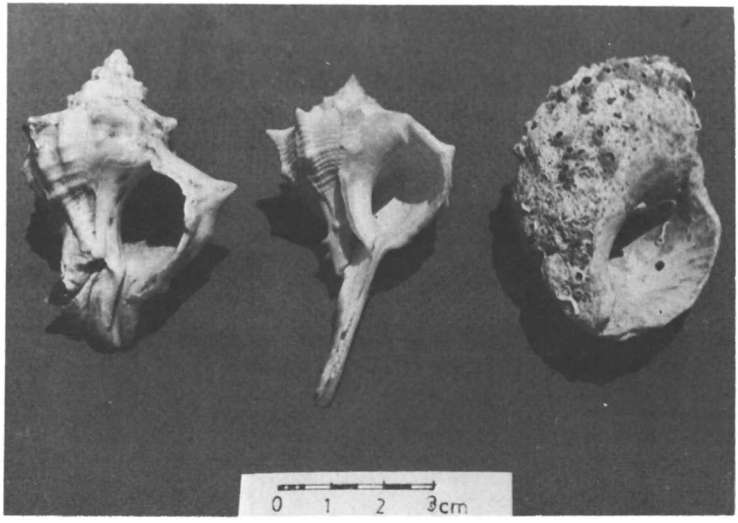

Figure 1. Shells of marine snails used in purple dyeing. Left to right: ***banded dye-murex*** (Truncolariopsis trunculus) *for* ***hyacinthine purple*** (tekhelet), ***spiny dye-murex*** (Bolinus brandaris) *for* ***Tyrian purple*** (argaman), *and the rock shell* Thais haemastoma *for* ***Tyrian purple*** (argaman).

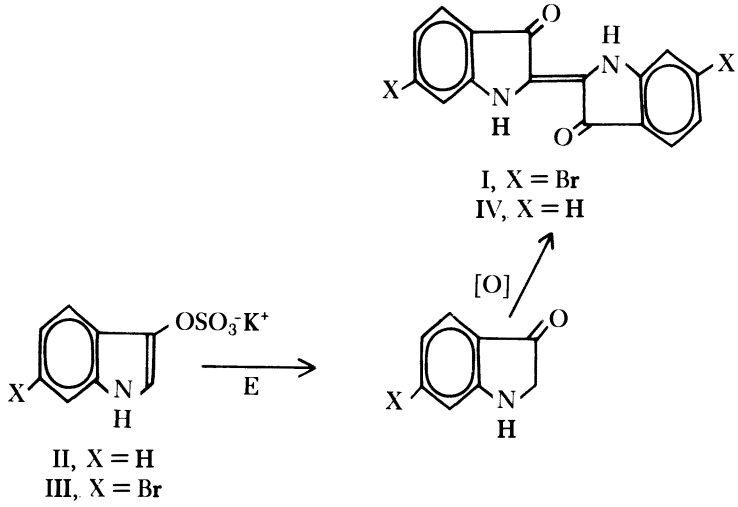

Scheme I. Major pathway for the transformation of natural colorless precursors obtained from banded dye-murex to hyacinthine purple (tekhelet). ***I**, 6,6′-dibromoindigotin; **II**, potassium indoxyl sulfate; **III**, potassium 6-bromoindoxyl sulfate; **IV**, indigotin; E, enzymatic or acidic hydrolysis, and [0], aerobic oxidation. (Reproduced with permission from Ref. 7. Copyright 1981 Society of Dyers and Colourists.)*

Regarding hyacinthine purple, however, several different and mutually exclusive identifications have been mooted by various scholars (7) and are the following: indigo blue, Tyrian purple (6,6′-dibromoindigotin), Prussian blue (cyanide salt of iron), *Janthina* pigment (bile pigment), green color (Tyrian purple intermediate tyriverdin), yellow color (Luther's translation of *gelb*), and hyacinthine purple (from *Trunculariopsis trunculus*). This identification question is not solely an academic one of interest in archaeology and art conservation. The Bible requires Jewish worshippers to attach to the corner tassels of their prayer shawls a thread of hyacinthine purple (Numbers 15:38). This commandment has not been observed since the seventh century. Discovery of the authentic blue-purple for the renewal of this ritual is awaited expectantly in synagogues throughout the world. Figure 2 shows Jewish tassels that incorporate a thread dyed with Prussian blue in accordance with the practice of Radzin. This dye is clearly unacceptable as an authentic purple because it is a synthetic cyanide salt of iron that is in no way related in structure to natural molluscan purples (7). The tassels from a Karaite prayer shawl (Egypt) appear in Figure 3; each tassel comprises 32 cords, half of which were originally dyed blue, as may be shown by unravelling the knot. The Jewish tassel has only eight cords (Figure 2).

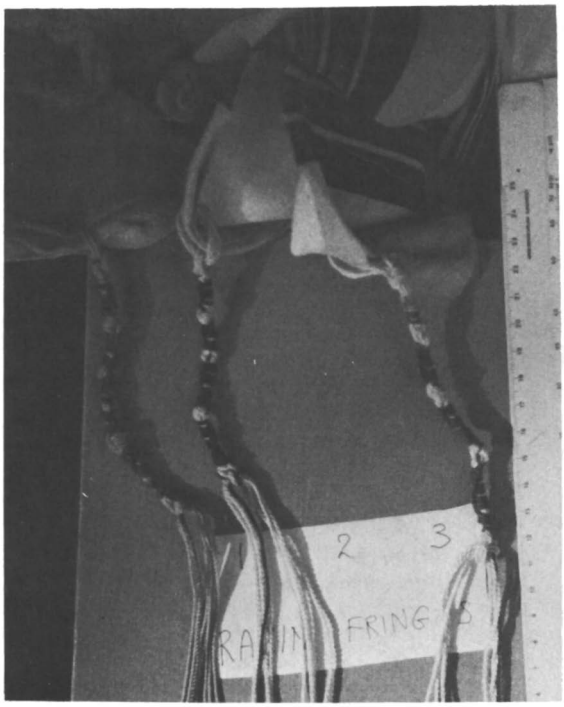

Figure 2. Corners of a traditional Jewish prayer shawl (tallit). *Three of its four corners are shown, each adorned with a tassel* (tzitzit) *of eight threads, one of which is dyed with Prussian blue, according to Radzin. 1 is older than 2 and 3, whereas 2 is older than 3, illustrating fading and varying strength of dyeings.*

Some views do not distinguish between Tyrian and hyacinthine purples, whereas others contend that hyacinthine purple is the vegetable dye indigo. The sources of this confusion are discussed in the following paragraphs.

First, the actual color of hyacinthine purple was uncertain. Ambiguities due to mistranslations of the biblical Hebrew *tekhelet* arose because no one had seen this textile for centuries. The result is the erroneous rendering of blue in most English bibles. The ancient Greek translation *hyakinthos* suggested to Luther a local flower and gem of the same name and led him to translate it as *gelb* or yellow. Furthermore, the word *tekhelet* has been revived in modern Hebrew to designate sky blue. Confusion was inevitable.

A second factor involves the usage of the term Tyrian purple. We have restricted it here to a particular type of shell purple that is

characterized chemically as 6,6′-dibromoindigotin. However, many authors use Tyrian purple as a generic term for all types of purples derived from shellfish, whatever the hue and chemical composition of the colorant. This usage includes hyacinthine purple and thus further confuses the issue of how to distinguish between the two principal purples of antiquity.

A third source of confusion has been the nature of the ancient forgery of *tekhelet* named *kela-ilan*. To have been such a successful imitation, *kela-ilan* must have been indistinguishable from *tekhelet*. It is generally accepted that *kela-ilan* was indigo, a blue vegetable dye. Accordingly, one is forced to conclude that hyacinth was blue. This conclusion excludes any seashell as its source because seashells give only purples. I have now demonstrated that this conclusion is untenable (*8*). The early midrash *Sifrei* in Numbers 15:41 states explicitly that *tekhelet* is forged by using a mixture of two materials, namely *kela-ilan* and a red colorant. The result is a purple. An authentic sample of *kela-ilan* dated A.D. 135 was found (*9*) in the Judean wilderness and is shown in Figure 4. For comparison, the dyeing obtained with the secretion from banded dye-murex (*Trunculariopsis trunculus*) is also shown in Figure 4. They

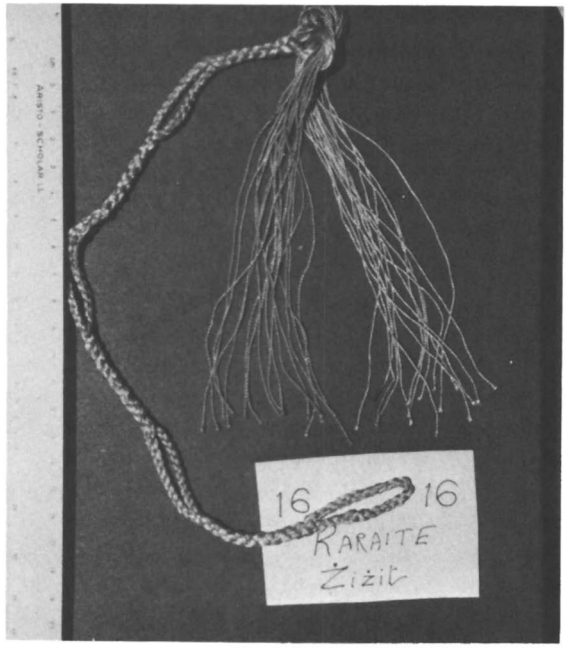

Figure 3. Single tassel from an Egyptian Karaite prayer shawl comprising 32 threads, half of which were originally dyed blue.

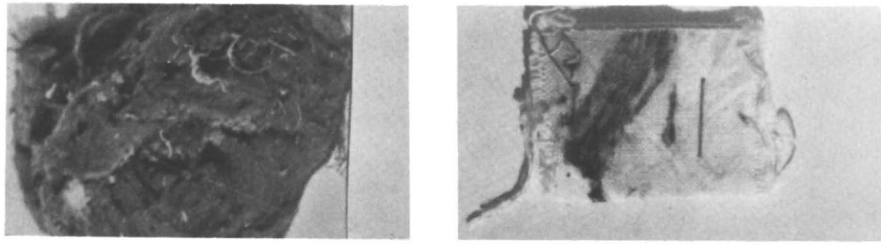

Figure 4. Left, kela-ilan *[archaic hyacinthine purple forgery* (9, 20)*] and right, contemporary hyacinthine purple from banded dye-murex. (Left photograph reproduced with permission from Ref. 20. Copyright 1968 Ciba-Geigy Review.)*

are indistinguishable violet colorings. ***Truncullariopsis trunculus*** is shown in Figure 1, left.

A thorough study of the subject reveals 12 criteria for identifying the snail that was the source of ancient hyacinthine purple, and these criteria are the following: (1) Phoenician seashell source (gastropod mollusk, conch, murex snail), (2) hyacinthine hue (bluish purple, violet), (3) color of ***kela-ilan*** (counterfeit ***tekhelet***), (4) unknown for 1500 years (ritual tassels' use), (5) distinguishable from ***argaman*** (Tyrian purple), (6) seasonal rarity, (7) coloration of shell, (8) stability and fastness of dyeing, (9) colorless secretion of live snails (artifact color), (10) comparison to grass, trees, the sea, and the sky, (11) technical feasibility [Doumet (*16*)], and (12) authentic historic specimens (Palmyra, Dead Sea). Banded dye-murex exhibits all these features, and must therefore be the elusive conch of *tekhelet* (*7*). This candidacy was, in fact, first proposed unobtrusively in 1842 by a Venetian scholar named Bartolomeo Bizio (*10*). Modern science has taken 140 years to vindicate his insight.

The colorant obtained from ***Truncullariopsis trunculus*** is a mixture of two dyestuffs, namely indigotin and 6,6′-dibromoindigotin. Indigotin is chemically indistinguishable from vegetable indigo blue, and 6,6′-dibromoindigotin is chemically indistinguishable from Tyrian purple (*11*, *12*). Together, however, these two chemicals form a unique violet, which was so sought after in antiquity.

Archaeologists have found shells of banded dye-murex used by the Phoenicians in purple dyeing at Sidon and Sarepta, whereas spiny dye-murex was used at Tyre (*13*). Figure 5 shows a whole *trunculus* beside a *trunculus* fragment from a Persian stratum at Appolonia. The *trunculus* fragment lost its spine when an ancient dyer broke the shell open in a characteristic fashion to remove the hypobranchial gland from within for extraction of the chromogenic mucus.

To ascertain whether the colors associated with Tyrian and hyacinthine purples can be made from the snails currently inhabiting the formerly Phoenician coast, I prepared crude dyes from hypobranchial glands of banded dye-murex and of the two Tyrian purple species, spiny dye-murex and *Thais haemastoma*. (Methanolic extracts of the glands were subjected to acidic hydrolysis (*12*) followed by exposure to sunlight for 2 h.) The snails were collected from the Mediterranean shore of northern Israel. In Figure 6, the blue-black specimen is from banded dye-murex, and the two reddish samples are from the Tyrian purple species. On purification by extraction in chloroform, the blue-black specimen yields a violet solution, whereas, the two reddish samples give a reddish purple, as shown in Figure 7. Figure 7 also shows a solution of synthetic indigotin for comparison. Although the fidelity of color reproduction in these prints is not exact, the species color differences are clearly demonstrated.

Spanier (*14*) has recently demonstrated a semiannual cycle in the availability of *trunculus* snails near Haifa. This cycle thus provides a biological basis for the proverbial seasonal rarity of the hyacinthine purple conchs. The snails bury themselves in the littoral sea bed in the

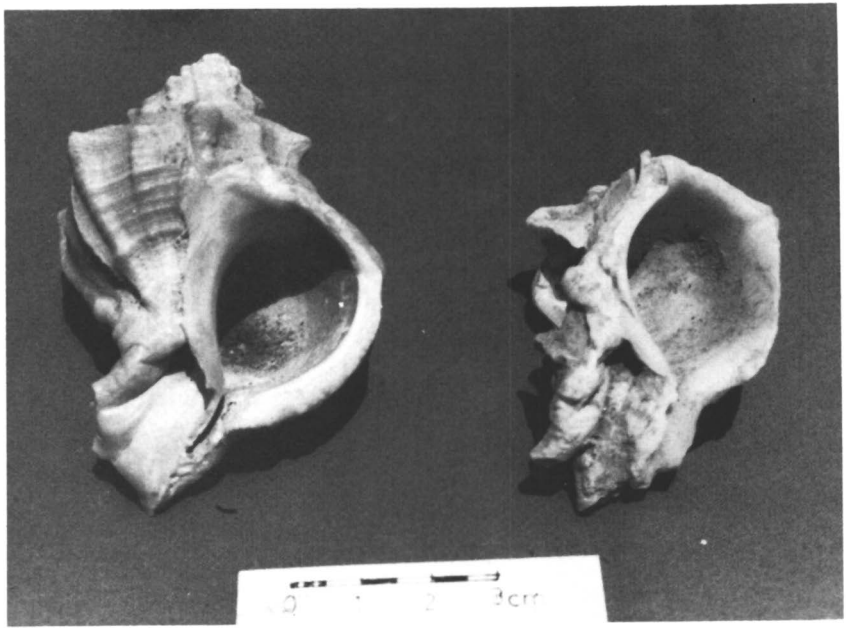

Figure 5. Left, a shell of banded dye-murex and right, a fragment of same species with spire broken off to permit excision of chromogenic gland (from a Persian stratum of I. Roll's excavation at Appolonia).

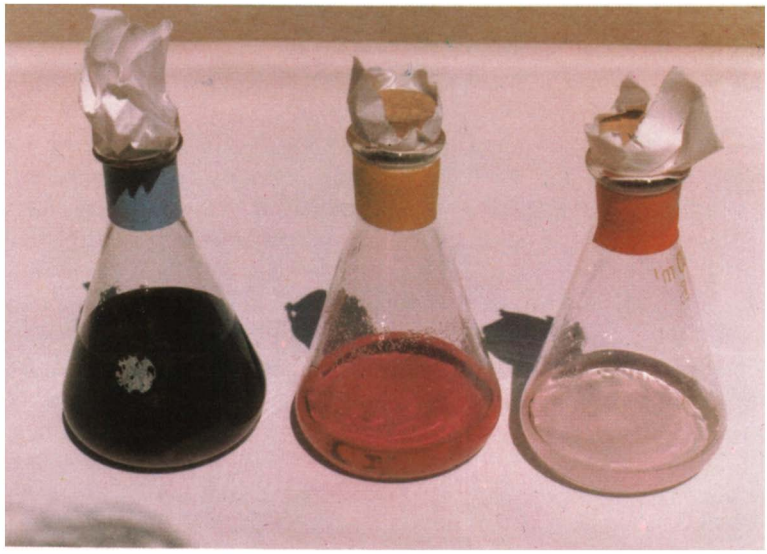

Figure 6. Crude colors developed from hypobranchial extracts of banded dye-murex (left, blue label), rock shell (center, yellow label), and spiny dye-murex (right, red label).

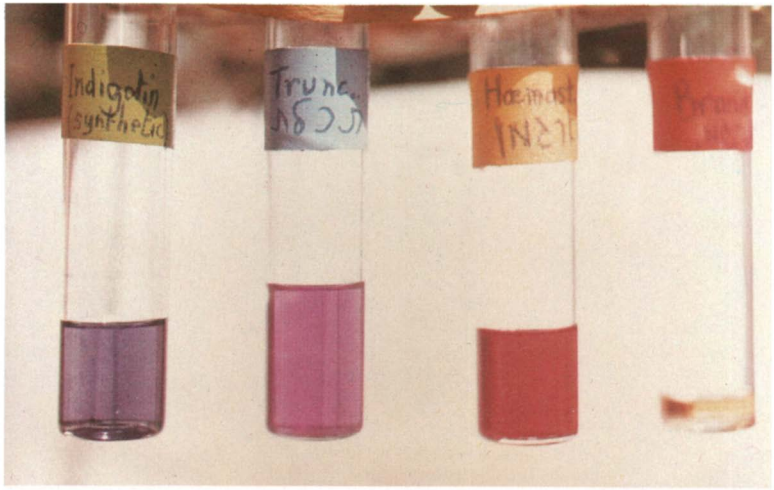

Figure 7. Green label: synthetic indigotin; blue, yellow, and red labels: purified extracts in chloroform solution of dyes from banded dye-murex, rock shell, and spiny dye-murex, respectively, prepared from the crude extracts of Figure 6.

summer and appear from the soil in the cold season. The stormy winter seas prevent shell fishing that thus may be practiced only at the commencement of fall and in early spring when the eastern Mediterranean is placid and the snails are exposed on the surface of the sea bed. The live shells are characteristically colored because of biological fouling (*6*), as shown in Figure 8.

The cryptic talmudic comparisons of the color of *tekhelet* to that of grass, trees, the sea, and the sky is understood now as reference to the chromatic sequence that occurs in nature when the colorless mucus from the snail, upon exposure to the elements, first becomes yellow, then gradually changes to green, followed by blue, and finally becomes violet (*15*).

In regard to the technical feasibility of having obtained hyacinthine purple from *Trunculariopsis trunculus* in antiquity, Doumet (*16*) recently demonstrated that he could dye wool with the crushed shells, following the "procedure of Tyre" as described by Pliny the Elder, who visited Judea in person. Only techniques and materials available to ancient artisans were used in this experiment.

The validity of the *trunculus* theory of the source of hyacinthine purple has now been corroborated by the identification of authentic archaeological remains of the dye on a textile from Palmyra some 1700 years old (*8*) and on a potsherd from the seventh century excavated near the Dead Sea.

The major natural precursors of hyacinthine purple in the hypobranchial gland are potassium indoxyl sulfate (Structure **II** in Scheme I) and its 6-bromo derivative (Structure **III** in Scheme I) (*12*). These are hydrolyzed and then aerobically oxidized to the final mixture of Structures **I** and **IV** (Scheme I).

The identification of purple dyes (*17*) is summarized in Table I.

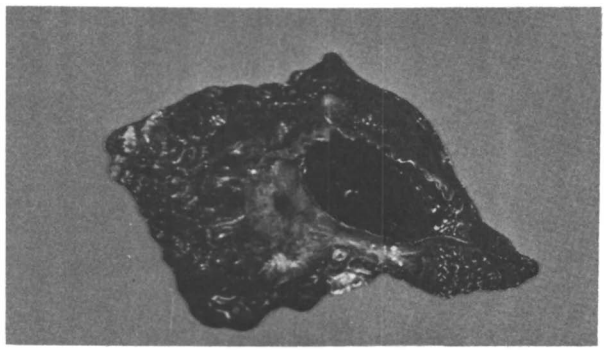

Figure 8. Biological fouling on shell of banded dye-murex (6). *(Reproduced with permission from Ref. 21. Copyright 1982 Weizmann Sci Press.)*

Published on February 1, 1986 on http://pubs.acs.org | doi: 10.1021/ba-1986-0212.ch010

Table I. Summary of the Identification of Purple Dyes

Name			
Biblical (Hebrew)	*Classical*	*Chemical*	*Marine Source*
Tekhelet	hyacinthine purple	6,6′-dibromoindigotin, indigotin	*Trunculariopsis trunculus*
Argaman	Tyrian purple	6,6′-dibromoindigotin	*Bolinus brandaris, Thais haemastoma*

Conclusions

Archaeological remains dyed with an indigotin and 6,6′-dibromoindigotin mixture corroborate the view that antique *tekhelet* was prepared from *Trunculariopsis (Murex) trunculus* (*8*).

The *trunculus* theory for the source of *tekhelet* provides archaeometry and historic conservation with malacological and chemical tests for distinguishing *tekhelet* dyeings from Tyrian purple (*18*).

The identification of *tekhelet* permits the development of a new textile product for the revival of Jewish ritual practices, such as dyed tassels for prayer shawls (*19*).

Acknowledgments

E. Spanier, Haifa University, provided the photographs for Figures 6 and 8 and kindly supplied the shellfish and dissected the hypobranchial glands. Ezra P. Gorodeski, Jerusalem, provided the Karaite tassel shown in Figure 3. The photographs for Figures 1, 4, 5, and 7 were taken by Y. Nattaf.

Notes Added in Proof

Tyrian purple (6,6′-dibromoindigotin) has been identified on potsherds excavated at Sarepta in Lebanon (22).

In contrast to the erroneous rendering of *tekhelet* as blue in English bibles based on the King James version of 1611, two modern translations of the Bible render it as violet (*23*, *24*).

Literature Cited

1. Born, W. *Ciba Rev.* **1937**, *4*, 106–29.
2. Sternlicht, M. *Israel Land and Nature* **1980**, *6(1)*, 17–21.
3. Eilat, M. "Economic Ties between Biblical Lands in the First Temple Period"; Bialik: Jerusalem, 1977 (in Hebrew; being translated by author).
4. Baker, J.T. *Endeavour* **1974**, *2*, 11–7.
5. Pfister, R. "Nouveaux Textiles de Palmyre"; Les Editions d'Art et d'Histoire: Paris, 1937.
6. Spanier, E.; Ziderman, I. *Mada* **1982**, *26*, 184–7 (in Hebrew).
7. Ziderman, I. *J. Soc. Dyers Colour.* **1981**, *97*, 362–64; Correction: *ibid.* **1982**, *98*, 247.
8. Ziderman, I.I. *Bull. Ame. Sch. Orient. Res.*, in press.
9. Yadin, Y. "The Finds from the Bar-Kokhba Period in the Caves of the Letters I"; Israel Exploration Society: Jerusalem, 1963; pp. 182–87.
10. Grimand de Caux; Gruby. *C.R. Hebd. Séances Acad. Sci.* **1842**, *15*, 1007–9.
11. Bouchilloux, S.; Roche, J. *Bull. Soc. Chim. Biol.* **1955**, *37*, 37–53.
12. Fouquet, H.; Beilig, H.-J. *Angew. Chem. Int. Ed. Eng.* **1971**, *10*, 816–17.
13. Reese, D.S. *Annu. Rep. Soc. Libyan Stud.* **1979–80**, *11*, 79–93.

14. Spanier, E. In "Developments in Arid Zone Ecology and Environmental Quality"; Shuval, H., Ed.; Balaban, I.S.S.: Philadelphia, 1981; pp. 65–70.
15. Dedekind, A. *Arch. Zool. Exp. Gen., 3e Serie* **1898**, *6*, 467–80.
16. Doumet, J. "A Study on Ancient Purple Colour"; Inprimerie Catholique: Beirut, 1980.
17. Ziderman, I.I. *Chem. Eng. News* **1983**. *61* (*24*), 88.
18. Ziderman, I.I. *Biblical Archaeol.*, in press.
19. Ziderman, I.I., In "Book of Tekhelet and Argaman"; Spanier, E., Ed.; Magnus: Jerusalem, in press.
20. Cover illustration, *Ciba Rev.* **1968**, issue 2.
21. Cover illustration, *Mada* **1982**, *26* (*4*).
22. McGovern, P. E.; Michel, R. H. *M.A.S.C.A. J.* **1984**, *3* (3), 67–70.
23. "New English Bible"; Oxford and Cambridge Univ. Presses, 1970.
24. "The Jerusalem Bible"; Darton, Longman and Todd: London, 1966.

RECEIVED for review November 26, 1984. ACCEPTED March 13, 1985.

11

Mordanted, Natural-Dyed Wool and Silk Fabrics

Light and Burial-Induced Changes in the Color and Tensile Properties

Howard L. Needles, Vicki Cassman, and Martha J. Collins
Division of Textiles and Clothing, University of California, Davis, CA 95616

Light and burial-induced weathering caused significant changes in the color and tensile properties of natural-dyed and mordanted-natural-dyed wool and silk fabrics. The degree and nature of light and burial-induced changes on these fabrics were dependent on the fiber type and the dye or dye-mordant combination used. Dyed wool samples were generally more colorfast to simulated sunlight from a filtered xenon source than mordanted-dyed wool samples, whereas the dyed silk samples were rendered more colorfast to light by mordanting. Soil burial caused darkening and large shade changes in dyed wool and silk fabrics due to soil ion-induced mordanting. Dyed-mordanted samples underwent smaller shade and depth of shade changes than unmordanted-dyed samples on burial, and chromium and copper mordants had the greatest effect.

DYE ANALYSIS IS AN IMPORTANT ANALYTICAL TOOL in the characterization of textiles of historical significance, but such analysis can be complicated by the aging process. Natural dyes found on historic textiles are not particularly lightfast or fast to soil burial conditions, and changes in the shade and depth of shade of dyed textiles can occur during these weathering processes. Mordanting of natural-dyed textiles with metal salts also can affect their color. In addition, the tensile properties of natural-dyed textiles can be affected by the dyeing-mordanting and weathering processes. Because the mechanisms of degradation are very different for weathering by light exposure versus burial in soil, color changes and changes in tensile properties are expected to differ depending on the weathering process used. The lightfastness of natural-

0065-2393/86/0212-0199$06.00/0

dyed textiles also is of importance to the textile conservator because light exposure during display or storage can critically affect the color and the tensile properties of the textile.

The lightfastness of natural dyes on fabric substrates has been the subject of numerous studies. However, the effect of mordants on the lightfastness of natural-dyed protein fiber substrates has received little attention. Some studies concerned with the effect of mordanting on the lightfastness of silk dyed with natural dyes have been conducted in Japan (*1–3*). Other studies have been concerned with the fastness of mordanted, natural-dyed protein fibers to artificial light as would be found in a museum setting (*4–6*). All these studies have established that mordants have a significant effect on the lightfastness of natural-dyed protein fibers.

Archaeological specimens of historic textiles found in burial sites are often exposed to the most severe conditions; exposure to bacteria, yeasts, algae, and fungi causes severe discoloration and degradation to the dyed textile (*7*). Although certain metal salts are known to have antimicrobial properties, little is known about the effect of mordants on burial-induced color changes in natural-dyed protein fibers. Nockert and Wadsten observed that wool stored near metal objects or ornaments shows less degradation on storage (*8*). They concluded that soil fungi and other organisms are killed by metal ions and particularly by copper ions.

To gain a better understanding of the effect of protein fiber type, dye, and mordant on sunlight and burial weathering processes, we dyed wool and silk with three phenolic dyes (found as major components in natural dye mixtures extracted from various plant sources) and post-mordanted samples of the dyed fabrics with five representative metal salts. We then exposed the unmordanted and the dyed-mordanted samples to simulated sunlight or soil burial and measured the differences in the color and tensile properties that resulted from these treatments.

Experimental

Materials. The wool fabric was a plain-weave worsted wool, style 6561, from Burlington Industries. The silk fabric was a degummed silk crepe, style 601, from Testfabrics, Inc. The dyes were $>95\%$ pure and were from the following sources: alizarin (C. I. Mordant Red 8) from Aldrich Chemical Co.; brazilin (C. I. Natural Red 24) from J. T. Baker Chemical Co.; and carminic acid (C. I. Natural Red 4) from H. Kohnstamm & Co., Inc. The five reagent grade metal salts used were aluminum potassium sulfate, stannous chloride, cupric sulfate, ferrous sulfate, and potassium dichromate from J. T. Baker Chemical Co.

Dyeing and Mordanting Procedures. All dyeing and mordanting was carried out with a Renigal laboratory dyeing machine, model ST. Fabric pieces

measuring 33 × 25 cm were weighed and wet out in aqueous 0.05% Triton X-100, a nonionic surfactant, for 2 h prior to dyeing. All dyebaths contained 2% dye, 3% sulfuric acid, and 10% sodium sulfate on weight of fabric (owf), and a liquor ratio of 100:1 was used. The fabric was entered into the dyebath at 45 °C, and the dyebath was brought to the boil and maintained at 100 °C for 1 h with constant agitation. The fabric samples were thoroughly rinsed with distilled water to remove unfixed dye and were allowed to air dry. Each dyed fabric sample was cut into 18 pieces. Three swatches of each dyed fabric were mordanted with different mordant solutions. Each mordant bath contained 1% mordant (owf), and a liquor ratio of 100:1 was used. The three swatches were entered into the mordant bath at 95 °C and were mordanted at this temperature for 1 h. The mordanted samples were thoroughly rinsed with distilled water and were allowed to air dry.

Light and Burial-Induced Weathering Tests. Dyed and dyed-mordanted wool and silk samples were exposed to weathering by light and burial by using the American Association of Textile Chemists and Colorists (AATCC) Test Methods 16E-1982 and 30-1981, respectively, with certain modifications. In the lightfastness test, fabric samples were exposed continuously in an Atlas weather-ometer, model Ci35-W, for 80 h by using simulated sunlight from a filtered xenon source with a borosilicate interfilter and soda line glass outer filter operating at an average black panel temperature of 63 °C and at an average relative humidity of 30%. During light exposure the samples received 85.6 $kJ/m^2/nm$ irradiation at 420 nm. In the burial test, the samples were buried 2.5 cm under a sandy loam soil containing 25% moisture at pH 7 at 28 °C for 14 days. The samples were thoroughly washed with distilled water and were air dried.

Color and Tensile Measurements. The color expressed as x, y, and Y color coordinates and color differences (ΔE) as measured for three or more samples by the AATCC Test Method 153-1978 using the CIELAB color difference formula and illuminant C were determined for all dyed and dyed-mordanted samples with a MacBeth MS-2000 color spectrophotometer. Tensile properties including breaking strength, percent elongation at break, and energy to break were measured for warp yarns from untreated and weathered dyed and dyed-mordanted samples with an Instron table model tensile testing machine by using a 1-in. gauge length and a crosshead speed of 1 in./min.

Results and Discussion

Mordant-Induced Color Changes. Mordanting had a profound effect on the shade (x, y) and the depth of shade (Y) of the dyed wool and silk fabrics (Table I). Alizarin, brazilin, and carminic acid all dyed the wool and silk to medium depths of shade.

Alizarin dyed both wool and silk to similar shades and depths of shade. Mordanting caused the alizarin-dyed wool and silk fabrics to become darker and to change shades; wool gave the greatest color differences. Shade changes were similar in alizarin-dyed wool and silk samples mordanted with the same mordant. Mordanting with chromium, copper, and iron caused the greatest changes in shade and depth of shade.

Table I. Mordant-Induced Color Changes in Dyed Wool and Silk Fabrics

	Wool				*Silk*			
Mordant	x	y	Y	ΔE	x	y	Y	ΔE
				Alizarin				
—	0.454	0.434	41.4	—	0.423	0.425	41.9	—
Al	0.433	0.358	27.9	37.0	0.399	0.347	28.3	35.4
Cr	0.483	0.372	7.3	52.1	0.429	0.328	10.6	52.5
Cu	0.347	0.280	8.4	72.8	0.336	0.303	13.3	57.2
Fe	0.345	0.321	7.6	67.0	0.361	0.335	7.3	57.0
Sn	0.518	0.375	16.2	38.8	0.408	0.373	36.1	23.1
				Brazilin				
—	0.357	0.368	49.6	—	0.372	0.386	45.9	—
Al	0.359	0.341	40.9	14.3	0.341	0.325	37.5	25.7
Cr	0.451	0.434	15.1	36.4	0.359	0.370	36.4	10.5
Cu	0.365	0.356	22.6	23.0	0.339	0.346	36.9	18.6
Fe	0.371	0.374	27.7	17.2	0.354	0.358	34.0	15.4
Sn	0.375	0.347	29.6	20.0	0.327	0.330	46.3	22.8
				Carminic Acid				
—	0.439	0.345	29.0	—	0.397	0.335	30.2	—
Al	0.343	0.303	33.7	28.2	0.330	0.317	38.6	20.7
Cr	0.453	0.436	15.4	33.7	0.359	0.365	34.6	21.9
Cu	0.326	0.311	18.6	35.7	0.328	0.318	31.3	21.0
Fe	0.337	0.335	14.8	36.9	0.351	0.361	21.8	25.5
Sn	0.405	0.308	16.0	21.9	0.343	0.321	37.5	16.5

Brazilin dyed silk to a slightly deeper shade than it dyed wool. The brazilin-dyed wool and silk almost always became darker on mordanting; the wool samples became much darker than the silk samples with all mordants except aluminum. Also, the changes in shade caused by mordanting were much less for the silk samples than for the wool samples. Mordanting of brazilin-dyed wool with chromium caused the greatest change in shade and the greatest deepening of shade.

Carminic acid dyed both wool and silk to similar shades and depths of shade. Mordanting of the carminic acid-dyed wool caused the samples to become deeper shades except when aluminum was used as the mordant. With the exception of iron, mordanting of carminic acid-dyed silk samples caused lightening as well as changes in shade in the dyed silks.

The mordanting process had a profound effect on the shade and depth of shade of the natural-dyed wool and silk. This result was expected because the metal ions used in mordanting complex with the dye on the fiber (*9*). Copper, chromium, and iron mordants gave the greatest color changes. The morphology and chemical structure of the protein fiber also affect the nature of the interaction between the dye

and the mordant, and the fiber may actually undergo reaction with the mordant. This reaction accounts for differences in the shade and depth of shade in wool and silk dyed and mordanted with the same dye-mordant combination.

Light-Induced Color Changes. Light-induced color changes in the dyed and dyed-mordanted wool and silk fabrics were dependent on the dye or dye-mordant combination used and the fiber type to which they were applied (Table II). The dyed wool samples were less light sensitive than the corresponding dyed silk samples. Mordanting of the dyed wool and silk samples generally caused them to undergo greater color and shade change on light exposure. This result was expected because mordanting in most cases caused the dyed sample to become much deeper in shade and thereby increased the amount of light absorbed by the sample on light exposure.

Samples dyed with alizarin showed little shade or depth of shade change on light exposure; however, mordanted-alizarin-dyed wool and silk samples were much more sensitive to simulated sunlight than were unmordanted samples. Mordanted-dyed silk samples were somewhat

Table II. Light-Induced Color Changes in Dyed and Dyed-Mordanted Wool and Silk Fabrics

	Wool				*Silk*			
Mordant	Δx	Δy	ΔY	ΔE	Δx	Δy	ΔY	ΔE
				Alizarin				
—	0.003	0.001	−0.5	1.4	−0.006	−0.006	−0.2	3.1
Al	−0.022	−0.003	3.5	6.1	−0.016	0.000	5.3	6.2
Cr	−0.078	−0.031	0.2	14.2	−0.016	−0.007	2.2	4.1
Cu	0.038	0.046	0.1	12.4	0.001	0.002	3.6	5.4
Fe	0.018	0.024	1.7	7.0	−0.007	−0.012	−3.4	7.3
Sn	−0.064	0.012	6.9	16.2	−0.042	−0.017	0.7	13.9
				Brazilin				
—	−0.001	−0.006	−1.4	2.8	−0.043	−0.048	1.3	20.0
Al	−0.028	0.009	12.2	15.1	−0.008	−0.005	8.2	10.3
Cr	−0.099	−0.063	−2.1	28.5	−0.030	−0.029	2.6	11.8
Cu	0.006	0.015	1.2	5.0	−0.010	0.001	3.6	4.7
Fe	−0.015	−0.002	10.9	10.1	−0.039	−0.035	3.7	14.5
Sn	0.004	0.011	−2.0	4.0	−0.003	0.003	0.9	2.8
				Carminic Acid				
—	−0.038	0.005	6.2	12.5	−0.032	0.003	6.5	11.7
Al	−0.012	0.016	7.2	11.7	−0.006	0.010	5.7	7.7
Cr	−0.106	−0.070	−2.6	31.1	−0.036	−0.036	5.7	14.5
Cu	0.021	0.028	2.4	9.2	−0.009	0.005	−0.8	5.1
Fe	0.010	0.016	4.2	7.4	0.005	0.009	0.0	3.5
Sn	−0.044	0.042	10.5	25.4	−0.008	0.012	7.3	9.2

less light sensitive than the corresponding wool samples. The mordanted-dyed silk samples underwent greater fading but less change in shade than the corresponding wool samples.

Brazilin-dyed wool was much more lightfast than brazilin-dyed silk; the dyed silk exhibited slight fading and a large shade change. Mordanted-brazilin-dyed wool samples were much more sensitive to light than was the unmordanted-dyed wool and showed differing changes in shade and depth of shade; chromium-mordanted wool had the poorest colorfastness. Mordanted-brazilin-dyed silks were less sensitive to light exposure than was the corresponding unmordanted-dyed silk; copper and tin-mordanted samples were the most lightfast.

Carminic acid-dyed wool and silk had similar sensitivities to light and showed considerable fading and color change. Chromium and tin-mordanted-brazilin-dyed samples showed much greater light sensitivity than the unmordanted-dyed wool and silk, and the other mordants had little effect or slightly improved the lightfastness of the samples.

The effect of dye and dye-mordant combinations on the lightfastness of wool and silk was quite variable. In many instances the presence of mordant on dyed wool samples tended to cause the fabric to become less lightfast, whereas the mordant on dyed silk samples that are sensitive to light tended to stabilize the dyed fabric to color change. Crews (*6*) found aluminum and tin mordanting of wool dyed with yellow natural dyes significantly increased the rate of photofading of the dyed fabrics. Watase (*3*) found that tin mordanting increased the rate of photodegradation of silk dyed with natural dyes, whereas chromium mordanting of these dyed silks had the least effect on photodegradation. In our study the effect of these mordants was much more variable, but tin and chromium mordanting in many instances caused greater light-induced color changes in the dyed fabrics than the other mordants studied.

Burial-Induced Color Changes. Burial of dyed and dyed-mordanted wool and silk fabrics had a profound effect on the color and depth of shade of the fabrics (Table III). Soil burial caused darking and extremely large changes in shade in most dyed fabrics, whereas the mordanted-dyed fabrics showed less deepening and change in shade than the unmordanted-dyed fabrics.

Burial of alizarin-dyed wool and silk resulted in extreme darkening and change in shade toward the purple. This extreme change may be due to mordanting of the samples during burial by ions contained within the moist soil. The mordanted-dyed wool and silk samples were much less susceptible to darkening and color change than unmordanted-alizarin-dyed samples; copper mordanting was most effective for the dyed wool, and chromium mordanting was most effective for the dyed silk.

Table III. Burial-Induced Color Changes in Dyed and Dyed-Mordanted Wool and Silk Fabrics

	Wool				*Silk*			
Mordant	Δx	Δy	ΔY	ΔE	Δx	Δy	ΔY	ΔE
				Alizarin				
—	−0.115	−0.137	−27.7	65.7	−0.072	−0.127	−24.2	55.6
Al	−0.033	−0.033	−5.2	15.3	−0.008	−0.026	−4.5	10.7
Cr	−0.050	−0.047	0.3	13.4	−0.010	−0.015	−1.3	5.1
Cu	0.024	−0.09	−2.2	7.8	−0.016	−0.034	−3.7	13.5
Fe	−0.008	−0.042	−2.0	11.7	−0.031	−0.022	5.5	10.4
Sn	−0.041	−0.026	−5.1	20.5	−0.020	−0.024	−10.9	14.9
				Brazilin				
—	−0.021	−0.029	−17.5	18.7	−0.033	−0.047	−13.1	22.2
Al	−0.016	0.009	−4.8	9.9	−0.007	0.010	−1.5	6.3
Cr	−0.071	−0.051	4.8	19.8	−0.019	−0.024	−0.1	8.9
Cu	−0.004	0.000	−3.7	4.4	0.000	0.004	−2.6	2.5
Fe	−0.021	−0.010	−0.6	6.0	−0.026	−0.024	0.6	9.8
Sn	0.012	0.010	−6.2	6.1	0.013	0.015	−6.5	7.1
				Carminic Acid				
—	−0.111	−0.038	−8.4	34.1	−0.060	−0.007	5.2	19.5
Al	0.010	0.026	−3.5	10.6	0.003	0.011	−3.1	5.1
Cr	−0.093	−0.073	5.5	28.0	−0.026	−0.039	0.3	14.4
Cu	0.014	0.006	−1.3	3.7	−0.003	0.008	3.3	5.0
Fe	−0.015	−0.016	−2.6	6.2	−0.035	−0.060	−1.3	13.5
Sn	−0.022	0.021	0.2	12.4	0.004	0.019	−2.1	8.1

Brazilin-dyed wool and silk underwent less darkening and shade change on burial than alizarin-dyed fabrics, and they became darker and more nearly like the shade of the mordanted-dyed samples. The mordanted-brazilin-dyed samples showed much less darkening and in most cases showed less color change than unmordanted-dyed samples on burial. Copper-mordanted wool and silk underwent the smallest degree of color change due to burial.

Carminic acid-dyed wool underwent extensive darkening and change in shade toward the purple on burial presumably because of soil ion-induced mordanting during burial. Although carminic acid-dyed silk underwent extensive shade change during burial, the fabric became somewhat lighter because of burial. Most of the mordanted-dyed wool and silk samples exhibited less shade change and depth of shade change than carminic acid-dyed samples; copper was most effective in preventing these changes.

The degree of shade and depth of shade change in the buried dyed wool and silk samples were quite dependent on the dye applied and the fiber type to which it was applied. The unmordanted-dyed wool and silk samples tended to undergo large changes in shade and deepening of

shade due to soil ion-induced mordanting on burial. Mordanting greatly reduced the magnitude of these color changes; chromium and copper mordanting resulted in the largest reductions. This result is consistent with the previous finding that copper ions tend to prevent burial-induced damage to textiles because of the antibacterial properties of copper (*8*). Also, the copper and chromium mordanted dyes may form more stable complexes that are less susceptible to ion exchange during soil burial.

Dyeing and Dyeing-Mordanting-Induced Changes in Tensile Properties. Dyeing and mordanting had a significant effect on selected tensile properties of wool and silk (Table IV). The elongations at break of yarns from dyed wools were significantly greater than those of undyed control wool, whereas the breaking strengths and energies to break of dyed silk yarns were significantly less than those of undyed

Table IV. Tensile Properties of Dyed and Dyed-Mordanted Wool and Silk Fabrics

	Wool			*Silk*		
Mordant	*Breaking Strength (g)*	*Elongation at Break (%)*	*Energy to Break (g-cm)*	*Breaking Strength (g)*	*Elongation at Break (%)*	*Energy to Break (g-cm)*
Undyed	419	44	320	117	41	56
			Alizarin			
—	424	54	383	101	48	44
Al	377	50	323	98	36[a]	38[a]
Cr	451	47	352	89[a]	36[a]	34[a]
Cu	397	55	365	89[a]	32[a]	33[a]
Fe	422	51	363	86[a]	29[a]	30[a]
Sn	266[a]	54	230[a]	86[a]	28[a]	29[a]
			Brazilin			
—	435	52	369	97	42	40
Al	395	53	357	87[a]	34[a]	35[a]
Cr	376	38[a]	235[a]	80[a]	28[a]	27[a]
Cu	390	48	320	87[a]	29[a]	30[a]
Fe	416	49	349	103	32[a]	39
Sn	288[a]	53	240[a]	93[a]	29[a]	30[a]
			Carminic Acid			
—	412	56	391	95	41	39
Al	391	52	353	86[a]	35[a]	33[a]
Cr	426	43[a]	305[a]	92	35[a]	31[a]
Cu	412	52	363	90	30[a]	29[a]
Fe	442	57	435	89	37	31[a]
Sn	286[a]	52	245[a]	87[a]	32[a]	29[a]

[a] Significant change in tensile property of mordanted-dyed sample was found in comparison to unmordanted-dyed sample at 95% confidence level.

control silk. Because the observed changes in tensile properties occurred for all the dyed samples, the dye-bath conditions themselves rather than the dyes are thought to cause the differences. The mordanting process also affected the tensile properties of the dyed wools in some instances and the tensile properties of the dyed silks in most instances. Mordanting of the dyed wools with chromium usually caused reductions in elongations at break and energies to break, whereas tin mordanting of wool caused reductions in breaking strengths and energies to break. Mordanting of the dyed silks with any of the mordants almost always caused reductions in breaking strengths, elongations at break, and energies to break.

Light-Induced Changes in Tensile Properties. The tensile properties of undyed wool were essentially unaffected by exposure to light for 80 h, whereas undyed silk was damaged by light exposure for the same periods (Table V). The dyed wool samples were also unaffected by light with the exception of carminic acid-dyed wool which showed a decrease in elongation at break. The dyed silk samples were damaged by light exposure to about the same degree as that found for undyed silk. All dyed wools mordanted with chromium and tin were damaged by light exposure, and large decreases in breaking strengths, elongations at break, and energies to break were found. Iron mordanting of the dyed wool samples also caused deterioration in tensile properties on light exposure except with brazilin-dyed wool. Mordanting of the dyed silk samples did not provide much protection from light-induced deterioration, but copper mordanted-dyed silk samples showed somewhat less loss in tensile properties on light exposure than the other mordanted-dyed silks.

Burial-Induced Changes in Tensile Properties. Burial of undyed wool caused a significant loss in breaking strength and energy to break, whereas a significant loss in the breaking strength and an increase in the elongation at break of undyed silk occurred because of burial (Table VI). The tensile properties of wool dyed with alizarin were unaffected by burial, whereas wool samples dyed with brazilin and carminic acid showed increased loss in tensile properties. Mordanting of the brazilin and carminic acid-dyed wools in many cases protected them from burial-induced losses in tensile properties; chromium and copper mordants provided the best protection on brazilin-dyed wool, and copper and iron mordants provided the best protection on carminic acid-dyed wool. Aluminum and tin mordanting of alizarin dyed-wool samples resulted in a greater loss in tensile properties on burial than that found for the unmordanted-dyed sample. This result suggests that these mordants negate the protective effect of this dye. The dyed silk samples showed

Published on February 1, 1986 on http://pubs.acs.org | doi: 10.1021/ba-1986-0212.ch011

Table V. Light-Induced Changes in the Tensile Properties of Dyed and Dyed-Mordanted Wool and Silk Fabrics

	Wool			*Silk*		
Mordant	Δ *Breaking Strength* (*g*)	Δ *Elongation at Break* (%)	Δ *Energy to Break* (*g-cm*)	Δ *Breaking Strength* (*g*)	Δ *Elongation at Break* (%)	Δ *Energy to Break* (*g-cm*)
Undyed	28	−5	−9	−40[a]	−17[a]	−40[a]
			Alizarin			
—	10	−4	−13	−45[a]	−17[a]	−33[a]
Al	14	−8[a]	−46	−51[a]	−7[a]	−30[a]
Cr	−79[a]	−24[a]	−250[a]	−48[a]	−4[a]	−27[a]
Cu	−13	−12[a]	−101[a]	−21[a]	3[a]	−17[a]
Fe	−62[a]	−18[a]	−182[a]	−56[a]	1	−24[a]
Sn	−9	−27[a]	−156[a]	−58[a]	−3[a]	−25[a]
			Brazilin			
—	−8	2	26	−37[a]	−9[a]	−28[a]
Al	11	−5	−18	−35[a]	−1	−25[a]
Cr	−19	−17[a]	−153[a]	−19[a]	10[a]	−14[a]
Cu	9	−5	−20	−17[a]	11[a]	−11[a]
Fe	−9	−4	−37	−87[a]	1	−35[a]
Sn	−5	−24[a]	−153[a]	−57[a]	−1	−24[a]
			Carminic Acid			
—	29	−14[a]	−48	−38[a]	−7[a]	−27[a]
Al	−10	−4	−42	−36[a]	−6[a]	−25[a]
Cr	−50[a]	−21[a]	−217[a]	−35[a]	−2	−29[a]
Cu	−5	−7	−52	−23[a]	1	−11[a]
Fe	−70[a]	−22[a]	−231[a]	−64[a]	−11[a]	−27[a]
Sn	−31	−24[a]	−168[a]	−58[a]	−4[a]	−25[a]

[a] Significant change due to light exposure of sample was found at 95% confidence level.

Published on February 1, 1986 on http://pubs.acs.org | doi: 10.1021/ba-1986-0212.ch011

Table VI. Burial-Induced Changes in the Tensile Properties of Dyed and Dyed–Mordanted Wool and Silk Fabrics

	Wool			*Silk*		
Mordant	*Δ Breaking Strength (g)*	*Δ Elongation at Break (%)*	*Δ Energy to Break (g-cm)*	*Δ Breaking Strength (g)*	*Δ Elongation at Break (%)*	*Δ Energy to Break (g-cm)*
Undyed	−184[a]	−13	−123[a]	−22[a]	4[a]	−12
			Alizarin			
—	−25	3	−1	−3	−13[a]	−6[a]
Al	−249[a]	−32[a]	−305[a]	−10[a]	31[a]	−10[a]
Cr	−54[a]	8	13	4	−5[a]	−5
Cu	15	0	29	4	−4[a]	−2
Fe	6	2	5	13[a]	6[a]	8[a]
Sn	−43[a]	−29[a]	−169[a]	14[a]	2	5
			Brazilin			
—	−206[a]	−32[a]	−301[a]	−1	−10[a]	−5
Al	−22	−6	−63	4	−4[a]	−5[a]
Cr	2	7	49	6	3	2
Cu	32	8[a]	71	0	−1	−2
Fe	−66[a]	−3	−88	0	−1	−4
Sn	−67[a]	−23[a]	−182[a]	6	2	4
			Carminic Acid			
—	−277[a]	−40[a]	−371[a]	4	−5[a]	−2
Al	−77[a]	−15[a]	−183[a]	4	0	2
Cr	−61	−1	−41	−9[a]	−1	−1
Cu	33	11[a]	117	−5	4[a]	2
Fe	−5	0	−6	3	−7[a]	−3
Sn	−105[a]	−26[a]	−202[a]	4	6[a]	4

[a] Significant change due to burial of sample was found at 95% confidence level.

smaller losses in breaking strengths and energies at break than undyed silk on burial; however, the dyed silks also showed significant decreases in elongations at break in comparison to undyed silk on burial. Mordants had a more variable effect on the tensile properties of dyed silk samples subjected to burial and generally did not provide a greater protective effect than dyeing alone.

Conclusions

This study shows that light and burial-induced changes in the color and tensile properties of protein fibers dyed with natural dyes and mordanted are dependent on the fiber type and the dye-mordant combination used on the fiber. This study also demonstrates that light-induced weathering of these materials is very different than burial-induced weathering. Knowledge of the dye-mordant combination used on a protein fabric provides useful information about the probable degree of deterioration expected in dyed-mordanted protein fabrics exposed to sunlight or burial and the sensitivity of natural dyed-mordanted protein fabrics to light-induced deterioration during museum exhibition. Information from this study and future studies of this type will assist the conservator in preservation and restoration of dyed and mordanted wool and silk fabrics of historical importance.

Literature Cited

1. Ishihara, M.; Sugio, K.; Mitsutome, Y. *Kagoshima-ken Kogyo Shikenjo Nenpo* **1974**, *21*, 34.
2. Shimizu, F.; Aida, G. *Sen'i Gakkaishi* **1971**, *27*, 182.
3. Watase, H. *Sen'i Seihin Shohi Kagaku* **1978**, *19*, 69.
4. Padfield, T.; Landi, S. *Stud. Conserv.* **1966**, *11*, 181.
5. Duff, D. C.; Sinclair, R. S.; Stirling, D. *Stud. Conserv.* **1977**, *22*, 161.
6. Crews, P. C. *J. Am. Inst. Conserv.* **1982**, *21*, 2, 43.
7. Nopitsch, W. *Ciba Rev.* **1953**, *100*, 3578.
8. Nockert, M.; Wadsten, T. *Stud. Conserv.* **1978**, *23*, 38.
9. Johnson, A. In "The Theory of Coloration of Textiles"; Bird, C. L.; Boston, W. S., Eds.; Dyers Co. Publications Trust: Bradford, England, 1975; p. 409.

RECEIVED for review November 26, 1984. ACCEPTED March 15, 1985.

12

Experimental Studies on the Effect of Aqueous and Nonaqueous Treatments on Historic Textiles

Manfred Wentz[1]
University of Wisconsin, Madison, WI 53706

Conservation of historic textiles may include aqueous and nonaqueous cleaning treatments. This study was undertaken to determine the effect of these cleaning treatments on fiber morphology of Tiahuanaco cotton and alpaca and on the colorfastness of naturally dyed wool. Scanning electron microscopy and X-ray diffraction analysis revealed that aqueous treatments alter the surface appearance and the crystallinity of these old fibers to a larger degree than nonaqueous treatments. Amino acid analysis showed that the amino acid content of the alpaca fibers is only slightly changed after the cleanings. The colorfastness of 11 naturally dyed wool samples to aqueous and nonaqueous treatments was generally excellent. Dry cleaning in commercial plants had a more severe effect on the colorfastness of the samples than laboratory treatments. Because the nonaqueous treatments changed the textile properties less than the aqueous treatments, dry cleaning may be a viable alternative in the conservation of historic textiles.

THE CLEANING OF HISTORIC TEXTILES is largely done by conservators who have gained practical experience in handling these often fragile objects. The main purpose of cleaning historic textiles is to restore their original appearance as much as possible and to prevent possible deterioration that may be caused by the presence of soils.

Two methods that are often used for cleaning are laundering and, to a more limited extent, dry cleaning. Laundering uses an aqueous medium, whereas dry cleaning uses a nonaqueous medium. Both procedures are not very well understood in the context of textile conservation, and better and more scientifically based methods are needed (*1*, *2*).

[1] Current address: University of North Carolina at Greensboro, Greensboro, NC 27412.

0065-2393/86/0212-0211$06.00/0

The first part of this study describes a series of experiments designed to answer some of the questions on how aqueous and nonaqueous treatments alter the morphology and chemical composition of fibers taken from a Tiahuanaco tapestry. The second part of this study focuses on the colorfastness to dry cleaning of naturally colored wool fabrics. This second study was undertaken because no information on the colorfastness of these types of colorants to dry cleaning could be found in the literature. A recently published paper (*3*) on drycleaning of historic textiles indicates that conservators are using this nonaqueous type of cleaning as a method of textile conservation.

I will briefly review some of the mechanisms of soil removal involved in aqueous and nonaqueous textile cleaning before proceeding to the experiments and results of this study. This discussion provides background information on the two methods of cleaning.

Mechanisms of Soil Removal

The exact composition of soils on historic textiles is complex and almost always unknown. Conservators are faced with the difficult task of selecting a method of cleaning.

On the basis of the degree and type of soiling, conservators can choose between localized or complete treatment of the item. Stain removal with solvents with or without additives is the method of choice if soils are localized and the general appearance of the rest of the textile is satisfactory. A systematic overview of methods of stain removal is given in the literature (*4*). The present discussion focuses on the method of complete immersion in the cleaning medium and on the principles of soil removal associated with this technique. Excellent summaries (*5*) on detergency in aqueous media exist, but detergency in nonaqueous media is not as well documented.

To initiate transfer of soil from the textile to the aqueous or nonaqueous cleaning medium, the textile must be completely wetted. This wetting is usually achieved by adding a surface-active agent to water to lower the surface tension so that the textile and the soils are brought into close contact with the liquid. The surface tension of the most popular nonaqueous solvent used in textile cleaning, tetrachloroethylene, is low enough to wet out the textiles (*6*). Once wetting is achieved, soil removal is initiated. The various steps involved in this process depend on the nature and the properties of the soils present. Table I gives a broad classification of soils encountered on textiles and classifies them according to their solubility properties. A listing of the basic colloidal processes involved in the two types of cleaning methods is also given in Table I. The mechanisms by which the four types of soils are removed from textiles will be discussed briefly.

Water-soluble soils are generally polar substances, such as sodium

Table I. Soils and Mechanisms of Soil Removal

Classification of Soils	*Method of Cleaning*	
	Laundering	*Dry Cleaning*
Water soluble	solution	solubilization
Oil soluble	solubilization	solution
Pigments, insoluble	suspension	suspension
Stains, insoluble	bleaching	spotting

chloride or sugars. They are soluble in water, but insoluble in the nonpolar dry-cleaning solvent. Oil-soluble soils are nonpolar substances, such as fats, oils, or sebum, which are soluble in the dry-cleaning solvent, but not in water. With the help of suitable surfactants, both types of soils can be solubilized in tetrachloroethylene or water.

Surfactants are organic molecules that possess a nonpolar hydrocarbon tail and a polar head. The polar head can be anionic, cationic, or nonionic. Because of the existence of the two moieties in one molecule, surfactants have limited solubility in polar and nonpolar solvents. Their solubility is dependent on the hydrophile–lipophile balance of their molecular structure. At a critical concentration, they form aggregates in either type of solvent. This colloidal aggregation is referred to as micellization, and the concentration at which it occurs is known as the critical micelle concentration. The term micelle was coined by McBain (*7*) to designate the aggregated solute. In water or other polar solvents, the micellar structure is such that the hydrophobic tails of the surfactant molecules are clustered together and form the interior of a sphere. The surface of the sphere consists of the hydrophilic heads. In nonpolar solvents, the orientation of the molecules is reversed.

The most important property of micelles in aqueous or nonaqueous solvents is their ability to dissolve substances that are insoluble in the pure solvent. In aqueous systems, nonpolar substances are solubilized in the interior of the micelles, whereas polar substances are solubilized in the micellar core in nonaqueous systems. This process is called solubilization. It can be defined as the formation of a thermodynamically stable isotropic solution with reduced activity of the solubilized material (*8*). It is useful to further differentiate between primary and secondary solubilization. The solubilization of water in tetrachloroethylene containing a surfactant is an example of primary solubilization. Secondary solubilization can be considered as an extension of primary solubilization because it refers to the solution of a substance in the primary solubilizate.

The removal of water-soluble soils from textiles during dry cleaning is an application of secondary solubilization (*9*). The practical significance of this concept was illustrated by Fulton et al. (*10*). They were able to demonstrate that in dry cleaning, the removal of sodium

chloride and glucose is greatly enhanced if a surfactant and small amounts of water are present. It is now well established that secondary solubilization is not only dependent on the activity of the solubilized water but also on the concentration and chemical nature of the surfactant forming the micelles (*9, 11*).

Insoluble pigment soils, such as clays or other particulate solids, are removed during cleaning from the fiber surfaces with the help of surfactants. In both cleaning systems, surfactants incorporate this type of soil into the micelles to form relatively stable suspensions to prevent the redeposition of soil onto the textile (*12*).

Stains, often colored, are not always removed by either immersion cleaning method. Bleach can be added during laundering; however, chemical damage to fibers is risked (*13*). Localized treatments may be the preferred way to remove colored stains in textile conservation. Manual stain removal, called spotting, is an integral part of professional dry cleaning because no simple, commercial procedure for bleaching textiles in the nonpolar solvent exists (*14*).

Experimental

Tiahuanaco Tapestry. A fragment of a classic Tihuanaco Middle Horizon tapestry (52145a-18046) was made available for this study by the Milwaukee Public Museum from the collection of Malcom K. Whyte. Figure 1 shows a

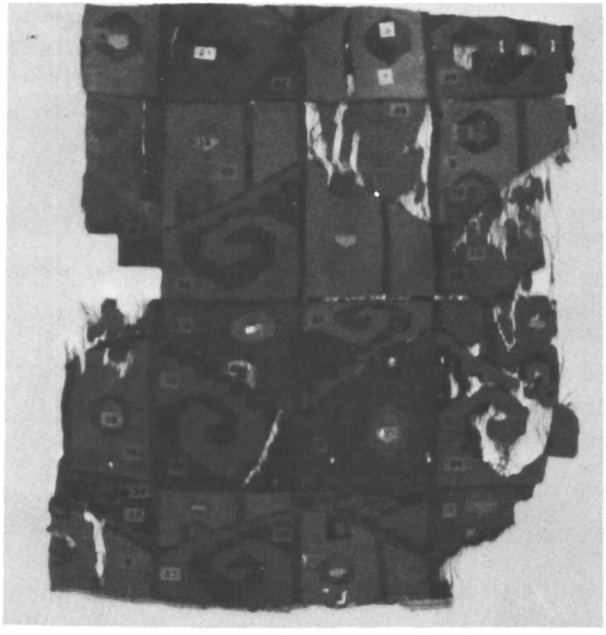

Figure 1. Tiahuanaco tapestry, Middle Horizon.

picture of the textile. Unfortunately, no excavation documents are available to trace the exact origin of the tapestry. The collection was appraised and evaluated by Bird (*15*) who has described the technical features of a similar artifact. The fabric comprises a combination of mostly alpaca and some cotton warps and alpaca wefts. Interlocking tapestry techniques were used to create geometric motifs of paired elements which include stepped frets or spirals with stylized profile heads. The main color areas are brown, gold-brown, black-brown, gold, red, green, and tan.

TREATMENTS. Small fabric samples were removed very carefully from the tapestry and transferred into glass vessels to which treatment liquids were added in sufficient amount to assure complete immersion. The samples remained for 1 h in these liquids. Distilled water and distilled water containing 1 g/L of Synperonic N, an ethoxylated nonylphenol, nonionic surfactant were used for aqueous treatments. Commercial grade tetrachloroethylene was selected for the nonaqueous treatments. All treatments were made at room temperature. After the samples were removed from the liquids, they were allowed to dry in open air at 21 °C and 65% rh.

ANALYSIS. Samples were analyzed before and after treatments. For scanning electron microscopy, samples were mounted on stainless steel stubs and coated with a 60% gold and 40% palladium alloy in a Denton DV-502 vacuum evaporator. A scanning electron microscope Joel model JSM-43 with an accelerating voltage of 10 kV was used. Photographs were taken with a Polaroid camera and type 55 films. Amino acid analysis was done on the alpaca fibers with the Durrum D 500 amino acid analyzer in the biophysics laboratory at the University of Wisconsin—Madison. Fiber samples of about 1 mg were hydrolyzed in ignition tubes with 6 N hydrochloric acid and 0.2% phenol and then were evacuated, sealed, and hydrolyzed at 110 °C for 24 h. Following hydrolysis, the samples were evaporated to dryness on a rotary evaporator and redissolved in a buffered (pH 2.2) citric acid solution. Aliquots were injected into the analyzer where the individual amino acids were separated and quantified by the ninhydrin method (*16*). X-ray measurements were made at the Forest Products Laboratory, U.S. Department of Agriculture in Madison, Wisconsin (*17*). X-ray diffractometer traces were taken on a Ryraku Denki goniometer by using nickel-filtered copper radiation between 10° and 30° for cotton and between 4° and 15° for alpaca. Samples, approximately 10 × 10 mm, were measured before and after treatments.

Colorfastness of Wool Dyed with Natural Colorants. For the second series of experiments, wool samples were colored with natural colorants. Wool fabrics No. 526 were obtained from Test Fabrics, and natural colorants were supplied by Cerulean Blue.

DYEING WITH NATURAL COLORANTS. The procedures followed are documented by van de Vrande (*18*). Details describing premordanting and the individual dyeing procedures for each natural colorant are summarized by Houg-Dobeck (*19*). Squared wool samples, 4 × 4 in., were premordanted in the appropriate amount of mordant in distilled water at a boil for 30 min at a liquor-to-cloth ratio of 50:1. Upon completion, the samples were transferred into the preheated dye bath. Stock solutions of each natural colorant were made by soaking the proper amount of the dry material in distilled water for 24 h. The extraction of the coloring matter was completed by boiling the solution for 10–15 min. The undissolved material was removed by filtration. Water was added to

the filtrate to obtain the needed amount of dye liquor to achieve the liquor-to-cloth ratio of 50:1. Dyeing proceeded in covered beakers at a boil for 1 h. After dyeing, all samples were rinsed thoroughly under hot, soft-running water until the rinse water was colorless. Each sample was dryed separately on white cardboards. Table II lists the types of colorants used in this study and color measurement data.

LABORATORY TREATMENTS. Colorfastness of the dyed wool samples was determined in aqueous and nonaqueous media. Colored samples were cut into 2- × 2-in. squares and sandwiched between multifiber fabrics (Test Fabrics) and undyed wool fabrics of the same dimensions. The fabrics were loosely sewn together by hand with white cotton thread. Two surfactants were chosen for the aqueous treatments: Tergitol NPX, a nonionic ethoxylated nonylphenol (Union Carbide) and Orvus WA, an anionic sodium alkyl sulfate (Proctor & Gamble). Solutions of 0.1% surfactant in distilled water were prepared. Tests were run in 250-mL Erlenmeyer flasks at a liquor-to-cloth ratio of 50:1. The flasks were placed in an Eberbach constant-temperature shaker bath adjusted to 30 °C and an agitation of 40 cycles/min. Treatment time was 1 h, after which the samples were opened and allowed to dry on blotter paper. This same procedure was used for the nonaqueous treatments. Commercial grade tetrachloroethylene (R. R. Street & Co.) with and without 1% Aerosol OT, the anionic surfactant sodium sulfosuccinate (Aldrich Chemical) was selected. The treated samples were removed from the liquids, opened, and dried on blotter paper in a ventilated hood.

FIELD STUDY. Dyed wool samples, 4 × 4 in., were sewn onto 20- × 20-in. undyed wool fabric. A white cotton fabric (80 × 80 print cloth) was sewn over the dyed samples so that the colored samples were between undyed wool and cotton test fabrics. Ten sample sheets were prepared. Two of each were sent to five different dry-cleaning plants in the Chicago area. The plants were

Table II. Color Measurement Data of Natural Colorants on Wool

	CIELAB Coordinates			
Natural Colorant	L	a	b	ΔE
Alkanet	34.29	3.88	−7.16	1.36
Annatto	71.20	17.21	57.02	2.47
Brazilwood	43.95	31.10	−1.37	3.86
Cochineal-alum	33.77	39.05	4.38	1.58
Cochineal-tin	38.43	42.28	14.39	2.66
Cochineal-chrome	25.53	13.27	−6.53	0.13
Cutch	46.54	11.06	26.56	0.59
Henna	48.84	11.06	26.56	0.98
Indigo	33.47	0.48	−13.78	0.66
Lac dye	51.52	32.40	5.65	1.86
Logwood	35.31	6.83	−12.37	2.53
Madder	66.68	21.85	22.45	0.21
Weld	75.48	−4.68	47.68	1.17

NOTE: ΔE is the color difference.

instructed to clean one of the sheets in the morning and one in the afternoon. Solvent samples were taken for analysis at the end of each test run.

VISUAL EVALUATION OF COLORFASTNESS. All samples were evaluated according to the American Association of Textile Chemists and Colorists (AATCC) rating system (*20*). The undyed wool, white cotton, and multifiber samples were rated with the AATCC gray scale for staining (AATCC Evaluation Procedure 2), and the dyed samples were rated with the AATCC gray scale for color change (AATCC Evaluation Procedure 1). Averages of ratings by two observers are reported.

INSTRUMENTAL COLOR MEASUREMENTS. When treated samples showed AATCC ratings of 4 or less, they were measured against the untreated samples on the Sargent-Welch SP8-200 UV-vis spectrophotometer with a diffuse reflectance sphere attachment. The instrument is interfaced with a Hewlett-Packard HP-85 computer and run by color measurement software. Spectral reflectance data at 10-nm intervals, tristimulus values, chromaticity coordinates, and CIELAB color difference were determined for these samples (*21*).

Results and Discussion

Tihuanaco Tapestry. The construction and historic origin of this type of tapestry is well documented (*15*). It is generally believed that the protein fibers are from the alpaca camelid. The alpaca has occupied a major position in the economic life of the Andean Plateau. The domestication of the alpaca may have begun in the Chavin Early Horizon culture around 800 B.C. Cotton was a trade item for the highland weavers and was frequently combined with alpaca. The tapestry studied here comes from Tiahuanaco culture which dominated most of Peru and parts of Bolivia between A.D. 800 and A.D. 1100. Preliminary tests under the stereomicroscope indicated that the fibers are extremely brittle and can be easily broken with a needle. It is not known if the textile was cleaned after excavation. Because the tapestry appears clean, it cannot be ruled that it has undergone a conservation treatment. The objective of this study was to gain information on how fibers taken from the old textile change their morphology and structure after treatments in aqueous and nonaqueous treatments. No attempt was made to immerse the whole textile fragment in one of the cleaning solutions. Microscopical analysis of carefully removed fibers indicated that the warp of the fabric consists of two-ply yarns made of protein or cotton fibers, whereas the weft appears to contain only two-ply yarns made of protein fibers.

SCANNING ELECTRON MICROSCOPY. Fiber samples were taken before and after treatments and observed under the microscope. Fibers were selected randomly, and no attempt was made to statistically document the findings. Figures 2 and 3 illustrate some of the noted characteristics of the cotton fibers. Figure 2 shows a cotton fiber from

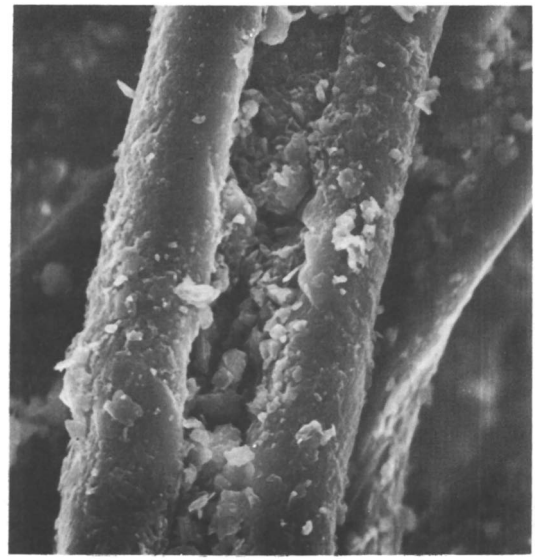

Figure 2. Cotton fiber (2250×) from Tiahuanaco tapestry, no treatment.

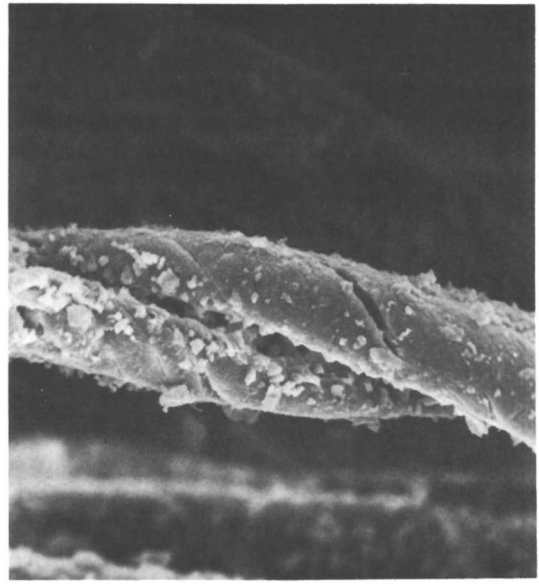

Figure 3. Cotton fiber (1125×) from Tiahuanaco tapestry, treated in distilled water.

the tapestry before treatment. It features the collapsed part of the kidney-shaped cotton fiber that consists of many particles of irregular shapes. Kassenbeck (22) described this concave part of the cotton fiber as the most accessible and reactive zone in the fiber cross section. This picture suggests that the disintegration of this historic cotton sample may have started in this fiber region. Figure 3 illustrates a convolution of a cotton fiber after treatment in distilled water. Two distinct helical breaks are present. This type of fiber cleavage was more visible on cotton fibers treated in aqueous systems and was not observed on cotton fibers treated in the nonaqueous solvent tetrachloroethylene. The breaks appear at acute angles of 30–35°. This finding suggests fibrillar separation of the secondary wall of cotton (23). Figure 4 shows protein fibers taken from the dark-brown weft before treatments. This picture shows that the cuticle cells of the fibers are no longer detectable and that irregularly shaped deposits exist on the fiber surfaces. Figure 5 illustrates the same type of fiber after dry cleaning. Here the treatment removed some of the surface deposits. The cross sections are round to oval and reveal characteristic medullas found in alpaca fibers. However, these pictures do not provide conclusive evidence that the protein fibers are indeed alpaca. The appearance and the dimensions of these fibers match those of alpaca and llama given by Harris (24).

AMINO ACID ANALYSIS. Protein fibers, such as wool and alpaca, consist of macromolecules that are naturally formed during the growth of the hair. These large molecules are actually copolymers of about 20

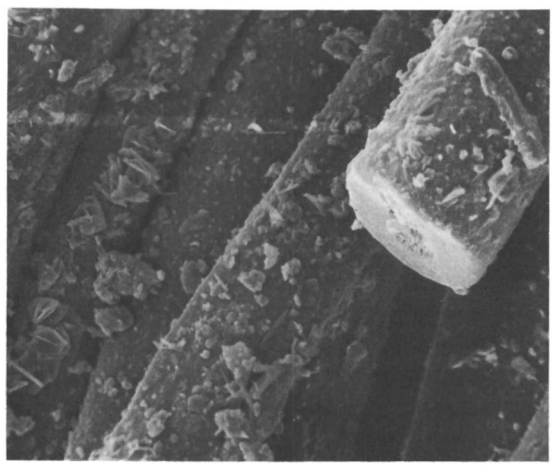

Figure 4. Protein fibers (700×) from Tiahuanaco tapestry, no treatment.

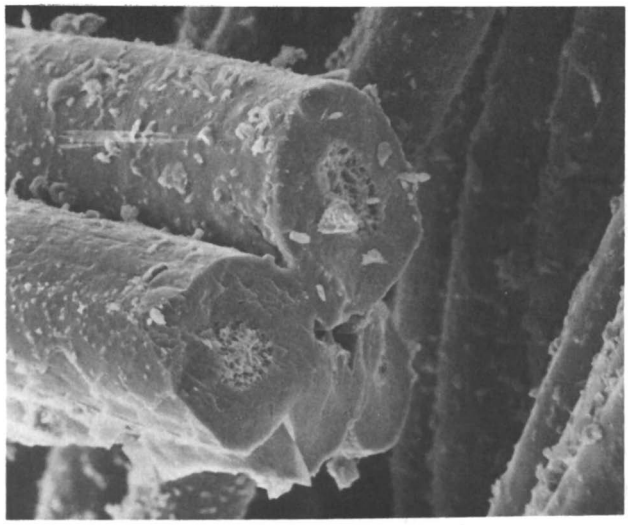

Figure 5. Alpaca fibers (800×) from Tiahuanaco tapestry, treated in tetrachloroethylene.

different amino acids linked together by peptide linkages. The sequence distribution of the amino acids in these natural polymers has a significant effect on fiber morphology as well as on the chemical reactivity of the fibers. Alexander et al. (*25*) have documented these interrelationships.

Mandelkern (*26*) provided an informative summary of the complex chemistry and morphology of protein fibers. Baer et al. (*27*) reported elemental analysis data obtained from 19 archaelogical pre-Columbian textile specimens. Although their findings suggest that generalized conclusions are not easily derived, their procedure was sensitive enough to detect changes in elemental analysis after washing. The analysis of amino acids was selected to address whether individual concentration changes occur as a result of treating old fibers in aqueous or nonaqueous systems. The first step in this sequence of analysis consisted of analyzing a contemporary alpaca sample and a sample taken from the Tiahuanaco textile. The analytical results agree reasonably well with data reported by Bradbury et al. (*28*), as summarized in Table III. The findings suggest that the protein fibers in the tapestry are alpaca. The data in the middle column represent averages of three, and the last column represents averages of two individual analyses. Table IV lists the control data from the original textile and average data obtained from three analyses after each treatment.

Only minor differences are found between aqueous and nonaqueous treatments. Note that the cystine content is slightly lower after

Table III. Amino Acid Composition of Alpaca Fibers

Amino Acids	*Bradbury et al. (28)*	*Contemporary Alpaca*	*Tiahuanaco*
Alanine	5.45	5.08	5.82
Arginine	6.95	7.16	6.99
Aspartic acid	6.45	5.99	6.66
Cystine	11.75[a]	5.74	3.32
Glutamic acid	13.40	13.55	16.51
Clycine	7.50	7.53	6.69
Histidine	0.80	0.77	0.56
Isoleucine	2.90	2.60	3.17
Leucine	7.25	7.17	7.99
Lysine	2.60	2.35	1.98
Methionine	0.40	0.50	0.39
Phenylalanine	2.40	2.55	2.42
Proline	7.20	7.03	6.90
Serine	10.60	10.82	8.13
Threonine	6.20	6.60	7.22
Tyrosine	2.25	2.35	1.98
Valine	5.50	5.35	6.18

NOTE: Values are reported in moles per 100 moles of amino acids.
[a] Bradbury (28) reported this value as ½ cystine.

Table IV. Amino Acid Analysis of Original and Treated Tiahuanaco Alpaca

Amino Acids	*Control*	*Water*	*Water and Surfactant*	*Tetrachloroethylene*
Alanine	5.82	5.99	6.00	5.75
Arginine	6.99	6.96	7.08	6.88
Aspartic acid	6.66	7.07	7.06	6.73
Cystine	3.32	2.61	2.61	3.08
Glutamic acid	16.51	17.29	17.24	15.97
Glycine	6.69	6.42	6.60	6.60
Histidine	0.56	0.70	0.64	0.47
Isoleucine	3.17	3.17	2.97	2.97
Leucine	7.99	8.39	8.10	7.88
Lysine	1.98	2.01	2.09	1.84
Methionine	0.39	0.40	0.33	0.43
Phenylalanine	2.42	2.43	2.40	2.43
Proline	6.90	7.10	6.99	6.52
Serine	8.13	8.20	8.46	8.11
Threonine	7.22	7.25	7.42	7.12
Tyrosine	1.98	2.09	2.05	2.18
Valine	6.18	6.12	6.18	5.75

NOTE: Values are reported in moles per 100 moles of amino acid.

the water treatments in comparison to the tetrachloroethylene treatments. Cystine forms covalent cross-links between adjacent polypeptide chains in keratin fibers and has a direct influence on the stress-strain behavior of wool. Robinson and Rigby (*29*) presented experimental data on the aging in keratin fibers involving thiol groups and disulfide cross-links and their effect on the stress–strain properties of protein fibers. In general, the results of the amino acid analysis suggest that the polypeptide composition of the old alpaca fibers in the Tiahuanaco tapestry has changed very little. It is reasonable to conclude that even if hydrolysis of the amide linkages between amino acids has occurred over time, the segments formed do not exhibit preferential solubility in either treatment system.

X-RAY DIFFRACTION. X-ray analysis has contributed greatly to the present knowledge of fiber morphology. The presence of both sharp and diffuse diffraction phenomena in the X-ray patterns of polymeric solids is generally accepted as evidence for a two-phase morphological model. In such a model, crystalline and amorphous regions are assumed to be present. Diffraction patterns provide information on lattice spacing, orientation, degree of crystallinity, crystallite size, and shape in polymers. X-ray diffraction data obtained with cotton by many researchers were recently summarized by Shenouda (*30*). This critical review demonstrated the complexity of this technique. In spite of the very extensive work on the fine structure of cellulose, none of the proposed morphological models adequately explain all the observed fiber properties.

Fibrous protein structure investigations applying X-ray diffraction and electron microscopy were reviewed by Blakely (*31*). Keratin fibers are made of three main structural components: the cuticle, the cortex, and the medulla. The medulla is only present in coarse fibers. The cortex forms the bulk of the fiber. Various morphological models have been proposed to explain the mechanical properties of keratin fibers. It is generally agreed that the cortex consists of fibrils in which protein molecules exist in helical and nonhelical regions.

This brief reference to the morphological architecture of cotton and wool fibers illustrates their complex nature. The use of X-ray diffraction in this investigation was not intended to yield quantitative information on the morphology of the historic fibers, but rather was intended to serve as a diagnostic technique to detect changes in morphology caused by the treatments. Any change induced by a conservation treatment is believed to affect mechanical fiber properties and should be minimized.

The X-ray equipment available for this study required a 10- × 10-mm sample size which had to be cut from the tapestry. Three samples were taken from the textile for this analysis. One of the samples served as a control before it underwent treatment. The samples were mounted

on glass slides with a double-sided adhesive, inserted into the specimen holder, and analyzed along the cotton warp and the alpaca weft. Figure 6 summarizes schematically the X-ray diffractive traces obtained from the Tiahuanaco cotton. The highest intensity of the untreated cotton appeared at a diffraction angle of 22.6° (2θ) which corresponds to the 002 reflection (*17*). The shape of the traces is indicative of cellulose I. Treatments in water and water containing 0.1% nonionic surfactant resulted in two peaks which Caulfield and Steffes (*17*) interpreted as an overlap of the 101 and the 002 reflections characteristic of cellulose II. These findings suggest that the aqueous treatments caused pronounced changes in morphology of this old cotton. In contrast, the tetrachloroethylene treatments did not change the diffraction pattern significantly.

Crystallinity indexes calculated according to the method described by Segal et al. (*32*) showed that the old cotton has a crystallinity of about 38%. Aqueous treatments increased the crystallinity of the historic cotton sample to about 45%. However, the crystallinity of contemporary cotton, which is about 70%, was not reached (*30*). This increase suggests that water acts as an internal plasticizer and allows a segmental reorientation which leads to an increase in crystallinity. Water-induced crystallization of amorphous cellulose fibers has been reported (*17*). Kalyanaraman (*33*) investigated orientation factors of cotton fibers from historic samples and found that the orientation values of the museums samples are smaller than the values of present-day cottons. He opined that cotton may have lost its orientation over time. In view of this

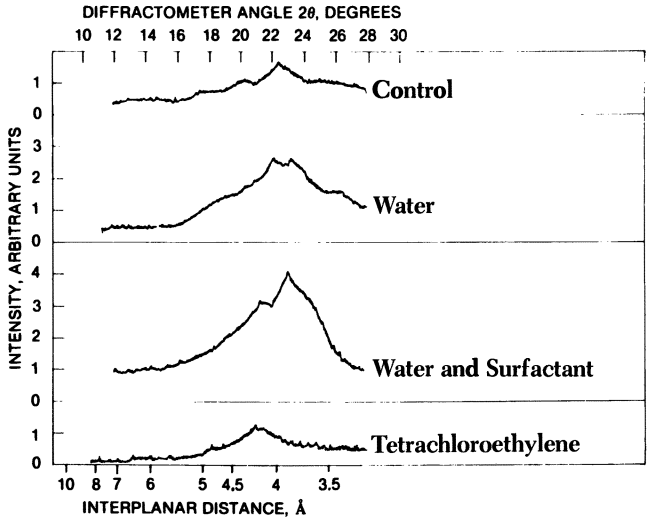

Figure 6. X-ray diffractive traces of Tiahuanaco cotton.

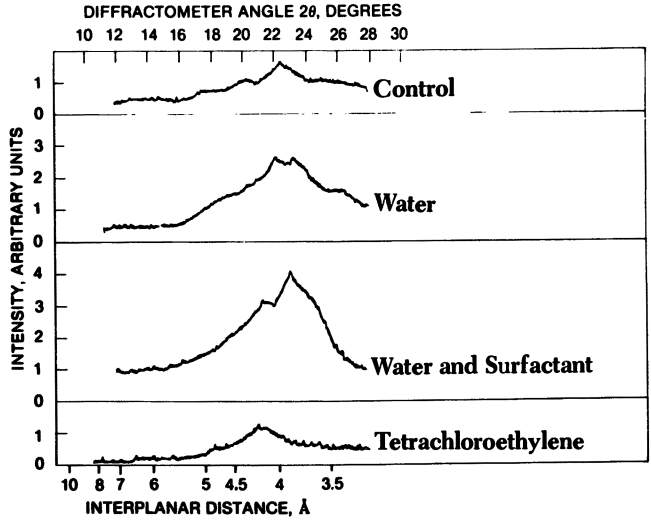

Figure 7. X-ray diffractive traces of Tiahuanaco alpaca.

interpretation, the aging of cotton may have caused a decrease in crystallinity of the cotton under investigation in this study. The implication for the textile conservator is that water treatments have a pronounced effect on the morphology of old cotton. This effect may be undesirable because internal stresses may develop upon wetting in water. Stress relaxation may have led to the helical fractures described earlier.

Figure 7 shows schematic reproductions of the shapes of the X-ray diffractive traces of alpaca observed after treatments in water and tetrachloroethylene. The reflections observed at about 9.8° (2θ) may indicate that the fibers contain ordered components having a specific helical configuration of the polypeptide chains (*31*). Aqueous treatments caused some changes in the intensities of the traces. In comparison, the nonaqueous treatment in tetrachloroethylene yielded a trace not much different from the control trace. On the basis of these observations, it is postulated that nonaqueous treatments affect the fiber morphology of historic cotton and protein fibers to a lesser degree than aqueous cleaning treatments.

Colorfastness of Wool Dyed with Natural Colorants. Before the synthesis of mauve by Perkins in 1856, all colorants used to color textiles were derived from natural resources. Brunello (*34*) comprehensively reviewed the types of natural colorants used prior to the evolution of the synthetic colorant industry. Colorfastness of natural colorants is of great

interest to the conservators. Several studies (*35*, *37*) on the lightfastness and washfastness of naturally colored textiles were done. However, studies (*38–40*) on the colorfastness to dry cleaning addressed only the fastness of synthetic colorants.

Cleaning of hydrophilic textiles in nonaqueous systems offers the advantage that the fibers do not swell as they do in aqueous cleaning solutions. As demonstrated earlier, morphological changes are minimized so that the physical properties of fibers are virtually unaltered. It follows that conservation treatments of historic textiles in nonaqueous systems may be a desirable alternative for conservators. However, such treatments raise the question of colorfastness of natural colorants to drycleaning. Because no information on this subject could be located, an experimental study was undertaken. For this study, wool was dyed with some of the more popular natural colorants listed in Table II. Color variations between samples dyed with the same colorant were minimal. This result is demonstrated by the low ΔE values in the last column in Table II. The ΔE values are quantitative measures of color differences in the CIELAB color space (*21*). The small numbers show that the natural colorants were applied evenly onto the wool samples. Conservators may question the practicality of using contemporary samples rather than historic ones. Contemporary samples are used because they are dispensable, whereas historic textiles are not dispensable. Studies of contemporary textiles are adding to the knowledge of conservation and provide a basis for informed decisions in the difficult task of historic textile conservation.

LABORATORY TREATMENTS. The results of the study on the colorfastness of the natural colorants on wool to laundering are summarized in Table V. The color change ratings were obtained by visually comparing the dyed samples after the treatments with the AATCC gray scale for color change. The staining ratings were made on the white fabrics by using the AATCC gray scale for staining (*20*). The results show that the dyed wool samples have very good colorfastness in both aqueous surfactant solutions. The differences are not statistically significant. These findings led to the conclusion that the anionic sodium alkyl sulfate surfactant, Orvus WA, and the nonionic ethoxylated nonylphenol surfactant, Tergitol NPX, do not cause significant color changes or staining of the natural colorants listed. The results of the dry cleaning study are given in Table VI. The ratings indicate that all samples have good colorfastness in the nonaqueous systems investigated. No statistically significant differences exist between the treatments in tetrachloroethylene with and without the anionic sodium sulfosuccinate surfactant, Aerosol OT.

FIELD STUDY. The use of large amounts of dry cleaning solvents in an environment without proper ventilation is not recommended because

Table V. Colorfastness of Naturally Dyed Wool to Laundering

Natural Colorant	*Orvus WA*		*Tergitol NPX*	
	Color Change	*Staining*	*Color Change*	*Staining*
Alkanet	5	5	4-5	4-5
Annatto	4-5	4-5	4-5	5
Brazilwood	5	5	5	4-5
Cochineal-alum	5	5	5	5
Cochineal-tin	5	5	5	4-5
Cochineal-chrome	5	5	5	4-5
Cutch	5	4-5	5	4
Henna	4-5	5	4-5	4-5
Indigo	4-5	4	4-5	4-5
Lac dye	3-4	5	4	5
Logwood	4-5	5	4-5	5
Madder	5	5	5	4-5
Weld	5	5	5	4-5

NOTE: Values are AATCC colorfastness ratings after treatments in 0.1% solutions of the indicated surfactants.

Table VI. Colorfastness of Naturally Dyed Wool to Dry Cleaning: Laboratory Study

Natural Colorant	*No Additive*		*1% Aerosol OT*	
	Color Change	*Staining*	*Color Change*	*Staining*
Alkanet	4-5	4-5	5	5
Annatto	5	5	4-5	5
Brazilwood	5	4-5	5	5
Cochineal-alum	5	5	5	4-5
Cochineal-tin	5	5	5	4-5
Cochineal-chrome	5	5	5	4-5
Cutch	4-5	4-5	4-5	4-5
Henna	5	5	5	5
Indigo	4	4-5	4-5	5
Lac dye	4-5	5	4-5	5
Logwood	5	5	4-5	5
Madder	5	5	5	5
Weld	5	5	5	5

NOTE: Values are AATCC colorfastness rating after treatments in tetrachloroethylene.

it may be hazardous to workers within the area (*41*). Because very few museums can afford commercial dry-cleaning equipment, conservators who would like to dry-clean historic textiles may have to use the services of a professional dry cleaner. To gain information on colorfastness to commercial dry cleaning, some tests were run under practical conditions.

The results in Table VII summarize the AATCC color change ratings after one treatment of each sample in five different plants, coded A to E. The ratings are generally lower than those observed in the laboratory study. This result suggests that the commercial dry-cleaning conditions are more severe on the color of naturally dyed wool. A variety of conditions may be responsible for this finding: detergent type and concentration, activity of solubilized water, solvent color, and nonvolatile residue, as well as machine-dependent parameters such as load factor, time of cleaning cycle, or drying conditions (*42*). Some of these variables were documented in this study, but no conclusive correlations could be established. Instrumental color measurement was done on

Table VII. Colorfastness of Naturally Dyed Wool to Dry Cleaning: Field Study

Natural Colorant	*Plant*				
	A	*B*	*C*	*D*	*E*
Alkanet	3.25	3.25	3.50	3.75	3.25
Annatto	5.00	5.00	5.00	4.75	5.00
Brazilwood	4.50	5.00	3.75	3.75	3.25
Cochineal-alum	5.00	5.00	4.75	4.50	4.50
Cochineal-tin	4.75	4.75	4.50	4.75	4.50
Cochineal-chrome	5.00	5.00	5.00	5.00	5.00
Cutch	3.75	4.25	3.75	4.00	3.75
Henna	3.50	3.75	4.25	4.25	4.25
Indigo	3.00	3.25	3.00	2.75	3.00
Lac dye	3.25	4.00	3.50	3.25	3.75
Logwood	4.00	3.25	3.75	4.00	3.75
Madder	4.50	5.00	4.25	4.75	4.50
Weld	3.75	4.25	4.50	4.50	4.00

NOTE: Values are AATCC colorfastness ratings.

Table VIII. Color Measurement of Naturally Dyed Wool After Dry Cleaning: Field Study (Plant A)

Natural Colorant	*CIELAB Color Differences*			
	ΔL	Δa	Δb	ΔE
Alkanet	2.06	−0.94	0.96	2.46
Cutch	−0.77	0.46	−0.13	0.90
Henna	2.65	−0.13	2.27	3.49
Indigo	5.34	−1.65	−0.13	5.58
Lac dye	2.65	−1.69	0.25	3.16
Logwood	−3.75	0.45	1.69	4.12
Weld	−0.53	0.33	−1.40	1.53

samples that gave ratings below 4. Typical results from plant A are shown in Table VIII. CIELAB color differences are listed individually for all three color coordinates (ΔL, Δa, Δb) along with the more conventional ΔE values. The individual color coordinate data are more informative because they give information on the shifts in hue as well as lightness in this opponent-color ordering system. For example, the indigo sample became lighter, and its hue shifted more toward green and blue after dry cleaning. The color difference expressed as ΔE merely describes the geometric distance of the color loci before and after treatments. The results indicate that indigo has the poorest color fastness, followed by logwood, henna, and lac dye. This finding suggests some of the coloring matter of these colorants has been removed or has interacted with solvent impurities to result in perceivable color changes. A summary of the pooled data obtained from this field study in each plant is given in Table IX. The second column lists one of the parameters measured in the plants, namely solvent transmittance. The dry-cleaning industry uses this concept as a control parameter for solvent color. It refers to the transmittance of the solvent at 500 nm in a 40-mm cuvette. The range from 45% to 76% represents typical practical dry-cleaning conditions (*6*). The data in Table IX demonstrate that despite variations in solvent color between plants, average wool color-change ratings are nearly the same in each plant. The staining on the adjacent white cotton and wool samples received high ratings. This result implies that the solvent conditions had only a minor effect on the appearance of the fabrics. Colorfastness data pooled according to treatments are given in Table X. Aqueous and nonaqueous treatments under laboratory conditions indicate that the colorfastness of the natural colorants on wool is excellent. The surfactants used in this study did not influence color change or staining significantly. Color change of these samples treated in dry-cleaning plants is more pronounced and differs significantly from the results obtained in the laboratory studies. Further details of this study and the statistical evaluation of the results are documented elsewhere (*19*).

Table IX. Average AATCC Colorfastness Ratings of Samples: Field Study in Five Dry-Cleaning Plants

Plant Code	*Solvent Transmittance (%)*	*Color Change of Wool*	*Staining*	
			Cotton	*Wool*
A	76	4.06 ± 0.75	4.88 ± 0.16	4.65 ± 0.16
B	61	4.29 ± 0.75	4.87 ± 0.13	4.55 ± 0.25
C	53	4.12 ± 0.63	4.80 ± 0.17	4.63 ± 0.19
D	46	4.15 ± 0.66	4.67 ± 0.24	4.53 ± 0.21
E	45	4.04 ± 0.65	4.70 ± 0.17	4.50 ± 0.20

Table X. Summary of Colorfastness Evaluation of Naturally Dyed Wool

Treatment	*Color Change*	*Staining*
Aqueous		
Orvus WA	4.80 ± 0.41	4.87 ± 0.23
Tergitol NPX	4.73 ± 0.32	4.87 ± 0.23
Nonaqueous		
Laboratory, no surfactant	4.83 ± 0.31	4.87 ± 0.23
Laboratory, Aerosol OT	4.80 ± 0.25	4.87 ± 0.22
Field study, five plants	4.17 ± 0.10	4.78 ± 0.19

NOTE: Values are AATCC colorfastness ratings.

Acknowledgments

I would like to thank Nancy Norton and Lori Houg-Dobeck for their help in the experimental part of this study; Daniel F. Caulfield, Forest Product Laboratory, U.S. Department of Agriculture, Madison, Wisconsin, for his assistance in the X-ray diffractive analysis; and John Stucker, R. R. Street Company, Oakbrook, Illinois, who facilitated the drycleaning field study. Appreciation is also extended to the Milwaukee Public Museum which provided the Tiahuanaco tapestry. Financial support for this study was obtained from the Graduate School of the University of Wisconsin—Madison and the Smithsonian Institution, Washington, D.C.

Literature Cited

1. Kajitani, N. In "Preservation of Paper and Textiles of Historic and Artistic Value"; Williams, J. C., Ed.; ADVANCES IN CHEMISTRY SERIES No. 164, American Chemical Society: Washington, D.C., 1977; p. 161.
2. Rice, J. W. In "Textile Conservation"; Leene, J. E., Ed; Smithsonian Institution: Washington, D.C., 1972; Chap. 4.
3. Bogle, M. *ICOM Comm. Conserv. Work. Group: Text. Ottawa* **1981**, 81/9/3.
4. Wentz, M.; Lloyd, A. D.; Watt, A. *Text. Chem. Color.* **1975**, *7*, 179.
5. Cutler, W. G. and Davis, R. C. "Detergency Theory and Test Methods"; Dekker: New York, 1975.
6. Martin, A. R.; Fulton, G. P. "Drycleaning Technology and Theory"; Interscience: New York, 1958; Chap. 5.
7. McBain, M. E. L.; Hutchinson, E. "Solubilization and Related Phenomena"; Academic: New York, 1955; Chap. 1.
8. Rosen, M. J. "Surfactants and Interfacial Phenomena"; Wiley: New York, 1978; Chap. 4.
9. Wentz, M.; Smith, W. H.; Martin, A. R.; *J. Colloid Interface Sci.* **1969**, *29*, 36.
10. Fulton, G. P., Lloyd, A. C., Loibl, F., Moore, G.; Reichhard, D. *ASTM-Bull.* **1953**, 129.

11. Kitahara, A.; Kon-no, K. *J. Colloid Interface Sci.* **1969**, *29*, 1.
12. Smith, W. A.; Wentz, M.; Martin A. R. *J. Am. Oil Chem. Soc.* **1968**, *45*, 83.
13. Burgess, H. D.; Hanlan, J. F. *J. II-CG.* **1980**, *4*, 15.
14. Wentz, M.; Cates, D. *Text. Res. J.* **1975**, *45*, 691.
15. Bird, J. B.; Skinner, M. D. *Text. Mus. J.* **1974**, *4*, 5.
16. Spackman, D. H.; Stein, W. H.; Moore, S. *Anal. Chem.* **1958**, *30*, 1190.
17. Caulfield, D. F.; Steffes, R. A. *Tappi* **1969**, *52*, 1361.
18. van de Vrande, I. "Wolle faerben mit Naturfarben"; Maier Verlag: Ravensburg, Germany, 1982.
19. Houg-Dobeck, L. M. S. Thesis, Univ. of Wisconsin, Madison, 1984.
20. Tech. Man. Am. Assoc. Text. Chem. Color. **1980**, *56*, Section 2.
21. Billmeyer, F. W.; Saltzman, M. "Principles of Color Technology", 2nd ed.; Wiley: New York 1981; Chap. 2.
22. Kassenbeck, P. *Text. Res. J.* **1970**, *40*, 330.
23. Duckett, K. E. In "Surface Characteristics of Fibers and Textiles", Part 1; Schick, M. J., Ed.; Dekker: New York, 1975; Chap. 2.
24. Harris, M. H. "Handbook of Textile Fibers", Harris Research Lab.: Washington, D.C., 1954; p. 72.
25. Alexander, P.; Hudson, R. F.; Earland, C. "Wool—its Chemistry and Physics", 2nd ed.; Franklin Publ.: New Jersey, 1963.
26. Mandelkern, L. "An Introduction to Macromolecules"; Springer-Verlag, New York: 1972; Chap. 6.
27. Baer, N. S., Delacorte, M.; Indictor, N. In "Preservation of Paper and Textiles of Historic and Artistic Value"; Williams, J. C., Ed.; ADVANCES IN CHEMISTRY SERIES No. 164, American Chemical Society: Washington, D.C., 1977; p. 261.
28. Bradbury, J. H. In "The Structure and Chemistry of Keratin Fibers"; Anfinson, C. B.; Edsal, J. T.; Richards, F. M., Eds.; Advances in Protein Chemistry, Vol. 27; Academic Press: New York, 1973.
29. Robinson, M. S.; Rigby, B. J. *Text. Res. J.* **1981**, *51*, 637.
30. Shenouda, S. G. In "Applied Fibre Science"; Happey, F., Ed.; Academic: London, 1979; Vol. 3; Chap. 7.
31. Blakely, P. R., *Ibid;* Chap. 11.
32. Segal, L.; Creely, J. J.; Martin, A. E., Jr.; Conrad, C. M., *Text. Res. J.* **1959**, *29*, 786.
33. Kalyanaraman, A. R. *Text. Res. J.* **1982**, *52*, 411.
34. Brunello, F. "The Art of Dyeing in the History of Mankind"; Neri Pozza Editore: Vicenza, Italy, 1973.
35. Padfield, T.; Landi, S. *Stud. Conserv.* **1966**, *11*, 181.
36. Duff, D.; Sinclair, R.; Sterling, D. *ibid* **1977**, *22*, 161.
37. Duff, D.; Sinclair, R.; Sterling, D. *ibid* **1977**, *22*, 170.
38. Hofenk-De Graff, J. H. *ibid* **1968**, *13*, 122.
39. Rhodes, W. K., *J.S.D.C.* **1964**, *80*, 23.
40. Johnson, A. E., *Text. Chem. Col.* **1974**, *6*, 275.
41. "Behavioral, Neurological and Physiological Effects of Perchloroethylene Exposure", NIOSH-HEW Contract Report No. HSM 99-73-35, 1974.
42. Wentz, M. and Jangetleiad, M. *Proc. AATCC Natl. Tech. Conf., Cherry Hill, N.J.* **1979**, 333.

RECEIVED for review January 11, 1985. ACCEPTED March 15, 1985.

Characterization of Metallic Yarns in Historic Persian Textiles by Microanalysis

Ian R. Hardin and Frances J. Duffield
Department of Consumer Affairs, Auburn University, Auburn, AL 36849

Scanning electron microscopy (SEM) and energy dispersive spectroscopy of X-rays were used to analyze the metallic content of 12 16th, 17th, and 18th century Persian textile fragments. This work was combined with historical research on the fragments and with optical microscopy studies to establish the era and provenance of the textiles. The SEM study revealed mechanical and chemical damage, as well as confirmed the mode of formation of the metallic threads. The X-ray work showed the threads to be silver, sometimes covered with gold. Sulfur and chlorine were present in many specimens; sulfur was present as a result of sulfur oxides in the air. Mercury was present in a number of samples, probably as residue from the gilding process.

A COLLECTION OF PERSIAN TEXTILE FRAGMENTS has been a part of the historic fabric collection in the Department of Consumer Affairs at Auburn University for a number of years. One of us (F. J. D.) initiated an investigation to determine how the fabrics came to be in the collection and what were their origins. The answer to the first question is incomplete. Apparently the textiles were originally donated to the Department of Textile Engineering by Oliver W. Brantley. Because of interest in the historic aspects, the collection was loaned to the Department of Consumer Affairs shortly thereafter. Brantley had made notes of identification that accompanied each of the 64 pieces in the collection. Just who Brantley was and how he came to possess the fabrics is still, after extensive inquiries, not known.

The purpose of this research was to assist in the authentication and identification of the fabrics in the collection. Much of the overall work had to do with the classification of the textiles with regard to fiber content, yarn construction, weaving technique, and place of origin or provenance. Through the use of microanalysis we were able to improve

0065-2393/86/0212-0231$06.50/0

the characterization of weaving techniques, analyze yarn construction, and determine the makeup of the metallic part of the yarns. The makeup of the metallic part of the yarns was determined by X-ray microanalysis and was also used to indicate possible origins of the metals.

Review of Literature

The textiles woven in Persia during the reign of Shah 'Abbas the Great (A.D. 1586–1628) were probably the most beautiful in the world of that time. The high regard held for these textiles was a result of the brilliant gold and silver threads, the sophisticated color schemes, the richness of the designs, and the readily apparent technical mastery. This mastery of weaving was a tradition in Persia (present day Iran). It began with the Achaemenian period of Cyrus the Great (529–550 B.C.) and reached a first apex during the Sassanian period (A.D. 226–642) (*1*).

Centuries of Islamic and Mongol rule followed, accompanied by a decline in textile quality. The Mongol invasion in the 14th century obliterated many of the cities that had been great weaving centers (2). Yarns from this period appear to be metallic, but they are actually membranes coated with gold or silver. Persian nationalistic pride was reestablished by Isma'il I in about A.D. 1500. During subsequent Safavid dynasties the quality of textile weaving once again reached a pinnacle. Under Shah 'Abbas II (A.D. 1642–1667) textiles became a commercial product as well as an art form.

The reason for the rise of these textiles as a commercial product was the new wealth in Europe that came with the exploration and colonization of the Americas. The tremendous increase in trade and the concomitant rise of merchant classes in Europe created a demand for the finest available textiles for garments, furnishings, carpets, and hangings. Persia was quite naturally sought as a source. Persian textiles of this period had delicate and elaborate designs created with a wide variety of colors. The weaves were much more complicated than European examples and remained so up until the end of the 17th century. The scale of use of metal threads in Persian textiles was matched only by Spain and Russia, and the metal threads used for background in Persia were seldom brocaded—an easier and less costly method. The use of flat metal strips, characteristic of the early Safavid era Persian textiles, was rarely seen in Europe before the late 16th century, and later European strips were always less brilliant than those in Persian textiles (3).

The greatly increased demand for Persian textiles caused the quantity of production to increase, and, almost inevitably, the quality of the textiles decreased. By the 18th century Persian textiles had declined

in technique as well as in design, whereas European and Far Eastern fabrics had become increasingly elaborate (*3*).

Historic textiles such as the Safavid Persian fabrics are worthy of study for several reasons. They deserve attention because of their beauty and the skill with which they were made, but they also stand as documents in the history of ideas (*4*), demonstrating continuities in cultural history. Generally, research done to establish the era, culture, and location of textile creations is based on a comparison of patterns in the weaving or knitting. The addition of metal threads to fabrics provides another means of identification because of variations in the way the metal may be incorporated into the fabric and the composition of the metallic component itself. Hoke and Petrascheck-Heim (*5*) point out that the chemical composition of the metallic threads may be dependent on their origins and thus assist in establishing the provenance of the fabrics themselves. An examination of historical literature indicates that Persia itself probably had little gold or silver for use in fabrics and that the metals were imported. Sir John Chardin (*6*), who traveled extensively in Persia in the mid-1600s, mentioned "gold-wire drawers" and "thread twisters", and gold brocades and velvets, but no sources of the metals. Kinnier (*7*), in his 1813 geographical memoir, alludes to mines of silver near Yezd (sic) that were not worked. Sources of gold and silver that were specified are India, Alleppo, Constantinople, Armenia, and Georgia. Sikes (*8*) stated that previous travelers said the cost for mining silver was more than the profit. All of these experiences give credence to the hypothesis that the gold and silver used in these textiles probably came from outside Persia via the many and active trade routes.

In general, four kinds of gold or silver threads appear in fabrics from the Middle Ages through the late Renaissance (*5*). They are (1) thin silver or gold wire woven into cloth; (2) thin sheets of silver or gold cut into narrow strips called lamellae and spun around a core of silk or linen; (3) gilt membrane strip for which very fine gold sheets are beaten onto an animal membrane, cut into lamellae, and wound onto a core of fibers; and (4) gilt leather or paper strip, produced like the membrane strip, but used as a flat strip instead of wound around a core.

Although the use of gold and silver metallic threads was fairly common in textiles for the wealthy, many of these fabrics are lost because of age and rotting. In addition, as Hoke and Petrascheck-Heim (*5*) indicated, these textiles were often burned to recover the precious metals.

Recent references to textiles that have gold and silver threads include the detailed volume on Persian textiles by Reath and Sachs (*3*) and work by France-Lanord (*9*), Werner and Summers (*10*), and Stouring-Neilsen (*11*). Except for Reath and Sachs (*3*), the articles deal

with descriptions of specific textiles or garments that incorporated metallic threads. Reath and Sachs (*3*) stated that Safavid silks were far richer and more complicated (compound weaves) than other contemporary fabrics. During this period, 1502–1736, Spain and Russia were the only countries that used metal thread as lavishly as Persia. European fabrics have large-scale designs composed of simple contours of two colors on a satin ground, whereas in Persia delicate and elaborate designs were executed in a wide range of colors.

Microscopic examinations of textiles containing gold and silver threads are few in number. The primary work seems to be that of Petrascheck-Heim (*12*) and Hoke and Petrascheck-Heim (*5*). Their research analyzed medieval textiles from graves in Germany and samples from various European locations that were supplied by several museums. These samples were examined by microprobe analysis in which the samples were bombarded with a focused electron beam to create backscattered and secondary electrons that were used for image formation. In addition, X-rays characteristic of the elements present in the sample were created by this bombardment. These allowed a microscopic analysis of the composition of the specimen. By combining the images formed from the electrons with the X-ray analysis and scanning electron microscopy (SEM), element-specific pictures were created. These clearly indicate varying elemental composition on the microscopic level. The elemental analysis on the German medieval textiles revealed that in several cases the metallic threads were probably of Oriental rather than European origin, a conclusion reached on the basis of silver-to-copper ratios in the threads. This conclusion agrees with the statement by Reath and Sachs (*3*) that Near Eastern metal thread contains much less copper than that from Europe.

Experimental

The textile pieces in the Brantley collection were subjected to historical research and microscopic analysis. These were done to verify the information already existing on the collection, to identify those fragments for which information was missing, to classify the fragments as textiles, and to identify the metallic threads that were part of the textiles.

The collection itself is made up of 64 fragments ranging in size from a 3.0- × 8.0-cm triangle to a 37.7- × 42.0-cm rectangle. Each fragment was accompanied by notes of identification, presumably written by Brantley.

Historical. A detailed visual examination of the textiles, both macroscopic and microscopic, was done to determine motifs, techniques of woven construction, color, and fiber content. Many literary sources were used to identify the fragments, including the "Survey of Persian Art" by Pope and Ackerman (*13*), "Persian Textiles and Their Techniques" by Reath and Sachs (*3*), plates from the volumes on Persian and Indian textiles by Riefstahl (*14*), and Bunt (*15*). In

addition, works by Emery (*16*) and Burnham (*17*) were used in the classification of the weaving techniques.

The collection pieces were examined and classified by dimensions, motifs, yarn construction, weaving technique, selvage, finish line, color, probable date, probable provenance, and presence or absence of metallic threads. After the initial classifications the pieces were taken to the Textile Museum in Washington, D.C., for comparison to extant Persian textiles in its collection. Comparisons were also done to pieces in the Hobart and Edward Small Moore Collection located at the Yale University Art Gallery.

Microscopic. The specimens in the collection were examined in detail by stereo light microscopy (7-40×) and by SEM (20-500×) with an AMR-100 electron microscope. Figure 1 shows a schematic for SEM indicating the generation of an electron beam at the cathode with the electrons accelerated toward the sample. The deflector coils cause the beam to be scanned back and forth across the sample, as indicated by the name. The impact of the electron beam on the sample has several effects. Back-scattered and secondary electrons escape from the specimen. Secondary electrons, especially, can be collected by the secondary electron detector. The signal generated by this device is fed to the cathode-ray tube (CRT) which is synchronized with the deflector coils. This process causes a "television" picture of the specimen. Outstanding resolution and depth of field are gained by this method.

X-ray. Another result of the electron beam striking the specimen in SEM is the generation of X-rays characteristic of elements present. Figure 2 shows an incident electron striking an atom and ejecting an orbital electron. The vacancy

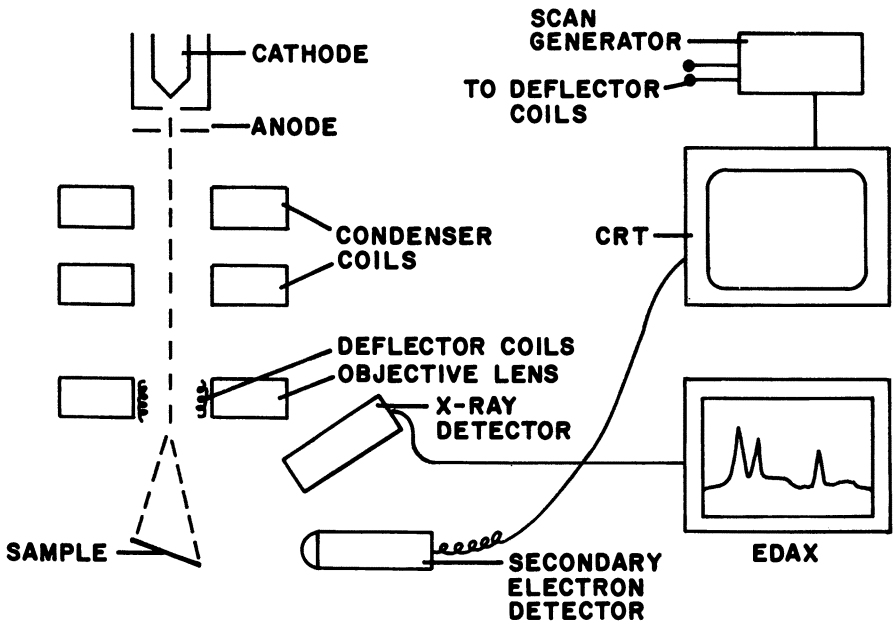

Figure 1. Schematic of SEM.

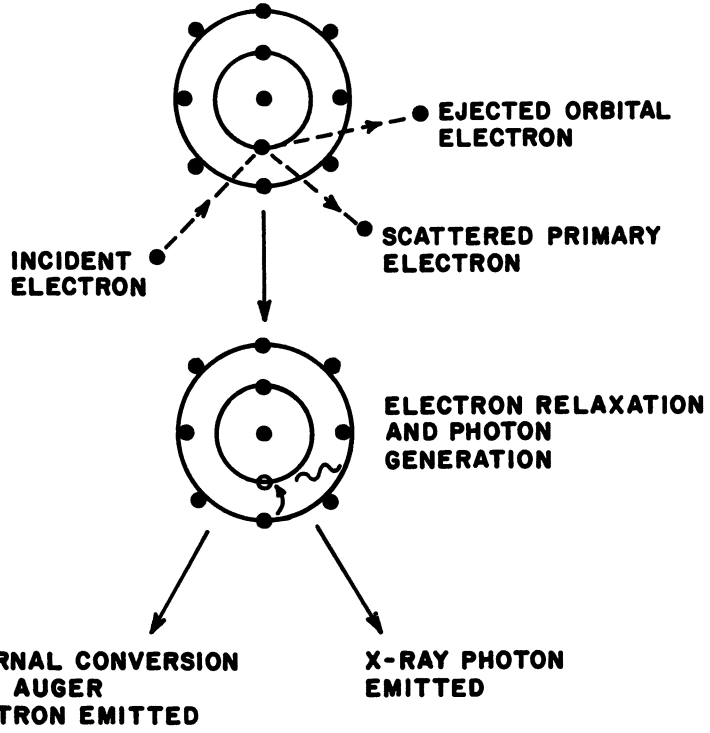

Figure 2. Production of X-rays and Auger electrons by electron bombardment.

created is filled by another orbital electron "falling" from an outer shell. As this transition occurs the electron loses an amount of energy equal to the difference in energies between the two shells. This energy is given off as an X-ray that is characteristic of the particular kind of atom and the transition in question. Figure 3 illustrates several of the more probable transitions, each of which gives off an X-ray of a definite wavelength and energy. The other possibility is internal conversion and production of an Auger electron. At the same time a continuum of X-rays with differing energies is created by the inelastic interactions of the electrons with the nucleus of the atom. These create a continuous background to the characteristic X-rays.

Figure 1 shows that the scanning electron microscope includes an X-ray detector with a crystal that separates the X-rays according to the characteristic energies. This method is called energy dispersive spectroscopy (EDS). An EDAX model 707A X-ray analyzer was employed for EDS. Both SEM and EDS were performed on specimens of yarn taken from the fragments in the Brantley collection. Characteristic energies of peaks in the spectra were cataloged. These peaks were then assigned to elements. These assignments for peaks were double-checked by examining compounds that contained the elements in question.

Correlation. The information gained from the historical analysis and from the microanalysis was examined for relationships between historically deter-

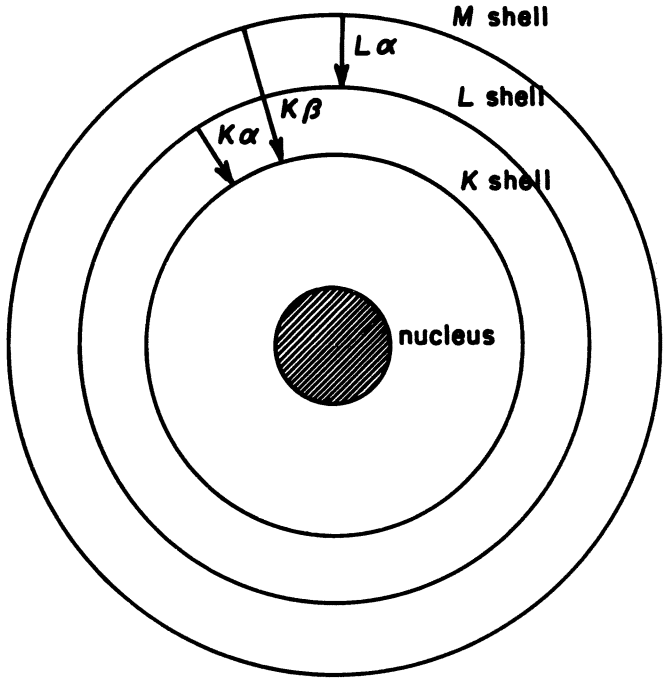

Figure 3. Electronic transitions in an atom.

mined provenances and the content of the metallic threads. We were particularly looking for differences in the elemental content of the metallic threads that might correlate with the provenances established by historical investigation. If, indeed, the different weaving centers received their silver and gold from differing outside sources, then a pattern of elemental analysis could assist further historical investigations.

Results and Discussion

Of the 64 fragments in the Brantley collection, 61 were found to be woven of silk, 1 was woven of silk and wool, 1 was woven of silk and cotton, and 1 was woven of cotton. Fifty of the samples contained metallic yarns; all were flat metal strips wound around silk yarns in a spiral fashion except one which was woven flat without the core. These metallic yarns were used both for ground fabric and for brocading.

Visual and optical microscopy established 14 different weaving techniques used within the collection. These included plain, twill, satin, brocade, velvet, double, and compound weaves. The design motifs represented in the collection included such flowers as centaureas, iris, four-o-clock, lilies, carnations, and roses. Other motifs commonly found were grape-leaf palmattes, quatrefoils, little birds, butterflies, and

various flowering shrubs and trees. By a combination of evidences from weave classification, motifs, and examination of extant examples, 43 of the fragments were assigned to the weaving centers of Abiana, Isfahan, Kashan, Mashad, and Yazd. Twenty-three fragments were assigned to Persia in general. The cities, along with the capital of Tehran, are shown on the map in Figure 4.

Optical Microscopy. Under the stereo microscope the intricacy and beauty of the weaves become readily apparent. Figure 5 shows some examples of fabrics that contain metallic yarns. Figure 5a has metallic wrapping that is very regular and spaced so as to pick up the color of the dyed fibers around which it is wrapped. Figure 5b, on the other hand, shows yarns in which the wrapping completely covers the enclosed fibers and produces more of a sheen in the fabric. Figure 5c shows a more random effect, whereas Figure 5d is a higher magnification view that shows more clearly how the metal thread is spiraled around the yarn.

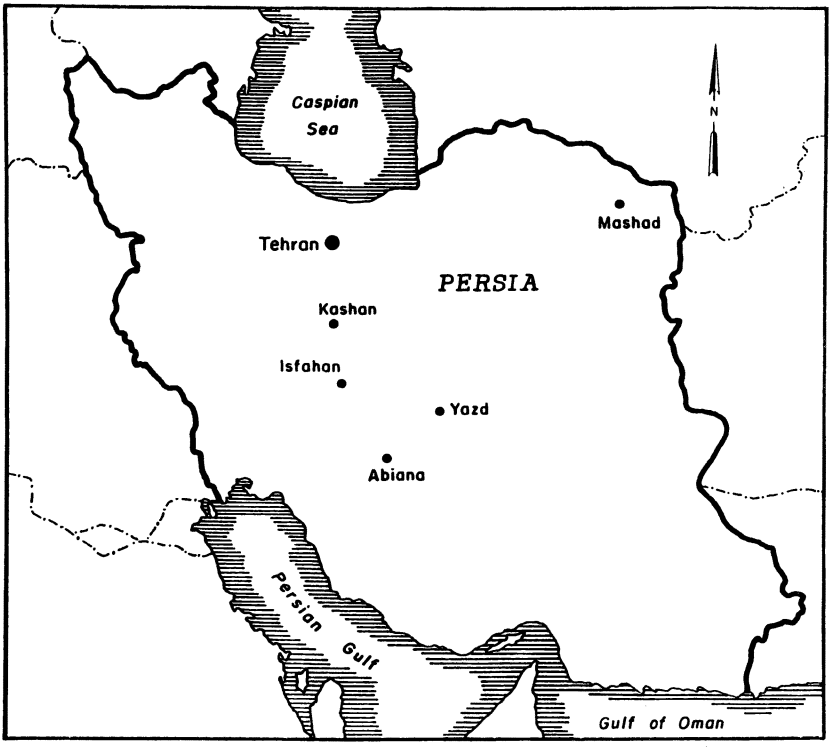

Figure 4. Map of Persia showing weaving centers.

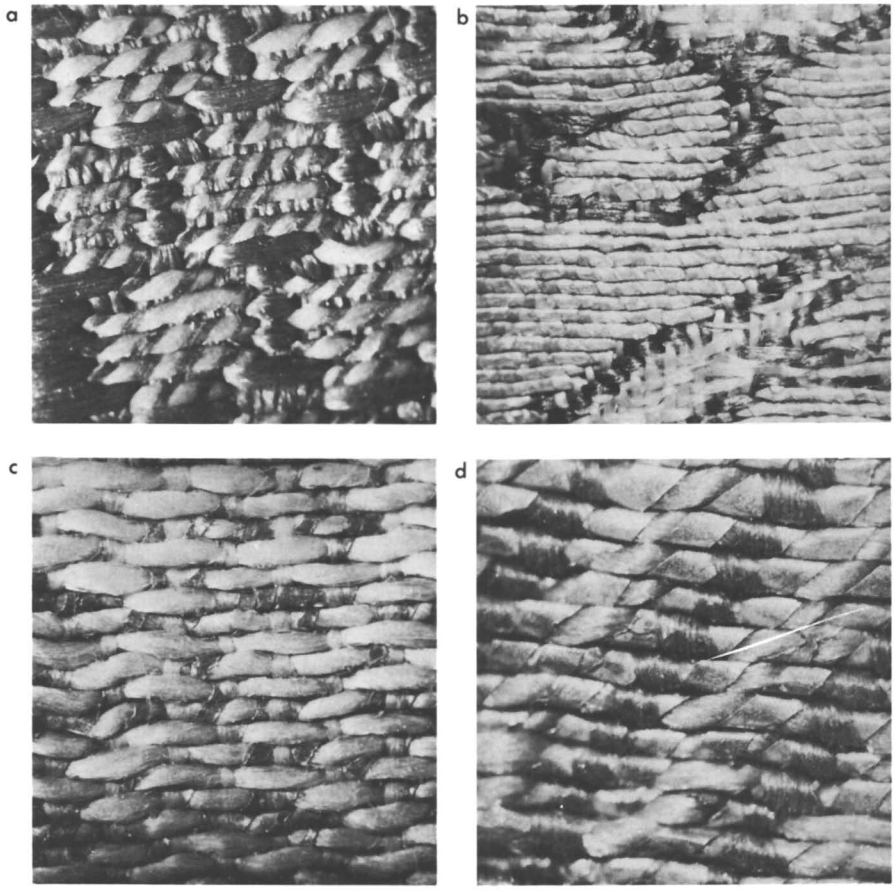

Figure 5. Optical microphotographs showing metallic yarns of specimen M-1 (a), TB-9 (b), TB-12 (c), and S-4 (d).

SEM. Of the 50 specimens containing metallic yarns, 11 were selected as representative of the group. These were examined by SEM and EDS. Examinations of individual threads from the specimens were done to establish the nature of the metallic thread wrapped around the silk fibers. Previous to the late medieval period, virtually all gold or silver threads were actually metals beaten very thin onto animal membranes, which were then cut into strips. As Persia became more prosperous, the higher quality pure metal strips were created and used. Often these metal strips were made by drawing metal wire to very fine diameters and then passing the wire through rollers to create the flat strip. Chardin's (*6*) references to gold wire drawers and thread twisters in 17th century Persia indicate that this method is probably that by which the metallic threads in this investigation were made.

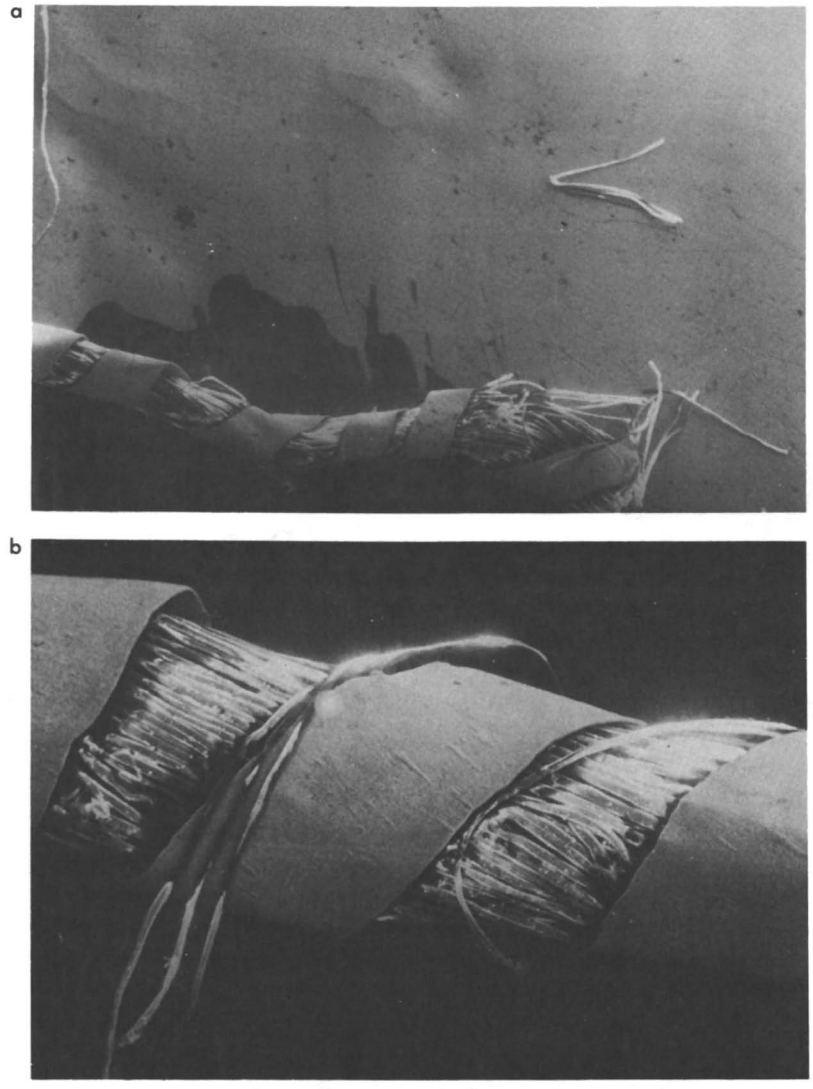

Figure 6. Photographs showing relative size of yarns (a = L-2; b = TB-12).

Figures 6a and 6b indicate the small size of the very fine threads in the study and emphasize the skill represented by their creation. In Figure 6a the outlines of the ear of Franklin Roosevelt on a dime can be seen to the right of the yarn. Figure 6b is a higher magnification shot of a yarn taken from the same sample. Figures 7a and 7b give further examples of the regularity of the threads and the way they were wrapped. Figure 7b, in particular, shows remarkable uniformity of

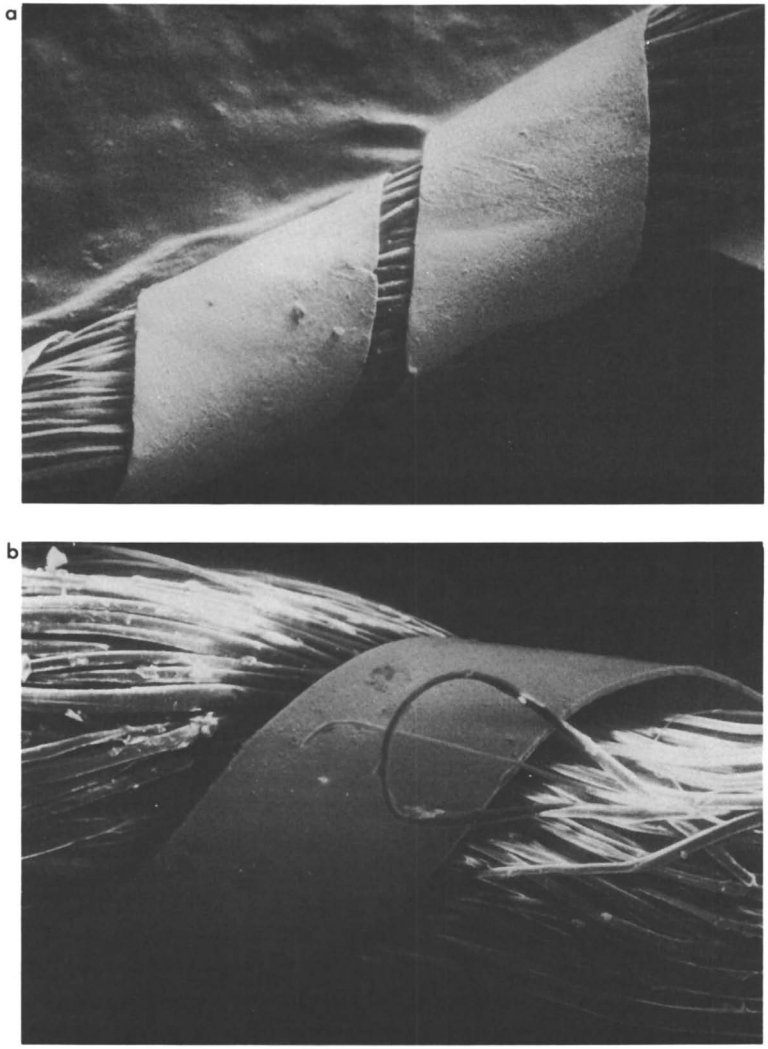

Figure 7. SEM photographs of metal-wrapped yarn (a = TB-10b; b = L-10).

thickness and regularity of the surface of the metallic wrapping. The charging evident in the photograph occurs because these specimens were prepared for X-ray examination and thus were not coated.

Not all the specimens were as uniform or as free from obvious damage. Figure 8 shows a typical yarn from a trimming band in the collection. Although the metal yarn surface appears undamaged, clear evidence of mechanical damage is indicated by a fold line running along

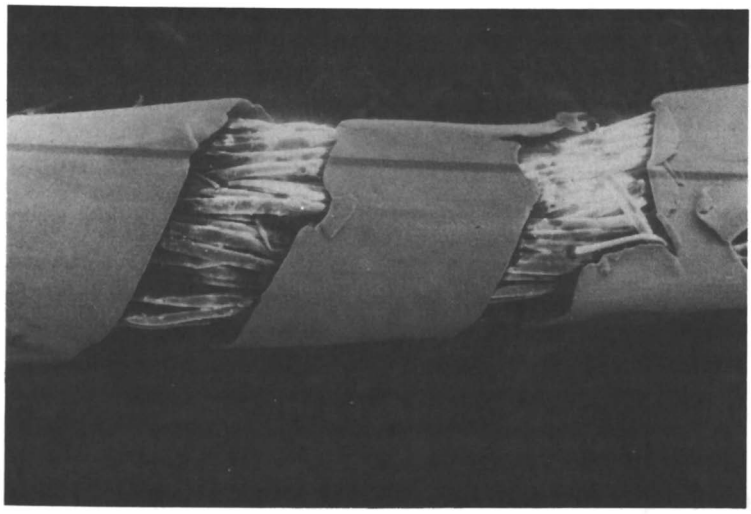

Figure 8. Yarn with mechanical damage (TB-2).

the yarn and tear damage to the wrap itself. Another trimming-band specimen is represented in Figure 9a. Here, the damage appears to be chemical rather than physical. In Figure 9b higher magnification of the same area gives clear indication of deposits formed by reaction with the metal, as well as what appear to be holes in the surface.

Figures 10a and 10b typify yet another form of damage to the metallic yarns. Figure 10a shows two areas, on the extreme right and extreme left, where a layer of metal seems to have broken off. Figure 10b is a higher magnification shot of the area on the left. In addition, the edges of the metal are much more irregular than those of other specimens. The irregularity of the edges might be caused by the formation process itself or may be the result of the corrosion evident on the surface. The delamination observed suggested first that this yarn might be a thin layer of metal on a membrane, rather than pure metal. X-ray analysis, discussed in detail later, showed that this was not the case. The material under the first layer has the same composition as the outer layer. The possibility is that these strips were not formed by flattening gold wire, but were made by hammering thin foil together and then cutting it into strips. This kind of delamination was observed on only a few specimens.

Delamination. As was mentioned earlier, specimen L-1 in Figure 10 had areas where delamination apparently had occurred. This observation suggested that the metal wrapping might be a membrane covered

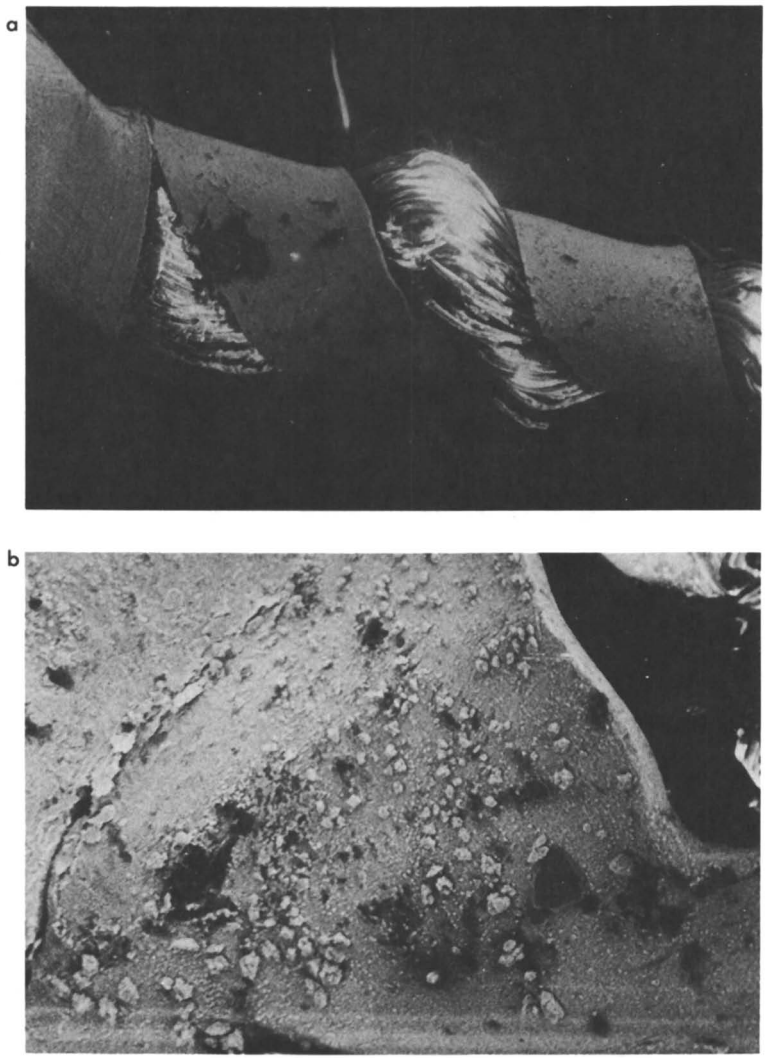

Figure 9. Deposits and holes caused by chemical attack (a = TB-13; b = TB-13).

with a thin layer of metal foil rather than solid metal. This composition would be unusual because the consensus among the historical sources was that, from the 16th to the 18th century in Persia, metallic yarns were exclusively all metal. Further examination of specimen L-1 involved X-ray mapping of the areas of the specimen where delamination had occurred. The results showed that the material underlying the removed layer had the same metallic composition of the upper layer and was not

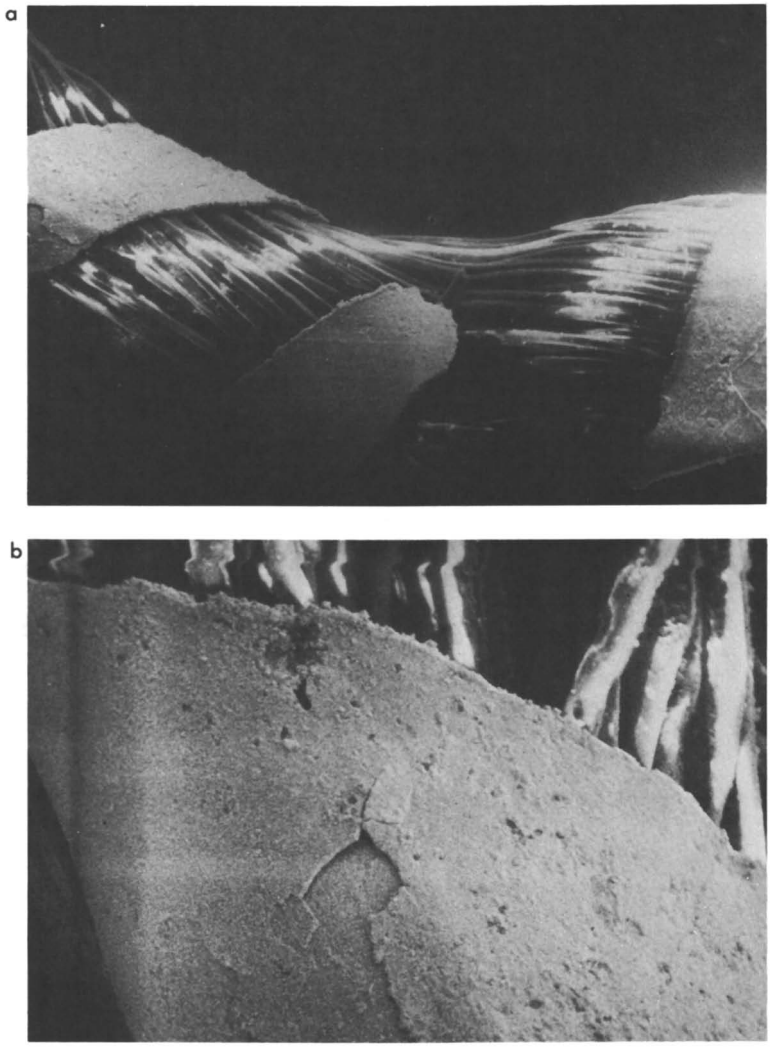

Figure 10. Delamination damage in metallic yarns (a = L-1; b = L-1).

animal membrane. The question of why the metal delaminated in the first place is, however, not resolved.

X-ray Analysis. The first step in X-ray analysis was to generate a full spectral analysis of each of the specimens. A typical example is the spectrum of specimen M-3 shown in Figure 11. Prominent peaks occur at 1.74, 2.24, 2.64, 2.98 and 3.16 keV. Although assignments for these peaks and others encountered in the work could be made from a chart,

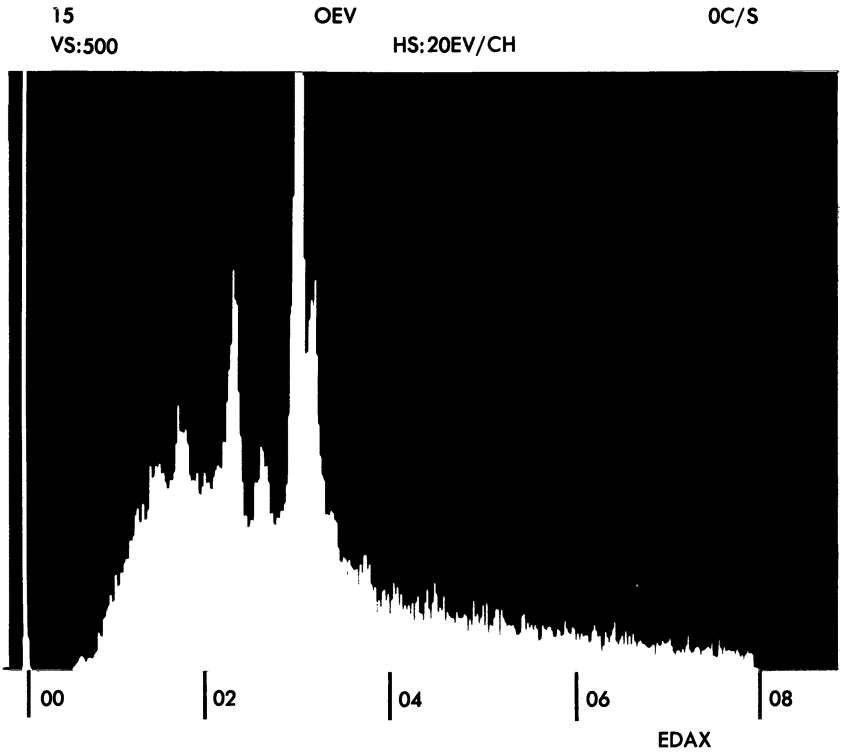

Figure 11. X-ray energy spectrum for specimen M-3.

it was felt that standards should be run for each of the peaks in question. Table I shows a list of elements and their energies of transition determined by experiment.

After the full X-ray spectrum was run, X-ray maps were generated to determine what parts of the specimen included the elements in question. Figure 8 is the SEM photo of specimen TB-2. Figure 12 is the full EDS spectrum of the same specimen, and distinct peaks appear at 1.74, 2.12, 2.20, 2.34, 2.62, 2.98, 3.16, and 3.30 keV. These peaks are the results of silicon, gold, mercury, sulfur, chlorine, and silver (three peaks), respectively. X-ray maps were generated at each of the energies noted to determine the sources of the signals. Two such maps are shown in Figures 13a (window at 2.98 keV) and 13b (window at 2.12 keV). The silicon appears to be present as sand, whereas the other elements are present in the metallic flat strip itself. This yarn has a very thin layer of gold over the silver strip. The mercury may very well be present because it was used in applying the gold in the first place. The process of "water gilding" used an amalgam of mercury to apply gold to the surface of silver (*18*). The mercury dissolved some of the silver and

Table I. Characteristic X-Ray Energies for Selected Elements

Element	*Transition*	*Energy (keV)*
Si	$K_{\alpha 1}$	1.74
Au	$M_{\alpha 1}$	2.12
Hg	$M_{\alpha 1}$	2.20
S	$K_{\alpha 1}$	2.31
Cl	$K_{\alpha 1}$	2.62
Ag	$L_{\alpha 1}$	2.98
	$L_{\alpha 1}$	3.16
Pd	$L_{\alpha 1}$	2.85
	$L_{\alpha 1}$	3.00
Mo	$L_{\alpha 1}$	2.36
	$L_{\alpha 1}$	2.44
Cu	$L_{\alpha 1}$	0.94
	$K_{\alpha 1}$	8.05

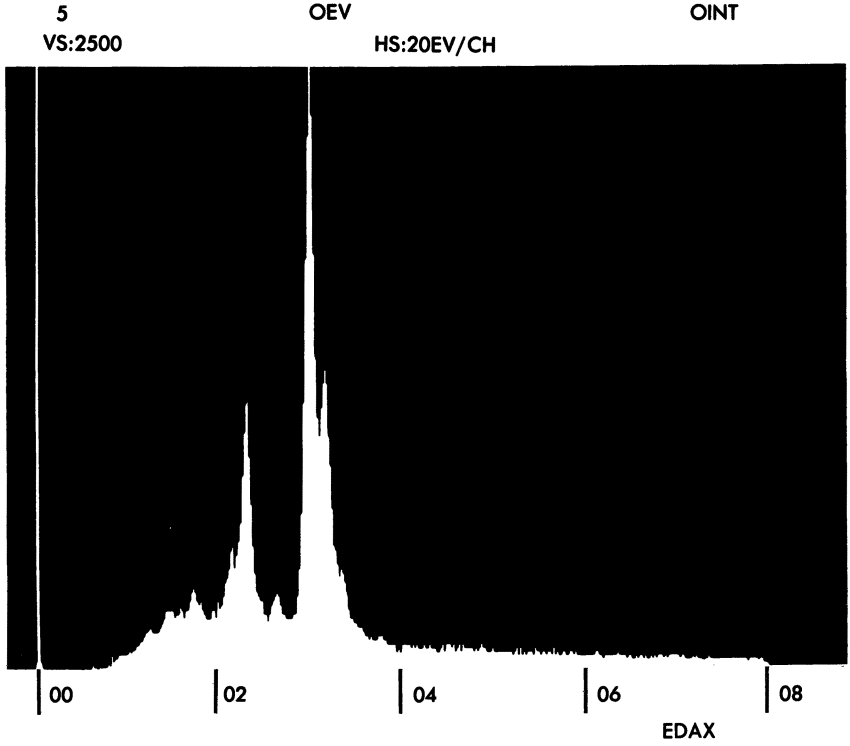

Figure 12. X-ray spectrum of specimen TB-2.

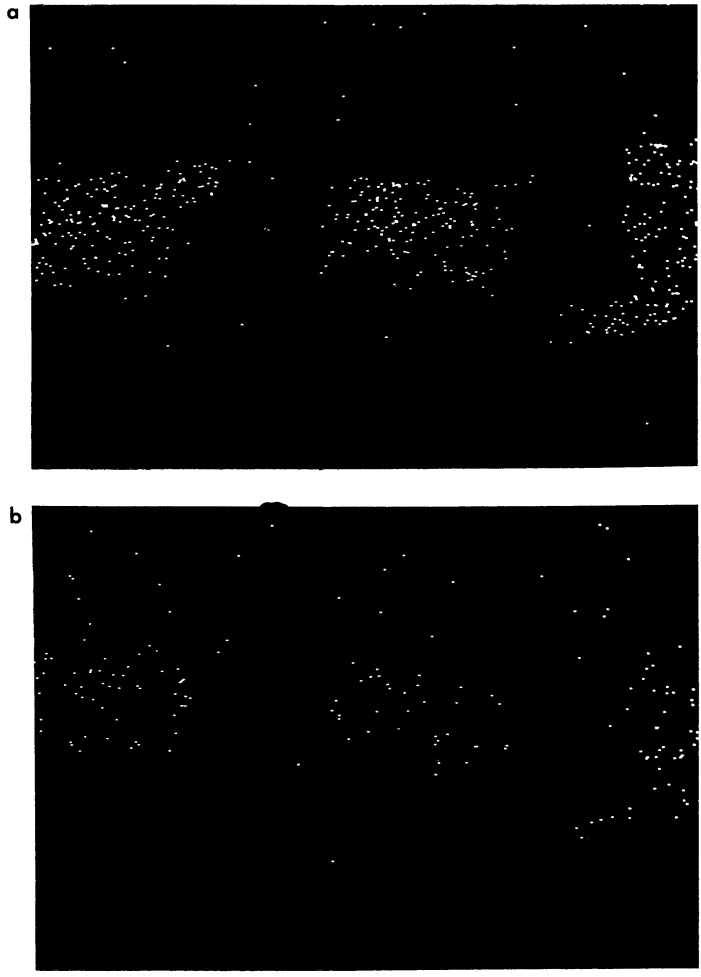

Figure 13. X-ray maps of silver (a) and gold (b) for TB-2.

helped to bond the two layers together (*5*). Also, the mercury may be the remnant of the gold mining process (*19*).

The presence of sulfur is probably the result of sulfur oxides in the air combining with the silver. These oxides are present whenever fossil fuels are burned, and they readily attack silver. Researchers (*5*) have stated that sulfur in such metallic yarns is the result of the breakdown of the silk protein, fibroin. This occurrence, however, is unlikely because silk contains almost none of the two sulfur-containing amino acids, cystine and methionine (*20*). The exact source of the chlorine present in the sample is less easy to explain. It is present in most, though not all,

specimens examined. One possible source might be salt used in dyeing the fibers around which the metallic strips are wound. Perhaps another source is perspiration from the past wearers of these garments.

The results for a specimen with a slightly different composition are presented in Figures 14 and 15. The SEM photo for specimen L-1 and the EDS spectrum are given in Figures 10a and 14, respectively. Figures 15a and 15b show the X-ray maps with the windows set at 2.98 keV (silver) and 2.36 keV (sulfur). Figure 14 shows peaks at 2.36, 2.98, 3.16, and 3.30 keV. Possible peaks occur at 2.12 keV (gold) and 2.62 keV (chlorine), but the indication is so weak that positive identification is difficult. Subsequent X-ray maps confirmed that the metallic wrapping contained silver and sulfur, as well as a small amount of chlorine, but no gold.

Results of microanalysis for typical specimens are listed in Table II. Every specimen examined was composed primarily of silver. A few of the specimens also contained gold, probably as a covering over the silver base. The presence of mercury in specimens TB-10A and TB-11, but not gold, is anomalous in view of the explanation given earlier for the

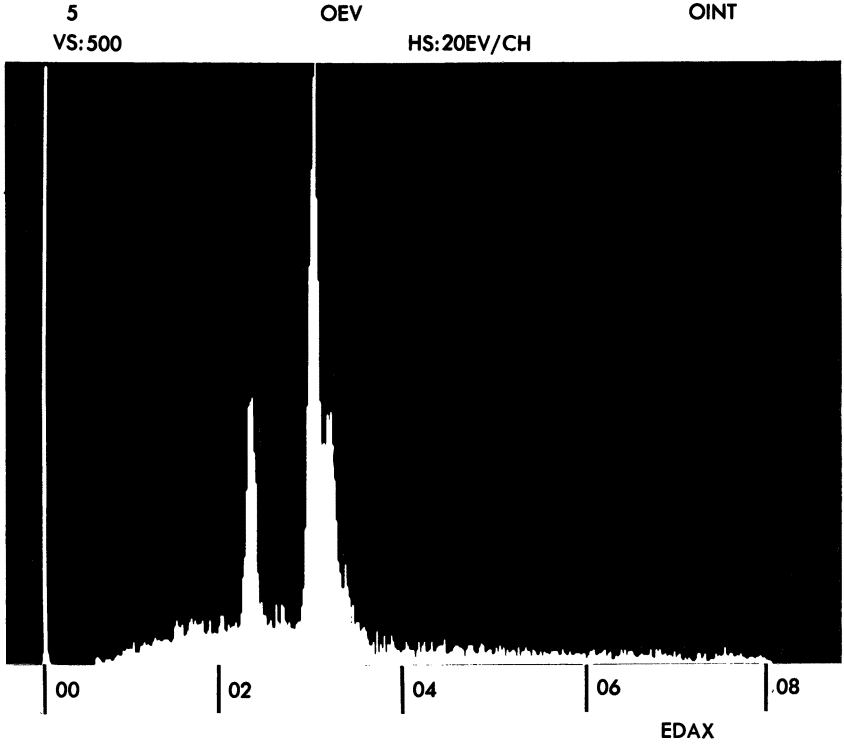

Figure 14. X-ray energy spectrum for specimen L-1.

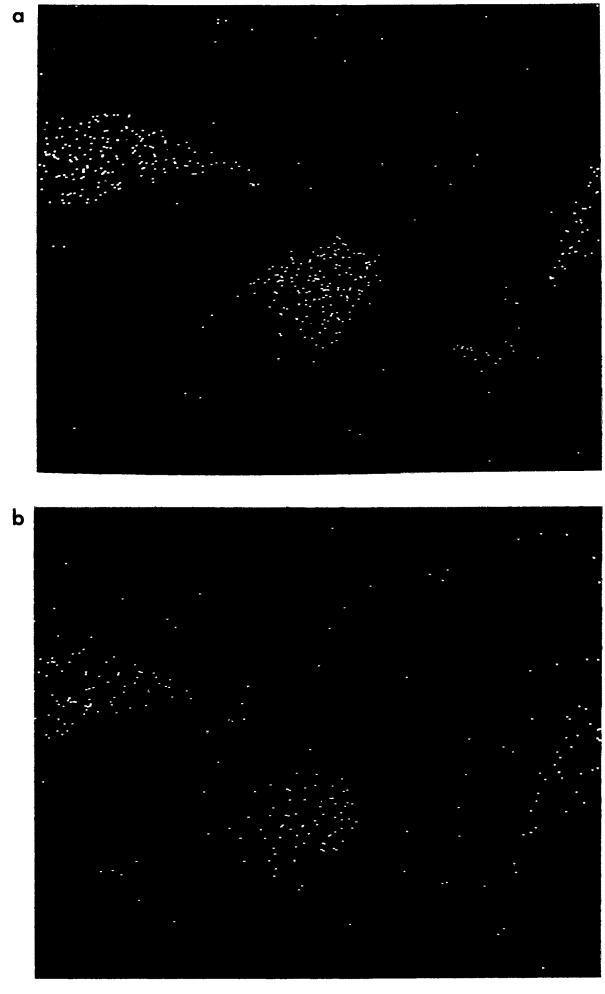

Figure 15. X-ray maps of silver (a) and sulfur (b) for L-1.

presence of mercury. One possibility is that a thin layer of gold could have been worn away. Because only limited sampling of each specimen was done, a bias of this kind could be induced. The ubiquitous presence of sulfur strongly suggests that the source was air pollution and that the absence for specimen L-5B is anomalous. Efforts to detect metals such as copper, paladium, and molybdenum in the specimens were unsuccessful. These metals have been mentioned in the literature as additives or impurities in gold and silver artifacts.

Interpretation of X-ray Spectra. The X-ray results must be interpreted carefully. Characteristic X-rays are generated from a substantial

Table II. Microanalysis of Metallic Threads

Sample	*Silver*	*Gold*	*Mercury*	*Chlorine*	*Sulfur*
L-1	●			●	●
L-2	●			●	●
L-5A	●			●	●
L-5B	●				
L-10	●			●	●
TB-2	●	●	●	●	●
TB-10A	●		●		●
TB-11	●		●		●
TB-12	●	●	●		●
TB-13	●	●	●	●	●
TB-13B	●			●	●
M-3	●	●		●	

NOTE: A ● denotes a positive finding.

fraction of the interaction volume formed by scattered electrons. This volume is close to the surface and usually extends only a few micrometers into the material. The X-ray generation range is given in one form by Anderson and Hasler (*21*):

$$\rho R = 0.064\ (E_o^{1.68} - E_c^{1.68})$$

where ρ is the density of the material, R is the range, E_o is the beam energy, and E_c is the critical ionization energy for characteristic X-rays. Thus, the X-ray spectrum detected represents only that material lying near the surface. The spectrum itself will be dependent on the uniformity of the material and, perhaps, on the accelerating voltage of the electron beam. As an example of the former, a sulfide layer on the surface of a silver wrapping could cause an erroneous quantitative estimate of elemental distribution. The surface layer may be relatively rich in sulfur, but deeper into the material sulfur may be absent. The same caution must be exercised with the specimens that contain gold and mercury. Because all of these elements are of high density, the X-ray spectra will be representative of only a fraction of a micrometer into the specimen, and not of the bulk specimen itself. If the accelerating energy is less than the energy needed to remove an electron, then the spectrum may lack high-energy peaks.

Historical Study Provenances. The provenances established by historical studies are listed in Table III. An attempt to link the results of the microanalysis to the provenances has been largely unsuccessful. The hypotheses that the different weaving centers received their precious metals from different sources and that the metals from these different

Table III. Provenances of Specimens Determined by Historical Studies

City or Country	*Specimens*
Abiana	S-4, S-14, M-3, L-12, TB-13
Isfahan	S-1, S-2, S-6, S-7, S-8, S-9, S-10, M-2, M-6, M-12, L-1, L-3, L-8, L-10, L-11, TB-3, TB-4, TB-16
Kashan	S-3, S-11, S-16, S-21, S-23, TB-2
Mashad	M-10, L-5, L-6
Persia, general	S-5, S-9, S-10, S-12, S-17, S-18, S-19, S-22, M-6, M-9, M-11, L-2, L-4, L-7, L-9, TB-1, TB-5, TB-6, TB-8, TB-9, TB-10, TB-11, TB-13, TB-15, TB-18, TB-19
Yazd	S-3, M-1, M-4, M-5, L-4, L-6

sources would have characteristic differences in the analyses were not proven. Further work in this area will require a more extensive range of samples, and even, perhaps, metals from art forms other than textiles.

Acknowledgment

This research was partially supported by an Auburn University Grant-In-Aid.

Literature Cited

1. Pope, A. U. "An Introduction to Persian Art Since the Seventh Century"; Scribner: New York, 1931.
2. Pope, A. U. "Masterpieces of Persian Art"; Dryden Press: New York, 1945.
3. Reath, N. A.; Sachs, E. B. "Persian Textiles and Their Techniques from the Sixth to the Eighteenth Centuries Including a System for General Textiles Classification"; Yale University: New Haven, 1937; p. 3.
4. Ackerman, P. *Ciba Rev.* **1953**, *98*, 3500, 3503-13.
5. Hoke, E.; Petrascheck-Heim, I. *Stud. Conserv.* **1977**, *22*, 49-62.
6. Chardin, J. "Sir John Chardin's Travels In Persia"; Repr. 1927 ed.; AMS Press: New York, 1972; pp. 268, 277, 278.
7. Kinnier, J. M. "A Geographical Memoir of the Persian Empire"; Repr. 1813 ed.; Arno Press: New York, 1973; pp. 40, 199, 224, 251, 319, 340.
8. Sikes, P. "A History of Persia—Volume I"; 3rd ed.; MacMillan: London, 1951; p. 34.
9. France-Lanord, A. *Conserv. Archaeol. Appl. Arts* **1975**, 15-18.
10. Werner, A. E. A.; Summers, G. A. C. *Archaeologica* **1971**, *103*, 136-47.
11. Stovring-Neilsen, S. *Medesser om Konservering* **1973**, *3 (3)*, 91-93.
12. Petrascheck-Heim, I. *Neus aus Alt-Villach, 7. Jahrbuch des Stadtmuseums Villach* **1970**, 56-190.
13. Pope, A. U.; Ackerman, P. "Survey of Persian Art"; Oxford University Press: London, 1965.

14. Riefstahl, R. E. "Persian and Indian Textiles from the Late Sixteenth to the Early Nineteenth Century"; E. Weyhe: New York, 1923.
15. Bunt, C. "Persian Fabric"; F. Lewis: Leigh-on-Sea, England, 1963.
16. Emery, I. "The Primary Structures of Fabrics"; Textile Museum: Washington, D.C., 1966.
17. Burnham, D. K. "Warp and Weft"; Royal Ontario Museum: Toronto, 1980.
18. *Sci. Am. Suppl.* **1984**, *17 (451)*, 7176.
19. Mora, E., personal communication, 1984.
20. "Handbook of Common Polymers"; Chemical Rubber Co.: Cleveland, 1971.
21. Anderson, C. A.; Hasler, M. F. *X-Ray Opt. Microanal. Congr. Int.* 4th **1965**; 310.

RECEIVED for review November 26, 1984. ACCEPTED March 28, 1985.

14

Characterization of Selected Prehistoric Fabrics of Southeastern North America

Lucy R. Sibley[1] and Kathryn A. Jakes[2]

[1]Department of Textiles and Clothing, Ohio State University, Columbus, OH 43210-1295

[2]Center for Archaeological Sciences, University of Georgia, Athens, GA 30602

Types of twined fabric structures composed of bast or phloem fibers and feathers were identified in prehistoric fabrics of southeastern North America by chemical and physical analyses and technical fabrication studies. Fabrics and either partially or completely mineralized pseudomorphs after fabric from the Tunacunnhee and Etowah sites in Georgia (dated respectively A.D. *150 ± 95 years and about* A.D. *1200) were examined. The work confirms the presence of at least two types of twined structures for the earlier Hopewell site and intricately constructed re-plied yarns and twined fabric for the later Mississippian one. The study of fabrics from both sites provides evidence of the kinds of materials produced and used by prehistoric peoples of the region during a 1000-year interlude.*

FABRICS USED BY THE ABORIGINAL PEOPLE of southeastern North America have not been studied extensively. Small fragments of cordage, fabrics, and matting have been recorded from various prehistoric sites in the region (*1–4*), but analytical and synthesizing efforts have focused on matters other than the study of these pieces or the study of their cultural implications. Because fabrics are manufactured and used by people, their examination can reveal information about those who produced them. A first step, however, is the analysis of fabric as fabric. The purpose of this project is this first step: to characterize selected examples of direct fabric evidence from the Tunacunnhee and Etowah sites in Georgia.

Direct fabric evidence means those forms of fabrics that are still organic and have retained their original fiber composition, and those that are partially or completely replaced by mineral compounds. Those replaced by mineral compounds, termed fabric pseudomorphs, result when fabrics in contact with metal are buried in a moist, soil environ-

0065-2393/86/0212-0253$07.00/0

ment, and corrosion of the metal over a period of time induces mineralization of the fibers. The physical shapes of fabrics are retained during the process (*5–6*). Pseudomorphs after fabric and partially mineralized fabric formations on Tunacunnhee copper ornaments, together with fabrics and partially mineralized fabrics from Mound C at Etowah, are the subject of this research.

Description of the Sites

Although both sites are in the same geographic area (Figure 1), they differ greatly in age and cultural expression. The Tunacunnhee site, dated A.D. 150 ± 95 years, represents the Hopewell tradition (*1*), whereas Etowah, in use between A.D. 900 and A.D. 1400, is considered to be of the Middle Mississippian period (*7*). Taken together, the two sites and their fabrics provide evidence of the kinds of materials produced and used by certain prehistoric people of the region. Both sites are expressions of major cultural traditions in southeastern North America, and both contain direct fabric evidence. These facts underscore the importance of

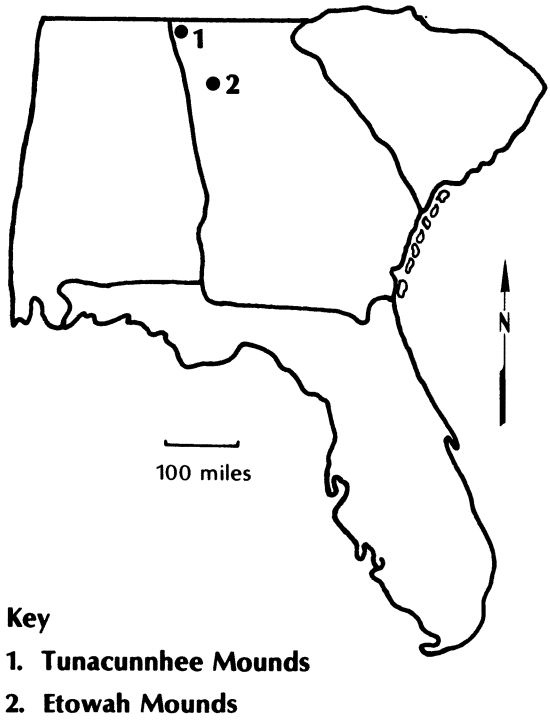

Figure 1. Map of region containing Tunacunnhee and Etowah sites.

the evidence. The Tunacunnhee site has one of the largest groups of Hopewell-type copper ornaments outside of Ohio (*1*), the nucleus of the tradition, and Etowah has long been considered a major Mississippian site with ties to Spiro Mound (and its textiles) in Oklahoma (*8–9*).

Tunacunnhee Site. The Tunacunnhee Mound and Habitation Site, located in Lookout Valley between Lookout and Sand Mountains in northwest Georgia, consists of numerous mounds of varying sizes and a habitation area adjacent to the mounds. Excavation of Mound C, the second largest of the aboriginal mounds, revealed a large submound burial pit, Feature 30 (F-30) with a number of items on its floor. Some of these items were a rectangular copper plate, two sets of bicymbal copper earspools[1], small beads, and a copper awl or pin (Figure 2) grouped together within what appeared to be a fabric bag or container. Fabriclike formations were observed on the plate and earspools (*1*) when the upper layer of the bag was removed for radiocarbon dating. Little remains of the lower layer. The copper plate, analyzed by Goad and Noakes (*10*), contained no other compounds that might have been

[1]The earspool was an ornament worn by aboriginal people. One type is the bicymbal earspool which consists of two discs in the shape of cymbals joined by a central shaft.

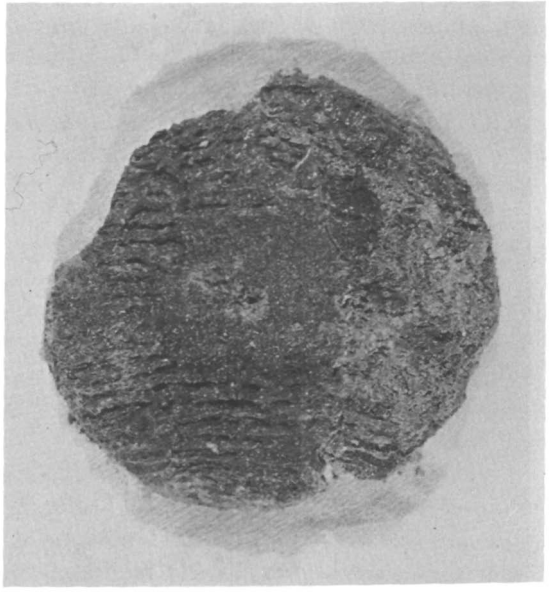

Figure 2. Earspool, F-30, Mound C, Tunacunnhee, 3.5 × 4.2 cm.

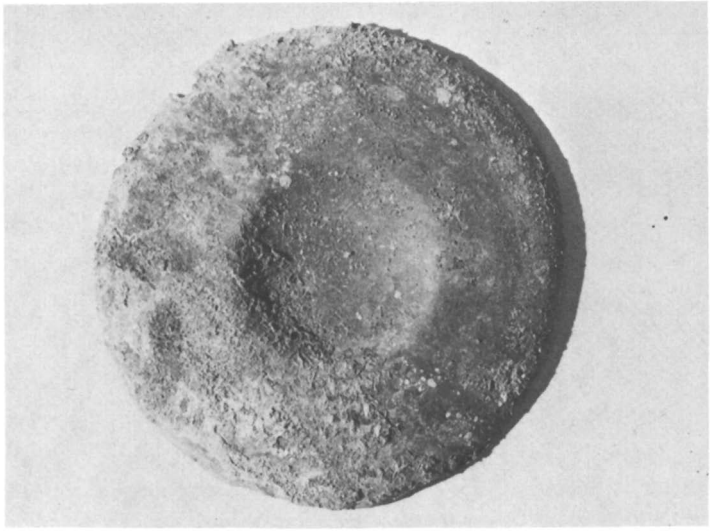

Figure 3. Earspool, F-33, Mound E, Tunacunnhee, 5.5 cm in diameter.

alloyed with copper. It did, however, contain some bromine (*1*). One set of earspools (east of plate) and the plate from F-30 were selected for study of fabric evidence.

The outer edge of another earspool (Figure 3), the second used in this investigation, comes from Mound E, whose boundaries overlap those of Mound C. Mound E is thought to be later in time because its earth fill is above that of Mound C (*1*). Near the center of Mound E is a submound burial pit, Feature 33 (F-33), with the remains of a male in an extended position (Burial 17). A number of high-status objects surrounded the male burial. The Mound E earspool, classified as Type B by Jefferies (*1*), differs in size and construction from the Mound C example.

Etowah Site. Also in northwest Georgia is the Etowah Mound Site, located near Cartersville, Georgia, on a flood plain of the Etowah River (*1*). The site consists of three large flat-topped or temple mounds, numerous small mounds, a few habitation sites, and a moat or ditch that runs into the river.

Interest in the Etowah site was heightened by the recovery in the 1920s of large numbers of objects from Mound C thought to be cult or religious art objects (*2*). Similar types of articles have been discovered at other Mississippian sites such as Moundville in Alabama and Spiro in Oklahoma. Although the whole religious complex of traits is designated as the Southeastern Ceremonial Cult or the Southern Cult, many feel that the Southern Cult may be traced to the Meso-American cultures.

Further exploration of Mound C in the 1950s revealed 75 burials and accompanying elite grave goods. As Kelly and Larson (2) noted, "no single mortuary structure in the Southern culture area has proved as rich in ritualistic paraphernalia as Mound C". The materials from which the objects were made are as varied as are the objects themselves. Shell, pottery, stone, wood, fabric, tortoise shell, and copper are represented in the elite burial goods from Mound C.

Direct Fabric Evidence

Three copper objects from the Tunacunnhee site with pseudomorphs after fabric adhering to their surfaces were selected for analysis. These were the copper plate, one set of earspools from Mound C (F-30), and a copper earspool from Mound E (F-33).

Additionally, three Etowah fabric fragments containing areas of partial mineralization were selected for the investigation. They were chosen to demonstrate the variation in structure among those fabrics recovered during the 1950s excavations. Currently, all three are thought to stem from a later phase of the mound's use. They are as follows: a bundle of fabric, Catalogue Number (Cat. No.) 840, Burial 57 (Figure 4); a clay-encrusted fabric, Cat. No. 1145, Burial 103 (Figure 5); and yarn adhering to a copper plate, Cat. No. 1156, Burial 110 (Figure 6).

Figure 4. Fabric Bundle, No. 840, Burial 57, Mound C, Etowah, 13.5 × 20 cm.

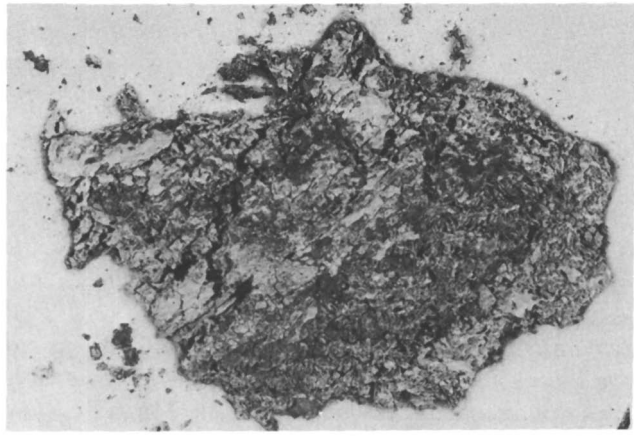

Figure 5. Fabric with feather-wrapped yarn, No. 1145, Burial 103, Mound C, Etowah, 10 × 15 cm.

Figure 6. Fragments of eagle dancer plate with yarn, No. 1145, Burial 110, Mound C, Etowah. The yarn group is approximately 3 cm long.

Experimental

To document their present condition, the six examples of direct fabric evidence from the two prehistoric sites were photographed with a Nikon F camera with a Nikkor microlens and Kodachrome type A and Panatomic X film. A Wild M400 photomacroscope with zoom settings yielding magnifications from 1× to 20.4×, a Wild MPS 55 electric control unit, fiber optics illumination, and Panatomic X and Kodachrome type A film were used in taking the photomicrographs.

Single small samples representative of each distinguishing feature from each object were cut and mounted for scanning electron microscopy. Each was carbon coated, and X-ray microanalysis [energy dispersive spectroscopy (EDS)]

was performed with an energy dispersive analysis of X-rays on International model 707B equipment. Elemental analyses reported are based on 3-G EDS determinations in areas of each representative sample. Subsequently, each sample was sputter coated with palladium to improve conductivity for photomicrography with a Cambridge S-4 stereoscan electron microscope.

Additional samples from some of the objects were studied by the Nomarksi differential interference contrast technique with a Zeiss photomicroscope II with oil immersion objectives.

Technical fabrication analyses were accomplished by study of the micrographs and examination of the objects using a Dolan-Jenner model 370 fiber optic inspection system with magnification to 9×. Fiber, yarn, and fabric data were compiled and studied. The result of these analyses are reported in this chapter.

Results

Fiber Identification. Identification of the fibers used in the fabrics from Tunacunnhee presents more difficulties than identification of those used from Etowah because most of the materials studied are pseudomorphs after fibers and no longer contain their original organic components. All that can be stated with confidence is that the Tunacunnhee materials exhibit pseudomorphs after bast fiber and after feathers. Table I is a summary of the fiber identification and elemental analyses performed. Because so little has been done to determine the process of pseudomorph development, elemental analyses are not known to indicate information concerning the previous organic state of the fibers, nor is it known how much the size of the fiber may have changed in replacement even though the shape was retained. The extent to which shape is preserved also is unknown. Therefore, species identification of

Table I. Fiber Identification and Elemental Analyses of Tunacunnhee Fabric Pseudomorphs

Object	*Fiber Identification*	*Elemental Analysis*[a]
Earspool, Mound C		
Disc	pseudomorph after bast (?)[b]	—
Shaft	pseudomorph after unknown fiber	—
Earspool, Mound E, disc	pseudomorph after bast (?)[b]	—
Breastplate, Mound C		Cu, Br[c]
Obverse	pseudomorph after unknown fiber	—
	pseudomorph after bast	*Cu*, S, Al, P, Si
Reverse	pseudomorph after bast	—
	pseudomorph after feather	*Cu*, Al, *P*, Si, *Ca*
Soil from site	—	*Al*, *Si*, *Fe*, Cu, K, Ti, Cu

[a] Elements that were present in significant quantities (large relative peak heights) are italicized; remaining elements were present in trace amounts (small relative peak heights).
[b] Questionable identification.
[c] Information was taken from Ref. 10.

bast fibers by physical structure such as dislocations or of feathers by nodes on barbules may be impossible. Until work is completed in defining how pseudomorphs form, identification of fibers from pseudomorphs, beyond gross generic classification, should be treated with some caution.

The outer surface of the earspools from Tunacunnhee Mounds C and E and the reverse side of the breastplate display pseudomorphs that have shapes characteristic of bast fibers (Figure 7). Typical of these fibers, the pseudomorphs occur in bundles of irregular size which are used as units in fabric production. The fibers are longer than staple and exhibit little of the twisting required for short fibers to produce a usable yarn. The fiber bundles of the bast group can be used with little processing in making fabrics.

On the observe side of the breastplate are fiber shapes that are smooth and separate and exhibit some crimp (Figure 8). Some evidence of longitudinal striations on the formations is present; inconsistency in size is found. They twist around each other while maintaining structural integrity. If the fiber shapes are bast, they have been subjected to some processing to separate them from their bundles. On the other hand, if the fibers occurred in the environment in somewhat the same structure as the pseudomorphs, that is, separate and individual, they would therefore be from a fiber class other than bast.

The central shaft of the Mound C earspool is wrapped with fiber pseudomorphs. The fiber shape has a flat, twisting, ribbonlike ap-

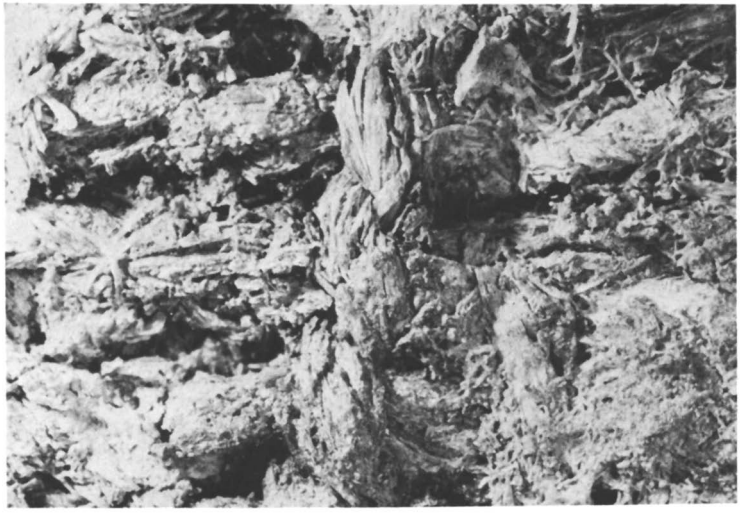

Figure 7. Pseudomorphs after bast from copper breastplate, F-30, Mound C, Tunacunnhee, 14×.

Figure 8. Pseudomorphs after undetermined fiber from copper breastplate, F-30, Mound C, Tunacunnhee, 6×.

pearance reminiscent of cotton. No final identification of these fiber pseudomorphs has been determined.

One section of the reverse side of the breastplate exhibits pseudomorphs after feathers (Figure 9). These pseudomorphs are striking in the fine detail of the barbules extending from the barbs. No identification of feather type has been made.

The Etowah fabric bundle (No. 840) contains fine yarns made of bundles of vegetable fibers typical of bast fibers. The core yarns of Etowah Mound C (EMC) No. 1145 also are bast, and they are wrapped with feathers. Figure 10 is an electron micrograph of the nodes on the barbules of these feathers. The copper plate EMC No. 1156 contains a twisted yarn of undetermined fiber composition; the fibers are smooth, untwisted, and long. Perhaps they are hair, but no scale structure was apparent on their surfaces. In the same area of the plate, some loose fibrous material adjacent to the yarn proved to be feather. In a second area of the plate, some fibrous material of undetermined type similar in appearance to that in the first area is present.

Further verification of the cellulosic versus proteinaceous character of the material may be derived from the elemental analyses, which are summarized in Table II. The feathers exhibit strong sulfur peaks as well as phosphorus, sodium, and calcium peaks. The bast fiber contains large amounts of phosphorus and calcium, typical of plant materials. Although the EDS of the bast fiber diplays sulfur, the relative peak height is small in comparison to other elements in this spectrum. The peak height of sulfur in the EDS of the feathers is so large relative to the

Figure 9. Pseudomorphs after feathers from copper breastplate, F-30, Mound C, Tunacunnhee, 12×.

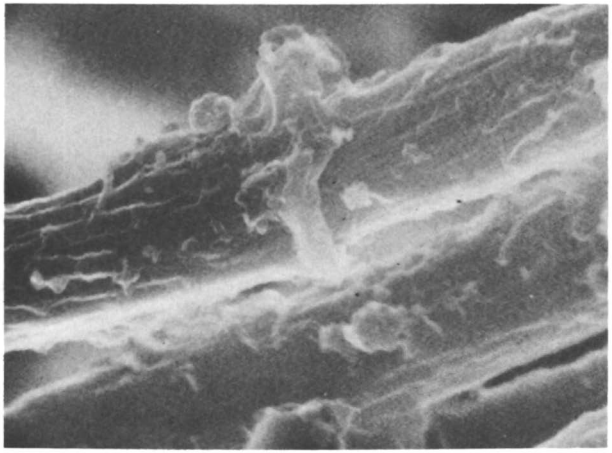

Figure 10. Feathers from yarn, No. 1145, Mound C, Etowah, scanning electron micrograph, 4725×.

peak height of other elements in this spectrum that perhaps the excess can be attributed to the cystine of the feather.

All of the materials contain copper and most contain iron, aluminum, and silicon. Their presence can be attributed to soil contamination or to impregnation of the fibers with products of copper corrosion. Further analyses currently are being conducted to identify the generic

Table II. Fiber Identification and Elemental Analyses of Etowah Mound Fabrics

Object	*Fiber Identification*	*Elemental Analysis*[a]
EMC No. 1156, copper breastplate	feather	*Na*, P, S, *Ca*, *Cu*
EMC No. 1145		
Core yarn	bast fiber	Al, Si, *P*, Cl, *Fe*, *Ca*, *Cu*
Wrapping yarn	feather	Na, Al, Si, P, Fe, S, *Cu*
EMC No. 840, twined fabric	bast fiber	*Al*, *Si*, P, S, K, Fe, Ti, *Ca*, *Cu*
Etowah copper celt[b]	—	*Cu*, *Fe*, *Si*, *Al*, *Mg*, Ni, Co, As, P
Soil sample (removed from EMC No. 1145)	—	*Al*, *Si*, *K*, Ca, Ti, Cr, Mg, *Fe*

[a] Elements that were present in significant quantities (large relative peak heights) are italicized; remaining elements were present in trace amounts (small relative peak heights).
[b] Information was taken from Ref. 11.

classification and species of the materials used in the fabrics from Etowah Mound C.

Yarn Evidence. Direct evidence of yarn usage from the Tunacunnhee site is in the form of pseudomorphs after fabric. The later Etowah site yields organic remains as well as pseudomorphic yarn shapes. With one exception, yarn pseudomorphs identified on the Tunacunnhee copper ornaments are derived from the bast fibers already noted. The fiber bundles typical of the stems of plants were used to produce slightly twisted (S-direction) yarns or yarns with no twist (*see* Table III). Evidence suggests that one system (System A, observe side of breastplate) is composed of short single fibers with crimp and is twisted together in a Z-direction (Figure 2). Underneath the feather pseudomorphs on the reverse side of the plate are fine yarns, some of which exhibit S-twist. No interworking of yarn and feather was discovered, although feather pseudomorphs were in association with yarn.

Yarns from the three Etowah examples exhibit greater variation from each other than do those of the Tunacunnhee. Although the basis for most of the yarns is a two-ply, S-twisted unit, the ways in which the units vary affect the resulting fabric structure (*see* Table IV). The simplest expression is found in the crumpled fabric bundle (No. 840, Burial 57) where two-ply, S-twisted yarns are used in both systems (Figure 11). Both sets of yarn exhibit a medium degree of twist (25–45°) and are derived from separate fibers twisted together. The System A yarn measures 0.175 mm, whereas the System B yarn is 0.135 mm. The yarns are uniformly brown.

A more complicated use of the two-ply unit is found in two clay-encrusted fabric fragments (No. 1145, Burial 103) from Etowah Mound

Table III. Yarn Evidence on Tunacunnhee Copper Ornaments

Object	*Yarn System*	*Yarn Unit*	*Direction of Twist*[a]	*Degree of Twist*
Earspool, Mound C				
Disc	A	fiber bundle	(\)	10
	B	fiber bundle	not discernible	—
Shaft	A	fiber bundle	(\)	10
Earspool Mound E				
Disc	A	fiber bundle	0	0
	B	two-ply	(/)	10–25
Breastplate, Mound C				
Obverse	A	twisted single fibers	(/)	10–25
	B	fiber bundles	(\)	10
Reverse	A	two-ply	(/)	10–25
	B	two-ply	(\)	10
	C	two-ply	(\)	10

NOTE: All fibers were probably bast fibers except for the shaft of the Mound C earspool and the obverse side (System A) of the Mound C breastplate, which were unknown fibers.
[a] (\) = S-twist; 0 = absence of attribute; and (/) = Z-twist.

Table IV. Yarn Evidence from Etowah

Object	*Yarn System*	*Fiber Twist*[a]	*Yarn Unit*[b]	*Direction of Twist*[a]	*Degree of Twist*
EMC No. 840	A	(\)	two-ply	(\)	25–45
	B	(\)	two-ply	(\)	25–45
EMC No. 1145	A	0	2–4 ply	(\)	10
		0	clustered	0	0
		0	1–2 unit	0	0
	B	0	1–2 unit	0	0
EMC No. 1156					
Area 1	A	0	2, two-ply	(/)	0
		0	re-plied	(\)	0
	B (?)	0	?	?	?
Area 2	0	0	plied (?), single (very fine)	(/)	?

NOTE: All fibers were probably bast fibers except for the clustered yarns of EMC No. 1145 and EMC No. 1156, System B, which were feather, and Area 2 of EMC No. 1156 which was an unknown fiber.
[a] (\) = S-twist; 0 = absence of attribute; (/) = Z-twist; and ? = not discernible under circumstances.
[b] Yarn number.

C. In each a core of yarns appears to be wrapped with featherlike structures, which are then bound to the core by a fine yarn with no twist (Figure 12). System A yarns measure 4.20 mm; the featherlike structures exhibit the characteristic shapes of downy barbules found on feathers, as indicated earlier. Scholtz (*12*) considers the complex yarns to be re-plied yarns because the core consists of plied yarns, and a wrapping yarn encircles the core unit. Modern textile specialists would classify yarns

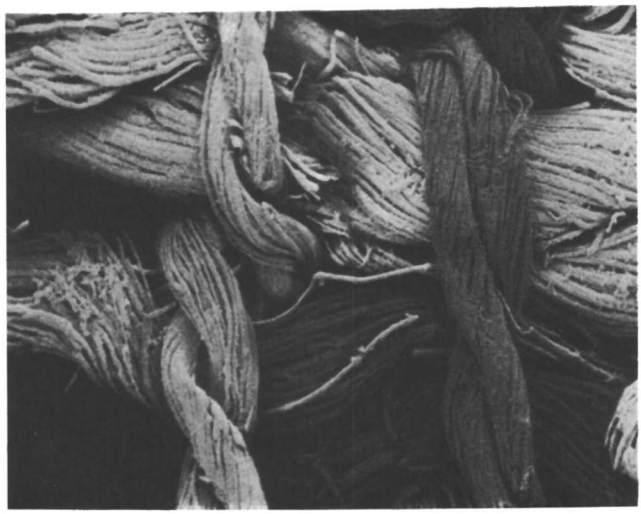

Figure 11. Alternate-pair twine, two-ply, S-twist yarns, No. 840, Burial 57, Etowah, scanning electron micrograph, 94×.

Figure 12. Re-plied yarn consisting of core with feather wrapped around it and held in place with binder, No. 1145, Mound C, Etowah, 6×.

such as these as complex if the core consisted of one yarn with effect and binder yarns spiraling around it (*13–14*). Yarns from a possible second system in the fabric consist of one to two units and have no twist. Much of the garment's structure is obscured by clay, and it is difficult to comment further.

The third fabric evidence from Etowah is attached to a copper plate, presumed to be an eagle dancer plate (No. 1156, Burial 110). Parts of it are pseudomorphic. In an area of the plate, one can observe dark fibers manipulated into yarns. The yarns are from only one system, and no obvious evidence of fabric structure is discernible. Nonetheless, the fibers are part of a re-plied or complex yarn type. Two singles are plied in a Z-direction to form a two-ply yarn. Then the yarn is twisted with another two-ply yarn in an S-direction; the result is a re-plied yarn (Figure 13). For the most part the yarns contain single smooth fibers. In certain areas the yarn has frayed and lost its re-plied configuration. Initial examination by scanning electron microscopy revealed downy barbules indicative of feathers on adjacent fibrous material.

A fragment of the eagle dancer plate exhibits pseudomorphs after yarn on its surface. In one area the remains of a fabric are apparent, but in another area numerous yarns are present in a random pattern. The area with the fabric remains has some finely plied yarns with Z-twist. Identifying the number of singles plied together was not possible. The other area contains fine single yarns with no twist.

Fabric Structural Evidence. For the most part the direct fabric evidence examined from the two sites consists of fibers and yarns within fabric structures rather than in matting or cordage. Two exceptions are the re-plied yarn occurring on the Etowah copper plate and the cords wrapped around the earspool shafts from F-30. Although the re-plied

Figure 13. Re-plied yarn: two-ply, Z-twisted yarns plied with another of the same in an S-twist direction, No. 1156, Mound C, Etowah, 1.5 mm diameter of single yarn, 12×.

yarn has no apparent fabric context, it may have been part of the fabric structure. The use of feather in an adjacent mat of fibers and its general treatment suggest that it did not exist separately as cordage. On the other hand, the pseudomorph wrapped around the earspool shaft must be considered as cordage. Its position and apparent functions would preclude any need for more complicated fabric structure.

Fabric structural evidence from both sites indicates twining as the typical means of producing fabric; however, the types of twining vary considerably. Twining occurs by the twisting and turning of one set of elements around another (*15*). In the interaction between the two systems, the active set encircles or encloses an inactive one (Figure 14). The interaction of twisting differs from the interlacing action found in weaving and the interaction found in cross-warp structures by the spiraling of the active set of elements.

Fabric evidence from the earlier site, as represented by pseudomorphs after fabric found on two copper earspools and a copper plate, is one of the simplest types of twining observed, namely, spaced twining. It can be seen on the upper surface of the earspool and on both surfaces of the plate from Mound C. Because no evidence indicated that yarn pseudomorphs had been dislodged, the original fabric structure is assumed to have consisted of spaced twining. The very nature of spaced twining requires action of the weft yarns rather than those of the warp;

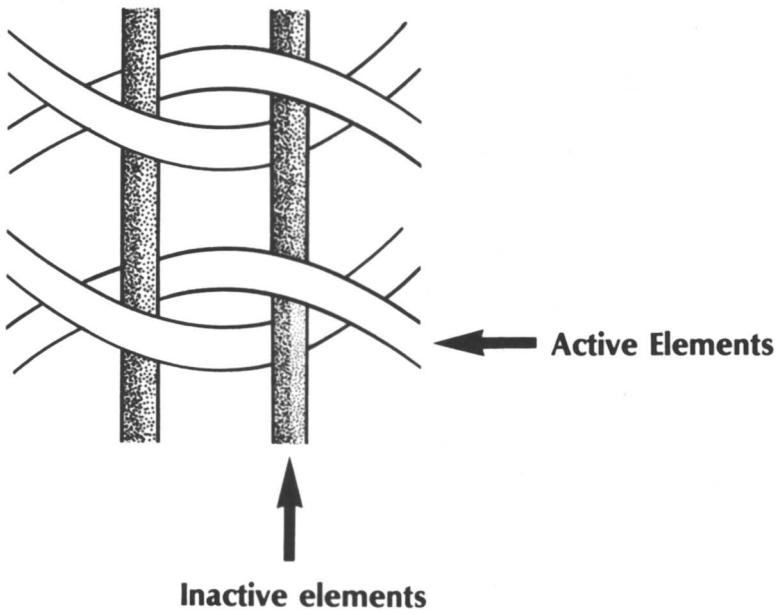

Figure 14. Schematic of twining.

hence, one may design the structure as spaced weft twining. The number of strands in each active set appears to be two, although corrosion products adhering to the surfaces of the pseudomorphs tend to obscure the exact shape.

The Mound C earspool also has pseudomorphs that may be related to an alternate-pair twine. If so, the earspool exhibits a variation that requires more foresight and planning than that associated with spaced weft twine. Alternate-pair twining involves an alternation of spans for the action pair (weft in this case) (*15*). Again, the corrosion obscures the evidence.

Particularly perplexing are the pseudomorphs after feathers found on the reverse side of the breastplate (F-30, Mound C). The cluster of feathers is in the central area of the plate on several of its fragments. It is adjacent to spaced weft twining, and a very finely twisted group of yarns is buried under the feather pseudomorphs. Careful examination to date reveals no interworking of yarn and feather.

Unlike the Mound C earspool, the fabric pseudomorphs on the Mound E earspool are less immediately identifiable. Although two systems of yarn can be observed, the particular order and type of interworking are not readily apparent. It may be a spaced weft twine because the distance between the yarns in both systems is slightly different. This particular earspool comes from the later mound. How much later is not known (*1*).

Of the three fabric examples from Etowah, the two with the more complicated yarn fabrication exhibit less in elaboration of fabric structures than does the one incorporating a simple two-ply, S-twist type of yarn. Both the re-plied, feather-core-binder yarn of No. 1145 and the eagle plate yarn of No. 1156 give little evidence of complex fabric structure. In the feather-core-binder yarn, the clay encrustation obscures fabric structural information. And in the eagle plate yarn, only the re-plied yarn and an adjacent fibrous mat remain.

The large re-plied yarns of No. 1145, moving in one direction and designated System A, can be identified, but the means by which they were interworked is hidden. Some yarns, possibly from a System B, appear at the outer edges of the clay just below the System A yarns, and another clay-encrusted area occurs approximately 5 cm above the System B area. Any interworking of the two systems is obscured. Furthermore, microscopic examination revealed no indication of interworking below the System A yarns. At some juncture, the System A yarns would have had to be interworked to achieve a cloak or headdress. An alternative is the use of the yarns as tassle-type entities that would swing freely from a belt or metal plate. This last possibility does not account for the second area of clay encrustation.

The re-plied yarns of the eagle dancer plate also pose a puzzle

concerning their former structure. They too may have been present as tassellike decorative features, and no System B yarns could be identified on the plate. However, a section that is little more than a mass of fibers near the yarns is present. The sample that was identified as feather was obtained from this area. An unusual feature of the re-plied yarns is the morphology of their component fibers, which was noted earlier.

Unlike the re-plied yarns for which fabric structure must be a conjecture, the yarns of the Mound C bundle (No. 840) are interworked in a fabric structure or structures. Although the bundle now is in pieces, it appears to have been a whole entity at the time of burial. Yarns, color, and character of structural variation support such an inference. The fabric structure of the bundle consists of at least four areas of pattern variation. It has an alternate-pair compact twining area exhibiting a pattern repetition that gives a sense of a rib rather than a twill (Figure 10). Adjacent to the alternate-pair compact twine is an area of cordlike sections anchored at either end by compact two-strand weft twine. No break in the yarns occurs as the pattern changes. Directly across the openwork from the compact alternate-pair twine is a band of the same two-strand weft. It is divided by a spaced twine section that incorporates transposed warp to achieve its effect (Figure 15). The outer edge of the band is finished. A fringe consisting of System A yarns hangs not from the finished edge but from the edge of the band next to the spaced area (Figure 16).

Other observations of interest to the understanding of this intricately designed fabric include the following: (1) The octagonal spaced open-

Figure 15. Openwork, No. 840, Burial 57, Etowah, 6×.

Figure 16. Fringe and band, No. 840, Burial 57, Etowah, 6×.

work is achieved by transposition of warp yarns, and some transposition of warp in the compact alternate-pair area occurs as well. (2) Both sides of the fabric are the same; this condition indicates the use of balanced units in the twining. (3) Two-ply, S-twist yarns appear in both systems. (4) Evidence suggests that the band section was added to the octagonal openwork area by the addition of yarns, each of which was incorporated into the compact weft twine of the band.

Conservation measures have not been taken for the fabric bundle, and it remains in a crumpled heap. All observations and comments are based upon the state of the fabric as it is now. Future work should lead to a better understanding of how these structurally varied areas fit together. The fabric was found underneath the skull of the human remains of Burial 57. Preliminary examination of similar fragments from the same burial at the Etowah Mounds Museum indicates the same fabric structural variation. These were, however, fragments found under the right and left arms as well as under the head.

Discussion

The discovery of pseudomorphs after spaced weft twining from the Tunacunnhee Burial Mounds site is not surprising. Twining as a structural process is widespread in America (*3, 8, 12, 16, 17*), and spaced weft twining is represented in a number of sites (*16, 17*). Furthermore, Jefferies (*1*) notes the presence of a bag in which the Mound C ornaments were coated. Initial photographs made of the objects in situ suggest that their spaced weft twining covered all the objects. Pseudo-

morphs after fabric then could well be the bag itself. One difficulty with this interpretation rests with the differences in yarn found on the breastplate and earspool. The System A formations on the obverse side of the breastplate do not exhibit the same fiber-bundle shape as those from the earspool (Table III); the fiber formations are distinct separate entities and exhibit some crimp and twisting together in a Z-direction. Scholtz (*12*) notes the presence of what she describes as "bast fibers which were separated into very fine fibers prior to being plied". The fibers she describes were identified as *Asclepias incarnata* or milkweed. The pseudomorphs after single, Z-twisted fibers on the breastplate may be from the milkweed originally.

That the reverse side of the breastplate exhibits diagonal patterning in the spaced weft twining is not unusual either. Twining as a technological process certainly offered a freedom of creative expression akin only to early tapestry-woven fabrics. Once a heddled loom is used, the spiraling encircling action of twining is no longer feasible. Thus, the presence of twining implies two considerations: the first is the lack of a heddled-loom technology, and the second is the lack of constraints found in the geometry of woven fabrics.

The Hopewell peoples did produce finely twined fabrics of various types (*12*, *18*). Church (*18*) indicates that the most common type found in three Ohio Hopewell mounds is a spaced alternate-pair weft twining. One instance of alternate-pair action was observed on the Tunacunnhee Mound C earspool, but the general corrosion of the earspool precluded clear identification.

Just as baffling is the presence of pseudomorphs after feathers in conjunction with spaced weft twined fabric and fine yarns; yet, no interworking of feathers into either fabric or yarn structures could be ascertained. The significance of the feathers is pertinent here. Their position only on the underside of the plate near its center may mean that the feathers were placed there for a special mortuary purpose and bear no relation to the fabric. On the other hand, the pseudomorphs after feathers could be part of one of the fabrics, surviving only because of their association with the copper. Fabric, feathers, and copper plate may be parts of ceremonial garb. The ornaments were not placed next to the skeleton, but rather they were beneath its remains and separated from it by soil fill. Church (*18*) also points out the presence of textiles or preserved textiles adhering to copper plates found on chest or loins of human remains in the Ohio Hopewell finds. She does not mention feathers as part of the plate-textile finds. Scholtz (*12*) has found feathers used in yarns recovered from the Ozark Bluff shelters, but the manipulation of the feathers appears to be closer to the Etowah fabric No. 1145 than to the feather pseudomorphs of Tunacunnhee.

By the Mississippian period at Etowah, fabric structures and their

accompanying technology apparently had become more elaborate than those of the earlier Middle Woodland Hopewell culture of Tunacunnhee, as revealed by examination of direct fabric evidence from the two sites. Both yarn and fabric structures from Etowah exhibit a complexity not present in the Tunacunnhee examples. Parallels with other Mississippian sites also support this observation (*8, 17*). Nevertheless, the elaboration is one of degree.

Although the discovery of fabrics from Etowah has been noted (*2, 19–24*), no attempt to identify the fibers has been reported. Because the Spiro Mound textiles are concurrent in history with those of Etowah Mound, the identification of fibers used at Spiro may be indicative of those used at Etowah. Whiford (*22*) lists three types of plant materials in the Spiro textiles. These are canebrake, paw paw, and milkweed. Of these, only the last one could be used to make fine cords and threads for intricate fabric construction; the first two are coarse materials used in matting and basketry. King and Gardner (*8*) report that most yarns used in Spiro fabrics were mixtures of many types of vegetable fiber and hair or feathers. The vegetable fiber provides stiffness and body; the hair or feathers are often wrapped on the surface to make the resulting fabric feel softer. The types of hair used included rabbit, squirrel or rat, buffalo, dog, horse or bear, fox, and muskrat. In laboratory reports separate from King and Gardner, Goodway indicated the use of spun feather and down while Laybourne identified the feathers as belonging to the *galliformes,* most likely turkey (*8*). Goodway further stated in her report that the identification of vegetable fibers used in the Spiro textiles is difficult because degradation has eliminated morphological structures such as nodes which are used to distinguish among them. Therefore, the vegetable fibers used were probably bast or leaf fibers because they occurred in bundles characteristic of these groups.

The Etowah people, like the Spiro people, incorporated feathers into yarns with structural permutations beyond what might have been used by the earlier Tunacunnhee–Hopewell people. Unlike the Spiro people, the Etowah people may not have spun down as described by King and Gardner (*8*), but rather they may have used the perhaps older tradition of core-feather-binder yarn to achieve their purposes. The feathers found in the yarns of No. 1145 show no twist or twist direction.

On the other hand, the loose feathers identified from Etowah No. 1156 could have been spun at one time, but they come from a mat of fiberlike material on which no yarn structures currently are evident. Their juxtaposition with the re-plied yarn (perhaps of animal hair) presents an anomaly because descriptions (*8, 12*) of other feather yarns do not include a re-plied yarn without a bast core. The yarn appears to be alike in all its parts. Its color, texture, and surface smoothness suggest an animal-hair fiber.

The twined Etowah fabric demonstrates an intricacy not seen in the earlier Hopewell fabrics. It appears to be related to other Mississippian fabrics identified as spaced octagonal openwork (*12*, *16*). Rachlin (*16*) notes that these gauzelike fabrics are not true gauze but rather are twined fabrics with transposed warp. They have their basis in the Woodlands period. In the case of the Etowah twined fabric, the spaced octagonal openwork is combined with compact alternate-pair twining (seen in Hopewell fabrics) and other variations designed to produce structural pattern design. Rachlin (*16*) points out that the octagonal openwork obtained by transposition of warp is a product of the Mississippian period in southeastern North America. She suggests that it may be a result of stimuli from Meso-American and South American gauze (*16*). King and Gardner (*8*) found numerous twined fabrics among the Spiro Mound group, but none appear to be of the complexity of the Etowah example. Future work will investigate the relationship between Etowah and Spiro fabrics.

Byers (*19*) reports analyses of Etowah fabrics that adhered to copper objects from Mound C. One was described initially by Willoughby (*23*) in 1932, and one was described by Moorehead (*24*) in the same year. Schematic illustrations of both fabrics bear a resemblance to fabric bundle No. 840, but differences also are seen. In the first of these fabrics, Byers indicates a spaced fabric with a System A (warp) as a single, two-ply, S-twist yarn and a System B (weft) as two, two-ply, S-twist yarns twining around the System A yarns. He notes that no selvage was present and that in certain areas Z-twist warp was used and provided a ribbed effect. Since his examination, the plate to which the fabric was attached has been cleaned.

The second example appears to be the same octagonal openwork as seen on the fabric bundle. It certainly resembles more closely the section of the Etowah bundle than other schematic illustrations (*9*, *12*, *16*). The intricately structured fabric bundle remains an example of high achievement in fabrics of the prehistoric peoples of southeastern North America.

Conclusions

Chemical and physical analyses of the six examples of direct fabric evidence raise more questions than are answered. Further work is required in determining the identity of the fibers, a task made more difficult by their degraded condition. Also, the presence of any dye and/or mordant in the fibers should be established. How pseudomorphs after fibers form must be defined to establish the extent of shape maintenance in replacement, the influence of chemical differences in fiber or in soil on the replacement minerals, the relationship between

pseudomorph size and original fiber size, and the relationship between the elemental composition of the pseudomorph and that of the original fiber.

Further analysis of the fabrication techniques employed in the production of these examples also is necessary. The Etowah bundle, for example, should be unfolded, while using correct conservation methods, and its structure should be subjected to detailed scrutiny. Only then can its relation to the fragments from the same burial on display in the Etowah Mound Museum and other Mississippian fabrics be known. When more data about the phenomenon of fabric pseudomorphism are obtained, then questions associated with the Tunacunnhee objects can be answered. Certainly the relationship between alternate-pair twined fabric found in both sites in Georgia deserves further study.

It is evident from the work completed, however, that direct fabric evidence, whether fabric or pseudomorph after fabric, contains much data about prehistoric fabrics of southeastern North America. The information gleaned from their study can be used to reconstruct the cultural implications of fabric manufacture and use among the prehistoric peoples of the region.

Acknowledgments

We wish to express our gratitude to James Whitney, Department of Geology, University of Georgia and the Wenner-Gren Foundation for Anthropological Research, for partial support of this work. We would like to acknowledge the assistance of William Rigsby, Center for Applied Ultrastructural Research, University of Georgia; and Chester dePratter, University of South Carolina. We are indebted to David Hally, Laboratory of Archaeology, University of Georgia; and to Lewis Larson, State Archaeologist, Georgia Department of Natural Resources, for permission to study the objects.

Literature Cited

1. Jefferies, R. W. "The Tunacunnhee Site: Evidence of Hopewell Interaction in Northwest Georgia"; Anthropological Papers of the University of Georgia No. 1; University of Georgia: Athens, Georgia, 1976; p. 1-3, 9-11, 14-15.
2. Kelly, A. R.; Larson, L. H. *Archaeology* **1957**, *10*, 39-48.
3. Holmes, W. H. "Annual Report"; Bureau of Ethnology: Washington, D. C., 1893; Vol. XIII, pp. 9-46.
4. O'Reilly, D. In "Excavations at Kolomoki: Season III and IV"; Sears, W. H., Ed.; University of Georgia Series in Anthropology No. 4; University of Georgia Press: Athens, Georgia, 1953; pp. 85-94.
5. Jakes, K. A.; Sibley, L. R. In "Archaeological Chemistry—III"; Lambert, J. B., Ed.; ADVANCES IN CHEMISTRY No. 205; American Chemical Society: Washington, D. C.; 1984; pp. 403-24.

6. Sibley, L. R.; Jakes, K. A., *Clothing and Textiles Research Journal* **1982** *1*, 24-30.
7. Hally, J. In "Early Georgia"; Society for Georgia Archaeology: Athens, Georgia, 1976; pp. 37-52.
8. King. M. E.; Gardner, J. S. In "The Research Potential of Anthropological Museum Collections"; Cantwell, A. E.; Griffin, J. B.; Rothschild, N. A., Eds.; Annals of the New York Academy of Sciences: New York, 1981; Vol. 376, pp. 123-39.
9. Willoughby, C. C. *The Missouri Archaeologist* **1952**, *14*, 107-24, 264-76.
10. Goad, S. I.; Noakes, J. In "Archaeological Chemistry—II"; Carter, G. F., Ed.: ADVANCES IN CHEMISTRY No. 171; American Chemical Society: Washington, D. C., 1978; pp. 335-46.
11. Hurst, V. J.; Larson, L. R. *Am. Antiq.* **1958-59**, 24; 177-81.
12. Scholtz, S. C. "Prehistoric Plies: A Structural and Comparative Analysis of Cordage, Netting, Basketry, and Fabric from Ozark Bluff Shelters"; Arkansas Archaeological Survey Publications in Archaeology, Research Series No. 9; University of Arkansas Museum: Fayetteville, Arkansas, 1975; pp. 20-22, 123, 133-34.
13. Joseph, M. L. "Essentials of Textiles"; Holt, Rinehart and Winston: New York, 1976; p. 147.
14. Hollen, N.; Saddler, J.; Langford A. L. "Textiles", 5th ed.; Macmillan: New York, 1979; p. 140.
15. Emery, I. "The Primary Structures of Fabrics: An Illustrated Classification"; The Textile Museum: Washington, D. C., 1966; pp. 180, 196-205.
16. Rachlin, C. K. *Indiana Hist. Bull.* **1958**, *35*, 67-79.
17. Kent, K. "Transactions"; American Philosophical Society; New Series: Philadelphia, Penn., 1957; Vol. 47; pp. 501-8.
18. Church, F. *Midcontinent Journal of Archaeology*. 1984, *9*, 1-25.
19. Byers, D. *Actas Mem., XXXV Congr. Int. Am.* **1964**, 1, 591-98.
20. Byers, D. *Am. Antiq.* **1962**, *28*, 206-16.
21. Larson, L. H. *J. Am. Antiq.* **1959**, *25*, 109-12.
22. Whitford, A. C. In "Anthropological Papers"; The American Museum of Natural History: New York, 1941; Vol. 38; pp. 7-22.
23. Willoughby, C. C. In "Etowah Papers"; Moorehead, W. K., Ed.; Yale University: New Haven, 1932; pp. 7-66.
24. Moorehead, W. K. "Etowah Papers"; Yale University: New Haven, 1932.

RECEIVED for review November 26, 1984. ACCEPTED March 15, 1985.

15

Replacement of Protein and Cellulosic Fibers by Copper Minerals and the Formation of Textile Pseudomorphs

Kathryn A. Jakes[1] and J. Hatten Howard III[2]

[1]Center for Archaeological Sciences, University of Georgia, Athens, GA 30602
[2]Department of Geology, University of Georgia, Athens, GA 30602

Pseudomorphs of copper minerals, within the corrosion encrustation of bronze and copper artifacts, faithfully duplicate fibers, yarns, and fabric construction of adjoining textiles. They are produced under conditions of chemical weathering at archaeological burial sites through the interaction of degrading fiber, corroding copper, and the resulting corrosion solution; Cu^{2+} enters the fiber, is bound by exchange and complexation along the polymer chains, and reacts with H_2O and available HCO_3^- to precipitate malachite, tenorite, and/or cuprite within, and subsequently replaces the fibers. This mechanism of fabric pseudomorph formation is based upon measurements of pH and redox potential during experimental fabric degradation and corrosion of Cu (simulating the zone of weathering) and upon Fourier transform infrared spectroscopy, ultraviolet-visible spectroscopy, scanning electron microscopy, and X-ray diffraction analyses of the fabric, precipitates, and incipient mineralization.

TEXTILE FABRICS FOUND in archaeological contexts can reveal a vast amount of information contributing to the understanding of the culture and technology of the ancient people who produced and used them. Yet, despite the significant evidence of technological advancement that textile fabrics can yield, their study is limited because few textiles survive the degrading forces of the burial environment. Fabric information from prehistoric cultures can be expanded greatly and extended farther back in time by the study of textile fabric pseudomorphs found as part of the corrosion encrustation of metal artifacts. These pseudomorph formations appear to retain the shape of the fibers, yarns, and fabrics, as well as those of feathers and leather, as the organic components are replaced, in a suitable burial environment, with mineral

0065-2393/86/0212-0277$06.00/0

compounds derived from associated metal artifacts. Pseudomorphic evidence is particularly useful when no organic textile materials are known from the same particular geographic areas and periods of history in which the pseudomorphs are discovered. The purposes of this chapter are to establish the need for the study of the process of pseudomorph development and to propose a mechanism for formation of pseudomorphs after protein and cellulosic fibers in association with copper.

As a form of direct fabric evidence, the physical shapes of textile fabric pseudomorphs have been studied to identify fiber type and yarn and fabric construction. Pseudomorphs of paired filaments in mineralized fabric formations found on Shang-period bronze weapons were determined to be replaced silk (*1*, *2*); S-and Z-twisted silk staple yarn pseudomorphs were identified as well as fabric constructions, including float yarns and a ribbed weave.

The identification of fiber preserved as pseudomorphs on prehistoric Amerindian copper objects proved more difficult. Yarn pseudomorphs composed of mineralized fiber bundles typical of some sort of bast fiber were observed, but identification beyond this gross generic classification was not possible (*3*). The details of construction of twined fabric pseudomorphs also are not well known because the pseudomorphs cannot be turned over for study of the reverse side. Similarly, the particular feather type of feather pseudomorphs cannot, as yet, be classified.

In addition to the analysis of physical structural characteristics of textile fabric pseudomorphs, chemical information has been obtained. On bronze and copper artifacts, the pseudomorphs are composed of malachite, tenorite, and cuprite (*1*, *2*), the formation of which probably requires moist conditions, a corrosive metal, and optimum fiber-metal contact (*1*). Trace elements in their structure vary from object to object and site to site (*1–3*), but the relationship of these elements and the fiber, metal, and soil composition is not yet known.

The Importance of Understanding Pseudomorph Development

In order that interpretations of prehistoric fabric use and manufacture are soundly based, it is necessary to demonstrate that minerals formed during postburial alteration of a fabric-metal association do, indeed, replace fabric components and duplicate faithfully the shapes of the fibers, yarns, and fabrics. The degree of detail to which this duplication occurs must be determined to establish limits to information that can be expected from fabric-pseudomorph study. For example, nodes on barbules of feathers, necessary for feather classification, have not been observed yet, but the mechanism of pseudomorph formation may be found capable of replicating such fine structures and thus prove useful in some archaeological studies. In addition, the relationship between pseu-

domorph size and the size of the original object (fiber, yarn, etc.) may bear on understanding either pseudomorph growth or the nature of the replaced precursor. Pseudomorphs after silk fibers on bronze implements are larger than fibers of silk, yet statistical analysis of pseudomorph size on two Shang-period bronze weapons did not indicate any relationship between replacement mineral, pseudomorph size, and original fiber size (*4*). More complete understanding of the character and development of pseudomorphs may allow future separation of the mineralized formations from the surrounding corrosion without destroying them so that the entire replaced object can be studied.

The study of pseudomorphs and how they form will reveal more than physical structural information. As greater understanding of the process of pseudomorph development and the interaction of geologic environment, fabric, and metal are attained, inferences concerning the influence of different fiber compositions and the effects of dyes and mordants in fabrics can be made. The influence of elements in the soil or the metal on the replacement process will also be learned. Once the process of pseudomorph formation is understood, this information can be directed toward predicting archaeological sites conducive to pseudomorph development, on the basis of preliminary assessment of site environmental conditions, and thus can promote the finding of archaeologically important evidence. An understanding of pseudomorph chemistry is necessary for making appropriate preservation and conservation decisions to protect both the pseudomorphs and the metal artifacts with which they are associated.

Degradation of Fabric and Corrosion of Metal Artifacts

The mechanism of fabric pseudomorph formation described herein is based on the influence of fiber internal structure; on experimental simulation of the geochemical conditions that should develop in the zone of weathering at archaeological sites; on resulting interaction of degrading fabric (silk and linen), solution, and corroding copper (representing bronze); and on incipient mineralization of fabric. Experimental hydrolysis and oxidation of silk with and without copper has been described previously (*4*, *5*); a similar experimental design was used in the study of linen (Testfabrics style L-53). Briefly, fabric or fabric plus copper is immersed in heated water through which air is bubbled. The oxidation-reduction potential (Eh) and pH of the solution are measured as the fabric degrades and the copper corrodes. Data are plotted on an Eh-pH diagram for the stability of copper species. Changes in composition of the fibers are monitored by IR spectroscopy, and changes in physical structure and mineralization are monitored by optical microscopy and scanning electron microscopy.

Internal Structure of Silk and Linen. Triangular-shaped silk filaments (called brins and composed of the protein fibroin) are embedded in a second protein (sericin) to form the bave unit. Microscopic examination of fabrics woven with the silk bave unit and subsequently cleaned of sericin reveals paired brin filaments. Fibroin contains 16 amino acids, and more than 80% of the polymer is composed of glycine, alanine, and serine only (*6*). Their small side groups allow chains of these amino acids to pack together closely to form the crystalline portions of the fiber. The bulkier amino acids, such as tyrosine, disrupt crystal order and produce the amorphous areas of the internal structure of the fiber.

Linen fibers processed from the bast plant stems contain 90% pure cellulose; the remainder is a mixture of lignins and hemicellulose (*7*). The regularity of the cellobiose unit and its rigidity in the chair form contribute to the regular packing of the cellulose chains and to the opportunity for hydrogen bonding through the hydroxyl units. Consequently, linen is highly crystalline in structure. Because the lumen is small and the fiber arrangement is very stiff and regular, the fiber does not collapse upon drying as cotton does. When moisture is absorbed, therefore, the fiber initially will not change its outer physical shape, as cotton will do.

The supramolecular structure of both fibers (Figure 1) is fringed fibrillar, and polymer chains pass repeatedly through crystalline, oriented, and amorphous regions. The crystal units are longer than they are wide, regularly distributed throughout the whole fiber, and show preferred orientation parallel to the long fiber axis. Silk is paracrystalline; linen is almost perfectly crystalline in its molecular arrangement (*6*).

As the fibers absorb water, the chains in the amorphous areas are pushed apart; the crystallites act as tie points to hold the chains together

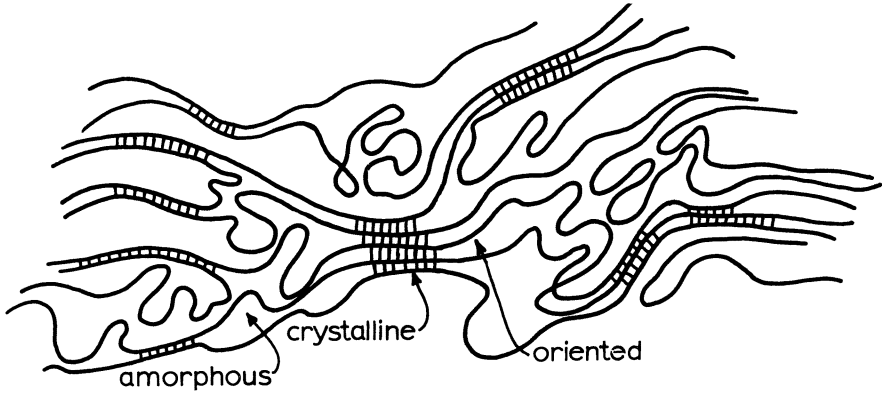

Figure 1. Fringed fibrillar internal structure of protein or cellulose.

(Figure 2). Silk fibers swell 19% in cross-sectional area, whereas linen swells 47% (*6*). Fiber swelling is limited by the interchain forces holding the polymers together in the crystalline areas; only when these forces are broken in degradation processes can the fiber swell more. Water is attracted by the peptide bonds of silk and by the cellulosic hydroxyls of linen. The first monolayer of water adsorbed by each polymer molecule is directly adsorbed and thus is tightly held in association with the polymer chain. Subsequent layers of water molecules are indirectly attached and thus are loosely held in association with other water molecules.

Effect of Fiber Degradation on the Corrosion Solution. Hydrolysis and oxidation of protein and cellulose have been described in the literature primarily with the focus on degradation in industrial processing conditions. In alkaline conditions, amino acids are released from silk in a chain unzipping mechanism; in acidic conditions, the scissions are random (*8, 9*). As the polymer deteriorates, free carboxyl and amine end groups are formed. Tyrosine oxidizes to a quinone; this reaction gives aged silk its yellow coloration. Amorphous areas of the fiber are attacked first.

Linen cellulose hydrolyzes at the acetal link. In acidic or neutral conditions, reducing oxycellulose is formed; in alkaline conditions, a nonreducing oxycellulose is formed. The new end groups produced, then, are aldehydic in the first case and carboxylic in the second case. Hydrolysis and oxidation are nonuniform; amorphous areas are attacked first (*10*).

For the purpose of this chapter, which is to interpret the interactions

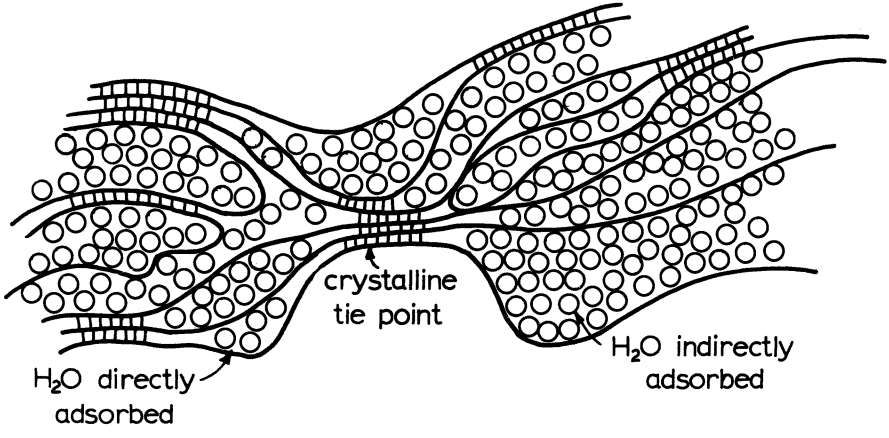

Figure 2. Fringed fibrillar internal structure of protein or cellulosic fiber swollen with water.

of degrading fabric and corroding metal in the geochemical framework of mineral (pseudomorph and metal artifact) associations in a groundwater environment, the experimental and analytical results are conveniently presented on an Eh-pH diagram, a graph that plots environmental redox potential, Eh, against pH. The Eh-pH diagrams quantitatively summarize the relative stability of pertinent geochemical species and can be used to interpret the conditions of redox potential and pH under which specific minerals form and to predict reactions and associations among minerals under changing conditions.

In the complex solutions of the natural geologic environment, the general oxidizing or reducing characteristics (redox potential, Eh) and the pH (Figure 3) are the result of combined effects of a number of redox, hydrolysis, and dissociation reactions among various geologic materials (e.g., ferrous and ferric minerals, sulfides, silicates, carbonates, organic material), atmospheric components (CO_2, O_2, H_2S), and water. Changes in Eh and pH of a particular geologic environment are brought about by varying influxes of meteoric waters and dissolved gases; by reaction of rock, sediment, and soil components; and by biologic activities. Degradation of the fibers by aerated waters and dissolution of these degradation products in the corrosion solution surrounding a metal artifact and impregnating the fibers produce a marked change in the geochemical environment by lowering the pH and raising the oxidation potential (*5*). These new conditions are imposed on the metal artifact and cause its corrosion and attendant formation of new mineral species as pseudomorphs and encrustation.

Copper Mineralogy and Geochemistry. The relations of the pseudomorph and encrustating copper minerals malachite, cuprite, tenorite, and azurite and of the metallic copper are displayed by Eh-pH diagrams constructed for the system Cu-H_2O-CO_2 (*5*), which is based on both the chemistry and mineralogy of the corroded bronze and copper artifacts and that of the experimental hydrolysis-oxidation solutions. The mineral species are plotted as stability fields of Eh and pH outlined by boundaries that represent Eh-pH equations for reactions between the species; these reaction equations were calculated from published thermodynamic properties of the pertinent minerals (*11, 12*). Further detail of the construction of this diagram and geochemical rationale for species represented are given in Reference 5.

The geochemical behavior of copper during chemical weathering and its experimental simulation can be interpreted from the Eh-pH diagram (Figure 4). Comparison of Figure 4 with Figure 3 shows that elemental copper should persist only in reducing geologic environments. Most near-surface geologic environments, however, are affected by aerated (oxygenated) surface waters or infiltrating meteoric water.

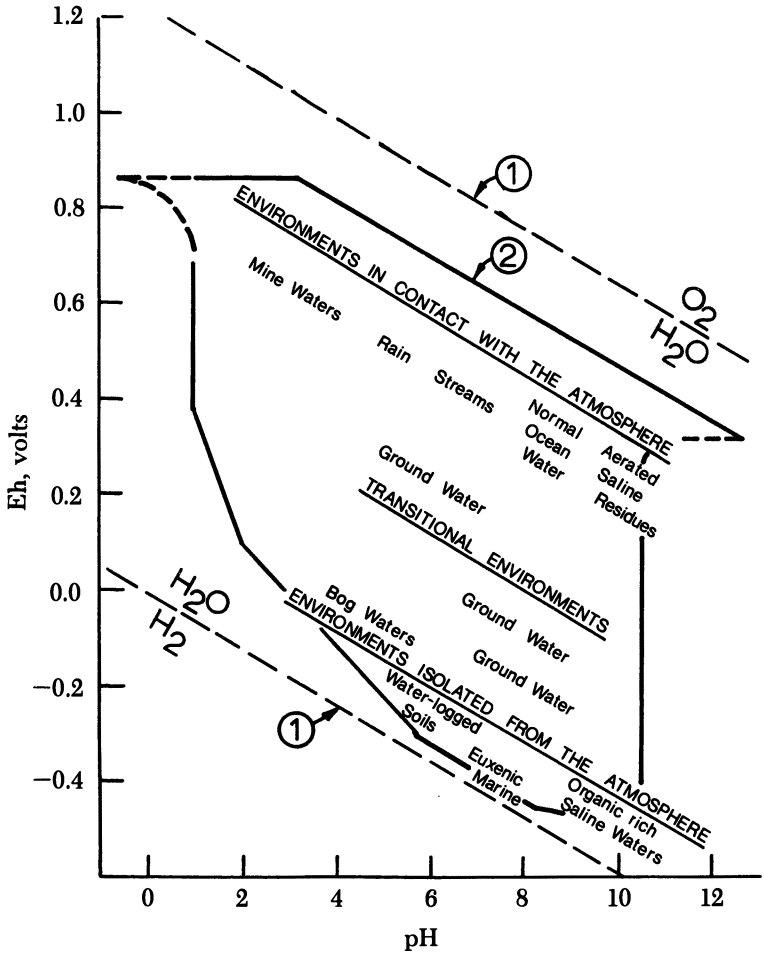

Figure 3. Eh and pH in natural environments: (1) stability limits of water; (2) outline of Eh-pH measurements of natural environments (13). *Typical geologic environments are identified* (14).

Geologic materials formed within or altered (weathered) by these oxygen-bearing waters are oxidized; the interaction of soluble oxidized materials and the near absence of reduced species produce high environmental Eh. Continued downward percolation of oxygenated water will gradually oxidize buried reduced materials—organic or metal artifacts as well as mineral deposits—as dissolved oxygen (as H_2O_2) is replenished by ground-water influx. In general, oxidation of metallic mineral deposits will exert either of two courses of Eh-pH change (*15*): (1) Oxidation of ferrous minerals (especially pyrite, FeS_2) will raise the

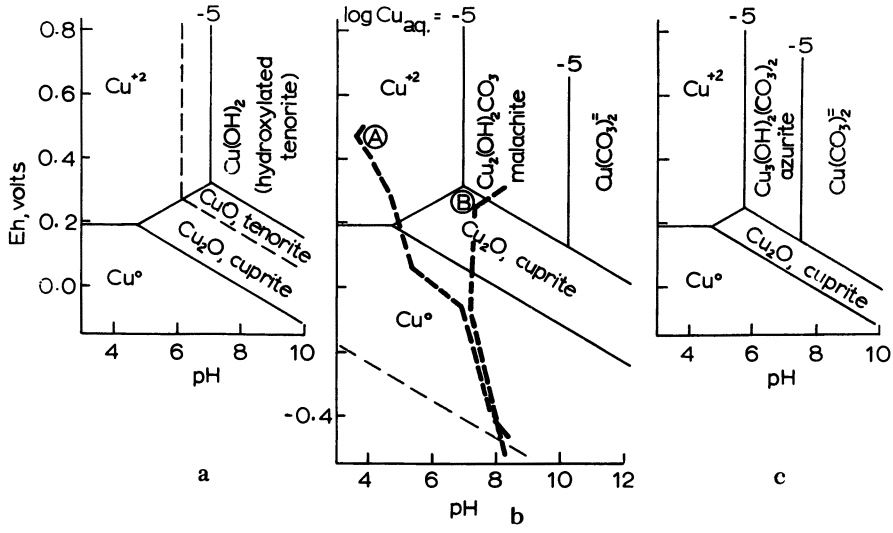

Figure 4. Eh-pH diagrams of the system Cu-H_2O-CO_2; $Cu^{2+} = 10^{-5}$ M. (a) $P_{CO_2} = 0$ atm; (b) $P_{CO_2} = 10^{-3.5}$ atm (equivalent to that of air); (c) P_{CO_2} = 1 atm. Traces A and B illustrate experimental aeration of a geochemical environment strongly influenced by oxidation of ferrous iron in the absence (A) and in the presence (B) of excess $CaCO_3$ (as limestone buffer) (15).

redox potential and lower the pH by hydrolysis of ferric iron (Figure 4b, Trace A). (2) If ferrous minerals are not present or if $CaCO_3$ (limestone, marble) is present in abundance as buffer against acid production, Eh will rise and little change in pH will occur (Figure 4b, Trace B).

Oxidation of the copper of bronze artifacts should raise the redox potential as cuprite, Cu_2O, is produced. If cuprite should undergo oxidation at a faster rate than elemental copper, simultaneous oxidation will raise the Eh through the cuprite stability field to produce either hydroxylated tenorite [$Cu(OH)_2$] or malachite [$Cu_2(OH)_2CO_3$] to form malachite at the expense of tenorite (compare Figures 4a and 4b). The stability of the malachite field with respect to the occurrence of $Cu(OH)_2$ is tenuous: If P_{CO_2} should become less than $10^{-4.02}$ atm, or HCO_3^- content should drop below $10^{-4.82}$ M, $Cu(OH)_2$ will form at the expense of malachite. Greater concentrations of HCO_3^-, from high P_{CO_2} of soils or from dissolution of carbonate minerals, are required in order for the mineral azurite to form (Figure 4c). Azurite, therefore, should not commonly be produced by the interaction of aerated ground waters and copper (bronze) artifacts.

Effect of Metal Corrosion on Fiber Degradation. The effect of the corrosion solution of copper on the progress of protein and cellulosic

degradation is not entirely clear. Copper is known to inhibit microbiological degradation, yet copper also acts as a catalyst of oxidative degradation. Both cellulose and protein bind copper ions: copper ion is exchanged for the proton of carboxyl groups in cellulose, under appropriate conditions. Copper binding by cellulose is also promoted by complexation with the hydroxyl groups (*10*). Copper ion binds with the NH_2 end groups of amino acids in silk, under the appropriate pH conditions, and subsequently will complex with free carboxyl end groups because the anionic carboxyl will be attracted to the cationic metal. Copper-ion binding by silk is also favored by complexation with amide linkages throughout the protein molecule (*16*). During experimental degradation of silk in the presence of copper, copper-ion adsorption was immediate and obvious (*5*); shortly after the introduction of silk to the corrosion solution, the silk turned green. The fibers, however, retained their shape in contrast to those treated under similar conditions without copper, which fibrillated along their length. Further experiments are being conducted to determine if an analogous result occurs in linen fibers.

Mechanism of Copper Pseudomorph Development after Protein and Cellulosic Fibers

Because protein and cellulosic fibers are buried in contact with copper metal objects, a chemical microsystem is established whereby the degradation of the fiber and the corrosion of the metal interact physically and chemically. As the corrosion solution impregnates and swells the fibers, polymer molecules in amorphous areas are spread apart but are prevented from complete dissolution by the resistant crystalline segments. Copper ion from the corrosion solution is bound to the polymers (Figure 5). As the fiber degrades and more end groups are formed, more copper is bound. Polymers expand further apart as interchain forces are reduced.

Fiber degradation, dissolution of degradation products, and oxidation of metallic copper alter the Eh and pH of the corrosion solution so that bound (and also free) copper ions will react with H_2O and available HCO_3^- to form one or more copper minerals. These minerals will precipitate in situ within the template of the fiber internal structure. In this manner, the shape of the fiber will be retained, although the size of the pseudomorph can become larger than that of the original fiber.

With this model of pseudomorph formation as a theoretical basis, it can be seen that the presence of large dye molecules, which can act as antioxidants or as blocks to fluid transfer, or the presence of metallic mordants, which can compete with copper ion, could be influential. Similarly, the impregnation of the fiber with other chemical species

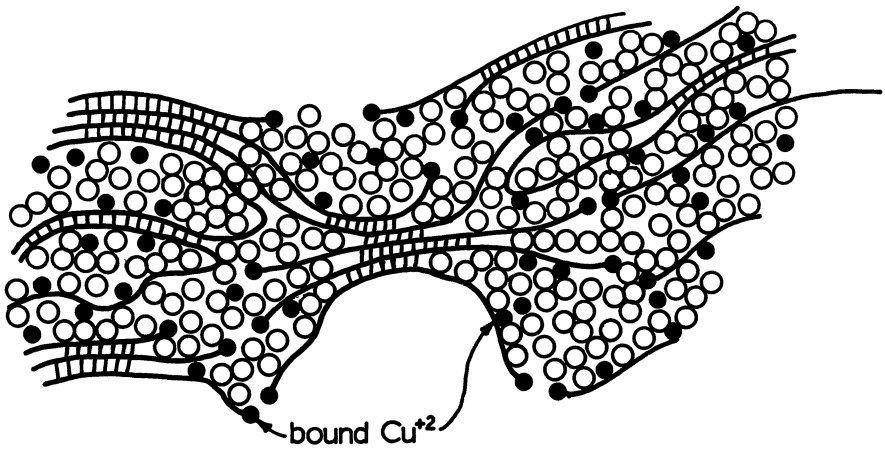

Figure 5. Fringed fibrillar internal structure of protein and cellulosic fiber impregnated by corrosion solution. Copper is bound to end groups and along the polymer chains and occurs also as free Cu^{2+} within the fiber.

from the ground water, the soil, and the corroding metal may have an effect on the resulting pseudomorph composition. These points are being studied in the current experimental series.

Conclusions

Textile fabric pseudomorphs can provide a wealth of information contributing to an understanding of ancient technologies and cultures. Delineation of the process of pseudomorph formation can expand this information by verifying the extent to which shape and object detail are maintained in replacement; by determining the relation between pseudomorph size and original fiber size; and by assessing the influence of other chemical species in the microenvironment, whether their source is fiber, metal, or soil. Knowledge of how pseudomorphs form will aid the anthropologist in reconstructing ancient use of fibers, yarns, and fabrics; the archaeologist in predicting the possibility of pseudomorphs on metal objects uncovered at a site; the conservator in handling the metal artifact with pseudomorphic evidence; and the geologist in understanding processes of fossilization by replacement.

Literature Cited

1. Jakes, K. A.; Sibley, L. R. In "Archaeological Chemistry III"; Lambert, J. B., Ed.; ADVANCES IN CHEMISTRY SERIES No. 205; American Chemical Society: Washington D.C., 1984; pp. 403–24.
2. Jakes, K. A.; Sibley, L. R. *Proc. Appl. Sci. in Examination of Works of Art.*, Museum of Fine Arts: Boston, Mass., 1983; in press.

3. Chapter 14 in this book.
4. Jakes, K. A. *Proc. Third Int. Symp. Archaeometry,* Smithsonian Institution: Washington, D.C., 1984; in press.
5. Jakes, K. A.; Howard, J. H. *ibid.*
6. Morton, W. E.; Hearle, J. W. S. "Physical Properties of Textile Fibers"; The Textile Institute: London, 1975; pp. 1–86, 223–64.
7. Peters, R. H. "Textile Chemistry, Vol. II"; Elsevier: New York, 1967; pp. 91–95.
8. Lucas, F.; Shaw, J. T. B.; Smith, S. G. In "The Silk Fibroins"; Anfinsen, C. B.; Anson, M. C.; Edsall, J. T.; Richards, F. M., Eds.; Advances in Protein Chemistry No. 13; Academic: New York, 1958; pp. 107–236.
9. Otterburn, M. S. In "The Chemistry of Natural Protein Fibers"; Asquith, R. S., Ed.; Plenum: New York, 1977; pp. 53–80.
10. McBurney, L. F. In "Cellulose and Cellulose Derivatives"; Ott, E.; Spurlin, H. M.; Grafflin, M. W., Eds.; Interscience: New York, 1954; pp. 99–163.
11. Robie, R. A.; Hemingway, B. S.; Fisher, J. R. *Geol. Surv. Bull. U.S. 1452* **1978**, 1–456.
12. Schindler, P. M.; Reinert, M.; Gamsjäger, H. *Helv. Chim. Acta* **1968**, *51*, 1845–56.
13. Baas Becking, L. G. M.; Kaplan, I. R.; Moore, D. *J. Geol.* **1960**, *68*, 243–84.
14. Garrels, R. M.; Christ, C. L. "Solutions, Minerals, and Equilibria"; Harper and Row: New York, 1965; p. 381.
15. Sato, M. *Econ. Geol.* **1960**, *55*, 928–61.
16. Gurd, F. R. N.; Wilcox, P. E. "Complex Formation Between Metallic Cations and Proteins, Peptides and Amino Acids"; Anson, M. C.; Bailey, K.; Edsall, J. T., Eds.; Advances in Protein Chemistry No. 11; Academic; New York, 1956; pp. 312–62.

RECEIVED for review November 26, 1984. ACCEPTED March 19, 1985.

16

Standards for Archival Materials

William K. Wilson and Susan Lee-Bechtold

National Archives and Records Services, Preservation Policy and Services Division, Washington, DC 20408

A suggested program for the development of standards under the administrative umbrella of a standards organization is presented. This procedure requires only leadership and the reprogramming of 0.1–1.0 worker years of conservator or scientist time in participating organizations. This process would generate the much needed manual of repair for conservators and tend to channel research in the direction of standards. Records keepers need standards in the following areas: (1) the preservation of collections: guidelines for storage, display, and security; (2) the restoration of records: guidelines for repair and specifications for materials used in restoration; and (3) the description of stable materials used in the generation of conservation of records: specifications for a wide variety of products such as paper, adhesives, and plastic films.

A STANDARD IS NOT AN END PRODUCT but a vehicle to assist records keepers in achieving the principal mission of their organizations, namely, to preserve information and to make this information available to others. The object of this chapter is to emphasize the need for records organizations to direct some of the efforts of their research and conservation laboratories toward the development of standards for records materials, to develop those standards in cooperation with a recognized standards organization, and to devise an improved mechanism for making use of specifications.

Although the bulk of our records are made on paper, records materials other than paper are multiplying and becoming more common. These materials have not been in existence long enough for scientists and conservators to have built up an adequate information bank concerning stability under conditions of use and storage. Difficulties may arise from unexpected interactions with the environment as well as minuscule and unnoticed variations in chemical structure. This situation is especially true of modern records substrates that frequently are combinations of

many different materials. The surprise occurrence of microfilm blemishes is an example of what may be in store in the future.

The data and concepts developed from research are useless to the records keeper unless they are translated into action. Examples of this action are a written procedure that can be used in the conservation laboratory and a specification that describes a product to be purchased for use in restoration. Some standards in the form of specifications for paper, laminating film, and photographic film are available. Standard procedures, developed in cooperation with a recognized U.S. standards organization for use in conservation laboratories, are not available.

Except in large organizations with quality control laboratories, no satisfactory mechanism for making use of specifications exists. This problem has two parts: (1) connecting suppliers with a large number of small-volume buyers, and (2) influencing the generators of records to use permanent materials. This problem has not been properly addressed because it requires the cooperation of a large number of organizations.

This chapter mostly emphasizes materials, procedures, and products for the creation, repair, and storage of records. This aspect is only part of the picture, as records materials are only the media for storage, retrieval, and use of information. Although we are aware of the need for, and of considerable activity in, areas such as buildings, equipment, automation, and archival arrangement and description, these subject areas are left to others who are more competent to address them. Technical standards for library and information science were covered in *Library Trends* (*1*), international standards for archives were discussed by Rhoads (*2*), and the general subject of standards for libraries and archives was developed by Clark (*3*).

The Role of Standards in Society

Much of the information in this section is taken from Reference 4. Standards play such a dominant role in everyday activities that one tends to forget that they exist. One may use a radio alarm clock, the accuracy of which is expressed through the use of standards traceable to the National Bureau of Standards (NBS). By international agreement, the time is referenced to the zero time meridian in Greenwich, outside of London. The radio operates on a frequency assigned by the Federal Communications Commission.

One may operate a faucet that is attached to the water supply by standard pipe threads to pipe of standard size. The purity of the water from the faucet is established within limits by a state, county, or city agency.

Interstate signing standards are the result of the efforts of the Engineering and Traffic Operations of the Federal Highway Administra-

tion. Campgrounds may be built according to standards developed by the Family Camping Federation of America. Gasoline is delivered by a pump, the accuracy of which has been certified by a state agency using requirements established by the National Conference on Weights and Measures of NBS.

Changes have been made in many office buildings to accommodate the handicapped according to Public Law 90-480, based on an American National Standards Institute (ANSI) standard developed by the National Easter Seal Society for Crippled Children and Adults.

The point to be made is that civilization as we know it today would collapse without a system of standards.

Who Develops Standards?

Standards may be developed by governments, standards organizations, companies, industries, technical associations, trade associations, professional societies, or even individuals. About 600 organizations in the United States are active in standardization for various reasons (*5*). These organizations may assist in the development of standards, they may issue standards, or they may disseminate standards.

At this point the concept of consensus in the development of standards must be introduced. No one person is likely to get everything in a consensus agreement that he or she wants, but the consensus represents a general compromise.

A company standard probably also will be a consensus standard, for example, a standard for the manufacture of an automobile. As the company has no desire to share information with its competitors, this standard will not be published. The consensus will be within the company: the engineers, the financiers, the stylists, and the quality control group. It is a serious consensus because the economic well being of the company depends on how well it balances all of these items.

Industry standards generally are produced by trade associations. A good example of industry standards is the collection of standard test methods produced by the Technical Association of the Pulp and Paper Industry (TAPPI), a professional and technical organization of the paper industry.

Standards may be generated by professional societies, such as the American Chemical Society, which maintains specifications for the purity of chemicals.

The full consensus standard is generated through the participation of all sectors that might have an interest in the standard: producers, users, ultimate consumers, and general interest groups. For example, a manufacturer of printing paper is a producer, the printer is the user of the paper, the ultimate consumer is the person who buys the book, and

representatives of a government laboratory or a university are in the general interest category. The user and the ultimate consumer may be the same, as is the case with the person who buys an automobile; or they may be separate persons, as is the case with the taxicab, in which the driver is the user, and the passengers are the final consumers.

The concept of user and ultimate consumer is especially important to the archivist and accounts for one of the most serious problems. The user, or primary consumer, buys the paper and makes the record. The ultimate consumer, or secondary consumer (the archivist), acquires the record and must live with the quality of the record received. Thus, the archivist is in a unique position of helplessness with respect to the quality of the materials on which the records are made. The librarian shares this unfortunate dilemma with the archivist.

Mandatory standards are issued by governments and may or may not be full consensus standards. Model building codes have been worked out by the full consensus procedure, and when they are adopted by a county or city government they become mandatory. The mandating by Congress in 1863 of a uniform railroad track gauge (from 33 different gauges) is an example of a mandatory standard that probably had little consensus input. The mandatory approach served to complete the unification of the country's railroad by the 1880s. This standard may have left much to be desired from a technical point of view, but the advantages of convenience, economy, and national security were far more important.

Definitions

The word standard has been used here in several different contexts, and several definitions are possible, depending on the situation. The definitions proposed by the American Society for Testing and Materials (ASTM) in "Form and Style for ASTM Standards" (1983) will be given here because much of the past development of standards for archival records materials has been through ASTM. In general, however, a standard is simply an agreed upon way of doing something.

As defined by ASTM, a *standard* is a document that has been developed and established within the consensus principles of the society and that meets the approval requirements of the ASTM procedures and regulations. The term standard is used as an adjective in the title of ASTM documents to connote specified consensus and approval (i.e., standard test methods, standard terminology).

Standard terminology provides for the definitions of terms or the descriptions of terms, as well as the explanations of symbols, abbreviations, and acronyms.

A *standard test method* is a definitive procedure for the identifica-

tion, measurement, and evaluation of one or more qualities, characteristics, or properties of a material, product, system, or service that produces a test result.

A *standard practice* is a definitive procedure for performing one or more specific operations or functions that do not produce a test result. We suggest that standards for the restoration of documents should fall in this category.

A *standard classification,* as it applies to materials, products, systems, or services, defines systematic arrangements or division into groups on the basis of similar characteristics, such as origin, composition, properties, or use. Papers may be classified according to composition, for example, groundwood, rag, and chemical wood-pulp papers. Papers also may be classified according to use, for example, printing, sanitary, packaging, and fine-writing papers.

A *standard specification* is a precise statement or a set of requirements to be satisfied by a product, material, system, or service. It indicates the procedure that determines whether the requirements given are satisfied.

Some of the materials and concepts of interest to archivists, and librarians as well, are categorized and listed as follows. The list is far from complete, but it illustrates the range of materials, products, and procedures susceptible to standardization.

1. Materials and products used in the storage of information: paper, books, leather, parchment, photographic materials, microfilm, motion picture film, magnetic tape, video tape, and sound discs (phonograph records).
2. Materials and products used in daily work: document boxes, display cases, file folders, map folders, and envelopes for prints and negatives.
3. Materials used in repair: adhesives such as hide glue, starch, cellulose gum, poly(vinyl alcohol), poly(vinyl acetate), and soluble nylon; encapsulating film; laminating film; deacidification chemicals; mounting board; reinforcing tissue; tape-splicing materials; and tape-cleaning materials.
4. Procedures and guidelines concerning information storage, display, and repair: test methods; lamination; encapsulation; storage (including cornerstones) with respect to temperature, relative humidity, and air pollution; display guidelines; use of products on which information is stored; reproduction; cleaning; bleaching; and deacidification.

This incomplete list needs no explanation. Standards are available for some of these items.

At this point one might ask, "What kinds of standards do archivists need?"

Definitions are urgently needed. For example, what is permanence? An answer to this question for paper records is given in each of the four ASTM specifications for permanent-record papers.

Procedures for repair of documents, which probably would be defined by ASTM as practices, are badly needed. A collection of guidelines could be used as a training manual as well as a laboratory manual.

Specifications are needed for the purchase of materials, such as laminating film, paper, and adhesives.

Test methods are required for the testing of materials purchased through specifications.

Potential Benefits of the Use of Standards

In the development of a standard, a laboratory group may perform the research on which the document is based, write a report, and present it to a committee with a draft standard. Or, if most of the information is available, a task group may write the standard. In any case, a committee reviews and provides input to the document, so the committee provides a much broader information base. All laboratories benefit from the combined expertise. Thus, organizations that participate in standards development are pooling their resources for the common good.

Standards that are developed through a national standards organization normally are recognized by all concerned as viable and useful documents. Usually a lot of work has gone into the development of a standard, and it has a broad base of support. An example of a standard that did not receive the recognition that it deserved is the Barrow specification for permanent and durable book papers (*6*). Although the merit of the document was recognized by archivists and librarians, its effectiveness was limited because it lacked the backup of a standards organization. It did not have a broad base of support.

Standards organizations usually require that their documents be reviewed every 5 years, and be revised, if necessary. A standard may remain essentially unchanged for 20 years if no reason is found to change it, but it may be changed frequently. The important point is that standards should not be allowed to fall behind the state of the art.

The economic benefits of standards can be considerable. To the archival community these benefits would be difficult to express in bookkeeping terms because the budget would not be appreciably different before and after standards. The benefits would accrue in the use of more stable materials, less need for repair in the future, and the presence of a focal point for gradual improvement in the conservation area.

A good collection of standards for the conservation laboratory

would allow the employment of lower grade personnel for the more routine tasks. At the same time, a standards manual would greatly accelerate the training of personnel.

Standards Organizations

Bodies Concerned Exclusively with Standards. ASTM and ANSI are concerned almost exclusively with standards that are developed by the voluntary consensus procedure, but they do not develop standards with their own staffs.

ASTM is one of the world's largest sources of voluntary consensus standards for materials, products, systems, and services (*4*). It is the primary management system for standards development in the United States and has more than 6100 standards under copyright. It currently has about 153 main technical committees (about 1935 subcommittees and sections) working on standards in diverse areas such as steel, plastics, textiles, sports equipment, consumer products, security systems and equipment, surgical inplants, and meat products.

ASTM standards are developed not by staff, but by those having expertise in specific areas who choose voluntarily to work within the ASTM system: producers, users, ultimate consumers, and representatives of government and academia. ASTM provides a forum within which these people can meet on a common ground to write standards that will best meet the needs of all interested parties. The ASTM system adheres strictly to the principles of due process and thus assures equal access to and equal voice in the standards forum and precludes discriminatory anticompetitive effects. Standards developed by ASTM committees are published in the 66-volume annual book of ASTM standards.

ANSI was founded in 1918 to coordinate standardization activities in the private sector, and today it is the coordinating organization in the U.S. national standards system. In contrast with ASTM it does not develop standards, but it does provide the mechanism for determination of need and arranges for competent organizations to perform the standards development work. The membership of ANSI consists of about 1000 companies and more than 200 trade, technical, professional, labor, and consumer organizations (*7*).

ANSI provides for the effective representation of U.S. interests in international standardization carried out by nontreaty organizations such as the International Organization for Standardization (ISO) and the International Electrotechnical Commission (IEC).

Approved American National Standards, which now number approximately 8500, encompass virtually every field and every discipline. The use of American National Standards is not mandatory. They become mandatory only when adopted or referenced by government. A

small fraction of ANSI's standards was developed by committees that operated under ANSI directly and used approved procedures (*8*). This activity is not encouraged and is now being returned to others for standards development, prior to review as American National Standards.

The Codes and Standards Division of the American Society for Mechanical Engineers is devoted exclusively to the development and maintenance of standards for pressure vessels, turbines, combustion engines, etc. Other smaller organizations that deal almost exclusively with voluntary standards are the Industrial Fasteners Institute, the Insulated Power Cable Engineers Association, and the Manufacturers Standardization Society of the Valves and Fittings Industry (*8*).

Trade Associations. Trade association standards normally are developed through a consensus of technical people in the industry, although user input also may be used to arrive at a consensus. Examples of trade associations that have produced standards are the Aerospace Industries Association, the American Petroleum Institute, the Association of American Railroads, and the Manufacturing Chemists Association. Some trade associations find it advantageous to develop standards under the sponsorship of a standards organization such as ASTM (*8*).

Professional and Technical Organizations. Organizations in this category that have produced many standards are the American Concrete Institute, the American Oil Chemist's Society, the American Society of Agricultural Engineers, the Institute of Electrical and Electronics Engineers, the Society of Automotive Engineers, and TAPPI (*8*). TAPPI is a professional and technical organization that develops standards for the paper industry. An organization of interest to archivists is the Association for Information and Image Management (AIIM), formerly the National Micrographics Association, which was formerly the National Microfilm Association. AIIM is a professional and technical organization as well as a trade association composed of about 10,000 individual professional members and more than 250 trade member companies. About 20 standards committees prepare standards in areas from terminology to quality and control to computer information interfaces (*9*). Although these standards are not concerned with permanence, they are useful in micrographics operations, especially in the maintenance of quality control through test charts (*9*). AIIM is the secretariat for ANSI Committee PH5, Micrographics.

NBS. NBS is not a standards organization in the sense of ANSI or ASTM. ANSI and ASTM provide the administrative and procedural framework, but not the technical capability. NBS contributes technical background for a host of standards on subjects ranging from time to safety.

NBS was created in 1901 to be the nation's central reference laboratory for measurements in the physical sciences and engineering. NBS develops, maintains, and/or disseminates hundreds of measurement standards including the fundamental standards for temperature, time, frequency, mass, length, amount of substance, and electrical measurements.

NBS is not a regulatory agency. It does not mandate or enforce standards, but it does provide the technical basis for the selection and application of standards by other agencies and by domestic and international voluntary standards organizations (*10*). NBS ensures that physical and chemical measurements within the United States can be traced to a consistent set of standards, reference methods, and reference materials that also are compatible with those used to regulate international trade.

By authority of the Brooks Act of 1965, NBS (*11*) has "responsibility for planning and managing a program of federal automatic data processing (ADP) standards and for the development of these standards . . . responsibility for providing scientific and technological advisory services to federal agencies regarding ADP."

NBS (*12*) maintains a comprehensive program on standard reference materials (SRMs): "SRMs are well-characterized, homogeneous, stable materials or simple artifacts with specific properties measured and certified by NBS. They are widely used in a variety of measurement applications, including the evaluation of the accuracy of test methods, improvement of measurement compatability among different laboratories, and establishment of measurement traceability to NBS. The Bureau currently has more than 1000 different SRMs available."

NBS coordinates the National Standard Reference Data System, which was established in 1963 as a nationwide program designed to give scientists and engineers easy access to critically evaluated data (*13*).

International Organizations. The two principal international standards organizations are ISO and IEC (*14–16*). Both were created in the 20th century, but the roots of IEC date to the 19th century.

IEC was formally created in 1906 to consider standardization of the nomenclature and ratings of electrical apparatus and machinery. In 1947, IEC became affiliated with ISO as its electrical division, but it maintained its technical and financial autonomy.

ISO had its roots in the International Federation of the National Standardizing Associations (ISA), which was created in 1926. ISA ceased to exist in 1942 and was succeeded by ISO, which was created in 1947 as the result of a conference held in London in 1946 to consider the establishment of an international organization whose object would be to facilitate the international coordination and unification of industrial standards.

Today more than 72 countries participate in the work of about 160

ISO technical committees to produce about 400 new or revised standards each year. Large numbers of standards have been developed in the areas of mechanical engineering, basic chemicals, nonmetallic materials, agriculture, and metals.

ISO work has been concentrated in the areas of terminology, dimensions, and test methods. A common technical language is an absolute requirement for effective communication and is especially needed in international standards work in which language barriers can cause not only comical but tragic situations.

ISO committees are listed in Reference 17. The following committees are of interest, or of potential interest, to archivists and librarians (the ISO committee numbers are given in parentheses): Paper, Board, and Pulps (6); Photography (42); Documentation (46); Metal Containers (52); Plastics (61); Applications of Statistical Methods (69); Office Machines (95); Computers and Information Processing (97); Packaging (122); Graphic Technology (130); Documents and Data Elements in Administration, Commerce, and Industry (154); and Micrographics (171).

These 12 subject areas represent some ground that might prove to be very fertile with respect to both national and international standards. As there is some momentum today to go the international standards development route and then the national route (*18*), the time is ripe for archivists to develop an interest in international standards.

An area that might be especially fruitful is the application of statistical methods. Because of the technical, social, and economic aspects of the problems, sufficient resources never will be available to conserve everything that should be conserved. Therefore, records keepers must know at all times what is in their collections, what needs restoration, the cost of restoration, the cost of storage, alternate procedures and the costs thereof, and the organizational structures necessary to get the tasks accomplished.

Regional Organizations. Regional organizations are international in membership but include countries in a specific geographical area. Most of them depend on and interact with ISO and IEC (*14, 16, 19*).

Federal, State, and Local Governments. Government bodies develop and use standards for many purposes, principally for procurement and regulation. For example, the Environmental Protection Agency sets standards for protection of the environment, the Department of Defense sets standards for procurement in those areas for which voluntary consensus standards do not apply, and the Office of Federal Supply and Services provides specifications for procurement of a host of products from erasers to office furniture. The Congressional Joint Committee on

Printing (JCP) provides specifications for printing and writing papers used throughout the federal government.

Standards Organizations of Special Interest to Archivists. Three standards organizations are of interest to archivists: ASTM, ANSI, and ISO. ASTM stands first in importance for the following reasons: (1) The wide range of technical expertise in many materials and product areas should cover most areas of interest to archivists. (2) The organizational structure of ASTM provides for the development of almost any kind of standard. (3) If ASTM standards are determined to be of national interest, they can become ANSI standards because ASTM follows a full consensus procedure in the development of standards. (4) Four specifications for permanent-record papers already have been developed through ASTM Committee D-6, Paper and Paper Products (*20*).

ANSI is of importance to archivists for the following reasons: (1) Archivists have collaborated with ANSI committees in the past in some areas, such as photography and library cards. (2) ANSI standards are recognized as national standards. (3) ANSI is the U.S. organization through which a group would work in participating in ISO. (4) ANSI Committee Z-39, National Information Standards Organization, formerly Library and Information Sciences and Related Publishing Practices, has operated for years in the development of standards in the library area. ANSI would not be the primary standards organization of interest to archivists because it does not develop standards.

ISO is of importance because it represents what could be the ultimate in technical cooperation among archivists throughout the world. This cooperation already has begun in the area of accelerated aging. Working Group 12, Accelerated Aging, under Subcommittee 2, Test Methods and Quality Specifications for Paper and Board, one of six subcommittees of ISO Committee 6, Paper, Pulp, and Board, has been functioning since 1974. The United States is convener of this working group.

A glance at the list of ISO committees of potential interest to archivists shows that ISO could be of great value. Participation in standards development in ISO assumes a strong technical background at the national level and a level of cooperation that allows the development of a national consensus in the areas of interest.

How Standards Are Developed Through a Standards Organization

Organization of ASTM Committees. The approximately 153 ASTM technical committees are divided into seven groups (*4*) (the number of committees in each group is given in parentheses): Ferrous Metals (5); Nonferrous Metals (10); Cementitious, Ceramic, Concrete,

and Masonry Materials (25); Miscellaneous Materials (33); Miscellaneous Subjects (45); Materials for Specific Applications (27); and Corrosion, Deterioration, and Degradation of Materials (4).

The miscellaneous materials committees include paint, paper, packaging, rubber textiles, and plastics. The miscellaneous subjects committees include emission spectroscopy, fire standards, appearance of materials, microscopy, and resource recovery. The materials for specific applications committees include electronics, tires, consumer products, and food-service equipment. The corrosion, deterioration, and degradation of materials committees include corrosion of metals, erosion and wear, and durability of nonmetallic materials.

The standards committees, such as D-6 Paper and Paper Products, are designed as main committees. The main committees are divided into subcommittees and task groups. Technical work in the preparation of a draft of a standard usually is done in a task group, although it may be done in a subcommittee. If the development of laboratory data is involved, the draft of a standard may be prepared by the project leader and submitted to a task group or perhaps directly to the subcommittee. The system is flexible, but within this flexibility ASTM adheres rigidly to the principles of due process.

Task group members usually are competent in a specific area of expertise. Task groups have no officers and usually are created on an ad hoc basis for a specific purpose. Task groups have no requirement for balance among participants.

Subcommittees consist of experts in specific areas related to the work of the main committee. The chairman may be a producer, a consumer, or a general-interest representative. Subcommittees must be balanced so that users and general-interest members outnumber producers and distributors.

The main committee is made up of the entire committee membership. The chairman cannot be a producer, although this restriction does not apply to the other officers. Main committees, like subcommittees, must also be balanced. The work of the main committee is guided by the executive subcommittee, which usually consists of the officers of the main committee, the subcommittee chairman, and perhaps several members at large. This executive subcommittee is a management subcommittee.

Establishment of Need and Development of Standards. Before standards can be developed, a need must be apparent to an institution, an individual, or to a professional society. This need can take many forms and can occur in several different contexts. At some point an individual, or a group of individuals, perhaps in a meeting, may realize that somebody ought to do something, and eventually action is initiated.

Historically, this something is contract research, or research in an in-house laboratory, to develop information in the subject area, and the need to develop standards may not be recognized at the time. For illustration, an imaginary scenario is developed in which the first step is for a small group of individuals representing several organizations to contact ASTM and request guidance and assistance. The group realizes that a standard is the desired end product.

A staff liaison person at ASTM in this subject area holds a conference in Philadelphia with representatives of the group. The staff liaison realizes that several consensus standards are needed in several closely related subject areas and suggests a meeting of organizations interested in, or potentially interested in, standards. To this list is added producers of the products of interest as well as government and university laboratories that maintain expertise in these particular materials areas.

At this point ASTM extends an invitation to all potentially interested parties to attend a planning and subsequent organizational meeting at ASTM in Philadelphia. Depending on the magnitude of the need, a new committee may be formed, or one or more subcommittees may be formed under an existing committee. In this example, it is assumed that a new committee is formed and approved by ASTM and that officers are selected.

At the first meeting of the new committee, ASTM staff members assist in the organization of the committee and in setting a course of action. It is agreed, for example, that five new standards are needed (a specification for an adhesive, and four standards for document storage), and this situation results in a natural division into subcommittees and task groups. Representatives of manufacturers point out that the information already is available for preparing two of these standards. Two task groups, consisting of technical experts in the areas of concern, are appointed to prepare these standards. It develops that two of the remaining three potential standards can be prepared after the development of information from questionnaires and a review of the literature. As these two are closely related, a single task group is assigned this responsibility.

The fifth need for a standard (a specification for an adhesive) presents more of a problem because some research is needed. How much work is needed can be determined only after some exploratory work is done. One of the organizations has a small research laboratory, and the representative of this organization volunteers to get this job done. At this point peer-group pressure takes over the situation. Ideally, within a year four draft standards are in the final stages of balloting, and laboratory work on the fifth has been completed.

This imaginary scenario can be extended to include the develop-

ment of guidelines for restoration procedures, which should be done by task groups of conservators with minor input by scientists and possibly suppliers of materials. These guidelines should be developed within the administrative framework of a standards organization. Many research problems should surface in writing guidelines for restoration.

The task groups write standards in the format prescribed by the standards organization. At this stage the technical content of the standard is determined, and competent performance can avoid trouble later. No official ballot is used at the task-group level in ASTM, but the consensus procedure still is active.

The draft standard is next reviewed by the parent subcommittee, and at this stage balloting becomes formal. Balloting is necessary to ensure that the standard has the proper review of due process so that it rests on a sound procedural foundation. The review at this stage usually is mostly technical.

Balloting at the main committee level may encounter difficulties other than technical objections, and negative votes may have a technical excuse that is not the real objection. ASTM takes the attitude that everyone comes to the committee table with a bias.

Negative ballots at the subcommittee level and the committee level must be resolved by a formal procedure. If the negative ballot can be resolved through an editorial change, a reballoting is not necessary. If the change is more than editorial, it must be called to the attention of all members of the subcommittee or committee. If a negative ballot is resolved through a substantive change, reballoting is necessary.

Evaluations by Other Organizations on Conservation Issues

The emphasis here will be on how standards might fit into the picture. Many recommendations for the development of standards have been made, but no plan has been suggested for developing and using them. Standards have been developed only on an ad hoc basis in the past.

The major point to be made is that a large number of problems could be solved by the development of consensus standards, through a voluntary standards organization, with little or no additional cost to the institutions involved.

Library professionals have been active in making recommendations and setting priorities in conservation. Although the library and archival professions are distinctly different, the records in their repositories are made on the same kinds of substrates.

National Conservation Advisory Council (NCAC) Report: Study Committee on Libraries and Archives. NCAC was established in 1973 to serve as a national forum for cooperation and planning among institutions and programs concerned with the conservation of cultural

property in the United States (*21*). The council, through study committees, has issued various reports on conservation needs in the United States and the desirability of establishing a national institute to assist in fulfilling these needs.

The work of the Study Committee on Libraries and Archives (*22*) under NCAC was concerned with the needs that are special to libraries and archives. One of the seven chapters in the booklet is devoted to standards.

The seventh recommendation of the study group reads in part (*22*), "The proposed national conservation institute should assist in the development of standards for conservation materials, environmental and storage conditions, and procedures for materials evaluation and testing."

"Standards of adequate and proper conservation treatment would appear to be the most direct, impersonal, and easily achieved means of protecting books and manuscripts. However, there are no standards of this type now in use. The most important single measure that can be taken to protect record materials is almost certainly to provide adequate environmental and storage conditions." Subsequently, the National Institute for Conservation (NIC) caused the formation of ANSI Subcommittee R, Environmental Conditions for Storage of Paper-Based Library Holdings, under Z39, National Information Standards Organization (*23*). A report, consisting of a review of the literature and a draft standard, has been submitted to NIC (*24*), and a standard should be issued within a few months.

A National Preservation Program: Planning Conference, Library of Congress. A 1976 planning conference for a national preservation program was sponsored by the Library of Congress, and the proceedings were published in 1980 (*25*). A summary was reported by Darling (*26*). A formal list of recommendations was not prepared and agreed upon by the group, but several important recommendations were made by individuals during the presentations and during the discussion periods. It is desirable to take a look at some of these earlier recommendations.

One of the participants spoke on three problems facing both archivists and librarians. The first is the need for a working manual for nonprofessional personnel engaged in repair. This working manual could be a collection of guidelines (standards) prepared by task groups of conservators and scientists within the framework of a standards organization such as ASTM. Standards for use by professionals would also be helpful.

The second comment about the increase in efficiency of the use of personnel if working manuals were available was well received.

The third point was developing a close, active relationship with appropriate manufacturers and suppliers of the materials that are used in

marking, repairing, and otherwise treating library and archival materials. This point strikes at the heart of the problems archivists and librarians have in making use of specifications. One could also include paper, binding materials, document boxes, etc., and eventually records substrates other than paper. The first step is to develop specifications for these materials, and the next step is to develop a mechanism for their use.

Preserving materials of the future was discussed considerably, and it was agreed that many problems could be prevented by printing all publications on permanent-durable paper. (This view was expressed by Robert Bahmer, Archivist of the United States in 1960, and led to the establishment of a research program at NBS that resulted in four specifications for permanent-record papers (*20*). It was also agreed that changing the system would not be easy because publishers have no incentive to change paper for printing. This area needs considerable attention.

As a postscript to the meeting, Norman J. Shaffer, then Chief of the Library of Congress Preservation Office, wrote in January 1980 in the preface of the proceedings of the December 1976 conference (*24*), "While the recommendations made at the planning conference are laudable and achievable at sometime in the future, day-to-day realities argue for doing now what can be done with available resources."

Historical Review of Preservation Programs. A history of problems and programs in preservation has been written by Darling and Ogden (*27*). This excellent review mentions most of the subjects discussed here and discusses the 1970s as a decade of analysis and development of conservation plans on a grand scale, starting with the Chicago Conference on the Graduate Library School, the proceedings of which were published in 1970 (*28*).

Two active programs supported by grants from the National Endowment for the Humanities (NEH) are mentioned in this review. The first is a program administered by the Association of Research Libraries, Office of Management Studies at Columbia University, to codify current practices and produce procedures and technical manuals together with a guided self-study planning process. A list of the publications generated from this grant is available (*29*). This effort is impressive in that the program includes everything that would be developed through a standards program. In fact, it would be the basis of a standards program.

The second NEH grant was awarded to the Society of American Archivists (SAA) in 1980 for the development of manuals and for an extensive series of workshops. A series of workshops has materialized, and two conservation manuals have appeared (*30*).

Plan of Action

What Needs To Be Done. Development and use of standards in the records area should be a continuing program and should be implemented with the attitude that the program still will be active 50 years from the date the first standard is issued. Action on the following items should be initiated: (1) The development of standards through a standards organization, such as ASTM, in the following areas: guidelines for restoration; guidelines for preservation, that is, storage, display, security, etc.; specifications for materials used in restoration; and specifications for materials used in the generation of records. (2) The development of a system for making maximum use of specifications for in-house purchasing. (3) The development of a public relations program to encourage the use of stable materials in the generation of records.

Attention should be given to the allocation of effort among the four types of standards mentioned in No. 1 and the type of expertise needed in writing them. Guidelines for restoration should be written by conservators assisted by scientists. Guidelines for preservation should be written by scientists in collaboration with conservators. Specifications for materials used in restoration should be developed through research and written by scientists; active participation of conservators and suppliers should be included. Specifications for materials used in the generation of records should be developed through research and written by scientists in collaboration with conservators and suppliers.

Restoration is the most fertile field in the conservation area for the preparation of standards. Archivists, librarians, and conservators have been begging for years for a manual of repair. A wealth of information is present in the various restoration laboratories in the United States and abroad. The missing ingredients are leadership and a framework within which to work. Both of these can be supplied by working within the administrative framework of a standards organization.

In 1976 The Institute of Paper Conservation initiated publication of *The Paper Conservator* (*31*). The object of this journal is to describe in detail, with illustration, various techniques for the repair of archival documents, books, and works of art on paper. The organization operates under the umbrella of the International Institute for the Conservation of Historic and Artistic Works.

Although this effort is not directed toward the development of standard procedures under the auspices of a national standardizing organization, the end product is of such quality that it could form the basis for committee action on the development of standards procedures.

Guidelines for preservation represent more of a problem in that recommendations for storage and display must (1) take into account a series of tradeoffs and (2) recognize that damage by any one parameter

(heat, light, humidity, dust) becomes a matter of degree rather than kind. All limits must be arbitrarily set.

Specifications for materials used in the restoration of records and in the generation of records must be the products of research laboratories. The development of a specification normally requires from 0.5 to 5 or even 10 worker years. Because the number of scientists who might be assigned to specifications research is small, the output must be very limited. A rough estimate is that one specification for two worker years of research would be a reasonable expectation, and two worker years of research time might be available each year. Although the productivity of this level is quite low, at the end of 10 years, 10 specifications would be available.

The development of a system for making maximum use of specifications for in-house purchasing is a problem for several reasons: (1) No specifications have been developed through a standards organization for materials used in restoration. (2) Even if such specifications were available, the quantities purchased would be so small that suppliers might not be willing, or able, to make special materials available at a reasonable price. (3) Although four ASTM specifications for permanent-record papers are available, archivists generate only a very small fraction of the records in their custody; the records usually are generated by others. A mechanism is badly needed to address these problems.

A public relations program to encourage the use of stable materials in the production of archival records is needed. Such programs have been initiated many times, but they have not been continuous and were ineffective. For example, at a 1980 meeting on the manufacture of alkaline-sized paper, a speaker was describing the advantages of paper made with an alkaline filler. One of the advantages was stability, but he said not to try to sell it on the basis of permanence because no one is interested. Professional people in the paper industry are not aware that a demand for permanent-record paper exists. The tragedy is that the demand usually is indirect because archivists seldom buy the paper for their records.

How Should the Program Be Implemented?. Implementing a standards program requires only that one organization take the lead and initiate action and that approximately 10 organizations agree to cooperate. Within 5 years the program should be highly productive. The steps in implementing a standards program are the following: One organization takes the initiative to become the lead organization. This lead organization writes a letter to a number (15–30) of archival organizations and libraries and suggests the development of a standards program, as indicated earlier. Assuming that 15 organizations respond to the letter, a questionnaire is prepared that asks for a listing of the procedures, materials, or products for which guidelines or specifications

are needed and inquires how much time of what grade personnel could be assigned. The response indicates the standards to be developed and how much personnel time in each organization is available. These representatives become an ad hoc committee. The next step is to write a letter to the chairman of the appropriate ASTM committee requesting the formation of a subcommittee entitled Guidelines for Conservation of Paper Documents. (This step is a formality because this subcommittee would be determined in advance.) After approval, a subcommittee chairman is appointed by the chairman of the committee, with the advice of the ad hoc committee. The chairman of the subcommittee then refers to the priority list from the questionnaire and the list of available personnel and appoints several task groups to write standards. During the writing of the first two or three guidelines, a format for all guidelines for restoration is developed. Formats for specifications are already available.

The development of a system for making use of specifications for institutional purchasing can be done in several ways: (1) Materials purchased against specifications may be tested in-house. Whether more than one organization in 100 has the resources to do its own quality control testing is doubtful. (2) A commercial testing laboratory could be used. This approach is acceptable, but the cost of testing might be greater than the cost of the materials. (3) A qualified products list (QPL) could be developed by having one or more laboratories test the products of interest; approved manufacturers would assure that they would not change their products without notice. This approach would require a loose organization among several institutions to handle the financing and administrative details. Although this approach certainly is plausible, it would require some cooperation. (4) Still another possibility is the concept of affidavits from manufacturers concerning whether their products meet specifications (certification statements).

For the development of a QPL program, one agency would need to take the lead and supply the director of the program as well as secretarial help. The director would arrange for the testing of materials and the collection of fees from participants of the program and would act as chairman of the committee administering the program.

A public relations program to encourage the use of stable materials for the generation of records should be a long-range, low-key program. Although paper represents the bulk of archival records, the publicity campaign must include other records materials as well. Twenty years from now nonpaper records will represent a substantially larger fraction of archival holdings.

Timetable for the Next 10 Years. One can estimate what might be accomplished in 10 years. There must be (1) a group of concerned conservators and scientists who believe in the program and are willing to

spend 0.1–1.0 worker years per organization per year on the program and (2) concerned managers who believe in the program and are willing to support it.

If the lead organization contributes 1 worker year per year of conservator time and a total of 2.0 worker years of scientist time, then in 10 years this time would add up to 20 worker years of conservator time and 20 worker years of scientist time.

Many restoration procedures probably would not require more than 1–2 months to prepare, but others might require as much as 2 or 3 years. If one assumes a median of 1 worker year, then at the end of 10 years 20 restoration procedures would be available. By the same line of reasoning, assuming that a specification would require 2 worker years for development, 10 specifications would be available at the end of 10 years.

As soon as the programs on the development of guidelines for restoration and the development of specifications are underway, possibly in 2 or 3 years, thought should be given to the development of a QPL program. This effort would be long term because resources are limited. This program would require not only rapport with suppliers but also substantial cooperation among organizations. Initial contacts with suppliers could be information sessions, although perusal of suppliers' brochures indicates cognizance of the needs of conservators. A void exists in uncertainty about the stability of materials, an area that has not been technically defined by archival organizations. This void can be filled partly through research and partly through contacts with manufacturers.

The publicity program should be initiated about 2 years after the start of the guidelines-specifications program. Although the program would change as personnel and conditions changed, it must be a continuing program to keep suppliers aware of the problem and to keep archivists, librarians, and the generators of records aware of available technology.

What Are the Expected Benefits? The expected benefits of a standards program for archival organization are summarized as follows:

1. Standards would encourage better communication among conservators, scientists, archival organizations, and suppliers of materials.
2. A collection of guidelines for repair would greatly simplify training and should result in much greater efficiency of operations.
3. A collection of guidelines for preservation would bring order out of chaos in this area and would result in less demand for expert consultation.

4. A collection of specifications would enable the purchase of stable materials for repair and permanent-record materials for making records.
5. Standards have a broad base of support because they are developed by personnel from several organizations.
6. Standards developed through a nationally recognized consensus standards organization are widely accepted and used.
7. Standards developed through a standards organization are not allowed to become obsolete.
8. Although the economic benefits of standards can be considerable, these benefits would be difficult to express in bookkeeping terms.
9. A standards program would represent a focal point for gradual improvement in the conservation area.
10. A standards program would enable archivists to develop maximum information through statistical procedures and make maximum use of conservation research facilities.

Potential Benefits of Advisory Panels. Many activities, from creation and conservation of records to providing the proper guidelines for their use and control, involve the services of specialists. It is not feasible for many archival organizations to have on staff the needed technical experts to participate in the activities of standards organizations. A carefully selected advisory panel for an archival organization, especially if a small research facility is available, can greatly increase the effectiveness of operations. Although probably a first, technical advisory panels could be used effectively with national and international archival organizations.

Summary of Available U.S. Documents

In comparison with need, the number of standards developed for archival records materials is minuscule. It is tragic that documents that are available are not widely used. Although organizational reasons may explain their nonuse, the level of awareness of their existence may be low.

Documents of interest to archivists and librarians are available from various sources. These documents will be discussed in the remaining sections.

ASTM Specifications. Four specifications for permanent-record paper (*20*) were developed at NBS through research sponsored by the National Archives and Records Service (NARS), other U.S. government agencies, and SAA. These also are ANSI specifications.

JCP Specifications. The U.S. Congressional JCP has published six government paper-specification standards for permanent-record paper (*32*). These specifications were written in the tradition of cotton or linen fiber, high folding endurance, and high cellulose purity as indicated by high α-cellulose content and low copper number.

ANSI Specifications for Library Cards. This paper was designed for a specific purpose for which both durability and permanence are important. Although the minimum pH of 5.5 does not provide maximum permanence, it makes possible the use of a sizing that can enhance durability (*33*).

Barrow Research Laboratory Specification for Book Paper. A specification developed by the Barrow Research Laboratory for permanent-durable book paper (*6*) contains a stringent requirement for retention of tearing resistance after 24 days of accelerated aging.

SAA Specification for Carbon Copies. The Paper Research Committee of SAA has developed a specification for permanent-durable paper for carbon copies (manifold paper) (*34*). This specification is patterned after Type I of ASTM D 3208, Specification for Manifold Paper for Permanent Records. The requirements are much tighter, however, and an accelerated-aging test has been added.

NARS Specification for Cellulose Acetate Laminating Film. Through research sponsored by NARS and other government agencies (at NBS), specifications were developed for a stable laminating film formulated from cellulose acetate (*35*). Unfortunately, these specifications never were processed through a standards organization.

TAPPI Testing Procedures. TAPPI publishes a comprehensive set of test methods for the evaluation of pulp, paper, paperboard, and paper-making materials. Several of these methods are useful to archivists, librarians, and conservators. As the cost of the complete set of standards is substantial, TAPPI has made available as a separate set a group of standards (*36*) entitled "TAPPI Standards and Suggested Methods Suitable for Use in the Examination of Paper for Books, Documents, and Works of Art on Paper".

ANSI Standards for Photographic Materials. A list of ANSI standards for photographic materials (*37*) is given in Table I. These standards cover a broad spectrum of need in the photographic area.

Current Activity on Book Paper. A committee under the sponsorship of the Council on Library Resources has been active since 1979 in

Table I. ANSI Standards for Photographic Materials

ANSI Standard	*Title*
PH1.25-1976	Specifications for Safety Photographic Film
PH1.28-1976	Specifications for Photographic Film for Archival Records, Silver-Gelatin Type on Cellulose Ester Base
PH1.41-1976	Specifications for Photographic Film for Archival Records, Silver-Gelatin Type on Polyester Base
PH1.42-1975	Methods for Comparing the Color Stabilities of Photographs (under revision)
PH1.43-1979	Practice for Storage of Processed Safety Photographic Film
PH1.45-1972	Practice for Storage of Processed Photographic Plates
PH1.48-1974	Practice for Storage of Black-and-White Photographic Paper Prints
PH1.51-1979	Dimensions for Micrographic Sheet and Roll Films
PH1.53-1978	Requirements for Photographic Filing Enclosures for Storing Processed Photographic Films, Plates, and Papers
PH1.60-1979	Specifications for Stability of Ammonia-Processed Diazo Photographic Film
PH4.8-1978	Methylene Blue Method for Measuring Thiosulfate and Silver Densitometric Method for Measuring Residual Chemicals in Films, Plates, and Papers

developing guidelines for stable book paper (*38*). These guidelines include a requirement for a minimum of 2% calcium carbonate. This committee, which later became ANSI Subcommittee S under Z-39, has finished the development of a standard for the permanence of book papers (*39*).

Literature Cited

1. Rush, J. E. "Technical Standards for Library and Information Science", in *Library Trends*, 1982, *31*, No. 2, Fall.
2. Rhoads, J. B. "Standardization for Archives," *UNESCO J. Inf. Sci.* 1981, Librarianship and Archives Administration, III 165, No. 3.
3. Clark, R. L., Jr. "Standardization and Technology in Archives-Library Relations"; Bowker: New York, 1976; pp. 133-40.
4. Standardization Basics, ASTM, 1979; Standardization Basics: Part 1, The What and Who of Standards, Standardization News V, No. 2, 24, 1977; Standardization Basics: Part 2, The People Process, and Principles of Standards Development, Standardization News V, No. 3, 21, 1977.
5. Toth, R. B. "Standards Activities of Organizations"; Special Publication 681, Aug; U.S. Dept. of Commerce, National Bureau of Standards; U.S. Government Printing Office: Washington, DC, 1984. Order no. 003-003-02602-6.
6. Barrow Restoration Laboratory, Virginia State Library, Richmond, Va., Specifications for Permanent Durable Book Papers, *American Archivist* 1975, July 1976, *38*, 405.
7. American National Standards Institute, Question and Answer Brochure, 1984. 1430 Broadway, New York, NY 10018; also conversation with ANSI representative Mar. 8, 1985.

8. ASTM Board Committee Report, The Voluntary Standards System of the United States of America; An Appraisal by the American Standards System of the United States of America; An Appraisal by the American Society for Testing and Materials, April, 1975.
9. "Facts About the National Micrographics Association", (now the Association for Information and Image Management); Assoc. for Information and Image Assoc., Silver Spring, Md.
10. "The International System of Units (SI)"; NBS Special Publication 330; U.S. Government Printing Office: Washington, D.C., 1981. Order No. 003-003-02380-9.
11. Thornton, M. Z. *ASTM Stand. News* **1978**, *6*, No. 10, 18.
12. Brochure of the National Bureau of Standards, 1984, p. 30.
13. Brochure of the National Bureau of Standards, 1984, p. 32.
14. "The Aims and Principles of Standardization"; Sanders, T. R. B., Ed.; International Organization for Standardization (ISO): Geneva, Switzerland, 1973.
15. "Standardization and Documentation: An Introduction for Documentalists and Librarians", (ISO): International Organization for Standardization Geneva, Switzerland, 1983.
16. "Directory of International and Regional Organizations Conducting Standards—Related Activities", NBS Special Publication 649; U.S. Government Printing Office: Washington, D.C., April 1983.
17. Kallmann, S. *ASTM Stand. News* **1979** 7, 21.
18. Williams, J. C. *ASTM Stand. News* **1981**, *9*, No. 3, 10.
19. McAdams, W. A. *ASTM Stand. News* **1978**, *6*, No. 11, 8.
20. Specifications for Permanent Record Papers, ASTM, D 3208 Manifold Papers, D 3290 Bond and Ledger Paper, D 3301 File Folders for Storage, D 3458 Copies from Office Copying Machines Annual Book of ASTM Standards, Vol. 15.09, 1985.
21. "Conservation of Cultural Property in the United States." National Conservation Advisory Council; Smithsonian Inst.: Washington, D.C., 1976. This first report of the NCAC describes the origins and objectives of the council and outlines national needs in conservation.
22. "Report of the Study Committee on Libraries and Archives", National Conservation Advisory Council; Smithsonian Inst.: Washington, D.C., 1978.
23. Voice of Committee Z39, April 1981, 3, No. 2, page 9. National Bureau of Standards: Gaithersburg, Md.
24. Wilson, W. K.; Wessel, C. J. "Guidelines for Environmental Conditions in Archives and Libraries", Report to National Institute for Conservation, Feb. 1984, National Archives and Records Service, Washington, D.C.
25. "A National Preservation Program, Proceedings of a Planning Conference"; Preservation Office; Library of Congress: Washington, D.C., 1980.
26. Darling, P. W. Report on Meeting held at the Library of Congress, Dec. 16–17, 1976, on National Planning for Preservation in the United States, Restaurator 1978, 2, 205.
27. Darling, P. W.; Ogden, S. "Problems Perceived to Programs in Practice: The Preservation of Library Resources in the U.S.A., 1956–1980"; Library Resources & Technical Services: January/March 1981; pp. 9–29.
28. *Libr. Q.* **1970**, *40*, 1–201.
29. Association of Research Libraries, Office of Management Studies: Washington, D.C. 20036.
30. Ritzenthaler, M. L. "Archives and Manuscripts: Conservation", 1983; Ritzenthaler, M. L.; Munoff, G. J.; Long, M. S. "Administration of Photographic Collections", 1984. Society of American Archivists: Chicago, Ill.

31. "The Paper Conservator" Institute of Paper Conservation: London, England.
32. "Congress of the United States, Joint Committee on Printing, Government Paper Specifications Standards, No. 8 April" Superintendent of Documents, U.S., Government Printing Office: Washington, D.C., 1977.
33. Z 85.1-1969 Standard for Permanent and Durable Library Catalog Cards.
34. *American Archivist* **1978**, *31*, 81, No. 1.
35. Wilson, W. K.; Forshee, B. W. "Preservation of Documents by Lamination, National Bureau of Standards Monograph No. 5". Out of print but copies may be obtained from Preservation Services Division, National Archives and Records Service, Washington, D.C., 1959.
36. "TAPPI Standards and Suggested Methods Suitable for use in the Examination of Paper for Books, Documents and Works of Art on Paper"; Technical Association of the Pulp & Paper Industry: Atlanta, Ga.
37. "Several specifications for photographic materials"; See Table 2; American National Standards Institute: New York.
38. Cole, J. Y. "Paper for Book Longevity, A report on a conference at the Library of Congress", Feb. 26, 1981, *Library of Congress Information Bulletin* **March 27 1981**.
39. ANSI Z39.48—1984 Permanence of Paper for Printed Library materials.

RECEIVED for review November 26, 1984. ACCEPTED March 15, 1985.

17

Monitoring the Autoxidation of Paper Using Photographic Materials

Vincent D. Daniels

British Museum, Department of Conservation, London WC1B 3DG, England

The autoxidation of organic materials may be detected by using photographic film sensitized by bathing in 0.05 M ammonium hydroxide. The mechanism of image formation is the interaction of the silver halide with oxygen-containing species, possibly hydrogen peroxide. The technique can be used to follow the rate of deterioration of materials, to test storage materials for photographs, and for nondestructive testing of objects.

THE PRINCIPAL TASK OF PAPER CONSERVATORS is to slow down the processes of deterioration that occur in the objects in their care. Paper artifacts are made from papers having a wide range of stabilities; some papers are quite permanent, whereas others degrade relatively rapidly. Additionally, the rate of deterioration of paper may increase because of improper storage conditions.

Many conservation treatments have been devised to slow down the rate of deterioration of paper. Often these treatments neutralize excess acidity in paper, which is an important factor in paper permanence. The probability of success with a new method is often determined by the use of accelerated aging tests and also by drawing parallels with existing methods thought to be effective. Many studies have investigated the best conditions for accelerated aging tests, but disagreement between laboratories is often found. However, even the best set of conditions produces a distortion of the results that would have occurred in ambient conditions.

Ideally, aging processes would be followed in ambient conditions, but the deterioration reactions are sufficiently slow so that finding techniques sensitive enough to follow them is difficult.

Oxidation and acid hydrolysis are the two principal deterioration mechanisms for paper, and recently chemiluminescence (CL) has been used to follow the oxidation of cellulosic materials at temperatures of 40 °C and below (*1*). CL is thought to be produced by the termination

0065-2393/86/0212-0317$06.00/0

step in a free radical chain reaction (*2*) as in the following sequence of steps:

$$\begin{aligned} &RH \longrightarrow R^{\cdot} + H^{\cdot} && \text{initiation} \\ &R^{\cdot} + O_2 \longrightarrow RO_2^{\cdot} \\ &RO_2^{\cdot} + RH \longrightarrow R^{\cdot} + RO_2H) && \text{propagation} \\ &2RO_2^{\cdot} \longrightarrow \text{stable products} && \text{termination} \end{aligned}$$

Hydrogen peroxide might be generated by reactions such as the following:

$$\begin{aligned} RO_2H &\longrightarrow RO^{\cdot} + OH^{\cdot} \\ 2OH^{\cdot} &\longrightarrow H_2O_2 \\ RO_2^{\cdot} + H_2O &\longrightarrow H_2O_2 + RO^{\cdot} \\ RO_2^{\cdot} + H_2O &\longrightarrow ROH + HO_2^{\cdot} \\ HO_2^{\cdot} + RH &\longrightarrow H_2O_2 + R^{\cdot} \end{aligned}$$

In the last reaction RH represents an organic molecule such as cellulose. Flameless reaction of organic compounds at low temperatures (autoxidation) is usually stated to proceed by the reaction paths just given. Peroxides are extensively involved in autoxidation. The formation of hydrogen peroxide during the slow oxidation of phosphorus, oil of turpentine, and metals by gaseous oxygen in the presence of water was studied by Schonbein as early as 1858 (*3*). Since then, hydrogen peroxide has been shown to be evolved during a wide range of aging processes; the ripening of pears (*4*) and tomatoes (*5*); the autoxidation of phenols, lignin, and xylan (*6*); the autoxidation of cellulose and primary alcohols (*7*); and the autoxidation of isopropyl alcohol (*8*). In the autoxidation of isopropyl alcohol, $HO_2^{\cdot}$ was shown to be the chain carrier; this species easily produces hydrogen peroxide by hydrogen abstraction.

The detection of organic peroxides or hydrogen peroxide offers a means of following the progress of autoxidation reactions. This chapter will describe how a method has been developed in which photographic film is used to detect the presence of hydrogen peroxide and perhaps other oxygen-containing species. Several examples will be given of the methods used in the examination of organic materials and in the testing of conservation processes. Oxidation is only one of the degradation processes occurring in paper, and it should be borne in mind that an ideal conservation treatment would slow down all deterioration including that occurring by acid hydrolysis.

Background

Soon after the discovery of the silver halide photographic plate, researchers found that light was not the only factor capable of forming a latent (developable) image on a photographic film. The first of these

discoveries was reported by Moser in 1842 (*9*). He noticed that certain bodies were capable of altering a silver iodide plate in the dark and assumed that some bodies were self-luminous. In 1896, Henri Becquerel discovered radioactivity because certain substances could form a latent image on a photographic plate, even when the substances were separated from the plate by black paper. While conducting research on the newly discovered radioactivity, William J. Russell rediscovered Moser's effect. Russell continued his investigations for several years and published many papers, the best of which appeared between 1897 and 1908 (*10*). He died in 1909.

Russell found that several types of materials could produce images. Of the metals, freshly abraded zinc, aluminum, magnesium, and cadmium gave strong images when they were in contact with photographic film. He demonstrated that the film was not exposed by light but by a chemical species. He found that hydrogen peroxide was capable of producing similar images and showed that it was formed during atmospheric oxidation of the metals just named.

Organic materials are also capable of forming images, and Russell found that wood, leaves, paper, paint, and certain oils were particularly active. Often substances that oxidize rapidly give a good Russell image, for example, drying linseed oil films, terpene oils, and resins. While conducting research on the origin of microblemishes on developed film, McCamy and Pope (*11*) found that hydrogen peroxide was evolved from certain greases, linseed oil, linoleic acid, turpentine, dipentene, pinene, benzaldehyde, rosin, cinnamaldehyde, and cardboard. All these substances produce strong Russell images and are capable of oxidizing easily.

Although the relationship between oxidation and the Russell effect is well founded, hydrogen peroxide cannot be considered as the only possible candidate for image formation as other peroxides, peroxide radicals, or single oxygen could be involved. In the case of freshly abraded metal, electrons (exoelectrons) could be responsible for image formation (*12*). However, both water and oxygen are necessary for exoelectron production. This requirement suggests that hydrogen peroxide may still be involved.

Production of Russell Images

Early workers involved in this area were able to use commercially available photographic films, but modern types are not suitable as they are made to be stable in storage. A method for studying the Russell effect with modern materials was developed at the Kodak (U.K.) Research Laboratory. Film for the present work was made according to the method published by Clifford (*13*). For the present work, Kodak

reproduction film type 2566 was used initially but was subsequently replaced by precision line film FP4. A sheet of film is immersed in 0.05 M ammonium hydroxide for 4 min and allowed to dry. The wet processing can be performed in a darkroom with Kodak 6B safelight illumination. Drying of the film takes about 2 h and is done in the dark in a light-tight box.

To obtain a Russell image, flat objects can be placed in direct contact with the film overnight. With thin, flat objects this imaging can be done conveniently inside an X-ray cassette. The film is developed by using conventional fixer and developer, in this case Ilford Phenisol and Hypam, respectively, each diluted to 20% by volume of the stock concentration. The mechanism of sensitization to hydrogen peroxide is not clear but may be due to an increase in silver ion concentration in the photographic emulsion (*14*).

Image production by hydrogen peroxide is probably brought about by reduction of the silver halide in alkaline conditions, for example, $2AgCl + H_2O_2 + 2OH^- \longrightarrow 2Ag + O_2 + 2Cl^- + 2H_2O$.

The Rate of Deterioration of Paper

Papers vary in their rate of oxidation; some give blacker images than others. Generally, high-lignin-content papers, such as those used to make newspapers and paperback books, give relatively dense images. This result supports the current view that lignin-containing papers are unstable and deteriorate by an oxidative mechanism. The Russell effect thus provides a means of studying the oxidation of paper and some of the factors that influence the rate of oxidation.

Light accelerates the deterioration of lignin-containing papers. This phenomenon was demonstrated by using the Russell effect. A piece of paper was removed from the inside of a paperback book that had been stored closed. A cardboard mask was made with a star-shaped hole cut in it. This mask was placed over the page, and the assemblage was exposed to normal laboratory daylight for a few minutes. A Russell image of the partly exposed sheet of paper is shown in Figure 1. The areas exposed to light are the star shape at the center and the top and bottom edges of the page. These show enhanced activity compared to the areas not exposed to light. It is easy to prove that the effect is not caused by CL or phosphorescence. If a piece of silica glass is placed between the film and the object under examination, complete blockage of activity is observed.

Exposure of other types of paper to light may enhance the image produced on the film, but sometimes no noticeable effect is seen. If the rates of deterioration of various types of paper are to be studied, then the type of storage prior to the experiment must be decided as it may

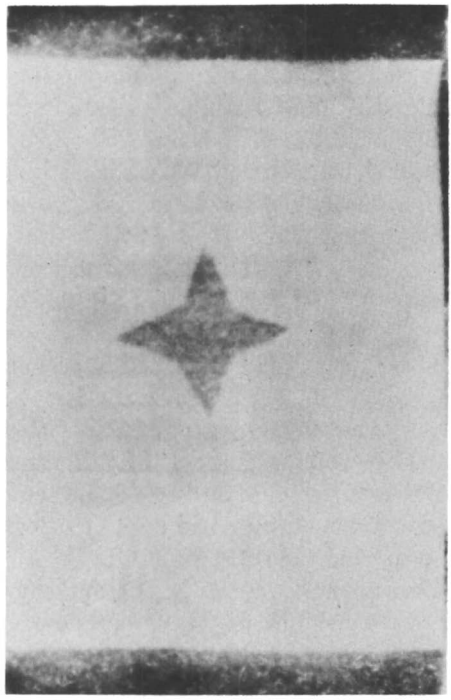

Figure 1. A Russell image of a page from a book. The paper has been exposed to light at the center, the top, and the bottom.

alter the result obtained. Sheets of paper stored in bulk often show yellowing at the edges; this result indicates that more oxidation has already taken place there than at the center. A Russell image of such a piece of paper shows more activity at the center than at the edge as more opportunity for oxidation is present at the center. The rate of oxidation in bulk storage could be limited by oxygen availability or could be accelerated by air pollution preferentially absorbed at the edge of a stack of paper. Subsequently, a single sheet can oxidize fastest at the center where the greatest amount of unoxidized material exists.

Testing Conservation Treatments

Oxidation is one of the major mechanisms for the degradation of paper, and the Russell effect has considerable potential as a tool for studying the way conservation treatments alter the progress of oxidation. Practically, the optical density of the images obtained could be determined by spectrophotometry, and a numerical comparison of sample images on the same sheet of film could be obtained. As yet, a mathematical

relationship between optical density and the release of hydrogen peroxide has not been determined. The sensitivity of the film is also variable and, thus, results on one sheet of film are not comparable with those on another unless a suitable standard is included on each occasion. So far, no suitable standard has been found.

When this research was started it was soon noticed that locally applied aqueous treatments produced inhomogeneous results on the Russell image of the treated area. This observation prompted further investigation. When a drop of water is applied to a piece of filter paper it spreads out and eventually dries. Under UV light the edge of the spot is seen to fluoresce. The Russell image shows intense activity in the fluorescent zone. Both fluorescence and Russell activity decrease over a period of several weeks. This phenomenon has been observed on wet-dry boundaries by chemists performing paper chromatography and by textile scientists. The effect is thought to be due to the movement of soluble impurities towards the edge of the spot and to evaporation of the water which somehow enhances the oxidation of substances in the paper (*15*). The study of paper conservation methods is aided by treating the samples by immersion in the solutions rather than by local application. This procedure seems to eliminate the effect described earlier if the paper is allowed to dry uniformly.

Alkaline earth deacidifying agents have been shown to have antioxidant properties for paper (*6*, *7*, *16*). A typical experiment that examines the antioxidant efficiency of chemical treatment will now be described. Discs of paper were cut into six segments. One of these was kept as a standard and the others were treated by immersion in one of the following: water, 2% sodium bicarbonate, 2% barium hydroxide in methanol, saturated calcium hydroxide solution, and 2% aluminum sulfate. The samples were removed from the solutions and allowed to dry on a glass plate. They were then stored in darkness for 3 days prior to examination. Four types of paper were studied in this series of experiments: filter paper, book paper of 1802, and two modern mechanical wood pulp papers—one from a paperback book and the other from a magazine. The results showed that all the deacidifying agents were effective antioxidants on all the papers, and sodium bicarbonate was the best of those examined. Aluminum sulfate was an effective antioxidant for papers high in cellulose, but it was not so useful for the other papers. However, aluminum sulfate is well known for its destabilizing effects, and it probably degrades paper by acid hydrolysis rather than by oxidation. Water washing produced no significant changes. A typical set of results is shown in Figure 2. In another set of experiments magnesium carbonate showed good antioxidant action toward paper, and copper acetate solution applied at 50 ppm was shown by the Russell effect to be a pro-oxidant in the three types of paper tested.

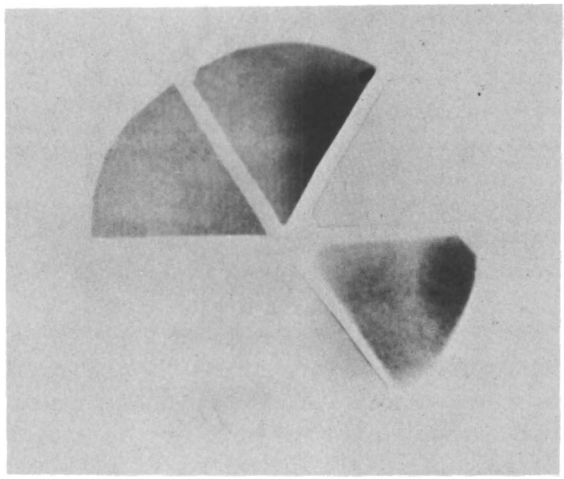

Figure 2. A Russell image of six segments of a 17th century book paper. Clockwise from the top the treatments were water, barium hydroxide, aluminum sulfate, calcium hydroxide, sodium bicarbonate, and no treatment.

These last two results are similar to those found by Williams (*17*); however, contrary to his results, no antioxidant effect was observed after 1% potassium iodide solution was applied to the paper.

Most experiments have been performed within days or weeks of preparation of the samples, but no significant changes in the activity of samples have been observed on storage. All the results in this section are for paper stored in darkness. In some cases different results may be expected for paper stored under illumination. For example, copper acetate is apparently an antioxidant for previously illuminated paper, but it is a pro-oxidant for dark storage. Similar results have been obtained for the oxidation of linseed-oil-containing verdigris (*18*).

Russell effect results for oxidation rates of paper seem to compare well with results obtained by conventional methods, but the Russell effect results were obtained at room temperature and other studies have mainly been done at elevated temperatures.

Testing Materials for the Storage of Photographs

McCamy and Pope (*11*) have established that both hydrogen peroxide and hydrogen sulfide have an accelerating influence on the deterioration of black and white photographic images and, in particular, microfilm. These oxidizing gases react with the silver image particles and cause microblemishes.

Routine methods are already available to test materials for their potential evolution of hydrogen sulfide (*19*); however, none exist for hydrogen peroxide. The Russell effect appears to be of use here as the sensitized film is exposed by hydrogen peroxide; the density of the image produced depends on the rate of evolution of peroxide and the contact time of the sample and film. By placing samples of materials to be tested in contact with the film, an image can be obtained and subsequently the materials can be ranked in order of their suitability.

It is not possible to produce film of reproducible sensitivity; thus, standards should be included against which new materials can be compared. Developing time also varies the density of the image produced. Two additional factors govern the density of the image produced. First, if the material has been exposed to light, the rate of oxidation of the material may be increased. Second, the hydrogen peroxide produced can diffuse through paper, and thus the image of two superimposed sheets of paper is greater than that of one. Figure 3 illustrates this fact. Thus, greater thicknesses of a porous material generally give a darker image.

Other Uses for the Russell Effect

Many types of objects give images of themselves with this technique. Sometimes these images reveal interesting features not easily obtainable by other methods. Two oil paintings have been examined. The cracks in the surface of the painting (the craqueleur) show up readily as black

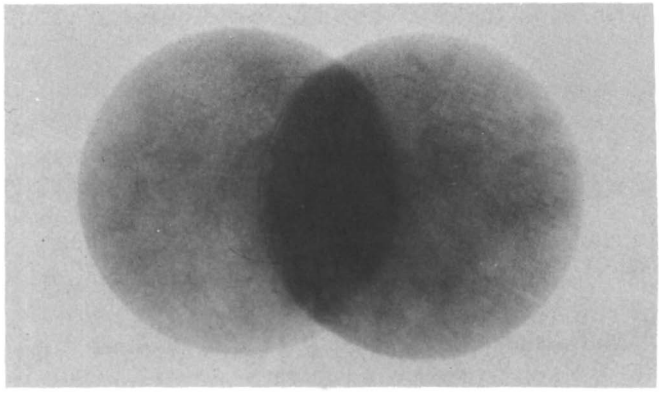

Figure 3. A Russell image of two partially superimposed filter papers.

lines on the photographic plate. The image itself is not revealed on old objects, but freshly applied paint should be detectable.

The writing on Burmese palm leaf manuscripts is made by piercing the surface of the leaf with a sharp stylus. This technique pierces the smooth outer surface and thus reveals the porous cell structure beneath. The writing is often difficult to see and is sometimes made visible by rubbing pigment into the indentations of the letters. By using the Russell effect the writing is rendered easily visible as black lines as the center of the leaf seems to oxidize much faster than the outer layer (Figure 4).

A possible use for the Russell effect is to detect areas of repair on museum objects. Epoxy and polyester resins produce strong images on a Russellgraph and can be easily detected against completely inert stone, ceramic, or metal. Used in this way, the technique is one of the few truly nondestructive testing methods as no incident energy is necessary to obtain the desired information.

The density of a Russell image from a paper object depends on the thickness of the paper. Some types of watermark are formed by localized thinning of the paper in the manufacturing process. A Russell image of such a piece of paper often reveals the watermark, but the image quality is not usually very good and better results can be obtained by light transmission or β-radiography. On the other hand it is possible, in principle at least, to obtain watermarks from paper attached to metals or stone through which passage of radiation would be very difficult.

Watermarks in sheets of paper can be revealed by an alternative technique. A freshly abraded sheet of aluminum acts as a strong source of image-forming particles. A sandwich is made of the paper under examination between the abraded metal surface and the photographic emulsion. The watermark and other features on the paper will be revealed if a variable attenuation of the image-forming particles occurs as they diffuse through the paper. This technique can sometimes yield results of the same quality as β-radiography (Figure 5).

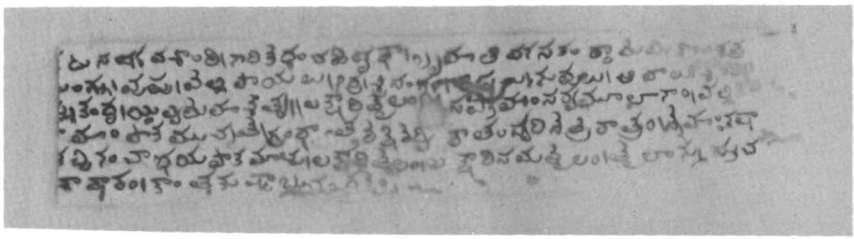

Figure 4. A Russell image of a palm leaf manuscript.

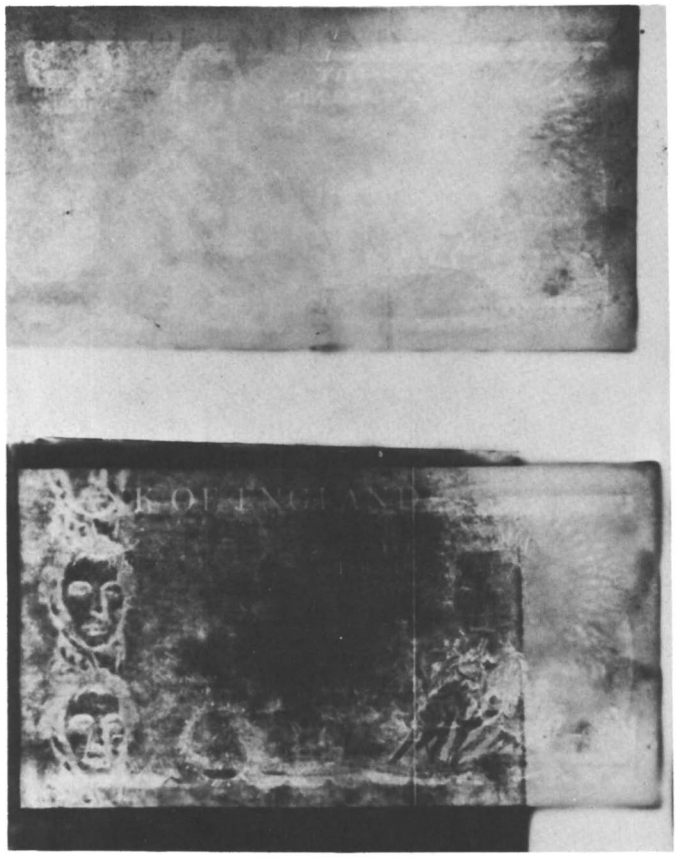

Figure 5. Top, a Russell image of a Bank of England £5 note; and bottom, the same image with a piece of abraded aluminum placed behind it to detect the watermark.

Literature Cited

1. Kelly, G. B.; Williams, J. C.; Mendenhall, G. D.; Ogle, C. A., In "Durability of Macromolecular Materials"; Eby, R. K., Ed.; ACS SYMPOSIUM SERIES No. 95; American Chemical Society: Washington, D.C., 1979, pp. 117-25
2. Hercules, D. M.; Hieffje, G. M.; Snyder, L. R.; Evenson, M. A. "Contemporary Topics in Analytical and Clinical Chemistry"; Plenum Press: London, 1977; Vol. I, pp. 83-85.
3. Partington, J. R. "A Textbook of Inorganic Chemistry", MacMillan: London, 1961; p. 197.
4. Brennon, T.; Frenkel J. *Plant Physiol* 1977, *59*, 411-16.
5. Warm, E.; Laties, G. C. *Phytochemistry* 1982, *21*, 827-31.
6. Ericeson, B.; Lindgren, B. O.; Theander, O. *Sven. Papperstidn.* 1971, *74*, 757-65.

7. Minor, J. L.; Sanyer, N. *J. Polym. Sci Part C* **1971**, *36*, 73-84.
8. Ohto, N.; Niki, E.; Kamiya *J. Chem. Soc. Perkin Trans. 2* **1977**, *13*, 1770-74.
9. Keenan, G. L. *Chem. Rev.* **1926**, *3*, 95-111.
10. Russell, W. J. *Proc. R. Soc.* **1897**, *61*, 424-33; **1898**, *63*, 101-12; **1899**, *64*, 409-19; **1904**, *74*, 131-34; **1906**, *B78*, 386-90; and **1908**, B, 376-81.
11. McCamy, C. S.; Pope, C. I., *J. Res. Nat. Bur. Stand. Sec. A* **1965**, 69A, 385-95.
12. Grunberg, L., *Brit. J. Appl. Phys.* **1958**, *9*, 85-93.
13. Clifford, R. D., *Chem. Ind. London* **1975**, 925.
14. Jenkins, R. L.; Farnell, G. C., *J. Phothogr. Sci.* **1976**, *24*, 41-9.
15. Fox, M. R., *J. Soc. Dyers Colour.* **1965**, *81*, 6-11.
16. Arney, J. S.; Jacobs, A. J.; Newman, R., *Repr. Am. Inst. Conserv. 7th Annu. Meet.*: **1979**, 10-17.
17. Williams, J. C.; Fowler, C. S.; Lyon M. S.; Merrill, T. L., In "Preservation of Paper and Textiles of Historic and Artistic Value"; Williams, J. C., Ed.; ADVANCES IN CHEMISTRY SERIES No. 164; American Chemical Society: Washington, D.C., 1977; pp. 37-61.
18. Rasti, F.; Scott, G., *Stud. Conserv.* **1980**, *25*, 145-157.
19. Daniels, V.; Ward, S., *Stud. Conserv.* **1982**, *27*, 58-60.

RECEIVED for review November 26, 1984. ACCEPTED March 12, 1985.

18

The Kinetics of Cellulose Deterioration

R. L. Feller, S. B. Lee, and J. Bogaard

Research Center on the Materials of the Artist and Conservator, Mellon Institute, Carnegie-Mellon University, Pittsburgh, PA 15213

The degradative scission of cellulosic chains can be regarded as taking place in two or three principal stages, frequently appearing to follow zero-order chemical kinetics, the situation in which an equal number of bonds are broken in a given length of time. Although these characteristics have been reported in the past—whether the degradation is essentially thermal, hydrolytic, photolytic, or photochemical in character—this concept of deterioration has not been widely stressed in the literature on conservation. In addition to reviewing the major publications on the subject, examples are provided from the literature and from recent laboratory findings concerning ways in which kinetic analysis may provide new insights into the process of cellulose deterioration under the influence of heat and light.

ACID-CATALYZED HYDROLYTIC DEGRADATION of cellulose proceeds according to the principles of chemical kinetics. Nonetheless, concepts of kinetics have not been widely applied in the literature concerning the conservation of cellulosic materials. Thirty years ago, McBurney (*1*) provided an excellent exposition of this subject. We will review the subject in the light of developments since that time (*2*) and will present examples from the literature and from our own work to illustrate ways in which an analysis of the kinetics of chain scission can help conservators better understand the deterioration of cellulose-based materials.

Experimental

Exposure of Bleached Pulp. Bleached pulp, based on 50% hardwood and 50% softwood kraft, jordaned to a Canadian standard freeness of 300–350 mL, was kindly supplied by Andrew Chase of the University of Maine. Unaged handsheets made from this pulp contained 85% α-cellulose (*3*) and 5% hot-1%-alkali-soluble matter (*4*). In the experiment illustrated in Figure 1, sheets were exposed in the Atlas 6500-W xenon-arc Fade-ometer equipped with Pyrex-glass filters; the air temperature was 31 °C, and the relative humidity was 27%; the black-panel temperature was 65 °C. Halfway through the reported period of

0065-2393/86/0212-0329$06.00/0

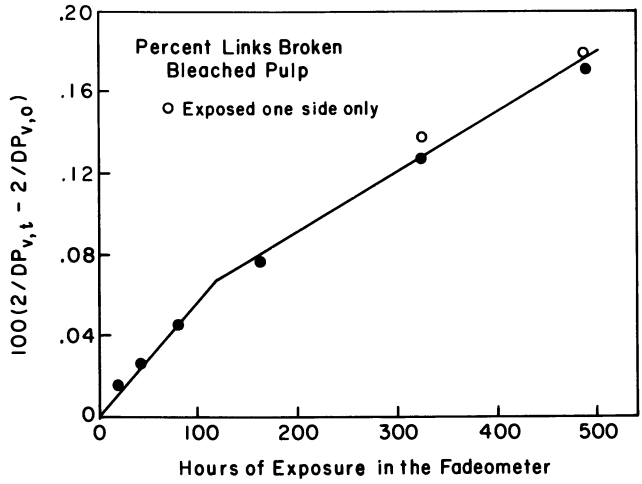

Figure 1. Change in $2/DP_v$ with time of exposure of bleached-sulfate-pulp handsheets in xenon-arc Fade-ometer.

exposure, sheets were turned over to ensure that both sides were equally exposed. This procedure made such little difference in the plots of the simplified rate equation used that handsheets were exposed on one side only in subsequent experiments.

Oxidation of Pulp. In the experiment reported in Figure 2, the bleached pulp stock was chemically modified prior to the formation of handsheets. The stock was first oxidized by dichromate as follows: After a short period of pretreatment in a 0.2 N solution of oxalic acid at a pulp consistency of 3%, the pulp was filtered and potassium dichromate was added to yield a 0.1 N solution. The pulp was allowed to react at room temperature for 30 min and then was filtered and washed. Thereafter the oxidized pulp was soaked overnight in oxalic acid and then was filtered and washed again.

Following chromate oxidation, the pulp was divided. One part was further oxidized by soaking the pulp overnight at 2% consistency in chlorous acid. The other portion was reduced by soaking it overnight in a 0.01 M solution of sodium borohydride (SBH). After these treatments, the samples were washed, and handsheets were prepared.

Carboxyl content was determined by the magnesium-ion-exchange method (*5*). For chlorous acid-treated pulp, the carboxyl group concentration was found to be 14.8 meq/100 g; for sheets reduced with SBH, the carboxyl group concentration was 3.4 meq/100 g. Neither had any significant aldehyde group content; the copper number (*6*) of the chlorous acid sheets measured 0.9 meq/100 g; that of the SBH sheets measured 0.3 meq/100 g.

Handsheets were exposed in the Fade-ometer for periods up to 299.0 h.

Thermal Degradation. Whatman No. 42 ashless filter paper has a basis weight of 92 g/cm^2, an α-cellulose content of 98%, and a solubility in hot 1%

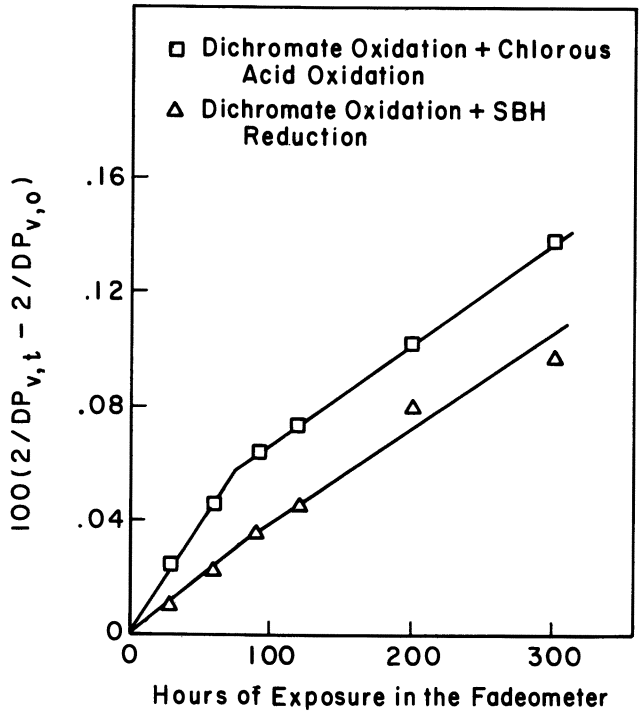

Figure 2. Change in $2/DP_v$ *with time of exposure. Photochemical deterioration of bleached-pulp handsheets, both oxidized and SBH reduced, in Fade-ometer.*

sodium hydroxide of 1.5%. Test sheets were first exposed under BLB fluorescent black lights. The lamps, which emit primarily near-UV radiation, were mounted 3½ in. above the samples. In the paper-testing room maintained at 50% rh and 21.1 °C (70 °F), the temperature of sheets under the bank of lamps reached about 24 °C.

After exposure to the BLB lamps, the papers were thermally aged at 90 °C and 50% rh for 3–30 days.

Viscosity Determination. Viscosities were measured in 0.5 M cupriethylenediamine (CED) at 25 °C with a Cannon-Fenske viscometer, size 100 (7). From these measurements, the intrinsic viscosity was determined according to the American Society for Testing and Materials (ASTM) Standard D1795. Values for the viscosity-average degree of polymerization were obtained by multiplying the intrinsic viscosity by 190.

All samples were first reduced with SBH to minimize possible degradation of the aged pulps which might occur during measurement of viscosity because of the presence of alkali-sensitive linkages. The paper was weighed, disintegrated in a blender, and dispersed in a 0.04% solution of SBH. At a pulp consistency of 0.2%, the suspension was left overnight, filtered, and washed. The pulp cake was then ready to be dissolved in the CED solution.

Kinetic Laws

For many years it has been the custom to follow the degradation of cellulose simply by measuring the fall in viscosity, as illustrated in Figure 3 (*8*). A number of researchers have pointed out, however, that it is not the intrinsic viscosity but the inverse, the intrinsic fluidity (more precisely, the inverse of the degree of polymerization), that is the significant unit to use in studying the degradation of linear polymers; this measurement is related to the number of bonds broken (*9–12*). Thus, McBurney (*1*) pointed out that, when the data in Figure 3 are plotted in terms of the change in intrinsic fluidity, the results demonstrate clearly that no decrease occurs in the rate at which the chains are being broken (Figure 4). Moreover, chain breakage is occurring at identical rates both in the case of the high-molecular-weight surgical cotton and the hydrocellulose of lower molecular weight.

If one considers the number of bonds between monomer units in a

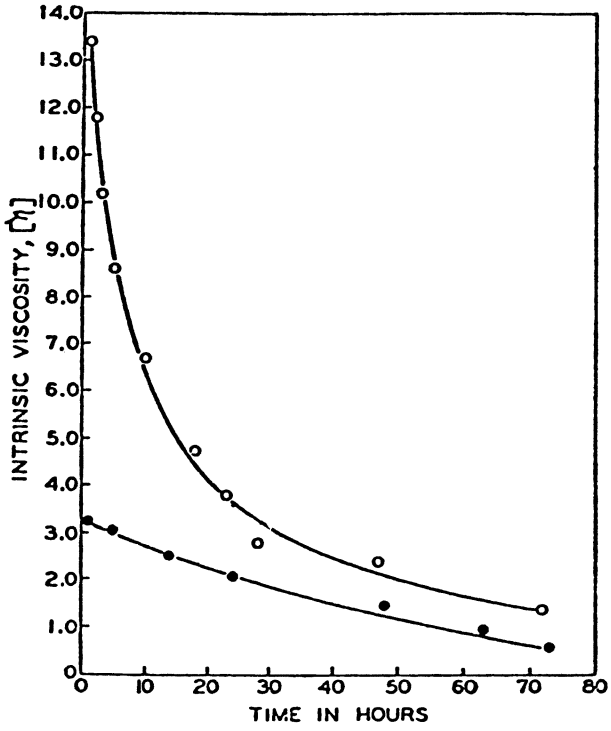

Figure 3. Change in intrinsic viscosity of cellulose during homogeneous hydrolysis in H_3PO_4 solutions at 20 °C. Key: ○, surgical cotton; ●, hydrocellulose. (Reproduced with permission from Ref. 1. Copyright 1954 Wiley.)

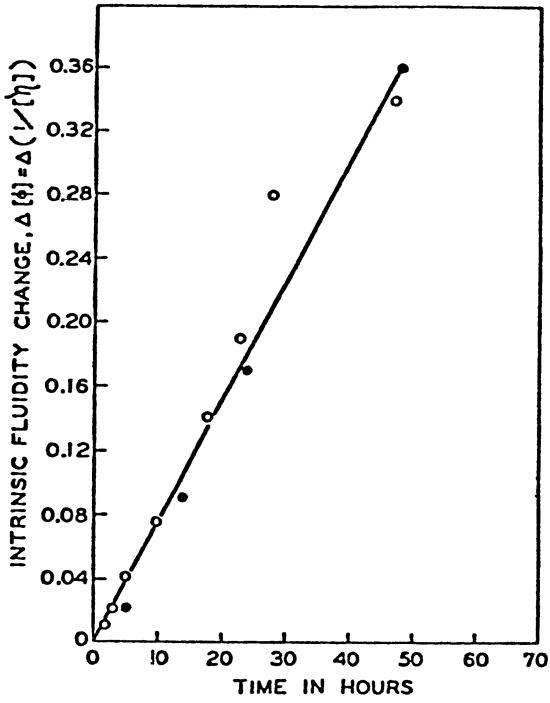

Figure 4. Data in Figure 3 plotted in terms of intrinsic fluidity. Key: ○, surgical cotton; ●, hydrocellulose. (Reproduced with permission from Ref. 1. Copyright 1954 Wiley.)

linear chain polymer that may be broken per unit of time, expressed in terms of the total number available, N, one may propose that random scissioning of bonds obeys a first-order kinetic rate law:

$$dN/dt = k'N \tag{1}$$

where t is the time and k' is the observed rate constant. This relationship may also be expressed in terms of the fraction of the total number of available bonds, $1 - 1/DP_n$, where DP_n is the number-average molecular weight:

$$d(1 - 1/DP_n)/dt = k'(1 - 1/DP_n) \tag{2}$$

The integrated form of this equation yields the familiar linear first-order rate equation in which ln stands for the logarithm to the base e, and the subscripts o and t refer to the initial value of DP_n and to the value at any time, t, respectively:

$$\ln(1 - 1/DP_{n,o}) - \ln(1 - 1/DP_{n,t}) = k't \quad (3)$$

At very low degrees of degradation, when only a small fraction of the bonds have been broken, Equation 3 can be simplified (*1*) to yield

$$1/(DP_n)_t - 1/(DP_n)_o = \alpha kt \quad (4)$$

The factor α is a measure of the accessibility of the bonds (*13*), and k is the specific rate constant for the rate of breaking of normal 1C–O–4′C bonds in the anhydroglucose chain (k' in Equations 1–3 equals αk). The expression $100[1/(DP_n)_t - 1/(DP_n)_o]$ gives the percentage of the initial number of bonds that have been broken. Equation 4 is also the equation that would apply if an equal number of bonds were broken in equal periods of time, that is, at a constant rate of chain scissioning (zero-order kinetics). Conformance to Equation 4, therefore, cannot be taken as proof of first-order kinetic behavior (*12*).

Many researchers have employed Equation 4 to follow the early stages of degradation of cellulose and other linear polymers and have applied Equation 3 when extending the investigation ot an advanced state. [Since the meeting of the International Council of Museums (ICOM) Committee on Conservation in Leningrad and Moscow, 1963 (ICOM Report 63–24), L. Santucci has been using a function of the type $\log (F_o/F) = a(1/DP - 1/DP_o)$ to express changes in DP and folding endurance, F (*14*, *15*).] Figure 5 shows a typical set of curves, plotted according to Equation 4, taken from the work of Daruwalla and Narsian (*16*), concerning the heterogeneous hydrolysis of cotton and of regenerated cellulose in 1 N hydrochloric acid. As these and other researchers have pointed out, the results are typical of the kinetic data related to the degradation of paper and textiles; the course of the heterogeneous degradation of cellulose by acid hydrolysis, and by photochemical and enzymatic attack as well, seems to display two distinct stages: a fast initial stage followed by a significantly slower one (*17*, *18*).

One may suggest that there are not two but at least three major stages in the overall hydrolytic degradation of cellulosic fibers, extending from the initial attack to the final point when all of the cellulosic material has been converted to soluble fragments. The first, rapid stage is considered to represent an attack on a small fraction of the 1C–O–4′C bonds in the cellulosic chain that are particularly sensitive to scissioning. These have frequently been designated as weak links. The second, slower stage essentially represents the attack on the normal 1C–O–4′C bonds located in the amorphous regions of the fibers. The final major stage represents the much slower rate of attack on the cellulose that is bound into the crystallite bundles or zones that usually make up a significant fraction of the fibers. This last stage of hydrolytic attack

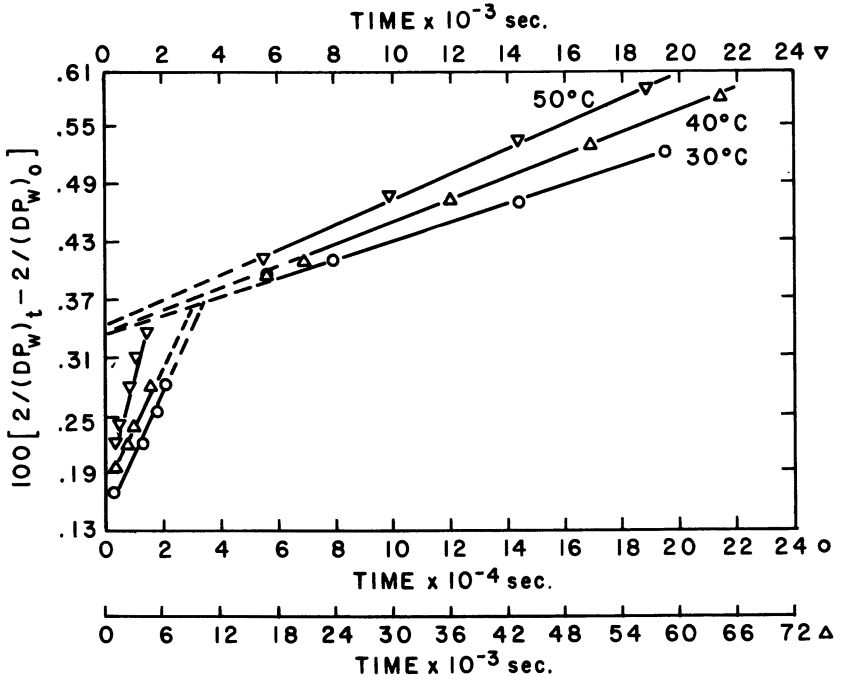

Figure 5. Data regarding heterogeneous hydrolysis of regenerated cellulose in 1 N hydrochloric acid at different temperatures. (Reproduced with permission from Ref. 16. Copyright 1966 TAPPI.)

begins at a condition close to the leveling off degree of polymerization (LODP) (*19, 20*). We will review the evidence that supports these concepts.

The Rapid Initial Stage

Perhaps it would be convenient to label the initial stage of hydrolytic degradation as the weak-link stage. However, this label tends to focus attention on the possible existence of a specific type of chemical bond and thus draws consideration away from other factors that may influence the phenomenon. Instead, we prefer to call the first stage simply the rapid initial stage, regardless of what may prove eventually to be its cause or causes.

In the 1940s and 1950s, a distinguished body of research grew out of the attempts of researchers (*2, 8–11*) to demonstrate that certain links in cellulose were particularly sensitive to rupture. Many speculated as to what these links might be. Eventually it was shown that none of the especially weak links were apparent when the hydrolysis was carried out under homogeneous conditions, such as can be accomplished by dissolv-

ing the cellulose in concentrated phosphoric acid. Under the conditions of heterogeneous hydrolysis, however, a modest number of highly sensitive linkages could be demonstrated. These are now thought to be the result of physically induced strains in the bonds (*19*, *21*).

As these concepts were being developed, Marchessault and Rånby (*22–24*) came to believe that the presence of oxidized groups in the pyranose rings would also be the cause of an increased ease of hydrolysis, attributable to inductive effects of the neighboring 1C–O–4′C bond. Figure 6 illustrates Rånby's (*24*) demonstration, in the case of oxidized cotton cellulose degraded under homogeneous conditions, of a rapid initial stage of hydrolysis, a phenomenon that could practically be eliminated by SBH reduction. He also demonstrated a similar effect of SBH in the case of wood cellulose (Figure 7).

An initial period of rapid hydrolysis is usually most apparent during

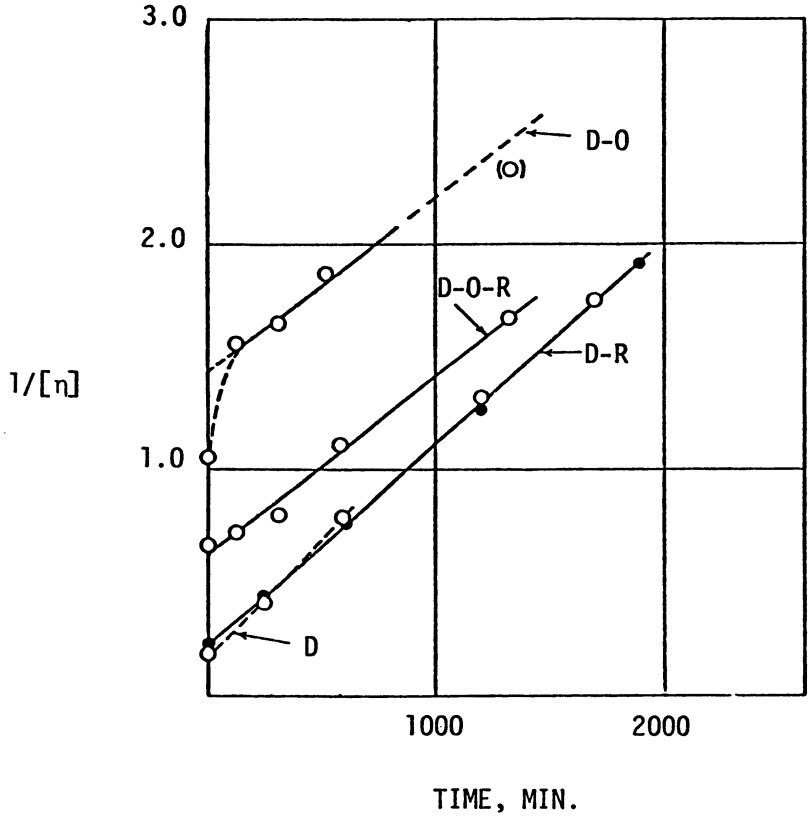

Figure 6. Rate of homogeneous hydrolysis of cotton cellulose in 81.25% phosphoric acid (D), chromate-oxidized cellulose (O), and SBH-reduced cellulose (R). (Reproduced with permission from Ref. 24. Copyright 1961 Wiley.)

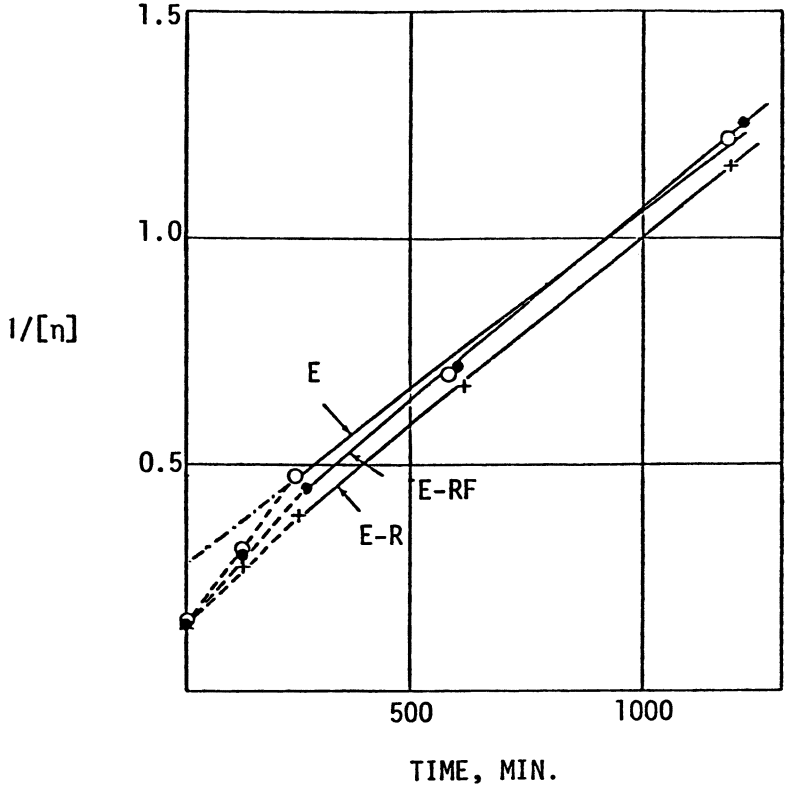

Figure 7. Rate of homogeneous hydrolysis in 81.25% phosphoric acid, expressed in terms of intrinsic fluidity, 1/[η]. Key: E, purified wood cellulose; RF, SBH-treated cellulose reduced in fiber form; and R, SBH-treated cellulose reduced as a gel. (Reproduced with permission from Ref. 24. Copyright 1961 Wiley.)

the heterogeneous hydrolysis of cellulose regenerated from solution. As many as 12–28 particularly sensitive links per 10,000 normal bonds can be introduced, apparently because of physical strains at the folds in the cellulosic bundles (*11, 13, 21, 24*). The relative rate of breaking these strained bonds is said to be about 10,000 times the rate of normal 1C–O–4′C bonds. In contrast, Rånby's (*24*) bonds that were sensitized by the inductive effects of neighboring oxidized units, observed during homogeneous hydrolysis, appear to be only about three to four times more sensitive than the normal bonds.

The Second Stage: Accessibility

In plots of the inverse of DP_n against time during heterogeneous hydrolysis, a second stage is usually observed in which scissioning also appears

to be linear with time, although it proceeds at a noticeably slower rate. Sharples (*11*) has suggested that this second stage represents the breaking of the 1C–O–4′C bonds between the normal anhydroglucose units located in the amorphous regions of the fibers. Because the amorphous component represents only a fraction of the total fiber, the observed scissioning will appear to take place at a lower overall rate than would be the case if all bonds were equally available. During this second stage the ratio of the observed rate, k', relative to the rate of breaking of bonds in cellopentaose (a soluble cellulose polymer), k, is considered to represent the accessibility, α, of the particular cellulose fiber under test (*see* Equation 4) (*11*). On this basis, the accessibility of cotton is found to be about 9–20%. In contrast, cotton that has been swollen by various treatments prior to hydrolysis can yield accessibility values from 22% to as high as 67%. Such figures agree qualitatively with the percentage of amorphous material in the fibers determined by methods such as moisture regain and X-ray diffraction.

If one considers the rate of hydrolysis of wood cellulose, in which the degree of crystallinity may be lower than in cotton fibers and in which bonds involving units other than glucose, such as xylose and mannose, may be present, the inherent rate of breaking of bonds in the proposed second stage can be expected to be greater than in the case of pure cellulose. A number of workers have pointed out that wood cellulose, under homogeneous conditions, is indeed hydrolyzed at a greater rate, as clearly displayed in Figure 8 (*2*). These data and Rånby's (*24*) data indicate that scissioning in wood cellulose occurs as much as two times faster than in cotton.

Whether one can effectively analyze the first or the second stages of scissioning in terms of weak links or of greater accessibility, or whether both factors contribute to each stage, is a matter for further consideration. Nonetheless, the rate at which 1C–O–4′C bonds are broken in the second stage is expected to be influenced in a major way both by accessibility and by the presence of bonds involving pentoses and hexoses other than glucose.

The Final Stage: Attack on Crystallites

In the earliest investigations of hydrolysis, it was readily observed that the *DP* of the cellulose fell rapidly to a low value, commonly designated as the leveling off degree of polymerization (LODP), beyond which further degradation proceeds at an extremely slow rate (*19,20*). Modern theories of fiber structure envision that the chains of cellulosic molecules are arranged in ordered and in disordered regions and that, furthermore, in the highly ordered regions the chains are aligned in small zones or regions that are called crystallites. These crystalline regions are pictured

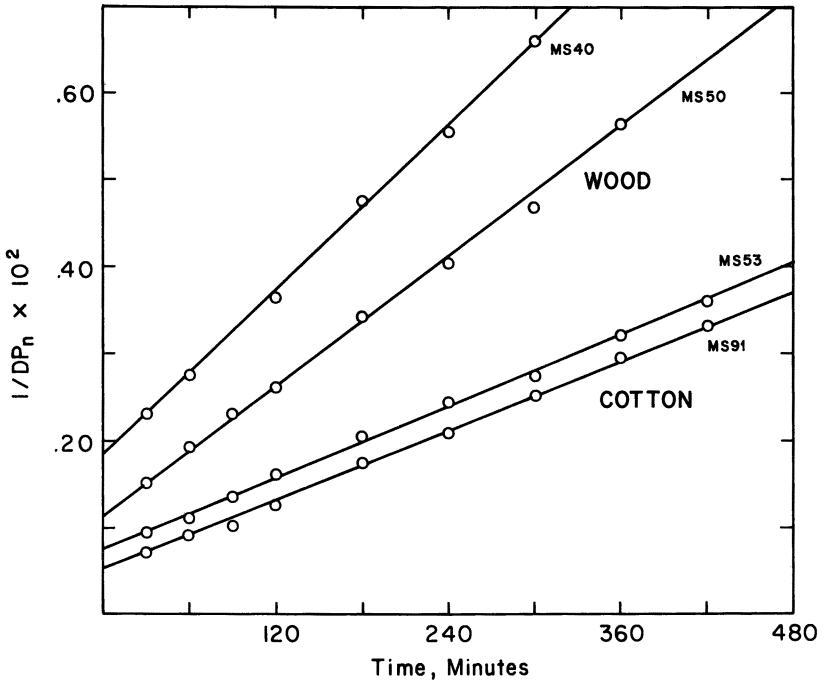

Figure 8. Homogeneous hydrolysis in phosphoric acid, illustrating enhanced rate for wood pulp (MS40, 50) compared to that of cotton samples (MS51, 91). (Reproduced with permission from Ref. 2. Copyright 1971 Wiley.)

as involving chain segments that have been folded back and forth upon themselves to form relatively discrete bundles. As a first approximation, the average length of the chain segments in the aligned bundles corresponds to the LODP. Thus, when hydrolytic attack has thoroughly disintegrated the material in the amorphous region, the so-called microcrystalline cellulose consisting largely of the described crystallite bundles is left. Within these, scissioning proceeds at a much slower rate and depends in part on the size of the crystallites. Further attack is on their surfaces; therefore, disintegration is fastest for the residue of fibers such as rayon, which normally have LODP values below 100, and is much slower for the residual material from cotton, which frequently has an LODP of around 200 (number average) (*20*).

Stages in Deterioration

In recent years, our laboratory has begun to stress that the deterioration of organic materials rarely takes place uniformly in time but tends instead to occur in stages (25). It is natural to ask if one or more of the

stages just outlined is of practical significance to the conservator. We believe they are. The stages described here, however, are not related to those observed in autoxidation; the stages in autoxidation usually involve a different reaction mechanism.

Figure 9 shows the 1943 data of Davidson (*26*) on the hydrolysis of cotton cellulose at 20 °C. The increase in fluidity with time suggests three stages: the period between points O and A may represent the rapid, initial, weak-link stage; that from A to B may represent the attack on the normal 1C-O-4′C bonds; and that from B to C may represent the slow-

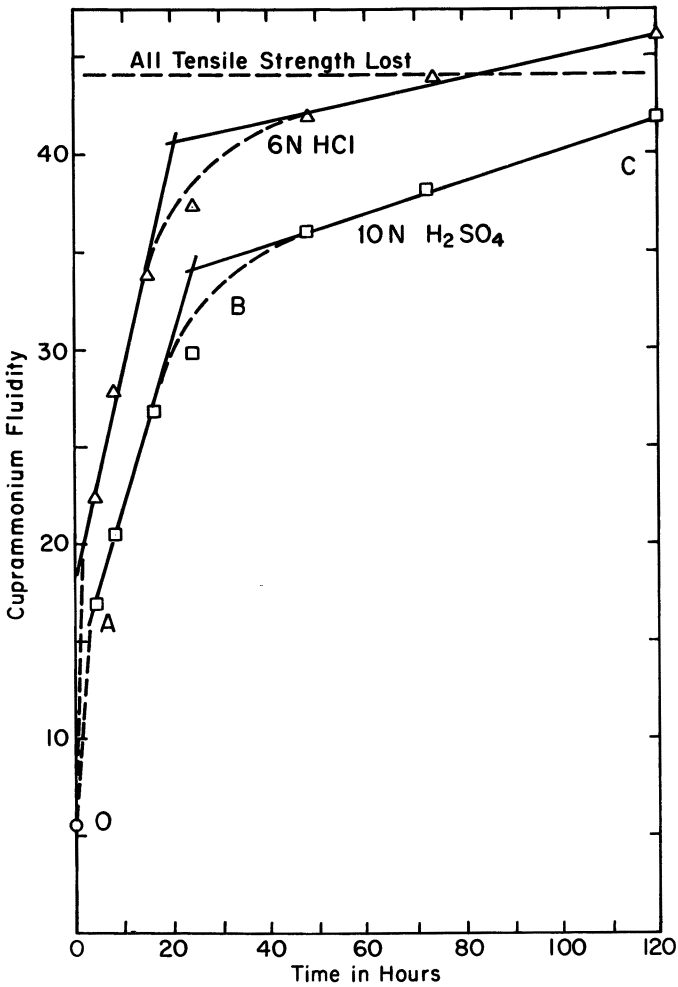

Figure 9. Data showing the change in cuprammonium fluidity of cotton cellulose in acids at 20 °C. (Reproduced with permission from Ref. 26. Copyright 1943.)

ing down period as disintegration approaches the LODP. Davidson (*26*) reported that tensile strength became negligible at a fluidity of about 45; Figure 9 shows that the proposed stages occur before all strength is lost.

Daruwalla and Narsian (*16*) regarded two stages to be of practical importance. They stated (*16*), "For all the fiber substances examined, that is, cotton, cotton treated with swelling agents, and cellulosic substances regenerated from different solvents, there exists two rates of heterogeneous hydrolysis. . . . The initial apparent rate of acid action (K_1) is about 1600–2300 times higher than that of the subsequent stage of hydrolysis (K_2)." Their principal findings regarding the heterogeneous attack on regenerated cellulose, illustrated in Figure 10, indicate two-stage behavior for enzymatic and acid-catalyzed hydrolysis, as well as for decomposition by 2540-Å radiation.

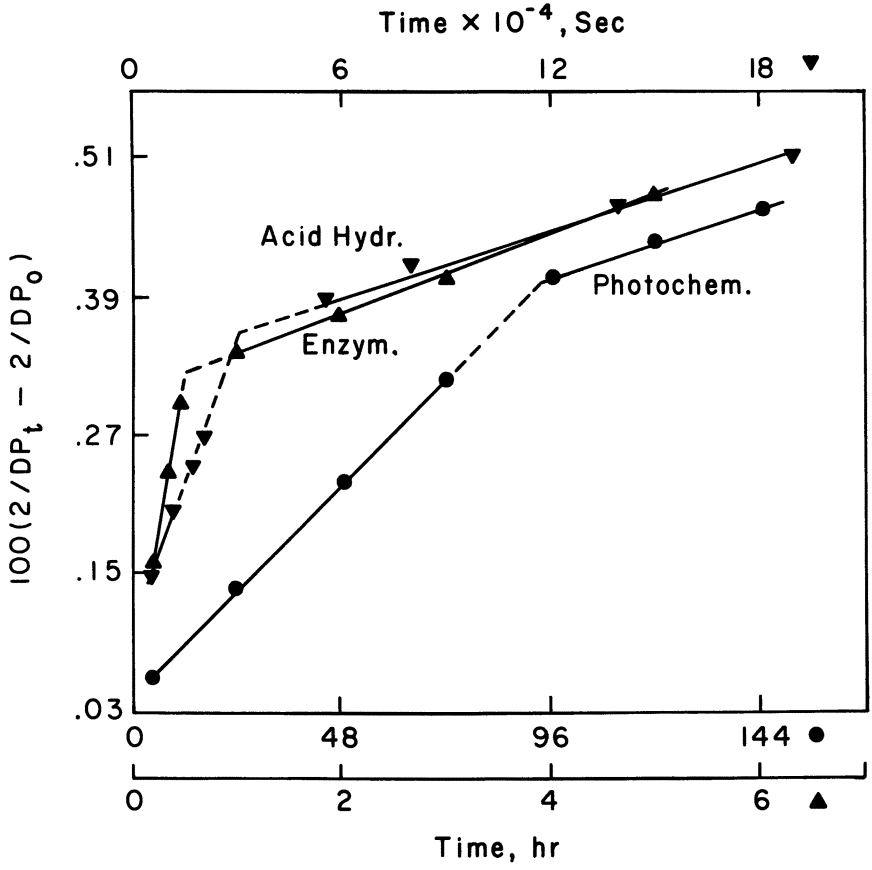

Figure 10. Data on the heterogeneous acid hydrolysis, enzymatic hydrolysis, and photochemical decomposition of regenerated cellulose. (Reproduced with permission from Ref. 16. Copyright 1966 TAPPI.)

The numbers on the vertical axis of Figure 5, and in Figures 1, 2, and 10–12, refer to the percentage of bonds broken. One may evaluate the extent of degradation at any point in these curves by recalling the percentage of 1C–O–4′C bonds that need to be broken in cotton automobile-tire cords before all strength is lost, a subject investigated by Conrad et al. (*27*) in 1951. Essentially using Equation 4, they came to the conclusion that only 0.3% of the bonds in cotton cords needed to be broken before complete loss of strength occurred. Upon consideration one finds that the calculations that led to this conclusion were based on viscosity-average molecular weights, DP_v. Hence, we may estimate, based on number-average molecular weights, DP_n, that the figure should be twice this percentage, or about 0.6%. From Figure 10, we see that the apparent break in the curves occurs when only about 0.33–0.39% of the bonds have broken. Thus, we have additional confirmation that the observed change in rate takes place well before all useful strength is lost.

The two segments in the curves in Figures 5 and 10 may represent the proposed second stage and the beginning of the third, marked-slowdown stage as the LODP is approached; the breaks occurred at DP_v levels between 400 and 470 (*16*), close to reported values of LODP in cotton ($DP_n = 200$–235).

Stages also seem to occur during thermal degradation at high temperatures (*28*). Figure 11, taken from the work of Shafizadeh and Bradbury (*29*), indicates three stages before a DP_n of 200 is reached. Shafizadeh and Bradbury (*29*) described their results as follows: "An initial small deviation (possibly due to some weak links) is followed by a linear portion, indicating random bond scission, and then a slackening off in the rate of DP_n decrease occurs beginning at $DP_n \simeq 250$, corresponding to a $DP_w = 500$."

Results

Several years ago we began to express the results of our thermal and photochemical degradation experiments in terms of Equation 4. Figure 1 shows some of the initial data obtained, relating to exposure of test sheets in the Fade-ometer. Just as Daruwalla and Narsian (*16*) observed, there seems to be a break in the curve. If the first stage indeed represents weak links, about 3 such bonds per 10,000 in the original cellulosic chain (0.03%) are apparent, a figure similar to the fraction of labile acid-sensitive links determined by Sharples (*21*) and labile photochemically sensitive links reported by Daruwalla (*16*) when radiation at 2540 Å was used.

Figure 2 shows the results of a second photochemical study. Handsheets made from bleached sulfate pulp were first oxidized with dichromate solution and then with chlorous acid; following dichromate oxida-

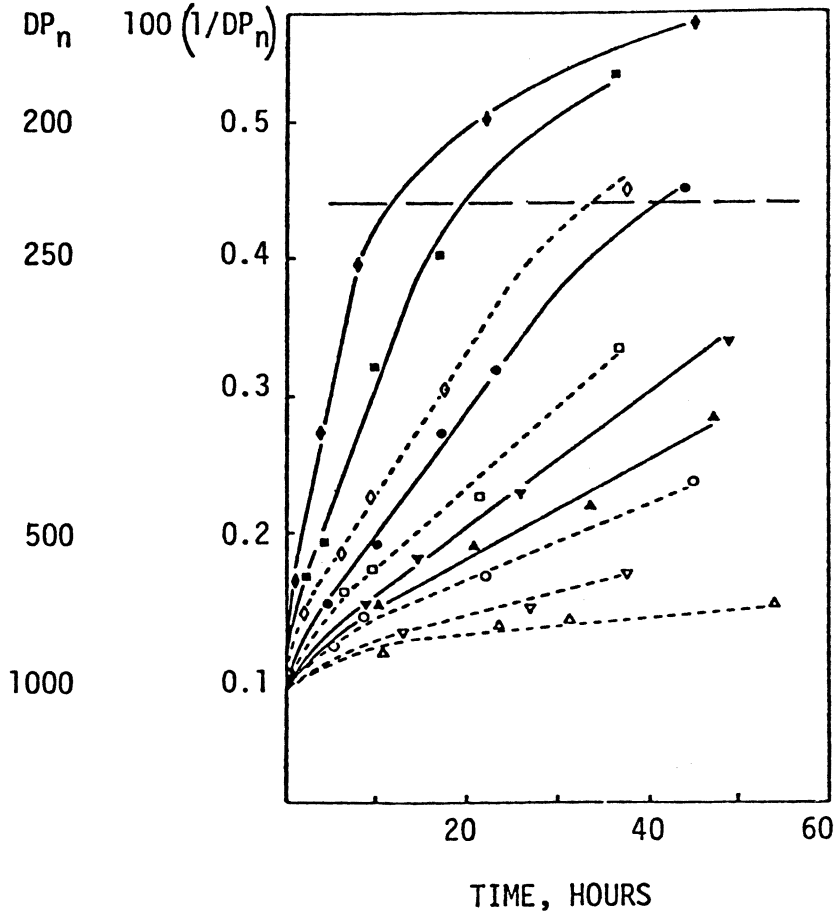

Figure 11. Change in $1/DP_n$ with time for cellulose heated in air and in nitrogen at 150–190 °C. Key: open symbols represent N_2; filled symbols represent air; △, ▲, 150 °C; ▽, ▼, 160 °C; ○, ●, 170 °C; □, ■, 180 °C; ◇, ◆, 190 °C. Reproduced with permission from Ref. 29. Copyright 1979 Wiley.)

tion, the pulp was reduced with SBH. The data again suggest a rapid initial stage followed by a slower one. Moreover, after SBH reduction, intended to remove carbonyl groups that might be the cause of increased sensitization of neighboring 1C–O–4′C links, we found the initial stage practically eliminated. This finding corresponds to related findings of Rånby for homogeneous hydrolysis (Figures 6 and 7) (*24*).

Figure 12 shows results of a thermal-aging experiment. Sheets of Whatman No. 42 filter paper were first exposed to near-UV radiation (BLB fluorescent black lights), after which they were subjected to oven

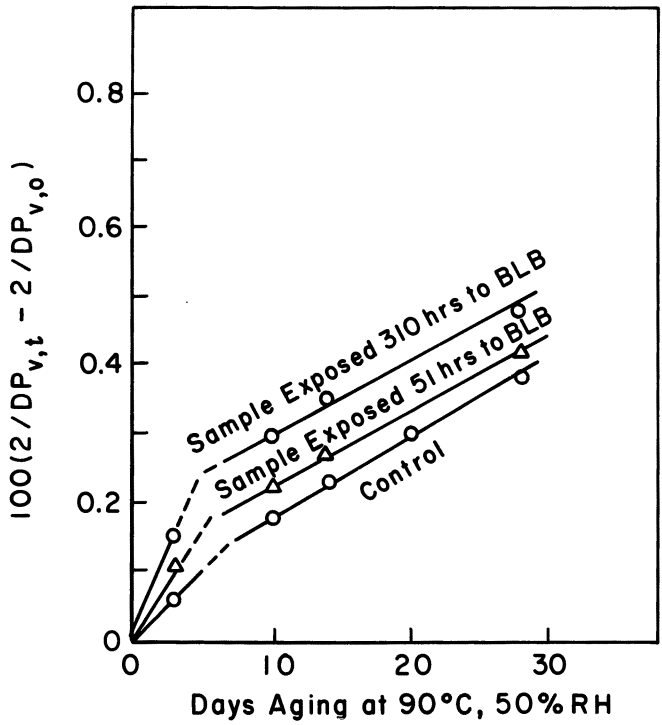

Figure 12. Change in $2/DP_v$ *during thermal degradation of Whatman No. 42 filter paper previously exposed to near-UV radiation (BLB fluorescent black lamps), compared to control sample.*

aging. The longer the period of exposure was, the greater the postulated initial stage. If one considers the later data points to represent a linear rate of chain breaking, then the intercepts at time zero imply that a certain fraction of the bonds were particularly sensitive to rupture, perhaps because of a rapid initial stage that occurred before less than 0.2% of the bonds were broken, well in advance of the loss of all useful strength.

Exposure to near-UV radiation in air leads to the formation of carbonyl groups on the cellulosic chain (*30*). These groups may weaken neighboring bonds as a result of inductive effects and could thus be the explanation of the increase in the initial stage of thermal deterioration with increased exposure to UV. If the second stage does indeed represent the rate of attack on the normal 1C-O-4′C bonds in the amorphous regions of the cellulose, then it is not surprising that the slopes (the rates of bond breaking) in the later part of the experiment are virtually the same. Kinetic analysis thus seems to provide new insights into the process of deterioration. It is one thing to state simply that exposure to near-

UV radiation causes high-α-cellulose pulps to become more sensitive to thermal deterioration; it is quite another thing to suggest that exposure to light primarily increases the initial rapid stage.

Discussion

To express the results in terms of a few distinctly linear stages is a simplification. We have reviewed a number of factors that can influence the ease of chain scissioning. A point that we have not discussed, however, is the fact that several researchers (*31*, *32*) have suggested that high-molecular-weight native celluloses may have a significant crystallite or chain-dislocation unit of the order of $DP_n = 500$. The overall rate must certainly represent transitions between the predominating influence of one or another of the factors noted.

We further realize that the slowest rate shown in many of the curves here may be an artifact resulting from the use of simplified Equation 4; if Equation 3 is applied, a noticeable break between the end of the second stage and the beginning of the final stage (crystallite attack) may be put off to a much more advanced degree of degradation if a discontinuity in the experimental data appears at all.

Whether it is useful to analyze the scissioning of cellulosic chains in terms of two, three, or more stages remains for further investigation. Regardless of what future investigators may conclude, our purpose here has been, first, to remind conservators and conservation scientists that relatively simple means are at our disposal for interpreting the deterioration of cellulose in terms of intrinsic fluidity and the laws of chemical kinetics. In particular, the initial stages of chain scissioning appear to follow zero-order kinetics in which a constant number of 1C–O–4′C bonds tend to be broken in a given length of time. Second, when expressed in these terms, the overall course of bond scissioning can be considered to take place in a number of reasonably well-defined stages.

When nothing remains but microcrystalline cellulose, no physical strength is present. Therefore, the rate of attack during the final stage described here will be of little practical concern to the conservator. Nonetheless, if the course of degradation is plotted in accordance with Equation 4, the onset of this last stage, an apparent slowdown as the LODP is approached, may indeed begin before all practical strength is lost.

Although the concepts outlined in this chapter are particularly appropriate for the interpretation of hydrolytic deterioration of cellulose, they show promise as an aid in the interpretation of thermal, photochemical, photolytic, and enzymatic degradation as well. Equations 3 and 4 are generally applicable to the scissioning process in linear polymers (*33*, *34*).

Acknowledgment

The Research Center gratefully acknowledges the assistance of a grant from the National Endowment for the Humanities to facilitate the preparation of an annotated bibliography concerning this topic and two related topics, which is planned for publication elsewhere.

Literature Cited

1. McBurney, L. F., In "Cellulose and Cellulose Derivatives", Part I; Ott, E.; Spurlin, H. M.; Grafflin, M. W., Eds.; Interscience: New York, 1954; p. 99.
2. Sharples, A., In "Cellulose and Cellulose Derivatives", Vol. V; Part V; 2nd ed.; Bikales, N. M. and Segal, L., Eds.; Wiley: New York, 1971, pp. 991-1006.
3. TAPPI Standard T203 os-74, "Alpha-, Beta-, Gamma-Cellulose in Pulp".
4. TAPPI Standard T212 os-76, "One Per Cent Sodium Hydroxide Solubility of Wood and Pulp"
5. Sjöström, E.; Haglund, P. *Svensk Papperstidn.* **1961**, *64*, 438.
6. TAPPI Standard T430 os-75, "Copper Number of Pulp, Paper, and Paperboard".
7. TAPPI Standard T230 os-76, "Viscosity of Pulp (Capillary Viscometer Method)".
8. Hiller, L. A., Jr.; Pascu, E. *Text. Res. J.* **1946**, *16*, 564-70.
9. af Ekenstam, A. *Ber. dtsch. Chem. Ges.* **1936**, *69*, 553-59.
10. Schulz, G. V.; Löhmann, H. J. *J. Prakt. Chem.* **1941**, *157*, 238-82.
11. Sharples, A. *J. Polym. Sci.* **1954**, *14*, 95-104.
12. Bryce, W. A. J.; Greenwood, C. T. *J. Polym. Sci.* **1957**, *25* (111), 480-83.
13. Sharples, A. *J. Polym. Sci.* **1954**, *13*, 393-401.
14. Santucci, L. *Boll. Ist. Patol. Libro* **1963**, *22*, 67.
15. Ibid. **1966**, *25*, 51.
16. Daruwalla, E. H.; Narsian, M. G. *Tappi* **1966**, *49* (3), 106-111.
17. Daruwalla, E. H.; D'Silva, A. P.; Mehta, A. C. *Text. Res. J.* **1967**, *37* (3), 147-60.
18. Daruwalla, E. H.; D'Silva, A. P.; Tandon, G. N. *Text. Res. J.* **1967**, *37* (3), 160-71.
19. Chang M. M. Y. *J. Polym. Sci.* **1974**, *12*, 1349-74.
20. Millett, M. A.; Moore, W. E.; Saeman, J. F. *Ind. Eng. Chem.* **1954**, *46*, 1493-97.
21. Michie, R. I. C.; Sharples, A.; Walter, A. A. *J. Polym. Sci.* **1961**, *51*, 85-98.
22. Marchessault, R. H.; Rånby, B. G. "Weak Links as Inductive Effects in the Hydrolysis of Cellulose", Proceedings 2nd Cellulose Conference, Syracuse, 1959; pp. 33-52.
23. Marchessault, R. H.; Rånby, B. G. *Svensk Papperstidn.* **1959**, *62*, 230-240.
24. Rånby, B. G. *J. Polym. Sci.* **1961**, *53*, 131-40.
25. Feller, R. L. In "Preservation of Paper and Textiles of Historic and Artistic Value"; Williams, J. C., Ed. ADVANCES IN CHEMISTRY SERIES No. 164, American Chemical Society: Washington, D.C., 1977; pp. 314-35.
26. Davidson, G. F. *J. Text. Inst.* **1943**, *34*, T87-T96.
27. Conrad, C. M.; Tripp, V. W.; Mares, T. *Text. Res. J.* **1951**, *21*, 726-39.
28. Fung, D. P. C. *TAPPI* **1969**, *52*, 319-21.
29. Shafizadeh, F.; Bradbury, A. G. W. *J. Appl. Polym. Sci.* **1979**, *23*, 1431-42.

30. Reine, A. H.; Arthur, J. C., Jr. *Text. Res. J.* **1970**, *40*, 90.
31. Elema, R. J. *J. Polym. Sci. Symp. 42* **1973**, 1545–62.
32. Max-Figini, M.; Coun-Matus, M. *Makromol. Chem.* **1981**, *182*, 3603–16.
33. Montrol, E. W. *J. Am. Chem. Soc.* **1941**, *63*, 1215–20.
34. Davis, A.; Golden, J. H. *Die Makromol. Chem.* **1964**, *78*, 16–23.

RECEIVED for review November 26, 1984. ACCEPTED March 13, 1985.

19

Fourier Transform IR Spectroscopy and Electron Spectroscopy for Chemical Analysis

Use in the Study of Paper Documents

David N.-S. Hon

Department of Forestry, Clemson University, Clemson, SC 29631

Theories and instrumentation of Fourier transform IR spectroscopy and electron spectroscopy for chemical analysis are briefly reviewed. The possibility of using these techniques in detection and analysis of acid impurities distributed at surfaces of paper documents produced during the period from 1790 to 1983 is demonstrated. Results show that all of the papers tested contained carboxylic groups. The carboxylic acids found in the paper of 1790 are the results of oxidation and aging. Acids in other papers are due to fiber oxidation as well as the presence of rosin acids. These techniques show promise as nondestructive methods for elucidating chemical characteristics of surfaces of paper documents.

PAPER-MAKING TECHNOLOGY has undergone extensive development in the past 200 years. The change of fiber resource from cotton and linen rags to wood fibers and the use of alum rosin sizes have significant adverse effects on the permanence and durability of paper materials (*1*). For example, the presence of hemicelluloses and lignin residues in wood pulps introduces acid impurities. Delignification and bleaching of wood fibers inescapably oxidize and degrade cellulose and hemicelluloses. The oxidized products usually contain acidic functional groups. In addition, acidity in paper may increase because of air pollutants it may absorb such as sulfur dioxide and nitrogen dioxide (2). Photooxidative effect can also increase the acidity of paper (3). Unfortunately, these acid impurities are the prime cause of poor aging properties of paper documents. Embrittlement and discoloration of paper documents in storage are aging

0065-2393/86/0212-0349$06.00/0

phenomena caused primarily by "intrinsic" acids present in the paper or formed later in the paper during storage (*4*).

The measurement of acidity in paper documents with cold- and hot-water extraction frequently distorts and damages the paper fibers and printing inks. Many paper conservators and museum curators have long desired a reliable and rapid method for the detection of acidity of paper documents in a nondestructive manner so that they can determine the acidity routinely to screen out valuable book documents for deacidification or other necessary preservation treatments. The objective of this chapter is to introduce two spectroscopic techniques, namely, Fourier transform IR spectroscopy (FTIR) and electron spectroscopy for chemical analysis (ESCA), for chemical analysis of paper surfaces. The effectiveness of these techniques in analyzing and determining the presence of acidic functional groups on paper documents is demonstrated.

Experimental

Materials. Book papers dating from about 1790 to 1983 and provided by the Library of Congress were used. The book documents were selected at approximately 10-year intervals and are listed in Table I. Whatman filter paper was used as a cellulosic sample. The fiber sources of the paper documents were determined by a staining technique developed by Graff (*5*). The aluminon test (*6*) and Raspail test (*7*) were performed to determine the presence of alums and rosins, respectively, in paper documents. For comparison purposes, pH values of paper documents were obtained by cold-distilled-water extraction of 1 g of paper for 1 h.

Table I. Selected Book Documents for Study

Year	*Title*
1790	Tableau General de L'Empire Othoman
1834	Report from the Select Committee on the Expedition to the Arctic Seas
1871	Annual Report of the Commissioner of Patents, Volume I
1881	*The Federal Reporter,* Volume 5
1891	*The Federal Reporter,* Volume 46
1899	*Transactions of the American Society of Civil Engineers,* Volume XLI
1909	*Le Monde Actuel*
1920	*Tier-Chemie, Volume 3*
1929	The Encyclopedia Britannica (14th Edition)
1939	*The Scientific Monthly,* Volume XLIX
1949	*Waveforms*
1959	Information Transmission, Modulation, and Noise
1969	Chemical Reactions in Solvents and Melts
1978	Search for Identity
1983	Physical Chemistry

Measurements. A Nicolet 20DX FTIR spectrometer was used to obtain 2-cm^{-1} resolution spectra for the 4600-400-cm^{-1} region. The spectrometer was equipped with a liquid-nitrogen-cooled mercury-cadmium-telluride detector. The sample chamber was allowed to come to equilibrium with a continuous nitrogen purge prior to data collection. A Harrick fixed-angle attenuated reflectance attachment with an internal reflectance crystal made of thallium bromoiodide (KRS-5, 45° face-out angle) was used.

ESCA spectra were measured with a Du Pont model 650 electron spectrometer with a MgKα X-ray source, equipped with a multichannel analyzer and data-reduction system. The samples were analyzed for the carbon ls (C_{ls}) and oxygen ls (O_{ls}) peaks. When energy excitements for particular functionalities were made, the C_{ls} peak for hydrocarbon species was used as the reference and was assigned the value of 285.0 eV to compensate for the charging effect. The C_{ls} peaks were analyzed by digitizing them and then using a curve-fitting procedure (*8*).

Background

In the past, although FTIR and ESCA were known to offer a great deal of information on specific chemical functional groups of surfaces, little application was made of these analytical tools in the field of conservation and restoration science and technology. A survey of instrumental analysis citations since 1953 in the conservation literature showed that only one FTIR work was published in *Studies in Conservation* in 1977 and two ESCA papers were published in *Archaeometry* in 1976. None appeared in Arts and Archaeology Technical Abstracts (AATA).

The purpose of this chapter is to provide scientists and technologists engaging in conservation and restoration research with adequate background material for an understanding of FTIR and ESCA and their chemical applications. I hope that this chapter will generate interest in research using these instruments as routine analytical tools for surface analyses of materials of historic value.

Background on FTIR. IR spectroscopy is one of the most important methods for the identification and characterization of chemical structures (*9–11*). Its greatest use lies in its unique application to the identification of chemical functional groups from vibrational spectra. However, the energy limitations of a conventional IR spectrometer are generally not suitable for polymeric analysis. Fortunately, the energy limitation can be minimized by using interferometers of the Michelson type rather than the conventional prism and grating instruments. This technique is called Fourier transform spectroscopy.

The Michelson interferometer is shown schematically in Figure 1. It consists of two mutually perpendicular plane mirrors, one of which can move at a constant rate along the axis and one of which is stationary. Between the fixed mirror and the movable mirror is a beam splitter where a beam of radiation from an external source can be partially

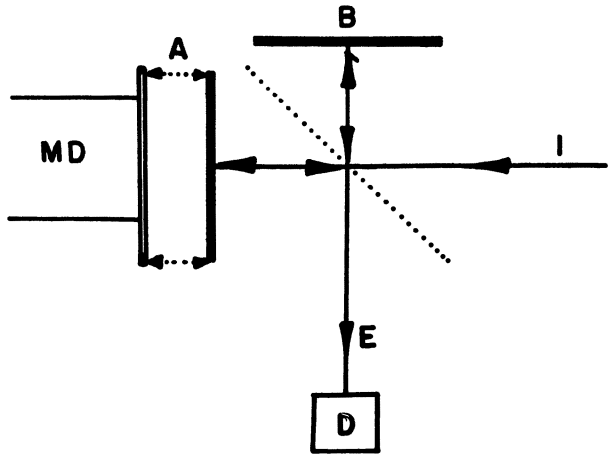

Figure 1. Diagram of a Michelson interferometer. Key: I, unmodulated incident beam; A, moving mirror; B, stationary mirror; E, modulated exit beam; D, detector; MD, mirror drive.

reflected to the fixed mirror and partially transmitted to the movable mirror. After each beam is reflected back to the beam splitter, it is again partially reflected and partially transmitted. Thus, a portion of the beams that traveled in the path to both the fixed and movable mirrors reaches the detector. If the two path lengths are the same, then no phase difference between the beams occurs, and they combine constructively for all frequencies present in the original beam. For different path lengths, the amplitude of the recombined signals depends on the frequency and the distance the mirror moved. For example, low frequencies interfere destructively (they have a phase shift of 180°) for relatively large movements of the mirror, whereas high frequencies require relatively small movements for this condition to occur. The resulting interferogram contains information on the intensity of each frequency in the spectrum. This data can be calculated by a mathematical operation known as the Fourier transform to yield the IR spectrum.

FTIR has several important advantages over conventional methods. The most important of these is the efficient and rapid collection of data. FTIR is also less susceptible to stray radiation. In addition, because a computer is necessary to obtain the Fourier transform, many scans can easily be performed to improve the signal-to-noise ratio (noise adds as the square root of the number of scans, whereas signals add linearly). Digital subtraction (that is, point-by-point subtraction of the separate spectra by a computer) can also be used to produce good difference spectra.

In summary, the important advantages of the FTIR spectrometer are listed as follows:

1. Multiplexing of spectral information (Fellgett's advantage): Information from all frequencies in the spectrum is gathered simultaneously.
2. Enhanced spectral throughput (Jacquinot's advantage): Because no entrance and exit slits of the monochromator are used, the amount of energy falling on the detector is greatly enhanced.
3. Frequency accuracy (Connes' advantage): Because the instrument uses a laser to monitor the position of the moving mirror in the main interferometer, the frequency of the measured spectrum is very accurate.

The IR spectra of solid samples usually are recorded in transmission either by pressing samples into KBr pellets or grinding samples up as Nujol mulls. These two techniques are not considered suitable for surface analysis of paper documents. Fortunately, some information can be obtained by using internal and external reflectance techniques. Only the internal reflectance technique or the so-called attenuated total reflectance (ATR) technique will be discussed here.

ATR can be used to analyze samples with rough surfaces such as wood, paper, and polymers. ATR techniques involve the placement of the sample papers on two sides of an internal reflectance crystal and then reflecting the IR beam through the crystal. As the beam is reflected through the crystal, a small amount of the sample is penetrated. The depth of penetration is determined by the index of refraction of the internal reflectance crystal, face-out angles, and the angle at which the IR beam enters the face of the crystal. Internal reflectance crystals having higher incident angles result in decreasing depths of penetration of the IR beam into the sample. Accordingly, the beam will lose energy at those wavelengths at which the material absorbs because of an interaction with the penetrating beam. This attenuated radiation, when measured and plotted as a function of wavelength, will give rise to an absorption spectrum characteristic of the material and resembling an IR spectrum obtained in the normal manner.

Background on ESCA. ESCA is one form of the general class of electron spectroscopy (*12–14*). The fundamental principles are reviewed here.

ESCA involves the energy analysis of electrons ejected from matter by incident radiation with X-ray photons. It allows the investigation of electronic structure because it provides a picture of core-level electron

binding energy for solids. The characteristic electron energies allow elemental analysis as well as chemical-state identification. In addition, photoelectron spectroscopy probes only the surface region of solids.

The basic ESCA experiment is illustrated in Figure 2. The solid sample is placed on a mound in a high vacuum and is irradiated with low-energy X-ray photons. Absorption of these X-ray photons results in prompt emission of photoelectrons from atomic orbitals having binding energies less than the energy of the X-ray photons. The total energy of an X-ray photon must be equal to the energy required to remove an electron from the atom, that is, the electron's binding energy plus the kinetic energy of the electron when it leaves the atom. This kinetic energy is what the electron spectrometer measures. In commercial electron spectrometers, this subtraction is carried out electronically so that spectra are produced directly in binding energies. Although the X-rays may penetrate deep into the sample, electrons emitted in the bulk of the material soon lose their energy through repeated collisions so that only atoms in a surface layer of very limited depth contribute to the intensity of measured electron emission. Figure 3 depicts this schematically. The escape depth varies as a function of electron kinetic energy and the type of materials being tested. It is normally in the range of 50–100 Å for organic materials. The energy of the emitted electrons thus characterizes the elements present in the surface layer, and the intensity of the signal indicates their abundance. Although quantitative measurements are seldom feasible, the relative abundances of elements in the surface region may be determined from the relative ESCA peak areas. Chemical information available in ESCA spectra beyond the elemental composition is due to the chemical-shift effect. This effect occurs because of the different chemical environments of the atoms in organic polymeric

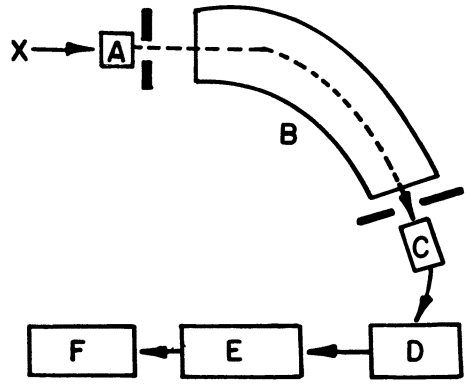

Figure 2. Diagram of an ESCA spectrometer. Key: X, X-rays; A, sample; B, electron analyzer; C, detector; D, amplifier; E, computer; F, recorder.

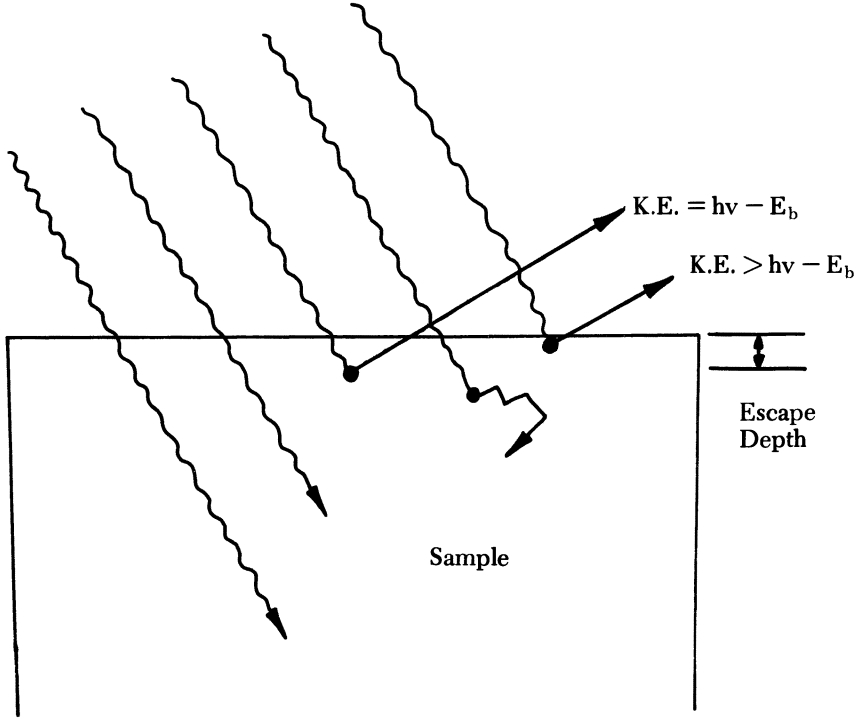

Figure 3. Escape characteristics of photoelectrons. Effective analysis depth is 10–100 Å.

materials. Some binding-energy shifts for the C_{1s} and O_{1s} transitions are summarized in Table II.

Many scientists have proven that the ESCA technique is very sensitive to surface constituents. Although ESCA has been used to identify the surface chemistry of various polymeric solids, its application to wood fiber and paper is relatively new (*15–17*).

Results and Discussion

Chemical Characteristics of Paper Documents. From the earliest times up to the present day, the substances used as vehicles for writing have been numerous. Ancient paper documents were basically made from rags of cotton and linters; cellulose is the major chemical constituent (*1*). Modern papers, however, are made of wood fibers, which usually are composed of cellulose, hemicelluloses, and lignin (*1*). In addition, for most of the modern papers, fillers, sizing agents, and other additives are used to improve paper properties (*1*).

The paper documents that were tested for this study were composed of softwood and hardwood cellulosic fibers. All of them were

Table II. Some Binding-Energy Shifts for C_{1s} and O_{1s} ESCA Transitions

Compound	*Binding Energy (eV)*
C_{1s}	
$(CH_2)_n$	283.3-285.3
RCH_2OH	285.5-287.5
RCH_2OR	285.8-287.8
RCOOR	288.0-290.0
RCOOH	288.1-290.1
O_{1s}	
RCH_2OH	532.2-534.2
RCOR	531.2-533.2
RCOOH	532.2-534.2
RCOOR	533.7-535.7

bleached. The pH values of these papers ranged from 4.95 to 7.1. With the exception of the 1790 paper, all the papers showed positive reactions with aluminon and Raspail tests. This result suggests that alum-rosin sizes were used for all these papers. The extent of surface treatments on papers with sizing agents, fillers, and additives was determined by the degree of wettability of paper fibers with water. The results of the paper surface analyses are summarized in Table III.

FTIR Spectra of Paper Documents. Good quality IR spectra can be obtained with the FTIR spectrometer and the ATR accessory without

Table III. Chemical Characteristics of Paper Documents

Sample	*Source*	*pH*	*Alum*	*Rosin*	*Wettability*
Cellulose	n	6.5	−	−	G
1790	rag	5.9	−	−	G
1834	softwood	5.3	+	+	G
1871	hardwood	5.1	+	+	G
1881	hardwood	5.0	+	+	M
1891	hardwood	5.3	+	+	M
1899	softwood	5.0	+	+	G
1909	softwood	4.4	+	+	M
1920	softwood	5.1	+	+	G
1929	hardwood	5.3	+	+	G
1939	softwood	5.1	+	+	G
1949	softwood	5.1	+	+	G
1959	hardwood	5.3	+	+	G
1969	hardwood	5.1	+	+	P
1978	hardwood	5.3	+	+	M
1983	hardwood	7.1	n	n	P

ABBREVIATIONS: n, no test made; +, present; −, absent; G, good; M, moderate; P, poor.

any complicated sample preparation. Typical FTIR spectra of pure cellulosic paper and papers of 1891 and 1969 are shown in Figure 4. The IR spectra of all the paper documents tested showed no absorption bands at 1610 and 1510 cm^{-1}. This result suggests that none of the papers contained detectable amount of lignin residues (*18*). Because detecting the oxidized and acidic functional groups in paper documents was of interest, only absorption bands relevant to these functional groups were analyzed. The results for specific functional groups of interest detected from paper documents are summarized in Table IV. These results show that aldehyde groups exhibiting two sharp bands at 2901 and 2852 cm^{-1} (*19*) were present in the paper documents of 1790, 1871, 1891, 1909, 1959, 1978, and 1983. This finding implies that acidic hydrolysis took place on these papers because one consequence of the hydrolysis of cellulosic fiber is the production of aldehyde-reducing end groups. However, without measuring the absolute value of the degree of polymerization of cellulosic polymer in these papers, it is difficult to predict to what extent the papers were degraded. The absorption band at 1720 cm^{-1} due to the carbonyl function of carboxylic groups was exhibited by most of the papers tested here, except papers of 1871, 1891, 1909, and 1959. Because most of the papers tested contained rosin acids as the sizing agent, it is difficult to distinguish whether the carboxylic acid is derived from fibers as a result of oxidation and aging or from rosin acids. Papers containing carboxylic groups also exhibited a

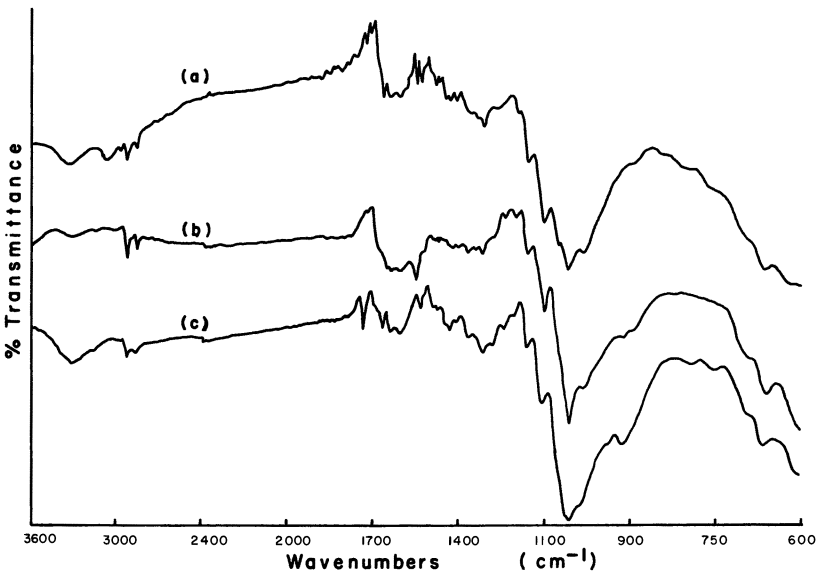

Figure 4. FTIR spectra of (a) cellulose, (b) 1891 paper, and (c) 1969 paper.

Table IV. FTIR Spectra of Paper Documents

	Absorption Bands (cm^{-1})				
Sample	*3310*[a]	*2910-2852*[b]	*1720*[c]	*1600*[d]	*1425*[d]
Cellulose	B	1, S	N	W	W
1790	S	2, S	W	W	VW
1834	B	1, B	S	W	S
1871	S	2, S	N	W	W
1881	S	1, B	S	W	S
1891	B	2, S	N	W	W
1899	B	1, B	S	W	S
1909	B	2, S	N	W	W
1920	B	1, B	S	W	S
1929	S	1, B	S	W	S
1939	B	1, B	S	W	S
1949	S	1, B	S	VW	S
1959	S	2, S	N	VW	W
1969	B	1, B	S	W	S
1978	B	2, S	W	S	W
1983	S	2, S	S	S	W

ABBREVIATIONS: B, broad; S, strong; W, weak; VW, very weak; N, none.
[a] Due to OH groups.
[b] Due to aldehyde group (2 bands) or CH vibration (1 band).
[c] Due to carbonyl of carboxylic groups.
[d] Due to carboxylic ions.

strong absorption band at 1600 cm^{-1} due to the carboxylate ions, which are possibly derived from rosin acids.

ESCA Spectra of Paper Documents. The ESCA spectra of all paper documents consisted of a singlet O_{1s} peak (529.92 eV) and a C_{1s} peak made up of different components. A typical ESCA spectrum of the C_{1s} peak for pure cellulose is shown in Figure 5. Two high-energy binding shoulders are visually discernible; these indicate the occurrence of a chemical shift due to the different environments of the carbon atoms in cellulose. This C_{1s} spectrum is essentially superimposed with three components and can be resolved by a Du Pont 310 curve: The principal peak (C_2) arising at 287.0 eV is assigned to C-O bonds, the higher energy shoulder (C_3) at 289.5 eV is assigned to C=O or O-C-O bonds, and the lower energy shoulder (C_1) at 285.0 eV is assigned to carbon bonded only to carbon and hydrogen (*20*). The C_3 peak is possibly due to the cyclic hemiacetal linkage of the cellulose. From the relative size of the oxygen and carbon ESCA peaks, the ratio of oxygen atoms to carbon atoms in the surface of cellulose can be calculated (normalization factor was 2.65 for the oxygen-to-carbon ratio). This ratio gives a direct measure of the surface associated with oxygen; a high oxygen content normally signifies a surface that has been oxidized.

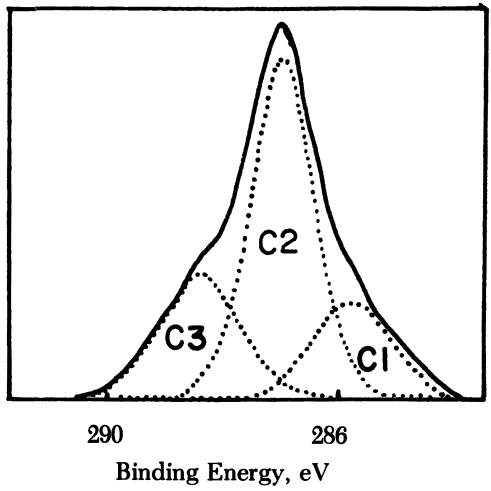

Figure 5. ESCA spectrum of pure cellulose.

Theoretically, cellulose has the gross formula $C_6H_{10}O_5$, and thus the oxygen-to-carbon ratio should be 0.83. The ESCA experimental data obtained in this study gave an oxygen-to-carbon ratio of 0.78. This result can be due to the deposition of impurities of hydrocarbon nature at the cellulosic surface.

The ESCA spectrum of 1790 paper exhibited a line shape similar to that of cellulose (Figure 6). In addition to C_1, C_2 and C_3 components, an extra component, C_4, was found at the higher energy binding, which could be due to the carboxylic groups generated at the paper surface (*12*). The oxygen-to-carbon ratio was 0.81, which was a little higher than that of pure cellulose (0.78). This result implies that the 1790 paper was oxidized during more than 100 years of storage and usage.

The ESCA spectra of the paper documents from 1834 to 1978 were very similar to 1790 paper. All of them exhibited four components at the C_{1s} peak with different intensities (Table V). The oxygen-to-carbon ratios of these paper documents were much lower than those of the pure cellulose and the 1790 paper. This result can be due to the rosin sizes used for these papers. Rosin is aromatic in nature; it is high in carbon-to-carbon and carbon-to-hydrogen bonds. Consequently, the oxygen-to-carbon ratio is reduced. Likewise, the C_4 component at higher energy binding appears to be due to the O=C-O bonds of carboxylic groups present in rosin acids or could be due to the oxidation of paper surfaces. Because no rosin size was used for 1790 paper, the C_4 component in that particular paper is due to the carboxylic group, which is an end product of cellulosic oxidation. Unfortunately, on the basis of ESCA spectra, determining whether the C_4 component is derived from rosin or from carboxylic groups is not possible.

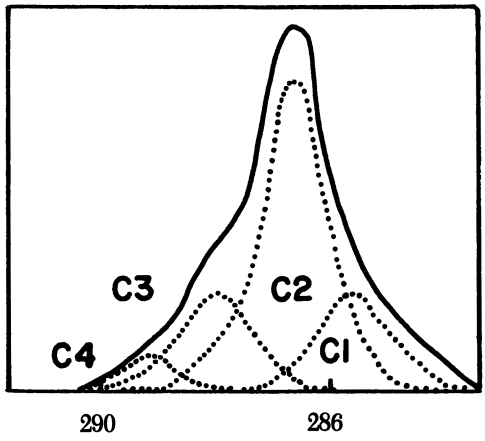

Figure 6. ESCA spectrum of 1790 paper.

Table V. Analysis of ESCA Carbon 1s Peaks

		Position (eV)			
Sample	*Oxygen:Carbon*[a]	C_1	C_2	C_3	C_4
Cellulose	0.78	285.0	285.6	287.9	—
1790	0.81	285.0	286.5	287.9	289.0
1834	0.58	285.0	286.5	287.9	289.1
1871	0.46	285.0	286.6	287.9	—
1881	0.56	285.0	286.5	287.9	289.1
1891	0.48	285.0	286.6	287.9	—
1899	0.55	285.0	286.5	287.8	289.0
1909	0.47	285.0	286.6	287.9	—
1920	0.57	285.0	286.5	287.8	289.0
1929	0.55	285.0	286.5	287.8	289.0
1939	0.55	285.0	286.5	287.8	289.0
1949	0.57	285.0	286.5	287.8	289.0
1959	0.47	285.0	286.6	287.9	—
1969	0.53	285.0	286.5	287.9	289.1
1978	0.48	285.0	286.6	287.9	—
1983	0.51	285.0	286.5	287.8	289.1

[a] Calculated value of cellulose from the empirical formula is 0.83.

Conclusions

The acidic impurities, whether they were generated in paper fibers because of oxidation or because of rosin acids deposited at fiber surfaces, were straightforwardly monitored by FTIR-ATR and ESCA. The presence of aldehyde groups as a consequence of cellulosic hydrolysis

and carboxylic groups was detected by FTIR. The presence of carboxylic acid and rosin acids was also detected by ESCA. FTIR and ESCA techniques have thus proved to be useful nondestructive methods for the identification of acidic impurities. These techniques show great potential for future studies of the conservation and restoration of surface materials of historic value.

Literature Cited

1. Hon, D. N.-S. In "Preservation of Paper and Textiles of Historic and Artistic Values II."; Williams, J. C., Ed.; ADVANCES IN CHEMISTRY SERIES No. 193; American Chemical Society: Washington, D.C., 1981; p. 119.
2. Hudson, F. L.; Grant, R. L.; Hockey, J. A. *J. Appl. Chem.* **1964**, *14*, 444.
3. Hon, D. N.-S. *J. Polym. Sci. Polym. Chem. Ed.* **1979**, *17*, 441.
4. Smith, R. D. CHEMTECH **1981**, *14*, 414.
5. Graff, J. H. "A Color Atlas for Fiber Identification"; The Institute of Paper Chemistry: Appleton, Wisconsin, 1940.
6. "Treatise on Analytical Chemistry"; Kolthoff, I. M.; Elving, P. J., Eds.; Interscience Encyclopedia: New York, 1959; Part II, Vol. 4.
7. Tech. Assoc. Pulp Paper Ind. "Rosin in Paper and Paperboard." T408 os-61.
8. Briggs, D. "Handbook of X-ray and Ultraviolet Photoelectron Spectroscopy"; Heyden: London, 1977; Chapt. 4.
9. Griffiths, P. R. "Chemical Infrared Fourier Transform Spectroscopy"; Wiley: New York, 1975.
10. Bell, R. J. "Introductory Fourier Transform Spectroscopy"; Academic: New York, 1972.
11. Miller, R. G. J.; Stace, B. C. "Laboratory Methods in Infrared Spectroscopy," Heyden: London, 1972.
12. Window, H.; Ho, F. F. "Applied Electron Spectroscopy for Chemical Analysis"; Wiley-Interscience: New York, 1982.
13. Siegbahn, K.; Nordling, C.; Fahlman, A.; Nordberg, R.; Hamerin, K.; Hedman, J.; Johansson, G.; Bergmark, T.; I. Karlsson, S. E.; Lindberg, B. *Nova Acta Regiae Soc. Sci. Ups. Ser. IV* **1967**, Vol. 4.
14. Hercules, D. M. "ESCA and Auger Spectroscopy"; ACS Audio Course; American Chemical Society: Washington, D.C., 1979.
15. Dorris, G. M.; Gray, D. G. *Cellul. Chem. Technol.* **1978**, *12*, 721.
16. Mjoberg, P. J. *Cellul. Chem. Technol.* **1981**, *15*, 481.
17. Hon, D. N.-S. *J. Appl. Polym. Sci.* **1984**, *29*, 2777.
18. Hon, D. N.-S. *J. Polym. Sci. Polym. Chem. Ed.* **1984**, *22*, 2227.
19. Conley, R. J. "Infrared Spectroscopy"; Allyn and Bacon: Boston, 1972; 2nd Ed.
20. Dorris, G. M.; Gray, D. G. *Cellul. Chem. Technol.* **1978**, *12*, 9.

RECEIVED for review November 26, 1984. ACCEPTED March 25, 1985.

Gel Permeation Chromatography

Use in Estimating the Effect of Water Washing on the Long-Term Stability of Cellulosic Fibers

Helen D. Burgess

Conservation Processes Research, Canadian Conservation Institute, Ottawa, Ontario, Canada, K1A 0M8

A gel permeation chromatographic (GPC) procedure using agarose gel and tris(ethylenediamine) cadmium dihydroxide to give a high-resolution separation of cellulose is described. The GPC technique was used to compare the long-term stability of naturally aged cotton textile fibers washed in distilled-deionized water, tap water, calcium bicarbonate (20 ppm), or calcium sulfate (20 ppm). The results, which were verified by viscometry, showed that tap water or calcium sulfate washed fibers exhibited less degradation after accelerated thermal aging (70 °C, 50% rh, 70 days) than the untreated control. The distilled-deionized water or calcium bicarbonate washed fibers showed greatly increased deterioration relative to the control.

WATER WASHING IS OF CENTRAL IMPORTANCE to both paper and textile conservation. The cleaning action of even a brief immersion in water improves the appearance of an artifact and removes any water-soluble materials that may be harmful to the chemical and physical stability of the fibers. However, the influence of the water quality, including such factors as pH and type and quantity of dissolved materials, upon the long-term stability of cellulosic fibers is not well understood, although recent research (*1-3*) has addressed a number of important questions arising from this problem.

These studies provided the first step to understanding some of the factors that can influence the permanence and durability of fibers. However, many questions remain unanswered. One of the most im-

portant considerations is whether these conclusions, drawn from experiments performed on new materials, are valid for historic artifacts. The partially degraded state of naturally aged fibers, with its concomitant changes in morphological structure and functional group levels, can be expected to contribute considerably to the sensitivity of cellulose to oxidative and hydrolytic (both acid- and base-catalyzed) mechanisms of degradation. Evidence supporting this reasoning may be seen in the literature dealing with color reversion (*4–7*). In these papers, the importance of the degree of degradation in influencing the rate of change of some pertinent chemical or physical property is very well illustrated.

Another point that must be raised is whether any experiments performed on paper fibers can be applied without reservation to linen or cotton textiles. If any differences exist they would relate to the influence of fiber length (textile fibers are generally longer) and structure (the random nature of the paper web versus the regularity imposed on textiles by the spinning and weaving process) upon chemical reactivity. The more extensive processing of paper fibers as well as the possible presence in the paper of undesirable components (e.g., lignin, hemicellulose, or extractives) would also impede valid comparison.

The legitimacy of comparisons between paper and textiles, as well as the ability to apply the results of a limited series of experiments to general conservation recommendations, is going to be very much determined by the depth of our understanding of the chemical changes taking place. Therefore, the most valid method of determining the effect of water washing on fiber stability will be one that can be related to a degradative process that influences both the chemical and physical properties of cellulose. Probably the most suitable technique is one that measures polymer length. Any method that involves the determination of molecular weight or degree of polymerization (DP) will permit chain scission—the ultimate result of both oxidative and hydrolytic degradation. If one is mainly concerned with chemical changes, the viscometric average DP (DP) is an ideal technique because of the relative ease, accuracy, and sensitivity of the analytical procedure. However, physical parameters such as breaking strength, flex lives (fold endurance), and toughness are much more accurately described by knowledge of the molecular weight distribution than they are by $\overline{DP}$ (*8*). Therefore, the examination of a problem relating to fiber degradation (with its concern with both physical and chemical changes) can best be accomplished by the distribution analysis.

Although this method of analysis is of obvious value on the basis of theoretical considerations, its useful application could only be achieved after solving a number of problems. The most important of these was to arrive at a suitable solvent system and to find a gel type that was

compatible with the particular solvent. These difficulties have greatly inhibited progress in the field. Most of the available literature deals with systems in which the cellulose was first nitrated or acetylated so that a convenient organic solvent could be used. However, these modifications are very degradative and almost certainly have contributed to the problem of getting good chromatographic resolution. Therefore, the best answer to these difficulties was to use a chemically stable solvent that was able to dissolve cellulose without excessive deterioration of the fiber. The colorless, odorless cadmium ethylenediamine solvent, tris-(ethylenediamine)cadmium dihydroxide (Cadoxen), seemed to be the most suitable solvent for the task.

Cellulose solvents such as tris(ethylenediamine)cadmium dihydroxide present difficulties with most conventional gel permeation chromatographic (GPC) gels: carbohydrate-based gels such as the Sephadexes swell too strongly; the cross-linked polystyrene gels such as Styragel do not swell enough; and the porous silica or glass-based gels break down in the alkaline aqueous solvents used to dissolve cellulose (*8*). Considerably more success was shown to be possible with the very rigid cross-linked agarose gels, Sepharose Cl (Pharmacia) (*9–12*). The analyses described in this chapter were based on this last choice.

The carbohydrate being eluted from a GPC column can be detected by a number of physical or chemical means (e.g., variation in refractive index or viscosity and colorimetric or fluorometric spectroscopic analysis). For the purpose of these experiments, the cellulose was tagged with a fluorescent label, dichlorotriazinylaminofluorescein (DTAF), which permits easy detection of very small quantities. The chromatographic system was set up to allow for convenient analysis of cellulose with a maximum resolution of the molecular weight distribution and a minimum of change to the sample.

With the help of this powerful technique, an effort was made to answer a few of the questions that exist concerning the effect of water washing on the long-term stability of cellulosic fibers. These questions include the following: (1) Can the conclusions published in the existing literature be applied to textiles and to fibers that are partially degraded by natural aging? (2) Can the beneficial effect of washing with tap water or dilute calcium hydroxide be ascribed (a) to the formation of a complex between the calcium cation and some component of the cellulose fiber and thus make oxidative attack more difficult or (b) to the prevention of acidic hydrolysis by the alkaline nature of calcium carbonate or calcium hydroxide?

These points were investigated by a series of experiments involving the water washing of a Peruvian cotton textile that was approximately 800 years old. Various treatments were tested by subjecting suitable size samples to washing with tap water, reagent grade distilled-deionized

water, calcium bicarbonate (20 ppm), or calcium sulfate (20 ppm). Suitable controls were included. The long-term stability of the fibers was assessed by comparing distribution data before and after accelerated thermal aging. The data obtained by the GPC techniques were verified by the determination of the viscometric $\overline{DP}$.

Experimental

Treatment Sequence. The textile used for the experiments was unbleached and undyed cotton. The fragment was plain weave and had a thread count of 17 × 12/cm (warp × weft), and the yarns were spun with a "Z" twist. The textile was dated from about A.D. 1100 to A.D. 1350 and was attributed to the Peruvian central coast. It was only moderately dirty and was in excellent condition.

All aqueous treatments were performed at 25 °C. Suitable size pieces were washed for 120 min in one of two sources of running water: The first source was a reagent grade water purified from tap water by a high-capacity Corning AG11 distillation apparatus that fed distilled water into a Barnstead Nanopure system. This deionizing purification setup consisted of high-capacity, ultrapure, and organic-removal cartridges set up in tandem. The second water source was Ottawa's tap water which had a water hardness of approximately 42 ppm made up of about 35 ppm of calcium and 7 ppm of magnesium.

After this initial treatment, the piece washed in the distilled-deionized system was divided into three parts: one was not further processed, and the other two were washed for an additional 60 min in one of two solutions containing 20 ppm of calcium (0.5 mM). These solutions were prepared from neutral calcium sulfate or calcium hydroxide converted to calcium bicarbonate by bubbling carbon dioxide gas through the solution for 60 min.

After the treatments were completed, the five pieces representing the five different washing sequences were cut into two halves: one was kept as a treatment control and was analyzed without further processing, and the other was subjected to accelerated thermal aging for 70 days at 70 °C and 50% rh. An untreated control was also included as part of both the unaged and aged sample groups. Each of the 12 pieces (unaged and aged) was at least 125 cm^2 and weighed 2 g.

Determination of $\overline{DP}$. $\overline{DP}$ was determined by using a Fenske viscometer equilibrated at 30 °C with tris(ethylenediamine)cadmium dihydroxide as the solvent for cellulose. This solvent was prepared in accordance with the method of Donetzhuber (*13*). All measurements were done in triplicate. The reported $\overline{DP}$ data were calculated from the mean intrinsic viscosities $[\eta]$ by using the following relationship (*14*):

$$[\eta]_i = 1.84 \times 10^{-2} (\overline{DP})^{0.76}$$

Preparation of Labeled Carbohydrate. Labeled cellulosic fibers were prepared by suspending approximately 100 mg of the cotton to be analyzed in 5 mL of 100 mM sodium carbonate that contained 3 mg of DTAF. The DTAF was prepared according to the method of Barskii et al. (*15*). The suspension was stirred for 18.0 h at room temperature.

Unreacted label was removed by rinsing with distilled-deionized water. After drying at room temperature, the samples were stored in a desiccator in the dark.

Labeled dextrans for calibration purposes were prepared by dissolving (in 15 mL of 100 mM Na_2CO_3) five dextran standards (100 mg each) of the following average molecular weight distributions: 10,000; 40,000; 70,000; 500,000; and 2,000,000. After stirring overnight, unreacted label was removed by exhaustive dialysis of the solution with water. The solution was freeze-dried, and the modified yellow dextrans were reclaimed.

Determination of Molecular Weight Distribution. A 1.6- × 95-cm column of Sepharose Cl-4B in 50% tris(ethylenediamine)cadmium dihydroxide (1:1 with water) was prepared and equilibrated by elution with six column volumes of 50% tris(ethylenediamine)cadmium dihydroxide. Downward flow with a pressure head of 125 cm was used.

Each sample to be analyzed was dissolved in tris(ethylenediamine)cadmium dihydroxide (1 mL) by stirring overnight, and then water (1 mL) was added. A 1-mL aliquot (concentration < 1.0%) was applied to the column, and elution proceeded with a pressure head of 100 cm and flow rate of 10 mL/h. A Turner 111 fluorometer (excitation filter 2A plus 47B and emission filter 8 plus 65A) fitted with a flow-through door allowed for automatic continuous monitoring of carbohydrates as they were eluted. Relative fluorescence was automatically recorded on a linear strip recorder. Fractions of 3 mL were collected on a FC-80K Gilson microfractionator. Typically, each sample was analyzed several times, usually at different concentrations, to ensure the reproducibility and accuracy of the data. A calibration run using the labeled dextrans was performed a minimum of one time per week.

Results and Discussion

GPC Column Calibration. The chromatography of a typical calibration run is shown in Figure 1. The successive elution of molecules of diminishing size is shown from left to right across the profile: peaks

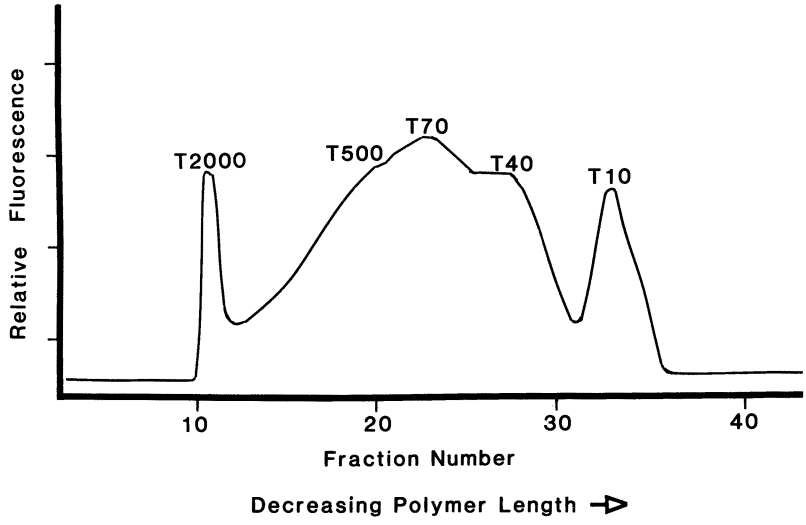

Figure 1. GPC of Dextran T calibration standards.

representing the T2000, T500, T70, T40, and T10 dextran standards (correlating to a molecular weight average of 2,000,000; 500,000; 70,000; 40,000; and 10,000, respectively) are clearly visible.

This separation occurs because the rate of travel of the individual molecules down the GPC column is dependent upon their ability to pass through the pores within the gel beads. The result is that the carbohydrate sample comes down the column at a rate proportional to the length of the polymer chain. The "apparent" size of an individual molecule (i.e., the size as observed by a GPC technique) is also going to be determined by the shape the polymer chain takes when it is dissolved in the solvent being used. Therefore, a column that is going to be used to fractionate cellulose should be calibrated with the best available polysaccharide standards. The Dextran T fractions from Pharmacia (mainly α-1,6 polymers of D-glucopyranose) have hydrodynamic properties in solution that are similar to those of cellulose and are the best commercially available materials for this task. The other synthetic polymer standards (e.g., polystyrene) will not give as accurate data, in absolute terms, unless the calibration is carried out according to Benoit's universal calibration concept (*16–18*).

A plot of log molecular weight versus fraction number of the central point of each dextran peak (Figure 2) yielded a straight line with a statistical "measure of fit" greater than 0.99, which is very close to the theoretical value of 1.00. This calibration curve can be used to determine the molecular weight distribution of subsequent chromatographic runs of cellulose samples of unknown distribution. Only very slight shifts in

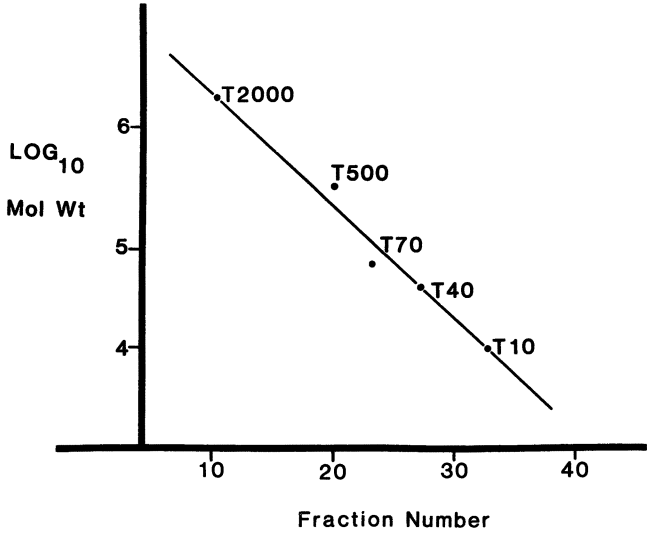

Figure 2. GPC calibration curve using Dextran T standards.

this linear plot were observed when the successive calibration runs performed during the course of the experiments were compared. For ease of comparison, all the chromatograms reported in this chapter were normalized to the calibration run obtained approximately midway through the experimentation period.

The data points for T500 and T70 fractions did not fall directly on the line as did the T2000, T40, and T10 dextrans. This pattern was consistently noted in every calibration curve obtained from these experiments and also from previous GPC data acquired by us with this particular system. The uniformity of this observation suggests that there may be some problem with the average molecular weight that the manufacturer attributes to the T500 and T70 fractions. It also illustrates the great difficulty that workers in the field will have in obtaining well-characterized polymer fractions of narrow molecular size distribution. However, the extreme reproducibility of the chromatography of these standards offers considerable reassurance that comparisons among samples of cellulose of unknown molecular weight distributions will be valid.

Determination of Molecular Weight Distribution. All of the unaged material, including both untreated and treated textiles, gave similar chromatographic profiles. Therefore, the data for the unaged cotton control shown in Figure 3 can be considered to be representative of both washed and unwashed samples. The implication from these observations is that the washing processes had little immediate effect on the molecular weight distribution. The aged samples, however, had very significant differences which are very easily apparent. Also, all of the aged samples showed obvious signs of degradation relative to the unaged control. This result is expected and is a necessary prerequisite to drawing any conclusions concerning the long-term stability of the cellulosic fibers.

The types of changes that were observed after the accelerated aging are illustrated by the comparison of the molecular weight distribution of the untreated controls before and after aging (Figure 3). Comparison of all the chromatograms illustrated in this chapter is facilitated by dividing the profiles into three areas of interest: (1) a high molecular peak section coming off the column at fraction numbers 11–15 having a molecular weight of 2,000,000 to about 850,000 ($\overline{DP}$ = 12,350–5250), (2) a large central peak at fraction number 17 or 18 which corresponds to a molecular weight of about 500,000, and (3) a pair of peaks covering the lower molecular weight range at approximately fraction numbers 29 and 33 and correlating to a molecular weight of about 35,000 and 13,000, respectively ($\overline{DP}$ = 216 and 80).

Changes in the high molecular weight range were observed by noting any alterations relative to the large central peak. Figure 3 clearly

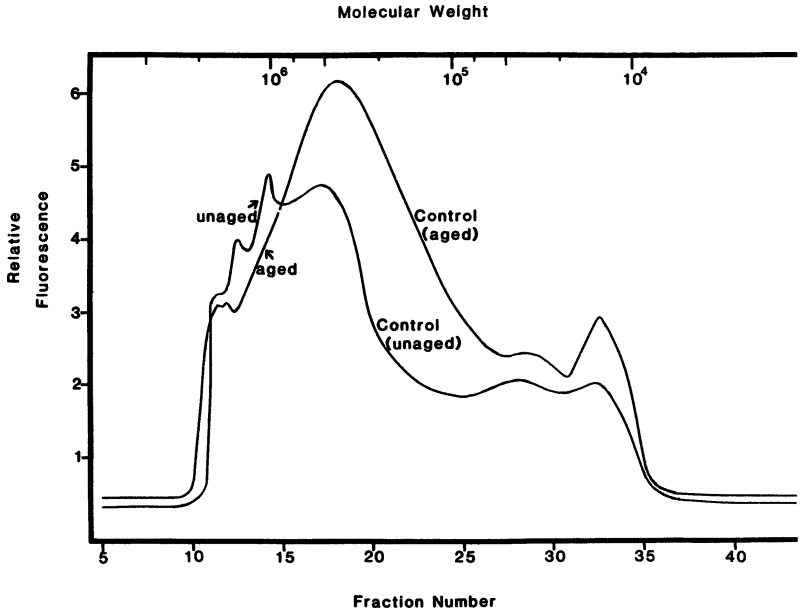

Figure 3. GPC of unwashed cotton samples before and after accelerated thermal aging.

shows how the aging process will result in the drastic loss of this high-DP material. Further evidence of changes due to thermal aging were noted by comparing the height of the two peaks in Area 3: in the unaged cellulose they were approximately the same, whereas in the aged materials the lower molecular weight peak, at fraction number 33, had increased in size relative to the other at fraction number 29. All of the changes evident in these observations may be interpreted as being the result of polymer-chain cleavage to produce shorter molecules of lower molecular weight (i.e., degradation of fibers).

The four washed samples that were aged did not give molecular weight distribution data identical to the aged control. The conclusion is that the washing process was having an impact on the long-term stability of the fibers. This effect can be seen by careful interpretation of the chromatograms shown in Figures 4 and 5. The results for the tap water and calcium sulfate (20 ppm) are in Figure 4, whereas Figure 5 illustrates the data obtained for distilled-deionized water and calcium bicarbonate (20 ppm) washing methods.

Figure 4 shows that very similar results were obtained from tap water and calcium sulfate washing. The distribution profiles show that the results fall somewhere between the unaged and aged controls depicted in Figure 3. The following observations are pertinent: (1) The

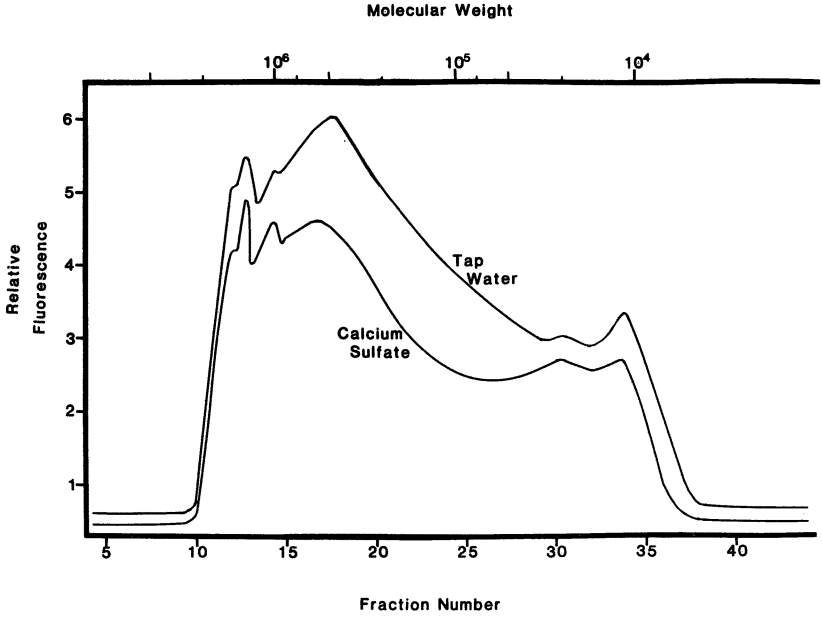

Figure 4. GPC of cotton samples washed in tap water or calcium sulfate (20 ppm) after accelerated thermal aging.

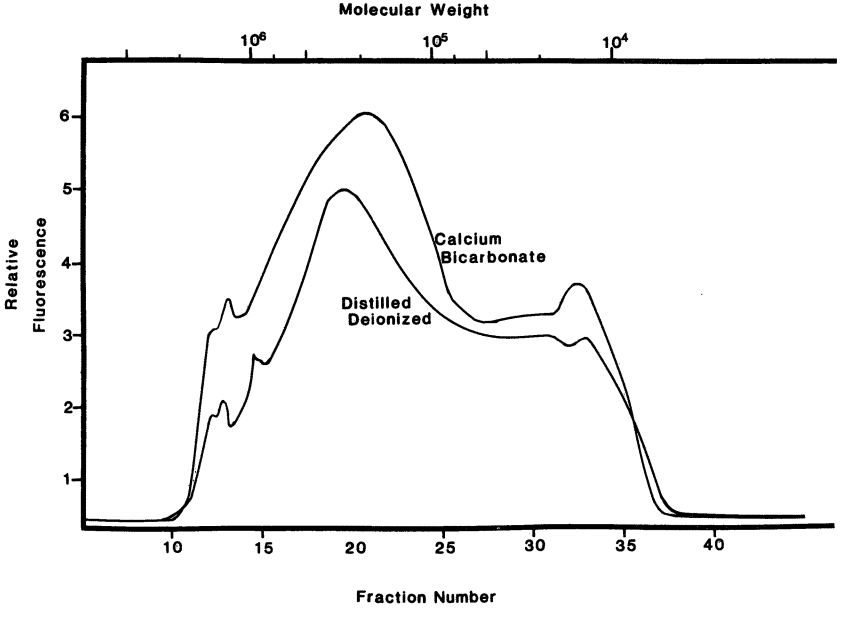

Figure 5. GPC of cotton samples washed in distilled-deionized water or calcium bicarbonate (20 ppm) after accelerated aging.

high molecular weight peaks at fraction numbers 11–15 were relatively large in comparison to the central peak at number 17. This result bore more similarity to the unaged control than to the aged fibers. (2) The height of the two peaks centered at fraction numbers 30 and 33 was slightly more than half of the height of the large peak at fraction number 17 (i.e., peak height ratio of Area 3 to Area 2 $\cong$0.5). The ratio for the aged, untreated control was also about 0.5, whereas the ratio for the unaged control was closer to one-third.

These comments lead one to conclude that the aged fibers treated with tap water or calcium sulfate washing have deteriorated relative to the unaged material but have not deteriorated as much as the aged control sample. In terms of conservation choices, the implication is that these two types of washing will actually improve the permanence and long-term stability of cellulosic fibers. This statement must be qualified by the consideration that any artifact to be washed must meet the necessary criteria of having sufficient mechanical strength and an absence of water-sensitive components.

The aged fibers that were previously washed with distilled-deionized water or 20 ppm of calcium bicarbonate showed similar results (Figure 5), but the degree of degradation was significantly higher than that seen with either tap water or calcium sulfate. The main difference between these two chromatograms and those in Figure 4 was in the elution of the high molecular weight material at fraction numbers 11–15: drastically reduced quantities were observed relative to the tap water or calcium sulfate treated cotton. The peak height ratio of Area 3 to Area 2 was slightly over 0.5, similar to that observed for all of the other aged samples. The conclusion is that the samples extensively washed with distilled-deionized water or the calcium bicarbonate system did not have as good long-term stability as cellulosic fibers washed with aqueous calcium sulfate or tap water.

Determination of the Viscometric $\overline{DP}$. The conclusions reached by the GPC experiments were verified by a separate determination of the viscometric $\overline{DP}$ (Table I). This analytical method does not give as full an understanding of the changes occurring during fiber deterioration as does a distribution analysis, but it will allow for a good quantitative comparison of samples. The main points that should be made from this data are the following: (1) The textile samples underwent a significant drop in average polymer length during accelerated thermal aging. (2) The aged samples that had been previously washed in either distilled-deionized water or 20 ppm of calcium bicarbonate showed DP values that were similar and drastically lower than the thermally aged untreated control. (3) The aged samples that had been previously washed in either Ottawa tap water or 20 ppm of calcium sulfate showed DP values that

Table I. The Viscometric Average Degree of Polymerization ($\overline{DP}$) of Cellulosic Fibers Washed in Water

Sample	$[\eta]_i$	$\overline{DP}$
Unaged, untreated control	5.75	1918
Aged, untreated control	4.81	1516
Aged, Ottawa tap water	4.93	1566
Aged, calcium sulfate (20 ppm)	4.86	1536
Aged, distilled-deionized water	3.68	1064
Aged, calcium bicarbonate (20 ppm)	3.76	1096

were similar and somewhat higher than the thermally aged untreated control.

The most likely explanation for the deleterious effect of distilled-deionized water is that the very pure water used was able to solubilize and remove constituents of the fiber that protect against oxidative attack. The divalent cations such as magnesium and calcium were probably the vital components being removed. This conclusion correlates well with published research in the pulp and paper field that shows that decreased degradation of cellulose occurs during oxygen bleaching if alkaline earth salts are added (*19–23, 25, 26*). Several mechanisms have been proposed to account for this effect: (1) The alkaline earth salts are able to complex free radicals (e.g., peroxides) and prevent them from taking part in the degradation phenomena (*19, 20*). (2) The alkaline earth salts are able to adsorb or complex transition metals (e.g., copper or iron) (*21–23*) which are known to catalyze the oxidative degradation of cellulose (*24*). (3) A specific interaction occurs between the salt and some easily oxidized portion of the glucose monomer. Oxidation is prevented by complex formation involving an unoxidized site (*25*) or via a direct stabilization of a primary oxidized derivative of cellulose (*26*). In either event, the swelling of the cellulose and the accessibility of the fibers may also be greatly affected and thus change the susceptibility of the cellulose to oxidation.

The poor performance of the calcium bicarbonate treated fibers is not so readily understood. However, a very likely explanation is the greatly increased sensitivity of naturally aged (and hence partially degraded) cellulose to alkaline materials. One may speculate that the calcium carbonate that was formed in the fibers was acting as an initiator of depolymerization reactions that are base catalyzed.

Alkaline degradation reactions are largely controlled by the carbonyl content of cellulose (*27–29*). Because the carbonyl levels go up as natural aging proceeds, one should expect that an 800-year-old textile would be much more likely to be adversely affected by alkali than would new, unoxidized cellulose. The vast majority of the conservation

studies that show the beneficial effects of alkaline treatments such as deacidification have been done with new materials. The results described in this chapter indicate that serious difficulties could be involved in applying information obtained from contemporary cellulosic studies to conservation treatments of much older museum artifacts.

A question must be raised as to why the tap water and the calcium bicarbonate washing treatments give such different results. The alkaline pH of the tap water suggests that calcium carbonate or bicarbonate is present and that the final product deposited in the fiber should be similar to that obtained with the pure bicarbonate solution. However, the chemical makeup of any city tap water is very complex and must contain a number of components that could affect the stability of cellulose. For example, the municipal treatment plant in Ottawa adds large amounts of alum (aluminum sulfate) to the water to settle particulate matter. Because alum makes the water very acidic, lime is then added to raise the pH. The result is that a large amount of calcium sulfate is present in the tap water and must affect the overall chemistry of the salts deposited in the fibers. One may further speculate that the anions present can influence the stability of cellulose as much as the cations. Any comprehensive understanding of the factors involved must include all parameters.

Conclusions

The degree of sensitivity that the textile fibers showed (both to the accelerated aging and to the different washing treatments) demonstrated that cellulose from cotton and linen textiles can be expected to be as susceptible to degradative processes as are the more extensively studied rag fiber papers. Therefore, much of the literature concerning treatments carried out on paper substrates should be applicable to textile conservation. However, it is still important to exercise caution in applying results from wood pulp papers to textile artifacts.

The results discussed in this chapter support the view that calcium or magnesium salts can be beneficial to the longevity of cellulosic materials. Removal of these components by washing with distilled or deionized water will be detrimental to a cellulosic artifact. However, conservators should not see these results as encouragement to use tap water in their washing treatments. Even areas having good tap water experience large seasonal variations of most constituents of the water as well as sporadic heavy metal contamination from pipes and water mains. These factors are not conducive to reliable high-quality water which conservation treatments require.

The data showing a large difference in fiber stability between the calcium bicarbonate and calcium sulfate treated samples were contrary

to what might have been expected on the basis of previously published studies. This disagreement can probably be ascribed to the age of the fibers used in the experiments. However, reliable general recommendations concerning the choice between neutral salts (of magnesium or calcium) and the traditional alkaline solutions cannot be based upon a single set of experiments performed on one type of cellulosic fiber. At the same time, revision is necessary of any previous conceptions regarding the complete safety of adding small amounts of magnesium or calcium bicarbonate (or hydroxide) to the wash water during the cleaning of historic artifacts. It is unlikely that the alkaline solutions could pose any problems with new materials, but evidence indicates that, in certain situations, the long-term stability of older fibers would be impaired.

Acknowledgments

I would like to thank Charles E. Llewellyn for donating the Peruvian textile used in these experiments. I would also like to acknowledge the help of J. C. McCawley, Chief, Conservation Processes Research, Canadian Conservation Institute, both in the preparation of this manuscript and in the performance of the experiments.

Literature Cited

1. Tang, L.; Jones, N. *J. AIC* **1979**, *18*, 61-81.
2. Tang, L. In "Preservation of Paper and Textiles of Historic and Artistic Value II"; Williams, J. C., Ed.; ADVANCES IN CHEMISTRY SERIES No. 193; American Chemical Society: Washington, D.C., 1981; pp. 63-86.
3. Nelson, J., et al *J. AIC* **1982**, *21*, 59-76.
4. Rapson, W. H.; Hakim, K. A. *Pulp Pap. Mag. Can.* **1957**, *58*, 151-57.
5. Rapson, W. H., et al *Tappi* **1958**, *41(8)*, 442-47.
6. Hosokawa, J. et al; *J. Jpn. Wood Res. Soc.* **1978**, *24(9)*, 638-42.
7. Corbi, J. C.; Rapson, W. H. *Pulp Pap. Mag. Can.* **1964**, *65*, 467-72.
8. Segal, L. In "Advances in Chromatography", Giddings, J. C. et al, Eds.; Dekker: New York, 1975; Vol. 12, pp. 32-59.
9. "Sepharose Cl: For Gel Filtration and Affinity Chromatography"; Technical Publication; Pharmacia Fine Chemicals: Uppsala, Sweden, 1975; p. 8.
10. Burgess, H. D. "The Degradation of Cellulose in Conservation Bleaching Treatments"; M.A.C. Thesis, Art Conservation Programme, Queen's Univ., Kingston, Canada, 1979.
11. Bose, A. "Aqueous Size Exclusion Chromatography of Non-Derivatized Cellulose: Application of Excluded Volume Concepts to Calibration"; Ph.D. Thesis, Purdue Univ., LaFayette, IN, 1980.
12. Burgess, H. D. *Prepr. 9th Inter. Congr. IIC* **1982**; pp. 85-88.
13. Donetzhuber, A. *Sven. Papperstidn.* **1960**, *63*, 447-48.
14. Segal, L.; Timpa, J. D. *Sven. Papperstidn.* **1969**, *72*, 656.
15. Barkii, V. E., et al *Izv. Akad. Nauk SSSR Ser. Biol.* **1968**, *5*, 744.
16. Benoit, H.; Grubisic, Z.; Rempp, P.; Decker, D.; Ziliox, J. G. *J. Chim. Phys.* **1966**, *63*, 1507.

17. Grubisic, Z.; Reibel, L.; Spach, G. *C.R. Hebd. Sceances Acad. Sci.* **1967**, *C246*, 1690.
18. Grubisic, Z.; Rempp, P.; Benoit, H., *J. Polym. Sci. Part B* **1967**, *5*, 753.
19. Croon, I.; Andrews, D. H. *Tappi* **1971**, *54*, 1893.
20. Samuelson, O. *Das Papier* **1970**, *24*, 671.
21. Robert, A.; Viallet, A. *Rev. ATIP* **1971**, *25(3)*, 237–41.
22. Gilbert, A. F.; Paulovova, E.; Rapson, W. H. *Tappi* **1973**, *56(6)*, 96–99.
23. Samuelson, O.; Stolpe, L. *Sven. Papperstidn.* **1974**, *77*, 16–26.
24. Ericsson, B.; Lindgren, B. O.; Theander, I.; *Sven. Papperstidn.* **1971**, *74*, 757.
25. Swan, B.; Akerblom, I. *Sven. Papperstidn.* **1977**, *80(11)*, 346–49.
26. Defaye, J.; Gadelle, A. *Pulp Pap. Mag. Can.* **1974**, *75(11)*, 394–97.
27. Golova, O. P.; Nosova, N. I. *Russ. Chem. Rev. Engl. Transl.* **1973**, *42(4)*, 327–38.
28. Richards, G. N. In "Cellulose and Cellulose Derivatives"; Bikales, N., Segal, L., Eds.; Wiley-Interscience: New York, 1971; Vol. V, Part V; pp. 1007–14.
29. Haskins, J. F.; Hogsed, H. J. *J. Org. Chem.* **1950**, *15*, 1264.

RECEIVED for review November 26, 1984. ACCEPTED April 17, 1985.

Influence of the Hemicellulose Fraction on Thermal and Photochemical Discoloration of Paper

S. B. Lee and R. L. Feller

Research Center on the Materials of the Artist and Conservator, Mellon Institute, Carnegie-Mellon University, Pittsburgh, PA 15213

Hemicelluloses and oxidized saccharidic components can lead to enhanced thermally induced discoloration. To demonstrate whether these substances would also increase discoloration under photochemical circumstances, hemicellulosic fractions from four different pulps were isolated. Filter paper sheets were saturated with these fractions to evaluate the tendency of these components to cause discoloration under fluorescent daylight and black-light lamps and under the conditions of thermal aging at 90 °C and 50% rh. Whereas thermal darkening was intense, only negligible changes in color occurred under the light sources. Similar results were observed with a series of handsheets containing reduced levels of γ-cellulose.

HEMICELLULOSE IS A MAJOR CONTRIBUTOR to the thermally induced darkening of bleached pulp (*1*). Rollinson (*2*) found the rate of formation of colored, acidic, water-soluble material to parallel discoloration of the pulp and also observed that the water-soluble components accounted for 50–60% of the discoloration that occurred during accelerated thermal aging; about 23% of these components were demonstrated to be oligosaccharides composed of simple sugars typical of hemicellulose. The effect of hemicelluloses has also been studied with model compounds (*3*, *4*); all aldoses and glucuronic acid were found to contribute to thermally induced discoloration. In contrast, relatively little attention has been given to the influence of hemicelluloses upon photochemically induced discoloration. As part of our general studies on the effect of light on paper, the present investigation was designed to compare the discoloration induced—thermally and photochemically—as a result of the presence of hemicellulosic materials.

Test sheets were prepared principally from Whatman No. 42 filter

0065-2393/86/0212-0377$06.00/0

paper saturated with hemicellulosic fractions that had been isolated from various unaged or thermally aged pulps by LiOH extraction (5). Another set of test sheets was prepared by saturation of filter paper with commercially prepared arabinogalactan and especially isolated acetylxylan. (The term "added-on" will be used to refer to the occlusion of the various fractions to the filter paper as a result of saturation.) Finally, a series of handsheets was made from the pulps of different γ-cellulose contents (10.5–1.5%) that were obtained by the extraction of bleached sulfate pulp with different strengths of caustic solution. The various test papers thus prepared with different concentrations of hemicellulosic components were evaluated for their tendency to discolor upon exposure to visible and near-UV radiation (daylight and black-light fluorescent lamps) and to heat.

Experimental

Extraction of Hemicelluloses from Various Pulps. The extraction procedure followed was that of Giertz and McPherson (*6*). Fifteen grams of unaged pulps [four kinds in all: bleached kraft pulp (BP), unbleached kraft pulp (UBP), unbleached groundwood pulp (GP), and chlorited UBP] was treated with 290 mL of 10.9% lithium hydroxide solution for 1 h at room temperature and was stirred intermittently (*see* Table I for the characteristics of the pulps). After the samples were diluted to about 1 L, the insoluble material was filtered off. The extract (filtrate) was neutralized to pH 6 with 2 M phosphoric acid (300 mL) and was allowed to stand overnight. The precipitated lithium phosphate and β-cellulose were separated by filtration. The filtrate was then concentrated to about 175 mL under reduced pressure at 30–40 °C. Salts present in the system were further precipitated with methanol and separated by filtration. The filtrate was again concentrated to about 60 mL. The filter paper was immersed into this concentrate to saturate the test sheets.

This procedure was applied also to BP, UBP, and GP samples that had been thermally aged at 90 °C and 50% rh for 20 days prior to extraction. The transmittances of 5% solutions of the neutral extracts at 460 nm, obtained with a Bausch and Lomb Spectronic 20 spectrophotometer, are noted in Table II. Whatman No. 42 filter paper was used as the substrate for the extracted material. When the sheets were dipped in the 60-mL concentrate, the pickup was found to be about 15%.

Hemicellulose Samples. Two water-soluble hemicellulosic samples were used: (1) acetyl-4-*O*-methylglucuronoxylan (molecular weight = 30,000) from white birchwood, isolated by the extraction of chlorine holocellulose with dimethyl sulfoxide and (2) arabinogalactan, Stractan from St. Regis Paper Company (arabinose:galactose = 1:6; molecular weight ≅ 60,000), prepared by the water extraction of heartwood of western larch. Both samples were kindly provided by T. E. Timell (SUNY).

Preparation of Pulp Having Different γ-Cellulose Contents. Unbleached pulp (50% hardwood kraft–50% softwood kraft) was subjected to chloriting treatment to remove lignin. The chemicals and conditions employed were the following: 25 g of sodium chlorite, 12.5 mL of glacial acetic acid, a pulp consis-

Published on February 1, 1986 on http://pubs.acs.org | doi: 10.1021/ba-1986-0212.ch021

Table I. Characteristics of Stock Pulps Used

Sample	*Description*	*Initial Reflectance at 457 nm (%)*	*Lignin Content (%)*	*Initial Hot-1%-Alkali Solubility (%)*	*Copper Number*
BP	50% hardwood kraft–50% softwood kraft	83.6	0.24	5.0	0.5
UBP	50% hardwood kraft–50% softwood kraft	30.8	4.4	3.7	0.6
GP	—	57.0	29.1	15.6	2.9

NOTE: Copper number is defined as the number of grams of metallic copper reduced from the cupric to cuprous state by 100 g of pulp fibers.

Table II. Light Transmittances of Neutralized Extracts at 5% Solids

Sample	*Extract from Unaged Sample*	*Extract from Heated Sample*[a]
BP	96	94
GP	2	35
UBP	46	50
Chlorited UBP	91	—

NOTE: Values are the percent transmission at 460 nm, 1-cm cell.
[a]Hemicellulose fractions from pulp stock heated at 90 °C and 50% rh for 20 days.

tency of 10%, a temperature of 75–80 °C, and a reaction period of 30 min. This treatment produced a pulp having 1.06% lignin which was then extracted with different concentrations of alkali to adjust the γ-cellulose content, as indicated in Table III (*12*). The extractions with caustic were carried out at a pulp consistency of 2%.

After caustic extraction, the pulp was separated by filtration (except the 17.5% alkali-treated pulps, which were first diluted and then decanted), 500 mL of 10% acetic acid was added, and the mixture was allowed to soak for 1 min before filtration. This procedure was repeated with a second 500-mL portion of 10% acetic acid. The material was then washed several times until it was acid free. From the pulps thus prepared, handsheets were made at the basis weight of 75 g/m^2.

Exposure to Light Sources. Three different light sources principally were used: (1) a bank of six General Electric high-output daylight fluorescent lamps, (2) a bank of six fluorescent BLB blacklights, and (3) an Atlas 6500-W xenon-arc Fade-ometer with Pyrex filters. Measurements of the output of the lamps indicated about 6.3% near-UV radiation (relative to UV plus visible radiation) in the Fade-ometer, 3.8% under daylight fluorescent lamps, and 86% under the BLB lamps. The brief tests with short-wave UV radiation (involving 254-nm emission) were done with mineral-inspection mercury-vapor lamps that had the dark-blue long-wavelength filters removed. These lamps previously had been used to investigate the depolymerization of methacrylate polymers by short-wave UV radiation.

The fluorescent lamps were mounted 3 ½ in. above the samples in a room maintained at 50% rh and 21.1 °C (70 °F). Under these conditions the temperature of the handsheets reached 24 °C. In the 6500-W Fade-ometer, the air temperature was 31 °C, the relative humidity was about 27%, and the black-panel temperature was 65 °C.

Table III. Characterization of Chlorite-Treated and Caustic-Extracted Pulps

Treatment Conditions for Caustic Extraction	*Composition of Resulting Celluloses (%)*		
	γ-Cellulose	*α-Cellulose*	*β-Cellulose*
Sample unextracted after chloriting	10.5	88.0	1.5
1% NaOH, 80 °C, 2 h	8.8	88.4	2.8
5% NaOH, 20 °C, 1 h	5.1	93.2	1.7
17.5% NaOH, 20 °C, ½ h	1.5	96.8	1.7

Results

Filter Paper with Hemicellulosic Fractions Added On. Hemicellulose fractions were isolated from unaged and thermally aged papers by extraction with LiOH, following the procedure described by Giertz and McPherson (*6*). The changes in postcolor number $[100(K/S) - (K/S)_0]$ (*7*) for various test sheets during exposure to visible and UV radiation and to heat are shown in Figures 1a, 1b, and 1c for material extracted from

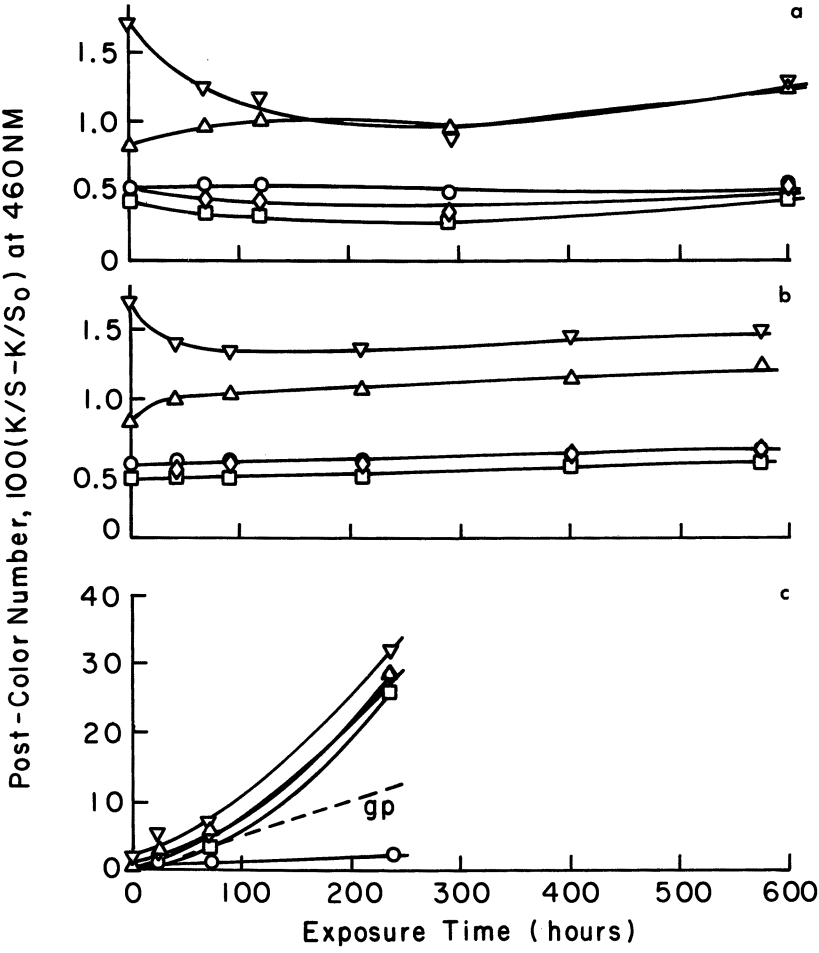

Figure 1. Changes in postcolor number of filter-paper sheets with 15% add-on of hemicellulose fractions derived from various pulps. For comparison, the thermal discoloration of a test sheet of groundwood pulp, gp, is shown. The initial postcolor number represents the increase in color over that of the untreated filter paper: a, daylight fluorescent lamps; b, black-light fluorescent lamps; c, heat (90 °C and 50% rh). Key: ○, blank filter paper; □, BP; △, GP; ▽, UBP; ◇, chlorited UBP.

unheated samples and then added on to the filter paper by immersion in a suspension of the neutralized extract. [The value for K_o/S_o is obtained from the reflectance, R, at 460 nm of a stack of six sheets of the sample papers, according to the relation $K/S = (1 - R)^2/2R$. KS_o is the initial value, and $(K/S)_t$ is the value following exposure or other treatment.] The net gain of added-on material was 15% on a dry-weighted basis. Figures 2a, 2b, and 2c show the results for sheets impregnated with hemicellulosic

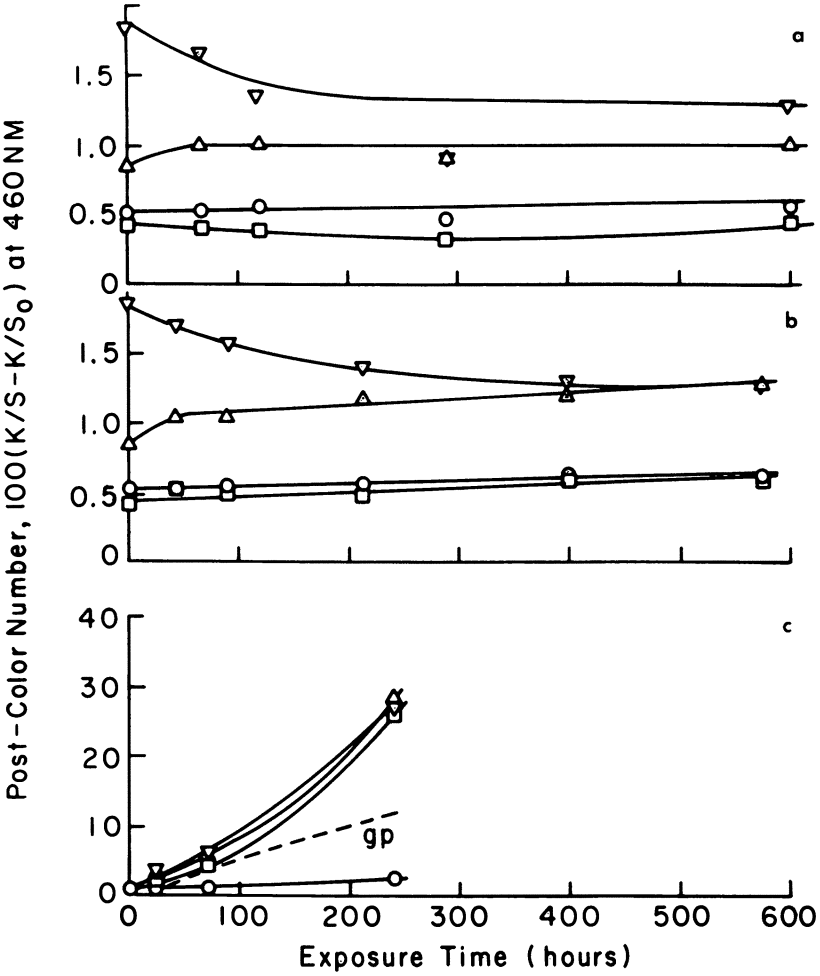

Figure 2. Changes in postcolor number of filter-paper sheets with 15% add-on of fractions from thermally aged hemicellulose derived from various pulps. For comparison, the thermal discoloration of a test sheet of groundwood pulp, gp, is shown. The initial postcolor number represents the increase in color over that of the untreated filter paper: a, daylight fluorescent lamps; b, black-light fluorescent lamps; c, heat (90 °C and 50% rh). Key: ○, blank filter paper; □, heated BP; △, heated GP; ▽, heated UBP.

fractions extracted from thermally aged pulps (pulp stocks were aged at 90 °C and 50% rh for 20 days before extracts were prepared). Twice as much material was extracted from the thermally aged sheets with LiOH as was obtained from the unaged stock. This result is similar to the finding of Giertz and McPherson (*6*) that increased material could be extracted from aged sheets. Table II, which gives the transmittances of the extract solutions at 5% solids, shows that the darkness of the extract solutions decreased in the order GP > UBP > chlorited UBP > BP. Colored alkali-soluble materials formed during thermal aging have been investigated by Lewin et al. (*8*).

The initial *K/S* values in the graphs of Figures 1a, 1b, 2a, and 2b depended on the type of pulp extracted and on the quantity of material added on. (The initial postcolor number represents the increase in color over that of the untreated filter paper.) The papers impregnated with the extract from the UBP tended to bleach during the first 100 h of photochemical exposure—the same result that we previously observed with the UBP pulp itself—and then a leveling off occurred. The extract material from the GP tended to darken, probably because of the lignin present. In the case of test sheets containing the added-on hemicellulosic material extracted from the BP and from the chlorite-treated UBP, the color scarcely changed, possibly because of the negligible presence of lignin. For these extracted substances, we found little difference in the behavior of the samples under daylight or under BLB black-light fluorescent lamps (Figures 1a, 1b, 2a, and 2b). Little discoloration also was observed when these samples were exposed to mercury-vapor lamps that emitted considerable radiation at 254 nm.

In contrast, marked and very similar darkening occurred upon the thermal aging of added-on test sheets at 90 °C and 50% rh, regardless of the particular hemicellulosic extract (Figures 1c and 2c). For comparison, the behavior of handsheets made solely from groundwood pulp (gp), notorious for its tendency to discolor, is shown in each figure.

Arabinogalactan and Acetylxylan Added on Test Sheets. Filter paper that had been dipped into suspensions of arabinogalactan and of acetylxylan to the extent of a 3% weight gain (3% add-on) was subjected both to humid (50% rh) and to dry thermal aging at 90 °C and also to exposure to various light sources. As shown in Figures 3 and 4, thermal aging darkened the test sheets considerably under humid conditions, whereas only moderate discoloration occurred under dry conditions. This behavior confirms the effects of humidity on the thermal-aging behavior of model hemicellulosic decomposition products, as reported by Rapson and Corbi (*4*), and of kraft pulps, as reported by Chang and Kondo (*1*). Exposure to visible and near-UV radiation caused no marked change in color.

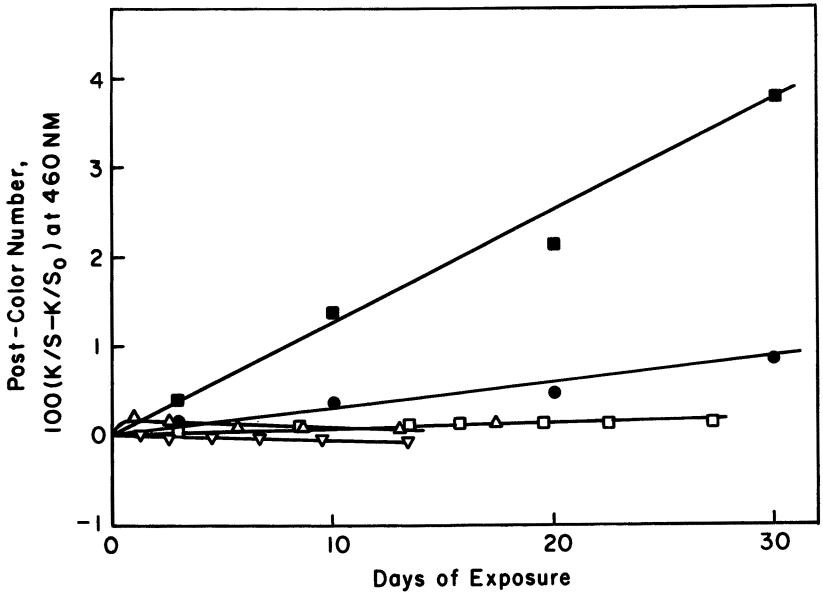

Figure 3. Postcolor number of filter papers saturated to a level of 3% add-on with arabinogalactan. Key (thermal discoloration): ■, 50% rh and 90 °C; ●, 0% rh and 90 °C; and (photochemical discoloration): □, daylight fluorescent lamps; △, BLB fluorescent lamps; ▽, Fade-ometer.

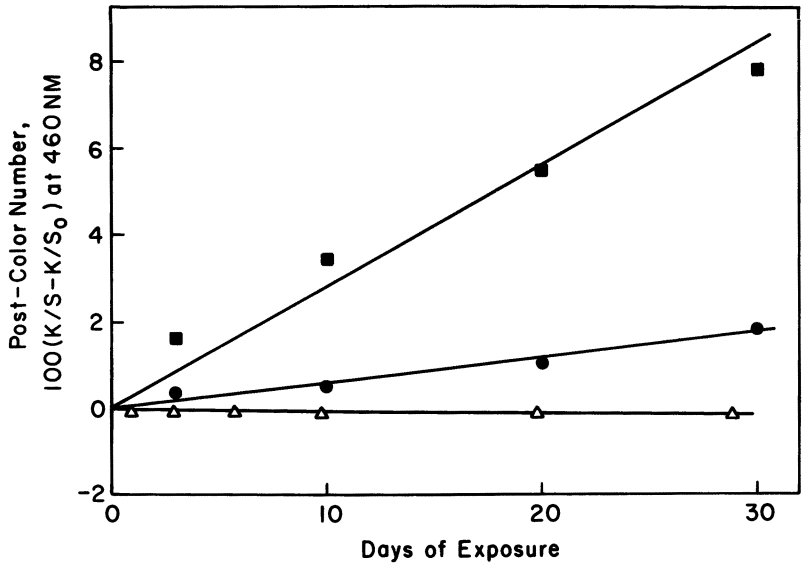

Figure 4. Postcolor number of filter papers saturated to a level of 3% add-on with acetylxylan. Key (thermal discoloration): ■, 50% rh and 90 °C; ●, 0% rh and 90 °C; and (photochemical discoloration): △, BLB fluorescent lamps.

Handsheets Made from Pulp Having Different Concentrations of γ-Cellulose. Figure 5 shows that a handsheet made from unextracted UBP darkened considerably upon thermal aging at 90 °C and 50% rh, whereas handsheets based on alkali-extracted pulps from this stock discolored only moderately. The results are similar to the findings of Giertz and McPherson (*6*) that treatment with alkalis, which tends to remove hemicelluloses, increases the brightness stability during thermal aging (*6*). Regardless of the γ-cellulose level in these test sheets, exposure to visible and near-UV radiation scarcely affected the color, even though changes in chemical composition could be detected (*9, 10*). Little discoloration was observed when these same samples were exposed to mercury-vapor lamps that emitted considerable radiation at 254 nm. Similar results were reported by Yasuda et al (*11*) when various monosaccharides were irradiated with a mercury-vapor lamp that emitted radiation between 250 and 400 nm (*11*).

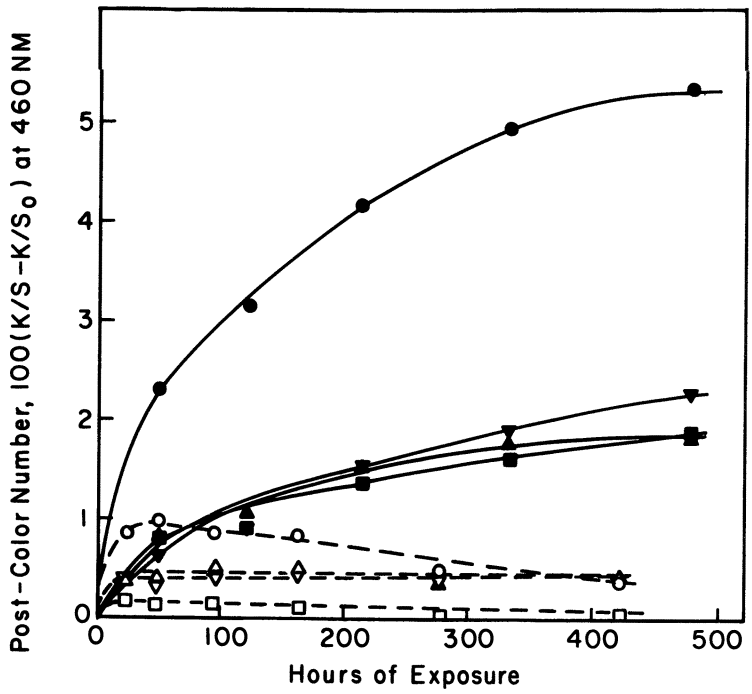

Figure 5. Postcolor number of test sheets of various contents of γ-cellulose that were prepared from UBP by extraction with alkali. The 10.5% sample is the starting material. Key (percent γ-cellulose): ●,○, 10.5; ■,□, 8.8; ▲,△, 5.1; and ▼,▽, 1.5. Dark symbols represent thermal discoloration; light symbols represent photochemical discoloration.

Conclusion

Tests using hemicellulosic extracts from several different pulp stocks indicate that little if any discoloration is caused by exposure of these components to visible and near-UV radiation or even radiation at 254 nm (UV). In the continuing quest to understand the causes of discoloration in paper, these results support the contention that the tendency of hemicelluloses to lead to discoloration is primarily a thermally induced effect.

Literature Cited

1. Chang, F.-J.; Kondo, T. *J. Jpn Wood Res. Soc.* **1971**, *17* (4), 160.
2. Rollinson, S. M. *Tappi* **1955**, *38* (3), 186.
3. Beélik, A. *Pulp Paper Mag. Canada* **1976**, *68* (3), T135.
4. Rapson, W. H.; Corbi, J.-C. *Pulp Paper Mag. Canada* **1964**, *65* (11), T459.
5. Hamilton, J. K.; Quimby, G. R. *Tappi* **1957**, *40* (9), 781.
6. Giertz, H. W.; McPherson, J. *Svensk Papperstidn.* **1956**, *59* (3), 93.
7. Tongren, J. C., *Paper Trade J.* **1938**, Technical Association Section, *107* (8), 34.
8. Albeck, M.; Ben-Bassat, A.; Epstein, J. A.; Lewin, M. *Tex. Res. J.* **1965**, *35* (9), 836.
9. Lewis, H. F.; Fronmuller, D. *Paper Trade J.* **1945**, *121*, 25.
10. Lee, S. B.; Feller, R. L. unpublished data.
11. Yasuda, S.; Nagaoka, M.; Hanzawa, M. *Res. Bull. Coll. Expt. For., Hokkaido Univ.* **1974**, *31* (1), 1.
12. Kaustinen, O. A.; Jappe, N. A. *Pap. Puu* **1960**, *42* (9), 485.

RECEIVED for review November 26, 1984. ACCEPTED April 25, 1985.

22

The Influence of Copper and Iron on the Permanence of Paper

Chandru J. Shahani and Frank H. Hengemihle

Preservation Research and Testing Office, Library of Congress, Washington, DC 20540

The aging of bleached kraft paper containing copper and iron species adsorbed from their aqueous sulfate solutions has been compared before and after a neutralization treatment with sodium bicarbonate. The observed rates of degradation were slower after the neutralization treatment. A decrease in the catalytic effect of the iron species was observed. However, the efficiency of the copper-catalyzed degradation reaction was enhanced after neutralization, although the concomitant decrease in the acidic hydrolysis component led to an overall increase in stability. The effect of chelation on the catalytic activity of metals was also investigated by studying the influence of copper(II) and iron (III) acetylacetonates on the stability of paper. Copper (II) acetylacetonate was observed to be a more active catalyst than the species adsorbed from ionic solutions, whereas iron(III) acetylacetonate did not catalyze the degradation of paper.

THE ADVERSE EFFECT OF TRANSITION METALS on the permanence of paper was first reported 50 years ago. Since then, this subject has attracted rather limited attention (2, 3). On the other hand, considerable work has been reported on the catalytic effect of these metals on the oxidation of cellulose and its model compounds in alkaline reaction systems, which simulate experimental conditions in alkaline bleaching and pulping processes (*4-19*). It is tempting to extrapolate this wealth of data on autoxidation of cellulose and celluloselike reaction systems in alkaline media to autoxidation phenomena that occur during the natural aging of paper. Indeed, similarities do exist between the reaction mechanism by which cellulose degrades in highly alkaline media and the complex process by which cellulose ages under ambient conditions. However, the diverse experimental conditions prevalent in these reaction systems suggest the

exercise of caution and restraint in the application of practical inferences drawn from the alkaline pulping of cellulose to the natural aging of paper.

Trace concentrations of iron, copper, and manganese are generally present in wood, the primary source of most modern paper. Because of its high affinity for transition metal species, cellulose tends to preferentially adsorb these species during its processing from wood chips to pulp and then to paper. The metallic impurities may be adsorbed as corrosion products, which result from the wear of manufacturing equipment, or from process chemicals and water. Fortunately for the antiquarian and the historian, their interest in limiting the concentration of metal-catalyst species in paper coincides with that of the manufacturer. In the presence of metallic impurities, the efficiency of oxidative and reductive bleaching processes is reduced as these metals catalytically decompose and waste the bleaching agent. The metals can deposit in paper in the form of darkly colored compounds and thereby decrease its brightness (*20*). In addition, the paper becomes increasingly susceptible to color reversion during storage so that the shelf life of the paper decreases. Therefore, considerable effort is generally undertaken by the paper maker to decrease the content of metallic impurities in process solutions and water. The entire pulping and paper-making operation can increase the level of contamination from iron as much as 12-fold if no effective treatment is applied (*20*). Generally, most commercial paper contains a significant level of metallic contaminants.

Entwistle et al. (*21*) orginally adapted a general free radical mechanism to the autoxidation of alkali cellulose. The reaction mechanism presented below for the interaction of cellulose with oxygen was proposed by Shafizadeh and Bradbury (*22*):

Initiation	$\text{Initiator, I} \longrightarrow \text{I}\cdot$	(1)
	$\text{I}\cdot + \text{O}_2 \longrightarrow \text{IOO}\cdot$	(2)
	$\text{Cell-H} + \text{I}\cdot \longrightarrow \text{Cell}\cdot + \text{IH}$	(3)
	$\text{Cell-H} + \text{IOO}\cdot \longrightarrow \text{Cell}\cdot + \text{IOOH}$	(4)
	$\text{Cell-H} + \text{O}_2 \longrightarrow \text{Cell}\cdot + \text{HOO}\cdot$	(5)
Propagation	$\text{Cell}\cdot + \text{O}_2 \longrightarrow \text{Cell-OO}\cdot$	(6)
	$\text{Cell-OO}\cdot + \text{Cell-H} \longrightarrow \text{Cell-OOH} + \text{Cell}\cdot$	(7)
Formation of Products	$\text{Cell-OOH} \longrightarrow \text{Cell-O}\cdot, \text{Cell-OO}\cdot$	(8)
	$\text{Cell-O}\cdot, \text{Cell-OO}\cdot \longrightarrow \text{Products}$	(9)
	$\text{Cell-OOH} \longrightarrow \text{Products}$	(10)

The hydrogen abstraction from the cellulosic chain has been proposed to occur predominantly at the C_1 position. Oxygen absorption can then lead

to the formation of a peroxy radical at this position, as in Reaction 6. This situation can lead to the cleavage of the glucosidic bond and the formation of an alkoxy radical on the neighboring glucose unit:

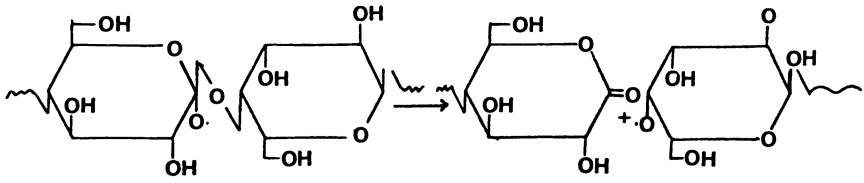

Transition metal species can accelerate this chain of events by catalyzing the homolytic decomposition of cellulosic peroxide molecules (*5*):

$$\text{Cell-OOH} + M^{n+} \rightarrow \text{Cell-OO}\cdot + H^+ + M^{(n-1)+} \quad (11)$$

$$\text{Cell-OOH} + M^{(n-1)+} \rightarrow \text{Cell-O}\cdot + OH^- + M^{n+} \quad (12)$$

This mechanism appears to be most commonly reported for transition-metal-catalyzed autoxidation of organic substrates. However, at least a few other possibilities exist (*23*). The effect of oxygen absorption and subsequent oxidation and cleavage of cellulosic chains on the permanence as well as the appearance of paper can be very significant. The absorption of even the smallest amounts of oxygen is known to produce a substantial loss in mechanical properties of polymeric materials. In the case of paper, oxygen absorption leads to a decrease in the degree of polymerization, color reversion, and a loss in mechanical properties.

The basic reaction mechanism for the autoxidation process just presented provides a useful frame of reference for a discussion of this reaction system. However, much needs to be learned about the interaction of cellulose with a composite system that includes oxygen, water, and metallic contaminants. A better understanding of this reaction system is essential for the development of practical measures for the inhibition of the autoxidative degradation of paper.

Several workers have observed the inhibition of autoxidative degradation of cellulose or its model compounds in the presence of magnesium compounds (*8–14, 18*). However, the mechanism for the observed inhibition process has been a matter of some controversy. Some workers have attributed their observation to the stabilization of peroxides by magnesium compounds (*8, 9, 11*). Robert has suggested that the metallic catalysts are adsorbed on or coprecipitated with magnesium hydroxide (*13*). Other workers are convinced that the

metallic catalysts are deactivated through the formation of a complex with magnesium (*10, 12*). Experimental evidence for the formation of a magnesium–iron complex in highly alkaline slurries has been reported by Gilbert et al. (*14*) and Isbell et al. (*18*). No experimental evidence is forthcoming for the formation of magnesium complexes with iron or copper species in paper.

In work (*3*) reported earlier from these laboratories, the copper-catalyzed oxidative degradation of paper was shown to be inhibited by treatment with magnesium bicarbonate solution. The possibility of the deactivation of copper ions by complex formation with magnesium species was considered. However, other work in these laboratories showed that paper impregnated with copper could not be stabilized upon treatment with magnesium acetate solution (*24*). Moreover, the earlier work (*3*) showed that a calcium bicarbonate treatment also effectively stabilized paper, although it appeared to be not equally effective. Several experimental factors, such as particle size, relative concentrations, and the chemical form of the two carbonates finally deposited in paper, could have contributed to the small differences in their stabilizing influence. Thus, it is uncertain at this stage if the retardation of the copper-catalyzed degradation of paper can be positively attributed to the formation of a copper–magnesium complex.

Arney et al. (*25*) observed that the buffering of paper with calcium carbonate retards oxygen-independent degradation reactions as well as those induced by oxygen. Furthermore, one must consider that deacidification treatments with both magnesium and calcium bicarbonate solutions stabilize paper against the degradative effect induced in the presence of copper species, whereas magnesium acetate is totally ineffective. These observations appear to suggest that the neutralization of acidity in paper probably serves to retard not only acidic hydrolysis of cellulose but also the copper-catalyzed autoxidation process. Therefore, this work has been extended to study the effect of a neutralization treatment on the stability of paper samples containing copper and iron species. To exclude the interaction of copper or iron with any other metallic species, no other metallic species were introduced in the neutralization process. Acidic species in paper were reacted with sodium bicarbonate, and the test samples were washed thoroughly to remove soluble sodium salts.

The reactivity of metals in Reactions 11 and 12 can be influenced by the gegenion or by complexing agents (*26–29*). Generally, coordinated metals are less reactive. Thus, the cobaltic ethylenediaminetetraacetic acid complex is not reduced by hydroperoxides (*30*), although cobaltic carboxylates are reduced very rapidly (*28, 31*). Coordination of metallic catalysts has been generally employed for their deactivation (*32*). On the other hand, researchers (*10*) have reported that the coordination of tran-

sition metal species can enhance their catalytic activity in cellulosic systems. Therefore, it was of interest to investigate further the influence of coordination on the catalytic effect of copper and iron in the present system. The rate of degradation of paper samples containing ionic copper and iron species adsorbed from their aqueous sulfate solutions has been compared with that of samples containing the corresponding acetylacetonate chelates.

Experimental

Materials and Regents. Paper samples employed in this study were 8- × 10-in. sheets cut from a continuous portion of a single roll or JCPA-60 bleached kraft paper. This paper had been manufactured from a pulp mixture consisting of 70% bleached southern kraft and 30% bleached hardwood kraft. The paper contained 13% clay materials, which are composed mainly of titanium dioxide. It also contained 212 ppm of iron and 66 ppm of copper and had a pH of 5.4. All chemicals employed were analytical reagent grade. Water used for the washing of paper samples and the preparation of solutions had a minimum resistivity of 15 MΩ.

Chemical Treatment of Paper. Test samples were treated with aqueous copper(II) or iron(II) sulfate solutions or with nonaqueous copper(II) or iron(III) acetylacetonate solutions. All chemical treatments were designed to obtain extensive and uniform penetration into the paper structure. To facilitate contact between paper and solution and to provide physical support, test samples were interleaved with fibrous sheets of nonwoven polyester. Sorption of metal species from aqueous media was achieved by immersion of paper samples into the solution of choice for 16–18 h. The metal-catalyst content of paper was varied by adjusting the solution concentration. The concentration of the aqueous metal salt solutions was varied from 10^{-3} to 10^{-1} M. One liter of solution was used for every 25 sheets of paper. At the end of the treatment period, paper samples treated in aqueous media were washed with water.

Paper sheets individually supported on the webbed polyester sheets were immersed in a water bath for a minimum of 1 h. The washing procedure was repeated three times. Test papers that were to be further subjected to a neutralization treatment were immersed in a 10^{-2} M sodium bicarbonate solution for 1 h. Subsequently, these test papers were also washed in three changes of water. The chemical treatments, as well as the washings, were intermittently punctuated with gentle agitation. Finally, the treated paper sheets, while still supported on nonwoven polyester, were placed on blotting papers to drain and then were air dried between acid-free paper.

Absorption of metallic acetylacetonates was carried out by immersing test papers in nonaqueous solutions of the iron(III) or copper(II) compound. In both cases, the solution concentration was 5×10^{-3} M. Iron(III) acetylacetonate was dissolved in acetone, and a mixture of acetone and chloroform (1:1) was used to dissolve copper(II) acetylacetonate. Test samples were immersed in metallic acetylacetonate solutions for 30 min and then were air dried.

Accelerated Aging and Testing of Paper. Test samples were subjected to accelerated aging under dry (100 °C) as well as humid (90 °C, 50% rh) conditions. At the end of the aging period, the samples were conditioned at 72 °F and 50% rh

for at least 24 h before testing. The Massachusetts Institute of Technology fold endurance was measured in accordance with the Technical Association of the Pulp and Paper Industry (TAPPI) Standard Test Method T511, with the exception that the load used was 500 g instead of the specified 1 kg. Fold-endurance measurements were made in both machine and cross directions. The pH of the paper was determined by a cold-extraction technique based upon the TAPPI Standard Test Method T509. A slurry containing 1.0 g of paper in distilled water was made up to 100 mL. The paper sample was macerated in a Waring blender for 1 min. The slurry was allowed to stand for 5 min before its pH was measured. Brightness levels were determined by measuring blue reflectance with a Photovolt model 670 reflection meter. The metallic content of paper samples was determined by atomic absorption using a carbon rod atomizer with a Varian model AA-6 spectrometer.

Results and Discussion

The stabilities of bleached kraft paper samples containing copper and iron species were compared before and after neutralization. Paper samples with copper(II) and iron(II) species adsorbed from their sulfate solutions were treated with sodium bicarbonate solution to neutralize acidic species. Excess sodium bicarbonate was washed away. Thus, no extraneous cations were introduced in this treatment, and the formation of any complex with the transition metal species was thereby precluded. Therefore, any stabilization observed as a result of this treatment can be ascribed only to the neutralization of acidic species in the test paper. A decrease in acidic content would inevitably enhance the stability of paper toward acidic hydrolysis. The stability of the test samples may be further influenced if the neutralization treatment affects the nature of the catalytic species or if the acidic species in paper also participate in the oxidation process.

To address a diverse but related concern, the effect of chelation of adsorbed copper and iron species on the catalytic degradation of paper was investigated. The stability of paper containing copper and iron species adsorbed from ionic solutions was compared with that of paper containing the acetylacetonate chelates of these metals. Nonpolar acetylacetonate complexes of metals have no affinity for adsorption on paper. These copper and iron chelates are neither adsorbed nor chemically bonded to the paper matrix.

Before the treated samples were subjected to accelerated-aging conditions, their pH values were measured. These data, along with the corresponding metallic contents, are shown in Table I for selected samples. The differences in pH values of the treated and control samples tend to be rather small. Samples containing metallic species adsorbed from aqueous sulfate solutions show a reduction in pH of less than one-half of a pH unit. The sodium bicarbonate-treated samples show some decrease in acidic content, but they are not neutral.

Table I. pH Values of Selected Paper Samples

Treatment	*Metal Content (ppm)*	*pH*
None	—	5.5
Water wash	—	5.6
$CuSO_4$	395	5.2
$CuSO_4$	138	5.4
$CuSO_4$, $NaHCO_3$	382	5.6
$CuSO_4$, $NaHCO_3$	151	6.0
$Cu(acac)_2$	302	5.5
$FeSO_4$	475	5.0
$FeSO_4$, $NaHCO_3$	453	5.8
$Fe(acac)_3$	566	5.5

NOTE: Aging period was 16 days.

Tang and Jones (*33*) and Nelson et al. (*34*) have shown that the washing of paper by immersion in pure water can adversely affect its permanence. Some papers were shown to have an appreciably lower stability after washing with deionized or distilled water, whereas they remained relatively unaffected after washing in tap water. Similarly, Eirk (*35*) demonstrated that the immersion of paper in organic solvents can also affect its permanence. These observations suggest that the adsorption of catalytic species from a solvent bath, as practiced here, must lead to a compound effect on the permanence of test samples. To focus this study on the catalytic effect of copper and iron species, it was necessary to exclude as far as possible the influence of the solvent wash on the permanence of paper. Therefore, the stability of paper samples containing different metallic species was compared with that of control samples washed with the same solvent or solvent mixture as that used in the sorption of the metallic catalysts.

To facilitate this comparison, we have defined two aging parameters. The *relative lifetime, X,* corresponds to an 87.5% reduction in the initial fold value of a paper sample, or three half-lives, during accelerated aging. The length of this aging period shows a good correspondence with the initial rate of loss of fold endurance. The relative lifetime encompasses a fraction of the total life span of a paper sample that is long enough to remain unaffected by the shape of the fold-endurance curve during the initial aging period, and yet small enough to disregard an extended tailing period. For test samples that were too stable to degrade by three half-lives over the experimental accelerated-aging period, extrapolation of the aging curve for fold endurance was necessary to evaluate the relative lifetime. This aging parameter affords an effective measure of stability and a convenient point of comparison for a variety of fold-endurance curves. A good correspondence was generally

observed between relative lifetime values and initial rates of loss of fold endurance.

The ratio of the relative lifetime of metal-impregnated test samples to the corresponding value for the appropriate control is represented by the term *relative stability*, Z. Thus, relative lifetime = X = three half-lives; relative stability = Z = X(sample)/X(control). Except for the treatment being evaluated, the control sample was subjected to exactly the same treatment as the test sample. A comparison of relative stability ratios attempts to exclude the effect of the solvent wash while giving due consideration to the effect of the metallic treatments. When the stability of a sample is not influenced by its treatment, the value of the relative stability parameter would ideally equal unity. On the other hand, the stronger the catalytic effect on the degradation process, the closer it would be to zero. The subscripts h and d appended to the parameters X and Z indicate humid and dry accelerated-aging conditions, respectively. This treatment of data is not of exclusive significance. Other procedures, equally relevant, can be successfully applied.

Data on the folding endurance of samples subjected to accelerated aging are shown in Tables II–VIII. Selected data are also presented in Figures 1–5, which show the decline in folding endurance along the machine direction. Relative lifetime, X, and relative stability, Z, values computed from these data are shown in Tables IX–XI.

An examination of the data in Table II and Figure 1 on paper samples washed with different solvents and aged under humid conditions shows that washing with deionized water does have an adverse effect on the stability of paper. Samples washed with acetone or a mixture of acetone and chloroform also age faster than untreated paper in the presence of moisture. Under dry accelerated-aging conditions, however, the observed effect of washing on the stability of paper is remarkably different, as can be seen from the data in Table III and Figure 2. All of the washed samples show an appreciable gain in stability. A comparison of the relative stability values Z_h and Z_d for the solvent-washed samples in Table IX crystallizes the contrast in accelerated-aging trends observed under humid and dry aging conditions.

Under humid aging conditions, the sodium bicarbonate treatment appears to maintain the original stability of the test paper in spite of the subsequent water wash. A loss in stability as a result of the washing process may be compensated by a corresponding gain due to the neutralization of acidic species and a consequent decrease in the rate of acidic hydrolysis. The stabilizing effect of the neutralization treatment is clearly evident under dry accelerated-aging conditions. The relative stability values under dry and humid aging conditions are 2.65 and 1.05, respectively. This contrast in the effects of the solvent wash and neutralization treatments on the stability of JCPA-60 paper under humid

Published on February 1, 1986 on http://pubs.acs.org | doi: 10.1021/ba-1986-0212.ch022

Table II. Fold-Endurance Data for Control Samples Aged at 90 °C and 50% rh

None			*Water*			*$NaHCO_3$*			*Acetone*			*Chloroform and Acetone*		
	Folds			*Folds*			*Folds*			*Folds*			*Folds*	
Days	*MD*	*CD*	*Days*	*MD*	*CD*	*Days*	*MD*	*CD*	*Days*	*MD*	*CD*	*Days*	*MD*	*CD*
0	724	372	0	752	311	0	809	327	0	816	347	0	688	324
2	607	314	2	658	243	2	661	306	2	560	201	2	534	177
6	449	213	5	501	204	3	626	201	7	269	186	7	314	191
9	308	184	8	249	72	6	540	236	9	237	165	9	230	183
13	185	131	13	25	25	13	360	184	11	159	81	11	211	130
20	71	74	16	14	9	17	257	164	15	69	65	15	94	89
22	57	75	19	10	16	23	107	73	18	24	43	18	57	66
33	17	36	29	5	14	28	28	56	28	16	38	28	21	45

NOTE: Column headings indicate the wash treatment used. MD denotes machine direction; CD denotes cross direction.

Published on February 1, 1986 on http://pubs.acs.org | doi: 10.1021/ba-1986-0212.ch022

Table III. Fold-Endurance Data for Control Samples Aged at 100 °C

None			*Water*			*$NaHCO_3$*			*Acetone*			*Chloroform and Acetone*		
	Folds			*Folds*			*Folds*			*Folds*			*Folds*	
Days	*MD*	*CD*	*Days*	*MD*	*CD*	*Days*	*MD*	*CD*	*Days*	*MD*	*CD*	*Days*	*MD*	*CD*
0	724	372	0	752	372	0	809	327	0	816	347	0	688	320
2	574	289	2	604	250	2	680	298	2	630	247	2	588	288
6	386	211	5	495	238	3	654	302	7	456	198	7	414	208
9	288	154	8	521	182	6	739	278	9	368	162	9	375	197
13	226	96	13	351	132	13	548	233	11	370	192	11	324	155
20	115	71	16	308	160	17	413	248	15	255	132	15	261	132
22	84	61	19	255	98	23	498	188	18	252	110	18	208	120
33	40	44	29	129	87	28	329	164	28	128	83	28	128	81

NOTE: Column headings indicate the wash treatment used. MD denotes machine direction; CD denotes cross direction.

Published on February 1, 1986 on http://pubs.acs.org | doi: 10.1021/ba-1986-0212.ch022

Table IV. Fold-Endurance Data for Paper Samples Treated with Aqueous Copper(II) Sulfate Solution

685 ppm of Cu			*591 ppm of Cu*			*395 ppm of Cu*			*138 ppm of Cu*		
	Folds			*Folds*			*Folds*			*Folds*	
Days	*MD*	*CD*	*Days*	*MD*	*CD*	*Days*	*MD*	*CD*	*Days*	*MD*	*CD*
				Aging Conditions: 90 °C and 50% rh							
0	691	278	0	710	308	0	716	432	0	855	437
2	186	103	1	438	181	1	563	233	1	777	464
5	1	6	2	178	131	2	428	233	2	641	298
8	0	0	3	67	45	3	273	158	3	476	222
			7	0	1	4	232	120	4	339	164
						7	10	10	7	158	64
									10	13	18
									14	12	11
				Aging Conditions: 100 °C							
0	691	278	0	710	308	0	716	432	0	855	437
2	399	182	1	408	238	1	750	336	1	743	302
5	211	112	2	450	190	2	746	379	2	708	330
8	89	12	3	403	158	3	591	274	3	731	316
13	18	11	7	151	70	4	609	279	4	739	240
16	15	9	9	112	55	7	520	219	7	601	267
19	1	2	11	48	41	13	395	137	10	534	187
			15	32	28	17	207	86	14	316	143

NOTE: MD denotes machine direction; CD denotes cross direction.

Published on February 1, 1986 on http://pubs.acs.org | doi: 10.1021/ba-1986-0212.ch022

Table V. Fold-Endurance Data for Paper Samples Treated with Aqueous Copper(II) Sulfate and Sodium Bicarbonate Solutions

694 ppm of Cu			*604 ppm of Cu*			*382 ppm of Cu*			*151 ppm of Cu*		
	Folds			*Folds*			*Folds*			*Folds*	
Days	*MD*	*CD*	*Days*	*MD*	*CD*	*Days*	*MD*	*CD*	*Days*	*MD*	*CD*
Aging Conditions: 90 °C and 50% rh											
0	801	271	0	822	324	0	864	340	0	894	278
2	539	251	2	490	173	1	567	274	1	650	280
3	419	212	3	373	169	2	413	241	2	563	253
6	86	67	6	81	57	3	423	233	3	563	275
						4	294	139	4	548	189
						7	113	66	7	361	109
						13	0	0	10	244	106
									14	161	74
Aging Conditions: 100 °C											
0	801	271	0	822	324	0	864	340	0	894	278
2	792	327	2	603	271	1	803	352	1	620	263
3	766	343	3	663	235	2	848	282	2	697	313
6	693	295	6	680	226	3	740	363	3	612	294
13	533	241	13	500	230	4	664	273	4	754	302
17	587	233	17	485	186	7	598	253	7	620	236
23	449	203	23	449	199	13	456	169	10	597	246
						17	483	183	14	500	220

NOTE: MD denotes machine direction; CD denotes cross direction.

Table VI. Fold-Endurance Data for Paper Samples Treated with Aqueous Iron(II) Sulfate Solution

1410 ppm of Fe			*1170 ppm of Fe*			*475 ppm of Fe*		
	Folds			*Folds*			*Folds*	
Days	*MD*	*CD*	*Days*	*MD*	*CD*	*Days*	*MD*	*CD*
			Aging Conditions: 90 °C and 50% rh					
0	783	377	0	851	391	0	797	331
2	186	103	1	438	181	1	563	233
5	1	6	2	178	131	2	428	233
8	0	0	3	67	45	3	273	158
			7	0	1	4	232	120
						7	10	10
			Aging Conditions: 100 °C					
0	783	377	0	851	391	0	797	331
2	310	170	1	460	307	1	678	274
5	123	71	2	380	165	2	569	240
8	33	42	3	308	129	3	519	213
13	7	15	7	99	82	4	467	234
16	8	9	9	41	44	7	302	167
19	4	4	11	19	32	13	196	130
29	2	4	15	20	11	17	108	78

NOTE: MD denotes machine direction; CD denotes cross direction.

Table VII. Fold-Endurance Data for Paper Samples Treated with Aqueous Iron(II) Sulfate and Sodium Bicarbonate Solutions

1360 ppm of Fe			*1190 ppm of Fe*			*453 ppm of Fe*		
	Folds			*Folds*			*Folds*	
Days	*MD*	*CD*	*Days*	*MD*	*CD*	*Days*	*MD*	*CD*
			Aging Conditions: 90 °C and 50% rh					
0	808	328	0	713	307	0	771	305
2	521	284	2	499	217	1	573	260
3	524	269	3	577	179	2	531	198
6	466	233	6	439	178	3	569	223
13	149	102	13	155	96	4	434	205
17	11	27	17	5	15	7	431	180
						13	159	113
						17	40	40
			Aging Conditions: 100 °C					
0	808	328	0	713	307	0	797	305
2	763	294	2	768	279	1	678	332
3	719	298	3	684	219	2	569	286
6	651	328	6	637	206	3	519	324
13	528	259	13	510	186	4	467	328
17	493	251	17	523	190	7	302	251
23	456	200	23	364	179	13	196	220
						17	108	160

NOTE: MD denotes machine direction; CD denotes cross direction.

Table VIII. Fold-Endurance Data for Paper Samples Treated with Metallic Acetylacetonate Solutions

90 °C and 50% rh			*100 °C*		
Aging Time (days)	*Folds*		*Aging Time (days)*	*Folds*	
	MD	*CD*		*MD*	*CD*
	302 ppm of Cu(II)				
0	676	510	0	676	310
1	599	220	1	560	264
2	340	220	2	554	251
3	253	153	3	562	200
7	3	11	7	405	266
9	1	2	9	331	197
			11	388	166
			18	225	111
	566 ppm of Fe(III)				
0	703	330	0	703	330
1	587	309	1	594	243
2	446	245	2	591	301
3	400	218	3	457	230
7	296	190	7	455	184
9	252	154	9	371	176
11	163	119	11	163	190
18	108	71	18	180	143

NOTE: MD denotes machine direction; CD denotes cross direction.

and dry accelerated-aging conditions suggests that the reaction mechanisms by which this paper ages in the presence and absence of moisture are not identical.

Data on accelerated aging of test samples in the presence of iron and copper species have been compiled in Tables IV through VIII. Selected data from these tables are also illustrated in Figures 3 to 5. The accelerated-aging data have been used to evaluate relative lifetime and relative stability values presented in Tables X and XI. Generally, the metal-catalyst content of the paper samples studied here is appreciably higher than the level of contamination that one may encounter in commercial papers. The intent is to highlight and compare otherwise subtle differences in the stability of paper that may result from a change in the chemical environment around the catalytic sites.

Accelerated-aging data for test samples containing metallic species adsorbed from aqueous iron(II) and copper(II) sulfate solutions show that under humid as well as dry aging conditions the rate of degradation increases with increasing metal content. Therefore, chemical treatments

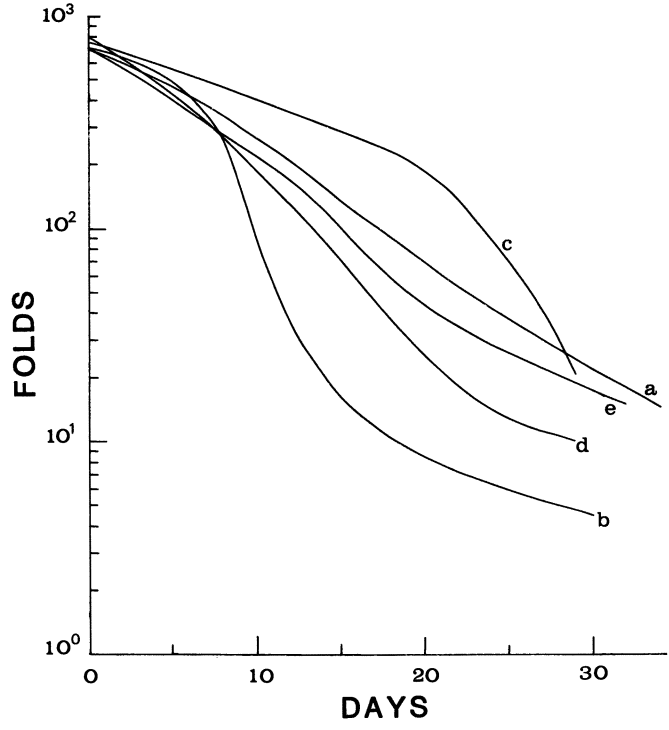

Figure 1. Accelerated aging of control samples at 90 °C and 50% rh. a, no washing; b, water wash; c, $NaHCO_3$ and water wash; d, acetone wash; e, acetone and chloroform (1:1) wash.

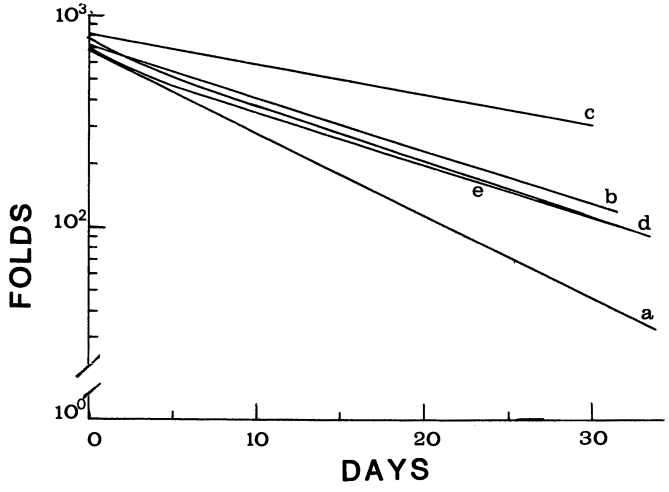

Figure 2. Accelerated aging of control samples at 100 °C. a, no washing; b, water wash; c, $NaHCO_3$ and water wash; d, acetone wash; e, acetone and chloroform (1:1) wash.

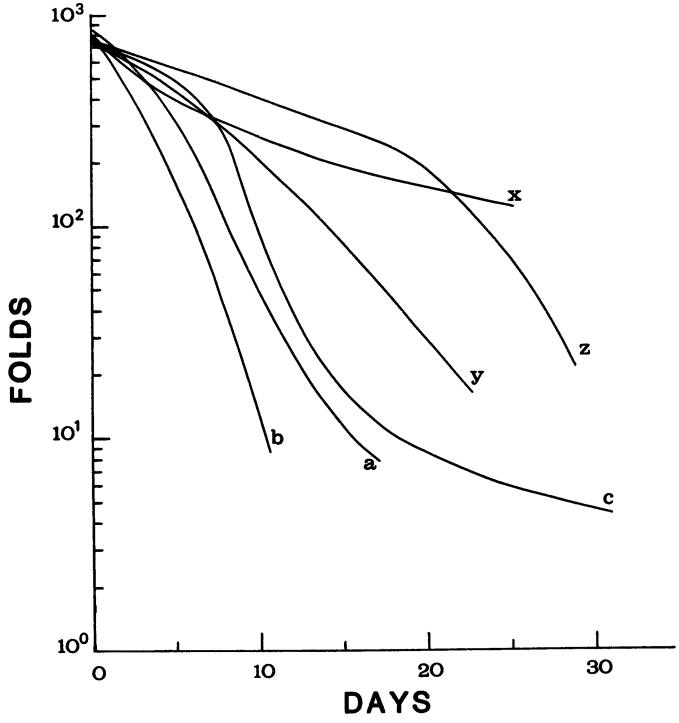

Figure 3. Accelerated aging of samples treated with metal salt solutions and aged at 90 °C and 50% rh. Chemical treatments: a, $CuSO_4$; b, $FeSO_4$; c, water-washed control; x, $CuSO_4$ and $NaHCO_3$; y, $FeSO_4$ and $NaHCO_3$; z, $NaHCO_3$ and water-washed control. Metal contents: a, 138 ppm of Cu; b, 475 ppm of Fe; x, 151 ppm of Cu; y, 453 ppm of Fe.

that extract metal-catalyst species from paper would be likely to extend its life.

In the absence of moisture, the observed rates of degradation are invariably slower, even though the temperature under these aging conditions is 10 degrees higher. Nevertheless, the relative lifetime values clearly demonstrate that copper and iron species adsorbed from sulfate solutions do catalyze the oxidation process in a dry aging environment. This observation was contrary to our expectation because earlier observations had suggested that in the copper-catalyzed system the presence of moisture was essential for the progress of the oxidation process (3). Indeed, as can be seen from Table XI, the catalytic effect of copper is not evident at lower concentrations. The rate of copper-catalyzed degradation may be so slow under these experimental conditions that it is masked by other degradative reactions.

In the case of both copper and iron compounds, the influence of the chemical environment on the catalytic effect of the metal is unmistak-

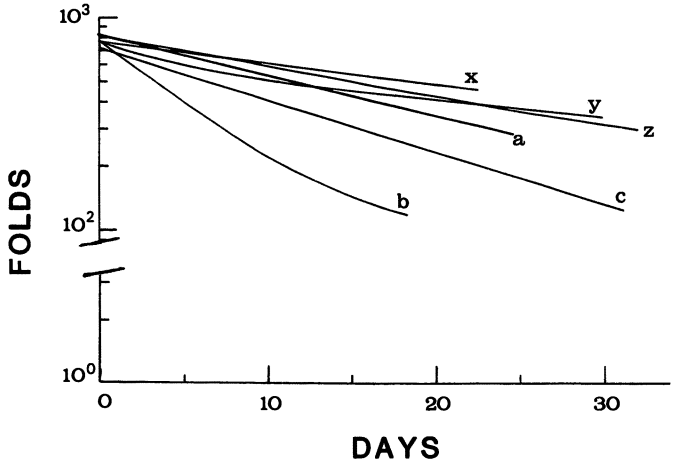

Figure 4. Accelerated aging of samples treated with metal salt solutions and aged at 100 °C. Chemical treatments: a, $CuSo_4$; b, $FeSO_4$; c, water-washed control; x, $CuSO_4$ and $NaHCO_3$; y, $FeSO_4$ and $NaHCO_3$; z, $NaHCO_3$ and water-washed control. Metal contents: a, 138 ppm of Cu; b, 475 ppm of Fe; x, 151 ppm of Cu; y, 453 ppm of Fe.

able. An examination of the relative lifetime values, X_h and X_d, in Tables X and XI shows that both iron- and copper-catalyzed systems achieve an appreciable increase in stability upon neutralization. This gain in stability as a result of the neutralization treatment is observed under humid as well as dry accelerated-aging conditions.

The effect of the neutralization reaction on the rate of metal-catalyzed degradation can be assessed in isolation from its effect on the acidic hydrolysis component by a comparison of the relative stability values before and after the sodium bicarbonate treatment. In the iron-catalyzed system, the relative stability values observed after the bicarbonate treatment are appreciably higher, especially at higher metal concentrations. The catalytic effect of iron for the autoxidative process may be reduced. However, the iron species adsorbed from the sulfate solution may itself be acidic. In such a case, neutralization of this acidic moiety would reduce the rate of acidic hydrolysis. Some metal salts, such as alum, are known to increase the acidic content of paper and accelerate its hydrolytic degradation (*36*).

A substantial increment in the relative lifetime values of copper-impregnated samples is also observed after sodium bicarbonate treatment (Table XI). Thus, the copper-catalyzed system also benefits from the neutralization process. However, the change in relative stability values does not compare as favorably. A small but consistently adverse effect upon relative stability indicates that unlike iron species, ionic copper species can be more effective catalysts at lower acidic concentra-

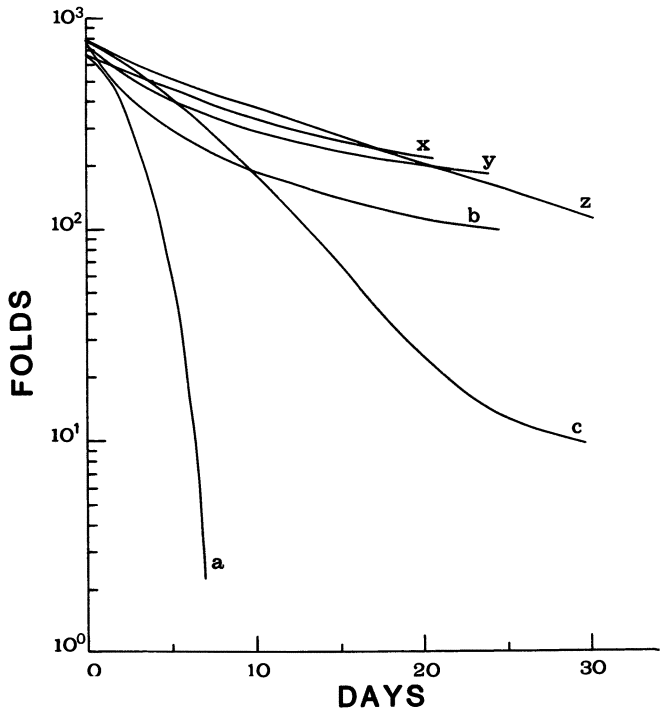

Figure 5. Accelerated aging of samples containing metal acetylacetonates. Samples a, b, and c were aged at 90 °C; x, y, and z were aged at 100 °C. Treatments: a, x: $Cu(acac)_2$; b, y: $Fe(acac)_3$; c, z: acetone-washed controls. Metal contents: a, x: 302 ppm of Cu; b, z: 566 ppm of Fe.

Table IX. Aging Parameters for Control Samples

Sample Treatment	X_h *(days)*	Z_h	X_d *(days)*	Z_d
None	26.4	—	25.8	—
Water	11.3	0.426	35.4	1.37
$NaHCO_3$	27.8	1.05	68.4	2.65
Acetone	13.6	0.516	34.2	1.34
Acetone and chloroform (1:1)	17.1	0.647	31.5	1.22

NOTE: X_h and Z_h values are for samples aged at 90 °C and 50% rh; X_d and Z_d values are for samples aged at 100 °C.

tions. Thus, the neutralization treatment does stabilize paper contaminated with copper species. However, a higher gain in stability would be expected in the absence of copper. The observed decrease in relative stability upon neutralization is so small that, from a practical standpoint, a similar increase in the catalytic effect of trace concentrations of copper

would not detract significantly from the overall gain in stabilization of paper upon deacidification.

Under accelerated aging in a dry environment at 100 °C, the relative lifetimes are appreciably larger than those observed under humid aging at 90 °C. However, the effect of aging conditions on relative stability does not follow a consistent trend. For iron species adsorbed from a sulfate solution, and for the iron(III) acetylacetonate system, the relative stabilities in the presence and absence of moisture are generally of the same order. On the other hand, the copper(II) acetylacetonate system, which has a relative stability value of 0.223 under humid aging conditions, assumes a value of 0.952 in a dry environment. Thus, in this reaction system, the presence of water molecules appears essential for the catalytic mechanism. The aging of paper in the presence of copper species adsorbed from a sulfate solution presents a complex picture. At higher metallic concentrations, the relative stabilities are comparable in humid and dry aging experiments. However, under dry aging conditions, the relative stability increases sharply as the copper concentration decreases. In this system, relative stabilities in humid and dry environments are of the same order at higher copper concentrations, whereas they contrast appreciably at lower concentrations.

After the bicarbonate treatment, both copper and iron species exhibit no catalytic activity in the absence of moisture. In fact, at higher concentrations, the copper species appears to stabilize paper in a dry environment. The neutralized copper species may be basic enough to retard degradation due to acidic hydrolysis. This observation suggests that water molecules must be involved in the reaction mechanism that prevails under humid aging conditions. The contrast in the relative stabilities of the neutralized systems under humid and dry aging conditions suggests that a simultaneous reduction in acidic and moisture content serves best to stabilize bleached kraft paper against metal-catalyzed oxidative degradation.

Rates of degradation observed in the presence of ionic iron and copper systems have been compared with those obtained for the respective acetylacetonate chelate systems in Tables X and XI. Lower relative lifetime and relative stability values are observed for the copper(II) acetylacetonate catalyzed system than those obtained in the presence of higher concentrations of the ionic copper species. A similar increase in the catalytic efficiency of copper upon coordination has been reported by Ericsson et al. (*10*). However, iron(III) acetylacetonate shows no catalytic effect at all. This observation of contrary effects on the stability of paper with the same chelates of two highly active transition metal catalysts is most interesting. Unlike the relatively stable octahedral iron(III) acetylacetonate molecule, the tetrahedral, tetracoordinate copper(II) chelate could accept two more ligands if it were to assume an

Table X. Aging Parameters for Paper Treated with Iron Solutions

Sample Treatment	*Iron Content (ppm)*	X_h *(days)*	Z_h	X_d *(days)*	Z_d
$FeSO_4$	1410	2.40	0.213	5.55	0.157
$FeSO_4$	1170	3.00	0.264	7.14	0.202
$FeSO_4$	475	6.36	0.565	19.5	0.551
$FeSO_4$, $NaHCO_3$	1360	13.2	0.474	64.8	0.974
$FeSO_4$, $NaHCO_3$	1190	13.9	0.501	83.1	1.22
$FeSO_4$, $NaHCO_3$	453	17.3	0.625	66.9	0.978
$Fe(acac)_3$	566	17.7	1.04	29.0	0.847

NOTE: X_h and Z_h values are for samples aged at 90 °C and 50% rh; X_d and Z_d values are for samples aged at 100 °C.

octahedral configuration. Conceivably, the driving force for such an occurrence can result from a gain in the ligand field stabilization energy due to a Jahn-Teller distortion (*37*). Most of the reactants in the autoxidation reaction sequence presented earlier are oxygenated species. These species can function as electron-pair donors to bond to the central copper atom. The simultaneous coordination of two reactants on the catalyst molecule would considerably enhance the probability of their interaction. The same reactants would also coordinate to the copper atom in the absence of the acetylacetonate ligands. In such a case, however, they may not find themselves in close enough proximity to react because they can occupy any of the six positions in the coordination sphere of the metal atom. The bidentate nature of the acetylacetonate ligands assures that in their presence, the other two ligands coordinate in adjacent positions.

Table XI. Aging Parameters for Papers Treated with Copper Solutions

Sample Treatment	*Copper Content (ppm)*	X_h *(days)*	Z_h	X_d *(days)*	Z_d
$CuSO_4$	685	2.60	0.231	9.95	0.281
$CuSO_4$	591	3.10	0.275	8.00	0.226
$CuSO_4$	395	4.62	0.410	33.2	0.939
$CuSO_4$	138	7.80	0.697	36.0	1.02
$CuSO_4$, $NaHCO_3$	694	5.42	0.195	98.1	1.43
$CuSO_4$, $NaHCO_3$	604	5.58	0.201	87.6	1.28
$CuSO_4$, $NaHCO_3$	382	6.80	0.245	67.8	0.991
$CuSO_4$, $NaHCO_3$	151	17.25	0.622	73.5	1.07
$Cu(acac)_2$	302	3.81	0.223	30.0	0.952

NOTE: X_h and Z_h values are for samples aged at 90 °C and 50% rh; X_d and Z_d values are for samples aged at 100 °C.

The catalytic free radical reaction mechanism cited earlier and the explanation just given present a likely sequence of events. However, they do not present a complete picture. Neither suggests any essential interaction between the metallic catalyst and water molecules. Yet, a comparison of the catalytic effect of copper(II) acetylacetonate in the presence and absence of moisture presents a striking contrast. It has already been demonstrated that neutralized ionic copper species actively catalyze degradative reactions in a humid aging environment. In a dry aging environment they are inactive, or at higher concentrations they even have a stabilizing effect on paper. Indeed, even in the absence of metallic catalysts, it has been seen that a solvent wash, which had a destabilizing effect under a humid aging environment, appeared to have a small but consistent and measurable beneficial effect under a dry aging environment. The stabilizing influence of the bicarbonate neutralization treatment was also much more significant in the absence of water. These observations are based upon work with a single paper. It cannot be presumed that similar trends would be observed with other papers, or cellulose itself. Nevertheless, it has been clearly demonstrated that, in at least some of the experimental systems studied here, bleached kraft paper degrades by different reaction mechanisms in the presence and absence of water. Data obtained here cannot be reconciled with the premise that water serves only to accelerate the rate of degradation, while the order of relative stabilities observed in its absence remains unchanged. On the other hand, Block (*38*) has presented evidence to suggest that cellulose ages by the same reaction mechanism under humid as well as dry aging environments. A better understanding of the role of water in the degradation of cellulose is needed.

The effect of metallic contaminants on the color reversion of paper has received considerable attention (*39–41*). In this work, paper samples containing copper and iron in comparable concentrations were selected for a limited study of the influence of their nature on color reversion in paper. These data are presented in Table XII. The extent of color reversion generally corresponds to the observed loss in permanence. However, one notable exception to this general trend is seen: The samples containing copper adsorbed from a copper(II) sulfate solution and subsequently treated with sodium bicarbonate lose brightness faster on humid aging than does the corresponding sample containing iron. Under dry aging of the same samples, paper containing the iron species is subject to a greater degree of color reversion than the sample containing copper. Paper samples with these copper and iron species in a near neutral environment show relative stability values close to unity; that is, the catalytic effect of the metals on the degradation of paper is minimal, if any. Thus, in some cases in which the catalytic effect of metallic contaminants on physical properties of paper may not be noticable, color reversion can be affected.

Table XII. Effect of Metals on Color Reversion

Treatment	Metal Content (ppm)	Brightness (%)		
		Unaged	Humid Aging	Dry Aging
None	—	78	68	73
Water wash	—	78	70	74
$CuSO_4$	395	77	61	74
$CuSO_4$	138	78	68	75
$CuSO_4$, $NaHCO_3$	382	77	63	74
$CuSO_4$, $NaHCO_3$	151	78	68	74
$Cu(acac)_2$	302	77	59	74
$FeSO_4$	475	74	63	69
$FeSO_4$, $NaHCO_3$	453	73	66	71
$Fe(acac)_3$	566	78	70	75

NOTE: Aging period was 16 days.

Some useful practical inferences can be drawn from this work for the conservation treatment of bleached kraft paper.

In most cases, a simultaneous reduction in acid and moisture content may provide the most convenient as well as efficient treatment for the stabilization of bleached kraft paper against oxidative degradation catalyzed by copper and iron contaminants.

A deacidification or buffering treatment, which would impart an alkaline reserve to paper, may stabilize it not only against acidic hydrolysis but also against iron-catalyzed degradation. An especially significant application would be in the treatment of documents written in acidic iron gall ink. Frequently, such writing eats through paper as a result of acidic hydrolytic and iron-catalyzed oxidative degradation of the cellulosic substrate. Deacidification of these documents may serve to retard both causes of degradation and thus prevent the ink from eating through the paper matrix. At the same time, conservators must be cautioned that a slight change in the color of the ink due to the decrease in acidity would not be surprising.

The data obtained here show a gain in the catalytic efficiency of copper species after a neutralization treatment. However, at the trace concentrations of copper that are found in most paper, this effect would be so small that it can be disregarded.

Treatment with chelating agents would stabilize paper if it were to succeed in extracting the metallic contaminants from paper. If, on the other hand, chelating agents were retained within the paper matrix by bonding to the metallic species, predicting whether such treatment would stabilize the paper or further accelerate its degradation would be difficult.

Literature Cited

1. Richter, G. A. *Ind. Eng. Chem.* **1935**, *27*, 432.
2. Langwell, W. H. *Tech. Bull. Tech. Sect., Brit. Paper and Board Makers' Assoc.* **1952**, *29*, 21-28, 52; **1953**, *30*, 170; **1955**, *36*, 199-207.
3. Williams, J. C.; Fowler, C. S.; Lyon, M. S.; Merrill, T. L. in "Preservation of Paper and Textiles of Historic and Artistic Value"; Williams J. C., Ed.; ADVANCES IN CHEMISTRY SERIES No. 164, American Chemical Society: Washington D.C., 1977; p. 37.
4. Robert, A.; Traynard, P.; Martin-Borret, O. U.S. pat. 3,384,533, 1968.
5. Robert, A.; Viallet, A.; Rerolle, P.; Andreolety, P. *Paper Trade J.* **1968**, *152*, 49.
6. Noreus, S. E. O.; Samuelson, H. O. Swedish pat. 314 584, 1968; Canadian pat. 901 221, 1972.
7. Rowlandson, G. *CPPA Chemical Pulping and Bleaching Conference Preprints* **1971**, p. 57.
8. Croon, I.; Andrews, P. H. *Advances in Oxygen Bleaching, Part I*, Chemetics Ltd., 1971.
9. Samuelson, O.; Stoppe, L. *Svensk Papperstidn.* **1969**, *72*, 662; **1971**, *74*, 545.
10. Ericsson, B.; Lindgren, B. O.; Theander, O. *Svensk Papperstidn.* **1971**, *74*, 757.
11. Samuelson, O. *Papier* **1970**, *24*, 671.
12. Pierron, M. P. *Bull. Soc., Chem. France* **1950**, *17*, 291.
13. Robert, A.; Viallet, A. *A.T.I.P.* **1971**, *25*, 238.
14. Gilbert, A.; Pavlova, E.; Rapson, W. H. *Tappi* **1973**, *56*, 95.
15. Sinkey, J. D.; Thompson, N. S. *Paper. Puu* **1974**, *56*, 473.
16. McCloskey, J. T.; Sinkey, J. D.; Thompson, N. S. *Tappi* **1975**, *58* (2), 56.
17. Landucci, L. L.; Sanyer, N. *Tappi* **1975** *58* (2), 60.
18. Isbell, H. S.; Parks, E. W.; Naves, R. G. *Carbohydrate Res.* **1975**, *45*, 197.
19. Manoocheri, M.; Samuelson, O. *Svensk Papperstidn.* **1973**, *76*, 486.
20. Hart, J. R. *Tappi* **1981**, *64* (3), 43.
21. Entwistle, D.; Cole, E. H.; Wooding, N.S. *Textile Res. J.* **1949**, *19*, 609.
22. Shafizadeh, F.; Bradbury A. G. W. *J. Appl. Polym. Sci.* **1979**, *23*, 1431.
23. Hipp, C. J.; Busch, D. H. "Coordination Chemistry"; Vol. 2; Martell, A. E., Ed.; ACS MONOGRAPH SERIES No. 174; American Chemical Society: Washington, D.C., 1978; p. 221-475.
24. Williams, J. C.; Merrill, T. L., Preservation Research and Testing Office, Library of Congress, Washington, D.C., unpublished data.
25. Arney, J. C., Jacobs, A. J., Newman, R., Preprints, *Seventh Annu. Meet. Am. Inst. Conserv.* 1979.
26. Denisov, E. T.; Emanuel, N. M. *Russian Chem. Rev.* **1960**, *29*, 645.
27. Kochi, J. *J. Am. Chem. Soc.* **1962**, *84*, 1193.
28. Hiatt, R.; Irwin, K. C.; Gould, C. W. *J. Org. Chem.* **1968**, *33*, 1430.
29. Onuma, K.; Wada, K.; Yamashita, J.; Hashimoto, H. *Bull. Chem. Soc. Jpn* **1967**, *40*, 2900.
30. Richardson, W. H. *J. Am. Chem. Soc.* **1965**, *87*, 247.
31. *Ibid.* **1965**, *87*, 1096.
32. Ingold, K. U. in "Oxidation of Organic Compounds-I"; Mayo, F. R., Ed.; ADVANCES IN CHEMISTRY SERIES No. 75; American Chemical Society: Washington D.C., 1968; p. 296-305.
33. Tang, L. C.; Jones, N. M. M. *J. Am. Inst. Conserv.* **1979**, *18*, 61.
34. Nelson, J.; King, A.; Indictor, N.; Cabell, D. *J. Am. Inst. Conserv.* **1982**, *21*, 59.

35. Eirk, K. *Bull. Am. Group, Intern. Inst. Conserv.* **1972**, *12*, 82.
36. Wilson, W. K.; Parks, E. J. *Restaurator* **1980**, *4*, 1–55.
37. Cotton, F. A.; Wilkinson, G. "Advanced Inorganic Chemistry" Interscience Publishers: New York, 1967; p. 683.
38. Block, I., *ICOM Comm. Conserv., Prepr. 7th Triennial Meet* **1984**, p. 84.9.7.
39. Czepiel, T. P. *TAPPI* **1960**, *43* (*4*), 289.
40. Kleinert, T. N.; Marracini, L. M. *Svensk. Papperstidn.* **1962**, *65*, 126; **1963**, *66*, 126; **1966**, *69*, 69; **1966**, *69*, 159.
41. Hon, D. N.-S. In "Preservation of Paper and Textiles of Historic and Artistic Value"; Williams J. C., Ed; ADVANCES IN CHEMISTRY SERIES No. 164. American Chemical Society: Washington, D.C., 1977; p. 119.

RECEIVED for review February 20, 1984. Accepted June 10, 1985.

Published on February 1, 1986 on http://pubs.acs.org | doi: 10.1021/ba-1986-0212.ch023

23

Accelerated Aging of Cellulosic Textiles at Different Temperatures

The Effect of Tetrahydridoborate Reduction

Ira Block and Hye Kyung Kim

Department of Textiles and Consumer Economics, University of Maryland, College Park, MD 20742

Measurements of tear strength and color change were made on a set of cotton cloths to study the rates of degradation under accelerated aging in a dry oven at temperatures ranging from 100 to 150 °C. Fabrics treated with either sodium or tetramethylammonium tetrahydridoborates were degraded at rates about one-half that of untreated controls. These results were consistent over the temperature range. Calculation of the activation energy (E_a) by different methods showed $E_a = 25.5 \pm 1.5$ kcal, in keeping with measurements made by others at lower temperatures.

SODIUM TETRAHYDRIDOBORATE, first used as a reducing agent for carbonyl species by Chaikin and Brown (*1*) in 1949, was shown to be effective as a reducing agent for the aldehyde groups in polysaccharides in 1952 (*2*) and was reported to be effective in stabilizing oxycellulose in 1953 (*3*). Head (*4*), in 1955, studied the use of $NaBH_4$ on both oxycellulose and hydrocellulose and showed that a dilute, unbuffered solution was highly effective in removing aldehydes and stabilizing the materials. In 1965, Varshney and Luner (*5*) reviewed the literature on the use of $NaBH_4$ and other tetrahydridoborates in the manufacture of paper and discussed their use as bleaching agents and their ability to stabilize pulps against both alkaline and acidic treatments. In 1980, Tang et al. (*6*) and in 1982, Burgess (*7*) reported results of investigations on the use of tetrahydridoborates for paper conservation.

Only very recently, however, has tetrahydridoborate reduction been considered to be more than just a bleaching method in the conservation of cellulosic textiles and paper. To some extent, the delay in studying the

0065-2393/86/0212-0411$06.00/0

use of the reduction process was due to the belief that carboxylic acids, formed during the oxidation of cellulose, were the major cause of its decay. Block (*8*, *9*), however, demonstrated that although deacidification and buffering with an alkaline material were useful in extending the lifetime of new cellulosic textiles, the treatment was no more effective than rinsing in deionized water for protecting aged textiles.

That carboxylic acid groups on the cellulosic chain play a minor role in the decay of the material is not surprising. As Davidson and Standing (*10*) and Davidson and Nevell (*11*) showed, acidic oxycelluloses are unstable because the carboxylic acids are converted to water-soluble, low molecular weight species. Thus, in old cellulosic textiles, the acidic species are removed from the fabric upon washing, and deacidification is not necessary. Kerr et al. (*12*) and more recently Hackney and Hedley (*13*) have provided independent evidence of the correctness of this view. Paper that has been subjected to sulfite pulping or that contains alum or rosin, which may form acids, responds well to deacidification because the additives are being neutralized.

If the carboxylic acids on the cellulosic chain are not the major cause of the thermooxidative decay of old cellulosic textiles, one must consider the carbonyl species, particularly the aldehydes on the C_2 and C_3 carbons. Nikitin (*14*) noted that "the primary autoxidation process is a reaction of molecular oxygen with aldehyde groups, which initiates a chain reaction resulting in more profound changes and decomposition of the molecule". Thus, reduction of the aldehyde groups should lead to improved stability of degraded cellulose.

In aqueous solution, tetrahydridoborates decompose as follows:

$$MBH_4 + 2H_2O \rightarrow MBO_2 + 4H_2 \quad (1)$$

whereas the carbonyl species in cellulose are reduced according to the following reaction:

$$C(=O)R + H_2 \rightarrow HC(OH)R \quad (2)$$

In this chapter, we report the results of a study on the use of tetrahydridoborate reduction in improving both the color and strength retention of cotton fabric artificially aged at temperatures ranging from 100 to 150 °C.

Experimental

Fabric. The fabric used in this work was a plain weave, 80 × 80 cotton print cloth weighing about 100 g/m^2 (Testfabrics, No. 400). The fabric was twice laundered and dried according to the American Association of Textile Chemists and Colorists (AATCC) Test Method No. 124-1978.

Tetrahydridoborate Treatment. Both 98%-pure $NaBH_4$ and 95%-pure tetramethylammonium tetrahydridoborate (TMA) were supplied by Alfa Products. Solutions (0.03 M) were prepared by adding weighed amounts of the solid to deionized water and diluting the solution to 1 L in a volumetric flask. After dissolution, the liquid was transferred to a shallow glass tray maintained at 25 °C in a water bath. Nine specimens of cloth cut to 10 × 10 cm and weighing about 9 g in toto were placed in the tray and allowed to float in the solution. Preliminary experiments showed that the results of the testing were not changed by soaking for periods longer than 20 min, nor was prewetting in water necessary. All samples were treated for 20 min. Control samples were soaked in deionized water at 25 °C for 20 min.

Following soaking, samples were rinsed with deionized water, squeezed gently, and allowed to air dry overnight on glass-fiber screens. All samples were stored in desiccators over silica gel prior to accelerated aging.

Accelerated Aging. Samples were removed from the desiccators and placed on glass-fiber screens in a forced-draft oven at the required temperature. Upon removal from the oven, samples were collected in a desiccator and then were transferred to a conditioned laboratory for testing.

Mechanical Testing. Tensile strength tests were performed with an Instron tensile tester as per the American Society for Testing and Materials (ASTM) D-1682, and tear testing was done with an Elmendorf apparatus as per ASTM D-1424 at 21 °C and 65% rh, after conditioning the specimens for at least 24 h. Results reported are the average of three tests.

Color Measurements. Color measurements were made on the samples with a Hunterlab model D25D2 color difference meter after conditioning. A white standard plate was used as a backing. Both fronts and backs of the cloths were measured three times, and the results were averaged. Color differences are reported in the LAB system.

Results and Discussion

Initial measurements of tensile strength and extension at break were erratic, as were calculations of energy to break. This problem led to an investigation of the correlation between tensile and tear testing; the results are shown in Figure 1. This figure demonstrates that the tensile strength of the cloth is not sensitive to baking time until tear strength has dropped below about 70% of the initial value. For cloths degraded beyond this point, a linear relationship exists between tensile and tear strengths. These results are analogous to those reported by Graminski et al. (*15*) for the tensile strength and folding endurance of paper. Their results showed that folding endurance was a more accurate measure of the degradation of the material. Furthermore, as noted by Taylor (*16*), ". . . in contrast to the role of tensile strength, tearing strength is directly involved in the assessment of serviceability" of cotton fabrics. Thus, because tear strength is more closely related to the performance of the cloth in actual use, and because it proved to be more sensitive to treat-

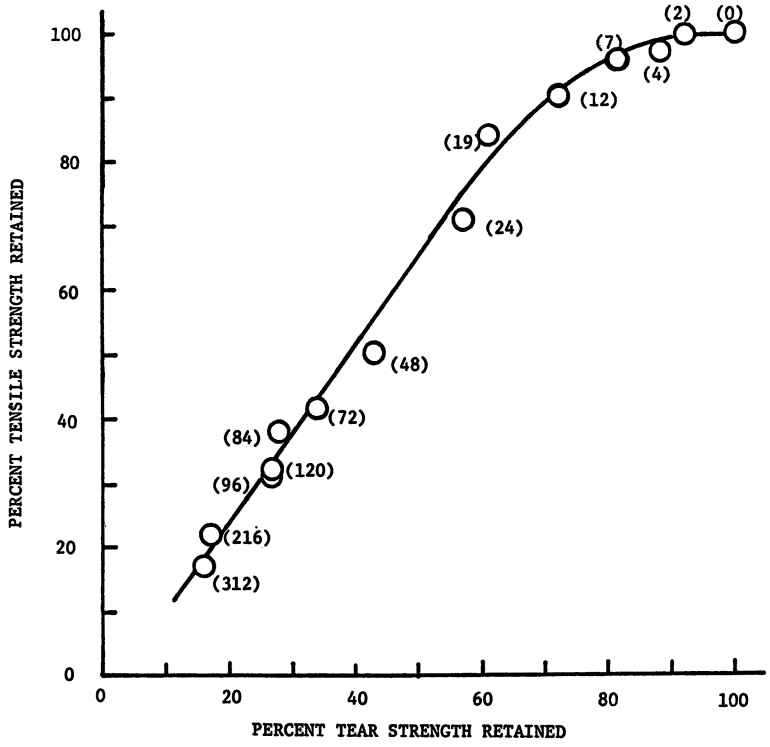

Figure 1. Comparison of strength retention by tear and tensile methods. Numbers in parentheses refer to baking time at 150 °C.

ment of the fabric than tensile strength, mechanical testing is reported in terms of this parameter.

Because changes in the relative humidity of the oven could affect the results, a study of the change in degradation rate as a function of relative humidity was conducted. Moisture was added to the air in the oven by permitting deionized water to seep through eight tubes perforated by 1-mm diameter holes along their length into a large shallow reservoir at the bottom of the oven. By adjusting the rate of water flow, the relative humidity could be controlled. The relative humidity was measured by use of wet-and dry-bulb thermometers and a psychrometric chart. The results, which are shown in Figure 2, indicate that the effect of relative humidity at 150 °C is small. (For further discussion of temperature and humidity effects in accelerated aging, *see* Reference 19).

A typical degradation curve for new and aged cloth is shown in Figure 3. This figure demonstrates that a TMA treatment is effective in slowing the rate of strength loss, even for cloth that has been artificially degraded to less than 60% strength retention. In addition, as shown in

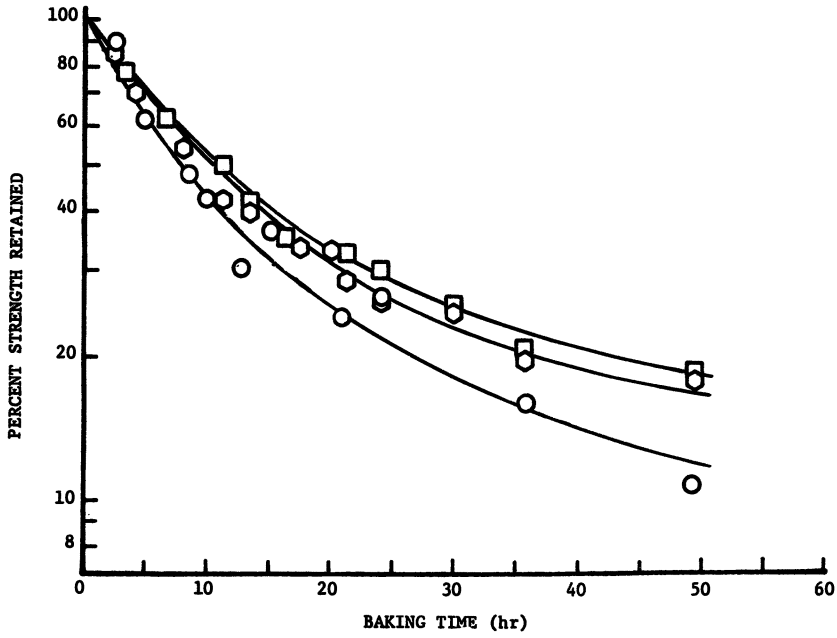

Figure 2. Percent strength retained vs. baking time for cotton fabric at 150 °C and varying relative humidity. Key: □, 1% rh (0.02 g/g); ⬡, 2% rh (0.08 g/g); ○, 10% rh (0.5 g/g).

Figure 4, the cloth is significantly whitened by the reduction treatment, and the more degraded it is, the greater the improvement in color.

Treatment with $NaBH_4$ shows a similar pattern. The rates of degradation of new cloth at temperatures ranging from 150 to 100 °C are shown in Figures 5–8. The plots are based on a statistical model that assumes first-order kinetics for depolymerization (*17*). They show that, in all cases, the treated fabric has been protected against thermooxidative degradation. Furthermore, the fact that the curves exhibit a linear portion indicates that strength loss is following first-order kinetics and may mean that changes in the mechanical properties are directly proportional to changes in the chemical state of the system.

Examination of Figure 5 shows that degradation in the early stages is linear with time but occurs at a rate somewhat higher than the rate of degradation found at later times. This phenomenon is observed at temperatures down to 120 °C. Apparently we are observing at least two phenomena, one in which the cellulosic chains are readily broken, and one in which the chains are more resistant to thermooxidative attack. It is not necessarily true that these results indicate different chemical mechanisms at work. Consider the model described by Rowland et al. (*18*) in which cellulose is a somewhat defective crystal composed of

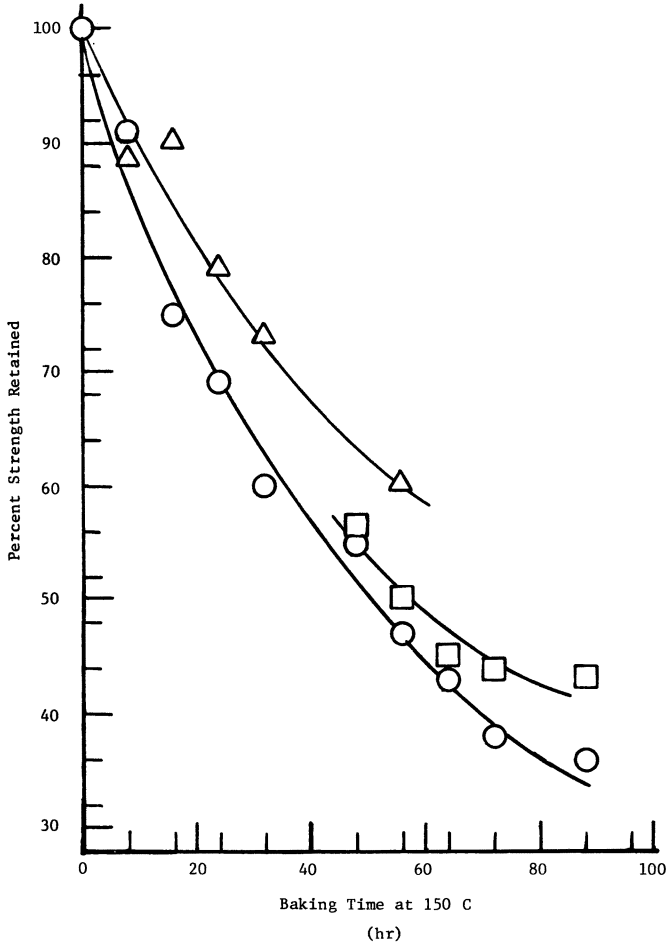

Figure 3. Strength retention vs. baking time for water-washed and TMA-treated cotton. Key: ○, new (untreated); △, baked 8 h (TMA treated); □, baked 48 h (TMA treated).

many disordered regions. We can postulate that the same chemical mechanisms are at work, but that they proceed at a much faster pace in the disordered regions than in the well-ordered regions. If this hypothesis is true, then as cellulosic fabrics age, their rate of degradation should continually decrease as less and less disordered material is available for reaction. Thus, we should find that cellulosic fabrics degrade to some point, and in the absence of mechanical forces, such as handling and rapid changes in humidity, they should hardly seem to degrade further. This situation may account for the longevity of ancient cloths, such as Egyptian burial garments, and may also indicate that very ancient cellu-

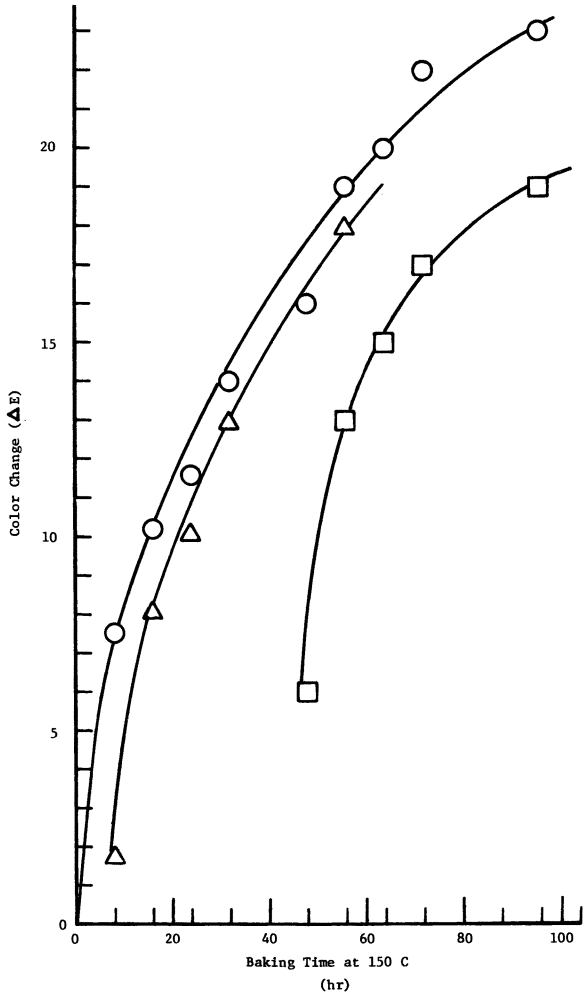

Figure 4. Color change vs. baking time for water-washed and TMA-treated cotton. Key: ○, new (untreated); △, baked 8 h (TMA treated); □, baked 48 h (TMA treated).

losic textiles do not require chemical treatment. A second consequence of this model—that old cellulosic textiles should be more crystalline than new ones—is well documented.

In Figure 8 we see another phenomenon occuring that was not evident in the work done at higher temperatures. The time scale here is much extended. In the beginning, the fabric seems to increase in tear strength before undergoing any losses. Once again the $NaBH_4$-treated material performs better than the water-washed material. We are likely observing a slow rearrangement of the morphology of the cellulosic

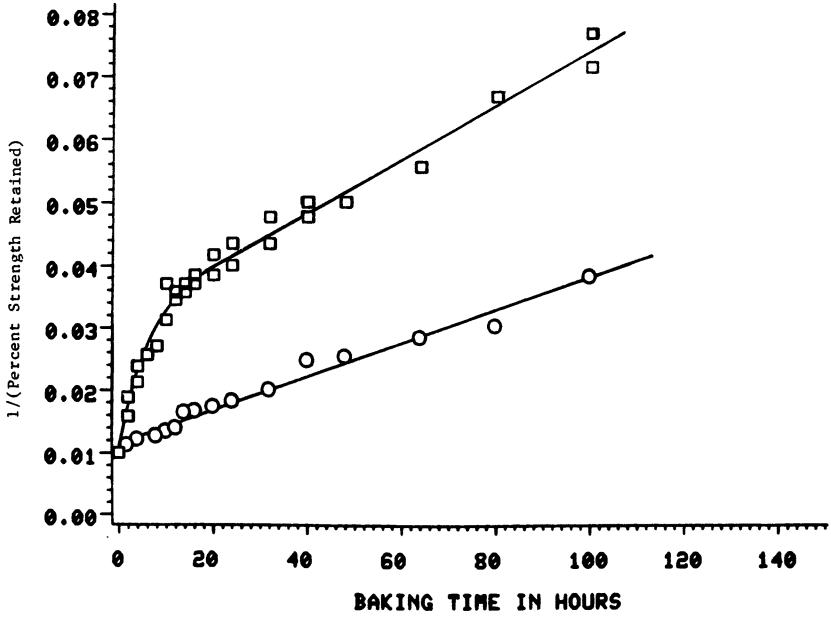

Figure 5. Aging of cotton fabric at 150 °C. Key: □, untreated; ○, treated with 0.05% $NaBH_4$.

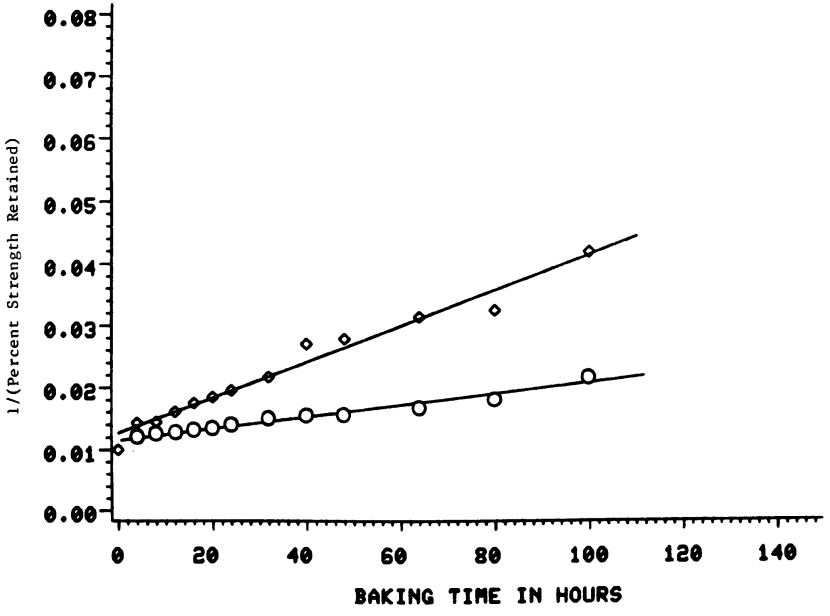

Figure 6. Aging of cotton fabric at 140 °C. Key: ◇, untreated; ○, treated with 0.05% $NaBH_4$.

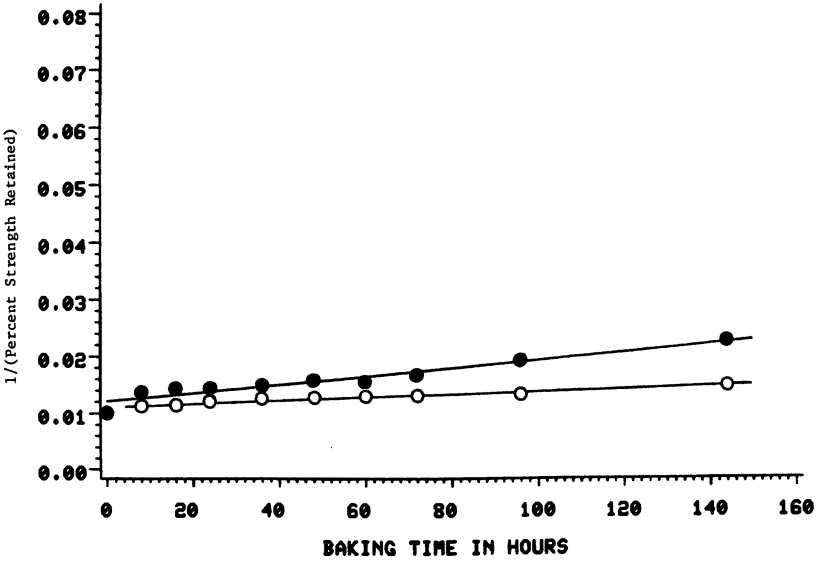

Figure 7. Aging of cotton fabric at 120 °C. Key: ●, untreated; ○, treated with 0.05% $NaBH_4$.

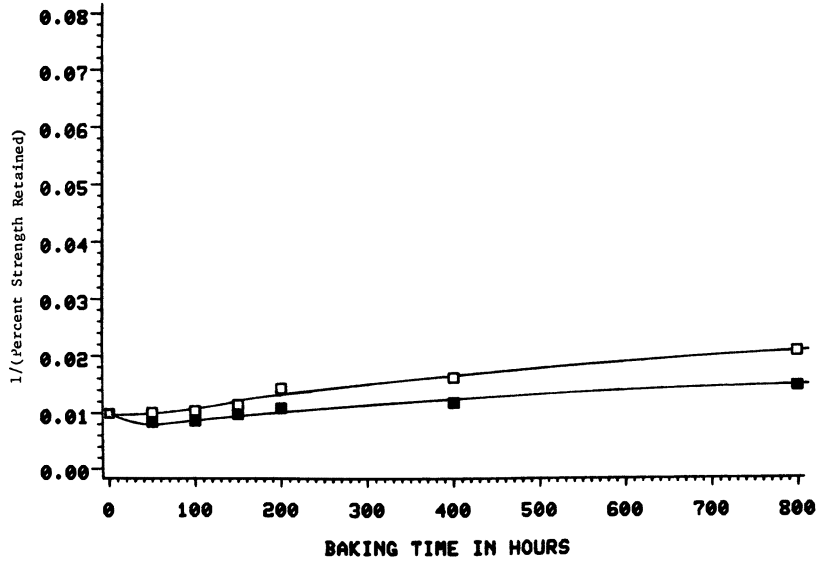

Figure 8. Aging of cotton fabric at 100 °C. Key: □, untreated; ■, treated with 0.05% $NaBH_4$.

chains within the fiber that leads to a reduction in internal stress and a concomitant increase in tear strength, although a restructuring of the yarns during thermal treatment is not impossible. This stress reduction occurs along with degradation, and in the early life of the fabric it leads to some improvement in mechanical properties. It is, however, soon surpassed by the deteriorating effects of depolymerization, so only at the lower temperatures is the phenomenon observed. At ambient conditions the molecular rearrangement is likely to be so slow that depolymerization is the overwhelming process.

Figure 9 is an Arrhenius plot of the results of the accelerated aging of new fabric at different temperatures. Regardless of the properties measured, long-term strength retention and short-term strength retention or color change (the slopes) for both treated and untreated cloth fell within the range of 25.5 ± 1.5 kcal/mol; no statistically significant difference between the highest and lowest values at the 0.05 or the 0.1 confidence levels was found. These results are in excellent agreement with the literature (*19*) and show that the reaction mechanisms do not change over the temperature range from 100 to 150 °C.

Tables I–IV summarize the preceding results in terms of the ratios of tetrahydridoborate-treated to water-washed cloth for color change and strength retention. Table I shows that the TMA treatment does little to affect the change in color of new or slightly degraded cloth, but it is quite effective for those cloths that have been aged significantly. Table II yields similar conclusions for $NaBH_4$, although $NaBH_4$ does not appear to do as well as TMA. This result indicates that extremely long

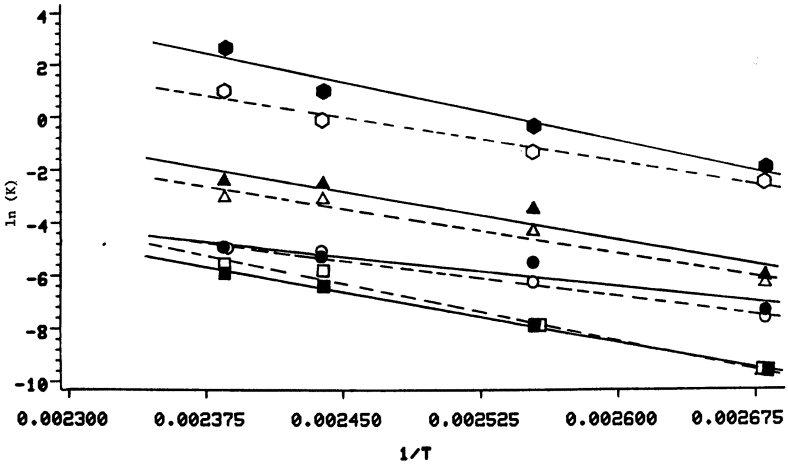

Figure 9. Arrhenius plot for cotton fabric. Key: ---, treated with $NaBH_4$; ———, untreated; ○, long-term strength retained; □, color change; △, short-term strength retained; ⬡, 1/(percent strength retained).

Published on February 1, 1986 on http://pubs.acs.org | doi: 10.1021/ba-1986-0212.ch023

Table I. Color Change: TMA-Treated Versus Water-Washed Cloths

Prebake Time (hours)	*Total Baking Time (hours)*										
	0	*8*	*16*	*24*	*32*	*40*	*48*	*56*	*64*	*72*	*96*
0	0.2	−0.8	−0.8	−3.7	—	—	−1.8	—	—	—	—
8	—	1.6	1.0	1.0	−1.0	—	—	−1.0	—	—	—
16	—	—	0.3	2.5	2.7	1.9	—	—	1.6	—	—
24	—	—	—	3.6	3.8	3.7	4.3	—	—	1.5	—
48	—	—	—	—	—	—	5.0	3.0	1.0	1.0	1.0

NOTE: Values are the differences in color change at 150 °C between new cloth that was washed with water and new cloth that was treated with TMA. Negative values mean that the water-washed cloth was less discolored than the treated cloth.

Table II. Color Change: $NaBH_4$-Reduced Versus Water-Washed Cloths

Baking Temperature (°C)	*Baking Time (hours)*	*Color-Change Difference*[a]
150	4	−5.6
	10	−8.7
	16	−6.9
	24	−7.0
	48	−11.0
140	8	0.0
	16	−0.9
	24	−1.3
	48	−1.0
	96	−2.4
	144	−2.6
120	16	1.1
	24	1.0
	96	0.0
	144	0.0
100	200	0.0
	400	−0.1
	800	−0.1

[a] Values are the differences in color change between new cloth that was washed with water and new cloth that was treated with $NaBH_4$. Negative values mean that the water-washed cloth was less discolored than the treated cloth.

aging times are required at lower temperatures before the results manifest themselves. Table III shows that the reduction treatment does significantly improve strength retention for older fabrics and is also useful for new ones, whereas Table IV indicates that $NaBH_4$ may be more beneficial than TMA.

Conclusions

Tetrahydridoborate reduction of cellulosic textiles improves color and strength retention. $NaBH_4$ appears to give better strength retention, whereas TMA seems superior in color retention. These results are independent of baking temperatures over the range from 100 to 150 °C, and humidity effects are small at elevated temperatures.

Acknowledgments

We wish to acknowledge the help of R. V. Kuruppillai in performing some of the experiments, the enlightening conversations with B. F. Smith, and the generous financial support of the National Museum Act, administered by the Smithsonian Institution.

Published on February 1, 1986 on http://pubs.acs.org | doi: 10.1021/ba-1986-0212.ch023

Table III. Percent Strength Retained: TMA-Treated Versus Water-Washed Cloths

Prebake Time (hours)	*Total Baking Time (hours)*										
	0	*8*	*16*	*24*	*32*	*40*	*48*	*56*	*64*	*72*	*96*
0	1.03	1.12	1.21	1.18	—	—	1.15	—	—	—	—
8	—	1.01	1.23	1.18	1.26	—	—	1.33	—	—	—
16	—	—	1.05	1.09	1.12	1.04	—	—	1.24	—	—
24	—	—	—	1.10	1.16	1.15	1.20	—	—	1.35	—
48	—	—	—	—	—	—	1.07	1.02	0.94	1.19	1.30

NOTE: Values are the percent-strength-retained ratios at 150 °C of cotton cloth treated with TMA to cotton cloth washed with water.

Table IV. Percent Strength Retained: $NaBH_4$-Reduced Versus Water-Washed Cloths

Baking Temperature (°C)	*Baking Time (hours)*	*Percent-Strength-Retained Ratio*[a]
150	4	0.90
	10	0.94
	16	1.67
	24	2.05
	48	2.12
140	8	1.11
	16	1.29
	24	1.33
	48	1.41
	96	1.76
	144	1.93
120	16	1.40
	24	1.55
	96	1.89
	144	2.14
100	200	1.07
	400	1.49
	800	1.89

[a] Values are the percent-strength-retained ratios of cotton cloth treated with $NaBH_4$ to cotton cloth washed with water.

Literature Cited

1. Chaikin, S. W.; Brown, W. G. *J. Am. Chem. Soc.* **1949**, *71*, 122.
2. Abdel-Akher, M.; Hamilton, J. K.; Montgomery, R.; Smith, F. *J. Am. Chem. Soc.* **1952**, *74*, 4970.
3. Meller, A. *TAPPI* **1953**, *36*, 366.
4. Head, F. S. H. *J. Text. Inst. Trans.* **1955**, *46*, T400. *J. Text. Inst. Trans.* **1955**, *46*, T584.
5. Varshney, M. C.; Luner, P. *TAPPI* **1961**, *44*, (44), 285.
6. Tang, L.; Troyer, M. A.; Williams, J. C. *Prepr. of the Sixth Annu. Conf., IIC—Canadian Group,* Ottawa, July 1980.
7. Burgess, H. D. *Prepr. Tenth Annu. Meet. of the AIC,* Milwaukee, May, 1982.
8. Block, I. *J. Am. Inst. Conserv.* **1982**, *22*, 25.
9. Block, I. *Prep. of the Contributions to the Wash. Congr. of the IIC,* September, 1982.
10. Davidson, G. F.; Standing, H. A. *J. Text. Inst. Trans.* **1951**, *42*, T141.
11. Davidson, G. F.; Nevell, T. P. *J. Text. Inst. Trans.* **1956**, *46*, T439.
12. Kerr, N.; Hersh, S. P.; Tucker, P. A.; Berry, G. M. In "Durability of Macromolecular Materials"; Eby, R. K., Ed. ACS SYMPOSIUM SERIES No. 95; American Chemical Society: Washington, D.C., 1979; p. 25.
13. Hackney, S.; Hedley, G. *Prepr. of the Seventh Triennial Meet. of the ICOM Comm. for Conserv.* Copenhagen, September, 1984.
14. Nikitin, N. I., In "The Chemistry of Cellulose and Wood"; J. Schmorak, Trans., Israel Program for Scientific Translations: Jerusalem, 1979; p. 171.

15. Graminski, E. L.; Parks, E. J.; Toth, E. E. In "Durability of Macromolecular Materials"; Eby, R. K., Ed.; ACS SYMPOSIUM SERIES No. 95, American Chemical Society: Washington, D.C., 1979.
16. Taylor, H. M. *J. Text. Inst. Trans.* **1959**, *50*, T161.
17. Jellinek, H. H. G. In "Aspects of Degradation and Stabilization of Polymers"; Elsevier: New York, 1978; p. 2.
18. Rowland, S. P.; Nelson, M. L.; Welch, C. M.; Hebert, J. J. *Text. Res. J.* **1976**, *46*, 194.
19. Block, Ira *Prepr. of the Seventh Triennial Meet. of the ICOM Comm. for Conserv.*, Copenhagen, September, 1984.

RECEIVED for review November 26, 1984. ACCEPTED March 13.

24

Stabilization of Paper Through Sodium Borohydride Treatment

Lucia C. Tang[1]

Preservation Research and Testing Office, The Library of Congress, Washington, DC 20540

The treatment of bleached kraft pulp with sodium borohydride followed by incorporation of basic calcium salts increased the stability of paper made from this pulp by 1.5–2.6 times. When manufactured paper, rather than pulp, was subjected to sodium borohydride treatment followed by washing with an aqueous solution of calcium hydroxide, the stability of the paper increased by as much as 4 times for groundwood paper and 30 times for bleached kraft paper.

THE DEGRADATION OF PAPER is a complex process. Besides acid hydrolysis, which appears to be the dominant degradative reaction under ambient conditions, oxidation contributes significantly to the degradation of the cellulosic matrix. Hydroxyl groups in the cellulosic macromolecule are oxidized to carbonyl and carboxyl groups (*1, 2*); this oxidation leads to the discoloration of paper (*3*) and a decline in its physical properties (*4, 5*). Oxidative degradation can occur in the manufacture of paper during pulping and bleaching operations. Trace metals introduced through contact with process chemicals, natural water sources, or metallic process units may further act as oxidation catalysts. Lignin residues, sunlight, UV light, air pollutants, heat, and humidity also facilitate the oxidation of cellulose in paper fibers.

Reducing agents, such as sodium borohydride, have been used extensively to improve brightness and other physical properties of pulp and paper (*6–17*). Sodium borohydride is a moderate reducing agent that selectively reduces compounds such as aldehydes and ketones to the corresponding alcohols, without affecting carboxylic acid groups (*6, 7, 12*). Rapson (*13*) reported that chlorine dioxide and/or sodium borohydride improved brightness stability during the processing of cellulosic

[1]Mailing address: 9116 Bells Mill Rd., Potomac, MD 20854.

pulp. Wade (*14*) proposed a combination of treatments with borohydride and ozone to bleach and brighten cellulosic fibers. Burr (*15*) demonstrated that small amounts of sodium borohydride and sodium hydroxide in wash water increased the strength of cotton fabric and prevented the deposition of iron in the fabric. Sodium borohydride has been employed to bleach paper and paper artifacts (*16, 17*). Bleaching of paper artifacts with dilute sodium borohydride solution has been successfully, although infrequently, attempted by paper conservators for several years.

In this work, the reducing action of sodium borohydride was combined with the stabilizing effect of mildly basic compounds of calcium and magnesium (*18, 19*) to enhance the permanence of paper. Washing of paper with dilute calcium hydroxide solution after treatment with sodium borohydride has been shown to greatly increase its stability (*20–22*). The effect of calcium hydroxide concentration in the wash solution has been investigated (*18, 23*). Jullander and Brune (*8*) showed that the presence of some metal salts, including those of calcium, increases the efficiency of borohydride reduction. This finding led me to investigate the stability of paper made from a pulp slurry containing sodium borohydride and calcium hydroxide or carbonate. The reduction of copper species in paper by borohydride ions was observed. The inhibition of this reduction process in the presence of magnesium bicarbonate was studied qualitatively.

Experimental

Materials. All test papers were obtained from a single roll or were made from pulp. The following test papers were used: (1) Foldur kraft paper, a bleached kraft paper made from 90% southern pine and 10% hardwood pulps, with 0.5% rosin size and 3% titanium filler; (2) newsprint paper made from 80% groundwood and 20% unbleached sulfite pulp; and (3) handsheets prepared from a 1:1 furnish of Weyerhaeuser New Bern softwood (NBS) and New Bern hardwood (NBH) bleached kraft pulps.

In the preparation of handsheets, the NBS:NBH furnish was soaked for 2 h in 0.0005% $Ca(OH)_2$ solution prior to the beating step. The pulp was then beaten in deionized water containing sodium borohydride (0.1% pulp weight) and 0.02% calcium hydroxide or 2.5% calcium carbonate (*22*). A Craftool Hollander laboratory beater was employed. Handsheets were prepared with a Noble and Wood brass sheet-making machine, which had been painted to prevent the contact of pulp with brass. The metal wire was overlaid with polyester fiber screening (75 mesh). Handsheets were also prepared from the same pulp furnish with the Noble and Wood brass sheet-forming machine before it had been painted. These papers had a copper content of 150 ppm as a result of contamination from the brass.

Preparation of Solutions. To provide a constant flow of 0.002% $Ca(OH)_2$ solution wash, a saturated calcium hydroxide solution was constantly diluted by using the chemical feeder technique (*18*). Other dilute calcium hydroxide solu-

tions were also prepared by appropriate dilution of 0.2% (saturated) calcium hydroxide solution with deionized water. Magnesium bicarbonate solution was prepared by passing a current of carbon dioxide into an aqueous slurry of basic magnesium carbonate (*19*).

Treatment of Papers. Foldur kraft and newsprint papers were prewet with 1:1 solution of denatured alcohol and distilled water before further treatment to facilitate their penetration. Test papers were treated with sodium borohydride by immersion in the appropriate solution for 30 min. The treated samples and untreated controls were then washed for 1 h in either a wash solution composed of dilute calcium hydroxide or in deionized water, or they were left unwashed.

Some Foldur kraft samples were preaged before borohydride treatment and further aging. Paper samples were subjected to accelerated aging at 100 °C in a dry oven for 14 h or at 90 °C and 50% rh for 7 h.

Aging Procedures. All treated and/or washed samples were air dried and conditioned at 70 °F and 50% rh before being subjected to accelerated aging in humid (90 °C and 50% rh) or dry (100 °C) circulating-air ovens for 1, 2, 3, and 5 weeks. Prior to testing, the oven-aged samples were again conditioned at 70 °F and 50% rh.

Determination of Physical Properties of Paper. BRIGHTNESS. The brightness was measured with a Photovolt model 670 reflectance meter. Measurements were made at 10 different places on both sides of the sheet, and the readings were averaged.

FOLDING ENDURANCE. The Massachusetts Institute of Technology folding endurance test was run at 0.5 kg of tension in the machine direction; 10 specimens were tested per sample, according to the Technical Association of the Pulp and Paper Industry (TAPPI) T511-su-69.

pH VALUES. A variation of the TAPPI cold-extraction procedure for the determination of pH (T435-su-68) of paper samples was employed. Specimens weighing 2.5 g and 250 mL of deionized water were mixed for 45 s in a Waring blender. The pH was measured with a Fisher Accumet model 320 pH meter and glass electrode standardized against a pH 7.00 buffer.

METAL CONTENT. Calcium, sodium, and boron contents of paper samples were determined by using a direct solid-sampling technique in conjunction with flameless atomic absorption spectroscopy (*20, 24*). A Varian Techtron AA-6 spectrophotometer was employed with a model 90 carbon rod atomizer. In addition to the direct solid-sampling technique, calcium content was also determined by digesting samples with concentrated hydrochloric acid for 30 min.

Results and Discussion

The effect of a reducing sodium borohydride treatment followed by a mildly alkaline wash on the physical properties and stability of paper was studied. Test papers were characterized by measuring their initial pH value, brightness, and folding endurance. Then they were subjected to borohydride treatment and washed with dilute calcium hydroxide solution or deionized water. The concentrations of sodium borohydride

and calcium hydroxide solutions were varied. These test papers were subjected to accelerated aging under dry as well as humid environments. The progressive loss in folding endurance and brightness was monitored intermittently. The effect of treatment variables was compared by computing relative permanence values. Plots of the logarithm of folding endurance versus aging time were employed to project the estimated lifetimes of samples and controls. *Estimated lifetime* is defined as the aging time required for the sample to retain only one double fold. The estimated lifetime of a sample divided by that of the corresponding control yields the *relative permanence*. These results are presented in Tables I and II.

Another measure of stability is the relative brightness retention. Variation of brightness was plotted against aging time. The initial slope of this line was computed by a least-squares treatment. The value of the slope for the control divided by the slope for the treated sample is defined as the *relative brightness retention*. These results are presented in Tables III and IV.

The results obtained for the treatment of Foldur kraft paper are shown in Table I. Generally, the folding endurance of the test papers increased as a result of the borohydride treatment. However, in the case of papers treated with 1.0% $NaBH_4$ without any subsequent washing, the folding endurance decreased markedly. The alkalinity in these papers probably led to hydrolytic degradation of paper. The 0.002% calcium hydroxide wash was just sufficient to neutralize (pH 7.0) the untreated Foldur kraft papers, although very little alkaline reserve was retained (0.18% $CaCO_3$ or 702 ppm of Ca). Because of the alkalinity of the borohydride solution (pH 9.5–10.0), treated sheets were alkalized to a greater or lesser extent (pH 6.2–9.5) depending upon the concentration of the solution employed.

In treating Foldur kraft papers with sodium borohydride, the relative stability of the treated paper was found to be related to its calcium and sodium content. Foldur kraft papers washed with 0.002% calcium hydroxide wash demonstrated about six to eight times the stability of samples left unwashed or washed with deionized water. Paper treated with 1.0% sodium borohydride, but left unwashed, degraded faster than the control sample. These samples had retained a large concentration of sodium (38.4%), whereas their calcium content had decreased from 445 to 143 ppm. The washing efficiency of deionized water and water containing 0.002% calcium hydroxide differed markedly in the removal of residual sodium from the 1.0% sodium borohydride-treated sheets. Treatment with 1.0% $NaBH_4$, followed by efficient washing with dilute calcium hydroxide, increased the relative permanence of Foldur kraft paper by about 27–33 times. This relative permanence was about four times that observed for paper subjected to calcium hydroxide washing

Published on February 1, 1986 on http://pubs.acs.org | doi: 10.1021/ba-1986-0212.ch024

Table I. Characterization and Aging of Foldur Kraft Paper

Treatment	*Washing*	*Initial pH*	*Calcium Content (ppm)*	*Sodium Content (ppm × 10^{-4})*	*Initial MIT Folds*	*Relative Permanence*	
						Dry Oven	*Humid Oven*
None	none	5.1	445	0.73	890	1.00	1.00
None	deionized water	5.7	292	0.14	1045	1.00	0.97
None	0.002% $Ca(OH)_2$	7.0	702	0.11	1050	8.43	5.71
0.01% $NaBH_4$	none	6.4	361	1.06	1255	4.35	2.88
0.01% $NaBH_4$	deionized water	6.2	465	0.64	1325	3.20	2.51
0.01% $NaBH_4$	0.002% $Ca(OH)_2$	7.2	684	0.10	1285	7.79	5.22
0.1% $NaBH_4$	none	9.0	418	5.65	960	25.8	11.8
0.1% $NaBH_4$	deionized water	7.5	425	1.61	1065	14.1	10.2
0.1% $NaBH_4$	0.002% $Ca(OH)_2$	7.6	713	0.19	1345	8.15	9.23
1.0% $NaBH_4$	none	9.5	143	38.40	20	1.3	1.3
1.0% $NaBH_4$	deionized water	7.9	228	2.6	1370	17.4	15.6
1.0% $NaBH_4$	0.002% $Ca(OH)_2$	7.7	779	0.72	1030	32.7	26.8

Published on February 1, 1986 on http://pubs.acs.org | doi: 10.1021/ba-1986-0212.ch024

Table II. Characterization and Aging of Newsprint Paper

Treatment	*Washing*	*Initial pH*	*Calcium Content (ppm)*	*Sodium Content (ppm × 10^{-4})*	*Initial MIT Folds*	*Relative Permanence*	
						Dry Oven	*Humid Oven*
None	none	5.2	845	1.4	340	1.00	1.00
None	deionized water	5.9	712	0.3	400	1.00	0.98
None	0.002% $Ca(OH)_2$	8.8	1883	0.2	450	2.67	2.63
0.01% $NaBH_4$	none	7.1	1053	5.50	460	1.97	1.89
0.01% $NaBH_4$	deionized water	5.5	882	1.82	540	1.54	1.84
0.01% $NaBH_4$	0.002% $Ca(OH)_2$	8.0	1581	0.2	480	2.57	3.63
0.1% $NaBH_4$	none	8.8	580	18.1	560	2.53	2.62
0.1% $NaBH_4$	deionized water	7.2	665	6.8	595	3.64	1.95
0.1% $NaBH_4$	0.002% $Ca(OH)_2$	7.9	1866	0.3	525	3.48	4.32
1.0% $NaBH_4$	none	9.2	265	60.5	10	0.88	0.92
1.0% $NaBH_4$	deionized water	8.0	205	11.7	600	4.07	1.57
1.0% $NaBH_4$	0.002% $Ca(OH)_2$	8.5	2135	1.5	600	3.87	3.36

Published on February 1, 1986 on http://pubs.acs.org | doi: 10.1021/ba-1986-0212.ch024

Table III. Brightness Retention of Foldur Kraft Paper

Treatment	*Washing*	*Initial Brightness*	*Final Brightness*		*Relative Brightness Retention*	
			Dry Oven	*Humid Oven*	*Dry Oven*	*Humid Oven*
None	none	75.6	66.0	56.4	1.00	1.00
None	deionized water	75.6	66.2	59.1	1.00	1.16
None	0.002% $Ca(OH)_2$	75.0	70.2	57.7	2.02	1.34
0.01% $NaBH_4$	none	76.5	69.8	64.0	1.43	1.49
0.01% $NaBH_4$	deionized water	77.0	70.3	60.7	1.43	1.17
0.01% $NaBH_4$	0.002% $Ca(OH)_2$	76.7	72.0	58.1	2.09	1.65
0.1% $NaBH_4$	none	77.7	72.0	55.0	1.83	0.90
0.1% $NaBH_4$	deionized water	79.2	72.7	58.0	1.51	0.88
0.1% $NaBH_4$	0.002% $Ca(OH)_2$	78.5	73.8	62.5	2.02	1.18
1.0% $NaBH_4$	none	79.2	74.0	32.8	2.06	0.41
1.0% $NaBH_4$	deionized water	80.5	73.8	57.7	1.46	0.81
1.0% $NaBH_4$	0.002% $Ca(OH)_2$	79.5	74.9	69.0	2.18	2.30

Published on February 1, 1986 on http://pubs.acs.org | doi: 10.1021/ba-1986-0212.ch024

Table IV. Brightness Retention of Newsprint Paper

Treatment	*Washing*	*Initial Brightness*	*Final Brightness*		*Relative Brightness Retention*	
			Dry Oven	*Humid Oven*	*Dry Oven*	*Humid Oven*
None	none	56.6	41.0	31.6	1.00	1.00
None	deionized water	56.2	41.0	34.4	1.03	1.30
None	0.002% $Ca(OH)_2$	51.9	43.1	37.5	1.55	1.51
0.01% $NaBH_4$	none	57.3	43.0	35.8	1.09	1.13
0.01% $NaBH_4$	deionized water	57.9	42.7	36.8	1.02	1.18
0.01% $NaBH_4$	0.002% $Ca(OH)_2$	52.4	43.3	39.2	1.49	1.65
0.1% $NaBH_4$	none	60.6	44.8	36.1	1.09	1.11
0.1% $NaBH_4$	deionized water	62.6	44.8	38.6	0.88	1.03
0.1% $NaBH_4$	0.002% $Ca(OH)_2$	59.1	46.0	43.9	1.24	1.66
1.0% $NaBH_4$	none	61.6	43.9	23.5	0.95	0.76
1.0% $NaBH_4$	deionized water	66.2	46.3	36.8	0.81	0.85
1.0% $NaBH_4$	0.002% $Ca(OH)_2$	62.3	47.2	38.9	1.04	1.06

alone. Papers treated with 0.1% $NaBH_4$ retained 5–6% sodium in paper. These paper samples showed a relative permanence value of 26, which is almost twice as high as that observed for the 0.1% $NaBH_4$-water-washed sample, and about three times the relative permanence of the $Ca(OH)_2$-washed sample. It appears that up to a point, increasing the sodium ion concentration stabilizes the paper. For papers treated with 1.0% $NaBH_4$ solution, calcium hydroxide wash provides the highest stability in comparison with unwashed or water-washed samples. Therefore, it is recommended that the concentration of aqueous sodium borohydride be limited to 0.1%, unless its use is followed by efficient washing and deacidification.

The effect of washing on borohydride treatment of newsprint paper is shown in Table II. As with Foldur kraft paper, improved initial folding endurance was observed; the higher solution concentrations produced the greater effects. Because newsprint exhibits much greater absorption than Foldur kraft, the 0.002% calcium hydroxide was sufficient to raise the pH of untreated newsprint from 5.2 to 8.8, with the retention of 0.47% $CaCo_3$ (1883 ppm of Ca). The relative permanence values for newsprint subjected to sodium borohydride treatment do not show as significant an improvement as that observed for Foldur kraft samples. As demonstrated by the atomic absorption data, retention of sodium is greater in newsprint than in Foldur kraft papers. The calcium hydroxide wash removed residual sodium from both treated and untreated papers, whereas the deionized water was not nearly as efficient. This observation is probably due to ion-exchange effects. Also, treatment with borohydride without subsequent washing lowered the calcium content of newsprint paper. Treatment of newsprint with either 0.1% or 1.0% $NaBH_4$ solution followed by 0.002% calcium hydroxide wash produced about 3.5–4 times the relative permanence of the control and about 1.5 times the stability of calcium hydroxide washing alone.

The results obtained for the brightness retention of borohydride-treated and washed Foldur kraft papers are presented in Table III. The sodium borohydride treatment increased initial brightness by up to 5 brightness units. Higher solution concentrations produced a greater brightening effect. Samples washed with 0.002% calcium hydroxide solution showed significant improvement in brightness retention. The combination of 1.0% $NaBH_4$ treatment followed by the calcium hydroxide wash produced significantly greater improvement in brightness retention on humid-oven aging than that conferred by calcium hydroxide washing alone. Under the same aging conditions, treatments with less concentrated borohydride solutions did not produce a significantly greater improvement in brightness retention than the $Ca(OH)_2$ wash. Brightness-retention values observed during accelerated aging in a dry oven also did not show a significant difference between a simple $Ca(OH)_2$ wash and borohydride treatment.

Table IV shows brightness retention of newsprint papers. Borohydride treatment increased initial brightness by as much as 10 brightness units. A decrease in brightness is generally observed when newsprint is subjected to a $Ca(OH)_2$ wash. Treatment with either 0.1% or 1.0% $NaBH_4$ followed by 0.002% calcium hydroxide washing also increased the brightness of newsprint. For the newsprint samples, the borohydride treatment did not produce a significantly greater improvement in brightness retention than the calcium hydroxide wash alone.

The results presented in Tables I and II showed that the treatment of Foldur kraft paper with 1.0% $NaBH_4$ followed by washing with 0.002% calcium hydroxide extended its permanence by as much as 32 times. It was of interest to investigate whether this increase in stability could be further extended by increasing the concentration of the $Ca(OH)_2$ wash solution. The results shown in Table V depict the aging properties of Foldur kraft paper washed with 0.002% and 0.007% $Ca(OH)_2$ solution. Although appreciable enhancement in relative permanence was observed for both concentrations, an increase in the $Ca(OH)_2$ concentration from 0.002% to 0.007% in the wash solution did not produce a significant gain in the stability of Foldur kraft paper. Brightness, as well as brightness retention, was significantly improved by washing with 0.002% $Ca(OH)_2$ solution, but no significant further gains were achieved by increasing the concentration of calcium hydroxide in the wash solution to 0.007%. Brightness retention was further improved by the combination of sodium borohydride treatment and aqueous calcium hydroxide wash. Again, the increase in brightness retention for the two concentrations of $Ca(OH)_2$ solution was the same within experimental error. Improvement in brightness retention results from stability gained through deacidification as well as through the reduction of chromophoric groups by borohydride treatment.

It was of interest to determine if sodium borohydride treatment could also stabilize degraded paper and restore its physical properties. The effect of borohydride treatment and subsequent $Ca(OH)_2$ wash on the stability of preaged paper was studied. These results are presented in Table VI. In all cases, borohydride treatment increased the brightness of preaged samples to values that were higher than their initial brightness. All treatment procedures, including $Ca(OH)_2$ wash, produced significant improvement in folding-endurance retention on accelerated aging. Borohydride treatment increased the stability of paper by as much as 20–34 times. The stability of paper treated with sodium borohydride solution and washed with $Ca(OH)_2$ was about twice that of paper subjected to the alkaline washing alone. No significant difference in folding-endurance retention was observed between 0.002% and 0.007% $Ca(OH)_2$-washed samples.

The stability of paper made from pulp reduced by sodium borohydride in the presence of calcium hydroxide or carbonate was studied.

Published on February 1, 1986 on http://pubs.acs.org | doi: 10.1021/ba-1986-0212.ch024

Table V. Effect of Calcium Hydroxide Wash Concentration on Aging of Foldur Kraft Paper

Treatment	$Ca(OH)_2$ Conc. (%)	Initial Folds	Relative Permanence		Initial Brightness	Relative Brightness Retention	
			Dry Oven	Humid Oven		Dry Oven	Humid Oven
None	none	1075	1.0	1.0	75.4	1.00	1.00
None	0.002	1430	12.3	8.3	75.4	1.68	1.42
None	0.007	1350	12.1	11.1	74.8	1.99	1.50
1.0% $NaBH_4$	0.002	1500	27.2	24.5	78.5	2.43	2.24
1.0% $NaBH_4$	0.007	1325	28.2	24.2	78.1	2.41	2.39

Table VI. Effect of Calcium Hydroxide Wash Concentration on Aging of Preaged Foldur Kraft Paper

Treatment	$Ca(OH)_2$ Conc. (%)	Initial Folds		Relative Permanence		Initial Brightness		Relative Brightness Retention	
		Dry Oven	Humid Oven	Dry Oven	Humid Oven	Dry Oven	Humid Oven	Dry Oven	Humid Oven
None	none	660	740	1.0	1.0	74.1	74.1	1.00	1.00
None	0.002	845	925	11.5	13.0	74.9	74.5	2.26	1.36
None	0.007	915	1000	11.2	12.8	74.7	74.1	2.53	1.53
1.0% $NaBH_4$	0.002	930	1030	23.3	26.1	78.7	78.7	2.87	2.20
1.0% $NaBH_4$	0.007	995	1005	18.5	34.0	78.7	78.2	2.82	2.26

NOTE: Papers aged in dry oven were preaged at 100 °C for 14 h; papers aged in humid oven were preaged at 90 °C and 50% rh for 7 h.

Bleached kraft pulp was beaten with 0.1% $NaBH_4$ and 0.02% $Ca(OH)_2$ or 2.5% $CaCO_3$. A higher concentration of $CaCO_3$ was necessary because calcium uptake from its slurry was not as efficient as that obtained with the more soluble hydroxide. These handsheets were subjected to accelerated aging and subsequent testing. The results obtained are presented in Table VII. The relative permanence of these paper samples with sodium borohydride incorporated during manufacture was observed to be 1.5–2.6 times that of samples prepared without borohydride. The stability gained through such treatment was appreciably smaller than that observed for Foldur kraft and newsprint papers subjected to borohydride treatment.

Papers with an appreciable copper content (50 ppm or higher) were observed to develop prominent, darkly colored spots upon treatment with sodium borohydride. These spots, which are brownish black or sometimes grayish green, are probably caused by the precipitation of copper boride (*25*) or some other reduced copper species (*26*). When paper with such colored spots was immersed in a 0.007% magnesium bicarbonate solution, the spots gradually disappeared within 1 h. In another set of experiments, handsheets were prepared with a Noble and Wood brass sheet-forming machine. Because of contamination from contact with the brass, these handsheets contained as much as 150 ppm of copper. These handsheets were first washed with 0.007% magnesium bicarbonate solution. Upon further treatment with 0.1% sodium borohydride solution, these papers did not develop any noticeable spots or stains. The copper content of this paper was monitored at each step of the treatment. During the first washing step, the paper lost 30–40% of the copper, but no further change in copper content was observed after the borohydride treatment or during a subsequent washing step. At the completion of the entire treatment, the paper still contained about 100 ppm of copper. Therefore, reduction in copper content alone cannot account for the inhibition of the precipitation of reduced copper species. The rate of reduction of copper species may be dependent upon acid concentrations. Neutralization of the acidity in paper by the mildly alkaline wash could have slowed the precipitation of reduced copper. Indeed, the liberation of hydrogen during the reduction step is considerably slower for papers that have been prewashed with a magnesium bicarbonate solution. Further work is needed to obtain a better understanding of the underlying reaction mechanisms. However, it is clear from these experiments that neutralization of acidity in paper is most desirable before subjecting paper to a borohydride treatment, especially if the paper contains copper species in a significant concentration. The beneficial effect of a dilute $Ca(OH)_2$ wash after the borohydride treatment also was amply demonstrated here. Indeed, conservators in the field have occasionally applied a similar sequence of borohydride treat-

Published on February 1, 1986 on http://pubs.acs.org | doi: 10.1021/ba-1986-0212.ch024

Table VII. Characterization and Aging of Paper from Borohydride-Treated Pulp

Pulp Additives[a]	*Brightness*	*pH*	*Ca (ppm)*	*Na (ppm)*	*B (ppm × 10^{-4})*	*Folds*	*Relative Permanence*
None	86	6.3	610	0.72	515	1610	1.0
0.1% $NaBH_4$ + 0.02% $Ca(OH)_2$	90	9.1	4690	1.10	595	1890	2.6
0.1% $NaBH_4$ + 2.5% $CaCO_3$	89	9.4	11470	1.10	595	1580	1.5

[a]Percent concentrations refer to proportions of pulp weight.

ment combined with washing steps using dilute calcium hydroxide or magnesium bicarbonate solution.

It has been shown here that the reducing action of sodium borohydride can be used effectively to stabilize paper as well as to increase its brightness. Aged paper was shown to regain its brightness and some of its lost strength. A washing step with dilute magnesium bicarbonate solution before the borohydride treatment was shown to inhibit the reduction of copper species. A washing step with dilute calcium hydroxide solution after the borohydride treatment was shown to prevent hydrolytic degradation that may result when more concentrated borohydride solutions are employed. Such a washing step imparts more stability than washing with water alone.

In spite of reports of limited success with borohydride reduction treatments in practice, I would like to add a word of caution. Sodium borohydride is a moderately strong reducing agent. Its interaction with inks and other media is not well understood at present. Therefore, this treatment should be used only when no other option is available. Even then, it should not be undertaken lightly. Testing of all media before treatment of artifacts is strongly recommended.

Acknowledgment

I wish to thank Chandru J. Shahani, Research Officer, for his helpful comments and assistance in the writing of this chapter.

Literature Cited

1. McBurney, L. F. "Cellulose and Cellulose Derivatives"; Ott, E.; Spurilin, H. M.; Graffin, M. W., Eds: Interscience: New York, 1954.
2. "The Bleaching of Pulp"; 3rd ed., revised. Dingh, R. P., Ed.; Technical Association of the Pulp and Paper Industry, Pulp Bleaching Committee: Atlanta, TAPPI, 1979.
3. Spinner, I. H. *TAPPI* **1962**, *45*, 495. Rapson, W. H.; Spinner, I. H. In "Bleaching of Pulp", TAPPI Monograph 27; Rapson, W. H., Ed.; Techn. Assn. Pulp Paper Ind.: New York, 1963. Virkola, N. E.; Vartianen, V. *Tappi* **1964**, *47*, 765. Kringstad, K. TAPPI **1969**, *52*, 1070.
4. Kimura, Y.; Kitano, A. *J. Jpn Wood Res. Soc.* **1956**, *2*(1), 28; *Abstr. Bull. Inst. Paper Chem.* **1957**, *27*, 508.
5. Zeronian, S. H.,; Hudson, F. L.; Peters, R. H. *Tappi* **1964**, *47*, 557.
6. Mayer, W. C.; Donofrio, C. P. *Pulp Pap. Mag. Can.* **October 1958**, 157–66.
7. Varshney, M. C.; Luner, P. *TAPPI* **April 1961**, Vol. *44*(4), 285–89.
8. Jullander, I.; Brune, K. *Svensk Papperstidn.* **October 1959**, *62*(20), 728–736.
9. Corbi, J. C.; Rapson, W. H. *Pulp Paper Mag. Can.* **1964**, *65*, T467.
10. Giertz, H. W.; McPherson, J. *Svensk Papperstidn.* **1956**, *59*, 93.
11. Marranci, L. M.; Kleinert, TR. N. *Svensk Papperstidn.* **1962**, *65*, 126; O'Brien, J. F. *Pap. Mill News* **1962**, *86*(39), 54, 56. Sanyal, A. K. *Indian Pulp Pap.* **1963**, *17*, 677.
12. "Sodium Borohydride". Ventron Div., Thiokol Corp. Danvers, Mass., 1979.

13. Rapson, W. H. Canadian Patent, 610,654 and 610, 655, December 13, 1960.
14. Wade, R. C. U.S. Patent 3,318,657, May 9, 1967.
15. Burr, F. K. U.S. Patent 3,081,265, March 12, 1963.
16. Burgess, H. D. "The Color Reversion of Paper After Bleaching", Preprints: The Conservation of Library and Archive Materials and the Graphic Arts; Cambridge, 1980 Conference, 171, (1980).
17. Roberts, M.; Etherington, D. "Bookbinding and the Conservation of Books", a dictionary of descriptive terminology; Library of Congress: Washington, D.C., 1982.
18. Tang, L. C. "Preservation of Paper and Textiles of Historic and Artistic Value II"; Williams, J. C., Ed.; ADVANCES IN CHEMISTRY SERIES No. 193; American Chemical Society: Washington, D.C., 1981; pp. 63–86.
19. Wilson, W. K.; Golding, R. A.; McClearen, R. H.; Gear, J. L. "Preservation of Paper and Textiles of Historic and Artistic Values II"; Williams, J. C., Ed.; ADVANCES IN CHEMISTRY SERIES No. 193; American Chemical Society, Washington, D.C., 1981; pp. 87–107.
20. Tang, L. C.; Troyer, M. A. *Technology and Conservation* **1981**, *2*, 40–45.
21. Tang, L. C.; Troyer, M. A. U.S. Patent 4,401,810, August 30, 1983.
22. Tang, L. C.; Troyer, M. A. *Proc. of the Techn. Assoc. of the Pulp and Pap. Ind.*, 1981 Papermakers Conference, Chicago, Illinois, April 6–8, 1981, pp. 77–84.
23. Tang, L. C. *J. Am. Inst. Conserv.* **1979**, *18*(2), 61–81.
24. Tang, L. C. *J. Am. Inst. Conserv.* **1978**, *17*(2), 19–32.
25. Hohnstedt, L. F.; Miniatas, B. O.; Waller, M. C. *Anal. Chem.* **1965**, *37*, 1163.
26. Paul, R.; Buisson, P.; Joseph N. *Comp. Rend.* **1951**, *232*, 627.

RECEIVED for review November 20, 1984. ACCEPTED March 14, 1985.

Glossary

alizarin An orange crystalline compound, insoluble in cold water; made synthetically from anthraquinone; used in the manufacture of dyes and red pigments. Also known as 1,2-dihydroxyanthraquinone. Found as a component in several natural dyes.

alpaca An artiodactyl of the camel family (Camelidae); economically important for its long, fine wool.

bast fiber Any fiber stripped from the inner bark of plants, such as flax, hemp, jute, and ramie; used in textile and paper manufacturing.

brazilin A bright-yellow compound obtained from brazilwood as a crystalline powder and used as a dye and indicator.

brazilwood A reddish wood obtained from several tropical American trees (genus *Caesalpinia*) of the legume family.

bave A term for the natural silk thread spun by the silkworm in making the cocoon. It contains two single filaments called brins that are bound together by a gelatinous gum called sericin.

brin A single filament of natural silk spun by the silkworm.

camelid Fibers of the camel family (Camelidae) including alpaca, camel, llama, and vicuña.

CIELAB An internationally accepted color space. CIE stands for Commission Internationale de l'Eclairage. LAB stands for coordinates l, a, and b, which are defined as mathematical coordinates in the three-dimensional color space. (Billmeyer, F. W.; Saltzman, M. "Principles of Color Technology", 2nd ed.; Wiley: New York, 1981; Chap. 2.)

color space A three-dimensional color-order system in which the shades and depths of shades of colored objects can be arranged, described, and distinguished from one another.

cutch A tannin colorant extracted from mangrove bark.

earspool A spool-shaped earplug worn buttoned through a hole in the earlobe, especially by the ancient Hopewell and Copena people.

jordan A machine or engine used to refine paper pulp, consisting of a rotating cone, with cutters, that fits inside another cone, also with cutters.

lake Any of a large group of dyes that have been combined with or adsorbed by salts of calcium, barium, chromium, aluminum, phosphotungstic acid, or phosphomolybdic acid; used for textile dyeing. Also known as color lake.

littoral Of, on, or along the shore.

madder The root of the madder plant (*Rubia tinctorium*), pulverized and used as source of glucosides to produce alizarin by fermentation. Also known as gamene.

malacology The study of mollusks.

mordant An agent, such as alum, phenol, or aniline, that fixes dyes to tissues, cells, textiles, and other materials by combining with the dye to form an insoluble compound. Also known as dye mordant.

natural colorants Dyes and pigments extracted from plant and mineral sources.

premordanting Adding or impregnating a mordant onto a textile before dyeing.

provenance Origin; derivation; source.

pseudomorph An altered mineral whose crystal form has the outward appearance of another mineral species. Also known as false form.

pseudomorph after fabric An altered mineral whose crystal form has replaced a textile fabric through mineralization to form an exact replica of that fabric.

vat dye One of the dyes that are easily reduced to a soluble and colorless form in which they easily impregnate fibers; subsequent oxidation produces the final color; examples are indigo and indanthrene blue.

AUTHOR INDEX

SUBJECT INDEX

AUTHOR INDEX

SUBJECT INDEX

B

C

D

E

F

G

H

I

J

K

L

M

N

O

P

Y